LEABHARLANN CHOLÁISTE NA TRÍONÓIDE, BAILE ÁTHA CLIATH | TRINITY COLLEGE LIBRARY DUBLIN
Ollscoil Átha Cliath | The University of Dublin

Terms and Conditions of Use of Digitised Theses from Trinity College Library Dublin

Copyright statement

All material supplied by Trinity College Library is protected by copyright (under the Copyright and Related Rights Act, 2000 as amended) and other relevant Intellectual Property Rights. By accessing and using a Digitised Thesis from Trinity College Library you acknowledge that all Intellectual Property Rights in any Works supplied are the sole and exclusive property of the copyright and/or other IPR holder. Specific copyright holders may not be explicitly identified. Use of materials from other sources within a thesis should not be construed as a claim over them.

A non-exclusive, non-transferable licence is hereby granted to those using or reproducing, in whole or in part, the material for valid purposes, providing the copyright owners are acknowledged using the normal conventions. Where specific permission to use material is required, this is identified and such permission must be sought from the copyright holder or agency cited.

Liability statement

By using a Digitised Thesis, I accept that Trinity College Dublin bears no legal responsibility for the accuracy, legality or comprehensiveness of materials contained within the thesis, and that Trinity College Dublin accepts no liability for indirect, consequential, or incidental, damages or losses arising from use of the thesis for whatever reason. Information located in a thesis may be subject to specific use constraints, details of which may not be explicitly described. It is the responsibility of potential and actual users to be aware of such constraints and to abide by them. By making use of material from a digitised thesis, you accept these copyright and disclaimer provisions. Where it is brought to the attention of Trinity College Library that there may be a breach of copyright or other restraint, it is the policy to withdraw or take down access to a thesis while the issue is being resolved.

Access Agreement

By using a Digitised Thesis from Trinity College Library you are bound by the following Terms & Conditions. Please read them carefully.

I have read and I understand the following statement: All material supplied via a Digitised Thesis from Trinity College Library is protected by copyright and other intellectual property rights, and duplication or sale of all or part of any of a thesis is not permitted, except that material may be duplicated by you for your research use or for educational purposes in electronic or print form providing the copyright owners are acknowledged using the normal conventions. You must obtain permission for any other use. Electronic or print copies may not be offered, whether for sale or otherwise to anyone. This copy has been supplied on the understanding that it is copyright material and that no quotation from the thesis may be published without proper acknowledgement.

The Role of Inflammation and Macrophage Accumulation in the Development of Obesity Induced Type 2 Diabetes Mellitus and the Possible Therapeutic Effects of Long Chain *n-3* Polyunsaturated Fatty Acids

A thesis submitted to the University of Dublin, Trinity College for the degree of Doctor of Philosophy (Ph.D.)

By

Elizabeth Oliver

February 2010

Institute of Molecular Medicine,
Trinity Centre for Health Science,
University of Dublin,
Trinity College.

Dedicated to my family

TRINITY COLLEGE
10 APR 2012
LIBRARY DUBLIN

9385

Declaration

I declare that the work in this thesis has not been previously submitted as an exercise for a degree to this or any other university.

I declare that this thesis, except where acknowledged, is entirely my own work.

I agree that Trinity College Library may lend or copy this thesis on request.



Elizabeth Oliver

15/2/2010

Date

Summary

Obesity gives rise to a state of chronic, low-grade inflammation characterised by inflamed white adipose tissue (WAT) with increased infiltration of macrophages termed adipose tissue macrophages (ATM). These ATM produce pro-inflammatory cytokines, which are proposed to alter the endocrine function of the WAT and disrupt insulin signalling. High intakes of long chain (LC) *n-3* polyunsaturated fatty acids (PUFA) such as eicosapentaenoic acid (EPA) and docosahexaenoic acid (DHA) are known to modulate immune cell function and may exert therapeutic effects on obesity induced insulin resistance and type 2 diabetes mellitus (T2DM). The objective of this thesis was to investigate the molecular mechanisms, which mediate the interaction between macrophages and adipocytes. An *in vivo* IL-1 type 1 receptor knock out (IL-1RI$^{-/-}$) mouse model followed by a series of *in vitro* experiments, including a co-culture of adipocytes and macrophages were examined. The effects of LC *n-3* PUFA treatment were assessed in adipocytes and macrophages both independently and in the co-culture system.

In chapter 3, an *in vivo* time-course experiment was established to study the molecular mechanism involved in the development of obesity-induced insulin resistance within immune compromised IL-1RI$^{-/-}$. We hypothesized that IL-1RI$^{-/-}$ mice will not only have a general reduction in inflammation but also a specific reduction in ATM due to a lack in IL-1 signalling. We speculated that this reduction in ATM would lead to increased insulin sensitivity within the WAT. After 16 weeks on a high-fat diet (HFD) the IL-1R1$^{-/-}$ mice cleared glucose more efficiently as determined by glucose tolerance tests (GTT) with significantly lower plasma insulin, triacylglycerol (TAG) and leptin levels relative to the WT. Importantly, pro-inflammatory cytokine and chemokine concentrations in the plasma, specifically interleukin (IL)-1β and CC Chemokine ligand (CCL)-5, were reduced. In addition, tumour necrosis factor (TNF)-α and monocyte chemotactic protein (MCP)-1 gene expression levels within the epididymal adipose tissue (EAT) of the IL-1RI$^{-/-}$ mice were also reduced. IL-1R1$^{-/-}$ mice exhibited significantly higher levels of insulin sensitive target genes such as glucose transporter (GLUT)-4 and insulin receptor substrate (IRS)-1 within the EAT, also signifying that these mice are more insulin sensitive. Additionally, IL-1R1$^{-/-}$ mice exhibited a leaner phenotype with smaller EAT adipocyte size.

In chapter 4 the effects of IL-1β treatment on inflammatory and insulin signalling *in vitro* within 3T3-L1 adipocytes were determined to verify the findings of the *in vivo* time-course experiment. This study demonstrated that IL-1β treatment induced a pro-inflammatory state within the adipocytes, which up-regulated mitogen-activated protein

kinase (MAPK) and nuclear factor (NF)-κB signalling and significantly induced IL-6 secretion. This was accompanied by reduced insulin sensitivity via a reduction in IRS-1 and GLUT4 expression. IRS-1 Serine phosphorylation was induced by IL-1β via the mammalian target of rapamycin (mTOR) pathways effectively inhibiting insulin signaling. This data correlated with observations in IL-1RI$^{-/-}$ mice, which exhibited increased insulin sensitivity and reduced inflammation.

In chapter 5 the effects of EPA and DHA on 3T3-L1 adipocytes and J774.2 macrophages *in vitro* were assessed. Chronic EPA treatment within 3T3-L1 adipocytes increased leptin and adiponectin secretion levels and improved insulin induced glucose uptake, suggesting EPA may have insulin sensitising effects. Conversely, DHA reduced GLUT4, inducing lipolysis and reducing the differentiation state of the 3T3-L1 adipocytes, indicating that DHA may have negative effects on adipocyte insulin sensitivity. However, DHA may induce anti-obesity effects by preventing further growth of WAT. The effects of LC *n-3* PUFA on J774.2 macrophages were more consistent, with EPA and DHA reducing inflammatory cytokine production while down-regulating MAPK and NF-κB signalling pathways. In the last chapters, co-culture of adipocytes and J774.2 macrophages was developed to study components of obesity induced insulin resistance. Furthermore, conditioned medium from the treated macrophages was incubated with the adipocytes. These models examined the effects of macrophages acutely (24 hour) and chronically (5 day) treated with EPA, DHA or DMSO vehicle control on adipocytes. Overall the data suggests that macrophage-derived soluble factors such as TNF-α, IL-6 and IL-1β promote a pro-inflammatory environment within the adipocytes in which inflammatory pathways such as NF-κB, ERK1/2 and p38 MAPK become up-regulated. These pro-inflammatory pathways cross-talk with the insulin signalling pathways leading to a reduction in adipocyte insulin signalling molecules such as GLUT4 and IRS-1, coinciding with reduced insulin induced glucose uptake and GLUT4 translocation to the cell membrane, indicative of insulin resistance. Furthermore, this work determined that pre-culturing macrophages with EPA and DHA attenuated the inflammatory effect while increasing insulin signalling markers and insulin sensitivity within the co-cultured adipocytes.

In conclusion, these results imply that obesity is associated with the generation of macrophage-derived soluble factors that promote a pro-inflammatory environment in which inflammatory pathways such as NF-κB and MAPK signalling become up-regulated. This leads to down-regulation in insulin sensitive markers such as GLUT4 and IRS-1 causing insulin-resistant adipocyte function, an effect attenuated by EPA and DHA.

Acknowledgements

I would firstly like to thank Prof. Helen Roche for giving me the opportunity to carry out this research and for her input and encouragement throughout my time in the Nutrigenomics lab. I would also like to thank Prof. Dermot Kelleher, Dr. Ross McManus, Dr. Aideen Long, Dr. Orla Sheils and the entire Steering Committee at Trinity College Dublin (TCD) for their support and input throughout the four year Ph.D. programme 'From Genes to Function'. I would also like to thank the Health Research Board for funding this research.

Many thanks to Prof. Kingston Mills and his Immune Regulation Research Group based at TCD who provided help setting up the IL-1R1$^{-/-}$ model. Additionally, I would like to thank the Bioresources Unit at TCD for housing the animals during the feeding study.

I would like to thank everyone in the Nutrigenomics lab, many of which have become valued friends. Thank you for your support and encouragement throughout the past three years. A special thanks to Dr. Clare Reynolds for her continuing advice and encouragement; Dr. Jane Ferguson and Annalouise O'Connor not only for the help and guidance over the gas chromatography but for being so supportive; Dr. Catherine Philips and Dr. Sinead Toomey for advice and guidance setting up the acute co-culture work; Dr. Mandy Claessens for help designing and setting up the initial IL-1RI$^{-/-}$ study; Karen Harford for her hard work and for facilitating the IL-1RI$^{-/-}$ work; Dr. Fiona McGillicuddy for her invaluable advice and support on many areas of my work. Not forgetting Dr. Cathal O'Brien, Dr. Vanessa Rungapamestry, Orla Finucane, Melissa Morine, Colm O'Grada, Emma Allott, Dr. Audrey Tierney and Dr. Jolene McMonagle, thanks guys!

Thanks to Dr Christine Cipolletta-Daly, Dr. Anthony Mitchell Davies, Jennifer Conroy based at TCD and Ann Cullen based at University College Dublin (UCD) for training and guidance with the confocal microscope work. Additionally, thank you to all the staff in the TCD Institute of Molecular Medicine and the UCD Conway Institute.

I would like to thank my friends and family, especially my parents and my brothers Lee, Martin and Rowan for their encouragement and support throughout my life.

Finally, I want to especially thank Robin Brady-Roche, he is terrific and I want to thank him for his continuous kindness, love and support.

Table of Contents

Declaration i

Summary ii

Acknowledgements iv

Abbreviations xi

Chapter 1 **General Introduction** **1**

1.1 Obesity **1**

1.1.1 Obesity, the metabolic syndrome and type 2 diabetes mellitus 1

1.2 Insulin and glucose homeostasis **2**

1.3 Quantifying insulin sensitivity **4**

1.3.1 Homeostasis model assessment and quantitative insulin sensitivity check index 5
1.3.2 Hyperinsulinemic euglycemic glucose clamp 5
1.3.3 Glucose tolerance test (GTT) 6

1.4 White adipose tissue: biology and function **7**

1.4.1 Subcutaneous and visceral adipose tissue 7
1.4.2 Lipid absorption and storage 9
1.4.3 Triacylglycerol synthesis and lipolysis 10

1.5 Adipokines: obesity and T2DM **13**

1.5.1 Adiponectin 14
1.5.2 Leptin 15
1.5.3 Resistin 17
1.5.4 TNF-α 19
1.5.5 IL-6 19
1.5.6 IL-1 20

1.6 Transcription factors: inflammation and insulin sensitivity **21**

1.6.1 Nuclear factor-κB 22
1.6.2 Peroxisome proliferator-activated receptors 24
1.6.3 Sterol regulatory element binding proteins 25
1.6.4 Transcriptional regulation of adipokines by cytokines 26

1.7 Obesity: a chronic pro-inflammatory state **27**

1.7.1 Immune cell recruitment into adipose tissue 27
1.7.2 Vascularization and hypoxia 29
1.7.3 Necrotic adipocyte death 29
1.7.4 Chemokines 29

1.8 Pro- and anti-inflammatory adipose tissue macrophages **30**

1.9 Insulin signalling **32**

1.9.1 Insulin receptor 32
1.9.2 Insulin receptor substrates 32
1.9.3 Phosphatidylinositol 3-kinase and protein kinase B/Akt 33
1.9.4 Glucose transporter 34
1.9.5 Insulin signaling and mitogen-activated protein kinase 35

1.10 Interactions between macrophages and adipocytes 36

1.10.1 Pro-inflammatory cytokines and adipocyte insulin signalling 37

1.11 Dietary fatty acids 38

1.11.1 Long chain polyunsaturated fatty acids and eicosanoid production 40
1.11.2 Membrane lipid composition and its impacts on cell signalling 42
1.11.3 Long chain polyunsaturated fatty acids and gene expression 45
1.11.4 The anti-inflammatory effects of LC *n-3* PUFA 46
1.11.5 Fatty acids and adipose tissue macrophages infiltration 47
1.11.6 Insulin sensitising LC *n-3* PUFA 47

1.12 Project Rationale 49

1.12.1 Project Hypothesis 49
1.12.2 Project Aims 50

***Chapter 2* Material and Methods 53**

2.1 Animal study 53

2.1.1 Animals and diets 53
2.1.2 Glucose tolerance test 54
2.1.3 Tissue and plasma collection 54
2.1.4 Adipocyte isolation 55
2.1.5 Determination of multiple cytokines using multi-analyte profiling 56
2.1.6 Determination of plasma triacylglycerol and non-esterified fatty acids 57
2.1.7 Determination of adipocyte size 59

2.2 Cell culture 60

2.2.1 3T3-L1 cell line 60
2.2.2 3T3-L1 sub-culture 60
2.2.3 Cyropreservation and revival of cells 61
2.2.4 Differentiation of 3T3-L1 61
2.2.5 J774.2 macrophages 62
2.2.6 Sub-culturing J774.2 macrophages 62
2.2.7 Cyropreservation and revival of cells 62
2.2.8 Cell enumeration and viability assessment 63
2.2.9 Preparation of fatty acids 63
2.2.10 Cell stimulation 63
2.2.11 Experimental design 64

2.3 MTT viability assay 67

2.4 Macrophage and adipocyte fatty acid composition analysis 68

2.4.1 Total lipid extraction 68
2.4.2 Transmethylation of macrophage and adipocyte lipid extracts 69

2.4.3 Gas chromatographic analysis of macrophage and adipocyte lipids 69

2.5 Oil red O staining in 3T3-L1 adipocytes 70

2.6 Glucose uptake analysis in 3T3-L1 adipocytes 70

2.7 RNA extraction and analysis 71

2.7.1 RNA extraction 71
2.7.2 Quantitation of RNA 72
2.7.3 Real-Time RT-Taqman® PCR: methodology 74
2.7.4 Preparation of RNA prior to cDNA synthesis 75
2.7.5 cDNA synthesis 75
2.7.6 Real-time TaqMan® PCR: reaction and analysis 76

2.8 Preparation of protein extracts and Western blotting 77

2.8.1 Isolation of total protein 77
2.8.2 Determination of protein concentration 77
2.8.3 Preparation of samples for gel electrophoresis and Western blotting 77
2.8.4 Sodium dodecyl sulphate polyacrylamide gel electrophoresis (SDS-PAGE) 78
2.8.5 Western blotting 78
2.8.6 Detection of antigens 78
2.8.7 Reuse of Western blots 79
2.8.8 Quantification of protein bands 79

2.9 Enzyme-linked immunosorbent assay 79

2.9.1 ELISA 80

2.10 Confocal microscopy 81

2.10.1 Preparation of 3T3-L1 adipocytes prior to confocal analysis 81
2.10.2 Confocal analysis 82

2.11 Data preparation and statistical analysis 85

***Chapter 3* The Effects of High Fat Diet Induced Obesity on Molecular Mechanisms Associated with Insulin Resistance *In Vivo* within IL-1 Receptor I Knockout Mice 86**

3.1 Introduction 86

3.2 Material and methods 90

3.2.1 Experimental design 90
3.2.2 Glucose Tolerance Test 90
3.2.3 Tissue and plasma collection 90
3.2.4 Adipocyte isolation 91
3.2.5 Determination of adipocyte size 91
3.2.6 Milliplex multi-analyte profiling 91
3.2.7 mRNA analysis (TaqMan® RT-PCR) 92
3.2.8 Data preparation and statistical analysis 93

3.3 Results 94

3.3.1 Phenotypic attributes of WT of IL-1RI$^{-/-}$ and WT mice at base line 94

3.3.2 Effects of a 16 week HFD on body weight, food intake and adipose tissue mass in IL-1RI$^{-/-}$ and WT mice 96
3.3.3 Effects of a 16 week HFD on glucose tolerance in male IL-1RI$^{-/-}$ and WT mice 99
3.3.4 Effects of a 16 week HFD on plasma hormone concentrations in IL-1RI$^{-/-}$ and WT mice 104
3.3.5 Effects of a 16 week HFD on plasma cytokine and chemokine concentrations in IL-1RI$^{-/-}$ and WT mice 110
3.3.6 Effects of a 16 week HFD on plasma triacylglycerol and non-esterified fatty acids levels in IL-1RI$^{-/-}$ and WT mice 113
3.3.7 Effects of a 16 week HFD on insulin sensitive target gene expression in the epididymal adipose tissue of IL-1RI$^{-/-}$ and WT mice 116
3.3.8 Effects of a 16 week HFD on inflammatory target gene expression in the epididymal adipose tissue of IL-1RI$^{-/-}$ and WT mice 122
3.3.9 Effects of a 16 week HFD on gene expression in the adipocytes of epididymal adipose tissue within IL-1RI$^{-/-}$ and WT mice 126
3.3.10 Effects of a 16 week HFD on adipocyte size in the epididymal adipose tissue of IL-1RI$^{-/-}$ and WT mice 127

3.4 Discussion 129

***Chapter 4* The Effects of IL-1β Treatment on Inflammatory and Insulin Signalling *In Vitro* within 3T3-L1 Adipocytes 141**

4.1 Introduction 141

4.2 Material and methods 146

4.2.1 Experimental design 146
4.2.2 Protein analysis and Western blotting 146
4.2.3 ELISA analysis 147
4.2.4 Oil red O staining 147
4.2.5 Glucose uptake assay 148
4.2.6 Data preparation and statistical analysis 148

4.3 Results 149

4.3.1 Effects of IL-1β treatment on insulin pathway protein expression in 3T3-L1 adipocytes 149
4.3.2 Effects of IL-1β treatment on ^{3}H glucose uptake in 3T3-L1 adipocytes 156
4.3.3 Effects of IL-1β treatment on lipid accumulation in 3T3-L1 adipocytes 158
4.3.4 Effects of IL-1β treatment on MAPK protein expression in 3T3-L1 adipocytes 159
4.3.5 Effects of IL-1β treatment on IκB-α protein expression in 3T3-L1 adipocytes 166
4.3.6 Effects of IL-1β treatment on adipokine secretion in 3T3-L1 adipocytes 169

4.4 Discussion 171

***Chapter 5* The Effects of EPA and DHA Treatment on Inflammatory and Insulin Signalling *In Vitro* within 3T3-L1 Adipocytes and J774.2 Macrophages 178**

5.1 Introduction 178

5.2 Material and methods 183

5.2.1 Experimental design 183
5.2.2 mRNA analysis (TaqMan® RT-PCR) 184
5.2.3 Protein analysis and Western blotting 185
5.2.4 ELISA analysis 185
5.2.5 Glucose uptake assay 186
5.2.6 Data preparation and statistical analysis 186

5.3 Results 187

5.3.1 Effects of EPA and DHA on adipokine secretion from 3T3-L1 adipocytes 187
5.3.2 Effects of EPA and DHA on insulin sensitive and inflammatory target gene expression in 3T3-L1 adipocytes 190
5.3.3 Effects of EPA and DHA on insulin sensitive and inflammatory target protein expression in 3T3-L1 adipocytes 194
5.3.4 Effects of EPA and DHA on glucose uptake in 3T3-L1 adipocytes 198
5.3.5 Effects of EPA and DHA treatment on cytokine secretion from LPS stimulated J774.2 macrophages 203
5.3.6 Effects of EPA and DHA treatment on inflammatory target protein expression in LPS stimulated J774.2 macrophages 209
5.3.7 The effects of acute EPA and DHA treatment on cytokine and adipokine secretion within a co-culture of J774.2 macrophages and 3T3-L1 adipocytes 215
5.3.8 The effects of acute EPA and DHA treatment on inflammatory and insulin sensitive target gene expression within a co-culture of J774.2 macrophages and 3T3-L1 adipocytes 220

5.4 Discussion 225

***Chapter 6* The Effects of LPS Stimulated Macrophages Pre-treated with EPA and DHA on Inflammatory and Insulin Signalling within 3T3-L1 Adipocytes of a Co-culture System 234**

6.1 Introduction 234

6.2 Material and methods 239

6.2.1 Experimental design 239
6.2.2 Macrophage and adipocyte fatty acid composition analysis 241
6.2.3 mRNA analysis (TaqMan® RT-PCR) 241
6.2.4 Protein analysis and Western blotting 241
6.2.5 ELISA analysis 242
6.2.6 Oil red O staining 243
6.2.7 Glucose uptake assay 243
6.2.8 Confocal GLUT4 translocation analysis 243
6.2.9 Data preparation and statistical analysis 245

6.3 Results 246

6.3.1 Effects of EPA and DHA treatment on J774.2 macrophage fatty acid composition 246
6.3.2 Effects of J774.2 macrophages pre-treated with EPA and DHA on 3T3-L1 adipocyte fatty acid composition within a transwell co-culture system 251
6.3.3 Effects of chronic EPA and DHA treatment on cytokine and adipokine secretion within a co-culture of J774.2 macrophages and 3T3-L1 adipocytes 254

6.3.4 Effects of LPS stimulated J774.2 macrophages pre-treated with EPA or DHA on inflammatory and insulin sensitive target gene expression within 3T3-L1 adipocytes of a transwell co-culture 257
6.3.5 Effects of LPS stimulated macrophages pre-treated with EPA and DHA on GLUT4 and IRS-1 protein expression in 3T3-L1 adipocytes 260
6.3.6 Effects of LPS stimulated macrophages pre-treated with EPA and DHA on insulin induced GLUT4 translocation to the membrane within 3T3-L1 adipocytes of a co-culture system 264
6.3.7 Effects of conditioned media from LPS stimulated macrophages (CM) pre-treated with EPA and DHA on ^{3}H glucose uptake within 3T3-L1 adipocytes 268
6.3.8 Effects of conditioned media from LPS stimulated macrophages (CM) pre-treated with EPA and DHA on 3T3-L1 adipocyte lipid accumulation and cell morphology 274
6.3.9 Effects of conditioned media from LPS stimulated macrophages (CM) pre-treated with EPA and DHA on MAPK protein expression in 3T3-L1 adipocytes 278
6.3.10 Effects of conditioned media from LPS stimulated macrophages (CM) pre-treated with EPA and DHA on IκB-α protein expression in 3T3-L1 adipocytes 286

6.4 Discussion 289

***Chapter 7* General Discussion 302**

References 311

AA	Arachidonic acid
ACC	Acetyl-CoA carboxylase
ACOD	Acyl-CoA oxidase
ACS	Acetyl-CoA synthetase
AdipoR	Adiponectin receptor
ADP	Adenosine triphosphate
AGPAT	1-acylglycerol-3-phosphate acyltransferase
ALA	α-Linolenic acid
AMPK	Adenosine monophosphate-activated protein kinase
ANOVA	Analysis of variance
AP	Activator protein
AT	Adipose tissue
ATGL	Adipocyte TAG lipase
ATM	Adipose tissue macrophages
ATP	Adenosine diphosphate
BAT	Brown adipose tissue
BMI	Body mass index
BSA	Bovine serum albumin
cAMP	Cyclic adenosine monophosphate
CCL	CC Chemokine ligand
CCR	CC Chemokine receptor
cDNA	Complementary deoxyribonucleic acid
CLA	Conjugated linoleic acid
CM	Conditioned media
CoA	Coenzyme A
COX	Cyclooxygenase
CPT	Carnitine palmitoyltransferases
CSF	Colony-stimulating factor
CVD	Cardiovascular disease
DAG	Diacylglycerol
DGAT	Diacylglycerol acyl-transferase
DGLA	Dihomo-γ-Linolenic acid
DHA	Docosahexaenoic acid
DHAP	Dihydroxyacetone-phosphate
DHAPAT	Acyl-CoA dihydroxyacetone-phosphate acyltransferase
DHAP-OR	Dihydroxyacetone-phosphate oxido-reductase
DIO	Diet induced obese
DMEM	Dulbecco's modified eagle medium
DMSO	Dimethyl sulfoxide
DNase	Deoxyribonuclease
DPA	Docosapentaenoic acid
EAT	Epididymal adipose tissue
ECACC	European collection of animal cell cultures
EDTA	Ethylenediaminetetraacetic acid
ELISA	Enzyme-linked immunosorbent assay
EPA	Eicosapentaenoic acid
ER	Endoplasmic reticulum
ERK	Extracellular signal-regulated kinases
ETA	Eicosatetraenoic acid
FA	Fatty acid
FABP	Fatty acid binding protein
FAS	Fatty acid synthase
FBS	Foetal bovine serum
FITC	Fluorescein isothiocyanate
FS	Frequently sampled
GF	Transforming growth factor
GHP	Growth hormone protein
GIR	Glucose infusion rate
GK	Glycerol kinase
GLA	γ-Linolenic acid
GLUT	Glucose transporter
GM	Granulocyte macrophage
GPAT	Glycerol-3-phosphate acyl-transferase
GPO	Glycerol phosphate oxidase
Grb	Growth factor receptor-bound protein
GSK	Glycogen synthase kinase
GTT	Glucose tolerance test
HDL	High density lipoproteins
HETE	Hydroxyeicosatetraenoic acid
HFD	High fat diet
HGP	Hepatic glucose production
HIF	Hypoxia-inducible factor
HOMA	Homeostasis model assessment
HRP	horseradish peroxidase

HSL	Hormone-sensitive lipase
IBMX	Isobutyl-1-methylxanthine
ICAM	Soluble inter-cellular adhesion molecule
IDL	Intermediate density lipoproteins
IFN	Interferon
IGF	Insulin-like growth factors
IKK	IκB kinase
IL	Interleukin
IL-1R	Interleukin-1 receptor
IL-1Ra	Interleukin-1 receptor antagonist
IL-1RAcP	Interleukin-1 receptor accessory protein
iNOS	Inducible nitric oxide synthase
IP	Intraperitoneal
IRAK	Interleukin-1 receptor associated protein kinase
IRS	Insulin receptor substrate
ITT	Insulin tolerance test
IV	Intravenous
IκB	Inhibitor of κB
JAK	Janus kinase
JNK	c-Jun N-terminal kinase
K_{ATP}	ATP-sensitive potassium channel
KC	Keratinocyte-derived chemokine
LA	Linoleic acid
LC	Long chain
LD	Lipid droplets
LDL	Low density lipoproteins
LFD	Low fat diet
LOX	Lipoxygenase
LPL	Lipoprotein lipase
LPS	Lipopolysaccharides
LT	Leukotrienes
LTB	Leukotriene
LXR	Liver X receptor
MAG	Monoacylglycerol
MAP	Multi-analyte profiling
MAPK	Mitogen-activated protein kinase
MCP	Monocyte chemotactic protein
MetS	Metabolic syndrome
MGL	Monoglyceride lipase
MIF	Macrophage migration inhibitory factor
MINMOD	Minimal model analysis
MIP	Macrophage inflammatory protein
mRNA	Messenger rebonucleic acid
mTOR	Mammalian target of rapamycin
MUFA	Monosaturated fatty acid
MyD88	Myeloid differentiation primary response gene
NEFA	Non-esterified fatty acids
NEMO	NF-κB essential modulator
NF-κB	Nuclear factor-κB
NK	Natural killer
NO	Nitric oxide
NSAID	Non-steroidal anti-inflammatory drug
OA	Oleic acid
ObRb	Lepin receptor
OD	Optical density
OGTT	Oral glucose tolerance test
PA	Palmitic acid
PAGE	Polyacrylamide gel electrophoresis
PAI	Plasminogen activator inhibitor
PAP	Phosphatidic acid phosphatase
PBS	Phosphate buffered saline
PG	Prostaglandin
PI3K	Phosphatidylinositol-3 Kinase
PK	Protein kinase
POD	Peroxidase
PP	Pancreatic polypeptide
PPAR	Peroxisome proliferator-activated receptor
PPRE	Peroxisome proliferator response element
PUFA	Polyunsaturated fatty acid
QUICKI	Quantitative insulin sensitivity check index
RANTES	Regulated upon activation, normal T cell expressed and secreted
RNA	Ribonucleic acid
ROS	Reactive oxygen species
rpm	Revolutions per minute

RT-PCR	Reverse transcription polymerase chain reaction
RXR	Retinoid X receptor
SAT	Subcutaneous adipose tissue
SDS	Sodium dodecyl sulphate
SEM	Standard error of the mean
Ser	Serine
SFA	Saturated fatty acids
SH	Src homology
SI	Insulin sensitivity index
SOCS	Cytokine signalling molecules
S-PE	Streptavidin-phycoerythrin
SRE	Sterol regulatory elements
SREBP	Sterol regulatory element–binding protein
STA	Stearidonic acid
STAT	Signal transducer and activator of transcription
SVC	Stromal vascular cells
T2DM	Type 2 diabetes mellitus
TAG	Triacylglycerol
TBS	Tris buffered saline
TEMED	N,N,N'N'-tetramethylethyledienediamine
Thr	Threonine
Thy	Tyrosine
TLR	Toll like receptor
TMB	Tetramethylbenzidine
TNF	Tumour necrosis factor
TNFR	Tumour necrosis factor receptor
TOLLIP	Toll interacting protein
TRAF	Tumour necrosis factor receptor-associated factor
TX	Thromboxane
TZD	Thiazolidinedione
UV	Ultraviolet radiation
VAT	Visceral adipose tissue
VCAM	Vascular cell adhesion molecule
VDCC	Voltage-dependent calcium channels
VLDL	Very low density lipoproteins
WAT	White adipose tissue
WHO	World health organisation
WT	Wild type

Chapter 1

General Introduction

1.1 Obesity

Obesity can simply be defined as a condition of excessive fat accumulation in adipose tissue which causes or exacerbates many health problems, both independently and in association with other diseases (Kopelman, 2000). Half of all adults and one in five children in Europe are now overweight; one third of these are obese (WHO, 2006). More than one million deaths in Europe annually are due to diseases related to excess body weight (WHO, 2006). This global epidemic of obesity results from a combination of genetic susceptibility, increased availability of high energy foods and decreased requirement for physical activity in modern society (Kopelman, 2000). Obesity is now considered a major contributor to the global burden of chronic disease and disability. This review will therefore firstly examine the role of obesity in the metabolic syndrome (MetS) and type 2 diabetes mellitus (T2DM). Secondly, this review will focus on the role of inflammation within obesity, exploring the molecular mechanisms that mediate the pro-inflammatory interaction between immune cells, predominantly the macrophages, and adipocytes in obesity and finally discuss how long chain (LC) *n-3* polyunsaturated fatty acids (PUFA) may attenuate this pro-inflammatory phenotype.

1.1.1 Obesity, the metabolic syndrome and type 2 diabetes mellitus

Obesity plays a central role in the metabolic syndrome (MetS), which includes hyperinsulinemia, hypertension, hyperlipidemia with an increased risk of cardiovascular disease (CVD) and T2DM. The adverse metabolic changes associated with obesity are mostly related to a reduction in sensitivity of the body's tissues to insulin, the state known as insulin resistance (Steinberger and Daniels, 2003). The risk of T2DM increases with greater body mass index (BMI; Table 1.1). The Nurses' Health Study Cohort found that after adjustment for age, BMI was the dominant predictor of risk for T2DM. The risk of diabetes increased five fold for women with a BMI of 25, 28 fold for those with a BMI of 30 and 93 fold for those women with BMI of 35 or greater, compared with women with a BMI of less than 21 (Colditz *et al.*, 1995). A strong positive association between overall obesity as measured by BMI and risk of T2DM was also found in men (Chan *et al.*, 1994). Men with a BMI of equal to or greater than 35 had a 42 fold increased risk of T2DM compared with men with a BMI less than 23. The association of obesity with the MetS and CVD risk is not only related to BMI but seems critically dependent on body fat

distribution. Individuals with greater degrees of central adiposity or visceral adipose tissue (VAT) develop MetS more frequently than individuals with a peripheral body fat distribution (Kissebah *et al.*, 1982).

Table 1.1 Classification of obesity based on BMI as determined by WHO

	BMI (kg/m^2)	**Obesity class**
Underweight	≤ 18.5	
Healthy	18.5 to 24.9	
Overweight	25.0 to 29.9	Grade 1
Obesity	30.0 to 39.9	Grade 2
Extreme obese	≥ 40	Grade 3

T2DM is characterized by peripheral insulin resistance, increased hepatic glucose production and impaired insulin secretion (Kahn and Rossetti, 1998). T2DM, once seen as a relatively mild ailment associated with ageing and the elderly, is now considered a chronic and debilitating disease. T2DM is ranked among the leading causes of blindness, renal failure, lower limb amputation and through its effects on CVD, it is also now considered one of the leading causes of death (IDF, 2009). The life expectancy of individuals with T2DM can be shortened by as much as 15 years, with up to 75% dying of CVD (Davies, 2005). Insulin is an essential hormone secreted by the pancreas; it affects a wide range of biological processes including glucose transport, glucose and lipid metabolism, cell growth, protein synthesis and gene expression in many different cell types and multiple organs including the liver, muscle and adipose tissue. Fundamentally, insulin resistance is a disordered state in which insulin inadequately stimulates glucose transport and in skeletal muscle and white apipose tissue (WAT) while inadequately suppressing hepatic glucose production (Reaven, 1995).

1.2 Insulin and glucose homeostasis

Blood glucose levels must be maintained within a precise range throughout the day, independently of dietary nutrient ingestion, in a process termed blood glucose homeostasis. This homeostasis involves a complex communication between different tissues, including the liver, skeletal muscle, adiposde tissue, brain and the endocrine pancreas (Fritsche *et al.*, 2008; Herman and Kahn, 2006; Rosen and Spiegelman, 2006). During the fasting state, insulin remains at low levels because plasma glucose concentrations are low. In this state, the levels of the counter-regulatory hormones, glucagon, adrenaline and corticosteroids are

increased to promote hepatic glucose production. In contrast, during the fed state insulin is increased. Insulin decreases blood glucose by promoting adipocyte and muscle glucose uptake, while suppressing glycogenolysis (conversion of glycogen to glucose) and gluconeogenesis (synthesis of glucose from non-carbohydrate precursor) preventing glucose production by the liver (Fritsche *et al.*, 2008).

The endocrine cells of the pancreas are grouped in the islets of Langerhans, which constitute approximately 1 – 2% of the pancreas mass. Islets are distributed throughout the organ in healthy human adults (Nadal *et al.*, 2009). The cells in the islets can be divided into α cells, which secrete glucagon, β cells, which secrete insulin, δ cells which secrete somatostatin and PP cells, which produce pancreatic polypeptide (Brissova *et al.*, 2005; Cabrera *et al.*, 2006). Furthermore, a small population of ghrelin-producing cells, ε cells, have also been identified (Prado *et al.*, 2004). The β cells are the most common and account for approximately 65 - 75% of the cell within the islets. The β cells are generally located in the centre of each islet, surrounded by the α, δ and PP cells (Ganon, 2005). However, the percentage of the different cell subpopulations and the islet cytoarchitecture vary between species. In rodent islets, β cells are the most abundant, 60 – 80% of the total number of cells; α cells account for 15 – 20%, while δ cells are less than 10% and PP-cells about 1%. In human islets, the proportion of δ and PP cells is similar to rodent islets, but the percentage of α cells is higher (35 – 45%) and the β cell percentage is lower (55 – 65%). Moreover, α and β cells are distributed evenly throughout the islet, suggesting that paracrine interactions between both types of cells may be more important in humans than in rodents (Brissova *et al.*, 2005; Cabrera *et al.*, 2006).

The main function of pancreatic β cells is the biosynthesis and release of insulin. The rate of insulin biosynthesis is controlled by many signaling molecules including neurotransmitters, hormones and nutrients, among which glucose is the most important (Nadal *et al.*, 2009). In response to short glucose stimulation, insulin biosynthesis is regulated by the increased translation of the pre- and pro-insulin transcript. However, after prolonged glucose exposure it is regulated via gene transcription (Permutt and Rotwein, 1983; Poitout *et al.*, 2006). Both transcriptional and translational regulation of insulin biosynthesis is essential to maintain the intracellular stores of insulin on a long-term basis (Nadal *et al.*, 2009). Glucose-induced insulin secretion is coupled to the metabolic state of the β cell. After transport into the cell, glucose is phosphorylated and shunted into glycolysis, which increases metabolic flux. This altered metabolic state leads to an increase in the ATP/ADP ratio that closes the plasma membrane-associated ATP-sensitive

potassium (K_{ATP}) channel. Closure of this channel depolarizes the membrane, leading to the activation of voltage-sensitive calcium (Ca^{2+}) channels, Ca^{2+} influx and insulin secretion (Newgard and McGarry, 1995) as described in Figure 1.1. Insulin resistance of skeletal muscle, liver and adipose in addition to dysfunction of pancreatic β cells are central abnormalities of T2DM.

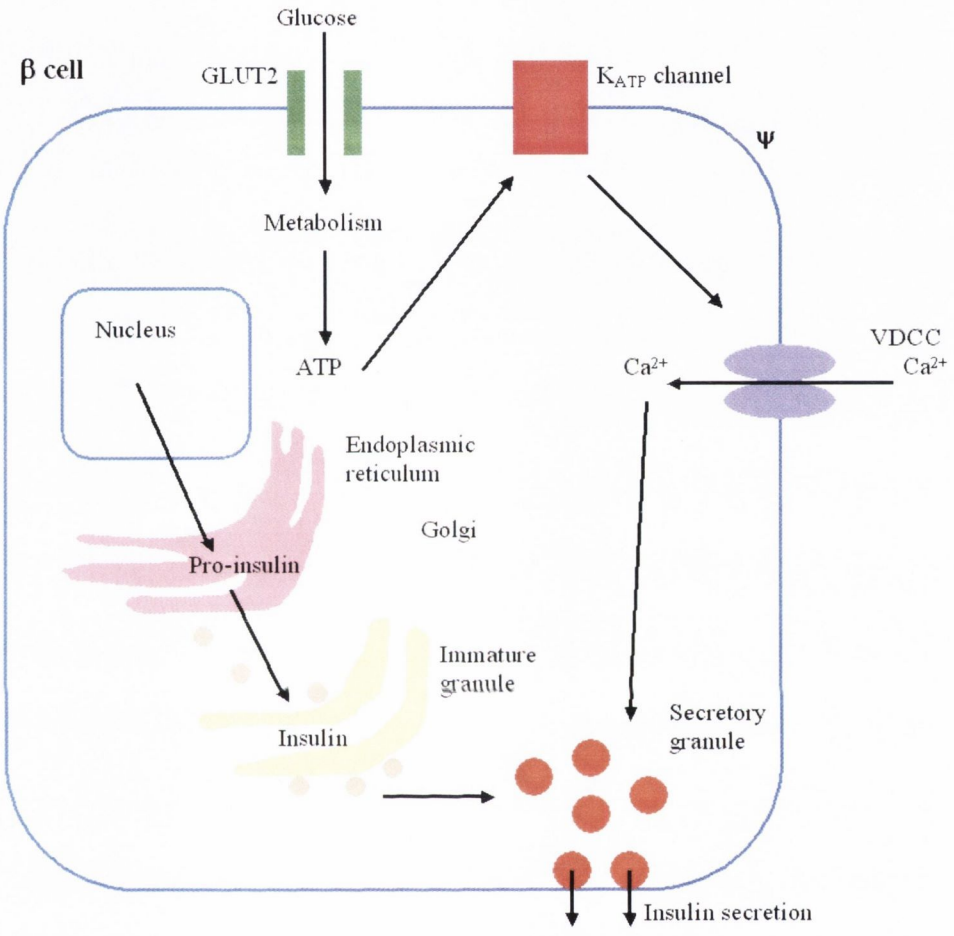

Figure 1.1 Insulin is synthesised in the rough endoplasmic reticulum (ER) of the β cells. It is then transported to the Golgi apparatus, where it is packaged in membrane-bound granules. Rising levels of plasma glucose cause transport of glucose into the cell via glucose transporters such as GLUT2. The increased levels of glucose increase glucose metabolism within the β cells causing an increase in the ATP/ADP ratio. The increase in ATP closes the ATP-sensitive potassium (K_{ATP}) channels, depolarizing the β cell membrane (ψ). This depolarization opens the voltage-dependent calcium channels (VDCC), allowing calcium influx. The rise in the intracellular calcium concentration in the β cell then triggers insulin granule exocytosis and insulin is passed into the blood. Adapted from Miki *et al.* 1999

1.3 Quantifying insulin sensitivity

The ability to dispose of glucose depends on the responsiveness of the pancreatic β cells to glucose and the sensitivity of the glucose utilizing tissues to the secreted insulin (Bergman *et al.*, 1981). Understanding the etiology of the various forms of impaired glucose

tolerance requires techniques for measuring both pancreatic responsiveness and insulin sensitivity, with a means to evaluate their relative contributions to overall glucose tolerance (Bergman *et al.*, 1981).

1.3.1 Homeostasis model assessment and quantitative insulin sensitivity check index

Mathematical handling of the fasting levels of glucose and insulin concentration has been used for the calculation of insulin sensitivity and secretion by introducing various indices, such as HOMA (homeostasis model assessment; fasting glucose [mMol/L] × fasting insulin [μU/mL])/22.5) and QUICKI (quantitative insulin sensitivity check index; 1/(log fasting glucose [mg/dL] + log fasting insulin [μU/mL]). Low HOMA values indicate high insulin sensitivity, whereas high HOMA values indicate low insulin sensitivity. Conversely, low QUICKI index values indicate low insulin sensitivity, whereas high QUICKI index values indicate high insulin sensitivity (Antuna-Puente *et al.*, 2008; Katz *et al.*, 2000; Matthews *et al.*, 1985). However, these simplistic approaches do not elucidate the dynamic state of the relationship between insulin sensitivity and secretion.

1.3.2 Hyperinsulinemic euglycemic glucose clamp

The glucose clamp technique, originally developed by DeFronzo *et al.* (1979), is widely accepted as the reference standard for directly determining metabolic insulin sensitivity in humans (DeFronzo *et al.*, 1979). Hyperinsulinemic euglycemic glucose clamp is conducted after an overnight fast in humans as described by Muniyappa *et al.* (2008). Insulin is infused intravenously at a constant rate. This constant insulin infusion results in a new steady-state insulin level that is above the fasting level or hyperinsulinemic (Muniyappa *et al.*, 2008). As a consequence, glucose disposal in skeletal muscle and WAT is increased, whereas hepatic glucose production (HGP) is suppressed. Under these conditions, a bedside glucose analyzer is used to frequently monitor blood glucose levels while 20% dextrose is given intravenously at a variable rate to "clamp" blood glucose concentrations in the normal range (euglycemic). An infusion of potassium phosphate is also given to prevent hypokalemia resulting from hyperinsulinemia and increased glucose disposal. After several hours of constant insulin infusion, steady-state conditions can typically be achieved for plasma insulin, blood glucose and the glucose infusion rate (GIR). Assuming that the hyperinsulinemic state is sufficient to completely suppress HGP, and since there is no net change in blood glucose concentrations under steady-state clamp conditions, the GIR must be equal to the glucose disposal rate (M). Therefore, whole body glucose disposal at a given level of hyperinsulinemia can be determined directly. M is typically

normalized to body weight or fat-free mass to generate an estimate of insulin sensitivity. Alternatively, an insulin sensitivity index (SI) derived from clamp data can be defined (Katz *et al.*, 2000).

In rodents, which have no true physiological fasting state, imposing a non-physiological fasting period leads to a significant decrease in body weight, depletion of hepatic glycogen content and improved insulin sensitivity (Muniyappa *et al.*, 2008). Therefore, under these non-physiological fasting conditions, plasma glucose and insulin levels may not attain steady-state conditions. Furthermore, it is likely that the glucose clamp technique in rodents is not as accurate and reliable as in humans due to small blood volumes (2 ml in mice) and limited sampling ability. Additionally, the glucose clamp is stressful in mice even with the use of anesthetics (Muniyappa *et al.*, 2008).

1.3.3 Glucose tolerance test (GTT)

The minimal model, developed by Bergman *et al.* (1979), provides an indirect measurement of metabolic insulin sensitivity and resistance on the basis of glucose and insulin data obtained during a frequently sampled intravenous glucose tolerance test (FSIVGTT) (Bergman *et al.*, 1979). After an overnight fast, an IV bolus of glucose is infused over 2 minutes starting at time 0. Blood samples are taken for plasma glucose and insulin measurements. These measurements are then subjected to minimal model analysis using the computer program MINMOD to generate an index of insulin sensitivity (SI) (Muniyappa *et al.*, 2008). The oral glucose tolerance test (OGTT) is a simple test widely used in clinical practice to diagnose glucose intolerance and T2DM. After overnight fast, blood samples for determinations of glucose and insulin concentrations are taken following a standard oral glucose load or a standard meal (Dalla Man *et al.*, 2005). The OGTT mimics the glucose and insulin dynamics of physiological conditions more closely than conditions of the glucose clamp or FSIVGTT. However, while the OGTT provides useful information about glucose tolerance, it provides little information about insulin sensitivity or resistance (Muniyappa *et al.*, 2008). In normal non-diabetic patients, blood glucose levels peak within 30 minutes to 1 hour following glucose ingestion. The peak in glucose levels triggers the release of insulin, which brings glucose levels back down to fasting levels within about 2 hours. In diabetics, the glucose peak is higher and they show a slower return to fasting levels (McCall and Tankersley, 2008). Furthermore, impaired glucose tolerance is reflected in a larger incremental area under the curve (AUC) of the plasma glucose disappearance curve.

In rodents GTTs can be conducted with more ease than the glucose clamp. However, unlike the clamp, these methods do not provide precise estimates of insulin sensitivity or tissue specific glucose disposal. The intraperitoneal (IP) GTT has an advantage over the OGTT in that it excludes incretin effects. An insulin tolerance test (ITT) can also be conducted in fasted animals, in which insulin is administered. Blood samples are taken for measurement of plasma glucose and insulin concentrations. For the ITT, the rate and magnitude of decline of plasma glucose concentration in response to an injection of insulin provide an estimate of insulin sensitivity. However, these tests can be stressful to the animals. In addition, imposing a non-physiological fasting state in rodents may complicate interpretation of results (Muniyappa *et al.*, 2008).

1.4 White adipose tissue: biology and function

The main role of WAT is the storage of triacylglycerol (TAG) during energy consumption and non-esterified fatty acid (NEFA) release when energy expenditure exceeds energy intake (Vazquez-Vela *et al.*, 2008). However, adipose tissue is increasingly viewed as an active endocrine organ with high metabolic activity. Adipose tissue produces a number of cytokines and bioactive molecules together termed as adipokines (Trayhurn and Wood, 2004). Some act in an autocrine or paracrine manner within the adipose tissue, while others are released into the systemic circulation and act as signalling molecules in other tissues such as the brain, liver, muscle and pancreas. Adipokines play an essential role not only in energy intake and regulation but also in metabolic processes such as angiogenesis, adipogenesis, extracellular matrix dissolution and reformation, steroid metabolism, immune response and hemostasis (Bays *et al.*, 2008).

1.4.1 Subcutaneous and visceral adipose tissue

WAT is composed of several subcutaneous and visceral adipose tissue (SAT and VAT) depots. In basic terms SAT is found just underneath the skin while VAT is found within the abdominal cavity and vital organs. Similarly, rodents have two main SAT depots; one anterior and one posterior lying in discrete anatomical locations while the VAT depots are located in the thorax and abdomen cavities (Figure 1.2; Cinti, 2005). The anterior SAT depot lies at the base of the forelimbs and extends into the base of the neck. The posterior SAT depot is located at the base of the hind legs. The thorax VAT lies around the heart and the aorta, while the abdominal VAT depots can be retro- or intraperitoneal. The omental depot is small in rodents, whereas the perigonadal depot or the epididymal adipose tissue (EAT) is well circumscribed, enveloped and bound to the epididymis by the peritoneal

leaflets in males, while in females, it surrounds the ovaries, uterus and bladder (Cinti, 2005).

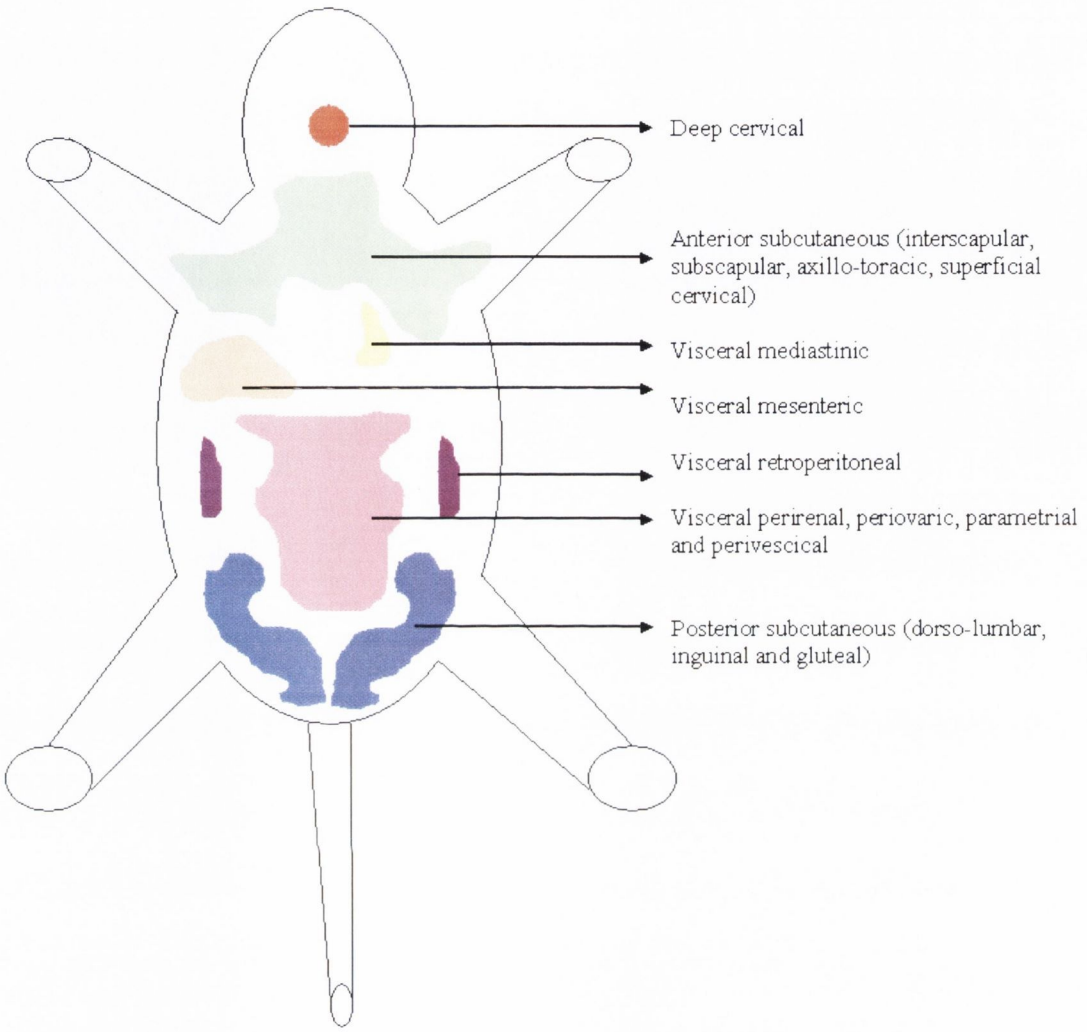

Figure 1.2 Subcutaneous and visceral adipose tissue (SAT and VAT) depot locations within rodents. Adapted from Cinti, 2005.

Interestingly, patterns of fat distribution within humans may confer additional risk for MetS (Despres *et al.*, 1989; Goodpaster *et al.*, 1997; Kelley *et al.*, 2000). In the health, aging and body composition (Health ABC) study, abdominal WAT comprising both VAT and SAT depots, in addition to muscle-associated VAT, were related to insulin resistance in older subjects, particularly in those who were of normal weight. Furthermore, accumulation of these regional WAT depots is characteristic of older people with T2DM and impaired glucose tolerance (Goodpaster *et al.*, 2003). Furthermore, numerous studies have indicated that abdominal WAT, particularly VAT, is a strong independent predictor of the MetS including symptoms such as hyperglycemia, dyslipidemia and hypertension (DeFronzo and Ferrannini, 1991; Despres *et al.*, 1990; Fujioka *et al.*, 1987; Kissebah *et al.*, 1982). The abdominal VAT is thought to be more metabolically active while acting as a

major source of adipokines, such as tumor necrosis factor (TNF)-α, interleukin (IL)-6 and monocyte chemoattractant protein (MCP)-1 (Tilg and Moschen, 2006). Importantly, SAT is also thought to play a major role in insulin resistance. The elevated insulin and glucose concentrations, in addition to T2DM, are significantly associated with hypertrophied SAT adipocytes of the abdomen in obese men and women (Berchtold *et al.*, 1972; Bjorntorp, 1971; Bjorntorp *et al.*, 1972; Imbeault *et al.*, 1999; Kissebah *et al.*, 1982; Morin *et al.*, 1998; Weyer *et al.*, 2000). These hypertrophied SAT adipocytes predict the development of T2DM, independent of obesity and insulin resistance (Weyer *et al.*, 2000). Additionally, obese pre-menopausal women with large SAT abdominal adipocytes are also more hyperinsulinemic and glucose intolerant than obese individuals with relatively smaller SAT abdominal adipocytes (Kissebah *et al.*, 1982).

1.4.2 Lipid absorption and storage

Lipids fulfill many roles in eukaryotes. Apart from being the main building blocks of cell membranes, they also carry out transport, signaling and storage functions. The most important compounds for energy storage in mammals are TAG (Schittmayer and Birner-Gruenberger, 2009). TAG are non-polar, water insoluble fatty acid trimesters of glycerol. Although most lipids are taken up in the form of TAG they must be degraded to NEFA and glycerol prior to absorption across the intestinal epithelium. This initial step is catalyzed by digestive lipases, pancreatic lipase, gastric lipase and aided by bile acids (Bodmer *et al.*, 1987; Canaan *et al.*, 1999; Chahinian *et al.*, 2006; Kleeberg, 1971; Semeriva and Desnuelle, 1976). The NEFA form mixed micelles with other lipids, e.g. monoacylglycerols and diacylglycerols, cholesterol, fat-soluble vitamins and lysophospholipids created by phospholipase A2 (Huggins *et al.*, 2002). These mixed micelles are absorbed by enterocytes located at the microvilli of the small intestine; TAG are reassembled into chylomicrons and then pass into the bloodstream via the lymphatic system. The chylomicrons are transported to other locations in the body by a highly complex lipid transport system, composed of five main classes of lipoproteins, i.e. chylomicrons, very low density lipoproteins (VLDL), intermediate density lipoproteins (IDL), low density lipoproteins (LDL) and high density lipoproteins (HDL) (Alonzi *et al.*, 2008).

Chylomicrons are broken down by lipoprotein lipase (LPL) in the capillaries of muscle and adipose tissue to NEFA, which then enter the cells. The chylomicron remnants, which have lost much of their TAG content, are taken up by the liver for disposal. Furthermore, the liver synthesizes TAG and cholesterol, and packages them as VLDLs

before releasing them into the blood. When VLDLs reach muscle and adipose blood vessels, the TAG are hydrolyzed by LPL to NEFA and taken up by surrounding muscle and adipose cells. During this process, the VLDLs become progressively denser and form LDLs. While most of the resulting LDLs are taken up by the liver for disposal, some circulate and distribute cholesterol to the rest of the body tissues. HDLs, which are also secreted from the liver and intestine, have the task of preventing lipid accumulation by removing surplus cholesterol from the tissues and transferring it to the LDLs. The dietary intake of both fat and carbohydrate, in excess of the needs of the body, leads to their conversion into TAG in the liver. These TAG are packaged into VLDLs and released into the circulation for delivery to the various tissues (primarily muscle and adipose tissue) for storage. Within the cell, NEFAs are either introduced to the β-oxidation cycle for energy supply (Berg, 2002), incorporated into phospholipids as basic building blocks for membranes (Loewen *et al.*, 2004) or reassembled to TAG for energy storage as lipid droplets (LD) (Bartz *et al.*, 2007). While in most cell types one of the main functions of LD is the removal of toxic concentrations of NEFA (Listenberger *et al.*, 2003), their major role in adipocytes is lipid storage. Therefore, adipocyte LD differ from those in other tissues in size and composition (Bartz *et al.*, 2007; Murphy and Vance, 1999; Zweytick *et al.*, 2000).

1.4.3 Triacylglycerol synthesis and lipolysis

In mammals, there are two main biochemical pathways for TAG biosynthesis: the monoacylglycerol pathway, which plays an important role in nutrient absorption in the small intestine and the glycerol-3-phosphate pathway, which is responsible for the majority of *de novo* TAG synthesis (Figure 1.3). Acyl-coenzyme A (Acyl-CoA) glycerol-3-phosphate acyl-transferase (GPAT) catalyzes the initial step of *de novo* TAG synthesis by converting glycerol-3-phosphate to lysophosphatidic acid. Lysophosphatidic acid is then acylated to form phosphatidic acid, followed by dephosphorylation to diacylglycerol (DAG). DAG is then converted to TAG, in acylation step catalyzed by acyl-CoA DAG acyl-transferase (DGAT). This pathway was largely identified by Kennedy and his coworkers in the 1950s (Kennedy, 1961; Weiss *et al.*, 1960). Lysophosphatidic acid can also be formed by the acylation of dihydroxyacetone-phosphate (DHAP) by CoA DHAP acyl-transferase and the subsequent reduction of 1-acyl-DHAP by DHAP oxido-reductase. However, the contribution of the DHAP pathway to TAG synthesis remains unclear (Coleman and Lee, 2004). The enzymes of TAG synthesis are integral membrane proteins of the peroxisomal, ER and mitochondria. Interestingly, during the development and

maintenance of obesity, over nutrition promotes TAG synthesis from increased substrate supplies while TAG biosynthetic enzymes are themselves up-regulated (Coleman *et al.*, 2000). For example, acetyl-coenzyme A synthetase (ACS)-1 mRNA is increased in adipose tissue from leptin deficient obese *ob/ob* mice compared with control littermates (Memon *et al.*, 1999). Importantly, in obesity, TAG accumulation in both adipose and non-adipose tissues is closely associated with several metabolic co-morbidities. TAG accumulation in muscle and pancreas occurs with insulin resistance (Goodpaster and Kelley, 1998; Koyama *et al.*, 1997) and islet cell dysfunction (Unger *et al.*, 1999), respectively, in T2DM both hepatic TAG synthesis in liver and VLDL secretion increase (Lewis, 1997). This data indicates that intracellular lipid accumulation might be causally linked to the pathogenesis of disordered energy homeostasis (Unger *et al.*, 1999).

While TAG synthesis occurs in multiple tissues, lipolysis is quantitatively the most predominant in WAT (Ahmadian *et al.*, 2007). During times of energy deprivation, WAT undergoes a shift toward greater net rates of lipolysis, which can be defined as the hydrolysis of TAG to generate NEFAs and glycerol (Figure 1.3) that are released into the vasculature for use as energy substrates by other organs. TAG are hydrolyzed to form DAG, then monoacylglycerol (MAG), with the liberation of a NEFA at each step; MAG is hydrolyzed to release the final fatty acid and glycerol. In times of energy need, such as fasting and exercise, adipocyte lipolysis is markedly increased by catecholamines that activate Gs-coupled receptors (Ahmadian *et al.*, 2007). These receptors, in turn, activate adenylyl cyclase to generate cyclic (c) AMP. Rising cellular concentrations of cAMP activate protein kinase A (PKA) that phosphorylates hormone-sensitive lipase (HSL). Interestingly, insulin is a potent inhibitor of lipolysis and acts primarily through its effect on phosphodiesterase and subsequent suppression of the formation of cAMP. Phosphorylation of HSL results in increased hydrolytic activity (Fredrikson *et al.*, 1981), translocation of HSL from the cytosol to the LD surface and enhanced TAG breakdown in the cell (Holm, 2003). Importantly, perilipin is an abundant adipocyte protein that exists in three isoforms (A, B and C), which are the products of differentially spliced transcripts from a single gene. It has been postulated that in the basal state, perilipin coats the lipid droplet and somehow interferes with HSL gaining access to the droplet (Londos *et al.*, 1995; Londos *et al.*, 1999; Souza *et al.*, 1998). Lipolytic activation of adipocytes is associated with polyphosphorylation of perilipin mediated by protein kinase A, which induces a change in the lipid droplet surface and the appearance of lipid microdroplets, allowing HSL access to core lipids (Clifford *et al.*, 2000; Londos *et al.*, 1999; Souza *et al.*, 1998). Martinez-Botas *et al.* (2000) observed that Perilipin$^{-/-}$ mice consumed more food

than control mice, but have normal body weight. These mice had smaller white adipocytes with elevated basal lipolysis. Perilipin$^{-/-}$ mice were also resistant to diet-induced obesity (Martinez-Botas *et al.*, 2000). Breeding the Perilipin$^{-/-}$ alleles into *db/db* mice reversed the obese phenotype by increasing the metabolic rate of the mice (Martinez-Botas *et al.*, 2000). These data demonstrate a clear role for perilipin in regulating lipolysis and energy balance.

Notably, Villena *et al.* 2004 identified and characterized a novel adipocyte TAG lipase called desnutrin (ATGL/desnutrin). In cells that contain fat stores, such as differentiated 3T3-L1 cells (Zimmermann *et al.*, 2004) and HeLa cells grown in oleic acid-rich medium (Smirnova *et al.*, 2006), desnutrin/ATGL is found tightly associated with the LD, as well as throughout the cytoplasm (Smirnova *et al.*, 2006; Villena *et al.*, 2004; Zimmermann *et al.*, 2004). Desnutrin/ATGL is regulated by nutritional and hormonal signals. In mice, desnutrin/ATGL expression is induced by fasting due to glucocorticoids, which are elevated during fasting and suppressed by re-feeding due to insulin (Kershaw *et al.*, 2006; Villena *et al.*, 2004). Furthermore, Villena *et al.* (2004) also observed that desnutrin/ATGL is down-regulated in *ob/ob* and *db/db* mice, further supporting a role for the enzyme in fat breakdown and contribution in the development of obesity (Villena *et al.*, 2004). Additionally, studies have shown that lipolysis is stimulated by adipokines such as leptin (Fruhbeck et al. 2001), TNF-α and IL-6 (Lyngso et al. 2002) indicating that inflammation can also contribute to metabolic disregulation.

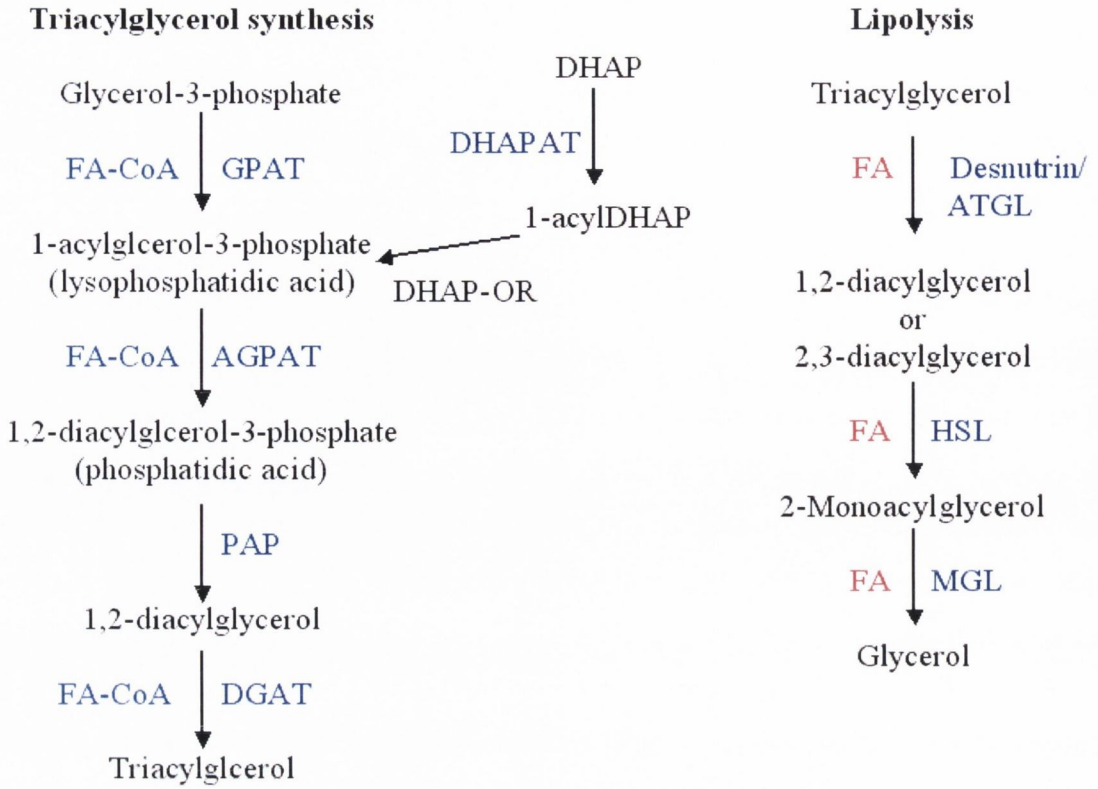

Figure 1.3 The enzymes of triacylglycerol synthesis and hydrolysis (AGPAT, 1-acylglycerol-3-phosphate acyltransferase; ATGL, adipose triacylglycerol lipase; CoA: coenzyme A; DGAT, diacylglycerol acyltransferase; DHAP, dihydroxyacetonephosphate; DHAPAT, acyl-CoA dihydroxyacetone-phosphate acyltransferase; DHAP-OR, dihydroxyacetone-phosphate oxido-reductase; FA, fatty acid; GPAT, glycerol-3-phosphate acyltransferase; HSL, hormone-sensitive lipase; MGL, monoglyceride lipase; PAP, phosphatidic acid phosphatase). Adapted from Ahmadian *et al.* 2007.

1.5 Adipokines: obesity and T2DM

Compared with WAT of lean individuals, adipose tissue of obese subjects expresses increased amounts of pro-inflammatory proteins such as TNF-α, IL-6, inducible nitric oxide synthase (iNOS), transforming growth factor (TGF)-β1, C-reactive protein, soluble inter-cellular adhesion molecule (ICAM), MCP-1, plasminogen activator inhibitor type 1 (PAI-I) tissue factor and factor VII (Fried *et al.*, 1998; Hotamisligil *et al.*, 1993; Perreault and Marette, 2001; Samad *et al.*, 1996; Samad *et al.*, 1997; Sartipy and Loskutoff, 2003; Visser *et al.*, 1999). Additionally, adiposity is negatively correlated with production of adiponectin, an insulin sensitising hormone that decreases hepatic gluconeogenesis and increases lipid oxidation in muscle (Arita *et al.*, 1999; Tomas *et al.*, 2002). Importantly, recent data suggests that in WAT, pro-inflammatory molecules are produced by stromal

vascular cells (SVC). The SVC fraction includes pre-adipocytes, vascular cells, such as endothelial cells and immune cells.

1.5.1 Adiponectin

Adiponectin is one of the most abundant adipose tissue specific factors; it exists most commonly in the plasma as a full-length protein although smaller, globular fragments also exist. Serum adiponectin levels are low in obese subjects and increase after weight loss. Importantly, adiponectin appears to improve insulin sensitivity (Lyon *et al.*, 2003; Scherer *et al.*, 1995) and hypoadiponectinemia may contribute to insulin resistance associated with obesity (Ouchi *et al.*, 1999). Recent studies also suggest that adiponectin has anti-inflammatory effects (Ouchi and Walsh, 2007). Interestingly, pre-treatment with adiponectin reduces lipopolysaccharide (LPS)-stimulated TNF-α production in human and porcine macrophages (Wulster-Radcliffe *et al.*, 2004; Yokota *et al.*, 2000). Adiponectin treatment also inhibits Toll-like receptor (TLR) mediated NF-κB activation in mouse macrophages (Yamaguchi *et al.*, 2005). Furthermore, adiponectin stimulates production of IL-10, an anti-inflammatory cytokine in porcine macrophages (Wulster-Radcliffe *et al.*, 2004). Importantly, pro-inflammatory cytokines have been shown to suppress adiponectin expression in adipocytes. TNF-α treatment suppresses adiponectin expression at the level of transcription in cultured 3T3-L1 adipocytes (Maeda *et al.*, 2001) and reduces the expression and secretion of adiponectin protein in primary human adipocytes (Kappes and Loffler, 2000). While treatment with insulin-sensitizing agents, thiazolidinediones (TZDs), that activate peroxisome proliferator-activated receptor-γ (PPAR-γ) is reported to increase expression and secretion of adiponectin in 3T3-L1 adipocytes while increasing plasma adiponectin levels in humans and obese mice (Combs *et al.*, 2002; Maeda *et al.*, 2001; Yang *et al.*, 2002; Yu *et al.*, 2002).

In addition, adiponectin can decrease insulin resistance by stimulating fatty acid oxidation and reducing TAG content in muscle and liver (Yamauchi *et al.*, 2001). Furthermore, studies indicate that adiponectin exerts its effects on energy homeostasis and glucose and lipid metabolism through phosphorylation and activation of adenosine monophosphate-activated protein kinase (AMPK), an enzyme typically activated by cellular stress (Hardie, 2003). Both globular and full-length adiponectin stimulate AMPK in skeletal muscle but only full-length adiponectin activates AMPK in liver (Yamauchi *et al.*, 2002). Activation of AMPK in liver reduces enzymes involved in gluconeogenesis leading to reduction of glucose levels (Berg *et al.*, 2001). It is also proposed that adiponectin could activate PPAR-α; this hypothesis is based on the observation that

treatment of lipoatrophic or obese diabetic mice with adiponectin or over expression of adiponectin in *ob/ob* mice resulted in increased expression levels of PPAR-α target genes such as CD36, acyl-coenzyme A (CoA) oxidase and uncoupling protein-2 (Yamauchi *et al.*, 2001). This could suggest that adiponectin increases fatty-acid combustion and energy consumption via PPAR-α activation, leading to decreased TAG content in the liver and skeletal muscle. Importantly, adipoR1 and R2 serve as receptors for globular and full-length adiponectin, mediating increased AMPK and PPAR-α ligand activities therefore leading to increased fatty-acid oxidation and glucose uptake (Combs *et al.*, 2003)

1.5.2 Leptin

Leptin is the product of the obese (*ob*) gene and is synthesized mainly in WAT. Leptin has been implicated in the regulation of food intake, energy expenditure and whole-body energy balance in rodents and humans (Houseknecht *et al.*, 1998). Importantly, leptin has been shown to act on a receptor site in the ventromedial nucleus of the hypothalamus to curb appetite and increase energy expenditure as body fat stores increase (Flier, 1997; Friedman and Halaas, 1998; Jequier and Tappy, 1999). In the fed, steady state, leptin expression and secretion reflect body fat mass in rodents and humans (Considine *et al.*, 1996; Frederich *et al.*, 1995; Maffei *et al.*, 1995) and are highly correlated with adipocyte size in lean and obese mice (Houseknecht *et al.*, 1996). Leptin concentrations decrease in response to short-term fasting and increase after re-feeding (Kolaczynski *et al.*, 1996a). Importantly, leptin concentrations are greatly elevated in obese subjects (Friedman and Halaas, 1998).

Patients with a complete deficiency of leptin due to mutations in the leptin gene express a phenotype of congenital obesity and show numerous endocrinological abnormalities, including insulin resistance and hypogonadotropic hypogonadism akin to the leptin deficient *ob/ob* mouse model (Montague *et al.*, 1997). Leptin administration has a potent effect on lipid metabolism, leading to a substantial reduction of fat mass within several days of administration (Halaas *et al.*, 1995; Pelleymounter *et al.*, 1995). Leptin treatment of animals has been shown to cause a dose-dependent decrease in food intake, loss of body weight, loss of fat depots, and an increase in energy metabolism (Levin *et al.*, 1996; Pelleymounter *et al.*, 1995). However, the vast majority of obese humans have high circulating leptin concentrations indicating that obesity is a leptin resistant state in humans (Ahima *et al.*, 2000; Friedman and Halaas, 1998; Mantzoros, 1999). Furthermore, endogenous leptin treatment is largely ineffective in reducing the body weight of obese

patients due to this state of leptin resistance, which develops rapidly in obese patients (Heymsfield *et al.*, 1999).

Although there are five different isoforms of its receptor, leptin exerts most of its physiologic functions by binding to the long form of its receptor, ObRb. Its signal transduction involves activation of the Janus kinase (JAK) and signal transducer and activator of transcription (STAT) pathway (Juge-Aubry *et al.*, 2005; Seufert, 2004). It is also likely that leptin activates mitogen-activated protein kinase (MAPK) pathways (Watowich *et al.*, 1996). A portion of circulating serum leptin is bound to a soluble Ob receptor (sOb-R), which in humans is generated by proteolytic cleavage of membrane bound leptin receptor. Leptin has been observed to inhibit insulin synthesis and secretion within the pancreatic β cells through several mechanisms including activation of ATP-dependent potassium channels, JAK/STAT signaling, interference with cAMP pathway, activation of phosphatidylinositol-3 kinase (PI3K) and inhibition of protein phosphatase-1 activity (Kieffer and Habener, 2000; Seufert, 2004; Siegrist-Kaiser *et al.*, 1997). Furthermore, in a bidirectional hormonal feedback loop (adipoinsular axis), *in vivo* and *in vitro* insulin has been shown *in vivo* to stimulate leptin secretion (Cusin *et al.*, 1995; Kieffer and Habener, 2000; Malmstrom *et al.*, 1996; Saladin *et al.*, 1995; Slieker *et al.*, 1996; Utriainen *et al.*, 1996; Vidal *et al.*, 1996).

Importantly, leptin has direct effects on WAT, including activation of the JAK/STAT pathway resulting in increased glucose utilization and lipolysis (Siegrist-Kaiser *et al.*, 1997). Leptin like adiponectin may also reduce excess lipid stores in organs such as the skeletal muscle and liver, which disrupts energy metabolism, impairing glucose oxidation and insulin response. Induction of leptin signaling in skeletal muscle activates AMPK, which phosphorylates and inactivates the enzyme acetyl-CoA carboxylase (ACC). ACC catalyzes the production of malonyl-CoA from acetyl-CoA. Malonyl-CoA inhibits carnitine palmitoyltransferases (CPT)-1, which transport long-chain fatty acyl-CoAs (LCFA-CoA) into the mitochondria prior to oxidation. Therefore, a reduction in Malonyl-CoA allows CPT1 levels to increase, resulting in increased mitochondrial lipid oxidation which in turn reduces the lipid content of cells and improves insulin sensitivity (Figure 1.4) (Moran and Phillip, 2003; Muoio *et al.*, 1997). Leptin like adiponectin may also stimulate fatty acid oxidation by activation of PPAR-α (Lee *et al.*, 2002). These protective effects of leptin may be lost in leptin resistant states such as obesity.

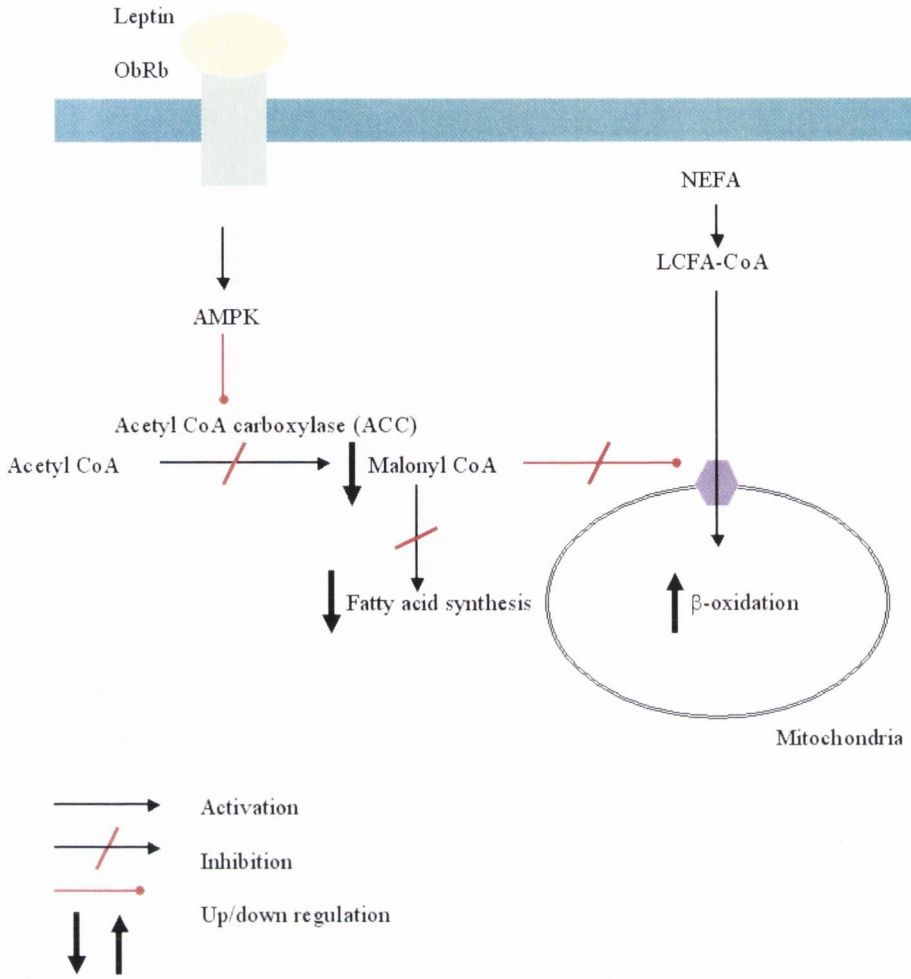

Figure 1.4 Activation of the leptin receptor ObRb activates adenosine monophosphate-activated protein kinase (AMPK), which phosphorylates and inactivates the enzyme acetyl-CoA carboxylase (ACC). ACC catalyzes the production of malonyl-CoA from acetyl-CoA. Malonyl-CoA inhibits carnitine palmitoyltransferases (CPT)-1, which transport long-chain fatty acyl-CoAs (LCFA-CoA) into the mitochondria prior to oxidation. A reduction in Malonyl-CoA allows CPT1 levels to increase resulting in increased mitochondrial lipid oxidation, which in turn reduces the lipid content of cells.

1.5.3 Resistin

Although murine and human resistin share more than 50% identity at the amino acid level, their expression patterns are different (Koerner et al., 2005). In mice, resistin is almost exclusively expressed in WAT in proportion to adipocyte differentiation and the amount of adipose tissue (Steppan et al., 2001). In humans, resistin is highly expressed in the bone marrow (Patel et al., 2003). In contrast to mice, only a low level of expression of resistin has been found in mature human adipocytes (Janke *et al.*, 2002; McTernan *et al.*, 2002a; McTernan *et al.*, 2002b; Savage *et al.*, 2001). Interestingly, the particular cells that express resistin in WAT appear to be within the non-fat SVC (Bo *et al.*, 2005; Janke *et al.*, 2002; Patel *et al.*, 2003).

Resistin appears to share several features with pro-inflammatory cytokines and can play a role in the regulation of inflammation and immunity (Tilg and Moschen, 2006). The expression of resistin is up-regulated during monocyte–macrophage differentiation, indicating a role for resistin in monocyte–macrophage function (Patel *et al.*, 2003; Savage *et al.*, 2001). Furthermore, it has been demonstrated that pro-inflammatory mediators such as TNF-α, IL-1β, IL-6 or lipopolysaccharide (LPS) can strongly increase the expression of resistin in peripheral blood mononuclear cells (PBMCs), suggesting a role for resistin in the process of inflammation (Anderson *et al.*, 2007; Bokarewa *et al.*, 2005; Kaser *et al.*, 2003; Lehrke *et al.*, 2004). While, Nagaev *et al.* (2006) demonstrated *in vitro* that resistin can induce the expression of pro-inflammatory cytokines IL-6, IL-8, and TNF-α within WAT (Nagaev *et al.*, 2006). Silswal *et al.* (2005) observed that incubation of both human and mouse macrophages with human recombinant resistin can increase the production of the pro-inflammatory cytokines through the induction of NF-κB (Silswal *et al.*, 2005). Additionally, resistin has been found to activate the MAPKs ERK and p38 in addition to PKB/Akt in several cell lines (Bertolani *et al.*, 2006; Calabro *et al.*, 2004; Kushiyama *et al.*, 2005; Mu *et al.*, 2006).

Interestingly, resistin has been shown to be increased in the mouse models of genetic and diet-induced obesity. The administration of resistin to healthy mice impaired glucose tolerance and insulin action while antibodies against resistin improve insulin action (Steppan *et al.*, 2001). Resistin has been shown to induce β cell apoptosis (Gao *et al.*, 2009) while in 3T3-L1 adipocytes, resistin attenuates the insulin-signaling pathway (Steppan *et al.*, 2005). In rat skeletal muscles, resistin inhibits insulin-stimulated glycogen synthesis and glucose uptake (Moon *et al.*, 2003; Pravenec *et al.*, 2003) perhaps due to a reduction in the intrinsic activity of glucose transporters (Pravenec *et al.*, 2003). Resistin also exerts its glucoregulatory effect by stimulating hepatic glucose output (Banerjee *et al.*, 2004; Muse *et al.*, 2004; Rajala *et al.*, 2003; Yang *et al.*, 2009). Resistin decreased insulin receptor and glycogen synthase activity while increasing the activity of glycogen phosphorylase; resulting in attenuation of glycogenesis and enhanced glycogenolysis leading to reduced glycogen content within the liver (Yang *et al.*, 2009).

Nevertheless, there are no differences in serum resistin levels among non-obese, obese and obese diabetic groups, despite wide variations in insulin sensitivity. Furthermore, resistin is not a significant predictor of insulin resistance when adjusted for adiposity (Degawa-Yamauchi *et al.*, 2003; Heilbronn *et al.*, 2004). However, resistin clearly plays a role in obesity-related sub-clinical inflammation.

1.5.4 TNF-α

TNF-α is a pleiotropic factor that exerts a variety of effects such as growth promotion, growth inhibition, angiogenesis, cytotoxicity, infammation and immunomodulation (Aggarwal and Natarajan, 1996). This cytokine is synthesized mainly by macrophages in response to invasive stimuli (Jue *et al.*, 1990). TNF-α is recognized by two different receptors, TNFR1 and TNFR2. Although the exact biological functions of the two receptors are still not fully understood, it has been suggested that TNFR1 plays an important role in both the pro-inflammatory and cytotoxic responses, while the other receptor may act to modulate the response generated by TNFR1 (Peschon *et al.*, 1998). TNF-α can either act in an autocrine or paracrine way at low concentrations or in an endocrine fashion when it is released in high concentrations.

In obese individuals and rodent models of obesity, TNF-α is over-expressed in WAT and muscle tissue (Hotamisligil *et al.*, 1995; Hotamisligil *et al.*, 1993; Saghizadeh *et al.*, 1996) at both the mRNA and protein level consistent with reports that circulating levels of TNF-α are increased in individuals with T2DM (Katsuki *et al.*, 1998; Pfeiffer *et al.*, 1997). Interestingly, Hotamisligil *et al.* (1997) showed that TNFR2 is over expressed in WAT of obese humans, with a strong correlation with BMI, hyperinsulinaemia and TNF mRNA levels in adipose tissue, while soluble receptors (sTNFR2) are elevated six fold in the obese subjects as compared with the healthy controls suggesting that TNFR2 may play a role in obesity by modulating the actions of TNF-α (Hotamisligil *et al.*, 1997). Furthermore, Uysal *et al.* (1997) generated obese mice with a targeted null mutation in the gene encoding TNF-α and also those encoding for the two TNF receptors (Uysal *et al.*, 1997). Interestingly, TNF deficient mice show a lower body weight and fat accumulation as compared to wild-type (WT) controls. The absence of TNF also resulted in significantly improved insulin sensitivity in both diet-induced obese mice and the *ob/ob* model of obesity. These results clearly indicate that TNF is an important mediator of insulin resistance through its effects on several important sites of insulin action.

1.5.5 IL-6

Several cell types are reported to produce IL-6; these include most cells of the immune system, endothelial cells, skeletal and smooth muscle cells, adipocytes, islet β cells, hepatocytes, microglial cells, astrocytes and a number of other cell types (Kamimura *et al.*, 2003). IL-6 was initially thought to be a pro-inflammatory cytokine mainly with effects within the immune system, however this understanding of IL-6 was simplistic (Kamimura

et al., 2003). In the adaptive and innate immune systems, IL-6 is involved in both amplification of and protection against inflammation (Jones *et al.*, 2001; Kamimura *et al.*, 2003). Therefore, inappropriate regulation of IL-6 may play a direct protective or deleterious role in both antigen-specific immune-mediated diseases and in diseases where IL-6 or other inflammatory factors cause a low-grade inflammation such as obesity induced T2DM (Jones *et al.*, 2001; Kamimura *et al.*, 2003; Pickup, 2004). IL-6 induces activation of the JAK/STAT pathway and MAPK pathways in both immune and non–immune-related cell types leading to increased expression of suppressors of cytokine signaling (SOCS) proteins and in particular SOCS-3, which exerts negative feedback on JAK/STAT signaling. Importantly, human adipose tissue is a major site of IL-6 secretion (Fried *et al.*, 1998; Mohamed-Ali *et al.*, 1997) accounting for 15 – 35% of the circulating levels (Mohamed-Ali *et al.*, 1997).

1.5.6 IL-1

The IL-1 family of molecules consists of two agonists, IL-1α and IL-1β, an IL-1 receptor antagonist (IL-1Ra), IL-1 receptors, type I and type II (IL-1RI and IL-1RII) and the IL-1 receptor accessory protein (IL-1RAcP) (Rock *et al.*, 1998). IL-1 signaling involves binding of either of the two ligands IL-1α or IL-1β to a common membrane-bound IL-1RI. Upon binding, the IL-1/IL-1RI signals through the transducing subunit, IL-1RAcP (Greenfeder *et al.*, 1995; Schreuder *et al.*, 1997; Vigers *et al.*, 1997). Activation of this complex involves the association of the adapter protein MyD88 to the cytoplasmic portions of the receptor subunits and activation of the IL-1 receptor associated protein kinase (IRAK) (Adachi *et al.*, 1998; Muzio *et al.*, 1997; Wesche *et al.*, 1997). These events ultimately lead to the activation and nuclear translocation of NF-κB, which is a crucial transcription factor for many IL-1 inducible genes. In addition, activation of PI3K, MAPKs and protein kinase C, as well as the generation of second messengers such as cyclic AMP, intracellular calcium and ceramide has been described (Arora *et al.*, 1995; Auron, 1998; Dinarello, 1996; Luo *et al.*, 1997).

IL-1β is a major pro-inflammatory cytokine that is primarily produced by blood monocytes, tissue macrophages and dendritic cells. B lymphocytes and natural killer (NK) cells also produce IL-1β (Dinarello, 2009; Martin and Wesche, 2002). Furthermore, an important pro-inflammatory property of IL-1β is its ability to increase the expression of adhesion molecules such as ICAM in mesenchymal cells and vascular cell adhesion molecule-1 (VCAM) in endothelial cells (Dinarello, 2009). Together with the induction of

chemokines, these properties of IL-1β promote the infiltration of inflammatory and immunocompetent cells from the circulation into the extravascular space and then into tissues, where tissue remodeling is the end result of chronic IL-1-induced inflammation (Dinarello, 2009).

Interestingly, expression of IL-1β is increased in WAT of both obese rodents and humans and its expression is correlated with the MetS (Salmenniemi *et al.*, 2004). Additionally, serum levels of IL-1Ra are significantly higher in obese compared with non-obese subjects, are highly correlated with insulin resistance and upon weight loss, the serum IL-1Ra levels decrease (Meier *et al.*, 2002). However, in contrast to this, in a human trial conducted by Larsen *et al.* (2007) treatment with IL-1Ra was demonstrated to improve glycemic control in patients with T2DM, which correlated with improved measures of β-cell secretory capacity. Similarly, Sauter *et al.* (2008) found that IL-1Ra treatment prevented diabetes *in vivo* in C57BL/6J mice fed a HFD for 12 weeks (Sauter *et al.*, 2008). Conversely, Matsuki *et al.* (2003) reported that a gene knockout of the IL-1Ra in mice caused leanness and resistance to diet-induced obesity, without any overt signs of illness (Matsuki *et al.*, 2003). While mature obese IL-1RI$^{-/-}$ mice were found to be insulin resistant, as evident by hyperinsulinemia, decreased glucose tolerance and decreased insulin sensitivity.

1.6 Transcription factors: inflammation and insulin sensitivity

Disregulation of transcription factors such as nuclear transcription factor (NF)-κB can lead to the constitutive over production of pro-inflammatory cytokines, which is associated with a number of chronic inflammatory disorders such as obesity induced T2DM (Beinke and Ley, 2004). Furthermore, insulin action in adipocytes also involves changes in gene transcription. Sterol regulatory element binding protein (SREBP)-1c plays a critical role in the actions of insulin to regulate adipocyte gene expression (Foretz *et al.*, 1999a; Kim *et al.*, 1998a; Shimomura *et al.*, 1999), by inducing genes involved in lipogenesis and repressing those involved in fatty acid oxidation. Additionally, peroxisome proliferator-activated receptor (PPAR)-γ also plays a crucial role in adipocyte differentiation, glucose metabolism and other physiological processes. Other transcription factors, including those of the forkhead family, may also play a major role in transducing insulin signals to the nucleus (Kops and Burgering, 1999).

1.6.1 Nuclear factor-κB

NF-κB is a multi-protein transcription factor whose regulatory targets include secreted inflammatory proteins such as cytokines and chemokines. Inflammatory stimuli including activation of Toll-like receptors (TLR), reactive oxygen species (ROS), ultraviolet radiation (UV) and pro-inflammatory cytokines promote NF-κB activation. In an unstimulated state, NF-κB resides in the cytoplasm, complexed with IκB. When activated, IKK directly phosphorylates IκB allowing NF-κB to be translocated to the nucleus, where it interacts with its DNA recognition sites to mediate gene transcription (Figure 1.4) (Devary *et al.*, 1993; Israel *et al.*, 1989; Medzhitov *et al.*, 1997; Schneider *et al.*, 1999). Importantly, obesity increases active, nuclear-localized NF-κB in liver and skeletal muscle and transcription of NF-κB target genes (Cai *et al.*, 2005; Yuan *et al.*, 2001). Additionally, during obesity enlarged adipocytes release increased levels of saturated fats which have been shown to activate TLR4 resulting in NF-κB activation, ultimately leading to augmented cytokine production (Suganami *et al.*, 2005; Suganami *et al.*, 2007b).

Interestingly, non-steroidal anti-inflammatory drugs (NSAIDs) increase insulin sensitivity within human patients (Arena *et al.*, 1978) and in rodent models such as Zucker *fa/fa* rats and *ob/ob* mice (Kim *et al.*, 2001a). These drugs are cyclooxygenase (COX) inhibitors, which are though to act as non-specific NF-κB and IKK-β inhibitors (Karin *et al.*, 2004). Additionally, high doses of salicylates, including sodium salicylate and aspirin, have been used to treat inflammatory conditions such as rheumatic fever and rheumatoid arthritis. These high doses are thought to inhibit NF-κB (Kopp and Ghosh, 1994) and its upstream activator IKK-β (Yin *et al.*, 1998), as opposed to working through COX, the classical targets of nonsteroidal anti-inflammatory drugs (NSAIDs). Interestingly, high doses of salicylates lower blood glucose concentrations (Baron, 1982; Reid *et al.*, 1957), although their potential for treating diabetes has been all but forgotten by modern biomedical science (Yuan *et al.*, 2001). Yuan and colleagues observed that high doses of salicylates reverse hyperglycemia, hyperinsulinemia and dyslipidemia in obese rodents by sensitizing insulin signaling (Yuan *et al.*, 2001). Activation or overexpression of the IκB attenuated insulin signaling in 3T3-L1 adipocytes, whereas IKK-β inhibition reversed insulin resistance. Furthermore, heterozygous deletion IKK-β1/2 protected against the development of insulin resistance during high-fat feeding and in obese *ob/ob* mice (Yuan *et al.*, 2001). In accord, targeted deletion of IKK-β in hepatocytes reduces obesity-induced hepatic inflammation and circulating inflammatory cytokines IL-1β and IL-6 (Arkan *et al.*, 2005; Cai *et al.*, 2005). Importantly, mice lacking IKK-β in hepatocytes retain liver insulin

responsiveness, while developing insulin resistance in muscle and fat in response to a high fat diet (HFD), obesity or aging (Arkan *et al.*, 2005). However, mice lacking IKK-β in myeloid cells retain global insulin sensitivity and are protected from insulin resistance (Arkan *et al.*, 2005). Therefore, these data indicate that IKK-β acts locally in liver and systemically in myeloid cells, where NF-κB activation induces inflammatory mediators that cause insulin resistance (Arkan *et al.*, 2005).

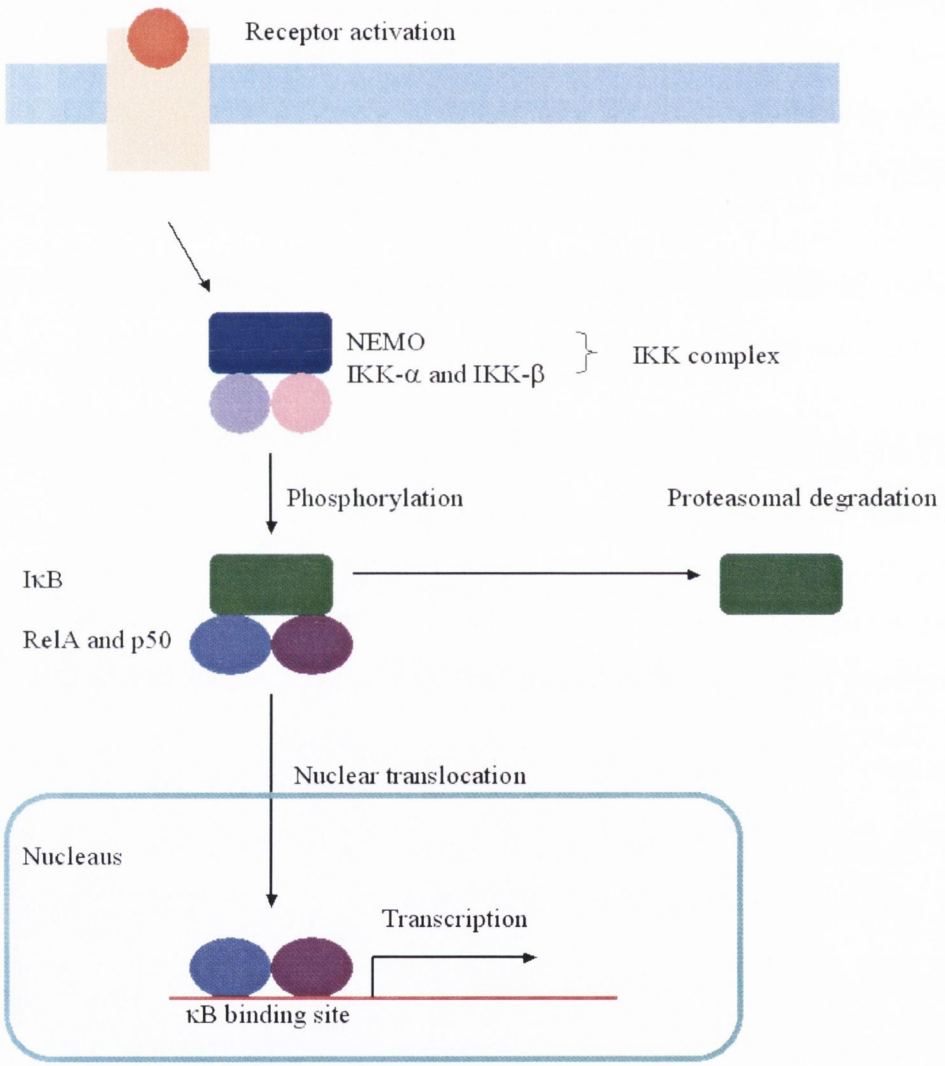

Figure 1.5 Model of the generic NF-κB activation pathway. The binding of ligand to a receptor leads to the recruitment and activation of an IKK complex comprising IKK-α and/or IKK-β catalytic subunits and two molecules of NEMO. The IKK complex then phosphorylates IκB leading to its degradation by the proteasome. Associated NF-κB dimmers are then released and translocate into the nucleus, where they bind to the promoter regions of NF-κB responsive genes to modulate their expression. Adapted from Beinke and Ley, 2004.

1.6.2 Peroxisome proliferator-activated receptors

PPARs are nuclear hormone receptors, initially described as molecular targets for compounds, which induce peroxisomal proliferation (Berger and Moller, 2002; Desvergne and Wahli, 1999). Three different isotypes of PPARs have been identified in various species: PPAR-α, -β and -γ (Berger and Moller, 2002; Desvergne and Wahli, 1999). PPAR-γ is mainly expressed in WAT and to a lesser extent in other tissues and cells throughout the body. PPAR-γ plays a central role in the process of adipocyte differentiation, peripheral glucose utilization and insulin sensitization (Braissant *et al.*, 1996; Chawla *et al.*, 1994; Jain *et al.*, 1998; Kliewer *et al.*, 1994). PPARs and the transcription factor CCAAT/enhancer-binding proteins (C/EBPs) transcriptionally transactivate adipose-specific genes, including adipocyte specific fatty acid binding protein (FABP)-4, fatty acid synthase (FAS), leptin, resistin and adiponectin (Combs *et al.*, 2002; Iwaki *et al.*, 2003; Mandrup and Lane, 1997). Jones and colleagues (2005) generated adipose specific PPAR-γ knockout mice (Jones *et al.*, 2005). These animals exhibited marked abnormalities in the formation and function of WAT and when fed a HFD these mice displayed diminished weight gain despite hyperphagia, diminished serum leptin concentrations and did not develop glucose intolerance or insulin resistance. Furthermore, PPAR-γ expression appears to be enhanced during the differentiation of monocytes into macrophages in response to pro-inflammatory mediators (Sacre *et al.*, 2005).

PPAR-γ is a ligand-activated transcription factor that binds to specific DNA sequences, known as peroxisome proliferator response elements (PPREs), in the promoter regions of the target genes only as an heterodimer with the retinoid X receptor (RXR) (Berger and Moller, 2002; Desvergne and Wahli, 1999; Feige *et al.*, 2006; Gearing *et al.*, 1993; Nolte *et al.*, 1998). In addition, PPAR-γ can regulate gene expression independently of PPRE, either by suppressing growth hormone protein-1 (GHP-1), a transcription factor involved in pituitary specific gene expression, or by interfering with the function of activator protein (AP)-1, signal transducer and activator of transcription (STAT)-1 and NF-κB (Feige *et al.*, 2006; Feinstein *et al.*, 2005; Ricote *et al.*, 1998b; Tolon *et al.*, 1998). Although no molecule has been demonstrated to serve as an endogenous ligand of PPAR-γ *in vivo*, several biological ligands or activators of PPAR-γ and other PPARs have been identified. Circumstantial evidence suggests that an endogenous PPARγ activator is produced during adipogenesis (Tzameli *et al.*, 2004), but efforts to purify such a ligand biochemically have proven problematic (Tontonoz and Spiegelman, 2008).

The long chain polyunsaturated fatty acids (LC *n-3* PUFA) and their oxidized derivatives, such as eicosanoid 8-S-hydroxyeicosatetraenoic acid (8S-HETE) and leukotriene B4 (LTB_4) selectively bind to and activate all three PPARs (Feige *et al.*, 2006; Willson *et al.*, 2000). PPAR-γ can be selectively activated by several prostanoids, such as 15-deoxy-Δ12, 14-prostaglandin J_2 (15d-PGJ_2) and 15-hydroxy-eicosatetraenoic acid (15-HETE), which are derivatives of arachidonic acid (AA) synthesized through the lipoxygenase pathway, as well as by nitrolinoleic acid derivatives (Feige *et al.*, 2006; Schopfer *et al.*, 2005; Willson *et al.*, 2000). Thiazolidinediones (TZDs) and tyrosine derivatives constitute the most well known synthetic ligands (Henke *et al.*, 1998; Lehmann *et al.*, 1995), while PPAR-γ affinity for some NSAID has also been reported (Lehmann *et al.*, 1997). TZDs are an established class of oral anti-diabetic agents and include pioglitazone and rosiglitazone.

1.6.3 Sterol regulatory element binding proteins

SREBPs are a family of transcription factors that have been associated with lipogenesis, adipocyte development (Kim and Spiegelman, 1996) and cholesterol homeostasis (Yokoyama *et al.*, 1993). When cells are in a sterol-depleted state, SREBP transcription factors are released from an ER membrane-bound precursor by a two-step proteolytic cleavage (Sakai *et al.*, 1996). After cleavage, SREBPs are translocated to the nucleus, where they bind to sterol regulatory elements (SREs) and/or E-boxes in the promoter region of target genes activating their transcription (Brown and Goldstein, 1997; Horton and Shimomura, 1999; Kim *et al.*, 1998a).

SREBP-1c is expressed in most human and mouse tissues with especially high levels in the liver, WAT, adrenal gland and brain (Shimomura *et al.*, 1997). Furthermore, SREBP-1c is expressed in cultured adipocyte cell lines (Shimomura *et al.*, 1997). In mouse WAT, SREBP-1c mRNA expression was dramatically reduced by fasting and elevated on re-feeding (Kim *et al.*, 1998a). Importantly, in cultured cells, SREBP-1c expression and activity are regulated by insulin (Azzout-Marniche *et al.*, 2000; Kim *et al.*, 1998a), leading to the hypothesis that it may be a major component of the transcriptional effects of insulin in target cells (Flier and Hollenberg, 1999; Osborne, 2000). Regulation of the expression of fatty acid synthase (FAS), lipoprotein lipase and leptin genes have been demonstrated to be mediated, partially by SREBP-1c (Boizard *et al.*, 1998; Foretz *et al.*, 1999b; Kim *et al.*, 1998a; Latasa *et al.*, 2000). Additionally, SREBP-1c has been shown to activate PPAR-γ by stimulating the production of its ligands (Kim *et al.*, 1998b) or by increasing its expression in adipocyte cell lines (Fajas *et al.*, 1999). In obese mice it has been shown that

the mRNA expression of SREBP-1c was decreased in WAT (Nadler *et al.*, 2000; Soukas *et al.*, 2000). Similarly, in obese humans the expression of SREBP-1c is significantly lower than in normal weight subjects (Kolehmainen *et al.*, 2001). Interestingly, weight reduction was associated with increased mRNA levels of SREBP-1c in obese subjects and could be ascribed to lowered action or concentration of insulin (Kolehmainen *et al.*, 2001).

1.6.4 Transcriptional regulation of adipokines by cytokines

Preliminary work suggests human inflammation may modulate individual adipokine levels (Anderson *et al.*, 2007). In a study by Anderson and colleagues (2007) lipopolysaccharide (LPS) treatment in human volunteers was found to not only increase blood and adipose cytokine levels but in adition increased plasma leptin, whole blood resistin and plasma resistin (Anderson *et al.*, 2007). Similarly, in mice, the administration of pro-inflammatory molecules such as LPS, TNF-α and IL-1, produced a prompt and dose-dependent increase in serum leptin levels and leptin mRNA expression in adipose tissue. Interetingly, anti-inflammatory cytokines such as IL-10 and IL-4 had no effect on leptin gene expression or serum leptin levels (Sarraf *et al.*, 1997). Furthermore, in a study by Kaser *et al.* (2003) resistin mRNA expression in human peripheral blood mononuclear cells (PBMC) was strongly increased by the pro-inflammatory cytokines IL-1, IL-6, TNF-α, and also by LPS (Kaser *et al.*, 2003).

Importantly, transcription factors SP1, LP1 and CCAAT/enhancer-binding protein (C/EBP) are thought to play a key role in the transcriptional activation of the leptin gene promoter (Mason *et al.*, 1998). These regulatory motifs are important for leptin gene expression because, in each case, point mutations resulted in two- to threefold reductions in leptin promoter activity (Mason *et al.*, 1998). Additionally, when multiple regulatory motifs were mutated there was an additive effect on inhibiting leptin promoter activity, indicating that each promoter regulatory site contributes independently to leptin gene transcription (Mason *et al.*, 1998). Transcriptional regulation of the leptin gene also seems to be controlled by PPARγ. Thiazolidinediones (TZD), pharmacological ligands for PPARγ, down-regulate leptin mRNA abundance in adipocytes (Lehmann *et al.*, 1995; Saltiel and Olefsky, 1996). Furthermore, Zhou *et al.* (2006) observed that C/EBPα activated resistin expression both in 293T cells and 3T3-L1 preadipocytes (Zhou *et al.*, 2006). Transcription factors C/EBP and PPAR work sequentially and cooperatively to stimulate the genetic events that result in differentiation (Cornelius *et al.*, 1994). However, some studies indicate that NF-κB p50 activation by inflammatory cytokines induces C/EBPα (Wang *et al.*, 2009). Furthermore, LPS has been shown to induce SP1 activation

via p38 MAPK causing up-regulation in IL-10 expression (Ma *et al.*, 2001). This indicates that inflammatory stimulus can induce transcription factors such as C/EBP and SP1, which may in turn up-regulate leptin and resistin expression *in vivo*.

1.7 Obesity: a chronic pro-inflammatory state

A major conceptual advance in the field of obesity-induced inflammation and insulin resistance was made by the discovery that obesity gives rise to a state of chronic, low-grade systemic inflammation with evidence of increased infiltration of macrophages into the adipose tissue. Weisberg *et al.* (2003) performed microarray analyses comparing WAT RNA profiles of various mouse models of obesity and identified a subset of genes consistently expressed in obese mice. Further analyses determined that this gene set, not typically expressed in adipocytes, was macrophage-derived (Weisberg *et al.*, 2003). In 2003 Weisberg and colleagues used immunohistochemical analysis of perigonadal, perirenal, mesenteric and SAT to show that the percentage of cells expressing the macrophage marker F4/80 (F4/80+) was significant and positively correlated with both adipocyte size and body mass. They observed that the F4/80+ cells are CSF-1 dependent, bone marrow-derived adipose tissue macrophages (ATM) (Weisberg *et al.*, 2003). Xu and colleagues (2003) reported similar findings and also showed that TZD treatment could repress the expression of macrophage-specific genes, providing an additional mechanism by which TZD treatment improves insulin sensitivity (Xu *et al.*, 2003). The ATM were shown to produce many of the pro-inflammatory molecules released by the WAT including TNF-α, nitric oxide synthase (NOS)-2 and IL-6 gene expression (Weisberg *et al.*, 2003). As discussed previously, pro-inflammatory cytokines such as TNF-α, IL-1β and IL-6 have been implicated in the development of insulin resistance and the pathophysiology of T2DM and obesity. In both humans and rodents, ATM accumulate in WAT with increasing body weight and their quantity correlates with measures of insulin resistance (Cancello *et al.*, 2005; Weisberg *et al.*, 2003; Xu *et al.*, 2003). In obese subjects ATM content is higher in VAT rather than SAT, consistent with the hypothesis that VAT plays a more prominent role in insulin resistance (Cancello *et al.*, 2006).

1.7.1 Immune cell recruitment into adipose tissue

Both adipocyte hyperplasia and hypertrophy can contribute to adipose tissue expansion; however, in adults, hypertrophy appears to predominate. Some of the consequences of hypertrophy include a reduction in vascularization, hypoxia and adipocyte cell death (Surmi and Hasty, 2008). These effects all combine to cause macrophage recruitment into

adipose tissue (Figure 1.6). Additionally, other immune cells such as neutrophils and T cells may enter WAT first and contribute to macrophage recruitment.

Weisberg *et al.* (2007) observed that cytotoxic T cells were present in large numbers within the adipose of both diet-induced obesity (DIO) and *ob/ob* obese mice relative to lean controls (Rausch *et al.*, 2008). In a recent study T regulatory (T_{reg}) cells were found to be highly enriched in the abdominal fat of normal mice, but their numbers were strikingly and specifically reduced at this site in insulin-resistant models of obesity (Feuerer *et al.*, 2009). Interestingly, a depletion of T_{reg} cells in 10 week old male mice was shown to induce a substantial decrease in insulin-stimulated insulin receptor tyrosine phosphorylation in epididymal adipose tissue (EAT) and liver (Feuerer *et al.*, 2009). Furthermore, insulin concentrations were significantly higher in T_{reg} cell-depleted mice, indicative of insulin resistance (Feuerer *et al.*, 2009).

Lynch and colleagues (2008) observed that obese patients have significantly less circulating natural killer (NK) and cytotoxic T lymphocytes (CTL) compared to lean controls (Lynch *et al.*, 2009). Within this study patients were classified into metabolically "healthy obese" or "unhealthy obese" groups, based upon standard cutoff points for blood pressure, lipid profile and fasting glucose. There were significantly higher levels of NK cells and CTL in the healthy obese group compared to the unhealthy obese group, independent of age and BMI. Interestingly, the NK cells were less activated in the healthy compared to the unhealthy group. They hypothesize that the significantly higher levels of CTL and NK cells, which express fewer inhibitory molecules, could protect against malignancy, infection and metabolic disease seen in obesity (Lynch *et al.*, 2009). Furthermore, Lynch and colleagues (2009) described an accumulation of functional invariant NK cells (iNKT) in human omentum. iNKT cells recognize lipid antigens presented by CD1d and respond rapidly by killing tumor cells and release cytokines that regulate adaptive immune responses. Importantly, omental iNKT-cell frequencies were lower in patients with severe obesity suggesting a novel role for the omentum in immune regulation (Lynch *et al.*, 2009).

Studies also indicate that neutrophil infiltration into WAT may precede macrophage infiltration. Neutrophil activation is a fundamental process in the innate immune response. Elgazar-Carmon *et al.* (2008) demonstrated neutrophils transiently infiltrate adipose tissue as early as 3 days after initiating a high-fat diet in mice (Elgazar-Carmon *et al.*, 2008).

1.7.2 Vascularization and hypoxia

Obese mouse models such as diet induced obese (DIO) mice and leptin deficient *ob/ob* mice have been used to demonstrate that hypoxia occurs in obese WAT (Hosogai *et al.*, 2007; Ye *et al.*, 2007). Decreased vascular density, which has been observed in obese mice (Voros *et al.*, 2005), may contribute to hypoxia. Importantly, it has been suggested that the ATM may act to stimulate angiogenesis in the adipose tissue (Pang *et al.*, 2008) and this could be a rationale for why the macrophages infiltrate into adipose tissue. Furthermore, mRNA and protein levels of hypoxia-inducible factor (HIF)-1α are elevated in adipose tissue of obese mice and obese humans, as are mRNA and protein levels for other hypoxia inducible genes (Hosogai *et al.*, 2007; Wang *et al.*, 2007; Wang and Zhang, 2008; Ye *et al.*, 2007). Ye and colleagues (2007) demonstrated *in vitro* that hypoxia may contribute to adipose tissue inflammation by showing that exposure of primary adipocytes and macrophages to hypoxia increases their expression of multiple inflammatory genes (Ye *et al.*, 2007).

1.7.3 Necrotic adipocyte death

Cinti and colleagues (2005) demonstrated that more than 90% of all macrophages in WAT are localized to dead adipocytes, where they fuse to form syncytia that sequester and scavenge the residual "free" adipocyte lipid droplets and ultimately form multinucleated giant cells, a hallmark of chronic inflammation. Adipocyte death increases in obese leptin deficient *ob/ob* mice 30 fold and obese humans exhibit ultra-structural features of necrosis (Cinti *et al.*, 2005). Necrotic like adipocyte cell death is a pathological hallmark of obesity and suggests that scavenging of adipocyte debris is an important function of the ATM in obese individuals (Cinti *et al.*, 2005).

1.7.4 Chemokines

Chemokines are small, chemotactic cytokines play a role in macrophage mobilization out of bone marrow and into many different tissues during the inflammatory process (Surmi and Hasty, 2008). Although they can be secreted by adipocytes, studies in which adipocytes were separated from the SVC have demonstrated that the majority of chemokine secretion in adipose tissue is from the SVC (Xu *et al.*, 2003). Therefore, expression of chemokines from ATM likely promote macrophage accumulation in the adipose tissue (Surmi and Hasty, 2008). Circulating concentrations of the chemokine monocyte chemotactic protein (MCP)-1 are increased in obesity subjects (Bruun *et al.*, 2005) and T2DM patients compared to non-diabetics (Christiansen *et al.*, 2005). Weisberg

and colleagues (2006) demonstrated that in obese mice matched for adiposity, MCP-1 receptor deficiency ($CCR2^{-/-}$) reduces ATM content, reduced the inflammatory profile of the adipose tissue, increased adiponectin expression, ameliorated hepatic steatosis, improved systemic glucose homeostasis and enhanced insulin sensitivity (Weisberg *et al.*, 2006).

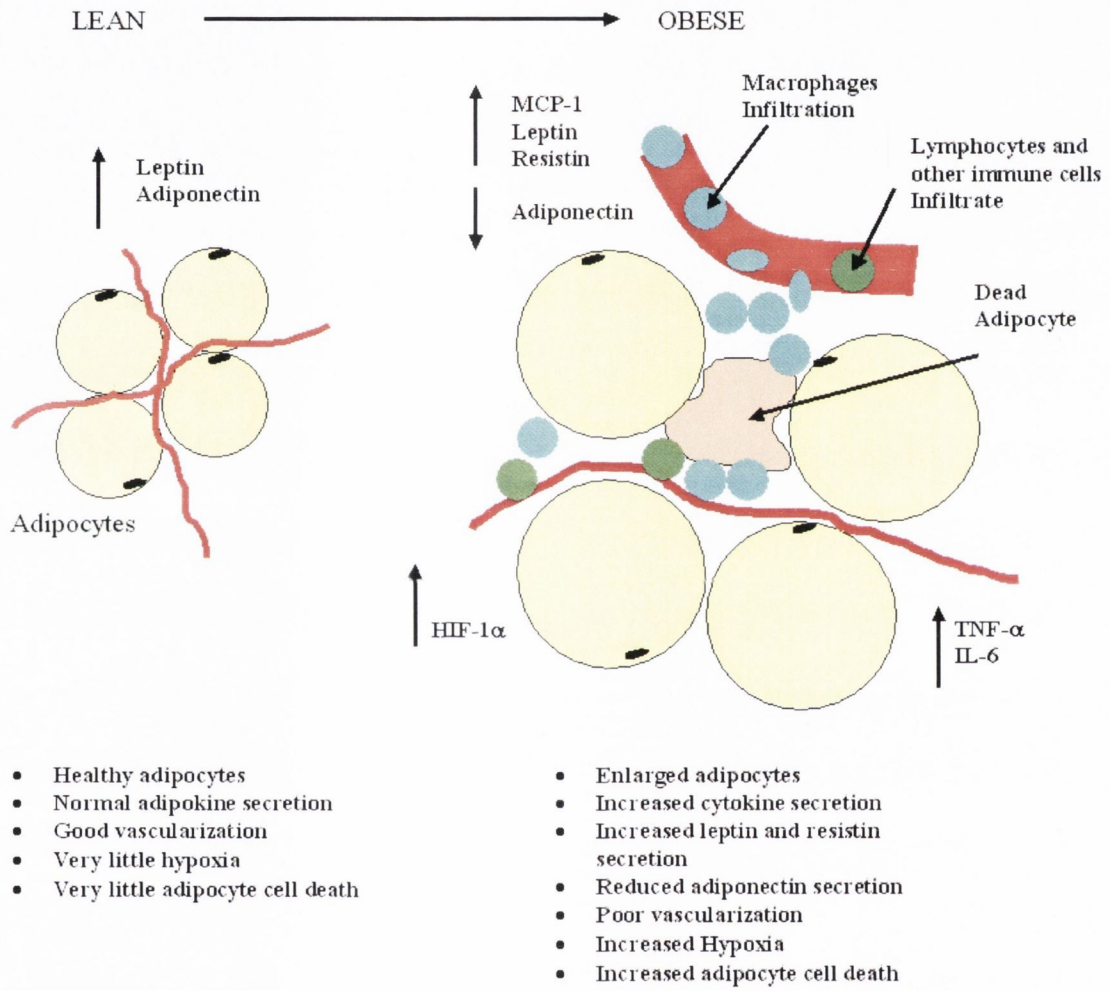

Figure 1.6 Increase in adipocyte size and poor vascularization of the adipose tissue leads to adipocyte cell death and hypoxia causing the release of pro-inflammatory cytokines and chemokines such as TNF-α, leptin and MCP-1 from the adipocytes and SVC. These pro-inflammatory modulators cause recruitment of macrophages and other immune cells into the adipose tissue exacerbating the inflammatory state.

1.8 Pro- and anti-inflammatory adipose tissue macrophages

The ability of macrophages to secrete both pro- and anti-inflammatory cytokines contributes to their dual role, furthermore ingestion of apoptotic cells has been shown to reprogram macrophages to become anti-inflammatory (Savill *et al.*, 2002). Different

stimuli activate macrophages to express distinct patterns of chemokines, surface markers and metabolic enzymes that ultimately generate the diversity of macrophage function seen in pro-inflammatory and anti-inflammatory settings (Lumeng *et al.*, 2007a). Macrophage activation has been defined across two separate polarization states, M1 and M2 (Gordon and Taylor, 2005; Mantovani *et al.*, 2004).

M1 or "classically activated" macrophages are induced by pro-inflammatory mediators such as LPS and interferon (IFN)-γ. M1 macrophages have enhanced pro-inflammatory cytokine production (TNF-α, IL-6 and IL-12) and generate reactive oxygen species such as nitric oxide (NO) via activation of iNOS. M2 or "alternatively activated" macrophages are generated *in vitro* by exposure to IL-4 and IL-13, they have low pro-inflammatory cytokine expression and generate high levels of anti-inflammatory cytokines IL-10 and IL-1 decoy receptor (Gordon and Taylor, 2005). Lumeng *et al* (2007) identified F4/80+CD11c+ populations of ATM or M1 macrophages in adipose tissue of obese mice that were not found in lean mice. ATM from lean mice expressed many genes characteristic of M2 macrophages, including IL-10. Interestingly, diet induced obesity decreased expression of these characteristic M2 genes in ATM and increased expression of genes such as those encoding TNF-α and iNOS which are characteristic of M1 macrophages. Lumeng and colleagues (2007) observed that ATM from obese $CCR2^{-/-}$ knockout mice, which have reduced macrophage infiltration into the adipose tissue, express M2 markers at levels similar to those from lean mice (Lumeng *et al.*, 2007b) suggesting MCP-1 and its receptor may be an important factor in regulating macrophage activation.

Interestingly, macrophage specific deficiency of PPAR-γ prevets the development of alternatively activated M2 phenotype (Odegaard *et al.*, 2007a). Macrophage PPAR-γ specific knockout mice showed a predisposition to diet induced weight gain, glucose intolerance and insulin resistance. Despite the increased adipose tissue mass, total ATM were reduced in the macrophage PPAR-γ specific knockout mice and this appeared to be due to a reduction in M2 macrophages. This suggests that M2 macrophages provide protection against diet induced insulin resistance and that PPARγ is fundamental to macrophages becoming the M2 phenotype. Human macrophage populations cannot always be classified simply as M1 or M2. However, it has been demonstrated that human ATM have both M1 and M2 characteristics, as evidenced by their secretion of both pro- and anti-inflammatory cytokines (Bourlier *et al.*, 2008; Zeyda *et al.*, 2007).

1.9 Insulin signalling

In insulin-resistant states, signal transduction via the insulin receptor is impaired with decreased activation of downstream intermediates, such as IRS-1 and Akt, resulting in reduced translocation of GLUT4 protein to the cell surface (Nguyen *et al.*, 2005). This results in a decrease in insulin-stimulated glucose transport and metabolism in adipocytes and skeletal muscle with impaired suppression of hepatic glucose output (Reaven, 1995). However, insulin has many more effects at both a cell signalling and gene expression level including its effects on carbohydrate, lipid and protein metabolism and therefore a decrease in insulin sensitivity undoubtedly has many serious and widespread consequences within the body.

1.9.1 Insulin receptor

The insulin receptor is necessary and sufficient to mediate insulin action. Humans and mice lacking insulin receptors are born at term, but do not survive long, suggesting that insulin receptors are essential for postnatal growth and fuel metabolism, but are not required for fetal metabolism (Accili *et al.*, 1999; Taylor, 1999). The complete insulin receptor is composed of two α- and two β-subunits, linked together by disulfide bonds. Insulin binds to the receptor's extracellular α-subunit, bringing the two α-subunits closer together. This conformational change enables ATP binding to the β-subunit's intracellular domain. ATP binding activates receptor autophosphorylation (Hubbard, 1997; Hubbard *et al.*, 1994), which enables the receptor's kinase activity toward intracellular protein substrates. There are numerous autophosphorylation sites in the β-subunit's intracellular domain. In addition to binding insulin, the insulin receptor can bind insulin-like growth factors (IGF-I and IGF-II). The affinity of IGF-I binding to the insulin receptor is approximately 100- to 1000-fold lower than insulin's affinity (De Meyts *et al.*, 1995). However, as circulating IGF-I levels are approximately 100-fold higher than those of insulin, the potential exists for IGF-I binding and acting through the insulin receptor.

1.9.2 Insulin receptor substrates

Insulin receptor substrates (IRSs) represent key elements in insulin and IGF actions (White *et al.*, 1985). Insulin, IGF-I and certain cytokine receptors phosphorylate IRSs. Phosphorylation of their tyrosine residues increases the affinity with which IRS proteins bind other signaling molecules. Each tyrosine-phosphorylated motif binds to a specific signaling molecule. In this way, protein complexes are formed, and various signaling pathways are engaged, providing a potential explanation for the diversity of insulin

signaling (White and Yenush, 1998). The IRS family is composed of four closely related members (IRS-1 to -4) (Lavan *et al.*, 1997a; Lavan *et al.*, 1997b; Sun *et al.*, 1991; Sun *et al.*, 1995) and a more distantly related homolog, Gab-1 (Holgado-Madruga *et al.*, 1996). Ablation of IRS-1 causes severe growth retardation with mild insulin resistance (Araki *et al.*, 1994; Tamemoto *et al.*, 1994), suggesting an important role of IRS-1 in both insulin and IGF actions. In contrast, ablation of IRS-2 causes combined insulin resistance in peripheral tissues and impaired growth of pancreatic β-cells (Withers *et al.*, 1998). Ablation of IRS-3 is devoid of a clear phenotype (Liu *et al.*, 1999), whereas ablation of IRS-4 is associated with modest growth retardation and insulin resistance (Fantin *et al.*, 2000). Finally, inactivation of Gab-1 has an embryonic lethal phenotype that suggests a role in hepatic growth factor, rather than insulin, signaling (Itoh *et al.*, 2000).

The phosphorylation state of IRS-1 appears to predict the ability of IRS-1 to mediate the insulin response (Aguirre *et al.*, 2000). Tyrosine phosphorylation of IRS-1 via the active insulin receptor leads to insulin signalling. Whereas, serine phosphorylation of IRS-1 via serine/threonine kinases results in an impaired ability of insulin to tyrosine phosphorylate IRS-1. Furthermore, activation of c-Jun N-terminal kinase (JNK) by pro-inflammatory cytokines inhibits insulin signaling, at least in part, by stimulating serine phosphorylation of IRS-1 (Aguirre *et al.*, 2000; Aguirre *et al.*, 2002).

1.9.3 Phosphatidylinositol 3-kinase and protein kinase B/Akt

Tyrosine phosphorylated IRS1/2 recruits the heterodimeric p85/p110 phosphatidylinositol 3-kinase (PI3K) at the plasma membrane, where it produces the lipid second messenger PIP_3, which in turn activates a serine/threonine phosphorylation cascade of PH-domain containing proteins (Alessi and Downes, 1998). PIP_3 targets include PDK1, the serine/threonine protein kinase B (PKB)/Akt, and the protein kinases C ζ and λ isoforms (Beeson *et al.*, 2003; Vanhaesebroeck and Alessi, 2000). Mechanistically, PDK1, PKB and PKCs, which all contain a PH-domain, are recruited at the plasma membrane by binding to PIP_3, PDK1 phosphorylates PKB and PKCs on a threonine residue located in the activation loop of the catalytic domain, causing their activation (Le Good *et al.*, 1998; Pullen *et al.*, 1998; Stephens *et al.*, 1998). PKB and PKC phosphorylate multiple down-stream effectors that promote diverse biological responses including glucose transporter (GLUT) 4 translocation at the plasma membrane (Khan and Pessin, 2002), glycogen synthesis via PKB mediated inhibitory phosphorylation of glycogen synthase kinase (GSK)-3, which negatively regulates glycogen synthase (Cross *et al.*, 1995), lipogenesis via up-regulation

of the expression of the fatty acid synthase (FAS) gene (Bourlier *et al.*, 2008), as well as a more general control of gene expression patterns (O'Brien *et al.*, 2001).

1.9.4 Glucose transporter

The facilitative glucose transporters (GLUT) are an energy-independent system that can only transport substrate down a concentration gradient. The primary function of the facilitative glucose carriers is to mediate the exchange of glucose between the blood and the cytoplasm of the cell. The class I facilitative transporters contain GLUT1–4, and these have been comprehensively characterized in terms of structure, function and tissue distribution. The class II facilitative transporters include GLUT5, GLUT7, GLUT9 and GLUT1; while the class III facilitative transporters comprise GLUT6, GLUT8, GLUT10, GLUT12 and HMIT.

GLUTl is widely expressed, but it is most abundant in fibroblasts, erythrocytes and endothelial cells with low levels of expression in muscle, liver and adipose tissue (Birnbaum *et al.*, 1986; Fukumoto *et al.*, 1988; Pardridge *et al.*, 1990). The GLUT2 is found in the liver, pancreatic β cells, small intestine and kidney (Thorens *et al.*, 1988). GLUT3 is found at highest levels in neuronal tissue and is considered the major GLUT responsible for transporting glucose into the brain and peripheral nerves (Kayano *et al.*, 1988; Nagamatsu *et al.*, 1992). In contrast, GLUT4 is predominantly expressed in adipose tissue and muscle (Furtado *et al.*, 2002). The GLUT1 and GLUT3 isoforms are thought to be responsible for basal or constitutive glucose uptake, while the GLUT2 isoform plays an important role in glucose homeostasis. Importantly, GLUT4 is primarily responsible for enhanced glucose uptake in response to insulin (Furtado *et al.*, 2002).

The intracellular movement of GLUT4 is complex and involves many organelles. Fundamentally, in the absence of insulin, GLUT4 is trapped in an intracellular circuit between endosomes and the *trans*-Golgi network (TGN). In the absence of insulin stimulation, GLUT4 is almost completely excluded from the plasma membrane. However, the addition of insulin, or exercise in the case of muscle cells, causes GLUT4 to shift from its intracellular location to the plasma membrane. Interestingly, disruption of GLUT4 expression in mice results in insulin resistance (Stenbit *et al.*, 1997) while over expression of GLUT4 ameliorates diabetes in the *db/db* mouse model (Brozinick *et al.*, 2001). Furthermore, insulin resistance is known to be associated with reduced glucose uptake and utilization by these tissues, and this has been related with reduced GLUT4 gene expression (Klip *et al.*, 1994). Conversely, several reports have found preserved or even increased glucose utilization in WAT and muscles at the beginning of the obesity syndrome (Krief *et*

al., 1988; Le Marchand *et al.*, 1978; Marangou *et al.*, 1986; Penicaud *et al.*, 1987; Stauffacher and Renold, 1969). It is possible that reduced GLUT4 content could be compensated for by increased insulin-induced translocation to the plasma membrane.

1.9.5 Insulin signaling and mitogen-activated protein kinase

On a parallel pathway, activated IRS1/2 recruit Grb2, which associates to SOS and activates the extracellular signal-regulated kinases (ERK)1/2 mitogen-activated protein kinase (MAPK) pathway (Van Obberghen *et al.*, 2001). The p38 and c-Jun NH_2-terminal kinase (JNK) stress-activated kinases have been shown to be phosphorylated/activated in response to insulin (Mussig *et al.*, 2005; Somwar *et al.*, 2000). The ERK1/2 do not seem to play a major role in mediating insulin's metabolic responses, however increased basal MAPK activity appears to contribute to the development of insulin resistance. Conversely, p38 MAPK activity has been proposed as a positive regulator of insulin action because of its capability to increase the uptake of glucose via GLUT4 (Somwar *et al.*, 2002).

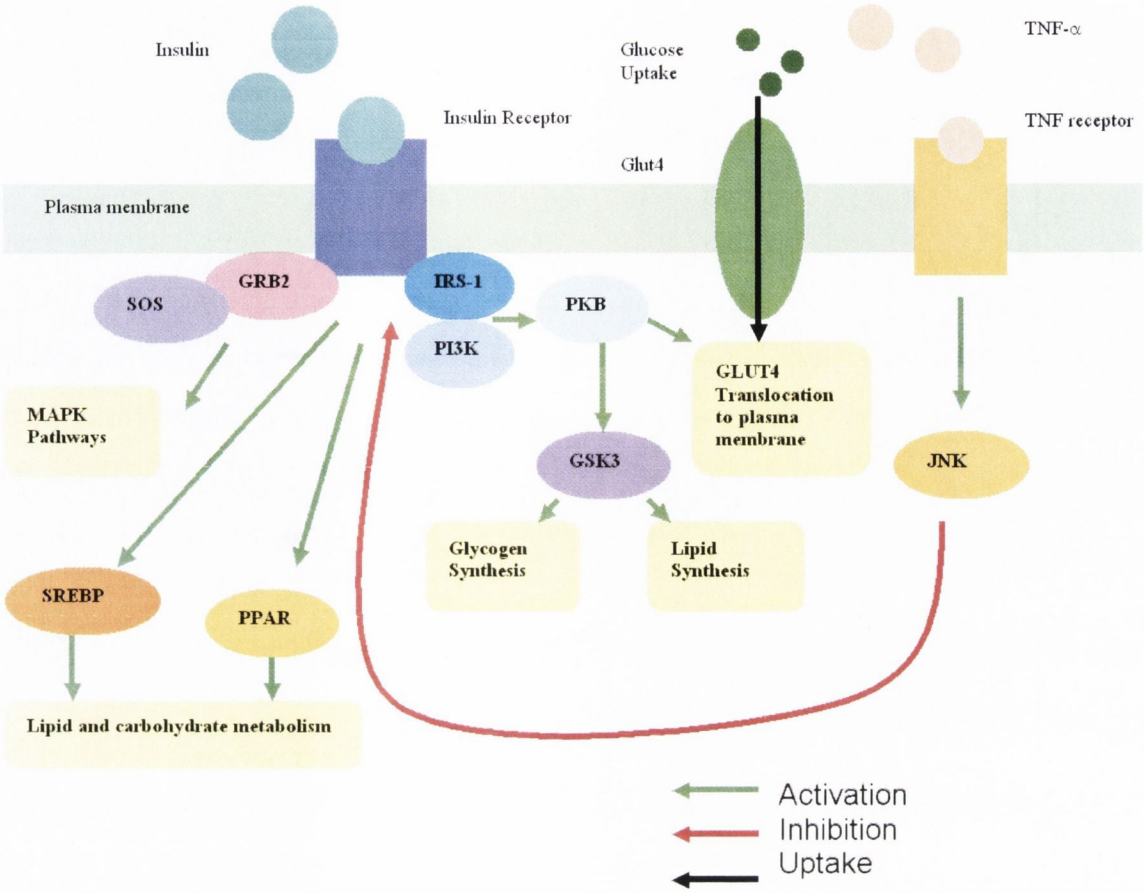

Figure 1.7 Activation of the insulin receptor evokes increased transcription of sterol regulatory element binding proteins (SREBP) and peroxisome proliferator-activated receptors (PPAR). Tyrosine phosphorylation of insulin receptor substrates (IRS)-1 and recruitment of Grb2 on the insulin receptor activate phosphatidylinositol 3-kinase (PI3K) and mitogen-activated protein kinase (MAPK) signalling. Combined these pathways regulate glucose, lipid and protein metabolism.

1.10 Interactions between macrophages and adipocytes

Lumeng *et al* (2007) examined how macrophages and adipocytes interact *in vitro* and whether macrophages can modify insulin responsiveness and glucose metabolism in adipocytes. Macrophage-secreted factors reduced insulin-stimulated glucose uptake in adipocytes via down-regulation of GLUT4 and IRS-1 (Lumeng *et al.*, 2007b). Furthermore, insulin-stimulated GLUT4 plasma membrane translocation was attenuated by macrophage-secreted factors. Treatment of macrophage-conditioned medium with TNF-α blocking antibodies partially reversed this insulin resistant state (Lumeng *et al.*, 2007b). TNF-α induces the expression of a variety of inflammatory cytokines in adipocytes, including IL-6, PAI-1, MCP-1 and TNF-α itself (Uysal *et al.*, 1997). Therefore, the induction of insulin inhibitory effects of TNF-α may not be direct. However, Lumeng *et al* (2007) showed that pro-inflammatory cytokines, such as IL-6, MIP-2 and MCP-1 were

induced in macrophages within a co-culture of adipocytes and macrophages (Lumeng *et al.*, 2007b).

1.10.1 Pro-inflammatory cytokines and adipocyte insulin signalling

TNF-α reduces insulin-stimulated receptor tyrosine kinase activity at low concentrations and can also decrease the expression of the insulin receptor, IRS-1 and GLUT-4 at higher concentrations as well as increase the phosphorylation of serine 307 of IRS-1, thus impairing its ability to bind to the insulin receptor and initiate downstream signaling (Rui *et al.*, 2001). IL-6, like TNF-α, exerted long term inhibitory effects on the gene transcription of IRS-1, GLUT-4 and PPAR-γ in adipocytes (Rotter *et al.*, 2003). This effect of IL-6 was accompanied by a marked reduction in IRS-1 protein expression and reduction in insulin-stimulated IRS-1 tyrosine phosphorylation coincident with impaired insulin stimulated glucose transport (Rotter *et al.*, 2003). Additionally, chronic *in vitro* treatment with IL-1β in 3T3-L1 adipocytes has been shown to decrease insulin induced glucose uptake by reducing the expression of GLUT4 and inhibiting its translocation to the plasma membrane (Jager *et al.*, 2007). This inhibitory effect was due to a decrease in the amount of IRS-1 and a decrease in tyrosine phosphorylation of IRS-1 (Jager *et al.*, 2007).

TNF-α and IL-6 also enhance the expression of suppressors of cytokine signalling (SOCS) molecules 1 and 3 that can attenuate insulin signalling by sterically hindering coupling of insulin receptor with IRS-1 (Ueki *et al.*, 2004b). SOCS proteins can also bind directly to IRS-1 facilitating its ubiquitation and subsequent degradation by the proteasome (Shi *et al.*, 2006a). Interestingly, the addition of the chemokine MCP-1 to differentiated adipocytes *in vitro* decreases insulin-stimulated glucose uptake and the expression of several adipogenic genes including GLUT4 and PPAR-γ. This may suggest that elevated MCP-1 may induce adipocyte dedifferentiation, which would contribute to a reduction in insulin sensitivity (Sartipy and Loskutoff, 2003). Several kinases including JNK (Aguirre *et al.*, 2000), mTOR and ERK (Gual *et al.*, 2003) have been implicated in the serine phosphorylation or deactivation of IRS-1 (Jager *et al.*, 2007). Many of these MAPK including JNK, ERK and p38 are activated by pro-inflammatory cytokines.

Additionally, TNF-α is also a potent inhibitor of adipocyte differentiation and can suppress the expression of some adipocyte-specific genes, such as PPAR-γ, in fully differentiated adipocytes (Xing *et al.*, 1997). Similarly, IL-1 has also been shown to inhibit adipocyte differentiation and induce lipolysis (Feingold *et al.*, 1992; Fried *et al.*, 1993; Gregoire *et al.*, 1992; Price *et al.*, 1986; Suzawa *et al.*, 2003); while a preliminary study

suggests that IL-6 may also increase lipolysis in human fat cells maintained in culture for 48 hours (Rotter *et al.*, 2003).

The transcription factor, NF-κB, plays a major role in inducing a range of inflammatory genes including COX-2, ICAM-1, VCAM-1, E-selectin, TNF-α, IL-1β, IL-6, iNOS, acute-phase proteins and matrix metalloproteinases in response to inflammatory stimuli (Chen *et al.*, 1999; Christman *et al.*, 1998). As discussed previously, NF-κB has an essential role in acute as well as chronic inflammation, which is activated by pro-inflammatory cytokines. Macrophage derived cytokines may therefore induce NF-κB activation within the adipocytes of the adipose tissue, exacerbating the pro-inflammatory environment. It is likely that TNF-α, IL-6 and IL-1β participate in concert with many other cytokines, chemokines and adipokines in the development of obesity induced T2DM.

1.11 Dietary fatty acids

Fatty acids are the basic structural components of TAG and are also found in phospholipids and cholesterol esters (Arab, 2003). TAG undergo hydrolysis to glycerol and non-esterifies fatty acid (NEFA) by lipases as described in section 1.4.3. Fatty acids are simple in structure, with a carboxyl group at one end and a methyl group at the other end of a carbon backbone. This backbone usually ranges between 6 and 24 carbons in length and is generally even-numbered (Arab, 2003). Fatty acids can be divided into three categories based on the presence of double bonds:

- Saturated fatty acids (SFA) have no double bonds and include palmitic acid (PA, 16:0).
- Monosaturated (MUFA) have a single double bond and include oleic acid (OA, 18:1).
- Polyunsaturated fats (PUFA) contain more than one double and include linoleic acid (LA, 18:2 *n-6*).

Many but not all fatty acids can be synthesized, lengthened or desaturated endogenously. Synthesis of fatty acids takes place in the cytosol. Synthesis starts with the carboxylation of acetyl CoA to manonyl CoA by acetyl CoA carboxylase. SFA are then synthesized from acetyl CoA and malonyl CoA via fatty acid synthase (FAS). Elongation by the FAS complex stops upon formation of palmitate (C16:0) (Stryer, 2000).

However, longer fatty acids are formed by elongation reactions catalyzed by enzymes on the cytosolic face of the ER membrane. Two-carbon units are sequentially added to the carboxyl end of both saturated and unsaturated fatty acids. Malonyl CoA is

the two-carbon donor in the elongation of fatty acyl CoA while the reaction is driven by the decarboxylation of malonyl CoA (Stryer, 2000). Fatty acids are also desaturated by enzyme systems in the ER membrane. Desaturation results in the formulation of a double bond. However, mammals lack the enzyme Δ-12-desaturase to introduce double bonds beyond C-9 and therefore require linoleic acid and α-linolenic acid (ALA, 18:3 *n-3*; Figure 1.8) in the diet.

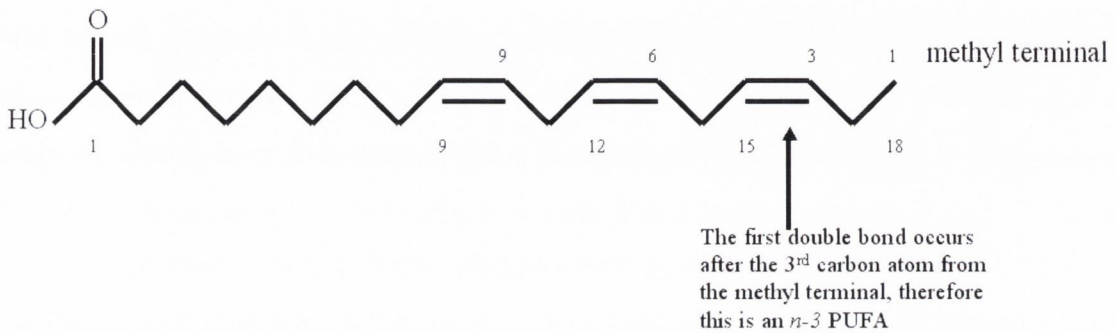

α-Linolenic Acid
9, 12, 15-Gammalinolenic Acid
18:3Δ9, 12, 15
18:3 *n-3*

Figure 1.8 Nomenclature schematic for polyunsaturated fatty acids (PUFA).

The *n-6* and *n-3* long chain (LC) PUFA are either obtained directly from the diet or derived from the metabolism of dietary LA and ALA (Leonard *et al.*, 2000). In animal tissues, Δ-6-desaturase converts LA into γ-linolenic acid (GLA, 19:3 *n-6*), to which an elongase system adds two carbon atoms to synthesize dihomo-γ-linolenic acid (DGLA, 20:3 *n-6*). In the *n-3* pathway, Δ-6-desaturase converts ALA into stearidonic acid (STA, 18:4 *n-3*), to which an elongase system adds two carbons to synthesize eicosatetraenoic acid (ETA, 18:4 *n-3*). A D-5-desaturase converts DGLA and ETA into AA and eicosapentaenoic acid (EPA, 20:5 *n-3*) respectively (Figure 1.8). Further elongation of EPA by two carbons results in the synthesis of docosapentaenoic acid (DPA, C22:5 *n-3*). It has generally been agreed that docosahexaenoic acid (DHA, 22:6 *n-3*) is synthesized through conversion of DPA by a Δ-4-desaturase (Figure 1.8). However, recent studies indicate that DHA can also be produced through an alternative pathway. DHA also has the potential to undergo some reverse metabolism known as retroconversion back to EPA. Overall, formation of *n-6* and *n-3* LC PUFA from their precursors LA and ALA requires at least three elongation steps and three or more different desaturases capable of utilizing LC PUFA as substrates (Leonard *et al.*,

2000). LA and ALA and their LC derivatives are important components of animal and plant cell membranes.

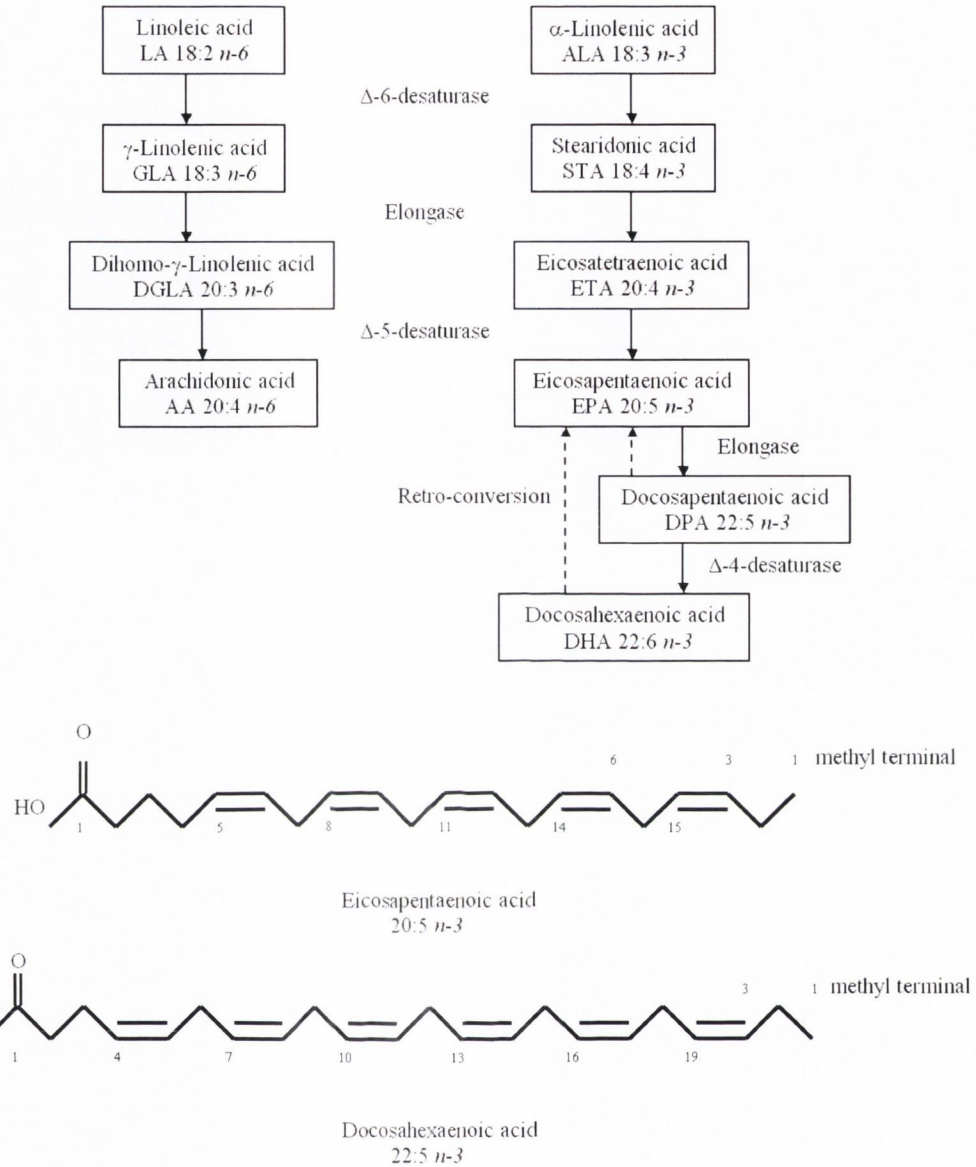

Figure 1.9 The common pathway for the synthesis of arachidonic acid (AA), eicosapentaenoic acid (EPA, 20:5 *n-3*) and docosahexaenoic acid (DHA, 22:5 *n-3*) from linoleic acid (LA, 18:2 *n-6*) and α-linolenic acid (ALA, 18:3 *n-3*) respectively. Retro-conversion is shown with broken arrows. Schematics for EPA and DHA are shown. Adapted from Leonard *et al.* 2000.

1.11.1 Long chain polyunsaturated fatty acids and eicosanoid production

The *n-6* and *n-3* fatty acids are converted into oxygen containing metabolites known as eicosanoids. Arachidonic acid (AA) is the dominant precursor; it is stored in cell membranes and can be mobilized by phospholipids and released in response to injury. Dietary sources rich in preformed AA include eggs and lean meats, such as poultry and fish. Importantly, when humans ingest fish or fish oil, the ingested EPA and DHA partially

replace the *n-6* fatty acids, particularly AA, in the cell membranes. Furthermore, EPA is a competitive substrate for the enzymes and products of AA metabolism. Therefore, the PUFA composition of cell membranes and subsequent eicosanoid metabolism is, to a great extent, dependent on dietary intake.

Eicosanoids include prostaglandins (PGs), thromboxanes (TXs) and leukotrienes (LTs). They are involved in modulating the intensity and duration of inflammatory responses (Calder, 2006). They are fast-acting, high-potency hormones that are produced locally and serve as second messengers. In general, eicosanoids formed from EPA via cyclooxygenase-2 and 5-lipoxygenase are anti-inflammatory, whereas those formed from AA are pro-inflammatory or show other disease-propagating effects (Bagga *et al.*, 2003). For example, prostaglandin-2 (PGE_2) produced by AA induces fever, pain, vasodilation and vascular permeability, while LTB_4 also produced by AA is chemotactic for leucocytes and induces the release of reactive oxygen species by neutrophils and inflammatory cytokines (TNF-α, IL-1β, IL-6) by macrophages (Lewis *et al.*, 1990; Tilley *et al.*, 2001). Furthermore, the eicosanoid metabolic products from AA are formed in larger quantities than those formed from LC *n-3* PUFA. Increased rates of AA metabolism lead to elevated levels of AA derived eicosanoids in both the blood and tissues of patients with a variety of inflammatory disorders (Kinsella *et al.*, 1990; Lewis *et al.*, 1990). The recognition that EPA and DHA have anti-inflammatory properties suggests that increasing their intake corrects the LC *n-6* and *n-3* PUFA balance and so may act to reduce the risk of inflammatory conditions and be of benefit to patients with inflammatory diseases (Calder, 2006; Sijben and Calder, 2007). Interestingly, recent studies have identified E-series resolvins, formed from EPA by a series of reactions involving cyclooxygenase-2 and 5-lipoxygenase. In addition, D-series resolvins and protectin are produced by a similar series of reactions involving DHA (Serhan *et al.*, 2008). These mediators appear to enable inflamed tissue to return to a state of homeostasis and have been shown to exert potent anti-inflammatory actions in many inflammatory cell types including neutrophils, macrophages, dendritic cells and T cells (Serhan *et al.*, 2008). However, their role is somewhat speculative particularly as their relevance *in vivo* remains to be fully established.

Additionally, Isoprostanes (iPs) are a class of natural products generated by the action of free radicals on PUFA (Morrow *et al.*, 1990; Pratico *et al.*, 1998). They are isomers of enzymatically formed prostaglandins, leukotrienes and epoxyeicosatrienoic acids (Lawson *et al.*, 1999; Morrow and Roberts, 1996). Unlike the enzymatic products of PUFA, they are formed initially *in situ* in the phospholipid domain of cell membranes, from which they are cleaved by phospholipases (Morrow *et al.*, 1992), circulated in

esterified and unesterified forms, and are excreted in urine. Although, iPs can be formed from many PUFA, research to date has focused almost exclusively on F2-iPs derived from AA. Several prostaglandin isomers isoprostanes (iPs) express biological activities *in vitro* (Elmhurst *et al.*, 1997; Takahashi *et al.*, 1992) and may act as incidental ligands at membrane receptors for prostanoids and at peroxisome proliferator-activated receptors (PPAR) in the nucleus (Kunapuli *et al.*, 1998; Pratico *et al.*, 1996). It is therefore important to be able to assess the extent of peroxidation of PUFA such as EPA and DHA.

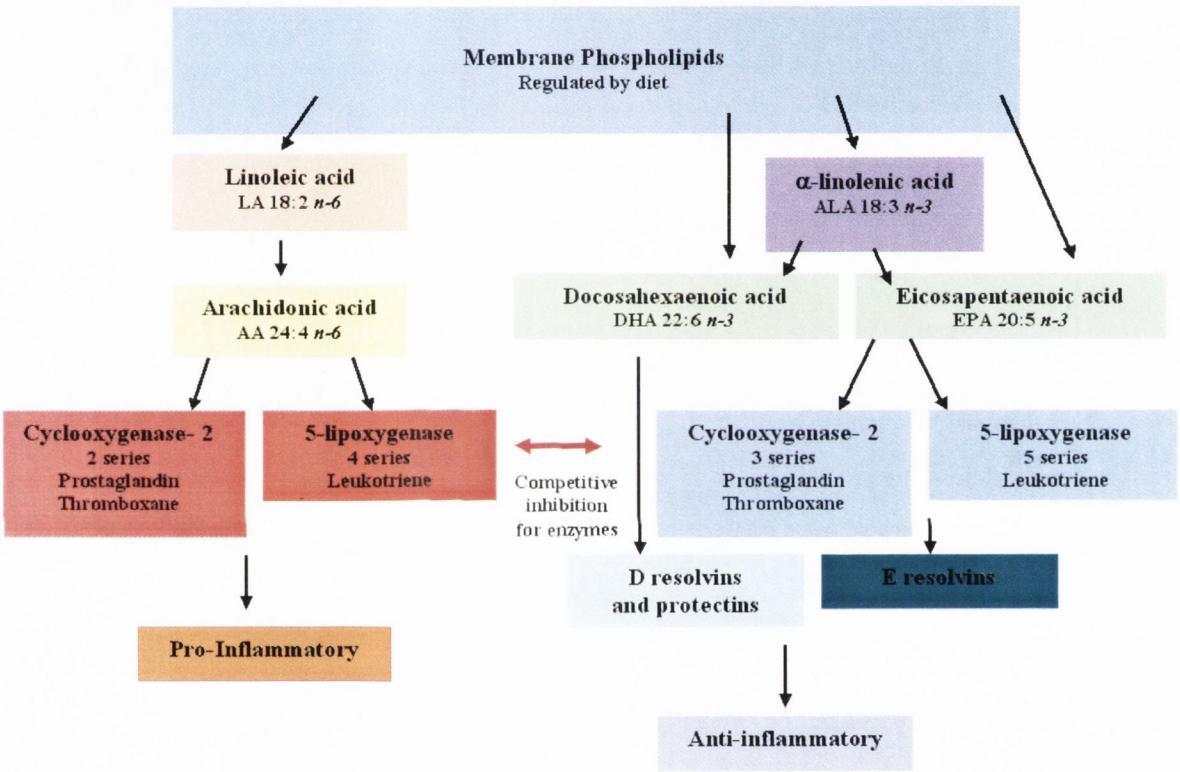

Figure 1.10 Mechanism of LC *n-3* PUFA anti-inflammatory action. Eicosapentaenoic acid (EPA) and docosahexaenoic acid (DHA) decrease the amounts of arachidonic acid (AA) available as a substrate for eicosanoid synthesis and inhibit their metabolism. EPA and DHA are also precursors to potent new families of mediators termed resolvins and protectins.

1.11.2 Membrane lipid composition and its impacts on cell signalling

Mammalian cell membranes consist of a lipid bilayer composed primarily of phospholipids and cholesterol. The cellular membrane is formed by polar lipids, which consist of a hydrophobic and a hydrophilic portion. The propensity of the hydrophobic moieties to self associate and the tendency of the hydrophilic moieties to interact with aqueous environments and with each other, is the physical basis of the spontaneous formation of membranes. This fundamental principle of amphipathic lipids is a chemical property that

enabled the first cells to segregate their internal constituents from the external environment (van Meer *et al.*, 2008). This same principle is recapitulated within the cell to produce discrete organelles (van Meer *et al.*, 2008). The major structural lipids in eukaryotic membranes are glycerophospholipids. Their hydrophobic portion is a diacylglycerol (DAG), which contains saturated or *cis*-unsaturated fatty acyl chains of varying lengths (van Meer *et al.*, 2008). The sphingolipids constitute another class of structural lipids, the hydrophobic backbone of which is ceramide (van Meer and Lisman, 2002).

Cell signalling induced hydrolysis of glycerolipids and sphingolipids produces a variety of lipid messengers. Some lipid messengers carry only one aliphatic chain and readily leave membranes; they signal through related membrane receptors (Meyer zu Heringdorf and Jakobs, 2007). In contrast, lipid messengers such as DAG and ceramide remain in the membrane and can recruit cytosolic proteins (Fernandis and Wenk, 2007). Lipid mediators are considered important in a wide range of processes involving cell-cell communication including host defense, inflammation, ischemia reperfusion, hemostasis and other vascular events. The activation of specific phospholipases is a critical early step in the biosynthesis of several structurally diverse lipid messengers. These phospholipases (PL) include PLA_2, PLD, PLC, and sphingomyelinase (Serhan *et al.*, 1996). Activation of these enzymes can be accomplished by either specific cell-surface receptors or by membrane perturbations such as in trauma or reperfusion injury. The lipid mediators produced include free fatty acids and their oxygenated products (e.g., eicosanoids), lysophospholipids, platelet activating factor (PAF), DAG, phosphatidic acid (PtdOH) and ceramide. These individual classes, some of which have extensive molecular diversity, are each implicated as essential mediators in a variety of tissue and cell functions (Serhan *et al.*, 1996).

Importantly, cytokines influence the production and actions of lipid messengers at several broad levels. They can 1) stimulate *de novo* biosynthesis of lipid messengers, 2) induce the enzymes that regulate lipid messenger biosynthesis and 3) act synergistically with a given lipid messenger to exert bioactions (Serhan *et al.*, 1996). Although less well documented, individual or groups of certain lipid messengers can likewise display a similar multilevel effect in the biosynthesis and actions of cytokines (Serhan *et al.*, 1996). For example several agonists induce sphingomyelin breakdown including TNF-α, IL-1 and interferon (INF)-γ. Functional consequences of sphingomyelin degradation include growth arrest, cell differentiation, apoptosis, decreased protein secretion, prostaglandin endoperoxide H synthase (PGHS)-II gene expression and production of prostaglandin (PG)

(Ballou *et al.*, 1996). Furthermore, ceramide is also implicated in mediating the actions of IL-1β, such as increased expression of IL-6 (Ballou *et al.*, 1996; Hannun and Obeid, 1995).

However, it is also expected that alteration in membrane lipid composition may lead to changes in lipid messenger production. Interestingly, Marignani and Sebaldt (1995) demonstrated that dietary enrichment with LC *n-3* PUFA induces marked changes in DAG metabolism in murine peritoneal macrophages. Within this study C57BL/6 mice were randomly assigned to either a corn oil (control diet) or LC *n-3* PUFA enriched diet. After four weeks macrophages were harvested and assayed for DAG. They observed that diet-induced LC *n-3* PUFA enrichment of membrane phospholipids resulted in decreased DAG formation. These changes may have significant implications for the normal second messenger function of DAG, namely the activation of PKC early in the receptor-mediated signal transduction cascade of many important intercellular agonists (Marignani and Sebaldt, 1995). Concurrent with this, Schley *et al.* (2007) determined that an EPA and DHA treatment in MDA-MB-231 human breast cancer cells decreased lipid raft sphingomyelin, cholesterol and DAG content and, in the absence of linoleic acid (LA), EPA and DHA increased raft ceramide levels (Schley *et al.*, 2007). It therefore seems likely that changes in lipid mediator formation may contribute to the anti-inflammatory mechanisms associated with dietary LC *n-3* PUFA supplementation.

Additionally, proteins that have important cellular functions, such as receptors, transporters, and enzymes are embedded in the lipid bilayer (Spector and Yorek, 1985). Consequently, modifications within the membrane lipid composition can affect many cellular functions and responses through regulation of the membrane proteins. Interestingly, an increase in the unsaturated fatty acid content of the membrane phospholipids affects the binding properties of the insulin receptor in Friend erythroleukemia and Ehrlich ascites cells (Ginsberg *et al.*, 1981; Ginsberg *et al.*, 1982). In both cases the cells enriched in unsaturated fatty acids contained an increased number of insulin receptors and exhibited a decrease in receptor binding affinity. The receptor number more than doubled when the cells were enriched with linoleic acid (18:2) (Spector and Yorek, 1985). In accord with this, insulin sensitizers such as bezafibrate (Matsui *et al.*, 1997) are known to increase the unsaturation of membrane lipids, and part of their beneficial action may be a membrane lipid mediated effect on the insulin receptor (Hulbert *et al.*, 2005). The activity and properties of a number of membrane bound enzymes has also been examined following lipid modifications in cultured cells. For example the activity of adenylate cyclase, a membrane bound enzyme that synthesizes the secondary messenger cAMP, is affected by changes in the composition of the phospholipid fatty acyl

chains and polar head groups. Its activity is also affected by changes in the cholesterol content of the plasma membrane.

The effects of lipid modification on cellular function are very complex. It is therefore not yet possible to make any generalizations or to predict how a given system will respond to a particular type of lipid modification. Many of the functional responses are probably caused directly by the membrane lipid structural changes, which affect either lipid fluidity or specific lipid domains. The conformation or quaternary structures of certain transporters, receptors and enzymes are most likely sensitive to changes in the structure of their lipid microenvironment, leading to changes in activity (Spector and Yorek, 1985). Changes in lipid membrane composition such as enrichment of LC *n-3* PUFA may have the potential to significantly alter second lipid messenger production and therefore alter intracellular signal transduction. These effects combined may therefore account, at least in part, for some of the less well understood actions of LC *n-3* PUFA.

1.11.3 Long chain polyunsaturated fatty acids and gene expression

The composition of LC *n-6* and *n-3* PUFA also affects gene expression and intercellular cell-to-cell communication. The balance of *n-3* and *n-6* PUFA is important for homeostasis and normal development within cells. PUFA rapidly modulate gene expression in different systems, by regulating transcription factors such as PPAR, liver X receptors (LXRs) and SREBP-1c (Jump, 2002; Schmitz and Ecker, 2008). These nuclear receptors play crucial roles in the regulation of the fatty acid metabolism. PUFA are potent PPAR activators, leading to the increased expression of genes responsible for fatty acid β-oxidation, such as acyl-CoA oxidase, fatty acyl-CoA synthetase and hydroxymethylglutaryl-CoA synthase (Benatti *et al.*, 2004; Jump and Clarke, 1999). Activators of PPAR have been shown to inhibit the activation of inflammatory genes, including TNF-α, IL-1β, IL-6, IL-8, cyclooxygenase (COX)-2, VCAM-1, iNOS, matrix metalloproteinases and acute-phase proteins (Jackson *et al.*, 1999; Jiang *et al.*, 1998; Marx *et al.*, 1999; Poynter and Daynes, 1998; Ricote *et al.*, 1998b; Takano *et al.*, 2000; Wang *et al.*, 2001; Xu *et al.*, 2001). Two mechanisms for the anti-inflammatory actions of PPAR have been proposed (Chinetti *et al.*, 2000; Delerive *et al.*, 2001). The first mechanism is that PPAR might stimulate the breakdown of inflammatory eicosanoids through induction of peroxisomal β-oxidation. The second mechanism is that PPAR might interfere with or antagonise the activation of other transcription factors, including NF-κB.

LC *n-3* PUFA can also down regulate the activity of NF-κB directly, which may provide an explanation of how LC *n-3* PUFA reduces inflammatory cytokine production

(Xu *et al.*, 2001). Xu *et al* reported that feeding mice fish oil resulted in a lower level of NF-κB in the nucleus of LPS stimulated spleen lymphocytes compared with feeding maize oil. Our group showed that in cell culture, pre-treatment of EPA and DHA significantly decreased LPS stimulated THP-1 macrophage TNF-α, IL-1β and IL-6 production compared to control cells (Weldon *et al.*, 2007). Furthermore, EPA and DHA down-regulated LPS-induced NF-κB/DNA binding in THP-1 macrophages by approximately 13%. DHA significantly decreased macrophage nuclear p65 expression and increased cytoplasmic IκB-α expression. This capacity for LC *n-3* PUFA to reduce pro-inflammatory cytokine production from inflammatory cells, such as macrophages, may have important potential to reduce the inflammation induced by the ATM in obesity, improving insulin resistance. Furthermore, we hypothesise that IL-1 has a strong involvment in ATM infiltration through its induction of chemokines. Therefore, a reduction in IL-1 expression caused by LC *n-3* PUFA incorportion into the membrane as discussed above could potentially reduce ATM accumulation during obesity.

1.11.4 The anti-inflammatory effects of LC *n-3* PUFA

Many human LC *n-3* PUFA intervention studies have shown anti-inflammatory effects in patients with chronic inflammatory conditions such as rheumatoid arthritis (Geusens *et al.*, 1994), asthma (Broughton *et al.*, 1997), Crohn's disease (Belluzzi *et al.*, 1996) and psoriasis (Mayser *et al.*, 1998); LC *n-3* PUFA have been shown to alleviate symptoms of each disease. The evidence for the beneficial effects of LC *n-3* PUFA within clinical trials is often conflicting and this may be due to factors such as the medical condition under analysis, the size of the study, the specific cytokines examined within the study, the study endpoints and the LC *n-3* PUFA dose. Many of these concepts are reviewed by Sijben and Calder (Sijben and Calder, 2007). On the basis of estimates from studies on Paleolithic nutrition and modern-day hunter-gatherer populations, it appears that humans have evolved while consuming a diet that was much lower in saturated fatty acids than the current Western diet (Eaton and Konner, 1985). Furthermore, the Paleolithic diet contained small and roughly equal amounts of *n-6* and *n-3* PUFA and much lower amounts of *trans* fatty acids compared to the current Western (Eaton and Konner, 1985; Simopoulos *et al.*, 1995). The current Western diet is very high in *n-6* fatty acids and this is thought to have detrimental health consequences.

1.11.5 Fatty acids and adipose tissue macrophages infiltration

Todoric *et al* (2006) demonstrated that many genes involved in inflammatory alterations were up-regulated in *db/db* mice fed a HFD rich in SFAs and MUFAs (HFD/S) compared with a low fat diet (LFD) (Todoric *et al.*, 2006). Adipose tissue infiltration with macrophages was markedly enhanced by HFD/S. Interestingly, inclusion of LC *n-3* PUFA in the diet (HFD/*n-3*) completely prevented macrophage infiltration induced by a HFD and altered inflammatory gene expression while reducing JNK phosphorylation in diabetic mice despite unreduced body weight. Furthermore, the HFD/S and HFD with LC *n-6* PUFA down-regulated expression and reduced serum concentrations of adiponectin, however this was not the case with LC *n-3* PUFA (Todoric *et al.*, 2006). These data suggest that beneficial effects of LC *n-3* PUFA on diabetes development could be mediated by their affect on ATM infiltration and subsequent inflammation. TLR4 may be an important regulator of this effect as observed by Todoric and colleagues as it has been shown to be a receptor for saturated fatty acids (SFA) and can mediate inflammatory cytokine production in macrophages exposed to PUFA (Lee *et al.*, 2001; Shi *et al.*, 2006b). LC *n-3* PUFA protect against SFA TLR4 induced inflammatory cytokine production (Lee *et al.*, 2003). Shi and colleagues (2006) showed female C57BL/6 mice lacking TLR4 have increased obesity but are partially protected against HFD induced insulin resistance (Shi *et al.*, 2006b). However, with a macrophage specific TLR4 knockout MθTLR4$^{-/-}$ there were no differences in macrophage accumulation in WAT or insulin sensitivity between MθTLR4$^{+/+}$ and MθTLR4$^{-/-}$ mice fed a HFD (Coenen *et al.*, 2009).

1.11.6 Insulin sensitising LC *n-3* PUFA

Epidemiologic studies have reported a low prevalence of impaired glucose tolerance and T2DM in populations consuming large amounts of LC *n-3* PUFA such as the Greenland Inuit and Alaskan natives (Adler *et al.*, 1994; Kromann and Green, 1980; Schraer *et al.*, 1999). However, much of the clinical evidence for the positive effects of LC *n-3* PUFA on insulin sensitivity are conflicting and as discussed previously this could be due to variable factors within study design, such as study endpoints and LC *n-3* PUFA dose or dietary advice given. Interestingly, Hu and colleagues (2003) examined prospectively the association between intake of fish and LC *n-3* PUFA on risk of CVD and total mortality among 5,103 female nurses with diagnosed T2DM (Hu *et al.*, 2003). Between 1980 and 1996, they documented 362 incident cases of CVD. Those who consumed fish at least one to three times a month had a 40% lower risk of developing CVD compared to women with

T2DM who ate fish less than once a month. Those who ate fish five or more times a week experienced a 64% reduction in CVD compared to those who ate fish less than once a month (Hu *et al.*, 2003). In contrast, a population study monitoring 36,000 non-diabetic Iowa women (between 55-69 years of age) over 11 years showed development of T2DM was positively associated with LC *n-3* PUFA (Meyer *et al.*, 2001). However, after adjustment for other dietary fat, only vegetable fat was related to T2DM risk and appeared protective. LC *n-3* PUFA have been shown to lower triacylglycerol (TAG) levels in subjects with T2DM or hypertriglyceridemia. Kesavulu and colleagues (2002) reported that supplementation of 1.8 g/day LC *n-3* PUFA for 2 months in 34 T2DM patients being treated with anti-diabetic drugs significantly reduced TAG levels however, supplementation increased HDL cholesterol levels (Kesavulu *et al.*, 2002).

Certain animal studies seem to suggest that LC *n-3* PUFA may affect muscle, liver and WAT differentially within the insulin resistant environment and this may reflect some of the inconsistent data observed. However, there is also some conflict of the positive effects of LC *n-3* PUFA in animal models of insulin resistance. Storlien and colleagues (1991) demonstrated that the substitution of fish oil for saturated or monounsaturated or LC *n-6* PUFA HFD (60% fat) in rats over 3 weeks completely prevented liver and muscle insulin resistance induced by the diets (Storlien *et al.*, 1991). Taouis *et al* (2002) showed that a HFD containing LC *n-3* or LC *n-6* PUFA given to Wistar rats induced hyperglycemia and hyperinsulinemia, signs of insulin resistance. A HFD enriched with LC *n-3* PUFA maintained GLUT4 content, insulin receptor, IRS-1 tyrosine phosphorylation and PI3-kinase activity in muscle, however not in the liver (Taouis *et al.*, 2002). A HFD enriched in LC *n-3* PUFA showed no change in GLUT4 and leptin mRNA within adipose tissue whereas GLUT4 and leptin mRNA expression was decreased in rats on a HFD enriched in LC *n-6* PUFA (Taouis *et al.*, 2002). Arguilera and colleagues (2004) induced a model of the metabolic syndrome in rats which showed increased body weights, systolic blood pressure, serum insulin, total lipids, triacylglcerol, cholesterol, non esterified fatty acids (NEFA), LDL, total proteins, albumin and serum TNF-α (Aguilera *et al.*, 2004). After fish oil administration, metabolic syndrome rats had significantly reduced blood pressure, serum insulin, TAG, cholesterol and NEFA (Aguilera *et al.*, 2004). However, there was no change in TNF-α concentration or fat accumulation, which seems counterintuitive. The exact composition of the HFD and the amount of LC *n-3* PUFA, specifically EPA and DHA, within the diet as well as the ratio of LC *n-6* to LC *n-3* PUFA may be a relevant factor in some of the conflicting information observed in these studies.

1.12 Project Rationale

Obesity produces a state of chronic, low-grade inflammation with increased infiltration of macrophages into the adipose tissue. These ATM have been shown both *in vivo* and *in vitro* to produce pro-inflammatory cytokines such as TNF-α, IL-6, IL-1β and MCP-1. These cytokines and chemokines most likely induce and enhance the activation of the MAPK (ERK, p38 and JNK) and transcription factors such as NF-κB in both the macrophages and adipocytes of the WAT. This inflammation causes down-regulation and decreased activation of insulin signaling proteins (GLUT4 and IRS-1), therefore blocking insulin action within the adipocytes and inducing a state of insulin resistance.

Interestingly, IL-1 signalling induces the production of many adhesion molecules and chemokines. IL-1 is also produced primarily by monocytes and macrophages (Dinarello, 2009; Martin and Wesche, 2002). These properties are thought to promote the infiltration of inflammatory and immunocompetent cells, from the circulation into WAT, leading to chronic IL-1-induced inflammation (Dinarello, 2009). IL-1 signalling may therefore pay a key role in the infiltration of ATM during obesity, leading to inflammation and insulin resistance.

LC *n-3* PUFA have been shown to influence gene expression (PPAR-γ and NF-κB) and eicosanoid production, reducing pro-inflammatory cytokine production from many different cell types, including macrophages. LC *n-3* PUFA may therefore offer a useful anti-inflammatory strategy to decrease obesity induced insulin resistance. However, the exact mechanisms between macrophages and adipocytes, both *in vivo* and *in vitro*, in addition to the effects of LC *n-3* PUFA on both cell types singularly and in combination, needs to be explored.

1.12.1 Project Hypothesis

We hypothesise that as macrophages infiltrate into the adipose tissue during obesity they secret pro-inflammatory molecules, which induce a pro-inflammatory state within adipocytes. We propose that this hightened state of inflammation inhibits insulin signalling in adipocytes leading to a state of insulin resistance. We further hypothesise that the IL-1RI$^{-/-}$ mice will have reduced ATM accumulation and will remain more insulin sensitive. Finally, we hypothesis that the incorporation of anti-inflmmatory LC *n-3* PUFA into the plasma membrane of the macrophages can attenuate the pro-inflmmatory state induced by the macrophages and improve insulin sensitivity within adipocytes.

1.12.2 Project Aims

Chapter 3: The Effects of High Fat Diet Induced Obesity on Molecular Mechanisms Associated with Insulin Resistance *In Vivo* within IL-1 Receptor I Knockout Mice

General aim:

- To establish an *in vivo* time-course experiment to study the molecular mechanism involved in the development of obesity-induced insulin resistance within immune compromised IL-1 type 1 receptor knock out mice (IL-1RI$^{-/-}$).

Specific aims:

1. To establish if lack of IL-1 signalling can protect against diet induced insulin resistance.
2. To determine if IL-1RI$^{-/-}$ mice have improved insulin sensitivity and a reduced pro-inflammatory state in the EAT throughout the 16 week HFD.

Chapter 4: The Effects of IL-1β Treatment on Inflammatory and Insulin Signalling *In Vitro* within 3T3-L1 Adipocytes

General aim:

- To determine the effects of IL-1β treatment on inflammatory and insulin signalling *in vitro* within 3T3-L1 adipocytes in order to verify the findings of the *in vivo* time-course experiment.

Specific aims:

1. To ascertain if an IL-1β treatment can induce inflammation and cellular stress in adipocytes.
2. To elucidate if insulin sensitivity is reduced in IL-1β treated adipocytes.

Chapter 5: The Effects of EPA and DHA Treatment on Inflammatory and Insulin Signalling *In Vitro* within 3T3-L1 Adipocytes and J774.2 Macrophages

General aims:

- To examine the effects of chronic EPA and DHA treatment on inflammatory and insulin signalling *in vitro* within 3T3-L1 adipocytes and J774.2 macrophages.
- To examine whether acute LC *n-3* PUFA pre-treatment of the J774.2 macrophages can attenuate the pro-inflammatory phenotype and improve insulin action within the 3T3-L1 adipocytes of the co-culture system.

Specific aims:

1. To define if chronic EPA and DHA treatment can improve insulin sensitivity in unstimulated 3T3-L1 adipocytes.
2. To establish if long term chronic EPA and DHA treatment has any potential pro-inflammatory or anti-inflammatory effects on unstimulated 3T3-L1 adipocytes.
3. To define the effects of chronic EPA and DHA treatment during differentiation, on insulin sensitivity and cell morphology.
4. To ascertain if chronic EPA and DHA treatment can reduce inflammation and cellular stress in LPS stimulated macrophages.
5. To elucidate if unstimulated or LPS stimulated macrophages can reduce insulin sensitivity and induce inflammation in adipocytes of a co-culture system.
6. To define if macrophages exert their effects on adipocytes via cellular contact or via secreted soluble molecules.
7. To define the anti-inflammatory and insuin sensitising effects elicited by an acute 24 hour EPA and DHA treament of the macrophages prior to co-culture with the adipocytes.

Chapter 6: The Effects of LPS Stimulated Macrophages Pre-treated with EPA and DHA on Inflammatory and Insulin Signalling within 3T3-L1 Adipocytes of a Co-culture System

General aims:

- To investigate the molecular mechanisms that mediate the interaction between J774.2 macrophages and 3T3-L1 adipocytes using an *in vitro* co-culture system.

- To examine whether chronic LC *n-3* PUFA pre-treatment of the J774.2 macrophages can attenuate the pro-inflammatory phenotype and improve insulin action within the 3T3-L1 adipocytes of the co-culture system.

Specific aims:

1. To verify the incorporation of LC *n-3* PUFA into the macrophages chronically pre-treated with EPA and DHA.
2. To confirm that the EPA and DHA is not present within the adipocytes of the co-culture and to assess any changes in their fatty acid composition.
3. To ascertain if chronic EPA and DHA treatment of the LPS stimulated macrophages can reduce inflammation in the co-culture system.
4. To discover if chronic EPA and DHA treatment of the LPS stimulated macrophages can reduce inflammation and cellular stress while up-regulating insulin signaling within the adipocytes co-cultured with the LPS stimulated macrophages.
5. To establish if chronic EPA and DHA treatment of the LPS stimulated macrophages can increase insulin induced glucose uptake within the adipocytes co-cultured with the LPS stimulated macrophages.
6. To elucidate if LPS stimulated macrophages can induce dedifferentiation and lipolysis within adipocyte of a co-culture system and to define if chronic EPA and DHA treatment of the LPS stimulated macrophages can attenuate these effects.

Chapter 2

Material and Methods

2.1 Animal study

2.1.1 Animals and diets

The targeting strategy for IL-1RI gene disruption has been previously described in detail (Glaccum *et al.*, 1997). IL-1RI$^{-/-}$ (C57BL/6 background sourced from Jackson Laboratories, ME, USA) and C57BL/6 wild type (WT) control (purchased from Harlan Laboratories, IN, USA) 6 week old male mice were held at the BioResources Unit of Trinity College Dublin under specific pathogen-free conditions. Ethical approval was obtained from the Trinity College Dublin Ethics Committee and the mice were maintained according to the regulations of the European Union and the Irish Department of Health, who govern the use of animals in research. IL-1RI$^{-/-}$ and C57BL/6 control mice were each fed a high-fat diet (HFD, 45% Kcal from fat; Research Diets Inc, NJ, USA; Table 2.1) for up to 16 weeks. Body weights were recorded every 2 weeks. Food intake was recorded as the difference between the weight of the food remaining in the food bin and the amount of pre-weighed food added every two weeks.

Table 2.1 The composition of the standard chow and high fat diets.

Diet	Chow		High Fat	
%	**g**	**kcal**	**g**	**kcal**
Protein	19.2	20	23.7	20
Carbohydrate	67.3	70	41.4	35.1
Fat	4.3	10	23.6	44.9
Total	90.8	100	88.7	100
kcal/gram	3.85		4.73	
Ingredient	**g**	**kcal**	**g**	**kcal**
Casein, 80 mesh	200	800	200	800
L-cystine	3	12	3	12
Corn starch	315	1260	72.8	291.2
Maltodextrin 10	35	140	100	400
Sucrose	350	1400	172.8	691.2
Cellulose, BW200	50	0	50	0
Soybean oil	25	225	25	225
Lard	20	180	-	-
Palm oil	-	-	177.5	1597.5
Mineral mix S10026	10	0	10	0
DiCalcium phosphate	13	0	13	0
Calcium carbonate	5.5	0	5.5	0
Potassium citrate, 1 H20	16.5	0	16.5	0
Vitamin mix V10001	10	40	10	40
Choline bitartrate	2	0	2	0
Total	1055	4057	858.1	4057

2.1.2 Glucose tolerance test

Glucose tolerance tests (GTT) were performed on C57BL/6 control mice and IL-1RI$^{-/-}$ mice at weeks 0, 4, 6, 12 and 16 of the HFD. Mice were fasted for 6 hours prior to the GTT. A 25% w/v glucose load (Sigma-Aldrich, Dorset, UK; 1.2 g/kg body weight) was administered with an intraperitoneal (IP) injection. Blood was sampled by tail bleed at time points 0, 15, 30, 60, 90 and 120 minutes after the glucose IP injection. Glucose was measured in mMol/L immediately with a glucose meter from Accu-Chek (Roche Ltd, Dublin, Ireland). Blood was collected in ethylenediaminetetraacetic acid (EDTA) coated capillary tube and spun at 15,000 rpm for 5 minutes; insulin levels were measured at time points 0, 30 and 60 minutes using a commercially available ELISA kit purchased from Mercodia (Uppsala, Sweden).

2.1.3 Tissue and plasma collection

Animals were fasted for 4 hours and culled by CO_2 inhalation at weeks 0, 6, 8, 12 and 16 of the HFD. Epididymal adipose tissue (EAT), visceral adipose tissue (VAT) from white adipose tissue (WAT), brown adipose tissue (BAT), skeletal muscle from the hind leg,

liver, kidney and pancreas samples were harvested. All tissue aliquots (~100 mg) for RNA and protein analysis were immediately snap frozen in liquid nitrogen and transferred to a freezer for storage at -80°C. A proportion of the EAT was prepared for adipocyte isolation and a second portion was placed in 10% neutral buffered formalin for histology. A fasting blood sample was taken from the heart using a needle and syringe. The syringe was coated with a layer of EDTA to prevent the blood from clotting. The blood was transferred into an eppendorf and centrifuged at 15,000 rpm for 5 minutes. The plasma was extracted, aliquoted and frozen at -80°C. Plasma adipokine and cytokine profiles were determined using a Milliplex multi-analyte profiling (Millipore, MA, USA). Plasma triacylglycerol (TAG) and non-esterified fatty acids (NEFA) were measured using commercially available enzyme assay kits (Randox, Co Antrim, Northern Ireland).

2.1.4 Adipocyte isolation

A portion of the fresh adipose tissue was sliced into small sections and transferred into 37°C 155 mMol/L NaCl (Sigma-Aldrich) in distilled water. NaCl was then removed using a needle and syringe and the adipose was incubated with collagenase buffer for 70 minutes in a shaking water bath at 37°C. The collagenase buffer consisted of Krebs Ringer bicarbonate buffer with 4% bovine serum albumin (BSA) and 2 mg/ml collagenase type II (Sigma-Aldrich). Krebs Ringer bicarbonate buffer consists of 118 mMol/L NaCl, 24.8 mMol/L $NaHCO_3$ (Sigma-Aldrich), 1.2 mMol/L KH_2PO_4 (Sigma-Aldrich), 4.8 mMol/L KCl (Sigma-Aldrich), 1.25 mMol/L $CaCl_2$ (Sigma-Aldrich), 1.2 mMol/L $MgSO_4$ (Sigma-Aldrich) and 10 mMol 4-(2-hydroxyethyl)-1-piperazineethanesulfonic acid (HEPES, Sigma-Aldrich) at pH 7.35 - 7.45. Collagenases are enzymes that break the peptide bonds in collagen; type II collagenase is suitable for the digestion and release of adipocytes (Fain, 1975; Rodbell, 1964). The adipose tissue was then flushed through a polypropylene filter (500 μm, Schleicher & Schuell MicroScience, Dassel, Germany) to separate the cells. The cells were then spun at 1,000 rpm for 5 minutes to separate the mature adipocytes from the stromal vascular fraction (SVF). The mature adipocytes float due to their high lipid content and therefore could be collected from the surface of the buffer. The adipocytes were washed with Krebs Ringer phosphate buffer (pH 7.4) with 1% BSA and spun at 1,000 rpm for 2 minutes. Adipocytes were collected and frozen in liquid nitrogen prior to storage at –80°C.

2.1.5 Determination of multiple cytokines using multi-analyte profiling

Multi-analyte profiling (MAP) allows simultaneous detection of multiple analytes within a small sample size. Adiponectin, granulocyte macrophage colony-stimulating factor (GM-CSF), interferon (IFN)-γ, interleukin (IL)-10, IL-12(p70), IL-13, IL-1β, IL-2, IL-4, IL-5, IL-6, IL-9, Insulin, keratinocyte-derived chemokine (KC), Leptin, monocyte chemotactic protein (MCP)-1, macrophage inflammatory protein (MIP)-1α, regulated upon activation, normal T cell expressed and secreted (RANTES) also known as chemokine (C-C motif) ligand (CCL)5, resistin and tumour necrosis factor (TNF)-α concentrations were determined in pg/ml. Plasma aliquots were prepared and shipped to Milipore for analysis (Millipore UK Ltd, Dundee, UK).

The Miliplex plate consists of wells containing polystyrene 5.6 μM microspheres. The microspheres are dyed with red and infra-red fluorophores in different ratios. Each ratio is used to uniquely identify each microsphere set. Each microsphere (or bead) set is coated with capture antibody specific to an antigen. A mixture of microspheres for specific antigens (capture bead stock) can be assessed within one analysis using 50 μl of plasma sample. The assay was performed in a 96-well filter plate. 25 μl of 1X capture bead stock was added to each well and washed twice in 200 ml 1X wash solution. Standards were reconstituted to working concentrations by serial 1:3 dilutions in assay diluent. 50 μl incubation buffer was added to each well followed by 100 μl standard into designated wells. 50 μl assay diluent followed by 50 μl samples was added to designated wells. The plate was covered and incubated for 2 hours at room temperature on an orbital plate shaker (500 - 600 rpm). During the incubation, the antigens from the plasma and standards became immobilized by the capture antibody on to the beads. The wells were washed twice and 100 μl of 1X biotinylated detection antibody was added to each well. The plate was covered and incubated for 1 hour on the plate shaker. The biotinylated detection antibody bound to the immobilised antigen. The wells were washed twice and 100 μl of 1X streptavidin-phycoerythrin (S-PE) was added to each well. The plate was covered and incubated for 30 minutes on the plate shaker. Finally, S-PE bound to the immobilized detection antibody completing the complex (Figure 2.1). The wells were washed three times with 200 μl working wash solution and then 100 μl working wash solution was added to each well and placed on the plate shaker for three minutes. The samples were subsequently analysed using the Luminex® 200™ analyzer (Luminex Corporation, TX, USA) and the data was assessed with xPonent Software (Luminex Corporation, TX, USA). The Luminex® 200™ analyzer is a dual laser, flow-based sorting and detection platform.

The beads are passed individually through a detection chamber; a 635 nm red laser excites the internal red/infra-red dyes and classifies the microsphere allowing identification of the antigen, while a 532 nm green laser excites the orange fluorophore of S-PE allowing quantification of the antigen. A standard curve was generated for each cytokine and chemokine and sample concentrations were calculated through the equation of the standard curve.

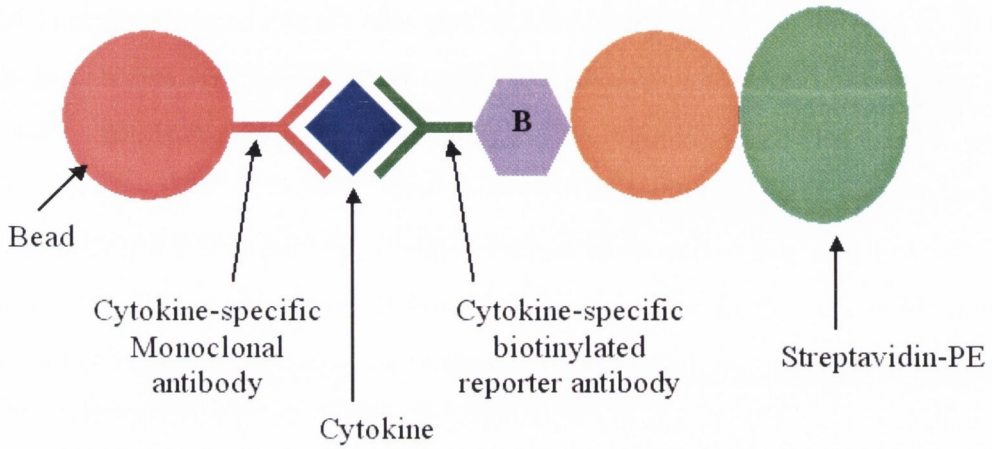

Figure 2.1 Microspheres (or beads) are dyed with differing concentrations of two fluorophores to generate distinct bead sets. Each bead set is coated with a cytokine-specific monoclonal antibody or capture antibody specific for one analyte or antigen. Captured antigen is detected using a biotinylated detection antibody and streptavidin-phycoerythrin (S-PE). A dual laser, flow-based sorting and detection platform allowed identification of and quantification of the antigen.

2.1.6 Determination of plasma triacylglycerol and non-esterified fatty acids

Plasma TAG and NEFA were measured using commercially available enzyme assay kits from Randox. Plasma TAG levels were measured using a colourimetric method (Tietz, 1990) as shown in Figure 2.2, in which TAG were hydrolized by lipoproteinlipase to produce glycerol and free fatty acids. The glycerol then participates in a series of coupled enzymatic reactions, in which glycerol kinase (GK) and glycerol phosphate oxidase (GPO) generate hydrogen-peroxide (H_2O_2). H_2O_2 reacts with 4-chlorophenol and 4-aminoantipyrine in the presence of peroxidase (POD) to form a quinoneimine dye (Jacobs and Vandemark, 1960; Koditschek and Umbreit, 1969; Trinder, 1969). The intensity of colour formed is proportional to the TAG concentration and can be measured photometrically between 480 nm and 520 nm.

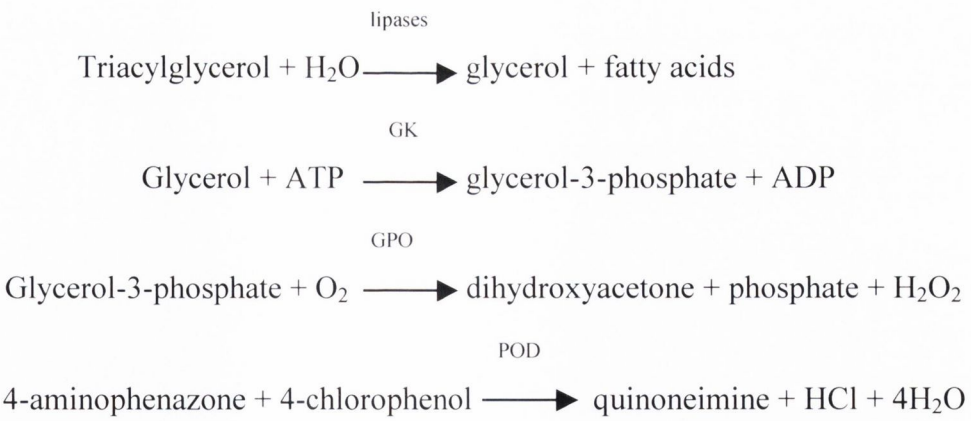

Figure 2.2 Triacylglycerol (TAG) was hydrolized by lipases to produce glycerol and free fatty acids. The glycerol then participates in a series of coupled enzymatic reactions, in which glycerol kinase (GK) and glycerol phosphate oxidase (GPO) generate hydrogen-peroxide (H_2O_2). H_2O_2 reacts with 4-chlorophenol and 4-aminoantipyrine in the presence of peroxidase (POD) to form a quinoneimine dye.

To measure TAG, the enzyme reagent containing 0.5 mMol/L 4-aminophenazone, 1.0 mMol/L ATP, lipases $\leq$ 150 U/ml, GK $\leq$ 0.4 U/ml, GPO $\leq$ 1.5 U/ml and POD $\leq$ 0.5 U/ml was reconstituted in 40 mMol/L (pH 7.6) Pipes Buffer containing 5.5 mMol/L 4-chlorophenol and 17.5 mMol/L Magnesium-ions. 3.5 µl of plasma sample or standard was incubated with 350 µl enzyme reagent in a 96-well plate for 5 minutes at 37°C. The absorbance of the samples and standards were measured at 500 nm against the reagent blank within 60 minutes using a SPECTRAmax®M2 microplate reader and SoftMax Pro® software (MDS Analytical Technologies, CA, USA). TAG concentration was calculated as mMol/L. Hypertriglyceridaemia is suspected from approximately 1.71 mMol/L.

Plasma NEFA levels were also measured using a colorimetric method as shown in Figure 2.3. This enzymatic method relies upon the acylation of coenzyme A (CoA) by NEFA in the presence of added acyl-CoA synthetase (ACS). The acyl-CoA produced is oxidized by added acyl-CoA oxidase (ACOD) with generation of H_2O_2. H_2O_2 in the presence of peroxidase (POD) permits the oxidative condensation of N-ethyl-N-(2hydroxy-3-sulphopropyl)m-toluidine (TOOS) with 4-aminoantipyrine, which forms a purple coloured adduct which can be measured colorimetrically at 550 nm (Matsubara *et al.*, 1983; Mulder *et al.*, 1983; Shimizu *et al.*, 1980).

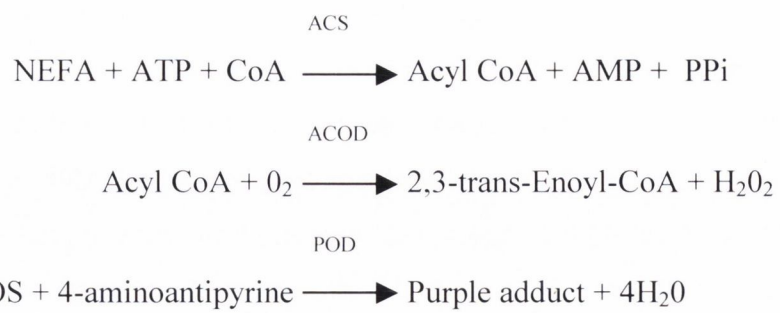

Figure 2.3 Acylation of coenzyme A (CoA) by non-esterified fatty acids (NEFA) in the presence of added acyl-CoA synthetase (ACS) produces acyl-CoA. Acyl-CoA is oxidized by added acyl-CoA oxidase (ACOD) with generation of H_2O_2. H_2O_2 in the presence of peroxidase (POD) allows oxidative condensation of N-ethyl-N-(2hydroxy-3-sulphopropyl)m-toluidine (TOOS) with 4-aminoantipyrine, which forms a purple coloured adduct.

Enzyme reagent 1 (R1) containing ACS ≥ 0.3 U/ml, Ascorbate oxidase ≥ 1.5 U/ml, 0.9 mMol/L CoA, 5.0 mMol/L ATP and 1.5 mMol/L 4-aminoantipyrine was reconstituted in phosphate buffer 0.04 mol/L (pH 6.9) with 3 mMol/L magnesium chloride and surfactant. Enzyme reagent 2 (R2) containing 0.3% (w/v) phenoxyethanol and surfactant was mixed with 10.6 mMol/L maleimide, ACOD ≥10 U/ml, POD 7.5 U/ml and 1.2 mMol/L TOOS. To measure NEFA, 5 µl of plasma sample or standard was incubated with 100 µl R1 and 200 µl R2 for 10 minutes at 37°C in a 96-well plate. The absorbance of the samples and standards was measured against the reagent blank after 10 minutes using a SPECTRAmax®M2 microplate reader and SoftMax Pro® software. NEFA concentration was calculated as mMol/L. Normal fasting plasma NEFA levels are between 0.1 - 0.9 mMol/L. Randox Assayed Multi-sera, Level 2 and Level 3 were used for quality control.

2.1.7 Determination of adipocyte size

A proportion of the EAT was placed in 10% neutral buffered formalin. Water was later removed from the tissue using progressively more concentrated ethanol (GPR Rectapur, VWR International, Belfast, Northern Ireland) followed by xylene (GPR Rectapur, VWR International) to remove the alcohol in a process known as dehydration in an automatic tissue processor (Leica TP 1020, Leica Microsystems, Ashbourne, Ireland). The samples were then embedded and placed in molten paraffin wax to replace the xylene using a Leica EG1150c (Leica). Sections of the tissue were cut on a Reichert-Jung 2030 (Leica) at 5 µm and placed on slides. The slides were then de-paraffinized and hydrated through solutions of xylene followed by methanol and then stained using an Auto Stainer XL (Leica). Slides were stained with hematoxylin (Sigma-Aldrich) and washed with water. The slides were

counterstained with eosin (Sigma-Aldrich). Hematoxylin stains the nuclei blue and eosin stains the cytoplasm pink. The stained slides were placed in ethanol and xylene to dehydrate the samples. Lastly, the slides were mounted in permount mounting media (Fisher Scientific, Dublin, Ireland) and covered with a coverslip. Images were taken on an Eclipse LV-Universal design microscope (Nikon Corporation, Tokyo, Japan) and the adipocyte area was measured in μm^2 using the NIS-Elements software (Nikon Corporation, Tokyo, Japan).

2.2 Cell culture

2.2.1 3T3-L1 cell line

The 3T3-L1 cell line was purchased from the European Collection of Animal Cell Cultures (ECACC, Salisbury, UK). Green and Kehinde derived the 3T3-L1 cell line from 3T3 mouse fibroblasts through clonal isolation. 3T3-L1 convert to adipocytes under defined culture conditions (Green and Kehinde, 1975). This conversion is a type of cellular differentiation, which occurs after the cells stop growing, at which time there is an increased incorporation of fatty acid precursors into triglycerides (Russell and Ho, 1976). The conversion involves the formation of numerous fat vacuoles, which coalesce into one large fat vacuole with time (Russell and Ho, 1976). 3T3-L1 cells are well characterised and are morphologically similar to fibroblastic pre-adipose cells found in adipose tissue and once differentiated, they exhibit virtually all the characteristics associated with mouse and human adipocytes present within adipose tissue (Cowherd *et al.*, 1999; Novikoff *et al.*, 1980). 3T3-L1 also express many of the same genes as adipocytes *in vivo* (Cowherd *et al.*, 1999). Furthermore, when injected into mice, 3T3-L1 pre-adipocytes differentiate and form fat pads, which are indistinguishable from normal adipose tissue (Green and Kehinde, 1979). 3T3-L1 cells are also sensitive to lipogenic and lipolytic hormones and drugs including insulin, which stimulates the uptake of glucose. 3T3-L1 cells offer an excellent model system for studying adipocytes.

2.2.2 3T3-L1 sub-culture

3T3-L1 cells were grown in dulbecco's modified eagle medium containing 4.5 g/L Glucose and 2 mMol L-glutamine (DMEM, Lonza Walkersville Inc, MD, USA) supplemented with 10% Foetal Bovine Serum (FBS, Gibco®, Invitrogen, Paisely, UK), 100 mg/ml streptomycin Sulfate and 100 µg/ml Potassium penicillin (Lonza Walkersville Inc). DMEM is rich in nutrients such as inorganic salts, amino acids, vitamins, D-Glucose, Sodium Pyruvate and the pH indicator Phenol Red. FBS is the portion of plasma remaining

after coagulation of blood. FBS is low in antibodies and rich in growth factors. The globular protein, bovine serum albumin (BSA), is a major component of FBS. Since commercial serum may vary between batches with regards to levels of antioxidants and growth factors, serum from the same batch was used throughout the course of the *in vitro* work. Penicillin-streptomycin is a broad spectrum bacteriostatic and bacteriocidal, with activity against gram negative and gram positive organisms. 3T3-L1 cells were grown in tissue culture treated, filter-vented cap 75 cm^2 flasks (Iwaki Seiyaku Co, Ltd, Tokyo, Japan) at 37°C and 5% CO_2 with 95% air in a humidified incubator (Thermo Elecron Corporation, OH, USA), until 70% sub-confluent. Sub-confluent cultured 3T3-L1 cells were split 1:10, once a week; cells were washed in phosphate-buffered saline (PBS, Gibco®, Invitrogen) and trypsinised to lift the adherent cells using 0.25% trypsin with EDTA (Lonza Walkersville Inc) in phosphate-buffered saline (PBS, Gibco®, Invitrogen). Once the cells began to lift trypsin activity was halted by the addition of the growth media; cells were centrifuged at 1,200 rpm for 5 minutes and transferred to new flasks.

2.2.3 Cyropreservation and revival of cells

To maintain healthy viable stocks, 3T3-L1 cells were grown until 70% sub-confluent, washed in PBS, trypsinised, centrifuged at 1,200 rpm for 5 minutes and the pellets re-suspended in 1 ml of cryopreservation media [90% FBS and 10% dimethyl sulfoxide (DMSO, Sigma-Aldrich)]. The suspension was immediately transferred into sterile cryovials (Nunc Plasticware, Life Technologies, Roskilde, Denmark). Cryovials were cooled to –80°C at -1°C/minute using a "Mr. Frosty" Freezing Container (Nalgene® Labware, Thermo Fisher Scientific, Roskilde, Denmark). The cryovials were then transferred to liquid nitrogen for long-term storage. Rapid thawing and dilution of the DMSO with growth media was ensured when re-establishing the vial stock.

2.2.4 Differentiation of 3T3-L1

3T3-L1 cells were grown until 70% sub-confluent, washed in PBS, trypsinised, centrifuged at 1,200 rpm for 5 minutes and re-suspended in 6 or 12-well plates (BD Biosciences, NJ, USA). To initiate differentiation, cells were grown to 100% confluency and then left for a further 2 days (Figure 2.4a). Differentiation was induced by adding 0.5 mMol 3-isobutyl-1-methylxanthine (IBMX, Sigma-Aldrich), 0.25 µMol dexamethoasone (Sigma-Aldrich) and 1 µg/ml insulin (Sigma-Aldrich) to the DMEM supplemented with 10% FBS and Penicillin-Streptomycin for 6 days (Figure2.4b). Differentiation media was then removed

and replaced with DMEM supplemented with 10% FBS and penicillin-streptomycin for 24 hours in preparation for experimental analysis.

a) b)

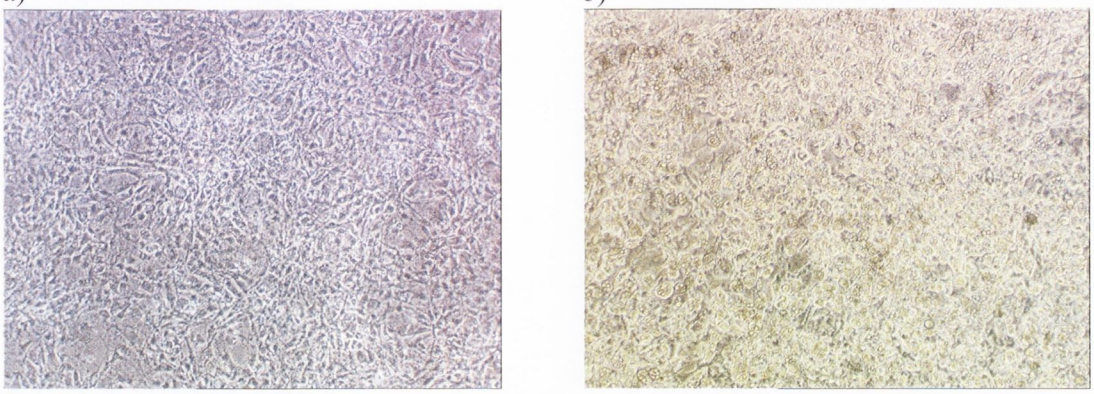

Figure 2.4 Confluent 3T3-L1 cells prior to differentiation (a) and 6 days post differentiation (b).

2.2.5 J774.2 macrophages

The J774.2 line was purchased from ECACC. J774.2 cells are a mouse BALB/c monocyte macrophage originally cloned from the ascites and solid tumour J774.1. J774.2 macrophages are well characterised and exhibit the cytologic, adherence and phagocytic properties of macrophages as well as expressing virtually all the characteristic genes associated with human macrophages (Ralph and Nakoinz, 1975).

2.2.6 Sub-culturing J774.2 macrophages

J774.2 cells were grown in DMEM containing 4.5 g/L Glucose and 2 mM L-glutamine supplemented with 10% FBS 100 mg/ml streptomycin sulfate and 100 μg/ml potassium penicillin. J774.2 cells are semi-adherent; some cells grew in suspension, some loosely attached to the surface while others flattened out and attached to the flask. J774.2 cells were grown in tissue culture treated, filter-vented cap 75 cm^2 flasks at 37°C and 5% CO_2 with 95% air in a humidified incubator, until 70% sub-confluent. Sub-confluent cultured J774.2 cells were split 1:4, two - three times a week by washing the cells and tapping the sides of the flasks to dislodge the cells. Cells were centrifuged at 1,200 rpm for 5 minutes and transferred to new flasks in preparation for experimental analysis.

2.2.7 Cyropreservation and revival of cells

To maintain healthy viable stocks J774.2 cells were grown until 70% sub-confluent, dislodged from the flask, centrifuged at 12,00 rpm for 5 minutes and the pellets re-suspended in 1 ml of cryopreservation media (90% FBS and 10% DMSO). The suspension

was immediately transferred into sterile cryovials. Cryovials were cooled to –80°C at -1°C/minute using a freezing container. The cryovials were then transferred to liquid nitrogen for long-term storage. Rapid thawing and dilution of the DMSO with growth media was ensured when re-establishing the vial stock.

2.2.8 Cell enumeration and viability assessment

Cell viability and yield were assessed prior to experiment set-up using Trypan blue solution (Sigma-Aldrich). Cells were stained with Trypan blue and counted on a haemocytometer under a light microscope using the protocol of Phillips and Terryberry (Phillips and Terryberry, 1957). Trypan blue assay is used to estimate the proportion of viable cells in a population. In a viable cell Trypan blue is not absorbed; however, it traverses the membrane in a dead cell. Hence, dead cells are shown as a distinctive blue colour under a light microscope. Since live cells are excluded from staining, this staining method is also described as a dye exclusion method.

2.2.9 Preparation of fatty acids

For the purpose of this *in vitro* study, stocks of fatty acids were prepared in DMSO. Eicosapentaenoic acid (EPA) and docosahexaenoic acid (DHA) were obtained from Sigma-Aldrich. 100 mMol of EPA and DHA was prepared, aliquoted and stored at -20°C. 3T3-L1 and J774.2 cells were treated with 50 μmol/L EPA or DHA while DMSO was used as a vehicle control. For all treatments, the final concentration of DMSO in culture medium was ≤ 0.1%.

2.2.10 Cell stimulation

Lipopolysaccaride (LPS) is a potent bacterial endotoxin and a specific activator of toll like receptor (TLR)-4, which induces inflammation within J774.2 macrophages. 1 mg/ml LPS from *Escherichia coli* dissolved in sterile pyrogen-free double distilled water was purchased from Alexis Biochemicals (Nottingham, UK) and stored at 4°C. IL-1β, a pro-inflammatory cytokine and activator of IL-1 receptor I (IL-1RI), was used to induce inflammation within the 3T3-L1 adipocytes. 5 μg of recombinant mouse IL-1β was purchased from R&D Systems (Abington, UK). The IL-1β was reconstituted in sterile PBS with 0.1% BSA and stored as 10 μg/ml 50 μl aliquots at –20°C.

2.2.11 Experimental design

In the first series of experiments, 3T3-L1 fibroblasts were differentiated into mature adipocytes as described in section 2.2.4. The cells were treated with 10 ng/ml IL-1β in serum free DMEM supplemented with antibiotics and 0.2% BSA for 5 minutes, 15 minutes, 30 minutes, 1 hour, 2 hours, 24 hours and 48 hours.

In the second series of experiments the effects of EPA and DHA on 3T3-L1 adipocytes and J774.2 macrophages were determined. 3T3-L1 fibroblasts were differentiated to mature adipocytes as described in section 2.2.4 and then treated with 50 μmol/L EPA, DHA or DMSO vehicle control in DMEM supplemented with 10% FBS and antibiotics for five days. Additionally, 3T3-L1 fibroblasts were differentiated as described in section 2.2.4 in the presence of 50 μMol/L EPA, DHA or DMSO vehicle control. Furthermore, J774.2 macrophages were treated with 50 μMol/L EPA, DHA or DMSO vehicle control in DMEM supplemented with 10% FBS and antibiotics for 5 days in 75 cm^2 flasks. 1 x 10^6 macrophages were then incubated with or without 100 ng/ml LPS in DMEM supplemented with 1% FCS and antibiotics for 15 minutes.

Finally, a series of co-culture and conditioned media (CM) experiments were conducted to examine the effects of J774.2 macrophages on 3T3-L1 adipocytes. In an acute LC *n-3* PUFA treatment co-culture system as depicted in Figure 2.5a, J774.2 macrophages were LPS stimulated (100 ng/ml) or unstimulated for 48 hours in DMEM supplemented with 10% FBS and antibiotics, after 24 hours LPS stimulation 50 μMol/L EPA, DHA or vehicle control was added. 3T3-L1 fibroblasts were differentiated into mature adipocytes as described in section 2.2.4. The media from the adipocytes and macrophages was removed and replaced with DMEM supplemented with 10% FBS and antibiotics. In a contact co-culture, mature fully differentiated 3T3-L1 adipocytes were incubated directly with the pre-treated macrophages; while in the transwell system pre-treated J774.2 macrophages were placed in permeable inserts above the fully differentiated 3T3-L1 adipocytes. Inserts allowed soluble molecules to circulate between cells however, direct cell contact was prevented.

In a chronic LC *n-3* PUFA treatment system as shown in Figure 2.5b, J774.2 macrophages were incubated with 50 μMol/L EPA, DHA or vehicle control for five days in DMEM supplemented with 10% FBS and antibiotics. In addition, during the final 48 hours of the LC *n-3* PUFA treatment macrophages were stimulated with 100 ng/ml of LPS. 3T3-L1 fibroblasts were differentiated into mature adipocytes as described in section 2.2.4. The media from the adipocytes and macrophages was removed and replaced with DMEM

supplemented with 10% FBS and antibiotics. In this transwell system pre-treated J774.2 macrophages were placed in permeable inserts above the fully differentiated 3T3-L1 adipocytes for 24 hours.

Additionally, a series of J774.2 macrophage conditioned media experiments were conducted as outlined in Figure 2.5c. J774.2 macrophages were pre-treated with 50 μMol/L EPA, DHA or vehicle control in DMEM supplemented with 10% FBS and antibiotics for three days. Subsequently, macrophages were then stimulated with 100 ng/ml LPS for 30 minutes, LPS stimulated macrophages were washed twice with sterile PBS after which the 50 μMol/L EPA, DHA or vehicle control in DMEM with supplements was replaced for a further 48 hours. Macrophage CM was collected and incubated with the mature differentiated 3T3-L1 adipocytes for 24 hours. Furthermore, macrophages were pre-treated with 50 μMol/L EPA, DHA or vehicle control in DMEM with 10% FBS and antibiotics for four days. Macrophages were then stimulated with 100 ng/ml LPS for 30 minutes, LPS stimulated macrophages were washed twice with sterile PBS after which 50 μMol/L EPA, DHA or vehicle control in DMEM with supplements was replaced for 24 hours. Macrophage CM was collected and incubated with mature differentiated 3T3-L1 adipocytes for 48 hours.

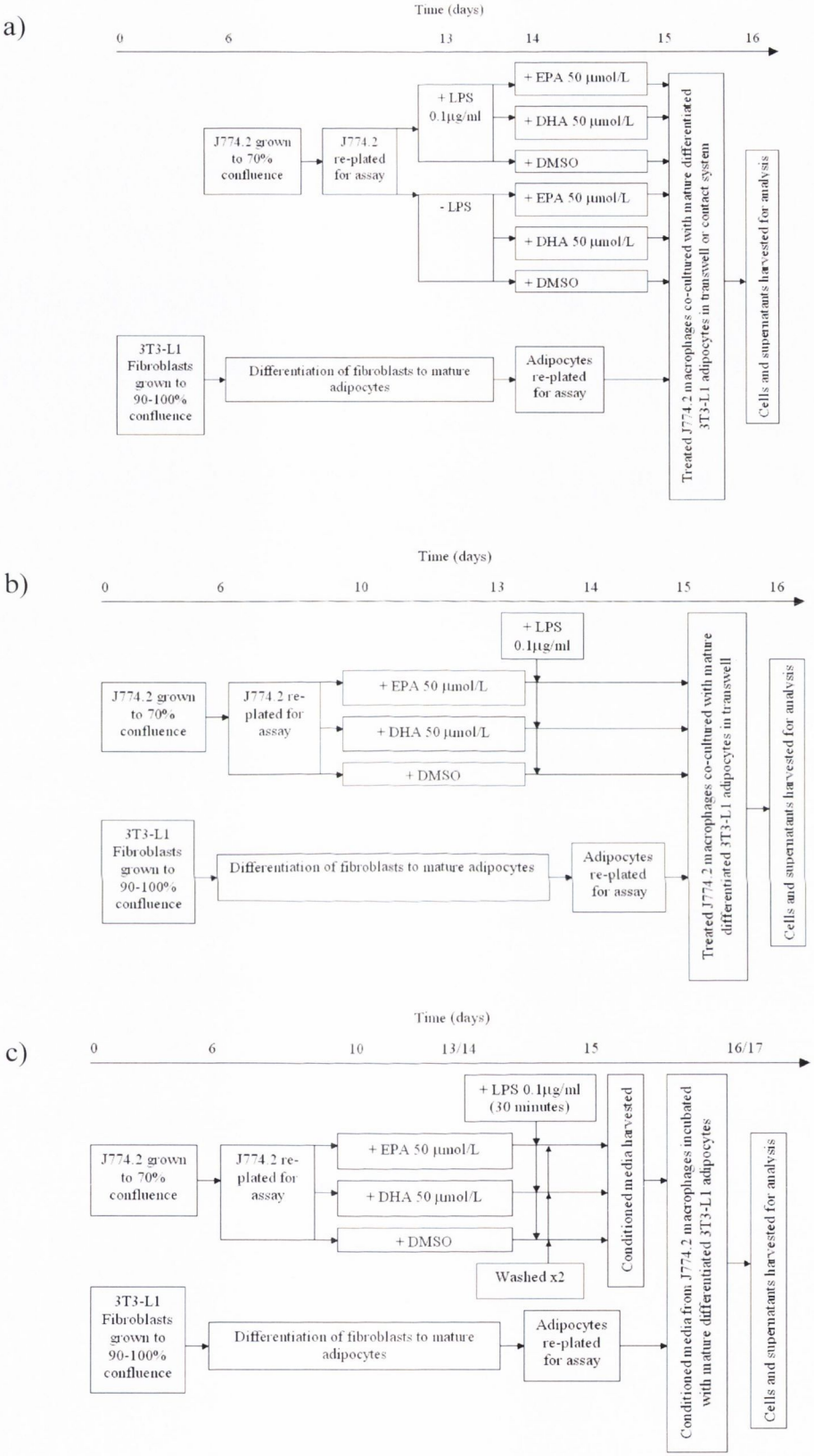

Figures 2.5 In the acute co-culture system (a), macrophages were stimulated with LPS (100 ng/ml for 48 hours) and treated with EPA/DHA (50 µMol/L for 24 hours) prior to co-culture for 24 hours. In the chronic system (b), macrophages were treated with EPA/DHA for 5 days and stimulated with LPS for 48 hours prior to co-culture for 24 hours. In the conditioned media (CM) experiments (c), macrophages were pre-treated with EPA/DHA for a total of 5 days and LPS stimulated for 30 minutes. CM was collected and incubated with the adipocytes for 24 or 48 hours.

2.3 MTT viability assay

The viability of 3T3-L1 adipocytes that receive media alone, 1 ng/ml IL-1β, 10 ng/ml IL-1β or 100 ng/ml IL-1β and J774.2 macrophages that receive media alone, 10 ng/ml LPS, 100 ng/ml LPS, 1 mg/ml LPS, 0.05% DMSO, 50 μMol/L EPA or 50 μMol/L DHA were quantified spectrophotometrically by an MTT-based *in vitro* toxicology assay kit (Sigma-Aldrich). The MTT system measures the activity of living cells via mitrochondrial dehydrogenases. MTT (3-[4,5-dimethylthiazol-2-yl]-2,5-dephenyltetrazolium bromide) is a tetrazolium salt that is incorporated into the mitochondria of living cells. Solutions of MTT dissolved in phenol red free balanced salt solutions are yellowish. In the presence of viable cells, mitochondrial dehydrogenases cleave tetrazolium rings yielding purple formazan crystals, which are soluble in acidified isopropanol. The amount of viable cell is directly proportional to the quantity of formazan formed.

1.5×10^5 adipocytes per well were differentiated in 96-well plates. The adipocytes were then incubated with IL-1β for 24 hours. 1.5×10^5 macrophages per well were cultured in 96-well plates and incubated with LPS for 48 hours. In addition, macrophages were cultured and incubated with DMSO, EPA or DHA in 75 ml^2 flasks for 3 days prior to transferral of 1.5×10^5 macrophages per well to 96-well plates for a further DMSO, EPA and DHA treatment for 48 hours. Control cells were left untreated. Wells containing medium alone were included as blanks. After a 4-hour incubation with 10 μl MTT, the formazan crystals were dissolved in 100 μl MTT solubilisation solution by repetitive pipetting. Absorbance was measured at 490 nm with a wavelength correction of 570 nm using a SPECTRAmax®M2 microplate reader and SoftMax Pro® software. The absorbance reading was obtained by subtracting the blanks from the sample value. Results are expressed as a percentage of untreated control cells. The treatment was rejected if the viability of the cells was lower than 95% of the control; the results are detailed in Table 2.2. However, it is of note that cell metabolism assays may produce misleading results if treatments alter the cellular metabolism by impairing energy metabolism or mitochondria function without killing the cell.

Table 2.2 The effects of IL-1β, LPS, DMSO and fatty acids on cellular viability. Adipocytes and macrophages were stimulated with IL-1β and LPS or treated with vehicle control and LC *n-3* PUFA as described. Results are expressed as percentage of untreated control cells (100%) and values represent mean and SEM, n = 3 - 16.

Cell type/Treatment	Cell viability %	SEM
3T3-L1 1 ng/ml IL-1β	99.86	5.66
3T3-L1 10 ng/ml IL-1β	99.50	6.47
3T3-L1 100 ng/ml IL-1β	89.26	6.013
J774.2 10 ng/ml LPS	109.51	2.12
J774.2 100 ng/ml LPS	97.07	2.47
J774.2 1 μg/ml	85.13	2.82
J774.2 DMSO 0.05%	100.32	0.99
J774.2 50 μMol EPA	95.81	0.65
J774.2 50 μMol DHA	95.03	1.00

2.4 Macrophage and adipocyte fatty acid composition analysis

2.4.1 Total lipid extraction

J774.2 cells were grown in 75 cm^2 flasks and treated with EPA and DHA for five days. Subsequently, the fatty acid treated macrophages were dislodged from the flask and centrifuged as described in 2.2.6. The pelleted cells were re-suspended in 1 ml of PBS and stored at –80°C for analysis. A proportion of the fatty acid treated macrophages were incubated with fully differentiated adipocytes in a transwell co-culture for 24 hours. Consequently, the macrophage treated adipocytes were washed twice with PBS then 1 ml of PBS was added to each well and the cells were quickly scraped using a cell scraper (Nunc Plasticware) and transferred to eppendorfs for storage at –80°C.

Lipid was isolated from cells in accordance with the Bligh and Dyer method (Bligh and Dyer, 1959). 400 μl of cell suspension was transferred into a 16 ml borosilicate glass test tube and 400 μl highly purified and deionized water, known as milliQ (Millipore, MA, USA) was added. 2 ml methanol (Sigma-Aldrich), 1 ml chloroform (Sigma-Aldrich), 40 μl 5mMol butylated hydroxy toluene (BHT) in ethanol (Sigma-Aldrich) and 100 μl 2 mg/ml solution of heptadecanoic acid (C17) was added to the solution. Heptadecanoic acid is used as an internal control to determine the quality of fatty acid extraction. The tubes were closed and vortexed for 1 minute. 1 ml milliQ water and 1 ml chloroform was immediately added and the solution was vortexed for 30 seconds. The tubes were centrifuged at 3,000 rpm for 15 minutes at 20°C to separate aqueous (lower) and organic (upper) phases. The

organic phase was transferred into a separate borosilicate tube using a glass pasteur pipette. 2 ml chloroform was added to the remaining aqueous phase and vortexed for 30 seconds. This was again centrifuged for 15 minutes at 3,000 rpm. The organic phase was removed and pooled with the previous isolate. The pooled organic phase was dried under nitrogen.

2.4.2 Transmethylation of macrophage and adipocyte lipid extracts

The lipid extract was treated with 1 ml methanol and 1 ml boron trifluoride (BF3; 14% in methanol, Sigma-Aldrich). The samples were vortexed for 30 seconds and placed in a water bath at 100°C for 40 minutes. Tube caps must be secure with no leaks and the samples must be repeatedly vortexed until complete dissolution of the lipid droplet. After 40 minutes the samples were cooled to room temperature. Subsequently, the resulting methyl esters were then extracted by adding 2 ml hexane (Sigma-Aldrich) and 2 ml milliQ water. The samples are vortexed for 10 seconds and the tubes were centrifuged at 2,000 rpm for 5 minutes at 10°C. Supernatants in the upper hexane phase were transferred to a new tube. 2 ml of hexane was added to the lower phase, vortexed for 30 seconds and centrifuged for 5 minutes at 2,000 rpm. The upper hexane phase was removed and pooled with the first supernatant. This aimed to optimise the methyl ester extraction. The pooled supernatant was dried under nitrogen and stored at –20°C until analysis by gas chromatography (GC).

2.4.3 Gas chromatographic analysis of macrophage and adipocyte lipids

The fatty acid methyl ester (FAME) composition of the J774.2 macrophage and 3T3-L1 adipocyte total lipids was analysed using a Shimadzu GC 2010 gas liquid chromatograph equipped with a flame ionisation detector, GC solutions software (Mason Technologies, Dublin, Ireland) and a fused silica capillary column (Omegawax, 30 m x 0.25 mm inner diameter, 0.2 μm film; Supelco Inc. PA, USA). The injector and the detector were kept at 250°C. The column oven temperature was held at 215°C for 45 minutes during the analysis and 1 ml of sample was injected into the GC; the carrier gas used was N_2. For each batch of samples a blank was prepared and run to act as a reference area value of the stock solution of heptadecanoic acid. Fatty acids were identified according to their retention times in comparison to two FAME standards (Supelco Inc). The fatty acid composition was represented as a relative percentage of the total quantified fatty acids.

2.5 *Oil red O staining in 3T3-L1 adipocytes*

Oil red O ($C_{26}H_{24}N_4O$) is a lysochrome (fat-soluble dye) diazo dye used for staining of neutral triglycerides and lipids. A stock solution of oil red O was prepared by resuspending 0.5 g of oil red O powder (dye content ≥ 75%; Sigma-Aldrich) into 100 ml of 100% isopropanol (Sigma-Aldrich). The solution was left to stir over night, away from light in a glass container. A fresh working solution was prepared by adding 6 ml of the stock solution to 4 ml of distilled water and then filtered. 3T3-L1 adipocytes were washed in PBS once and fixed in 10% neutral buffered formalin (Sigma-Aldrich). Cells were washed twice and the working solution of oil red O was added for 1 hour on an orbital shaker at low speed. Subsequently, cells were washed three times with water and observed under microscope (Nikon Corporation, Tokyo, Japan); images were taken using Matrox Intellicam (Matrox Electronic Systems Ltd, Quebec, Canada). In chapter 4 images were assessed using ImageJ, a public domain, Java-based, image processing program developed at the National Institutes of Health (Collins, 2007). Images were converted to 8-bit greyscale and a thresholded binary image was created to highlight the red stained regions, which were then measured as pixels and converted to percentage fold change. In chapter 6 oil red O stained adipocytes were washed and left to dry for 2 hours. Consequently, oil red O was extracted from the adipocytes with 100% isopropanol. Isopropanol was used as a blank and absorbance was measured at 500 nm using a SPECTRAmax®M2 microplate reader and SoftMax Pro® software. Values were expressed as percentage change relative to adipocytes.

2.6 *Glucose uptake analysis in 3T3-L1 adipocytes*

3T3-L1 adipocytes were incubated in serum free media with 0.2% BSA (fraction V, Calbiochem®, Merck Chemicals Ltd., Nottingham, UK) for 4 hours. Cells were then incubated in PBS with 0.2% BSA (fraction V) for 30 minutes prior to addition of 100 nMol of Insulin (Sigma-Aldrich) in PBS for 15 minutes, after which 5 μCi/ml of deoxy-D-glucose, 2-[^{3}H(N)] (Perkin-Elmer, MA, USA) in 1 mMol glucose (Sigma-Aldrich) was added to the cells and incubated for 10 minutes. Cells were then washed twice and lysed in radioimmunoprecipitation assay (RIPA) buffer containing protease inhibitor cocktail (Sigma-Aldrich). The samples were added to scintillation fluid (National Diagnostics Inc, GA, USA) and assayed for ^{3}H uptake as counts per minute (Tri-Carb 2900TR low activity liquid scintillation analyzer, Perkin-Elmer). The remaining lysates were stored at –80°C for western blot analysis. Values were expressed as either counts per minute or percentage change relative to insulin induced ^{3}H glucose uptake within 3T3-L1 adipocytes (100%).

2.7 RNA extraction and analysis

2.7.1 RNA extraction

Total RNA was extracted from EAT, adipocytes were isolated from EAT and 3T3-L1 adipocytes. In the acute co-culture model, total RNA was extracted from the adipocytes and macrophages in the contact system and adipocytes alone in the transwell system. In the acute co-culture total RNA was isolated using TRI Reagent® (Sigma-Aldrich). TRI Reagent is a mixture of phenol and guanidine thiocyanate and represents an improved version of the single-step method of Chomczynski and Sacchi (1987) (Chomczynski and Sacchi, 1987). It effectively disrupts and dissolves cell contents and maintains the integrity of RNA by inhibiting ribonuclease activity. Cells were washed to remove any non-adherent cells and lysed directly in the culture plates by adding 1 ml TRI Reagent®. Samples were incubated at room temperature for 5 minutes to allow complete dissociation of nucleoprotein complexes. The RNA homogenates were transferred to RNase-free microfuge tubes and 0.2 ml chloroform (Sigma-Aldrich) was added. The tubes were shaken vigorously for 15 seconds, incubated at room temperature for 15 minutes and centrifuged for 15 minutes at 12,000 rpm at 4°C to separate organic (lower) and aqueous (upper) phases. RNA was precipitated from the aqueous phase by incubating with 0.5 ml 100 % isopropanol (Sigma-Aldrich) for 10 minutes at room temperature. Samples were then centrifuged at 12,000 rpm for 10 minutes at 4°C. The resulting pellet was then washed with 1 ml 75% ethanol in RNase free water (Sigma-Aldrich). The RNA was air-dried for 10 minutes, resuspended in 20 µl RNase free water and stored at -80°C until further analysis.

Total RNA was also extracted from EAT and EAT isolated adipocytes using the RNeasy lipid tissue mini kit from Qiagen (West Sussex, UK). In the chronic EPA and DHA pre-treatment models total RNA was extracted from the 3T3-L1 adipocytes using the RNeasy mini kit from Qiagen. Adipose tissue samples were removed from –80°C storage. 100 mg was immediately placed directly into 1 ml QIAzol Lysis Reagent (Qiagen), in a flat based 7 ml tube with lid. The tissue was immediately homogenised using a rotor-stator homogeniser (Ultra Turray®, IKA, Staufen, Germany) until the sample was uniformly homogeneous (usually taking between 20 and 40 seconds). The homogenate was incubated at room temperature for 5 minutes to promote dissociation of nucleoprotein complexes. Adipocytes isolated from the EAT as described in section 2.1.4 were removed from –80°C storage and 1 ml QIAzol Lysis Reagent was added. The cells were homogenised using a needle and syringe. 200 µl of chloroform was added to the QIAzol Lysis and shake vigorously for 15 seconds. The homogenate was incubated at room temperature for 3

minutes and centrifuged at 10,000 rpm for 15 minutes at 4°C. The upper aqueous phase was transferred to a new collection tube. 600 µl of 70% ethanol (in RNase free water; Sigma-Aldrich) was added and mixed thoroughly by vortexing. 700 µl of the sample was transferred into an RNeasy mini spin column in a 2 ml collection tube (Qiagen) and centrifuged at 10,000 rpm for 15 seconds at room temperature. The flow through was discarded and the remaining sample was centrifuged within the same column. 3T3-L1 adipocytes were not treated with QIAzol but homogenised in 350 ml of RLT buffer using a needle and syringe, then transferred to a RNeasy column and spun at 10,000 rpm for 15 seconds.

700 µl RW1 buffer was added to the RNeasy columns from the EAT, EAT adipocytes or 3T3-L1 extraction process and centrifuged for 15 seconds at 10,000 rpm to wash the column. 500 µl RPE buffer was added onto the RNeasy spin column and centrifuged for 15 seconds at 10,000 rpm to wash the column further. 500 µl Buffer RPE was added again to the RNeasy spin column and centrifuge for 2 minutes at 10,000 rpm to dry the RNeasy silica-gel membrane. Finally, the RNeasy Spin Column was placed into a new 2 ml collection tube and centrifuged at full speed for 1 minute to completely dry the membrane. To elute the RNA from the column, the RNeasy column was transferred to a new 1.5 ml collection tube, 30 µl of RNase-free water was added directly onto the RNeasy silica-gel membrane and centrifuged for 1 minute at 10,000 rpm.

2.7.2 Quantitation of RNA

The concentration and purity of RNA within 3T3-L1 adipocytes was determined using a Nano-Drop® spectrophotometer (NanoDrop® UV-vis ND-1000, NanoDrop Technologies Inc., DE, USA). The "RNA-40" program was selected and 1 µl of blank (RNase free water) or sample was pipetted onto the measurement pedestal, the sampling arm was closed and the spectral measurements were made. When a measurement of a sample is taken, the intensity of light that has transmitted through the sample was recorded. The sample intensities along with the blank intensities were used to calculate the sample absorbance. The absorbance is measured at 260 nm and 280 nm. A 260/280 ratio of sample absorbance was used to assess the purity of RNA. A ratio of ~2.0 is generally accepted as "pure" for RNA. If the ratio is appreciably lower, it may indicate the presence of protein, phenol or other contaminants that absorb strongly at or near 280 nm. Sample concentration in ng/µl is calculated from the absorbance at 260 nm using the the Beer-Lambert equation.

The concentration and quality of RNA within the EAT and adipocytes isolated from EAT were assessed using an Agilent 2100 bioanalyzer (Agilent Technologies,

Cheshire, UK) and associated RNA 6000 Nano LabChip kits (Agilent Technologies). 550 µl of RNA nano gel matrix was prepared by centrifuging in a spin filter at 4,000 rpm for 10 minutes. RNA 6000 nano dye concentrate was vortexed for 10 seconds and spun down. 1 µl of dye was added to 65 µl of the filtered gel and centrifuged at 14000 rpm for 10 minutes. A new RNA Nano chip was placed on the chip priming station and 9 µl of the gel-dye mix was pipetted into the well marked. The chip priming station was locked and the plunger was pressed down slowly, after 30 seconds the plunger was released. An additional 9 µl of the gel-dye mix was added to two wells marked. 5 µl of the RNA 6000 nano marker was added to the rest of the wells. A ladder was heated to 70°C for 2 minutes and allowed to cool. 1 µl of the ladder was added to a specific well. 12 RNA samples were then loaded on to the chip and the chip was vortexed. The chip was inserted into the bioanalyser and a "eukarote total RNA nano series II" assay selected. Data is displayed as an electropherogram, the electropherogram of the ladder should contain 7 well-resolved peaks as shown in Figure 2.6a. The electropherogram of the RNA isolated from an EAT sample is shown in Figure 2.6b. The Agilent Expert software assigns a RIN number to each trace. The RIN number is assigned according to the strength of signal found between the 5S and 18S band, between the 18S and 28S bands, and after the 28S band. A RIN number of 10 is a perfect score and interpreted as excellent RNA. In these experiments a RIN of ≥ 5 was considered suitable for RT-PCR analysis.

a)

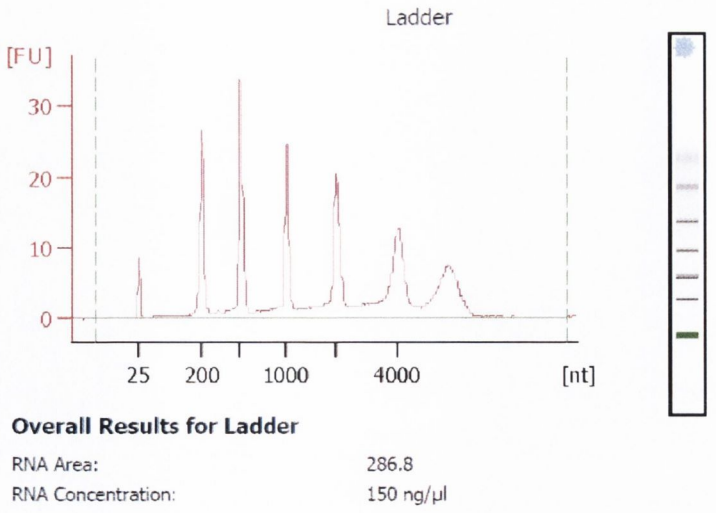

Overall Results for Ladder

RNA Area:	286.8
RNA Concentration:	150 ng/µl

b)

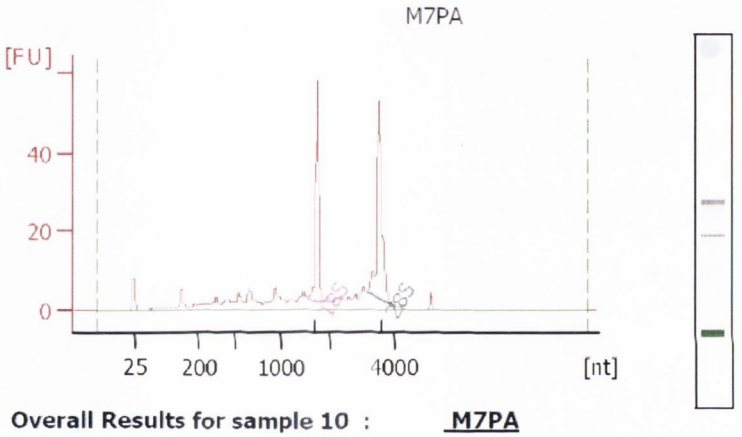

Overall Results for sample 10 : M7PA

RNA Area:	255.2
RNA Concentration:	133 ng/µl
rRNA Ratio [28s / 18s]:	1.4
RNA Integrity Number (RIN):	7.6 (B.02.04)

Figure 2.6 The electropherogram of the ladder (a) and the RNA isolated from an EAT (b).

2.7.3 Real-Time RT-Taqman® PCR: methodology

Real-time reverse transcriptase polymerase chain reaction (RT-PCR) is a rapid and sensitive method for the detection and quantification of PCR amplification while the reaction is occurring (i.e. in real time). Data is collected throughout the PCR process and reactions are characterised by the time when amplification of a target is first detected rather than the amount of target accumulated after a fixed number of cycles. TaqMan® chemistry uses a flurogenic probe to enable the detection of a specific PCR target product. Glyceralderhyde-3-phosphate (GAPDH) or 18S was used as the reference for all experiments. The use of such an endogenous control compensates for differences in the amount of starting material added to each reaction.

TaqMan probes are oligonucleotides that have a fluorescent reporter dye attached to the 5' end and a quencher moeity coupled to the 3' end. These probes are designed to hybridize to an internal region of a PCR product. In the unhybridized state, the proximity of the fluorescent reporter dye and the quench molecules prevents the detection of fluorescent signal from the probe. During PCR, when the polymerase replicates a template on which a TaqMan probe is bound, the 5'- nuclease activity of the polymerase cleaves the probe. This decouples the fluorescent and quenching dyes. Therefore, fluorescence increases in each cycle, proportional to the amount of probe cleavage. Both primer and probe must hybridize to the target for amplification and cleavage to occur which ensures non-specific amplification is not detected. The Ct is defined as the fractional cycle number at which the fluorescence generated by cleavage of the probe crosses a fixed threshold in the exponential phase of amplification. An inverse relationship is therefore observed between the amount of template present and the Ct. Samples that contain fewer copies of the target gene require a greater number of cycles (maximum is 40) to generate a detectable signal. Samples were quantified using either the standard curve method or the comparative Ct method as described in 2.7.6.

2.7.4 Preparation of RNA prior to cDNA synthesis

To eliminate any possible contamination of the RNA by genomic DNA, the samples were treated with a Turbo DNA-free™ kit (Perkin-Elmer Applied Biosystems, Warrington, UK). 1.5 μg of RNA was added to an RNase-free eppendorf, 1 ml of TURBO DNase and 0.1 times the RNA sample volume of TURBO DNase buffer was added to the RNA sample and mixed gently. The samples were incubated at 37°C for 20 minutes followed by the addition of 0.1 times the RNA volume of resuspended DNase inactivation reagent. The samples were then incubated for 2 minutes at room temperature and centrifuged at 15,000 rpm for 90 seconds and transferred to a new RNase-free eppendorf.

2.7.5 cDNA synthesis

1.5 μg DNase-treated RNA was reverse transcribed using a SuperScript® VILO™ cDNA synthesis kit (Invitrogen Corporation, NV Leek, Netherland) in a 26 μl reaction containing 4 μl of 5X VILO™ reaction mix containing random primers, $MgCl_2$ and deoxynucleotides (dNTPs), 2 μl 10X Superscript® enzyme mix containing reverse transcriptase and recombinant ribonuclease inhibitors and 1.5 mg RNA in 20 ml deionized, diethylpyrocarbonate (DEPC) treated water (Sigma-Aldrich). The reaction was carried out

at 42°C for 60 minutes and terminated by heating at 85°C for 5 minutes; samples were stored at -20°C. Reactions in which the reverse transcriptase was omitted served as negative controls.

2.7.6 Real-time TaqMan® PCR: reaction and analysis

RNA expression was quantified by real time PCR (RT-PCR) on an ABI 7700 or ABI 7700HT Sequence Detection System (Perkin-Elmer Applied Biosystems). For the early acute co-culture experiments an ABI PRISM 7700 sequence detection system was used with a 96-well plate. For all other experiments RNA was quantified using an ABI PRISM 7900HT sequence detection system and a 384-well plate. Each 10 μl of reaction contained 0.5 μl of cDNA, 5 μl TaqMan® 2 X Master mix, 0.5 μl TaqMan® pre-developed target primer probe kits with forward and reverse primers and 4 μl DEPC treated water. Insulin receptor substrate (IRS)-1, insulin receptor, glucose transporters (GLUT)-4, peroxisome proliferator-activated receptors (PPAR)-γ, sterol regulatory element–binding protein (SREBP)-1c, resistin, adiponectin, adiponectin receptor 1 and 2 (AdipoR1 and 2), TNF-α, IL-6, IL-1RI, IL-1RII, IL-1β, IL-1 receptor antagonist (Ra), MIP-1α and macrophage migration inhibitory factor (MIF) were investigated using pre-developed primer probe kits. All reagents necessary for running a TaqMan® RT-PCR assay were purchased from Perkin-Elmer Applied Biosystems. All reactions were performed in duplicate using the following conditions, 50°C for 2 minutes and 95°C for 10 minutes followed by 40 cycles of 95°C for 15 seconds and 60°C for 1 minute.

In chapter 5, for the analysis of the acute co-culture model, standard curves were constructed from the standard reactions for target genes and the enogenous control GAPDH by plotting values for Ct versus log cDNA input (ng). For each sample, results were normalised by dividing the amount of target gene by the amount of GAPDH and expressed relative to the appropriate control. In chapter 4, 5 and 6, the comparative Ct method or ΔΔCt method was used to calculate gene expression levels. This involves comparing the Ct values of the samples of interest with the control. The Ct values of both the calibrator and the samples of interest were normalized to 18S an internal control and expressed relative to the appropriate control group.

$$\Delta\Delta \text{ Ct} = \Delta \text{ Ct}_{,\text{sample}} - \Delta \text{ Ct}_{,\text{reference}}$$

Δ $\text{Ct}_{,\text{sample}}$ is the Ct value for any sample normalized to the internal control and Δ $\text{Ct}_{,\text{ reference}}$ is the Ct value for the calibrator also normalized to the internal control.

2.8 Preparation of protein extracts and Western blotting

2.8.1 Isolation of total protein

3T3-L1 adipocytes treated with fatty acids and 3T3-L1 adipocytes treated with J774.2 macrophages in a co-culture system as described in section 2.2.10, were prepared for protein extraction and analysis. After treatment cells were washed with sterile PBS and 1 ml of RIPA buffer with protease inhibitor cocktail (Sigma-Aldrich) was added to each well and incubated for 30 minutes at 4°C. Cells were then collected using a cell scraper, transferred to a sterile eppendorf and stored at -80°C until analysis. Prior to use these cells were centrifuged for 10 minutes at 1,500 rpm at 4°C to pellet cell debris. Supernatant containing the protein was then ready for analysis.

2.8.2 Determination of protein concentration

Concentrations of total protein were determined by Bradford assay using the Bio-Rad protein assay (Bio-Rad Laboratories Inc., CA, USA). The Bio-Rad protein assay is a dye-binding assay in which a differential colour change of a dye occurs in response to various concentrations of protein (Bradford, 1976). The absorbance maximum for an acidic solution of Coomassie® Brilliant Blue G-250 dye shifts from 465 nm to 595 nm when binding to protein occurs (Compton and Jones, 1985; Reisner *et al.*, 1975). 20 ml of reagent S per 1 ml of reagent A was prepared. 5 mg/ml, 2.5 mg/ml, 1.25 mg/ml and 0.65 mg/ml BSA standards were prepared in RIPA buffer. 5 µl of the standards and samples were placed in duplicate into a 96-well plate, 25 µl of working solution A and 200 µl of solution B were added to each well. After 15 minutes the absorbance was measured at 590 nm using a SPECTRAmax®M2 microplate reader and SoftMax Pro® software. The concentration of protein was determined using the BSA standard curve.

2.8.3 Preparation of samples for gel electrophoresis and Western blotting

10 µg of total protein and 1:6 6X loading buffer (420 mMol Tris-HCl pH 6.8, 30% v/v glycerol, 10% w/v SDS, 600 w/v mMol DTT, 0.012% w/v bromophenol blue; all purchased from Sigma-Aldrich) were boiled at 100°C for 5 minutes to denature proteins. The samples were immediately used for SDS polyacrylamide electrophoresis (PAGE).

2.8.4 Sodium dodecyl sulphate polyacrylamide gel electrophoresis (SDS-PAGE)

Proteins were separated using 10% acrylamide resolving gel.

- *Resolving gel:* 4.66 ml 30% acrylamide, bisacrylamide mix (Sigma-Aldrich), 3.5 ml 1.5 Mol Tris pH 8.8, 5.84 ml distilled water, 84 µl 10% ammonium persulphate and 8 µl TEMED.
- *Stacking gel:* 1.2 ml 30% acrylamide, bisacrylamide mix (Sigma-Aldrich), 1.9 ml 0.5 Mol Tris (pH 6.8), 4.5 ml distilled water, 54 µl 10% ammonium persulphate and 7.5 µl TEMED.

Acrylamide gels were cast between two glass plates. The glass plates were placed in a electrophoresis unit (Atto Corporation, Tokyo, Japan). Electrode running buffer (25 mM Tris Base, 192 mM glycine and 0.1% w/v SDS) was added to the unit. Samples and a dual colour standard from Bio-rad Laboratories Inc. were loaded and electrophoresis was carried out at 25 mA per gel for ~1 hour until the migration dye front had begun to run off the gel.

2.8.5 Western blotting

The semi-dry method for transfer of electrophoresed proteins to immobilizing membranes as described by Towbin *et al.* (Towbin *et al.*, 1979), was preformed using a Sammy semi-dry blot system (Schleicher and Schuell, Germany). Nitrocellulose transfer membrane (0.45 µm; Pall Corporation, NY, USA) and filter paper (Pierce Biotechnology Inc, IL, USA) were soaked in transfer buffer (25 mM Tris Base, 192 mMol glycine and 20% v/v methanol). The blot sandwich was prepared as follows: 6 sheets of filter paper pre-soaked in transfer buffer, nitrocellulose membrane pre-soaked in transfer buffer, gel and a further 6 sheets filter paper pre-soaked in transfer buffer. Care was taken to ensure the absence of air bubbles. Electrophoresis transfer was performed at 189 mA for 45 minutes.

2.8.6 Detection of antigens

Blots were incubated with a solution of 13 mMol TBS and 150 mMol NaCl with 0.01% v/v Tween 20 (Sigma Adrich) containing 5 % BSA for 1 hour. Blots were incubated with the primary antibody at a dilution of 1:1000 in TBS-Tween 20 containing 5% BSA overnight at 4°C. Rabbit monoclonal or polyclonal antibodies specific to phosphorylated insulin receptor (Tyr1158, Tyr1162, Tyr1163), GLUT4 (Millipore) protein kinase (PK)-B/Akt, phosphorylated Akt (Thr308), IRS-1, phosphorylated IRS-1 (ser636/639), inhibitor of κB (IκB)-α, phosphorylated-IκB-α (Ser32), phosphorylated c-Jun N-terminal kinase

(JNK)1/2 p54/46 (Thr183/Tyr185), p38 mitogen-activated protein kinase (MAPK), phosphorylated p38 MAPK (Thr180/Tyr182), phosphorylated p44/42 MAPK (ERK1/2, Thr202/Tyr204; Cell Signalling Technology®, MA USA), PPAR-γ (Abcam, Cambridge, UK), nuclear factor (NF)-κBp65, JNK1 p54 and p44 MAPK (ERK1; Santa Cruz Biotechnology Inc., CA, USA) were examined. Membranes were then washed six times for 5 minutes in TBS-Tween 20. Subsequently, the blot was incubated with peroxidase-conjugate secondary antibody (polyclonal goat anti-rabbit IgG-peroxidse-conjugate immunoglobulins; Santa Cruz Biotechnology Inc.) at a dilution of 1:2000 for 1 hour at room temperature. Blots were then washed 6 times for 5 minutes in TBS-Tween 20. All incubations were carried out on a rocking platform to ensure thorough mixing. Antigens were detected by incubating the membrane in a 1:1 solution of luminol/enhancer solution: stable peroxide solution (Supersignal® West Pico Chemiluminescent Substrate, Pierce Biotechnology, IL, USA) for 2 minutes at room temperature. Excess reagent was drained from the membrane, which was then placed between two sheets of transparent acetate in an autoradiography cassette before being exposed for 1 to 10 minutes. The films were developed using an XoGraph automatic X-ray processor (Healthcare Ltd., Gloucestershire, UK).

2.8.7 Reuse of Western blots

To probe for different proteins the blot was stripped. The blot was washed in TBS-Tween 20 washed three times for 10 minutes, then incubated with stripping buffer (Restore™, Pierce Biotechnology) for 10 minutes and washed in TBS-Tween 20 for a further six times for 5 minutes. After washing the blot was ready to use again, commencing with the blocking stage in Western blot protocol.

2.8.8 Quantification of protein bands

Protein bands were quantified by densitometry using the TINA software version 2.09c (Raytest, Straubenhardt, Germany) and protein levels were expressed as percentage change relative to adipocytes alone.

2.9 Enzyme-linked immunosorbent assay

Cell culture supernatants from 3T3-L1 adipocytes and J774.2 macrophages were removed and centrifuged at 2,000 rpm for 10 minutes to pellet dead cells. The supernatants were aliquoted and frozen at –80°C until subsequent analysis of cytokine and adipokine concentrations. Blood was collected during the GTT in a capillary tube at time points 0, 30

and 60 minutes post glucose IP. The blood was spun 15,000 rpm for 5 minutes and plasma collected, aliquoted, snap frozen in liquid nitrogen and stored at –80°C until subsequent analysis of insulin concentrations.

2.9.1 ELISA

The concentrations of TNF-α, IL-1β, IL-6, IL-10, adiponectin, leptin and resistin in the cell culture supernatants were determined using commercially available DuoSet ELISA development systems from R&D Systems. Insulin levels were measured using a commercially available ELISA kit purchased from Mercodia. The ELISAs were carried out as per manufacturer's instructions. For the R&D ELISAs, 96-well microtiter plates (Nunc) were coated with 100 µl per well of an anti-cytokine/adipokine capture antibody and incubated over night at room temperature. The plates were washed three times in wash buffer containing 0.05% Tween 20 in PBS (Sigma-Aldrich) and then blocked with 300 µl per well of blocking buffer containing 1% BSA in PBS (in the case of leptin 5% Tween 20 in PBS with 0.05% NaN_3) for 1 hour at room temperature to remove excess primary antibody and prevent non-specific binding. Plates were washed three times and 100 µl of samples or serially diluted standards were added and incubated at room temperature for 2 hours. Plates were then washed three times and 100 µl of biotinylated anti-cytokine detection reagent was added to each well and incubated at room temperature for 2 hours. Plates were washed three times and 100 µl per well of detection reagent or streptavidin conjugated horseradish peroxidase (HRP) diluted 1:200 was added for 20 minutes at room temperature and protected from light. The plates were washed three times and 100 µl per well of substrate solution [1:1 mixture of hydrogen peroxide and tetramethylbenzidine (TMB)] was added for 20 minutes at room temperature to allow the blue colour to develop. The reaction was stopped by adding 50 µl per well of sulphuric acid and absorbance was measured at 450 nm with a wavelength correction of 570 nm on a SPECTRAmax®M2 microplate reader with SoftMax Pro® software. A standard curve was constructed for each assay by plotting absorbance (optical density) values from the standards versus concentration of the standards. Sample concentrations were then calculated through the equation of the standard curve.

For the insulin ELISA, 96-well plates were pre-coated with anti-insulin capture antibody. 25 µl of calibrator was added to each well followed by 5 µl of pre-prepared standards or samples. 50 µl of enzyme conjugate-HRP solution was added to each well and the plate was incubated on an orbital shaker (700 - 900 rpm) for 2 hours at room

temperature. During incubation insulin in the sample reacts with peroxidase-conjugated anti-insulin antibodies and anti-insulin antibodies bound to the well. The plate was washed six times with the wash buffer to remove unbound enzyme labelled antibodies, 200 µl of TMB was added to each well and incubated for 30 minutes at room temperature and protected from light. Subsequently, 50 µl of acid stop solution was added to each well and gently mixed for 5 seconds on an orbital shaker. Absorbance was measured at 450 nm using a SPECTRAmax®M2 microplate reader and SoftMax Pro® software. The absorbance of the standards was plotted against the insulin concentration of the standards (log-log). Sample concentrations were then calculated through the equation of the standard curve.

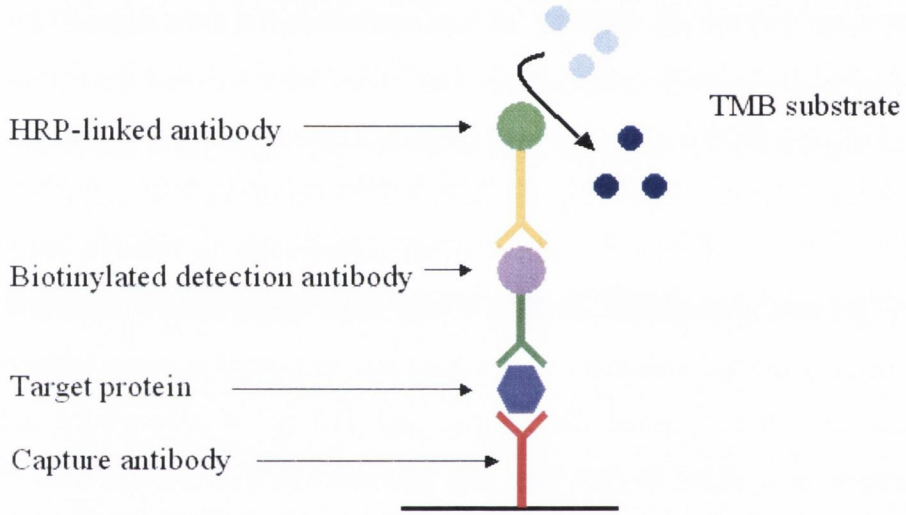

Figure 2.7 Sandwich ELISA in which a primary capture antibody is coated onto the surface of a 96-well plate. The target protein anneals to the immobilized primary antibody. A secondary dectection antibody containing an enzyme such as horseradish peroxidase (HRP) is then added which acts upon a substrate, such as tetramethylbenzidine (TMB), which becomes oxidized to produce a blue colour in direct proportion to the amount of target protein present. Oxidation is stopped using an acidic solution, which turns the solution yellow and can be measured using a microplate reader.

2.10 Confocal microscopy

2.10.1 Preparation of 3T3-L1 adipocytes prior to confocal analysis

Mature differentiated 3T3-L1 adipocytes were cultured on a 13mm cover glass (VWR International) within the lower compartment of a transwell co-cultured system. J774.2 macrophages were pre-treated with 50 µMol/L EPA, DHA or DMSO vehicle control for 5 days and stimulated with 100 ng/ml LPS during the final 48 hours of the LC *n-3* PUFA chronic treatment. The mature adipocytes were then co-cultured with the macrophages in a transwell system for 24 hours. The transwell insert containing macrophages was then removed and 10 nMol of insulin (Sigma-Aldrich) in media was added to each well and

incubated for 40 minutes as this was determined to be the optimal time to see colocalization of GLUT4 to the membrane. The confocal protocol used was based on a technique developed by Oatey *et al.* (Oatey *et al.*, 1997). The adipocytes were washed twice with PBS and fixed with 4% (Baqui *et al.*, 2003) paraformalderhyde for 30 minutes (Sigma-Aldrich) at room temperature. Subsequently, cells were washed three times and incubated with 5% BSA (Sigma-Aldrich) for 20 minutes at room temperature to minimise non-specific background staining. The cells were then washed three times with PBS and the cell surface proteins were labelled with 0.5 mg/ml EZ-link Sulfo-NHS-LC-biotin for 15 minutes at room temperature; cells were then washed six times and incubated with a 1: 100 dilution of Texas red avidin D (Peirce) for 30 minutes at room temperature. NHS-LC-Biotin is water soluble and binds to cell surface proteins (Baqui *et al.*, 2003), the negative charge of $-SO_4$ group keeps biotinylation localized at the cell surface so the reagent does not pass through the cell membrane. The avidin D bound to Texas red binds to the biotinylated molecule. The cells were washed six times and permeabilised using triton x-100 (0.1%, Sigma-Aldrich) for 20 minutes. The adipocytes were incubated with BSA (5%) for 20 minutes at room temperature. Subsequently, the cells were incubated with 1:100 dilution of an anti-rabbit GLUT4 antibody (Millipore) overnight at 4°C. At the end of the incubation period the cells were washed with PBS six times followed by a 1:200 dilution of corresponding FITC conjugated secondary goat anti-rabbit antibody (Abcam). The cells were washed ten times in PBS and the cover glass was flipped and mounted onto slides using a Dako mounting medium (Dako, CA, USA). Images were taken and co-localisation was analysed using a LSM510 META confocal microscope (Carl Zeiss MicroImaging Inc. NY, USA).

2.10.2 Confocal analysis

Within confocal microscopy, specimens are recorded as a digital image composed of a multi-dimensional array containing many volume elements, termed voxels, that represent three-dimensional pixels. The size of a voxel is determined by the numerical aperture of the objective, the illumination wavelength and the confocal detector pinhole diameter. An argon-ion laser and helium-neon laser are switched on and a multi-track configuration selected, which allows detection of two or more fluorophores. The adipocytes of interest with good staining were selected. Gain and offset is used to adjust light intensities to match the dynamic range of the detector. These adjustments assure that the maximum number of grey levels are included in the output signal with very little black (no signal) or white (saturated signal). After digitisation, the photon signal is displayed as shades of grey

ranging from black to white. A z stack was then taken; this is a stack of images focused at regularly placed intervals through the depth of an object of interest, allowing one to subsequently create renderings to visualize the entire sample in 1D or 3D. The co-localization of the two fluorescent probes within the adipocytes, FITC (fluoresces at ~488 nm with absorption at ~495 nm), which has green emission, and Texas red (fluoresces at ~615 nm with absorption at ~589 nm), which has red emission, are represented in the image (Figure 6.2) by pixels containing both red and green colour contributions. The images show scans collected from a detector channel filtered for the emission spectrum of FITC when excited at 488 nm with an argon-ion laser (a) and the channel filtered to gather fluorescence emission from Texas red excited with a 543 nm helium-neon laser (b). Digitally combining the two images reveals co-localization of the two fluorescence signals at the membrane (c).

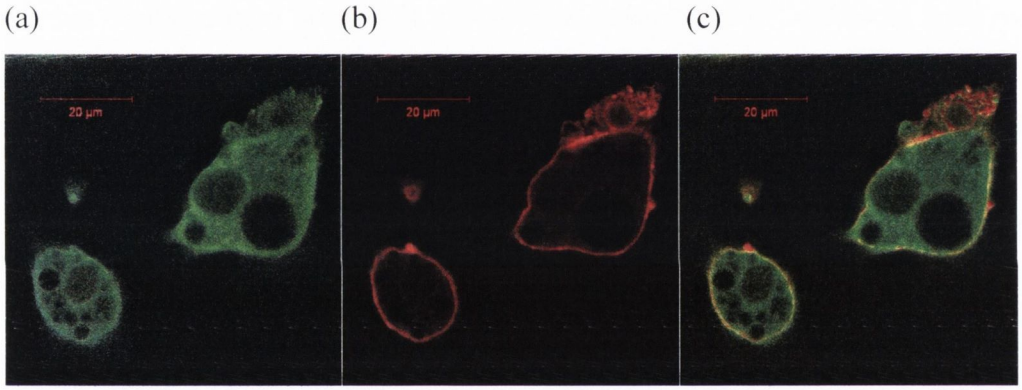

Figure 2.8 The co-localization (c) of the two fluorescent probes FITC (a) and Texas red (b) within the adipocytes.

Graphical display for co-localization analysis of the pseudocolored specimen images are represented by a scatterplot as shown in Figure 6.3, which correlates the relationship or association between two sets of data. The scatterplot graphs the intensity of one pseudocolor versus another for each pixel in the image, or a selected region of interest, on a two-dimensional histogram. One channel (green) is graphed along the **x**-axis, while the other (red) is plotted on the y-axis. Therefore, every pixel of the composite image is characterized by a pair of intensities distinguished as co-ordinates in a Cartesian system. Analysis of the distribution pattern generated by the intensity pairs enables identification of fluorophore co-localization.

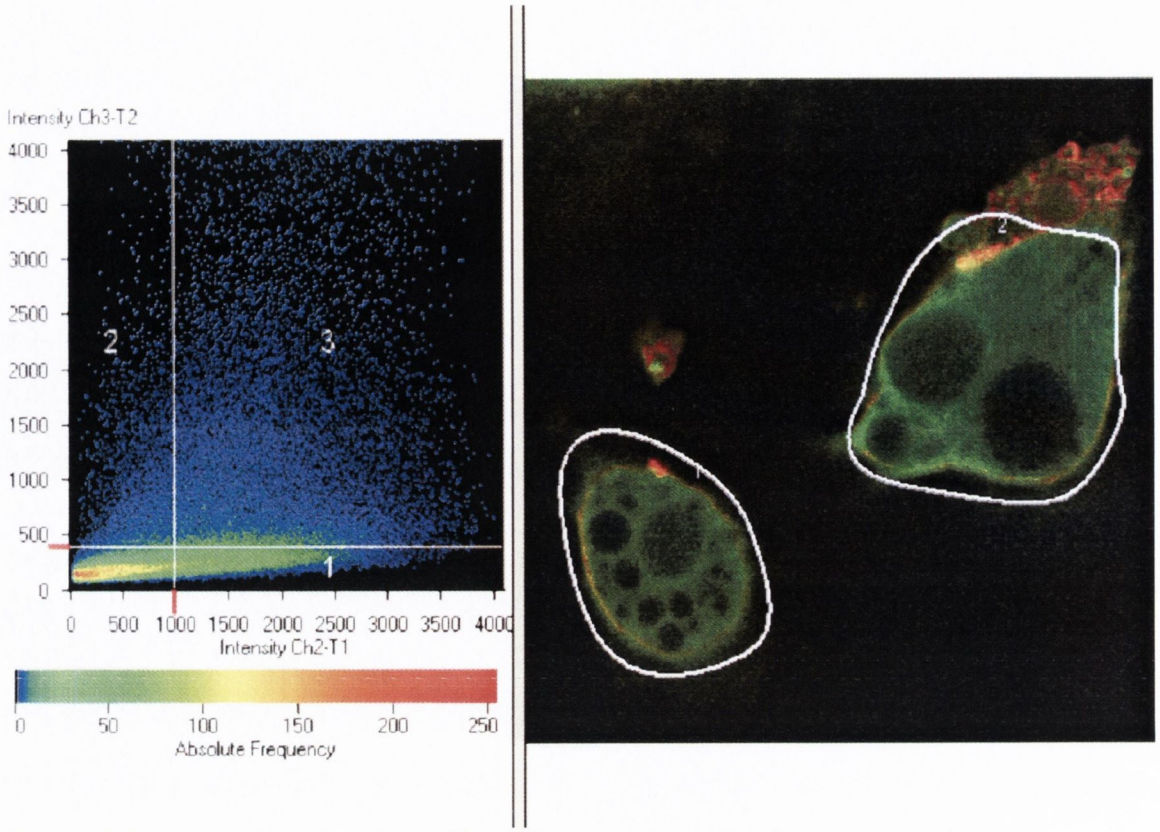

Figure 2.9 Co-localization of specific regions as represented by a scatterplot.

Pearson's correlation coefficient is one standard technique applied in pattern recognition for matching one image to another in order to describe the degree of overlap between the two patterns. Pearson's correlation coefficient is calculated according to the equation:

$$R_r = \frac{\sum_i (S1_i - S1_{aver}) \bullet (S2_i - S2_{aver})}{\sqrt{\sum_i (S1_i - S1_{aver})^2 \bullet \sum_i (S2_i - S2_{aver})^2}}$$

Where S1 is the signal intensity of pixels in the first channel and S2 is the signal intensity of pixels in the second channel. The values S1(average) and S2(average) are the average values of pixels in the first and second channel, respectively. In calculating Pearson's correlation coefficient, the average pixel intensity values are subtracted from the original intensity values. As a result, the value of this coefficient ranges from -1 to 1, with a value of -1 representing a total lack of overlap between pixels from the images and a value of 1 indicating perfect image registration. Pearson's correlation coefficient accounts only for the similarity of shapes between the two images, and does not depend upon image pixel intensity values. When applying this coefficient to co-localisation analysis, however, the potentially negative values are difficult to interpret. Values between –1 and 0 indicate some form of inverse relationship between the channels, as may occur when one channel is

very dim and the other bright (Pawley, 2006). Other coefficients provide further information regarding the nature of the co-localisation as well as being less sensitive to channel imbalances (Pawley, 2006).

2.11 Data preparation and statistical analysis

Data was reported as Mean ± SEM. Statistical analysis was performed with SPSS (SPSS Inc, IL, USA). The distribution of data for each variable was assessed and variables transformed to normalise the distribution of data if necessary. In chapter 3, Mauchly's test of Sphericity was used to validate repeated measure factor ANOVA of the plasma glucose levels between groups over time in the GTT. When the significance level of Mauchly's test was < 0.05 then sphericity could not be assumed. The correction used for violations of sphericity was Greenhouse-Geisser. Multiple comparisons were performed by one-way ANOVA. Significant inter-group differences were subsequently tested by post hoc Bonferroni statistical analysis. Independent Student's t-tests (2 tailed) were performed between the C57BL/6 WT control and the IL-1R1$^{-/-}$ groups. In chapter 4, 5 and 6 multiple comparisons were performed by one-way ANOVA. Inter-group differences were subsequently tested by post hoc Least Significant Difference (LSD) statistical analysis. In chapter 4 independent Student t-tests (2 tailed) were performed between the control and IL-1β treated cells. A statistical probability of $P \leq 0.05$ was considered statistically significant.

Chapter 3

The Effects of High Fat Diet Induced Obesity on Molecular Mechanisms Associated with Insulin Resistance *In Vivo* within IL-1 Receptor I Knockout Mice

3.1 Introduction

White adipose tissue (WAT) is a complex, essential and highly active metabolic and endocrine organ. Adipose tissue secretes an array of cytokines and adipokines that regulate body weight homeostasis, insulin sensitivity, and inflammation (Siiteri, 1987). During an obese state the adipose tissue becomes inflamed with increased infiltration of immune cells such as macrophages, which contribute to the local production of pro-inflammatory cytokines. These adipose derived pro-inflammatory cytokines are proposed to alter the endocrine function of the tissue and could impinge insulin signalling and action in adipocytes, liver and muscle leading to the development and/or aggravation of insulin resistance (Marette, 2003).

Many *in vitro* and *in vivo* studies have demonstrated the effects of interleukin (IL)-1 in reducing body mass and insulin sensitivity while IL-1 receptor antagonist (IL-1Ra) has been shown to suppress obesity induced insulin resistance; however numerous studies are conflicting and require further elucidation (Garcia *et al.*, 2006; Jager *et al.*, 2007; Larsen *et al.*, 2007; Matsuki *et al.*, 2003; Sauter *et al.*, 2008; Somm *et al.*, 2005). The IL-1 family is an important part of the innate immune system and consists of two agonists, IL-1α and IL-1β, a specific receptor antagonist called IL-1Ra, and two receptors, IL-1RI and IL-1RII. IL-1RI is biologically active while IL-1RII is biologically inert and functions as a decoy receptor (Colotta *et al.*, 1994). Importantly, IL-1β expression is increased in the WAT of obese subjects (Juge-Aubry *et al.*, 2004).

IL-1β is a major pro-inflammatory cytokine that is primarily produced by blood monocyte, tissue macrophages, and dendritic cells. B lymphocytes and natural killer (NK) cells also produce IL-1β (Dinarello, 2009; Martin and Wesche, 2002). Furthermore, an important pro-inflammatory property of IL-1β is its ability to increase the expression of adhesion molecules such as intercellular adhesion molecule-1 (ICAM) in mesenchymal cells and vascular cell adhesion molecule-1 (VCAM) in endothelial cells (Dinarello, 2009). Together with the induction of chemokines, these properties of IL-1β promote the infiltration of inflammatory and immunocompetent cells from the circulation into the extravascular space and then into tissues where tissue remodelling is the end result of chronic IL-1-induced inflammation (Dinarello, 2009). Therefore, IL-1 may pay an important role as macrophages and other immune cells infiltrate into the adipose tissue

during obesity leading to the inflamed state associated with type 2 diabetes mellitus (T2DM).

Chronic treatment with IL-1β i*n vitro* has been shown to decrease insulin sensitivity in adipocytes, and this is discussed in chapter 4. IL-1β may participate in concert with other cytokines, such as tumour necrosis factor (TNF)-α and IL-6, in the development of insulin resistant states (Jager *et al.*, 2007). Additionally, stimulation of cells by IL-1 agonist initiates the transcription of many other pro-inflammatory genes including IL-6 and IL-8 therefore increasing the pro-inflammatory environment of obese adipose tissue and adding to this concert of available cytokines. Interestingly, in a case/control study, individuals with detectable circulating levels of IL-1β and elevated levels of IL-6 had an increased risk to develop T2DM, compared with individuals with increased concentrations of IL-6 but undetectable levels of IL-1β (Spranger *et al.*, 2003). Furthermore, expression of both IL-1β and its receptor is increased in visceral adipose tissue (VAT) of obese subjects (Juge-Aubry *et al.*, 2004) and IL-1β levels are correlated with the metabolic syndrome (Salmenniemi *et al.*, 2004).

Serum levels of IL-1Ra are also significantly higher in obese compared with non-obese subjects and have a positive correlation with leptin concentrations and BMI (Meier *et al.*, 2002). Interestingly, IL-1Ra levels are highly correlated with insulin resistance and upon weight loss, the serum IL-1Ra levels decrease (Meier *et al.*, 2002). In a human trial conducted by Larsen *et al.* (2007) treatment with IL-1Ra was demonstrated to improve glycemic control in patients with T2DM, which correlated with improved measures of β-cell secretory capacity. At the doses used, there were no alterations in insulin sensitivity (Larsen *et al.*, 2007). However, Sauter and colleagues (2008) found that IL-1Ra treatment prevented diabetes *in vivo* in C57BL/6J mice fed a high fat diet (HFD) for 12 weeks (Sauter *et al.*, 2008). The IL-1Ra treatment improved glucose tolerance and insulin secretion. The HFD increased serum levels of free fatty acids, resistin and leptin, however the IL-1Ra treatment reduced these levels. In addition, IL-1Ra counteracted adiponectin levels, which were decreased by the HFD. Importantly, IL-1Ra protected islets from the HFD induced β-cell apoptosis and improved β cell proliferation and enhanced glucose-stimulated insulin secretion (Sauter *et al.*, 2008).

Conversely, Matsuki *et al.* (2003) reported that excess IL-1 activity due to gene knockout of the IL-1Ra in mice caused leanness and resistance to diet-induced obesity, without any overt signs of illness (Matsuki *et al.*, 2003). Correspondingly, Somm *et al.* (2005) found that the blood insulin:glucose ratio was significantly lower in IL-1Ra$^{-/-}$

animals, which is compatible with an increased sensitivity to insulin, reinforced by the fact that the insulin content and pancreatic islet morphology of IL-1Ra$^{-/-}$ animals were normal (Somm *et al.*, 2005).

In a recent study by Garcia *et al.* (2006), obese IL-1RI$^{-/-}$ mice with reduced IL-1 activity showed increased body weights after 5 - 6 months of age compared to WT. Obese IL-1RI$^{-/-}$ mice were found to be insulin resistant, as evident by hyperinsulinemia, decreased glucose tolerance and decreased insulin sensitivity. This obese phenotype was preceded by decreased leptin sensitivity, fat utilization and locomotor activity. Their explanation for the decreased leptin sensitivity is that leptin actions in the brain may be dependent on IL-1 (Garcia *et al.*, 2006). Leptin regulates energy balance through its actions in the brain on appetite and energy expenditure. Luheshi *et al.* (1999) injected leptin into rats intracerebroventricularly or peripherally and found it induces significant dose-dependent increases in core body temperature as well as suppression of appetite. Furthermore, injection of leptin increased levels of IL-1β in the hypothalamus of normal Sprague–Dawley rats. Central injection of IL-1Ra inhibited the suppression of food intake caused by central or peripheral injection of leptin and abolished the leptin-induced increase in body temperature in both cases. Importantly, they observed that IL-1RI$^{-/-}$ mice showed no reduction in food intake in response to leptin, therefore suggesting leptin action in the brain is dependent on IL-1 signaling (Luheshi *et al.*, 1999).

Both IL-1 agonists and the IL-1RI are expressed within the hypothalamus (Ericsson *et al.*, 1995; Quan *et al.*, 1994) and IL-1 is therefore proposed to play an important role in the responses to acute infectious illness. Infectious responses include negative energy balance, characterized by reduced food intake, weight loss, increased thermogenesis and fever (Garcia *et al.*, 2006). Interestingly, injection of IL-1 (Dinarello, 1996; Moldawer *et al.*, 1988; Plata-Salaman, 1994; Plata-Salaman *et al.*, 1988) like many other cytokines such as IL-6 (Plata-Salaman, 1988; Plata-Salaman, 1996), IL-8 (Plata-Salaman and Borkoski, 1993; Plata-Salaman and Borkoski, 1994), TNF-α (Fong *et al.*, 1989; Plata-Salaman, 1989) and IFNγ (Plata-Salaman, 1992) can induce anorexia. IL-1β induces anorexia when administered acutely or chronically into the brain in low doses (picomolar range) (Plata-Salaman *et al.*, 1996; Sonti *et al.*, 1996) whereas peripheral administration consistently requires much larger doses (microgram range), suggesting that IL-1β acts directly on the CNS (Plata-Salaman, 1989). In preclinical studies the effects of IL-1β in inducing anorexia were attenuated by the IL-Ra (Plata-Salaman and Ffrench-Mullen, 1992).

Somm and colleagues (2005) demonstrated that IL-1Ra$^{-/-}$ mice have a lean phenotype due to decreased fat mass, related to a defect in adipogenesis and increased

energy expenditure (Somm *et al.*, 2005). The adipocytes were smaller in these animals and the expression of genes involved in adipogenesis was reduced. Energy expenditure as measured by indirect calorimetry was elevated, and weight loss in response to a 24 hour fast was increased in IL-1Ra$^{-/-}$ animals compared with wild-type mice. Interestingly, Somm *et al.* (2005) observed that IL-1Ra$^{-/-}$ mice have an increase in food intake with respect to their body weight when fed a normal diet, and this is possibly the consequence of decreased blood leptin levels, reflecting reduced WAT stores (Somm *et al.*, 2005).

In summary, within the IL-1Ra$^{-/-}$ mice that presumably have an up-regulated IL-1 pathway there is a reduction in body weight and an improvement in insulin sensitivity. However, in IL-1R1$^{-/-}$ mice where the IL-1 pathway is most likely reduced there is increased body weight with insulin resistance. This seems counterintuitive to initial *in vivo* trials examining the effects of IL-1Ra treatment. IL-1Ra reduces IL-1 activity and improved glucose tolerance and insulin secretion suggesting it may have a potential therapeutic role in the treatment of T2DM. However, IL-1 agonists have been shown to produce weight loss and increase energy expenditure within whole organisms, which correlates with the reduction in body weight observed in the IL-1Ra$^{-/-}$ mice. Nevertheless, IL-1β treatment *in vitro* seems to reduce insulin sensitivity and markers of insulin sensitivity while up-regulating the pro-inflammatory state which does not correspond with the IL-1Ra$^{-/-}$ and IL-1RI$^{-/-}$ models as yet. It is clear the IL-1 pathway has multiple effects, depending on cell type and organ being examined within the obese state. Furthermore, the mechanism in which the IL-1 pathway is manipulated seems critical to the final obese and insulin resistant state observed. Previous work from our group demonstrated that IL-1RI$^{-/-}$ mice are partially protected against obesity induced insulin resistance (De Roos *et al.*, 2009).

3.2 Material and methods

3.2.1 Experimental design

As described in section 2.2.1, IL-1RI$^{-/-}$ (C57BL/6 background sourced from Jackson Laboratories) and C57BL/6 WT control (purchased from Harlan Laboratories) 6 week old male mice were held at the BioResources Unit of Trinity College Dublin under specific pathogen-free conditions. Ethical approval was obtained from the Trinity College Dublin Ethics Committee and mice were maintained according to the regulations of the European Union and the Irish Department of Health that govern the use of animals in research. IL-1RI$^{-/-}$ and C57BL/6 control mice were each fed a HFD (45% Kcal from fat) for up to 16 weeks. Body weights and food intake were recorded every 2 weeks.

3.2.2 Glucose Tolerance Test

GTTs were performed on C57BL/6 WT mice and IL-1RI$^{-/-}$ mice at weeks 0, 4, 6, 12 and 16 of the HFD as described in section 2.1.2. Mice were fasted for 6 hours prior to the GTT. A 25% w/v glucose load (1.2 g/kg body weight) was administered with an intra-peritoneal (IP) injection. Blood was sampled by tail bleed at time points 0, 15, 30, 60, 90 and 120 minutes after glucose IP injection. Glucose was measured in mMol/L immediately with a glucose meter from Accu-Chek (Roche Ltd.). Blood was collected in a capillary tube and spun at 15,000 rpm for 5 minutes; insulin levels were measured at time points 0, 30 and 60 minutes using a commercially available ELISA kit from Mercodia as described in section 2.9.1.

3.2.3 Tissue and plasma collection

At weeks 0, 6, 8, 12 and 16 of the HFD animals were fasted for 4 hours and culled by CO_2 inhalation. Epididymal adipose tissue (EAT), VAT from WAT, skeletal muscle from the hind leg, liver, kidney and pancreas samples were harvested. All tissue aliquots (~100 mg) for RNA and protein analysis were immediately snap frozen in liquid nitrogen and transferred to a freezer for storage at -80°C. A proportion of the EAT was prepared for adipocyte isolation and a second portion was placed in 10% neutral buffered formalin for histology. Fasting blood sample was taken from the heart using a needle and syringe. The blood was transferred into an eppendorf and centrifuged at 15,000 rpm for 5 minutes. The plasma supernatant was extracted, aliquoted and frozen at -80°C. Plasma adipokine and cytokine profiles were determined using Milliplex multi-analyte profiling from Millipore. Plasma triglycerides (TAG) and non-esterified fatty acids (NEFA) were measured using commercially available enzyme assay kits from Randox as described in section 2.1.6.

3.2.4 Adipocyte isolation

A portion of the fresh adipose tissue was taken and sliced into small pieces. A collagenase buffer containing Krebs ringer bicarbonate buffer with 4% BSA and 2 mg/ml collagenase was added to the adipose and incubated for 70 minutes in a shaking water bath at 37°C as described in section 2.1.4. The partially digested adipose tissue was then flushed through a polypropylene filter (500 μm) to separate the cells. The cells were then spun at 1,500 rpm for 5 minutes to isolate the mature adipocytes from the stromal vascular cells (SVF). The mature adipocytes float and therefore were collected from the surface of the buffer. The adipocytes were washed as described in section 2.1.4 and frozen in liquid nitrogen prior to storage at –80°C

3.2.5 Determination of adipocyte size

A proportion of the EAT was placed in 10% neutral buffered formalin. The histology techniques used are explained in more detail in section 2.1.7. Briefly, the samples were firstly dehydrated in an automatic processor. The samples were then embedded in paraffin wax and the tissue cut into 5 μm thick sections. The sections were placed on slides and de-paraffinized. Subsequently, the samples were hydrated and stained with Hematoxylin followed by eosinas. Hematoxylin stains the nuclei blue and eosin stains the cytoplasm pink. The stained slides were dehydrated and mounted. Images were taken on an Eclipse LV-Universal Design Microscope (Nikon Corporation) and the adipocyte area was measured in μm^2 using the NIS-Elements Software (Nikon Corporation).

3.2.6 Milliplex multi-analyte profiling

Multi-analyte profiling (MAP) allows simultaneous detection of multiple analytes within a small sample size. Adiponectin, granulocyte macrophage colony-stimulating factor (GM-CSF), interferon (IFN)-γ, IL-10, IL-12(p70), IL-13, IL-1β, IL-2, IL-4, IL-5, IL-6, IL-9, insulin, keratinocyte-derived chemokine (KC), Leptin, monocyte chemotactic protein (MCP)-1 also known as CC chemokine ligand (CCL)-2, macrophage inflammatory protein (MIP)-1α, regulated upon activation, normal T cell expressed and secreted (RANTES) also known as CCL5, resistin and TNF-α concentrations were determined in pg/ml. Plasma aliquots were prepared and delivered to Millipore for analysis (Millipore UK Ltd, Dundee, UK). The MAP technique used is explained in more detail in section 2.1.5. Briefly, the Millliplex plate consists of wells containing polystyrene microspheres. The microspheres are dyed with two fluorophores in different ratios; this is used to uniquely identify each

bead. Antibodies to the target molecules or capture antibody are immobilized on the specific microbeads. The plasma samples are then mixed with the microbeads and the target antigen molecules bind to the antibodies on the microbead forming an immune complex. Detection antibody is then added to the beads and this binds to the antigen. This is followed by streptavidin-phycoerythrin (S-PE), which binds to the detection antibody. The beads are then passed through a detection chamber (Luminex® 200™ analyser; Luminex Corporation). A red laser excites the internal red/infrared dyes and classifies the microbead allowing identification of the target antigen, while a green laser excites the orange fluorophore of S-PE allowing quantification of the antigen. The data is assessed with xPonent Software (Luminex Corporation). A standard curve is generated for each cytokine and chemokine within every assay and sample concentrations were calculated through the equation of the standard curve.

3.2.7 mRNA analysis (TaqMan® RT-PCR)

Total RNA was extracted from approximately 100 mg of adipose tissue or 500 µl of isolated adipocytes using RNeasy Mini kit from Qiagen as described in section 2.7.1. After extraction RNA was quantified using the Nano-drop and quality was assessed using the bioanlyser as described in section 2.7.2. RNA was deoxyribonucleic acid (DNase) treated and cDNA was synthesised using SuperScript® VILO™ (Invitrogen Corporation) as described in sections 2.7.4 and 2.7.5 respectively. RNA was quantified using an ABI PRISM 7900HT sequence detection system and a 384 well plate as described in section 2.7.6. Briefly, each 10 µl reaction contained 0.5 µl of cDNA, 5 µl TaqMan® 2 X Master mix, 0.5 µl TaqMan® pre-developed target primer probe kits with forward and reverse primers and 4 µl DEPC treated water. Insulin receptor substrate (IRS)-1, insulin receptor, glucose transporter (GLUT)-4, peroxisome proliferator-activated receptor (PPARγ), sterol regulatory element–binding protein (SREBP)-1c, resistin, adiponectin, adiponectin receptor 1 and 2 (AdipoR1 and 2), TNF-α, IL-6, IL-1RI, IL-1RII, IL-1β, IL-1Ra, MCP-1, MIP-1α, MIF and the endogenous control 18S were investigated using pre-developed primer probe kits. All reagents necessary for running a TaqMan® RT-PCR assay were purchased from Perkin-Elmer Applied Biosystems. The comparative Ct method or ΔΔCt method was used to calculate gene expression levels. The Ct values of both the control and the samples of interest were normalized to an appropriate endogenous housekeeping gene, in this case 18S, and expressed relative to the appropriate control.

3.2.8 Data preparation and statistical analysis

Data was reported as Mean ± SEM. Statistical analysis was performed with SPSS (SPSS Inc.). The distribution of data for each variable was assessed and variables transformed to normalise the distribution of data if necessary. The Mauchly's test of Sphericity was used to validate repeated measure factor ANOVA of the plasma glucose levels between groups over time in the GTT. When the significance level of the Mauchly's test is ≤ 0.05 then sphericity cannot be assumed. The correction used for violations of sphericity was Greenhouse-Geisser. Multiple comparisons were performed by one-way ANOVA. Significant inter-group differences were subsequently tested by post hoc Bonferroni statistical analysis. Independent Student's t-tests (2 tailed) were performed between the C57BL/6 WT and the IL-1R1$^{-/-}$ groups. A statistical probability of $P \leq 0.05$ was considered statistically significant.

3.3 Results

3.3.1 Phenotypic attributes of WT of IL-1RI$^{-/-}$ and WT mice at base line

The phenotypic attributes of both WT and IL-1RI$^{-/-}$ groups at base line of the 16 week HFD intervention are shown in Table 3.1. At week 0 of the study there were no significant difference in body weight, epididymal and visceral adipose tissue (EAT and VAT) mass, EAT adipocyte size, fasting plasma glucose, insulin, non-esterified fatty acids (NEFA), resistin, adiponectin, CC chemokine ligand (CCL)-5, IL-1β and TNF-α mRNA expression levels between groups.

However, fasting plasma triacylglycerol (TAG) and leptin concentrations were significantly reduced (53% and 67% decrease) in the IL-1RI$^{-/-}$ mice relative to the WT group ($P \leq 0.001$ and $P \leq 0.003$ respectively) at week 0 of the study. Interestingly, mRNA expression of GLUT4, IRS-1, PPAR-γ and monocyte chemotactic protein (MCP)-1 were significantly higher (6.7, 5.2, 2.2, and 6.3 fold increase) in the IL-1RI$^{-/-}$ mice relative to WT ($P \leq 0.001$, $P \leq 0.003$, $P \leq 0.013$ and $P \leq 0.001$ respectively) at base line.

Table 3.1 Phenotypic attributes of IL-1RI$^{-/-}$ and WT mice at week 0. At week 0 body weight (g), epididymal and visceral adipose tissue (EAT and VAT) fat mass (g) were recorded within WT and IL-1R$^{-/-}$ mice. EAT and VAT mass was measured after extraction from the mouse as a crude measure of fat deposition. EAT adipocyte size (μm^2) was measured at base line from microscope images taken of adipose sections stained with Hematoxylin and eosin. Fasting plasma glucose was determined in 6 hour fasted mice; glucose (mMol/L) was measured from a tail bleed. Fasting plasma insulin (pMol/L), triacylglycerol (TAG, mMol/L), non-esterified fatty acids (NEFA, mMol/L), leptin (pg/ml), resistin (pg/ml), adiponectin (pg/ml), CC chemokine ligand (CCL)-5 (pg/ml) and IL-1β (pg/ml) were measured in 4 hour fasted WT and IL-1RI$^{-/-}$ mice at base line using either enzyme assays or milliplex Multi-analyte profiling (MAP). mRNA expression of GLUT4, IRS-1, PPAR-γ, MCP-1 and TNF-α were also determined within the EAT at week 0 of the 16 week HFD study. RNA was harvested and mRNA levels were measured using RT-PCR. mRNA levels were normalized to 18S and the results are expressed as fold induction relative to WT. Values are expressed as mean ± SEM. *** $P \leq 0.001$, ** $P \leq 0.01$, * $P \leq 0.05$ relative to WT. An independent Student's t-test was performed on the IL-1RI$^{-/-}$ vs. WT.

	Wild Type			IL-1RI$^{-/-}$			
	n	**Mean**	**SEM**	**n**	**Mean**	**SEM**	**P value**
Body Weight (g)	25	22.84	0.34	20	23.18	0.85	0.69
EAT Mass (g)	10	0.39	0.02	9	0.37	0.05	0.66
VAT Mass (g)	10	0.31	0.03	9	0.28	0.04	0.60
Adipocyte Size (μm^2)	7	1071.31	89.72	10	1318.90	124.37	0.16
Plasma Glucose (mMol/L)	8	8.53	0.33	8	9.04	0.46	0.38
Plasma Insulin (pMol/L)	5	215.75	7.58	6	169.12	10.71	0.19
Plasma TAG (mMol/L)	6	0.87	0.04	6	0.40	0.06	0.00***
Plasma NEFA (mMol/L)	5	0.12	0.05	6	0.12	0.02	0.95
Plasma Leptin (pg/ml)	6	1631.67	98.01	6	530.36	54.91	0.00**
Plasma Resistin (pg/ml)	6	1700.83	55.16	6	1537.42	73.08	0.48
Plasma Adiponectin (pg/ml)	6	8258.33	228.12	6	7425.83	643.70	0.63
Plasma CCL5 (pg/ml)	6	90.08	3.44	6	118.01	12.16	0.39
Plasma IL-1β (pg/ml)	6	27.38	2.41	6	47.05	3.21	0.07
EAT GLUT4 (mRNA)	6	1.00	0.28	4	6.65	0.68	0.00***
EAT IRS-1 (mRNA)	6	1.00	0.31	4	5.17	1.06	0.00**
EAT PPAR-γ (mRNA)	6	1.00	0.18	4	2.24	0.36	0.01*
EAT MCP-1 (mRNA)	6	1.00	0.27	4	6.34	0.92	0.00***
EAT TNF-α (mRNA)	4	1.00	0.21	4	1.45	0.34	0.37

3.3.2 Effects of a 16 week HFD on body weight, food intake and adipose tissue mass in IL-1RI$^{-/-}$ and WT mice

The body weights and food intake of the IL-1RI$^{-/-}$ and WT groups during the 16 week HFD are presented in Figures 3.1 and 3.2 respectively. Body weight was significantly decreased in the IL-1R1$^{-/-}$ at week 6, 8, 10 and 12 of the HFD compared to WT ($P \leq 0.034$, $P \leq 0.040$, $P \leq 0.002$, $P \leq 0.013$ respectively). Interestingly, food intake was significantly higher at 8, 12 and 16 weeks HFD in the IL-1RI$^{-/-}$ mice compared to WT ($P \leq 0.010$, $P \leq 0.004$, $P \leq 0.002$).

The weights of EAT and VAT extracted from the WT and IL-1RI$^{-/-}$ groups at week 0 and 16 of the HFD are presented in Figure 3.3. After 16 weeks on the HFD both the IL-1RI$^{-/-}$ mice and WT mice showed a significant increase in EAT ($P \leq 0.001$ and $P \leq 0.001$) and VAT ($P \leq 0.009$ and $P \leq 0.001$) accumulation compared to corresponding week 0 groups. However, after 16 weeks on a HFD, IL-1RI$^{-/-}$ had significantly lower EAT (52% decrease) and VAT (59% decrease) mass compared to WT ($P \leq 0.002$, $P \leq 0.006$ respectively).

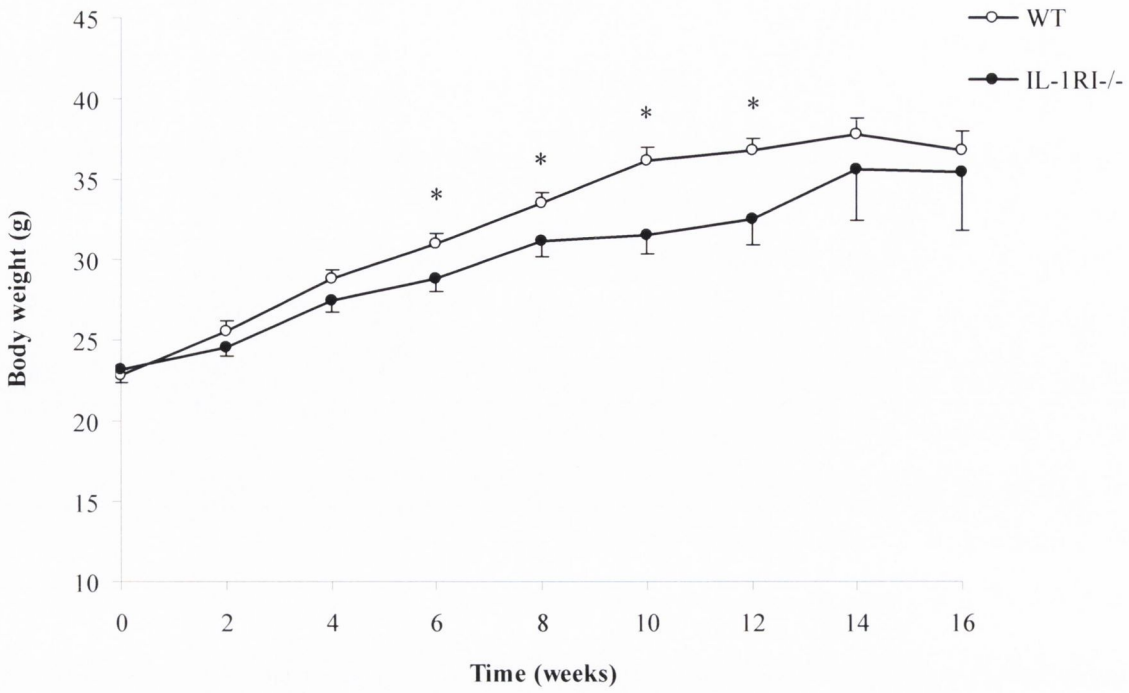

Figure 3.1 Effects of a 16 week HFD on body weight in male IL-1RI$^{-/-}$ and wild type (WT) mice. Body weight (g) was measured every 2 weeks, n = 6 - 25. Values are expressed as mean ± SEM. * $P \leq 0.05$ relative to wild type. An independent Student's t-test was performed on the IL-1R1$^{-/-}$ groups vs. the corresponding WT groups.

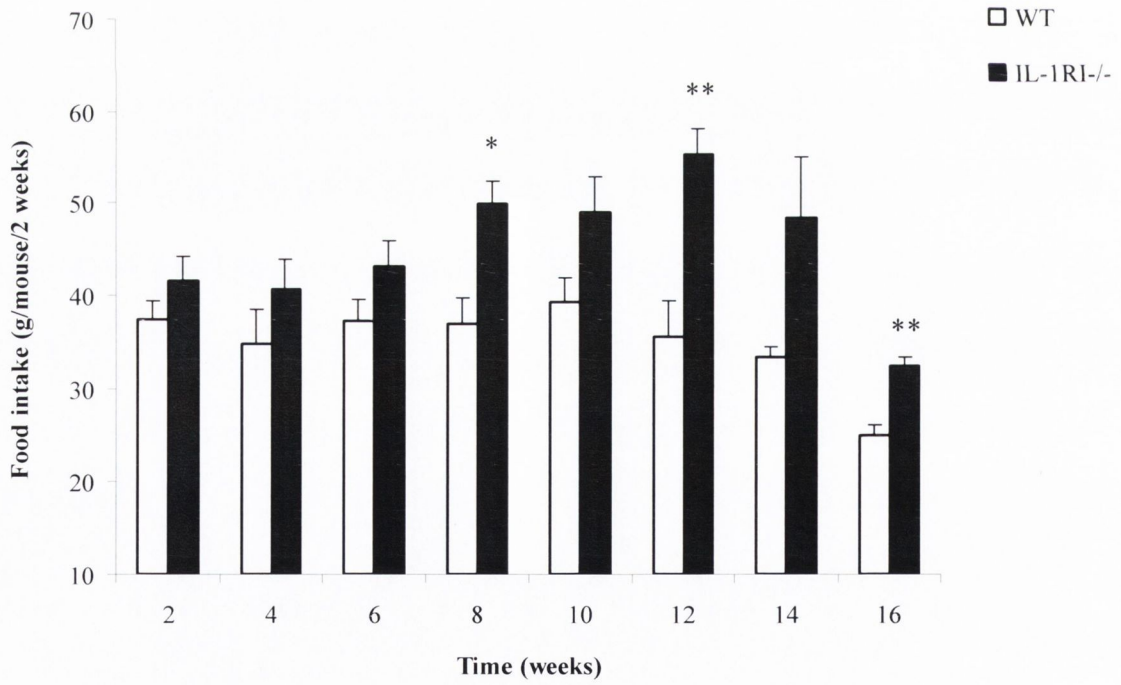

Figure 3.2 Effect of a 16 week HFD on food intake in male IL-1RI$^{-/-}$ and WT mice. Food consumption (g) was measured every two weeks for each cage and divided by the number of mice within the cage, n = 14 – 23. Values are expressed as mean ± SEM. * $P \leq 0.05$, ** $P \leq 0.01$, relative to wild type. An independent Student's t-test was performed on the IL-1R1$^{-/-}$ groups vs. the corresponding WT groups.

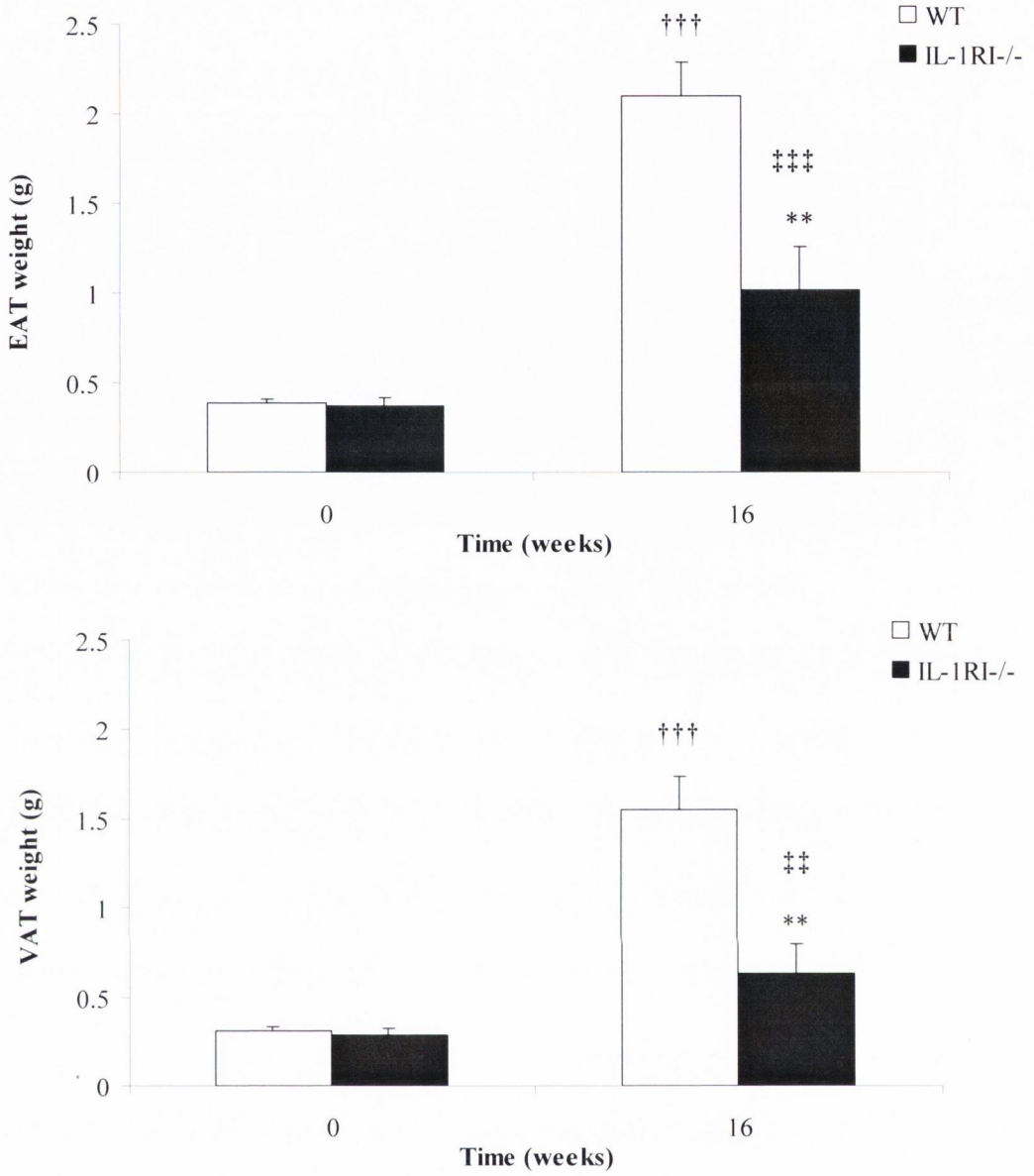

Figure 3.3 Effect of a 16 week HFD on epididymal and visceral adipose tissue (EAT and VAT) accumulation in male IL-1RI$^{-/-}$ and WT mice. EAT and VAT were weighed (g) after extraction from the mouse as a crude measure of fat deposition, n = 5 - 10. Values are expressed as mean ± SEM. ††† $P \leq 0.001$ relative to week 0 WT; ‡‡ $P \leq 0.01$, ‡‡‡ $P \leq 0.001$ relative to week 0 IL-1RI$^{-/-}$. ** Indicates $P \leq 0.01$, relative to wild type. An independent Student's t-test was performed between the IL-1R1$^{-/-}$ groups vs. the corresponding WT groups and within the IL-1RI$^{-/-}$ and WT groups week 0 vs week 16.

3.3.3 Effects of a 16 week HFD on glucose tolerance in male IL-1RI$^{-/-}$ and WT mice

The GTT in IL-1RI$^{-/-}$ and WT mice at week 0, 4, 6, 12 and 16 of the HFD are presented in Figures 3.4, 3.5, 3.6, 3.7 and 3.8 respectively. At week 0 the glucose response of the IL-1RI$^{-/-}$ group significantly differed ($P \leq 0.049$) from that of the WT group at week 0 as determined by repeated measures ANOVA. The IL-1R1$^{-/-}$ group had a significantly higher peak of glucose 15 minutes after injection (27% increase; $P \leq 0.023$) but then recovered 30 minutes post injection with no significant difference between groups at 30, 90 and 120 minutes. After 4 weeks on the HFD there was no significant difference in the glucose response between groups. However, after 6 weeks HFD the glucose response in IL-1RI$^{-/-}$ group significantly differed from the WT ($P \leq 0.008$). The plasma glucose levels 15 minutes post injection were significantly higher (17% increase) in the IL-1RI$^{-/-}$ group ($P \leq 0.050$). In contrast, at 60 and 120 minutes post injection the plasma glucose levels were significantly lower (23% and 24% decreases) in the IL-1RI$^{-/-}$ group compared to the WT group ($P \leq 0.049$ and $P \leq 0.035$ respectively), indicative of enhanced glucose clearance within the IL-1RI$^{-/-}$ mice. After 12 weeks HFD there was no significant difference between groups. Interestingly, after 16 weeks HFD the IL-1RI$^{-/-}$ group significantly differed from that of the WT group ($P \leq 0.022$). At 60 and 120 minutes post injection the plasma glucose levels were lower in the IL-1RI$^{-/-}$ group ($P \leq 0.052$ and $P \leq 0.056$ respectively).

Area under the curve (AUC) measurements of the glucose response over the 120 minute GTT are shown in Figure 3.9. Within the IL-1RI$^{-/-}$ group the glucose response significantly increased at week 12 and 16 of the HFD relative to week 0 ($P \leq 0.015$ and $P \leq 0.033$; Figure 3.9a). The glucose response was also increased at week 12 relative to week 4 of the HFD ($P \leq 0.037$). In the WT group the glucose response was significantly increased at weeks 6, 12 and 16 of the HFD relative to week 0 ($P \leq 0.001$, $P \leq 0.017$ and $P \leq 0.001$ respectively; Figure 3.9b). Furthermore, the glucose response was significantly increased at weeks 6 and 16 relative to week 4 ($P \leq 0.055$ and $P \leq 0.001$). However, there was no significant difference between groups at any of the weeks.

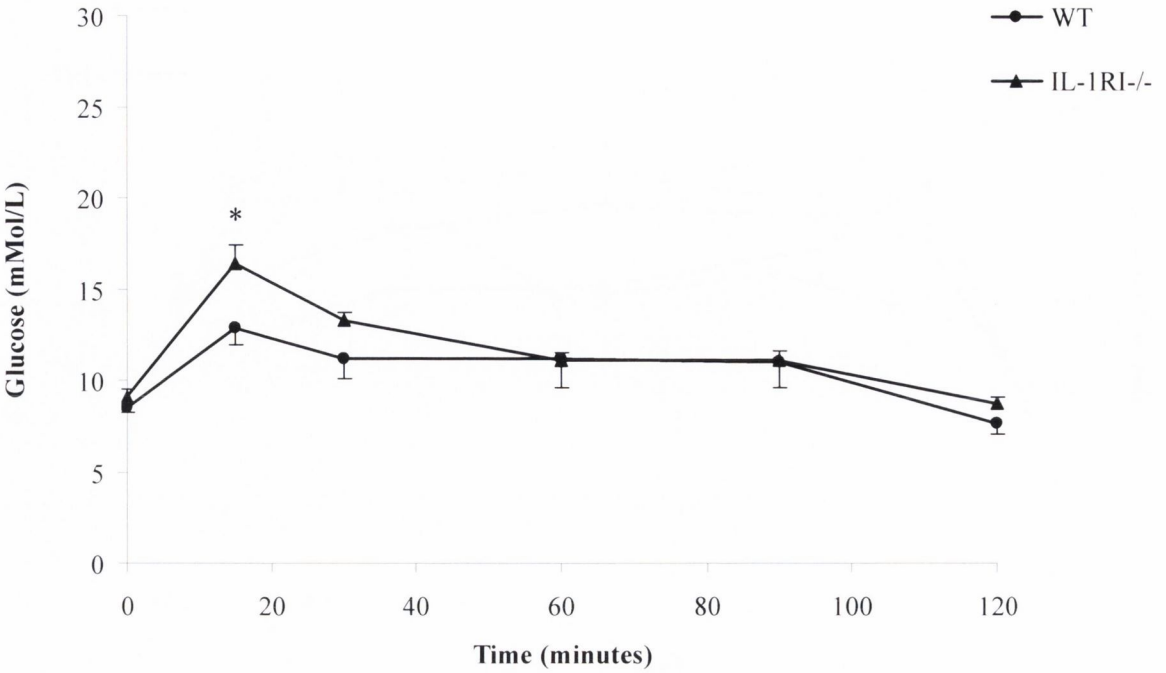

Figure 3.4 Effects of HFD on glucose tolerance in IL-1R1$^{-/-}$ and WT mice. At baseline a glucose load was administered to 6 hour fasted mice and glucose (mMol/L) was measured from a tail bleed blood sample at time points 0, 15, 30, 60 and 120 minutes post injection, n = 8. Values are means ± SEM. * $P \leq 0.05$ relative to WT. A repeated measure ANOVA was performed between groups. A significant inter-group difference was subsequently tested by independent Student's t-test (2 tailed).

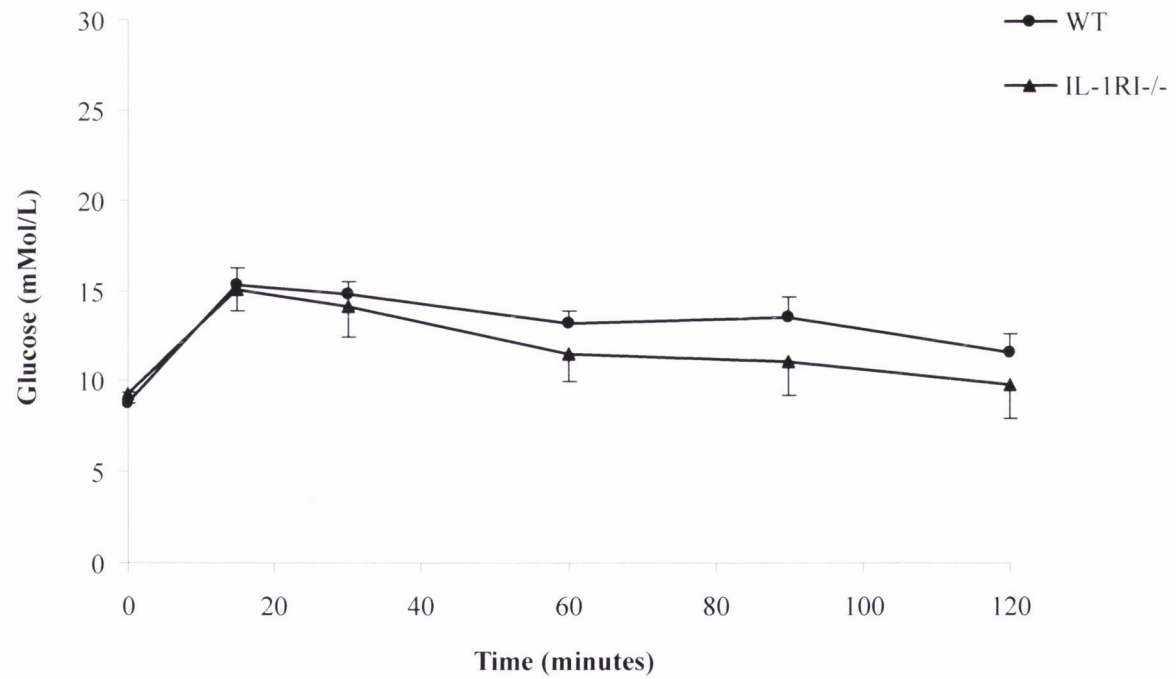

Figure 3.5 Effects of HFD on glucose tolerance in IL-1R1$^{-/-}$ and WT mice. After 4 weeks on a HFD a glucose load was administered to 6 hour fasted mice and glucose (mMol/L) was measured from a tail bleed blood sampled at time points 0, 15, 30, 60 and 120 minutes post injection. Values are means ± SEM, n = 6.

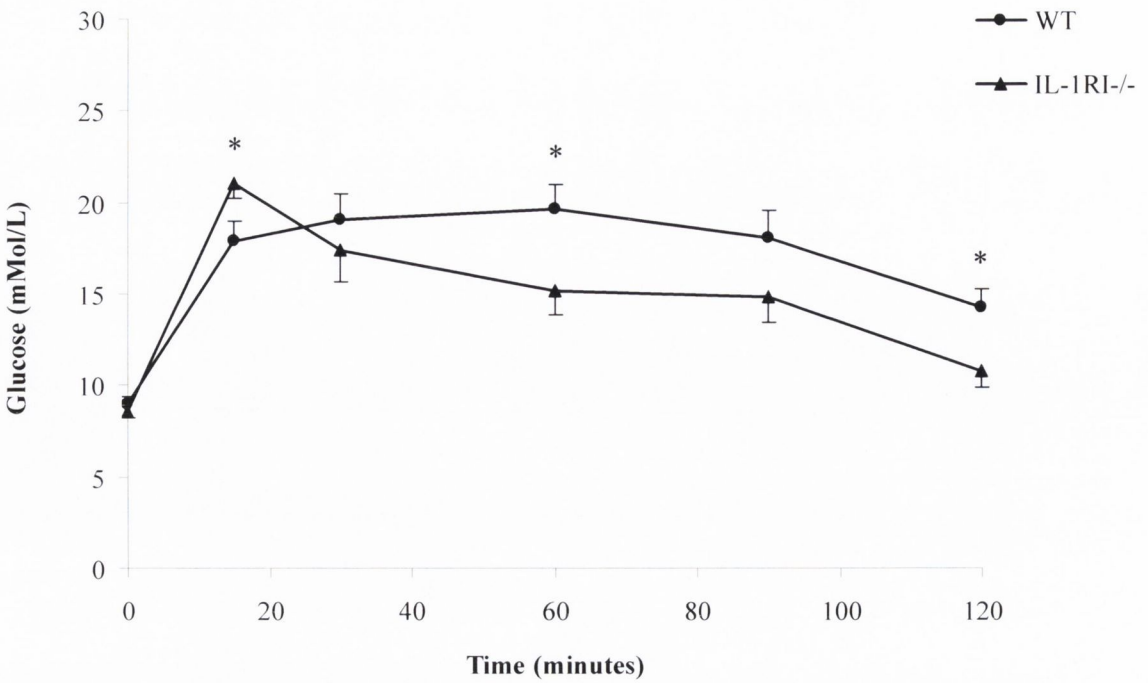

Figure 3.6 Effects of HFD on glucose tolerance in IL-1R1$^{-/-}$ and WT mice. After 6 weeks on a HFD a glucose load was administered to 6 hour fasted mice and glucose (mMol/L) was measured from a tail bleed blood sample at time points 0, 15, 30, 60 and 120 minutes post injection, n = 5 - 6. Values are means ± SEM. * $P \leq 0.05$ relative to wild type. A repeated measure ANOVA was performed between groups. A significant inter-group difference was subsequently tested by independent Student's t-test (2 tailed).

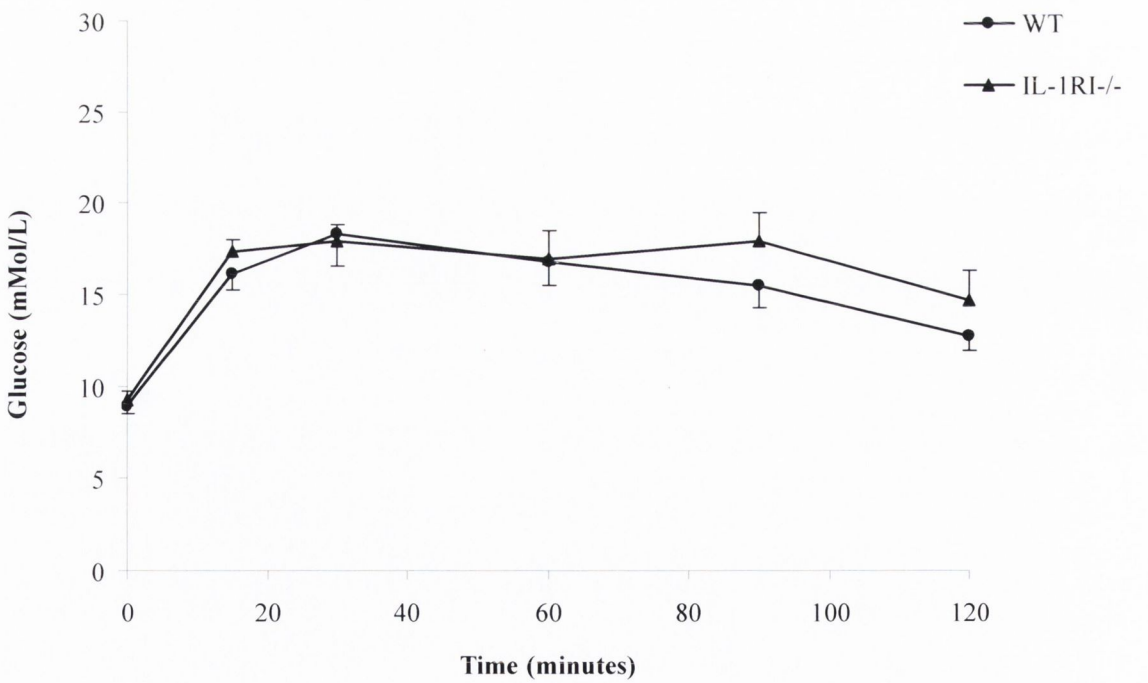

Figure 3.7 Effects of HFD on glucose tolerance in IL-1R1$^{-/-}$ and WT mice. After 12 weeks on a HFD a glucose load was administered to 6 hour fasted mice and glucose (mMol/L) was measured from a tail bleed blood sample at time points 0, 15, 30, 60 and 120 minutes post injection. Values are means ± SEM, n = 6.

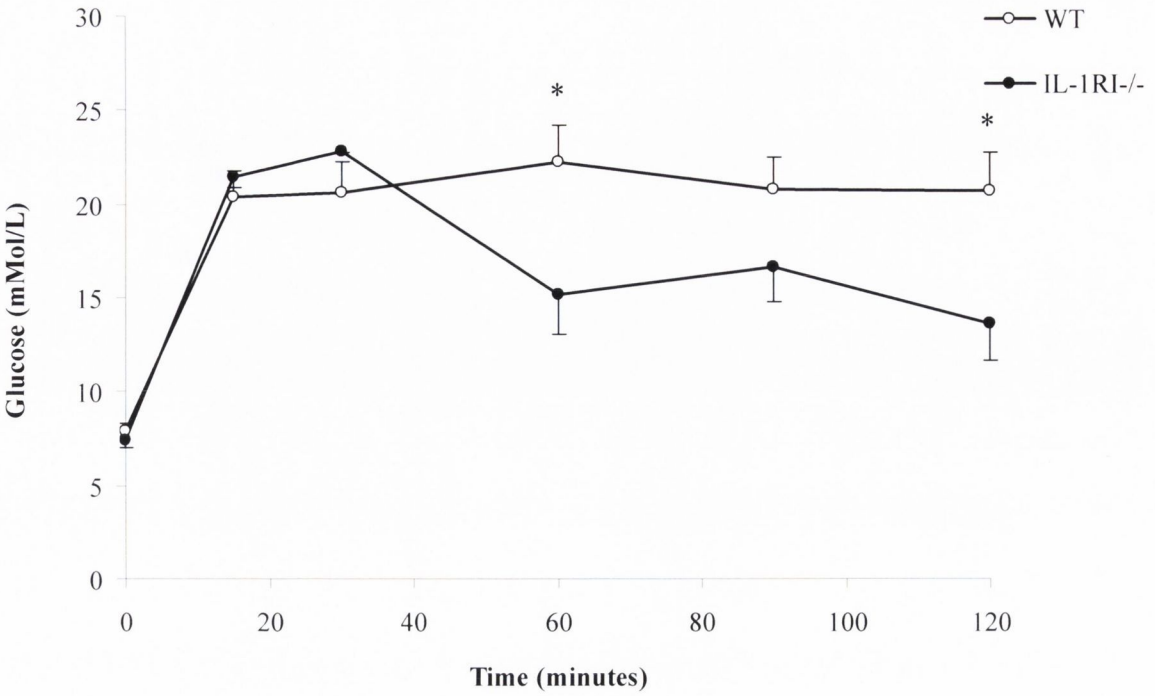

Figure 3.8 Effects of HFD on glucose tolerance in IL-1R1$^{-/-}$ and WT mice. After 16 weeks on a HFD a glucose load was administered to 6 hour fasted mice and glucose (mMol/L) was measured from a tail bleed blood sample at time points 0, 15, 30, 60 and 120 minutes post injection. Values are means ± SEM, n = 4 - 7. * $P \leq 0.06$ relative to wild type. A repeated measure ANOVA was performed between groups. A significant inter-group difference was subsequently tested by independent Student's t-test (2 tailed).

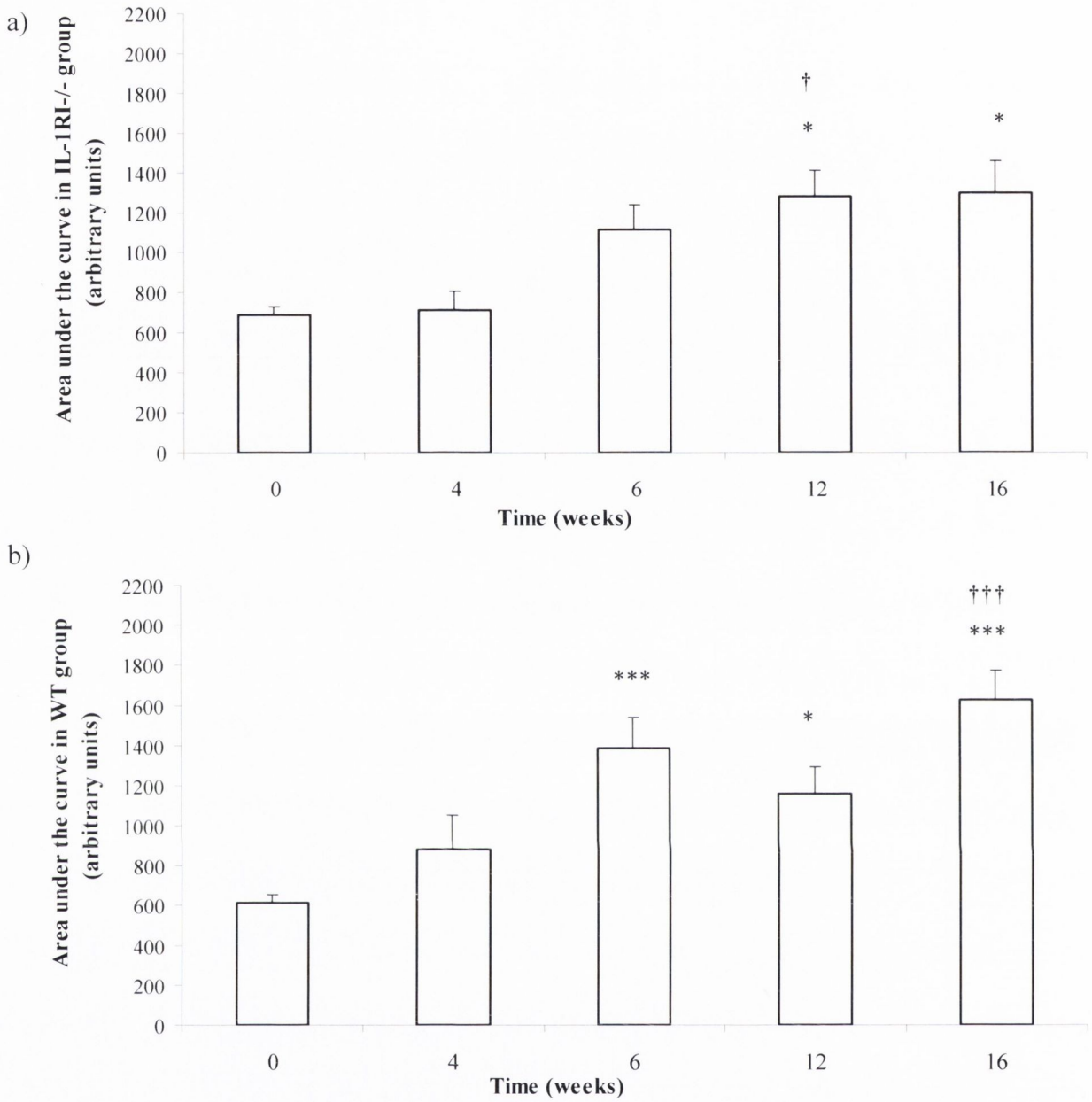

Figure 3.9 Effects of HFD on glucose tolerance in IL-1R1$^{-/-}$ (a) and WT (b) mice. Area under glucose curves during GTT (mMol/L × 120 minutes) at week 0, 4, 6, 12 and 16 of the HFD. Values are means ± SEM, n = 4 - 8. * $P \leq 0.05$, *** $P \leq 0.001$ relative to week 0; † $P \leq 0.05$, ††† $P \leq 0.001$ relative to week 4. A one-way ANOVA was performed between weeks within animal groups. Significant inter-group differences were subsequently tested by post hoc Bonferroni statistical analysis.

3.3.4 Effects of a 16 week HFD on plasma hormone concentrations in IL-1RI$^{-/-}$ and WT mice

Plasma insulin, resistin, leptin and adiponectin concentrations were assessed in fasting IL-1RI$^{-/-}$ and WT mice at week 0, 6, 8 and 12 HFD as presented in Figures 3.10, 3.11, 3.12, 3.13 and 3.14 respectively. Fasting plasma insulin concentrations (Figure 3.10) significantly increased (2.1 fold increase) from week 0 to 6 of the HFD in WT mice ($P \leq 0.020$). After 12 weeks HFD the IL-1RI$^{-/-}$ mice had significantly lower plasma insulin levels (31% decrease) as compared to WT ($P \leq 0.033$).

Fasting plasma leptin concentrations (Figure 3.11) significantly increased in the WT and IL-1RI$^{-/-}$ groups (15 fold and 9 fold increase) from week 0 to 12 ($P \leq 0.004$ and $P \leq 0.001$). However, fasting plasma leptin concentrations were significantly lower in the IL-1RI$^{-/-}$ mice at weeks 0, 6, 8 and 12 of the HFD (77%, 86%, 93% and 81% decrease) compared to WT ($P \leq 0.003$, $P \leq 0.004$, $P \leq 0.001$ and $P \leq 0.037$ respectively). Fasting plasma leptin levels corrected for body weight (Figure 3.12) increased in the WT and IL-1RI$^{-/-}$ group (10 fold and 6 fold increase) from week 0 to 12 ($P \leq 0.008$ and $P \leq 0.003$). However, fasting plasma leptin concentrations were significantly lower in the IL-1RI$^{-/-}$ mice at weeks 0, 6, 8 and 12 of the HFD (68%, 85%, 92% and 79% decrease) compared to WT ($P \leq 0.003$, $P \leq 0.005$, $P \leq 0.001$ and $P \leq 0.042$ respectively) when corrected for body weight. Furthermore, fasting plasma leptin concentrations corrected for body weight were significantly increased in the IL-1RI$^{-/-}$ mice at weeks 12 relative to week 8 of the HFD (73% increase) compared to WT ($P \leq 0.029$).

Fasting plasma resistin levels (Figure 3.13) significantly increased from week 0 to 6 (1.8 fold increase) of the HFD in the IL-1RI$^{-/-}$ mice ($P \leq 0.015$). Fasting plasma resistin levels were not significantly altered within the WT. Fasting plasma adiponectin levels (Figure 3.14) were also increased from weeks 0 to 6 (3.6 fold increase) and 0 to 12 (3.1 fold increase) of the HFD within the WT control mice ($P \leq 0.011$ and $P \leq 0.042$). Within the IL-1RI$^{-/-}$ group there was a significant increase in adiponectin levels (2.7 fold increase) from week 0 to 6 of the HFD ($P \leq 0.005$). After 12 weeks HFD there was a significant decrease in adiponectin levels (53% decrease) within the IL-1RI$^{-/-}$ group compared to the WT group ($P \leq 0.003$).

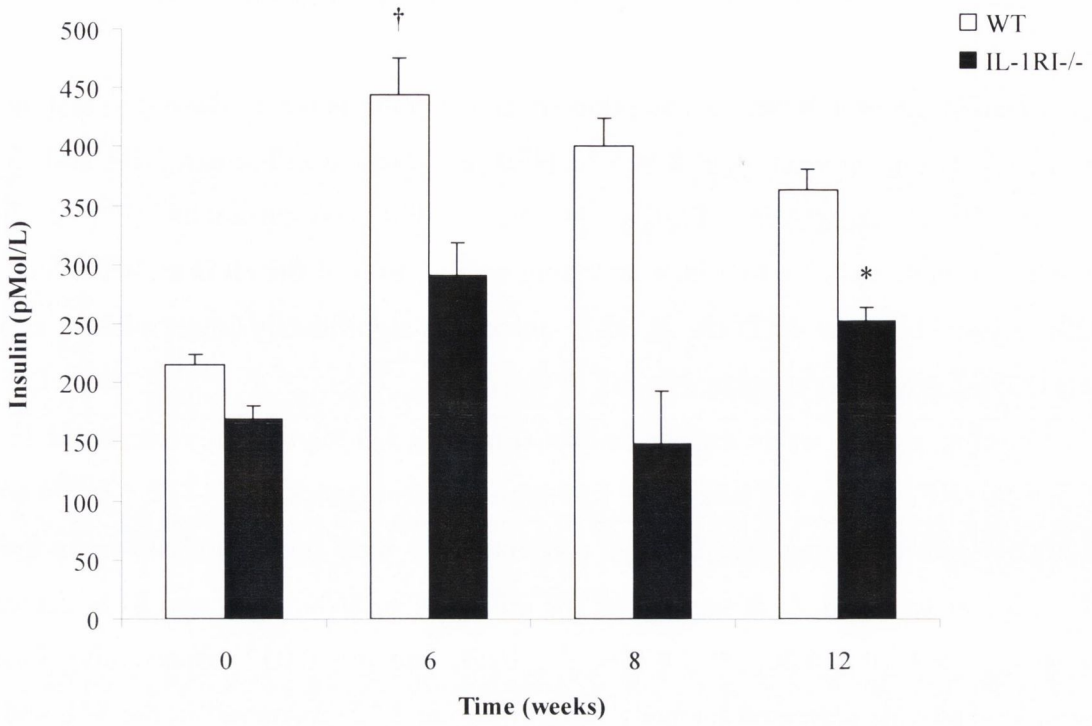

Figure 3.10 Effects of HFD on fasting plasma insulin levels in the WT and IL-1R1$^{-/-}$ mice. Fasting plasma insulin levels (pMol/L) were measured using milliplex MAP at week 0, 6, 8 and 12 of the HFD, n = 2 - 6. Values are means ± SEM. † $P \leq 0.05$ relative to week 0 WT; * $P \leq 0.05$ relative to WT. One-way ANOVA was performed within each group followed by post hoc Bonferroni testing. An independent Student's t-test was performed on the IL-1R1$^{-/-}$ groups vs. the corresponding WT group.

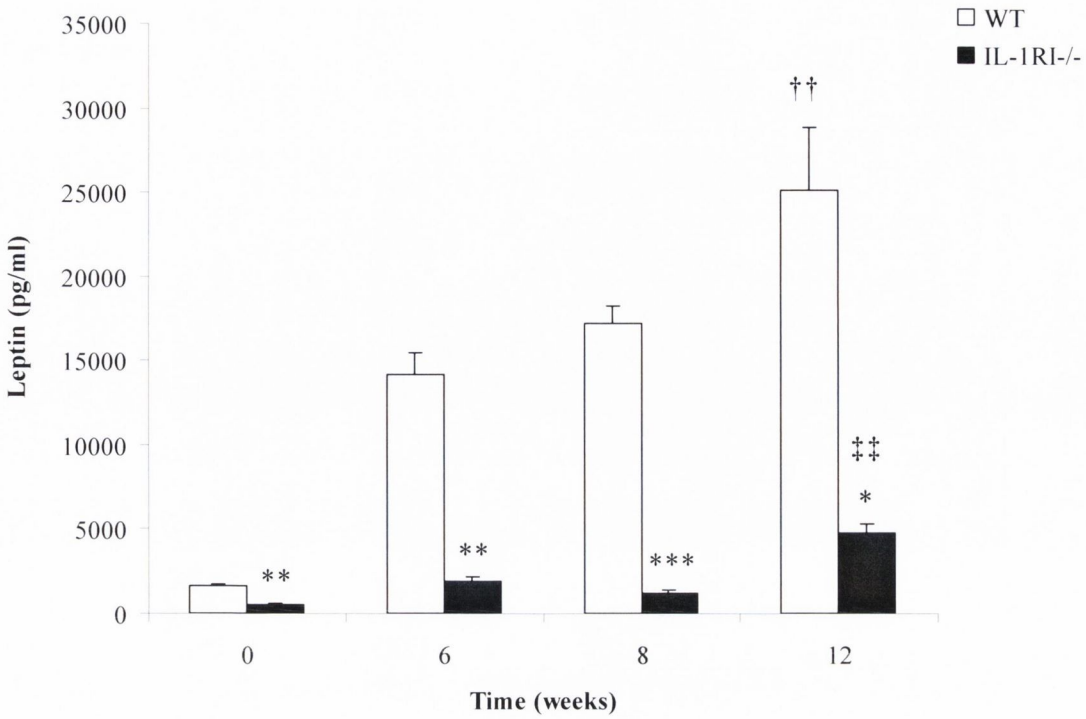

Figure 3.11 Effects of HFD on fasting plasma leptin levels in the WT and IL-1R1$^{-/-}$ mice. Fasting plasma leptin levels (pg/ml) were measured using milliplex MAP at week 0, 6, 8 and 12 of the HFD, n = 2 - 6. Values are means ± SEM. †† $P \leq 0.01$ relative to week 0 WT; ‡‡ $P \leq 0.01$ relative to week 0 IL-1RI$^{-/-}$; * $P \leq 0.05$, ** $P \leq 0.01$, *** $P \leq 0.001$ relative to WT. One-way ANOVA was performed within each group followed by post hoc Bonferroni testing. An independent Student's t-test was performed on the IL-1R1$^{-/-}$ groups vs. the corresponding WT group.

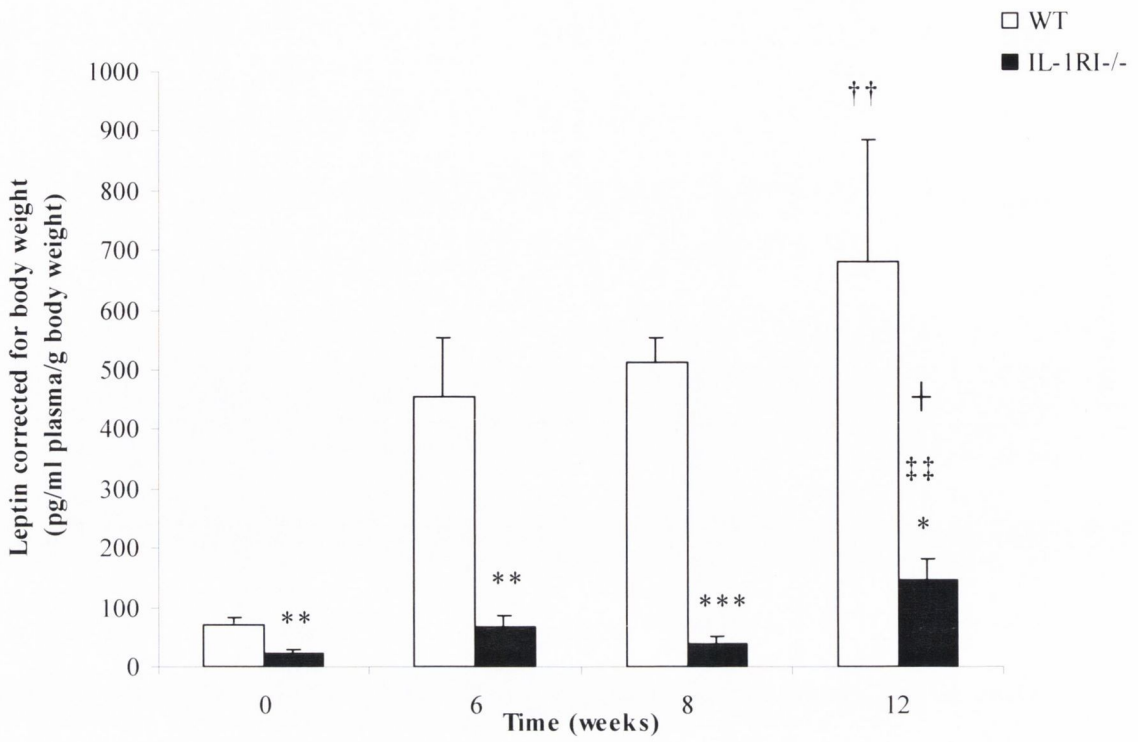

Figure 3.12 Fasting plasma leptin levels corrected for body weight in the WT and IL-1R1$^{-/-}$ mice during the HFD. Fasting plasma leptin levels (pg/ml) were measured using milliplex MAP at week 0, 6, 8 and 12 of the HFD, n = 2 - 6. Values are expressed relative to body weight and the graph shows means ± SEM. †† ≤ 0.01 relative to week 0 WT; ‡‡ P ≤ 0.01 relative to week 0 IL-1RI$^{-/-}$; ┼ P ≤ 0.05 relative to week 8 IL-1RI$^{-/-}$; * P ≤ 0.05, ** P ≤ 0.01, *** P ≤ 0.001 relative to WT. One-way ANOVA was performed within each group followed by post hoc Bonferroni testing. An independent Student's t-test was performed on the IL-1R1$^{-/-}$ groups vs. the corresponding WT group.

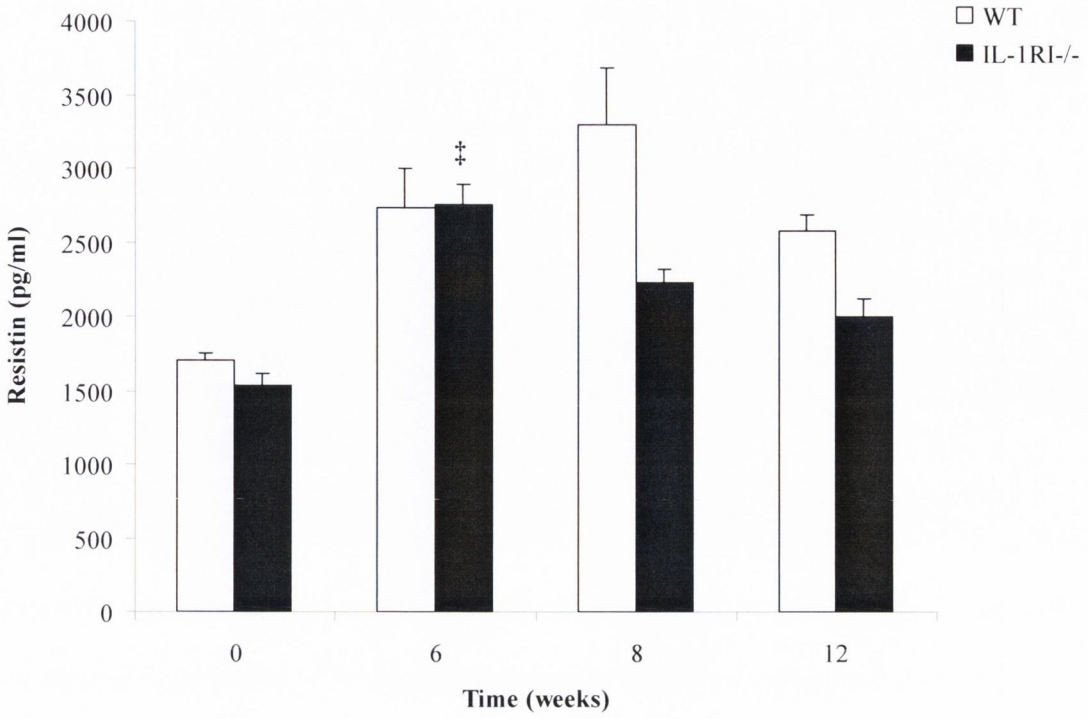

Figure 3.13 Effects of HFD on fasting plasma resistin levels in the WT and IL-1R1$^{-/-}$ mice. Fasting plasma resistin levels (pg/ml) were measured using milliplex MAP at week 0, 6, 8 and 12 of the HFD, n = 2 - 6. Values are means ± SEM. ‡ $P \leq 0.01$ relative to week 0 IL-1RI$^{-/-}$. One-way ANOVA was performed within each group followed by post hoc Bonferroni testing.

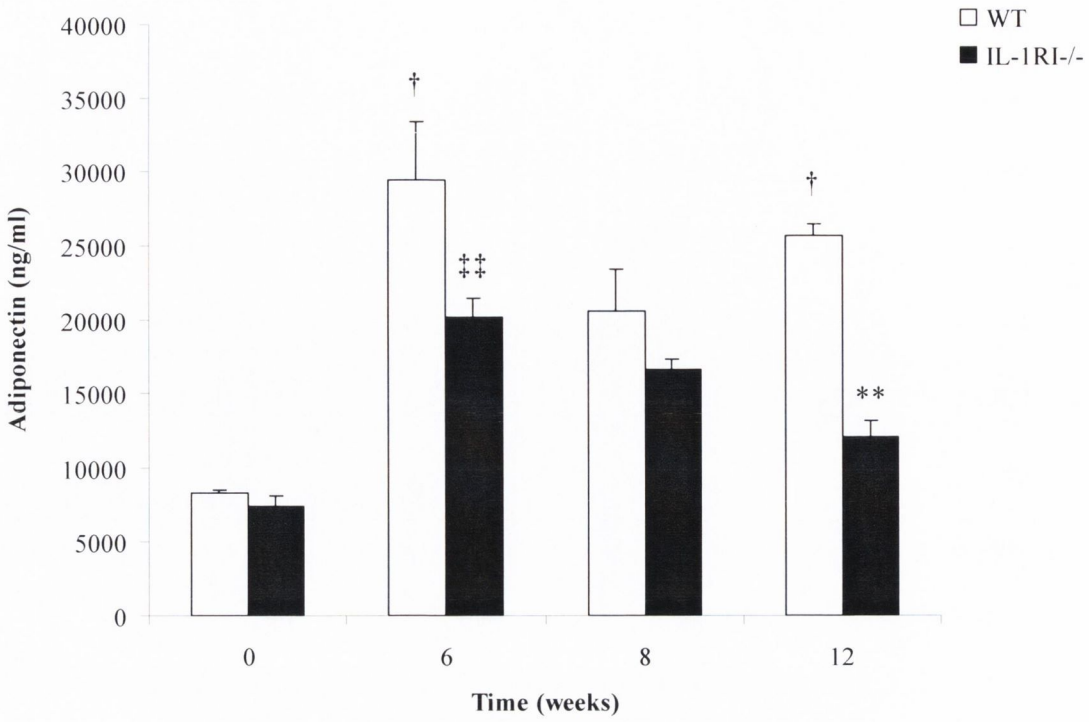

Figure 3.14 Effects of HFD on fasting plasma adiponectin concentrations in the WT and IL-1R1$^{-/-}$ mice. Fasting plasma adiponectin levels (ng/ml) were measured using milliplex MAP at week 0, 6, 8 and 12 of the HFD, n = 2 - 6. Values are means ± SEM. † $P \leq 0.05$ relative to week 0 WT; ‡‡ $P \leq 0.01$ relative to week 0 IL-1RI$^{-/-}$; ** $P \leq 0.01$ relative to WT. One-way ANOVA was performed within each group followed by post hoc Bonferroni testing. An independent Student's t-test was performed on the IL-1R1$^{-/-}$ groups vs. the corresponding WT group.

3.3.5 Effects of a 16 week HFD on plasma cytokine and chemokine concentrations in IL-1RI$^{-/-}$ and WT mice

Cytokines and chemokines within the plasma were also analysed using a Milliplex kit, however the plasma concentrations of TNF-α, IL-6, IL-4, IL-9, IL-10, IFN-γ and MCP-1 were undetectable throughout the study. However, levels of IL-1β and CCL5 were successfully analysed within the plasma of fasting IL-1RI$^{-/-}$ and wild type mice at week 0, 6, 8 and 12 HFD as presented in Figures 3.15 and 3.16. At week 6 of the HFD plasma IL-1β concentrations were significantly reduced (61% decrease) in the IL-1R1$^{-/-}$ group compared to the WT group ($P \leq 0.050$). Plasma IL-1β was not significantly altered over time within groups or between animal groups at weeks 0, 4, and 12 of the HFD. Plasma CCL5 concentrations were significantly increased 2.7 fold within the WT group at week 12 compared to week 0 WT ($P \leq 0.022$). Plasma CCL5 levels were was not significantly altered between animal groups at any of the time points. Interestingly, plasma IL-1β and CCL5 concentrations seem consistently lower within the IL-1RI$^{-/-}$ relative to the WT at week 6, 8 and 12, however not significantly.

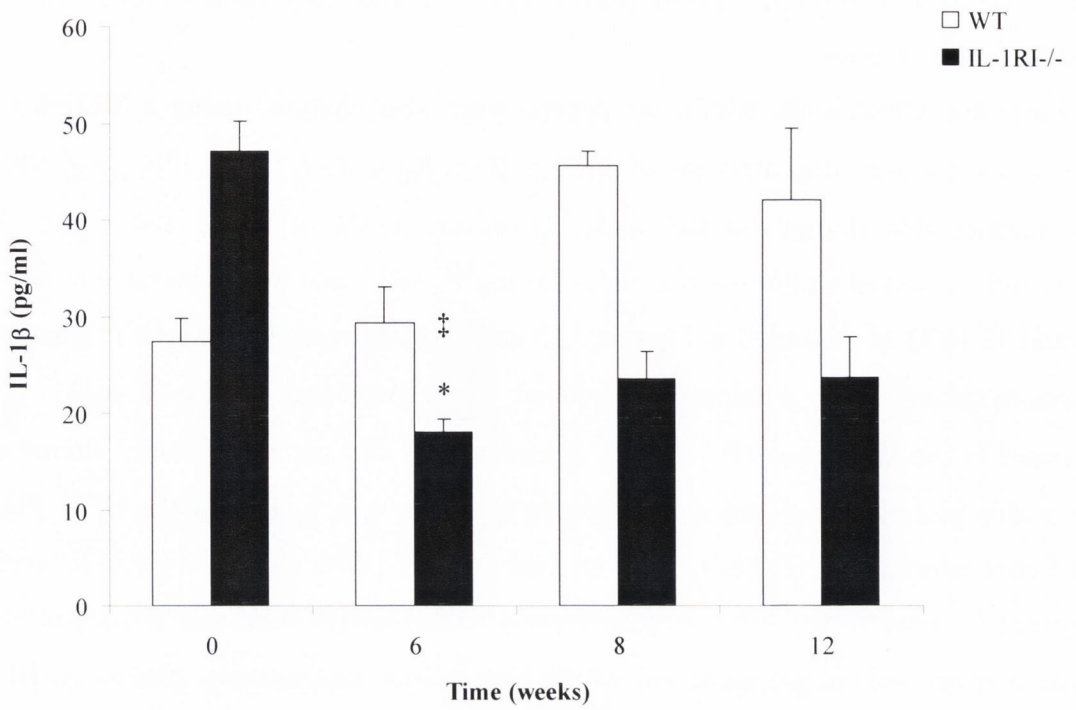

Figure 3.15 Effects of HFD on plasma IL-1β concentrations in the WT and IL-1R1$^{-/-}$ mice. Plasma IL-1β levels (pg/ml) were measured using milliplex MAP at week 0, 6, 8 and 12 of the HFD, n = 2 - 6. Values are means ± SEM. * $P \leq 0.05$ relative to WT; ‡ $P \leq 0.05$ relative to week 0 IL-1RI$^{-/-}$. One-way ANOVA was performed within each group followed by post hoc Bonferroni testing. An independent Student's t-test was performed on the IL-1R1$^{-/-}$ groups vs. the corresponding WT group.

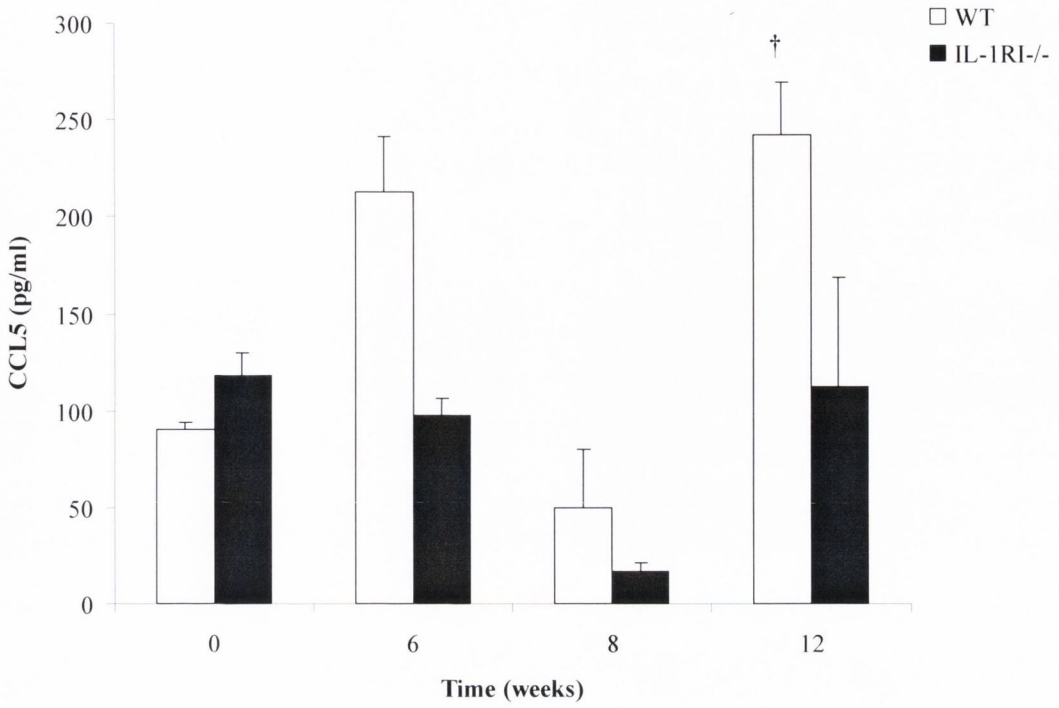

Figure 3.16 Effects of HFD on plasma CCL5 concentrations in the WT and IL-1R1$^{-/-}$ mice. Plasma CCL5 levels (pg/ml) were measured using milliplex MAP at week 0, 6, 8 and 12 of the HFD, n = 2 - 6. Values are means ± SEM. † $P \leq 0.05$ relative to week 0 IL-1RI$^{-/-}$. One-way ANOVA was performed within each group followed by post hoc Bonferroni testing.

3.3.6 Effects of a 16 week HFD on plasma triacylglycerol and non-esterified fatty acids levels in IL-1RI$^{-/-}$ and WT mice

Fasting plasma TAG and NEFA concentrations were analysed for week 0, 6, 8, 12 and 16 HFD in male IL-1RI$^{-/-}$ and WT mice as presented in Figures 3.17 to 3.20 respectively. Fasting plasma TAG levels (Figure 3.17) significantly increased (2.5 fold increase) at week 6 HFD relative to week 0 in the IL-1RI$^{-/-}$ group ($P \leq 0.040$). Plasma TAG concentrations also significantly increased in the WT group at weeks 6 and 8 (1.6 fold and 1.8 fold) of the HFD relative to week 0 ($P \leq 0.026$ and $P \leq 0.001$). Furthermore, plasma TAG levels decreased 27% at week 16 of the HFD relative to week 8 within the WT group ($P \leq 0.049$). At week 0 and 8 of the HFD plasma TAG concentrations were significantly reduced (54% and 76% decrease) in the IL-1R1$^{-/-}$ group compared to the WT controls ($P \leq 0.001$ and $P \leq 0.001$). Fasting plasma TAG levels corrected for body weight (Figure 3.18) were reduced in the IL-1RI$^{-/-}$ group (54% and 63% decrease) relative to the WT group at week 0 and 8 ($P \leq 0.001$ and $P \leq 0.001$). However, fasting plasma TAG concentrations were significantly decreased in the WT mice at weeks 12 (28% and 32% decrease) relative to week 6 and 8 of the HFD ($P \leq 0.039$ and $P \leq 0.018$) when corrected for body weight.

Fasting plasma NEFA levels (Figure 3.19) significantly increased in the IL-1RI$^{-/-}$ group at weeks 6, 8, 12 and 16 (3.1, 2.6, 3.0 and 2.7 fold increase) of the HFD relative to IL-1RI$^{-/-}$ week 0 ($P \leq 0.002$, $P \leq 0.04$, $P \leq 0.003$ and $P \leq 0.02$ respectively). Similarly, plasma NEFA concentrations significantly increased in the WT group at weeks 6, 8 and 16 (4.0, 3.5 and 3.9 fold increase) of the HFD relative to week 0 ($P \leq 0.005$, $P \leq 0.035$ and $P \leq 0.003$ respectively). However, there were no significant differences in NEFA levels between IL-1RI$^{-/-}$ and WT groups at all time points within the study. Fasting plasma NEFA levels corrected for body weight (Figure 3.20) were higher in the IL-1RI$^{-/-}$ group at week 0, 6, 12 and 16 of the HFD (3.3 fold, 2.25 fold, 2.8 fold and 2.0 fold increase) relative to the WT group ($P \leq 0.005$, $P \leq 0.022$, $P \leq 0.003$ and $P \leq 0.005$). However, fasting plasma NEFA concentrations when corrected for body weight were significantly increased (2.9 fold increase) in the WT mice from weeks 0 to 6 of the HFD ($P \leq 0.013$).

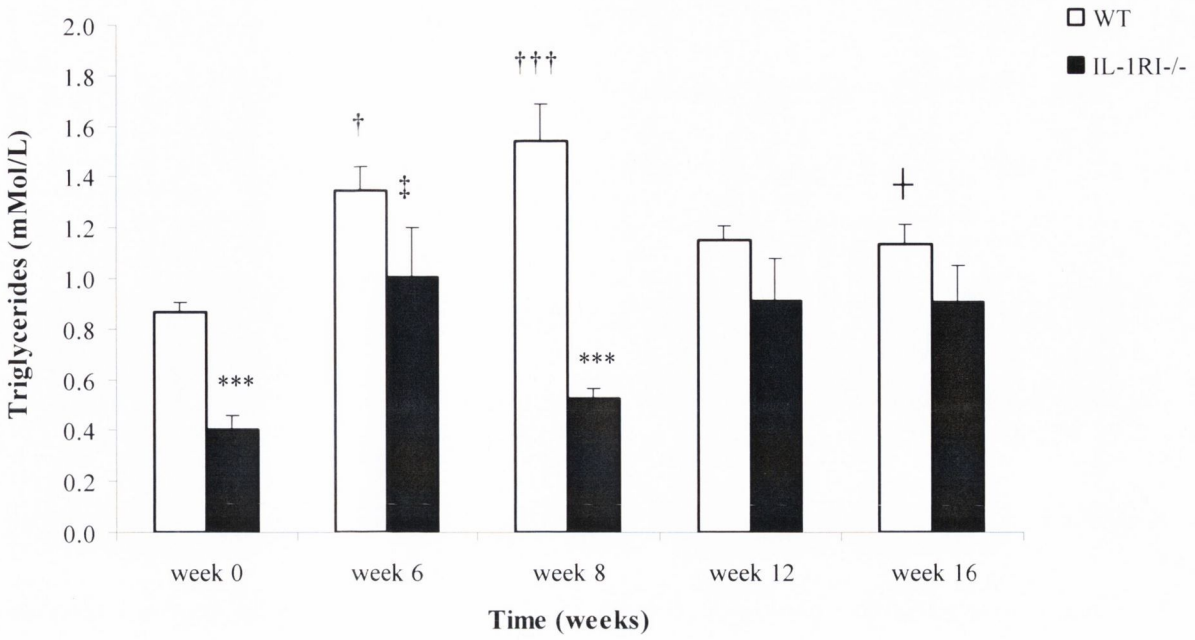

Figure 3.17 Effects of HFD on fasting plasma triacylglycerol concentrations in the WT and IL-1R1$^{-/-}$ mice. Plasma TAG levels (mMol/L) were measured using an ELISA at week 0, 6, 8, 12 and 16 of the HFD, n = 5 - 8. Values are means ± SEM. † $P \leq 0.05$, ††† $P \leq 0.001$ relative to week 0 WT; ‡ $P \leq 0.05$ relative to week 0 IL-1RI$^{-/-}$; + $P \leq 0.05$ relative to week 8 WT; *** $P \leq 0.001$ relative to WT. One-way ANOVA was performed within each group followed by post hoc Bonferroni testing. An independent Student's t-test was performed on the IL-1R1$^{-/-}$ groups vs. the corresponding WT group.

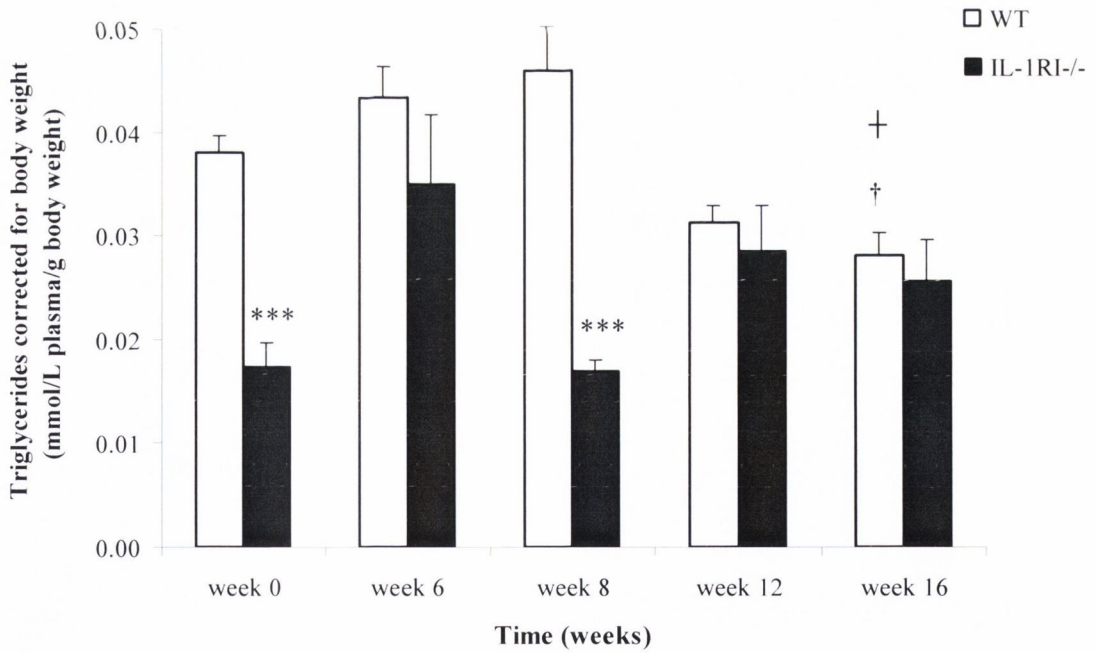

Figure 3.18 Fasting plasma triacylglycerol concentrations corrected for body weight in the WT and IL-1R1$^{-/-}$ mice during the HFD. Plasma TAG levels (mMol/L) were measured using an ELISA at week 0, 6, 8, 12 and 16 of the HFD, n = 5 - 8. Values are expressed relative to body weight and the graph shows means ± SEM. † $P \leq 0.05$ relative to week 6 WT; + $P \leq 0.05$ relative to week 8 WT; *** $P \leq 0.001$ relative to WT. One-way ANOVA was performed within each group followed by post hoc Bonferroni testing. An independent Student's t-test was performed on the IL-1R1$^{-/-}$ groups vs. the corresponding WT group.

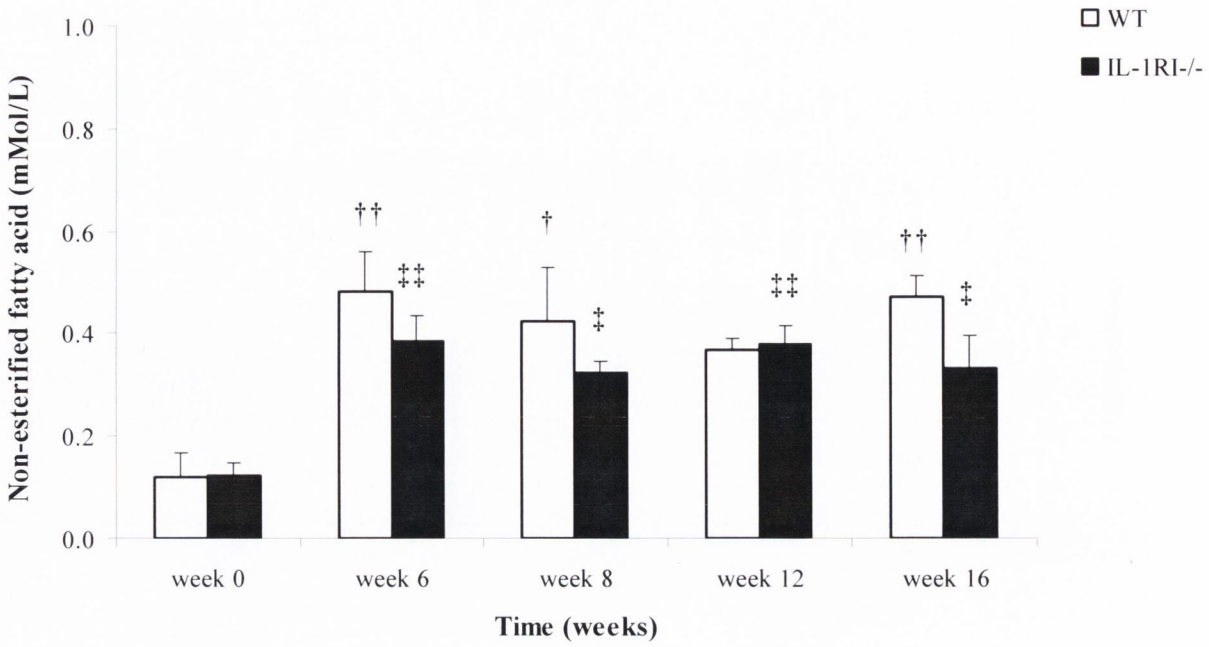

Figure 3.19 Effects of HFD on fasting plasma NEFA concentrations in the WT and IL-1R1$^{-/-}$ mice. Plasma NEFA levels (mMol/L) were measured using an ELISA at week 0, 6, 8, 12 and 16 of the HFD, n = 5 - 8. Values are means ± SEM. † $P \leq 0.05$, †† $P \leq 0.01$ relative to week 0 WT; ‡ $P \leq 0.05$, ‡‡ $\leq P$ 0.01 relative to week 0 IL-1RI$^{-/-}$. One-way ANOVA was performed within each group followed by post hoc Bonferroni testing.

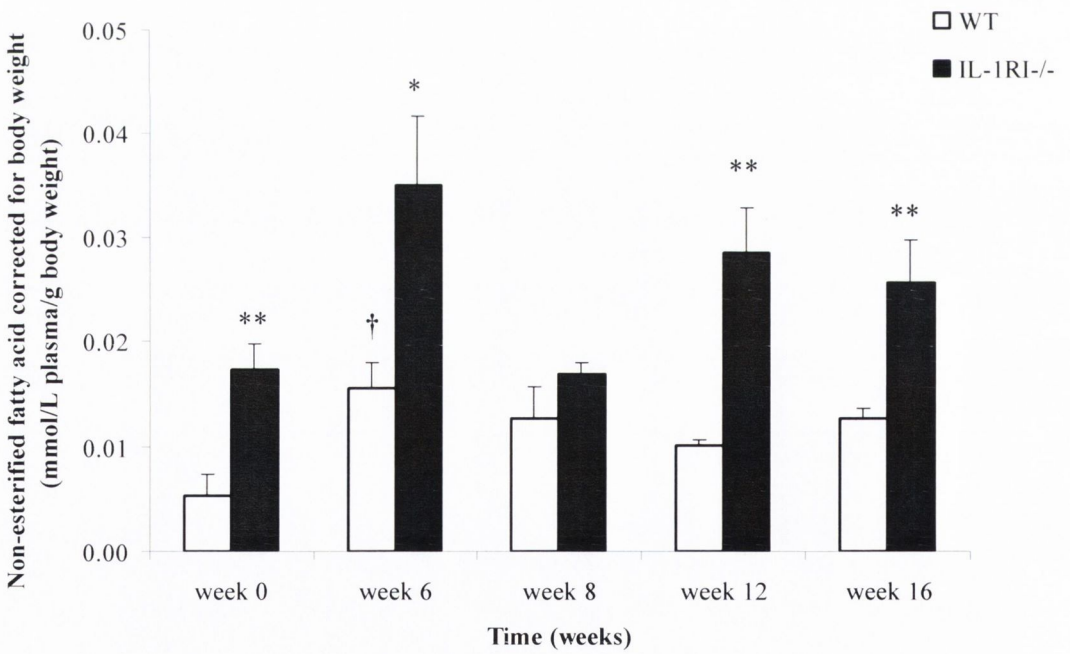

Figure 3.20 Fasting plasma non-esterified fatty acids concentrations corrected for body weight in the WT and IL-1R1$^{-/-}$ mice during the HFD. Plasma NEFA levels (mMol/L) were measured using an ELISA at week 0, 6, 8, 12 and 16 of the HFD, n = 5 - 8. Values are expressed relative to body weight and the graph shows means ± SEM. † ≤ 0.05 relative to week 0 WT; *** $P \leq 0.001$, ** $P \leq 0.01$, * $P \leq 0.05$ relative to WT. One-way ANOVA was performed within each group followed by post hoc Bonferroni testing. An independent Student's t-test was performed on the IL-1R1$^{-/-}$ groups vs. the corresponding WT group.

3.3.7 Effects of a 16 week HFD on insulin sensitive target gene expression in the epididymal adipose tissue of IL-1RI$^{-/-}$ and WT mice

GLUT4, IRS-1, PPAR-γ, adiponectin and resistin mRNA expression were measured at week 0, 6, 8 and 16 HFD in the epididymal adipose tissue (EAT) of male IL-1RI$^{-/-}$ and WT mice as presented in Figures 3.21, 3.22, 3.23, 3.24 and 3.25 respectively. RT-PCR analysis determined that GLUT4, IRS-1, PPAR-γ, adiponectin and resistin mRNA levels were significantly higher (6.6 fold, 5.2 fold, 2.2 fold, 11.2 fold and 7 fold) at week 0 of the study in the IL-1RI$^{-/-}$ group compared to the WT group ($P \leq 0.001$, $P \leq 0.003$, $P \leq 0.013$, $P \leq 0.001$ and 0.001 respectively). However, there were no significant differences in the gene expression levels of GLUT4, IRS-1, PPAR-γ, adiponectin and resistin between IL-1RI$^{-/-}$ and WT groups at weeks 6, 8 and 16 of the HFD. However, the Ct values of the insulin sensitive targets decrease over the course of the 16 week HFD in both WT and IL-1RI$^{-/-}$ mice, indicating an up-regulation in insulin sensitive target gene expression.

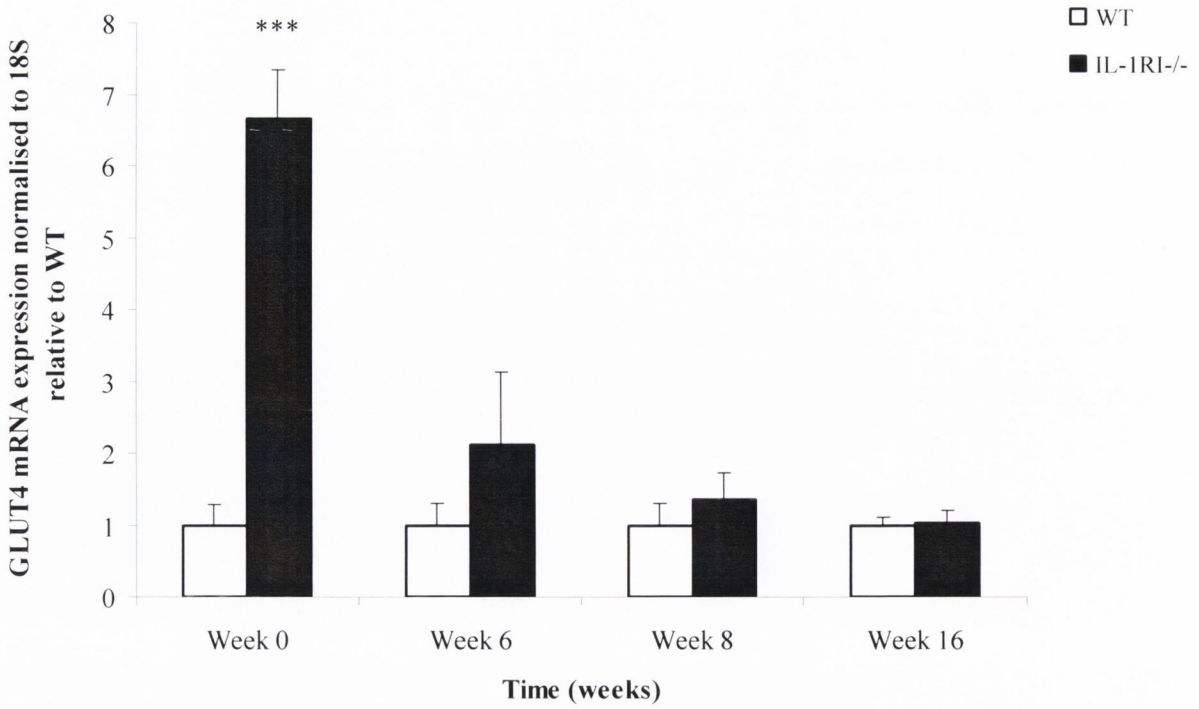

	WT		IL-1RI$^{-/-}$	
Week	**Δ Ct mean**	**SEM**	**Δ Ct mean**	**SEM**
0	15.03	0.37	12.31	0.14
6	11.84	0.43	11.32	1.04
8	10.62	0.38	10.52	0.59
16	10.67	0.16	10.68	0.21

Figure 3.21 Effects of HFD on GLUT4 gene expression within EAT of WT and IL-1R1$^{-/-}$ mice. GLUT4 mRNA levels were measured using Taqman RT-PCR at week 0, 6, 8 and 16 of the HFD. mRNA levels were normalized to 18S and the results are expressed as fold induction relative to the WT. The Δ Ct values are shown in the table. Values are means ± SEM, n = 3 - 6. *** $P \leq 0.001$ relative to WT. An independent Students t-test was performed on the IL-1R1$^{-/-}$ groups vs. the corresponding WT group.

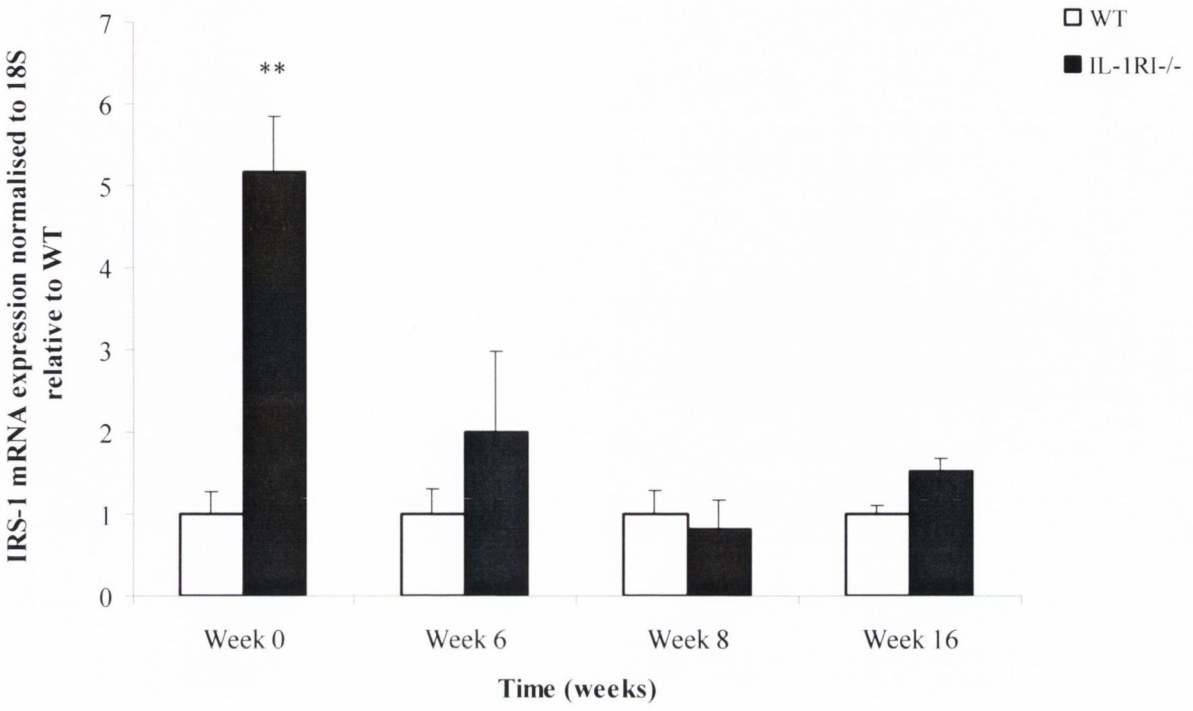

	WT		IL-1RI$^{-/-}$	
Week	**Δ Ct mean**	**SEM**	**Δ Ct mean**	**SEM**
0	16.80	0.49	14.55	0.36
6	15.16	0.54	14.61	0.93
8	13.74	0.41	14.33	0.44
16	12.42	0.12	11.96	0.26

Figure 3.22 Effects of HFD on IRS-1 gene expression within EAT of WT and IL-1R1$^{-/-}$ mice. IRS-1 mRNA levels were measured using Taqman RT-PCR at week 0, 6, 8 and 16 of the HFD. mRNA levels were normalized to 18S and the results are expressed as fold induction relative to the WT. The Δ Ct values are shown in the table. Values are means ± SEM, n = 3 - 8. ** $P \leq 0.01$ relative to WT. An independent Student's t-test was performed on the IL-1R1$^{-/-}$ groups vs. the corresponding WT group.

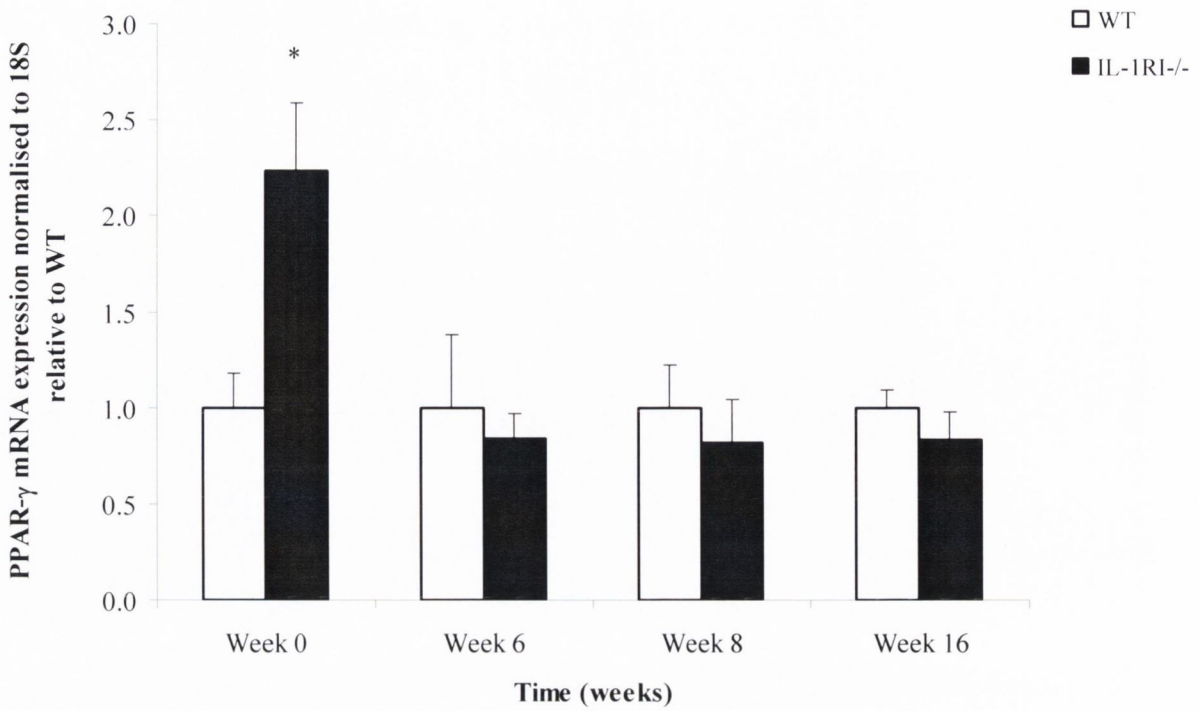

	WT		IL-1RI$^{-/-}$	
Week	**Δ Ct mean**	**SEM**	**Δ Ct mean**	**SEM**
0	17.61	0.27	16.50	0.20
6	14.96	0.49	15.25	0.22
8	14.43	0.32	14.90	0.34
16	10.69	0.12	11.04	0.23

Figure 3.23 Effects of HFD on PPAR-γ gene expression within EAT of WT and IL-1R1$^{-/-}$ mice. PPAR-γ mRNA levels were measured using Taqman RT-PCR at week 0, 6, 8 and 16 of the HFD. mRNA levels were normalized to 18S and the results are expressed as fold induction relative to the WT. The Δ Ct values are shown in the table. Values are means ± SEM, n = 3 - 6. * $P \leq 0.05$ relative to WT. An independent Students t-test was performed on the IL-1R1$^{-/-}$ groups vs. the corresponding WT group.

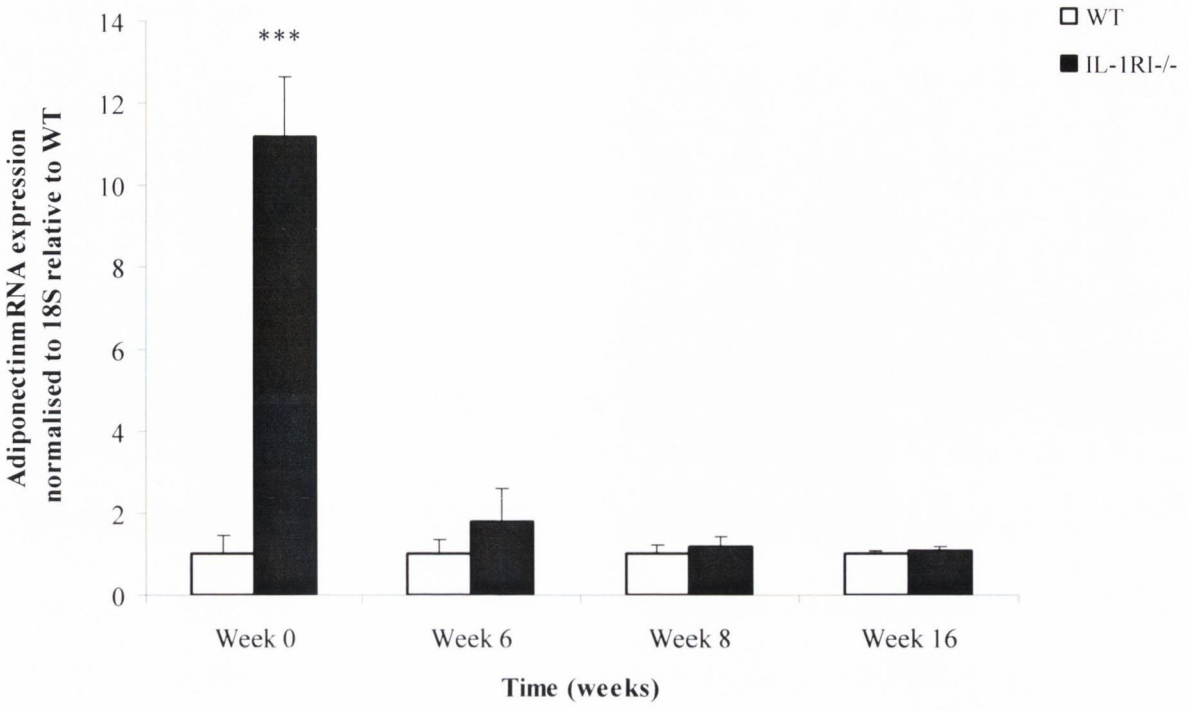

	WT		IL-1RI$^{-/-}$	
Week	**Δ Ct mean**	**SEM**	**Δ Ct mean**	**SEM**
0	10.89	0.2955	8.33	0.16
6	8.50	0.48	8.12	1.29
8	7.94	0.33	7.87	0.35
16	6.38	0.13	6.32	0.16

Figure 3.24 Effects of HFD on adiponectin gene expression within EAT of WT and IL-1R1$^{-/-}$ mice. Adiponectin mRNA levels were measured using Taqman RT-PCR at week 0, 6, 8 and 16 of the HFD. mRNA levels were normalized to 18S and the results are expressed as fold induction relative to the WT. The Δ Ct values are shown in the table. Values are means ± SEM, n = 3 - 8. *** $P \leq 0.001$ relative to WT. An independent Student's t-test was performed on the IL-1R1$^{-/-}$ groups vs. the corresponding WT group.

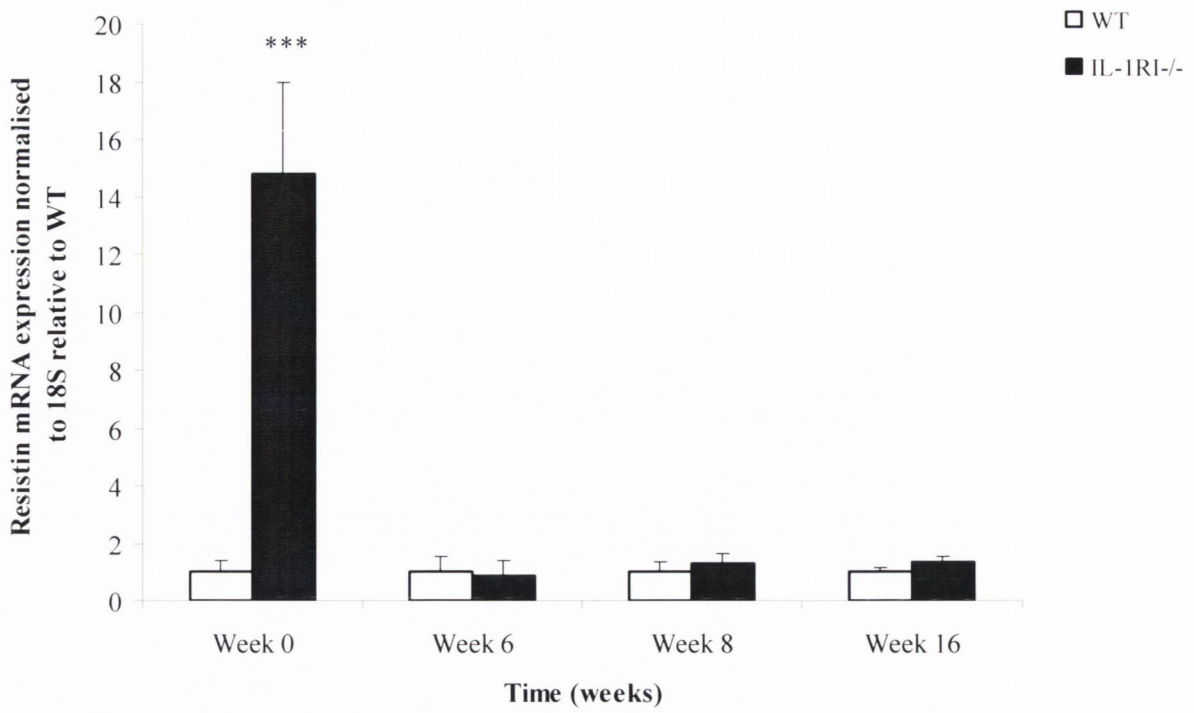

	WT		IL-1RI$^{-/-}$	
Week	**Δ Ct mean**	**SEM**	**Δ Ct mean**	**SEM**
0	14.25	0.62	10.47	0.32
6	11.54	0.70	12.44	0.99
8	11.41	0.42	11.33	0.52
16	8.16	0.19	7.80	0.20

Figure 3.25 Effects of HFD on resistin gene expression within EAT of WT and IL-1R1$^{-/-}$ mice. Resistin mRNA levels were measured using Taqman RT-PCR at week 0, 6, 8 and 16 of the HFD. mRNA levels were normalized to 18S and the results are expressed as fold induction relative to the WT. The Δ Ct values are shown in the table. Values are means ± SEM, n = 3 - 6. *** $P \leq 0.001$ relative to WT. An independent Student's t-test was performed on the IL-1R1$^{-/-}$ groups vs. the corresponding WT group.

3.3.8 Effects of a 16 week HFD on inflammatory target gene expression in the epididymal adipose tissue of IL-1RI$^{-/-}$ and WT mice

TNF-α, MCP-1 and MIF mRNA expression were measured for week 0, 6, 8 and 16 HFD in the EAT of male IL-1RI$^{-/-}$ and WT mice as presented in Figures 3.26, 3.27 and 3.28 respectively. Other inflammatory targets such as IL-1β, IL-1Ra, IL-6 and MIP-1α were examined with real time RT-PCR, however their expression was too low within the adipose to be accurately measured.

Interestingly, TNF-α mRNA levels were significantly lower (33% decrease) at week 16 of the HFD in the IL-1RI$^{-/-}$ group compared to the WT group ($P \leq 0.006$). MCP-1 (also known as CCR2) mRNA expression was significantly up-regulated (6.3 fold increase) in the IL-1RI$^{-/-}$ mice compared to WT at week 0 ($P \leq 0.001$). However, at weeks 6 and 8 of the HFD MCP-1 was significantly lower (82% and 72% decrease) in the IL-1RI$^{-/-}$ group relative to the WT group ($P \leq 0.028$ and $P \leq 0.024$ respectively). Furthermore, at week 16 of the HFD MCP-1 was lower (62% decrease) in the IL-1RI$^{-/-}$ group relative to the WT group ($P \leq 0.080$), however not significantly. MIF mRNA expression was significantly up-regulated (3 fold increase) in the IL-1RI$^{-/-}$ mice ($P \leq 0.043$) at week 8 relative to WT. Lastly, the Ct values of TNF-α and MIF gene expression reduced over the course of the 16 week HFD in both WT and IL-1RI$^{-/-}$ mice, however more appreciably in WT indicating a greater up-regulation in inflammatory target gene expression within these mice.

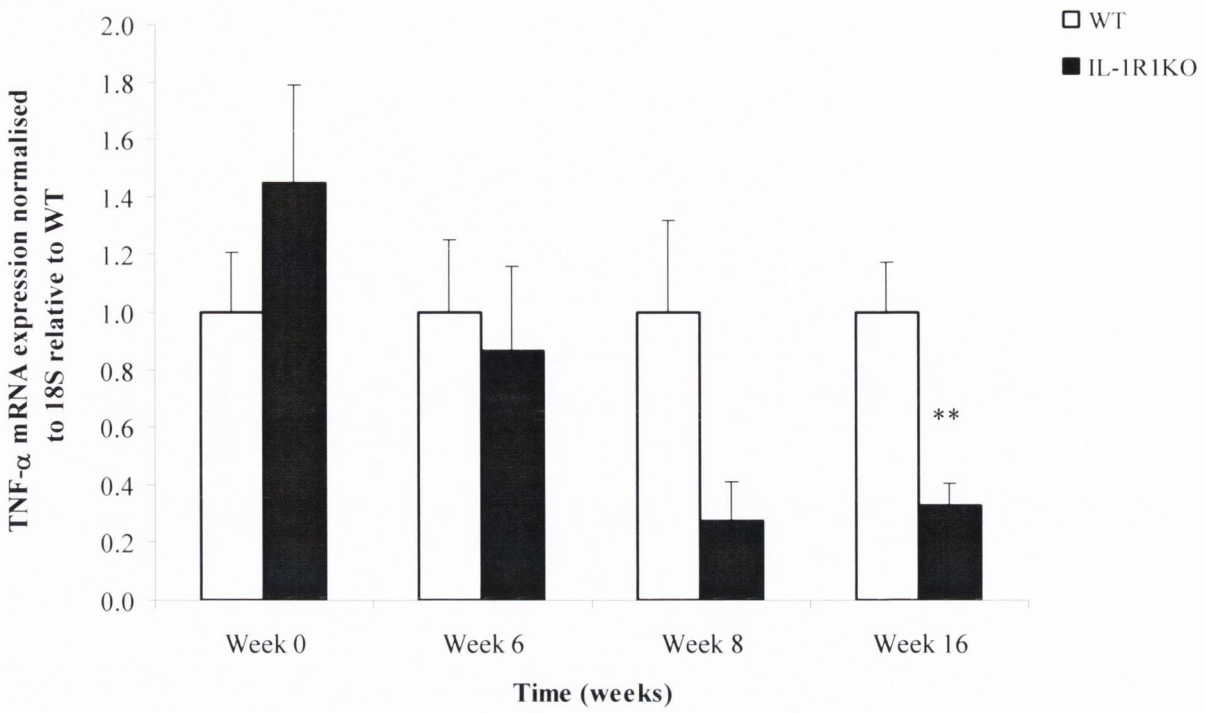

	WT		IL-1RI$^{-/-}$	
Week	**Δ Ct mean**	**SEM**	**Δ Ct mean**	**SEM**
0	22.30	0.30	21.87	0.30
6	20.65	0.36	21.12	0.68
8	19.75	0.45	21.97	0.70
16	15.67	0.23	17.46	0.35

Figure 3.26 Effects of HFD on TNF-α gene expression within EAT of WT and IL-1R1$^{-/-}$ mice. TNF-α mRNA levels were measured using Taqman RT-PCR at week 0, 6, 8 and 16 of the HFD. mRNA levels were normalized to 18S and the results are expressed as fold induction relative to the WT. The Δ Ct values are shown in the table. Values are means ± SEM, n = 3 - 6. ** $P \leq 0.01$ relative to WT. An independent Student's t-test was performed on the IL-1R1$^{-/-}$ groups vs. the corresponding WT group.

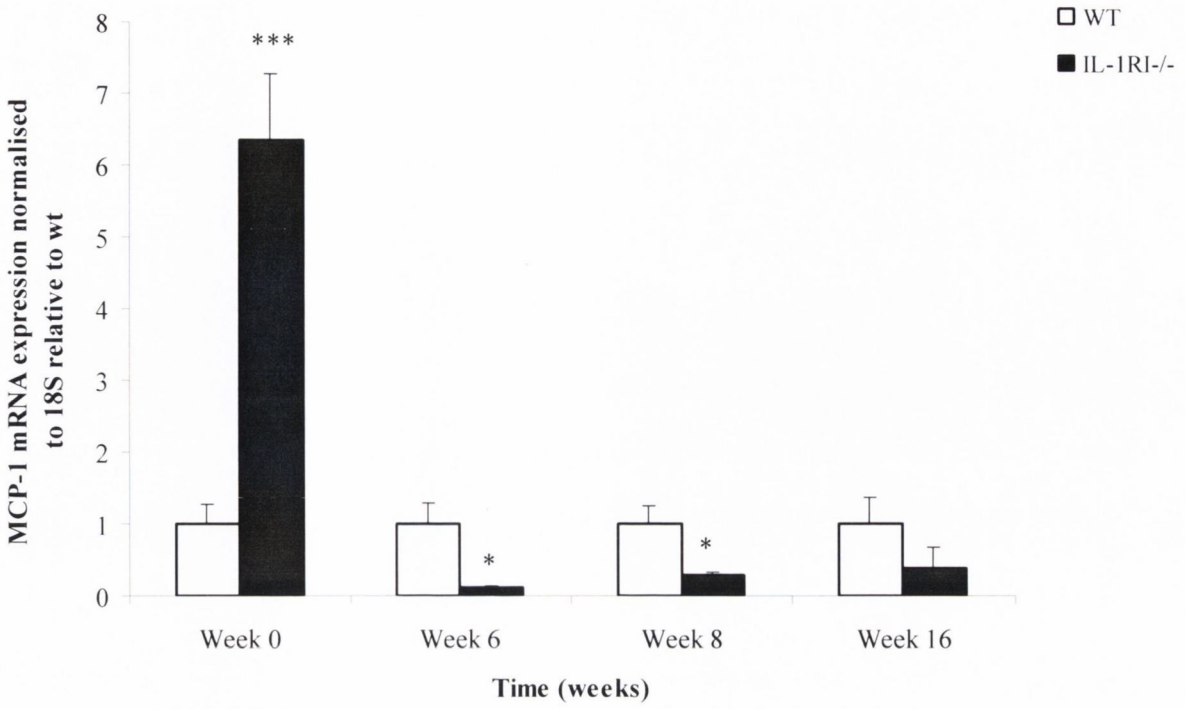

	WT		IL-1RI$^{-/-}$	
Week	**Δ Ct mean**	**SEM**	**Δ Ct mean**	**SEM**
0	21.53	0.49	18.92	0.25
6	16.81	0.51	19.85	0.11
8	17.62	0.38	19.59	0.35
16	12.59	0.80	15.26	0.81

Figure 3.27 Effects of HFD on MCP-1 gene expression within EAT of WT and IL-1R1$^{-/-}$ mice. MCP-1 mRNA levels were measured using Taqman RT-PCR at week 0, 6, 8 and 16 of the HFD. mRNA levels were normalized to 18S and the results are expressed as fold induction relative to the WT. The Δ Ct values are shown in the table. Values are means ± SEM, n = 3 - 6. * $P \leq 0.05$, *** $P \leq 0.001$ relative to WT. An independent Student's t-test was performed on the IL-1R1$^{-/-}$ groups vs. the corresponding WT group.

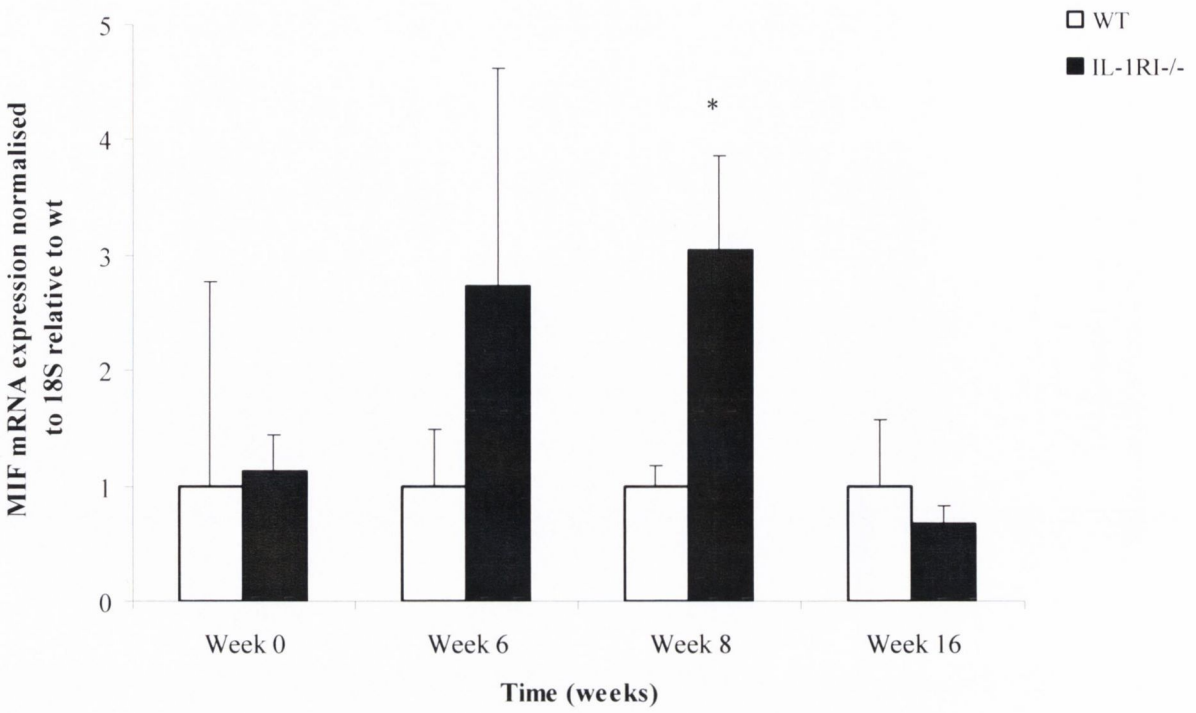

	WT		IL-1RI$^{-/-}$	
Week	**Δ Ct mean**	**SEM**	**Δ Ct mean**	**SEM**
0	19.14	1.41	19.19	0.50
6	18.09	0.92	17.34	0.97
8	18.35	0.25	16.94	0.37
16	11.80	0.42	12.53	0.32

Figure 3.28 Effects of HFD on MIF gene expression within EAT of WT and IL-1R1$^{-/-}$ mice. MIF mRNA levels were measured using Taqman RT-PCR at week 0, 6, 8 and 16 of the HFD. mRNA levels were normalized to 18S and the results are expressed as fold induction relative to the WT. The Δ Ct values are shown in the table. Values are means ± SEM, n = 3 - 6. * $P \leq 0.05$, *** $P \leq 0.001$ relative to WT. An independent Student's t-test was performed on the IL-1R1$^{-/-}$ groups vs. the corresponding WT group.

3.3.9 Effects of a 16 week HFD on gene expression in the adipocytes of epididymal adipose tissue within IL-1RI$^{-/-}$ and WT mice

An array of genes were measured in isolated EAT adipocytes of IL-1RI$^{-/-}$ and WT mice at week 16 of the HFD as presented in Table 3.2. The Δ Ct values show there was very little variation in gene expression between IL-1RI$^{-/-}$ and WT groups within the adipocytes at week 16 of the HFD. Interestingly, TNF-α and MCP-1 gene expression within the adipocytes were down-regulated although not significantly in the IL-1RI$^{-/-}$ group relative to WT ($P \leq 0.07$ and $P \leq 0.08$).

Table 3.2 Effects of HFD on gene expression within EAT adipocytes of WT and IL-1R1$^{-/-}$ mice. At week 16 of the HFD adipocytes were isolated from EAT and RNA was successfully harvested. mRNA levels were measured using RT-PCR at week 16 of the HFD. Δ Ct and P values are shown, n = 6 - 7. An independent Students t-test was performed on the IL-1R1$^{-/-}$ groups vs. the corresponding WT group.

	WT		IL-1RI$^{-/-}$		
	Δ Ct mean	**SEM**	**Δ Ct mean**	**SEM**	**P value**
GLUT4	12.81	0.36	13.13	0.43	0.64
IRS-1	14.64	0.32	14.71	0.34	0.84
Insulin receptor	14.81	0.36	14.86	0.40	0.90
SREBP-1c	15.18	0.40	15.47	0.33	0.39
PPAR-γ	13.17	0.32	13.16	0.35	1.00
Adiponectin	8.41	0.25	8.39	0.44	0.68
Adiponectin receptor 1	12.61	0.26	12.77	0.36	0.75
Adiponectin receptor 2	13.65	0.40	13.77	0.40	0.73
Resistin	10.14	0.38	10.05	0.57	0.71
Leptin	9.56	0.49	10.82	0.46	0.12
TNF-α	11.47	0.66	13.07	0.66	0.07
MCP-1	10.49	0.61	11.79	0.59	0.08
MIF	14.37	0.32	14.81	0.28	0.23

3.3.10 Effects of a 16 week HFD on adipocyte size in the epididymal adipose tissue of IL-1RI$^{-/-}$ and WT mice

Adipocyte size was measured for week 0, 6, 8, 12 and 16 HFD in the EAT of IL-1RI$^{-/-}$ and WT mice as presented in Figure 3.29. At 8 and 16 weeks of the HFD adipocytes size within the EAT was significantly lower (53% and 26% decrease) in the IL-1RI$^{-/-}$ mice compared to the WT mice ($P \leq 0.047$ and $P \leq 0.014$). Within the IL-1RI$^{-/-}$ group there was a significant increase in adipocytes size at week 12 (4.7 fold increase) of the HFD compared to week 0 IL-1RI$^{-/-}$ ($P \leq 0.012$). Interestingly, within the WT group there was a significant increase in adipocyte size at week 6, 8, 12 and 16 (5.8, 4.4, 6.8 and 5.5 fold increase) of the HFD compared to week 0 WT ($P \leq 0.001$, $P \leq 0.005$, 0.001 and $P \leq 0.001$ respectively). Furthermore, at week 12 of the HFD there was a significant increase (2.7 fold increase) in adipocyte size compared to week 8 WT ($P \leq 0.006$).

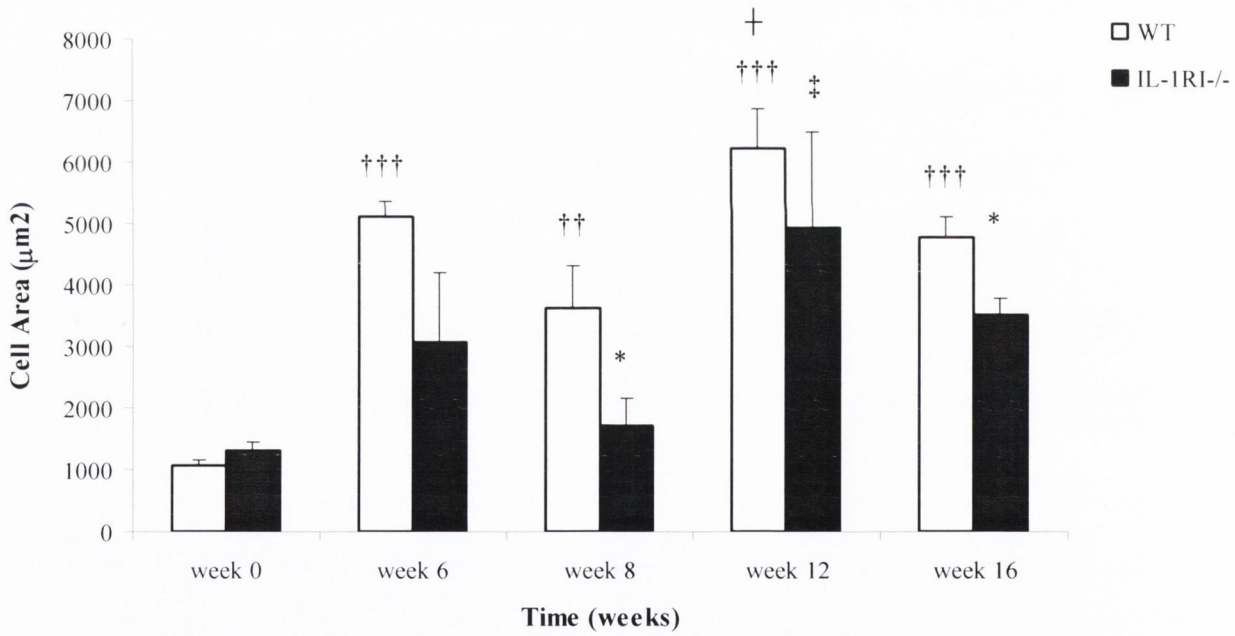

Figure 3.29 Effects of HFD on adipocyte area within EAT of WT and IL-1R1$^{-/-}$ mice. Slides were prepared and stained with hematoxylin and eosin. Microscope images were taken and adipocyte size was measured in μm^2 for week 0, 6, 8 and 16 of the HFD, n = 4 - 10. Values are means ± SEM. * $P \leq 0.05$ relative to WT; †† $P \leq 0.01$, ††† $P \leq 0.001$ relative to week 0 WT; ‡ $P \leq 0.05$ relative to week 0 IL-1RI$^{-/-}$; + $P \leq 0.05$ relative to week 8 WT. One-way ANOVA was performed within each group followed by post hoc Bonferroni testing. An independent Students t-test was performed on the IL-1R1$^{-/-}$ groups vs. the corresponding WT group.

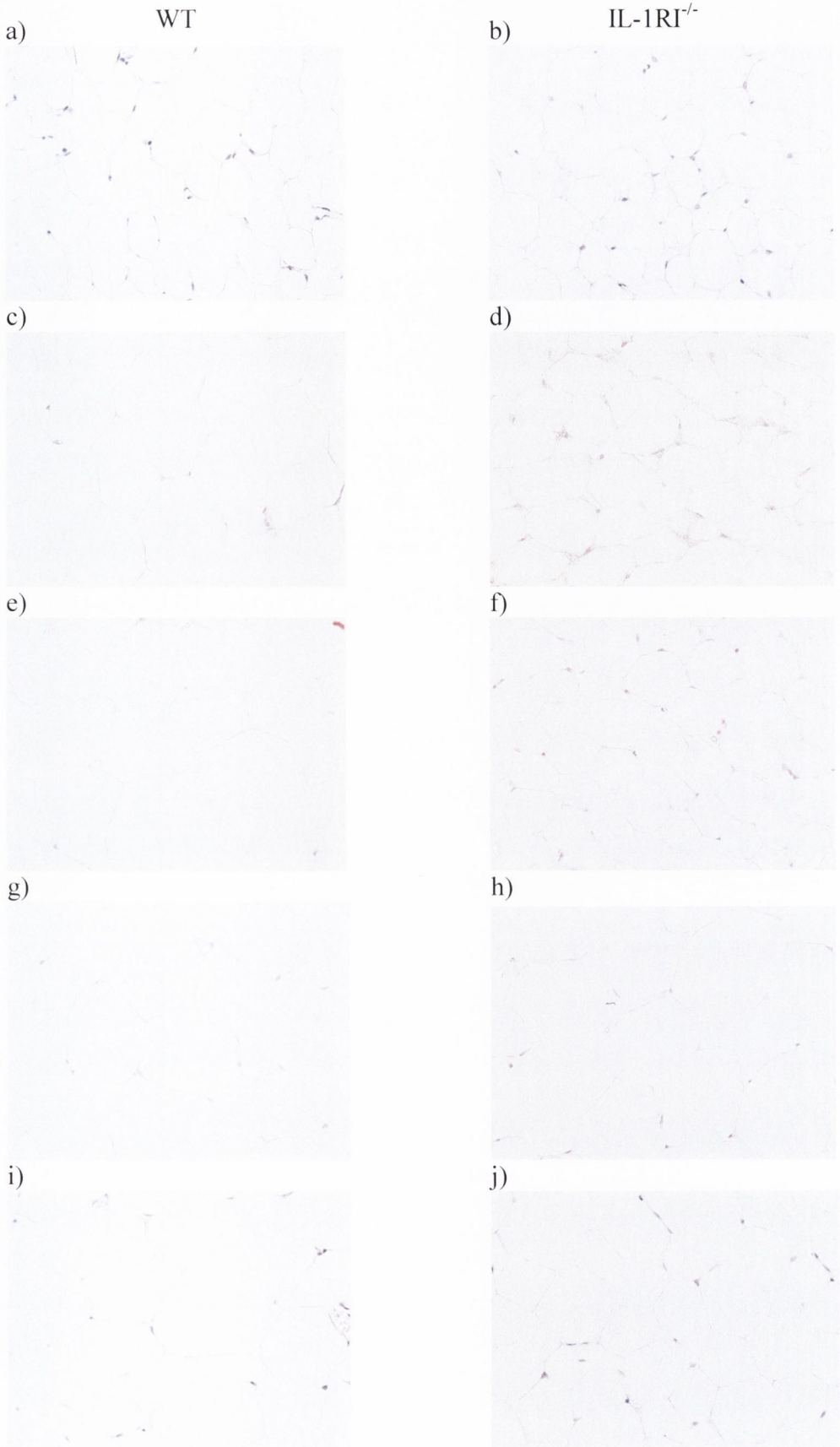

Figure 3.30 Effects of HFD on adipocyte area within EAT of WT and IL-1R1$^{-/-}$ mice. Slides were prepared and stained with hematoxylin and eosin. Microscope images were taken and adipocyte size was measured for week 0 WT (a) and IL-1RI$^{-/-}$ (b); week 6 WT (c) and IL-1RI$^{-/-}$ (d); week 8 WT (e) and IL-1RI$^{-/-}$ (f); week 12 WT (g) and IL-1RI$^{-/-}$ (h); week 16 WT (i) and IL-1RI$^{-/-}$ (j).

3.4 Discussion

IL-1 is thought to promote the infiltration of inflammatory and immunocompetent cells from the circulation into WAT leading to chronic IL-1-induced inflammation (Dinarello, 2009). IL-1 signalling may therefore pay a key role in the infiltration of ATM during obesity, leading to inflammation and the associated insulin resistance. We therefore hypothesized that IL-1RI$^{-/-}$ mice will not only have a general reduction in inflammation but also a specific reduction in adipose tissue macrophages (ATM) due to a lack in IL-1 signalling leading to increased insulin sensitivity within the WAT.

At base line, the WT and IL-1RI$^{-/-}$ groups showed no significant difference in body weight, EAT mass, VAT mass, EAT adipocyte size, fasting plasma glucose, insulin, NEFA, resistin, adiponectin, CCL-5, IL-1β and TNF-α mRNA expression levels. However, fasting plasma TAG and leptin concentrations were significantly reduced in the IL-1RI$^{-/-}$ mice relative to the WT group. Furthermore, mRNA expression of GLUT4, IRS-1, PPAR-γ and MCP-1 were significantly higher in IL-1RI$^{-/-}$ mice relative to WT. These differences may be partially due to the fact that the C57Bl/6 WT mice were from Harlan and the IL-1RI$^{-/-}$ mice were from Jackson and may have different genetic backgrounds. This discrepancy was due to misunderstandings within the various animal units we dealt with during the study and was not ideal. Furthermore, the IL-1RI$^{-/-}$ mice were bred in-house while the C57Bl/6 WT mice were acquired from Harlan. Even though the Harlan mice were given two weeks to become accustomed to the new environment, environmental difference prior to this may be linked to the differences observed in the groups. Furthermore, recent evidence suggests that the trillions of bacteria that normally reside within the human gastrointestinal tract, collectively referred to as the gut microbiota, affect nutrient acquisition and energy regulation; it further suggests that obese and lean people have different gut microbiota. These findings raise the possibility that the gut microbiota has an important role in regulating weight and may be partly responsible for the development of obesity in some people (Zhang *et al.*, 2009). Therefore, the differences at base line may be due to differences in the gut microbiota owing to distinct environmental conditions early in life. A clone library could be used to fingerprint the complex microbial community within WT and IL-1RI$^{-/-}$ mice to explore the differences. In future studies, more controls are necessary to reduce or remove these inter-group differences. However, the differences observed at base line could also be due to specific deletion of the IL-1RI gene.

In this study, it was found that both IL-1RI$^{-/-}$ and WT groups showed deterioration in their glucose uptake response throughout the 16 week HFD. However, within the WT

control group there was a greater deterioration in glucose response. At week 0, the peak plasma glucose concentrations (at 15 minutes) were higher, suggesting the IL-1RI$^{-/-}$ mice are perhaps less insulin sensitive. However, there was no difference in glucose levels at later time points (30-120 minutes), indicating that glucose clearance was not altered between groups. At week 6 of the HFD it was established that the IL-1RI$^{-/-}$ group showed an enhanced glucose uptake response relative to the WT group, suggesting the IL-1RI$^{-/-}$ mice are more insulin sensitive. Importantly, the IL-1RI$^{-/-}$ mice also show significantly lower body weight at week 6 compared to WT. This may indicate that the increased insulin sensitivity within the IL-1RI$^{-/-}$ mice at week 6 is weight dependent. At week 12, both IL-1RI$^{-/-}$ and WT have a similar reduced glucose uptake response and both show signs of insulin resistance. However, at week 16 the WT glucose response continues to decline while the IL-1RI$^{-/-}$ mice show almost no decline in their glucose uptake response. At week 16, there was no significant difference in body weight between IL-1RI$^{-/-}$ and WT (ranging from 30g to 42g) suggesting the increased insulin sensitivity within the IL-1RI$^{-/-}$ mice is not weight dependent. Interestingly, this may suggest at week 16 the WT mice undergo macrophage infiltration into the adipose causing a heightened state of inflammation and insulin resistance, which the IL-1RI$^{-/-}$ mice are protected from. However, the evidence supporting this conclusion is indirect and requires further analysis. Adipose tissue specimines could be examined using immunohistochemistry or flow cytometry to directly demonstrate that ATM and other immune cells such as T cells were altered throughout the 16 week HFD intervention.

In summary, these GTT data indicate that both IL-1RI$^{-/-}$ and WT mice are becoming increasingly more insulin resistant over the course of the 16 week HFD. However, WT control mice show a more significant decline in insulin sensitivity. Fundamentally, IL-1RI$^{-/-}$ mice remain more insulin sensitive at week 6 and 16 of the HFD compared to WT. In future studies it may be important to select mice within certain weight limits to control for both body weight and age.

Additional studies could examine the pancreatic β-cell function within WT and IL-1RI$^{-/-}$ mice. Islets could be isolated from the pancreas using collagenase and insulin secretion measured in response to glucose. The β-cells release insulin in two phases; in the first phase, insulin release is rapidly triggered in response to increased blood glucose while in the second phase there is a sustained slow release of newly formed insulin vesicles. Administration of the glucose during the GTT leads to a peak in blood glucose levels of around 15 minutes, causing an initial rapid release of insulin and leading to a quick decline in blood glucose. This is followed by a slow release of insulin from the pancreas, causing

glucose levels to drop gradually back to normal. At week 0 and 6 of the GTT the glucose peaks are higher within IL-1RI$^{-/-}$ mice suggesting they have an impaired first phase insulin response, however they recover more rapidly than WT suggesting an improved second insulin release phase. In humans the assumption has been generally made that the 30 minute response reflected first phase insulin release, whereas the 120 minute response reflected second phase insulin release. The earliest detectable defect in β-cell function is commonly thought to be a reduction in first-phase insulin release (Cerasi and Luft, 1967). This may suggest that at week 0 and 6 the IL-1RI$^{-/-}$ mice show symptoms of β-cell dysfunction. These mice with impaired β-cell function may be more likely to develop T2DM if exposed to other risk factors such as increased body weight. However, in opposition to this hypothesis, IL-1β administration has been shown to induce apoptosis in isolated rat and human pancreatic islet cells in addition to pancreatic β-cell lines (Bendtzen *et al.*, 1986; Kaneto *et al.*, 1995).

Alternatively, the low glucose peaks observed within IL-1RI$^{-/-}$ mice at week 0 and 6 may suggest the glucose injections, although accurately measured, were too low and did not induce a strong enough peak. However, the reduced glucose peak is not evident at week 4, 12 and 16 in IL-1RI$^{-/-}$ mice suggesting either a recovery of the β-cells or more accurate glucose injections. Importantly, WT mice show a general deterioration in their second phase insulin release as shown by the higher glucose levels at 120 minutes post IP glucose injection compared to the IL-1RI$^{-/-}$. This may indicate that during the course of the HFD, WT mice develop a state of reduced whole body insulin sensitivity with decreased glucose disposal as a result.

Unfortunately, the plasma insulin measurements made during the GTT show no peak in insulin (data not shown). This may suggest that the insulin peak was missed. In terms of improving the methodology, a hyperinsulinemic euglycemic clamp could be used to quantify insulin resistance more accurately. This measures the amount of glucose necessary to compensate for an increased insulin level without causing hypoglycemia and is the gold standard for insulin resistance analysis. Fasting plasma insulin concentrations were also assessed during the 16 week HFD study. Interestingly, fasting plasma insulin levels increased in the WT from week 0 to 6 of the HFD. Increased fasting insulin levels are suggestive of a state of insulin resistance. The pancreas increases production of insulin in a state known as hyperinsulinemia to try and compensate for the insulin resistant state. After 12 weeks HFD, IL-1RI$^{-/-}$ mice had significantly lower insulin concentration compared to WT suggesting the IL-1RI$^{-/-}$ mice are more insulin sensitive.

This study also examined body weight, food intake and fat mass within the IL-1RI$^{-/-}$ mice and WT controls. The data indicates that these factors are partially controlled by the IL-1 signaling pathway. Within this 16 week HFD study the body weights of the IL-1RI$^{-/-}$ mice were significantly lower at weeks 6 to 12 of the HFD. The food intake was higher at weeks 8, 12 and 16 of the HFD in the IL-1RI$^{-/-}$ groups compared to WT. This data may suggest that the IL-1R1$^{-/-}$ have a different metabolic rate or perhaps utilise the fat from the HFD in a different way to the WT group. However, at week 16 of the HFD there was no significant difference in body weight or food intake between groups. It would be interesting to measure the metabolic activity within these mice using a metabolic cage to discern any differences in metabolism between WT and IL-1RI$^{-/-}$ mice. This cage allows urine and faeces collection, oxygen consumption measurements and monitoring of animal movements. Additionally, a pair-feeding method could be used in which the amount of food consumed by the experimental animal is immediately delivered control animal. The methabolic cage and pair-feeding method could elucidate if the WT and IL-1RI$^{-/-}$ mice have differences in food intake or metabolism. Interestingly, EAT and VAT mass was lower in the IL-1RI$^{-/-}$ mice compared to the WT mice at week 16 of the HFD, suggesting the body composition of IL-1RI$^{-/-}$ mice differs from that of the WT. Analysis of body composition in IL-1RI$^{-/-}$ and WT controls could be further examined using dual-energy X-ray absorptiometry (DEXA) or magnetic resonance imaging (MRI).

The data from our study conflicts with studies by Garcia *et al* (2005) and Somm *et al* (2005). Somm *et al.* established that excess IL-1 activity due to gene knockout of the IL-1Ra in mice induces a lean phenotype due to decreased fat mass, while Garcia *et al.* established that IL-1RI$^{-/-}$ mice have a specific increase in body weight and fat mass (Somm *et al.*, 2005); (Garcia *et al.*, 2006). Somm *et al.* used an alternative model to examine the effects of IL-1 in obesity. They assume that IL-1Ra knockout mice have increased IL-1 activity however, this is not conclusively proven as there are no measurements of the IL-1RI or IL-1β in either the tissues or plasma. Furthermore, an excessively activated IL-1β pathway may not act in reverse to an inactive IL-1β pathway as may be expected.

There are also clear discrepancies between this study and the study by Garcia *et al* (2005). Within this study a HFD (45% energy as fat) was administered to IL-1RI$^{-/-}$ and WT from the age of 6 weeks for a 16 week duration. Garcia *et al.* (2005) used a standard chow control diet for 12 months. They found no significant change in body weight until 6 months of age. In 4 month old mice there were no significant changes in body fat content, however in 9 month old mice there was a significant increase in body fat content. They termed the younger 4 month old mice as pre-obese and the older 9 month old mice as

obese. This may suggest that age and diet are important factors within this IL-1RI$^{-/-}$ phenotype. Our data may suggest that within younger IL-1RI$^{-/-}$ mice there is protection against HFD induced obesity whereas Garcia *et al.* may have demonstrated that within older chow fed IL-1RI$^{-/-}$ mice the reverse is true with less protection against diet induced obesity.

Leptin is an important regulator of food intake and energy expenditure that links peripheral adipose energy stores to the hypothalamic satiety center and serves as a very sensitive marker of the body fat content and metabolic activity (Havel, 2002). Leptin concentrations increase with obesity and tend to decrease with weight loss. Levels of serum leptin are highly correlated with adipose tissue mass; and the increased expression of the *ob* gene in the adipocytes of obese subjects suggests that this is due to increased synthesis of leptin (Considine *et al.*, 1996). Zimmet *et al* (1996) report a link between serum leptin and levels of obesity among Western Samoans in the South Pacific, a population with a particularly high prevalence of severe obesity and T2DM (Zimmet *et al.*, 1996), suggesting leptin may increase the risk of developing obesity induced T2DM. Fasting plasma leptin concentrations increased in the WT and IL-1RI$^{-/-}$ groups at week 0 to 12. However, fasting plasma leptin concentrations were significantly lower in the IL-1RI$^{-/-}$ mice compared to controls. The increased leptin levels within the mice may correlate with the increased adipose tissue mass with the WT mice showing higher levels of both adipose and leptin. Furthermore, the increased leptin levels may have repressed food intake as observed within the WT mice. However, when the fasting plasma leptin levels were corrected for body weight a similar trend was observed to the uncorrected total fasting plasma concentrations. This suggests that body weight did not have a significant effect on leptin secretion in this model. The leptin levels were higher within the WT at base line indicating that the IL-1RI$^{-/-}$ mice express less leptin endogenously. This base line disparity may be due to genetic or environmental differences as discussed previously. The high leptin levels may indicate a state of leptin resistance in WT mice.

Interestingly, leptin may also be directly regulated by IL-1β. Faggioni *et al.* (1998) found that IL-1β mediates leptin induction during inflammation (Faggioni *et al.*, 1998). IL-1β deficient ($^{-/-}$) and IL-6 deficient ($^{-/-}$) mice were injected intra-peritoneally with LPS or subcutaneously with turpentine, as models of systemic or local inflammation respectively. In IL-1β$^{+/+}$ mice, both LPS and turpentine increased leptin mRNA and circulating leptin. In contrast, neither LPS nor turpentine increased leptin levels in IL-1β$^{-/-}$ mice. In IL-6$^{+/+}$ or IL-6$^{-/-}$ mice, turpentine increased leptin protein to comparable levels. They conclude that

IL-1β is essential for leptin induction by both LPS and turpentine in mice, but IL-6 is not (Faggioni *et al.*, 1998). This suggests that the IL-1RI$^{-/-}$ mice may lack leptin secretion and this may explain the low levels of plasma leptin observed within these mice.

Epidemiological evidence has indicated that circulating adiponectin levels are reduced in patients with insulin resistance, T2DM, obesity or cardiovascular disease (Arita *et al.*, 1999; Lindsay *et al.*, 2002; Lindsay *et al.*, 2003). Low plasma adiponectin levels in these disease states are accompanied by reduced adiponectin gene expression in adipose tissue (Hotta *et al.*, 2001; Weyer *et al.*, 2001). Fasting adiponectin concentrations significantly increased from week 0 to 6 and 0 to 12 of the HFD in WT mice. Within the IL-1RI$^{-/-}$ group there was a significant increase in adiponectin levels from week 0 to 6 of the HFD. These increases may correlate with the increased WAT mass and may also suggest both groups are maintaining some degree of insulin sensitivity. After 12 weeks HFD there was a significant reduction in the plasma adiponectin concentration within the IL-1RI$^{-/-}$, this may correlate with the lower WAT mass observed within these mice. It may suggest a reduction in insulin sensitivity within the IL-1RI$^{-/-}$ group at 12 weeks HFD, which correlates with the GTT data.

Fasting resistin levels significantly increased from week 0 to 6 of the HFD in the IL-1RI$^{-/-}$ mice, however there was no significant difference between groups. Human studies have reported positive correlations between serum resistin and body fat content (Zhang *et al.*, 2002). On the contrary, several studies have failed to demonstrate such correlations in rodents. Asensio *et al.* (2004) determined that mice fed a HFD had induced adipocyte differentiation, denoted by increased aP2 gene expression, a surrogate marker of differentiation, which positively correlated with resistin gene expression (Asensio *et al.*, 2004). Subsequently, in view of this and previous studies (Haugen *et al.*, 2001; Kim *et al.*, 2001b), it was suggested that elevated resistin expression was a result of adipocyte differentiation (Asensio *et al.*, 2004). It is of note that the resistin levels are increased at week 6 of the HFD while adipocyte size was moderately reduced at week 6 and significantly reduced at week 8 within the IL-1RI$^{-/-}$ group. Therefore, the increase in plasma resistin levels could have been caused by an increase in differentiation of pre-adipocytes to new smaller adipocytes as observed.

A wide range of cytokines and chemokines within the plasma were analysed, however the concentrations of several, such as TNF-α, IL-6, IL-4, IL-10, IFN-γ and MCP-1, were unexpectedly too low to be detected consistently throughout the study. In a recent study, plasma cytokine concentration was measured successfully using the Multiplex kit from untreated CD1 mice (Bobrowski *et al.*, 2005). Concentrations ranged from ~50-100

pg/ml for TNF-α, IL-6 and IL-10 to ~10 pg/ml for IFN-γ. Cytokines such as IL-6 are drastically increased 100 fold within obese mice such as untreated *ob/ob* (Terao *et al.*, 2008). Therefore, the plasma samples from our mice should have contained detectable levels of these cytokines suggesting an error during analysis. Millipore carried out this analysis and therefore we cannot be sure of the cause of this error. However, plasma IL-1β concentrations were shown to decrease significantly within the IL-1RI$^{-/-}$ group at week 6 compared to week 0. Furthermore, at week 6 of the HFD plasma IL-1β concentrations were significantly reduced in the IL-1R1$^{-/-}$ group compared to the WT group. IL-1β remains lower in IL-1RI$^{-/-}$ mice throughout the study and this may be due to decreased inflammation and macrophage accumulation into adipose tissue or caused by the lack of IL-1RI$^{-/-}$ signalling directly. Ilyin *et al.* (1996) examined IL-1β-induced profiles of IL-1β, IL-1 receptor type I and II (IL-1RI and IL-1RII) and IL-1 receptor antagonist (IL-1Ra) within the brain (Ilyin and Plata-Salaman, 1996). mRNA levels were highly inter-correlated within the same samples suggesting the operation of an IL-1β feedback system (Ilyin and Plata-Salaman, 1996). However, it is interesting to note that IL-1β was increased in the WT mice at week 6, which correlates with the reduced insulin sensitivity observed in these mice. It would be interesting to examine IL-1Ra expression within the WT and IL-1RI$^{-/-}$ mice during the 16 week HFD intervention to gain further insight into the IL-1 signalling pathway during diet induced obesity.

CCL5 was successfully measured in this study. Wu and colleagues (2007) observed that CCL5 was increased in WAT of murine and human obesity (Wu *et al.*, 2007). CCL5 and its receptors also contribute to macrophage recruitment and are implicated in the development and progression of atherosclerotic lesions (Appay and Rowland-Jones, 2001; Schober *et al.*, 2002). Systemic CCL5 concentrations were reported to be higher in obese individuals with T2DM or impaired glucose tolerance than in non-diabetic controls (Herder *et al.*, 2005). Interestingly, plasma CCL5 concentrations within our study showed an increase at week 12 compared to week 0 in the WT mice and not the IL-1RI$^{-/-}$ mice signifying that the control mice may have increased macrophage infiltration at week 12. This correlates with the idea that the IL-1RI$^{-/-}$ mice may have less ATM at week 16 and are protected from the insulin resistant state observed within the WT.

TAG play an important role in the metabolism as energy sources and transporters of dietary fat. Lipoprotein lipases break down TAG into NEFA and glycerol. NEFA can then be taken up by cells via the fatty acid transporter (FAT). Insulin resistance, dyslipidaemia and abnormal NEFA metabolism are common features found in subjects with the metabolic syndrome (DeFronzo and Ferrannini, 1991; Reaven, 1995). The

regulation of TAG and high-density lipoprotein (HDL) concentrations is not entirely understood, however there is abundant data demonstrating that these parameters are associated with insulin resistance (Frayn and Coppack, 1992; Laws and Reaven, 1992). Plasma TAG concentrations significantly increase in the WT group at weeks 6 and 8 of the HFD relative to week 0 but dropped at week 16 of the HFD relative to week 8, signifying the WT mice are most insulin resistant at week 8. While fasting plasma TAG levels significantly increased in the IL-1RI$^{-/-}$ group at week 6 relative to week 0 suggesting a reduction in insulin sensitivity at week 6. Fundamentally, fasting plasma TAG concentrations are reduced in the IL-1RI$^{-/-}$ group relative to the WT at week 0 and 8 indicating the IL-1RI$^{-/-}$ mice are perhaps more insulin sensitive. When fasting plasma TAG levels were corrected for body weight a similar trend was observed to the uncorrected total fasting plasma TAG level. This indicates that body weight did not have a significant effect on plasma TAG levels in these mice.

Total fasting plasma NEFA levels showed a similar trend to the TAG as expected. Although there were no significant differences in NEFA levels between IL-1RI$^{-/-}$ and WT groups at all time points. Interestingly, plasma NEFA levels were increased within the IL-1RI$^{-/-}$ mice at weeks 0, 6, 12 and 16 of the HFD when corrected for body weight. Increases in plasma NEFA could be interpreted as an increase in lipid oxidation. Stored fat within the WAT is likely mobilized in to NEFA and released into the plasma in an attempt to meet energy demands. As hypothesised earlier it is likely the IL-1RI$^{-/-}$ have a higher metabolism and an increased energy demand. The IL-1RI$^{-/-}$ mice appeared to have a leaner body mass with lower body weight, reduced adipose tissue mass and increased food intake. As discussed previously this hypothesis could be explored further with the use of metabolic cages. Furthermore, expression of lipases involved in lipolysis could be explored within the WAT.

The data from the GTTs and cytokine profiling may indicate that at week 16 the WT mice undergo macrophage infiltration into the WAT causing a heightened state of inflammation and a reduction in insulin sensitivity, which the IL-1RI$^{-/-}$ mice are partially protected from. Gene expression of insulin sensitive and inflammatory targets was therefore assessed within the EAT to further explore this hypothesis. GLUT4, IRS-1, PPAR-γ, adiponectin and resistin mRNA levels were significantly higher at week 0 of the study in the IL-1RI$^{-/-}$ group signifying that the EAT of the IL-1RI$^{-/-}$ mice are more insulin sensitive at this time point. PPAR-γ is a transcription factor, which regulates many genes involved in lipid and glucose metabolism. PPAR-γ also plays a key role in adipogenesis and adipocyte differentiation. Therefore the high level of mRNA at week 0 of the study in

the IL-1RI$^{-/-}$ group may indicate that the EAT contain an increased number of differentiated mature adipocytes with increased lipid and glucose metabolism. The adiponectin and resistin mRNA levels at week 0 do not correlate with the plasma concentrations observed, which could indicate that another adipose tissue depot such as the VAT is also important in controlling the plasma levels; additionally there may also be an inhibition in protein production within the EAT adipocytes at week 0. The expression levels of these insulin sensitive targets remain high at week 6 in the IL-1RI$^{-/-}$ mice, however not significantly. At week 8 and 16 the mRNA expression levels are not significantly different between IL-1RI$^{-/-}$ and WT groups. This suggests that the IL-1RI$^{-/-}$ EAT is initially more insulin sensitive compared to WT at week 0 but reduces to the normal levels expressed by the WT over the course of the HFD. It seems likely that the activity of the insulin targets are not necessarily regulated through transcriptional expression but through post-translational modification such as activational or inhibitor phosphorylation of the proteins. Furthermore, other depots of WAT such as the VAT may also play a key role in insulin sensitivity.

The gene expression of inflammatory targets was also assessed. TNF-α mRNA levels were found to be significantly lower at week 16 of the HFD in the IL-1RI$^{-/-}$ group. This suggests that the EAT of the IL-1RI$^{-/-}$ group is less inflammatory, possibly due to a reduction in ATMs and other immune cells due to the IL-1RI$^{-/-}$ phenotype. Furthermore, within the isolated adipocytes of the EAT there was a moderate reduction in TNF-α mRNA expression in the IL-1RI$^{-/-}$ group compared to the WT suggesting the adipocytes themselves are less inflamed. MCP-1 mRNA expression was also examined as MCP-1 is known to recruit immune cells such as monocytes to sites of tissue injury and infection. Interestingly, MCP-1 mRNA expression was initially up regulated in the IL-1RI$^{-/-}$ mice, however at weeks 6 and 8 of the HFD MCP-1 was significantly lower in the IL-1RI$^{-/-}$ group relative to the WT group. Concurrently, CCL5 a similar chemokine was established to be up-regulated within the plasma of the WT group at week 12 of the HFD. Additionally, within the isolated adipocytes of the EAT there was a moderate reduction in MCP-1 mRNA expression in the IL-1RI$^{-/-}$ group compared to the WT also suggesting the adipocytes are less inflamed after 16 weeks on a HFD. MIF is a pro-inflammatory cytokine, and plasma MIF concentrations are elevated in obese individuals. Conflictingly, MIF gene expression was found to be up-regulated in the IL-1RI$^{-/-}$ mice compared to WT mice at week 8 of the HFD suggesting the EAT from the IL-1RI$^{-/-}$ mice may be more inflammatory at week 8.

It was observed that adipocyte size within the EAT was significantly lower in the IL-1RI$^{-/-}$ mice at week 8 and 16 of the HFD. Interestingly, there was a significant increase in adipocyte size throughout the study within the WT group. This could suggest that the IL-1 pathway regulates the size or differentiation of adipocytes. Maffeis *et al.* (2007) found that increased adipocyte size was correlated with a reduction in insulin sensitivity and an increase in IL-6 and TNF-α plasma concentrations (Maffeis *et al.*, 2007). They propose that once the fat cell becomes hypertrophic, a cellular program is initiated, aiming to restrain further volumetric growth. Increased expression of cytokines and reduced synthesis of adiponectin lead to cellular insulin resistance, in the presence of which further growth of adipocytes is hampered severely. Hence, fatty substrates are redirected to other tissues, where the undesirable effects of lipotoxicity occur and ectopic fat deposition is favoured (Maffeis *et al.*, 2007). Within this study at week 16 inflammatory targets such as the adipose tissue TNF-α mRNA and plasma CCL5 were reduced within the IL-1RI$^{-/-}$ group which corresponds with the reduction in adpocyte size. Furthermore, the increased insulin sensitivity as observed in the GTT may reflect the decreased adipocyte size within the IL-1RI$^{-/-}$ group. It was determined that EAT adipocyte size was increased at week 12 within the IL-1RI$^{-/-}$ mice, correlating with the reduction in insulin sensitivity observed within the GTT data and indicating that larger adipocytes may be less insulin sensitive.

Additionally, Monteiro *et al.* (2006) determined that larger adipocytes are more prone to rupture and adipocyte cell death (Monteiro *et al.*, 2006). The increase in adipocyte cell size as observed in the WT group of this study could cause increased cell necrosis leading to increased infiltration of macrophages and therefore could reflect the increased inflammation of the adipose tissue and the reduction in insulin sensitivity observed. However, IL-1β is also an angiogenic factor and plays a role in tumor metastasis and blood vessel formation (Voronov *et al.*, 2003). In mice deficient in IL-1β, vascular endothelial cell growth factor (VEGF) cannot stimulate formation of blood vessels (Dinarello, 2009). The small adipocyte size could therefore be due to poor vascularisation.

In conclusion, IL-1RI$^{-/-}$ mice showed lower body weight and adipose tissue mass with higher food intake suggesting the IL-1RI$^{-/-}$ mice have increased metabolic activity and a lean body mass. The IL-1RI$^{-/-}$ mice remained more insulin sensitive with more efficient glucose clearance especially within phase 2 of insulin secretion from the pancreas. In comparison the WT mice undergo a steady decline in their glucose clearance over the 16 week HFD. At week 6 it seems likely that the increased insulin sensitivity within the IL-1RI$^{-/-}$ mice is due to their reduced body weight. However, at week 16 there was no significant difference between body weights suggesting the increased insulin sensitivity

within the IL-1RI$^{-/-}$ group is due to reduced inflammation and reduced macrophage infiltration within the adipose tissue. This is compounded by a reduction in IL-1β and CCL5 concentrations within the plasma in addition to reduced TNF-α and MCP-1 mRNA expression within the IL-1R$^{-/-}$ mice EAT particularly at weeks 12 and 16 suggesting these mice are less pro-inflammatory and that the adipose tissue may have less immune cell infiltration. Furthermore, IL-1RI$^{-/-}$ mice exhibited lower fasting plasma insulin and TAG levels suggesting these mice are more insulin sensitive. IL-1R1$^{-/-}$ mice exhibited higher levels of GLUT4, IRS-1, PPAR-γ and adiponectin gene expression at week 0 also signifying these mice are perhaps more insulin sensitive. Additionally, IL-1R1$^{-/-}$ mice exhibited smaller adipocyte size, a common feature of lean highly insulin sensitive adipose tissue. Plasma leptin levels were significantly lower in the IL-1RI$^{-/-}$ mice compared to WT, suggestive of the fact that the WT mice are leptin resistant while the IL-1RI$^{-/-}$ mice controls leptin secretion or perhaps reflects lower adipose tissue mass. High plasma leptin levels within the WT mice may also have reduced food intake. Plasma NEFA levels were increased within the IL-1RI$^{-/-}$ mice when corrected for body weight. Increases in plasma NEFA could be interpreted as an increase in lipid oxidation indicative of fat mobilized to meet energy demands. It is possible the IL-1RI$^{-/-}$ have a higher metabolism and have an increased energy demand.

This study has produced many interesting findings however further work is ongoing to elucidate this model in more depth. Analysis of genetically engineered mice is crucial for our understanding of the *in vivo* function of genes and proteins in the whole organism. In this study the knockout represents a powerful tool for elucidating IL-1 function in a model of obesity induced insulin resistance. However, in future studies conditional gene targeting applying the Cre/loxP-mediated recombination system could be used to evaluate how deletion of the IL-1RI gene in a specific cell-type such as macrophages can affect the onset of obesity induced insulin resistance. Furthermore, using this Cre/loxP-mediated recombination system, a gene can be deleted within subregions or specific cell types in the brain such as the hypothalamus. Cytokines such as IL-1 are thought to have important effects on behaviour such as appetite. Therefore, a blockade in the IL-1 signalling pathway in specific regions of the central nervous system (CNS) may have protective effects in terms of obesity induced insulin resistance and this could be explored using conditional gene targeted knockout mice.

Another system of examining IL-1 signalling within an obesity induced insulin resistance mouse model is to lethally irradiate, from a cesium gamma source, WT recipient mice and injected them with bone marrow cells from corresponding IL-1RI$^{-/-}$ mice. This

would establish the specific effects of IL-1 signalling within bone marrow derived immune cells such as the macrophages in terms of obesity induced insulin resistance. Correspondingly, IL-1RI$^{-/-}$ mice could be irradiated and injected with the bone marrow of WT mice. This would determine the specific effects of IL-1 signalling within the HFD induced insulin resistance correlating with tissues such as the adipose. These studies could add insight into the IL-1RI$^{-/-}$ model and identify the importance of IL-1 signalling in ATM during obesity induced T2DM.

Chapter 4

The Effects of IL-1β Treatment on Inflammatory and Insulin Signalling *In Vitro* within 3T3-L1 Adipocytes

4.1 Introduction

Recent studies show clear evidence that cytokines are not only produced by adipocytes but are also capable of inducing insulin resistance in these cells. The implications of many cytokines, such as tumour necrosis factor (TNF)-α and interleukin (IL)-6, in insulin resistance are well documented. Elevated levels of TNF-α have been hypothesized to induce insulin resistance in a variety of catabolic disease states, including cancer (McCall *et al.*, 1992), sepsis (Van der Poll *et al.*, 1991) and trauma (Ikezu *et al.*, 1997). Furthermore, direct exposure of healthy individuals, animals or isolated cells to TNF-α induces a state of insulin resistance (Feinstein *et al.*, 1993; Hauner *et al.*, 1995; Hotamisligil *et al.*, 1994a; Hotamisligil *et al.*, 1994b; Hotamisligil *et al.*, 1996; Lang *et al.*, 1992; Liu *et al.*, 1998). In obese individuals and rodent models of obesity, TNF-α is over-expressed in adipose and muscle tissue (Hotamisligil *et al.*, 1995; Hotamisligil *et al.*, 1993; Saghizadeh *et al.*, 1996) at both the mRNA and protein level, consistent with reports that circulating levels of TNF-α are increased in individuals with NIDDM (Katsuki *et al.*, 1998; Pfeiffer *et al.*, 1997). Additionally, levels of TNF-α expression strongly correlate with hyperinsulinemia and decreased insulin sensitivity. A number of *in vitro* studies, in adipocytes, suggest that TNF-α may act directly to down-regulate glucose transporter (GLUT)-4 gene expression, thereby decreasing insulin-stimulated glucose transport (Hauner *et al.*, 1995; Long and Pekala, 1996; Stephens and Pekala, 1991). TNF-α increases the serine phosphorylation of IRS-1. This mechanism reduces its tyrosine phosphorylation and activation by the insulin receptor (Gual *et al.*, 2005; Tanti *et al.*, 1994; Zick, 2001). Several mitogen-activated protein kinases (MAPK) including JNK c-Jun N-terminal kinase (Aguirre *et al.*, 2000), mammalian target of rapamycin (mTOR) (Gual *et al.*, 2003; Ozes *et al.*, 2001) and extracellular signal-regulated kinases (ERK) (Bouzakri *et al.*, 2003; Engelman *et al.*, 2000; Gual *et al.*, 2003) have been implicated in the serine phosphorylation of insulin receptor substrate (IRS)-1. TNF-α and IL-6 also enhance the expression of cytokine signalling molecule (SOCS) proteins that can attenuate insulin signaling by binding to the insulin receptors and reducing their ability to phosphorylate IRS proteins (Emanuelli *et al.*, 2000; Ueki *et al.*, 2004a). Alternatively, SOCS proteins can bind directly to IRS proteins, leading to their degradation (Rui *et al.*, 2002; Shi *et al.*, 2006a). Conversely, in 3T3-L1 adipocytes, acute treatment with cytokines such as TNF-α

can enhance IRS-1 tyrosine phosphorylation and its association to the p85 phosphatidylinositol-3 Kinase (PI3K) subunit (Guo and Donner, 1996) leading to an increase in glucose uptake via GLUT1. TNF-α is also a potent inhibitor of adipocyte differentiation and can suppress the expression of some adipocyte-specific genes such as peroxisome proliferator-activated receptor (PPAR)-γ in fully differentiated adipocytes (Xing *et al.*, 1997).

Similarly, studies have shown that human adipose tissue is a major site of IL-6 secretion (Fried *et al.*, 1998; Mohamed-Ali *et al.*, 1997) accounting for 15 – 35% of the IL-6 circulating levels (Mohamed-Ali *et al.*, 1997), whereas TNF-α, in contrast, is only secreted at very low levels by human fat cells (Mohamed-Ali *et al.*, 1997). Long term incubation with IL-6 has been shown to increase basal glucose transport in 3T3-L1 adipocytes, whereas acute stimulation had no effect (Stouthard *et al.*, 1996). IL-6 has been shown to impair both insulin action and the insulin-signaling pathway. IL-6, in contrast to TNF-α, does not appear to activate JNK or increase the phosphorylation of serine 307 or serine 612 of IRS-1. However, IL-6 similarly to TNF-α, inhibits the transcriptional activity and protein expression of several molecules related to insulin signalling and action, including IRS-1 and GLUT4 in adipocytes (Rotter *et al.*, 2003). Interestingly, a preliminary study suggests that IL-6 may increase lipolysis in human fat cells maintained in culture for 48 hours (Rotter *et al.*, 2003).

Interestingly, both TNF-α and IL-6 can reduce adiponectin secretion from adipocytes (Tilg *et al.*, 1994). Adiponectin is one of the most abundant adipose tissue specific factor and appears to improve insulin sensitivity and inhibit vascular inflammation (Lyon *et al.*, 2003). Serum adiponectin levels are low in obese subjects and increase after weight loss. Hypoadiponectinemia may contribute to insulin resistance and accelerated atherogenesis associated with obesity (Ouchi *et al.*, 1999). Therefore, the increased cytokine expression in adipose tissue may also be linked to the reduction in adiponectin secretion. Kaser *et al.* (2003) observed that within human peripheral blood mononuclear cells (PBMC) resistin mRNA expression is strongly increased by the pro-inflammatory cytokines IL-1, IL-6 and TNF-α. This suggests that in humans resistin may be a link between inflammation and insulin resistance (Kaser *et al.*, 2003). Initial studies in rodents suggest that resistin is up-regulated in obesity, this participating in the pathogenesis of insulin resistance (Ouchi *et al.*, 2003). Studies have also shown that IL-6 can induce the synthesis of IL-1Ra and IL-10 which suggests that IL-6 may have some anti-inflammatory properties (Steensberg *et al.*, 2003; Tilg *et al.*, 1994). Straczkowski *et al.* (2005)

demonstrated a significant positive association between circulating IL-10 levels and whole-body insulin sensitivity (Straczkowski *et al.*, 2005). The effects of IL-1Ra are more controversial as discussed in chapter 3.

Expression of IL-1β is also increased in adipose tissue of both obese rodents and humans and its expression correlates with the metabolic syndrome (MetS) (Salmenniemi *et al.*, 2004). As discussed in chapter 3 many *in vivo* animal models and human trials have examined the effects of the IL-1 pathway in obesity and insulin resistance however, much of this evidence is controversial. Several studies suggest potential up-regulation of IL-1 in IL-1Ra$^{-/-}$ mice can reduce body weight and increase insulin sensitivity (Matsuki *et al.*, 2003; Somm *et al.*, 2005). Additional studies propose that down-regulation of IL-1 in mice treated with IL-1Ra increases insulin sensitivity (Larsen *et al.*, 2007; Sauter *et al.*, 2008). In the case of IL-1RI$^{-/-}$ mice, some studies indicate that a high fat diet (HFD) reduces insulin sensitivity within these mice, while previous work from our group indicated that IL-1RI$^{-/-}$ mice are partially protected against obesity induced insulin resistance (De Roos *et al.*, 2009; Garcia *et al.*, 2006). However, *in vitro,* the effects of IL-1β on adipocytes are more consistent and consistent with the effects of other cytokines such TNF-α and IL-6. Chronic treatment with IL-1β in adipocytes has been shown to decrease insulin induced glucose uptake by reducing the expression of GLUT4 and inhibiting its translocation to the plasma membrane (Jager *et al.*, 2007). This inhibitory effect was due to a decrease in the amount of IRS-1 and a decrease in tyrosine phosphorylation of IRS-1 (Jager *et al.*, 2007). IL-1 has also been shown to inhibit adipocyte differentiation (Fried *et al.*, 1993; Gregoire *et al.*, 1992; Price *et al.*, 1986; Suzawa *et al.*, 2003) and induce lipolysis (Feingold *et al.*, 1992) consistent with the effects of IL-6. In a recent report treatment of mature 3T3-L1 adipocytes with IL-1β for six days did not modify their differentiation state (Lagathu *et al.*, 2006), however addition of the cytokine during the differentiation process markedly altered the adipocyte phenotype (Lagathu *et al.*, 2006; Ohsumi *et al.*, 1994).

After binding of IL-1α or IL-1β to the IL-1RI, the IL-1 receptor accessory protein (IL-1RacP) (Greenfeder *et al.*, 1995) binds to this receptor complex, myeloid differentiation primary response gene (MyD88) and toll interacting protein (TOLLIP) are then recruited to the receptor complex with subsequent addition of interleukin-1 receptor associated protein kinase (IRAK) (Huang *et al.*, 1997; Li *et al.*, 2001) and activation of tumour necrosis factor receptor-associated factor (TRAF)-6. TRAF6 is thought to activate the nuclear factor (NF)-κB pathway and MAPKs including ERK, JNK and p38 (Martin and Wesche, 2002) through a series of kinase and phosphorylation steps (Ninomiya-Tsuji *et*

al., 1999) leading to transcriptional activation by NF-κB and c-JUN (Figure 4.1). Interestingly, elevated activities of these MAPKs are found in adipocytes and muscles of obese and insulin resistant rodents and humans (Gual *et al.*, 2005). Jager *et al.* (2004) established that prolonged IL-1β treatment induced a sustained activation of ERK and p38 but not JNK, suggesting that an increase in IL-1β expression in adipose tissue could thus participate in the elevated activity of these kinases in obesity (Jager *et al.*, 2007). Activation of these kinases could be involved in the inhibitory effect of IL-1β on insulin-induced glucose transport. Activation of p38 was demonstrated to be involved in the down-regulation of GLUT4 expression (Carlson *et al.*, 2003). Jager *et al.* (2007) established that pharmacological inhibition of the ERK pathway totally prevented a decrease in IRS-1 mRNA and partially prevented the inhibition of IRS-1 protein expression induced by IL-1β treatment (Jager *et al.*, 2007). Furthermore, a recent study demonstrated that ERK1 deficient mice are more sensitive to insulin on a HFD (Bost *et al.*, 2005). It seems likely that IL-1β impairs adipocyte biology and may induce insulin resistance. IL-1β is a major pro-inflammatory cytokine that is primarily produced by tissue macrophages and may therefore act in concert with other cytokines and adipokines within the adipose tissue playing a major role in the development of obesity induced insulin resistance. However, due to inconsistent data from multiple *in vivo* models, it therefore seems necessary to begin a comprehensive elucidation of the specific effects of IL-1β in adipocytes *in vitro* not only on protein expression but adipokine and cytokine secretion, adipocyte differentiation and glucose uptake at multiple time points.

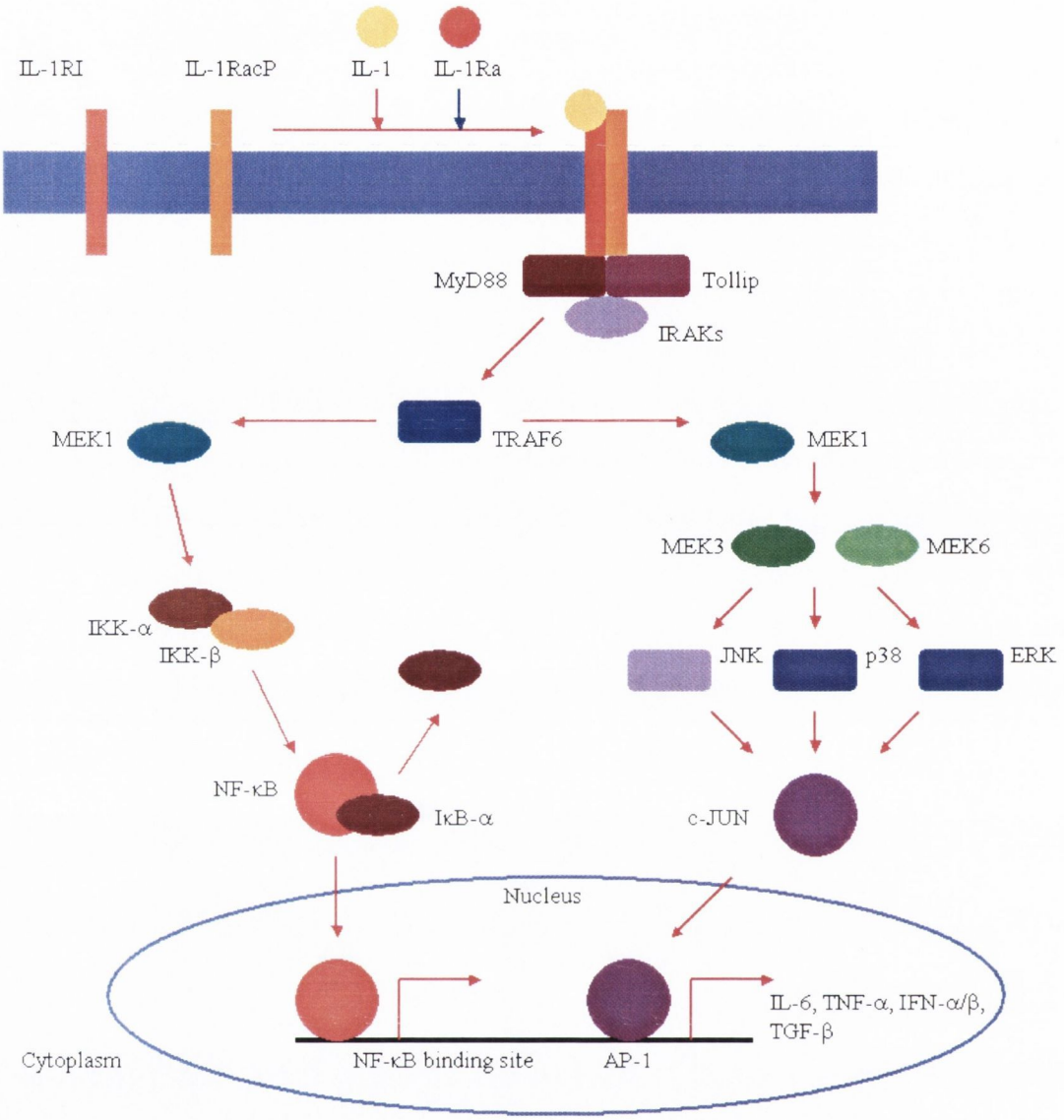

Figure 4.1 After IL-1 is bound a complex is formed between the type 1 receptor (IL-1RI) and the receptor accessory protein (IL-1RAcP). The cytosolic proteins MyD88 (Myeloid Differentiation primary response gene-88) and TollIP (Toll-Interacting Protein) are recruited to this complex, where they function as adaptors, recruiting IRAK (IL-1 Receptor-Associated Kinase). IRAK1, a serine-threonine kinase, activates and recruits TRAF6 (TNF Receptor-Associated Factors-6) to the IL-1 receptor complex. TRAF6 activates two pathways, which leads to the activation of transcription factors such as NF-κB and c-Jun.

4.2 Material and methods

4.2.1 Experimental design

3T3-L1 fibroblasts were differentiated to mature adipocytes as described in section 2.2.4. The cells were then stimulated with 10 ng/ml of IL-1β for 5 minutes, 15 minutes, 30 minutes, 1 hour, 2 hours, 24 hours and 48 hours as described in section 2.2.11. The 10 ng/ml dose was selected as previous studies have shown that cytokines such as IL-1α at a concentration of 10 ng/ml can induce insulin resistance within 3T3-L1 adipocytes (He *et al.*, 2006). Briefly, 3T3-L1 fibroblasts were grown to confluencey in 12-well plates and differentiation was initiated by culturing cells in the presence of insulin, dexamethasone and isobutyl-1-methylxanthine (IBMX) for six days. Differentiation media was removed and replaced with DMEM containing 10% FBS and penicillin/streptomycin for 24 hours. Fully differentiated adipocytes were then treated with 10 ng/ml of IL-1β in DMEM with penicillin/streptomycin and 0.2% BSA.

4.2.2 Protein analysis and Western blotting

Cells were washed in PBS and total cell lysates were extracted with RIPA buffer with protease inhibitor cocktail (Sigma-Aldrich) as described in section 2.8.1. Protein concentrations were assessed using the Bradford assay. 10 μg of protein was separated by electrophoresis through sodium dodecyl sulphate polyacrylamide (SDS-PAGE) gels and the proteins were then transferred to a nitrocellulose membrane as described in section 2.8.3 and 2.8.4. Details of the Western blotting and antigen detection techniques are described in sections 2.8.5 and 2.8.6. Briefly, membranes were blocked using 5% BSA in TBS with 0.1% tween 20 and then incubated overnight at 4°C with antibodies specific to GLUT4 (Millipore), phosphorylated-insulin receptor (Tyr1158, Tyr1162, Tyr1163), protein kinase (PK)-B/Akt, phosphorylated Akt (Thr308), IRS-1, phosphorylated IRS-1 (ser636/639), inhibitor of κB (IκB)-α, phosphorylated IκB-α (Ser32), phosphorylated-JNK1/2 p54/46 (Thr183/Tyr185), p38 MAPK, phosphorylated p38 MAPK (Thr180/Tyr182), phosphorylated p44/42 MAPK (ERK1/2, Thr202/Tyr204; Cell Signalling Technology®), JNK1 p54 and p44 MAPK (ERK1; Santa Cruz Biotechnology Inc.). Correct loading of protein was confirmed by blotting for actin (Sigma-Aldrich). Membranes were washed in TBS with 0.1% tween (Sigma-Aldrich) and then incubated with peroxidase conjugate anti-rabbit antibody (Santa Cruz Biotechnology Inc.) for 2 hours at room temperature. After further washing, immunoreactive bands were visualized using an enhanced chemiluminescence reaction (Supersignal® West Pico Cemiluminescent Substrate, Pierce Biotechnology). Membranes were exposed to film for 1 to 10 minutes

and processed using a XoGraph automatic X-ray processor (Healthcare Ltd.). The position of the band was confirmed by the inclusion of suitable molecular weight markers (Bio-Rad Laboratories). Protein bands were quantified by densitometry using the TINA software version 2.09c (Raytest, Straubenhardt, Germany) and protein levels were expressed as percentage change relative to adipocytes alone.

4.2.3 ELISA analysis

Supernatants were collected from the cells and ELISA analysis was carried out using commercially available kits from R and D Systems for leptin, resistin, adiponectin, TNF-α, IL-6 and IL-1β as described in section 2.9.1. Briefly, the primary or capture antibody specific to the antigen was coated to the walls of a 96-well microtiter plate. Standards were provided with the kits and were reconstituted to working concentrations by serial 1:2 dilutions in reagent diluent. Supernatant and standards were added directly to the 96-well microtiter coated with capture antibody and antigens became immobilized by the capture antibody. The secondary or detection antibody was added to the wells and bound to the immobilized antigen. The detection antibody was conjugated with horseradish peroxidase (HRP) and substrate tetramethylbenzidine (TMB) was added to each well. The immobilised HRP of the detection antibody acts on the TMB causing a blue colour to develop proportionally to the amount of antigen present. H_2SO_4 stops the oxidation of TMB and changes the blue colour to yellow. Absorbance of the wells was read in the microplate reader at 450 nm with a wavelength correction of 570 nm. A standard curve was constructed for each assay and sample concentrations were calculated through the equation of the standard curve.

4.2.4 Oil red O staining

A fresh working solution of oil red O was prepared as described in section 2.5. Adipocytes were washed in PBS and fixed in 10% neutral buffered formalin (Sigma-Aldrich). Cells were washed again and the working solution of oil red O was added. Cells were washed and observed under microscope (Nikon Corporation); images were taken using Matrox Intellicam (Matrox Electronic Systems Ltd.). Images were assessed using ImageJ, a public domain, Java-based image processing program developed at the National Institutes of Health (Collins, 2007). Images were converted to 8-bit greyscale and a thresholded binary image was created to highlights the red stained regions; these were then measured as pixels and converted to percentage fold change.

4.2.5 Glucose uptake assay

Glucose uptake was analyzed in 3T3-L1 adipocytes as described in section 2.6. Cells were incubated in serum free media with 0.2% BSA for 4 hours. Cells were then incubated in PBS with 0.2% BSA for 30 minutes prior to addition of 100 nMol of Insulin (Sigma-Aldrich) in PBS for 15 minutes, after which 5 μCi/ml of Deoxy-D-glucose, 2-[^{3}H(N)] (Perkin-Elmer) in 1 mMol glucose (Sigma-Aldrich) was added to the cells and incubated for 10 minutes. Cells were then washed twice and then lysed in RIPA buffer containing protease inhibitor cocktail (Sigma-Aldrich). The samples were added to scintillation fluid (National Diagnostics Inc.) and assayed for ^{3}H uptake as counts per minute (Tri-Carb 2900TR low activity liquid scintillation analyzer, Perkin-Elmer). The remaining lysates were stored at –80°C for western blot analysis.

4.2.6 Data preparation and statistical analysis

Data was reported as Mean ± SEM. Statistical analysis was performed with SPSS (SPSS Inc.). The distribution of data for each variable was assessed and variables transformed to normalise the distribution of data if necessary. Multiple comparisons were performed by one-way ANOVA. Significant inter-group differences were subsequently tested by post hoc Least Significant Difference (LSD) statistical analysis. Independent Student's t-tests (2 tailed) were performed between control and IL-1β treated cell. A statistical probability of $P \leq 0.05$ was considered statistically significant.

4.3 Results

4.3.1 Effects of IL-1β treatment on insulin pathway protein expression in 3T3-L1 adipocytes

A time course study examined the effects of IL-1β treatment (10 ng/ml) on IRS-1, phosphorylated IRS-1 (Ser636/639), phosphorylated insulin receptor (Tyr1158/Tyr116/Tyr1163), PKB/Akt, Akt (Thr308) and GLUT4 protein expression in 3T3-L1 adipocytes for up to 48 hours as presented in Figures 4.2 to 4.7.

Whole cell IRS-1 protein expression was significantly reduced in fully differentiated 3T3-L1 adipocytes treated with IL-1β for 15 minutes (16% decrease, $P \leq 0.026$), 30 minutes (16% decrease, $P \leq 0.024$), 60 minutes (20% decrease, $P \leq 0.009$), 120 minutes (22% decrease, $P \leq 0.004$) and 24 hours (21% decrease, $P \leq 0.006$; Figure 4.2). Conversely, IL-1β treatment of mature 3T3-L1 adipocytes significantly increased whole cell phosphorylated IRS-1 (Ser636/639) at 15 minutes (38% increase, $P \leq 0.007$), 30 minutes (44% increase, $P \leq 0.003$), 60 minutes (26% increased, $P \leq 0.045$) and 120 minutes (43% increase, $P \leq 0.003$). Phosphorylated-IRS-1 protein expression was also increased in adipocytes treated with IL-1β for 24 hours (25% decrease, $P \leq 0.058$) however not significantly (Figure 4.3).

Whole cell phosphorylated insulin receptor (Tyr1158/Tyr116/Tyr1163) protein expression was increased similarly in insulin stimulated 3T3-L1 adipocytes (32% increase) and insulin stimulated adipocytes treated with IL-1β for 48 hours (26% increase) compared to control adipocytes untreated with insulin ($P \leq 0.003$ and $P \leq 0.009$; Figure 4.4). A similar trend was observed for whole cell Akt protein expression in insulin stimulated 3T3-L1 adipocytes and insulin stimulated adipocytes treated with IL-1β for 48 hours (40% and 30% increase) compared to control 3T3-L1 adipocytes untreated with insulin (Figure 4.5). Interestingly, whole cell phosphorylated Akt (Thr308) protein expression was significantly increased 55% in insulin stimulated 3T3-L1 adipocytes relative to control unstimulated 3T3-L1 adipocytes ($P \leq 0.029$). Similarly, phosphorylated Akt protein expression was also significantly increased 76% in insulin stimulated 3T3-L1 adipocytes treated with IL-1β for 48 hours relative to control adipocytes ($P \leq 0.006$; Figure 4.6). Whole cell GLUT4 protein expression was significantly decreased 61% in insulin stimulated 3T3-L1 adipocytes treated with IL-1β for 48 hours relative to control 3T3-L1 adipocytes ($P \leq 0.009$; Figure 4.7). GLUT4 expression was decreased in insulin stimulated 3T3-L1 adipocytes treated with IL-1β for 48 hours relative to insulin stimulated 3T3-L1 adipocytes, however also not significantly.

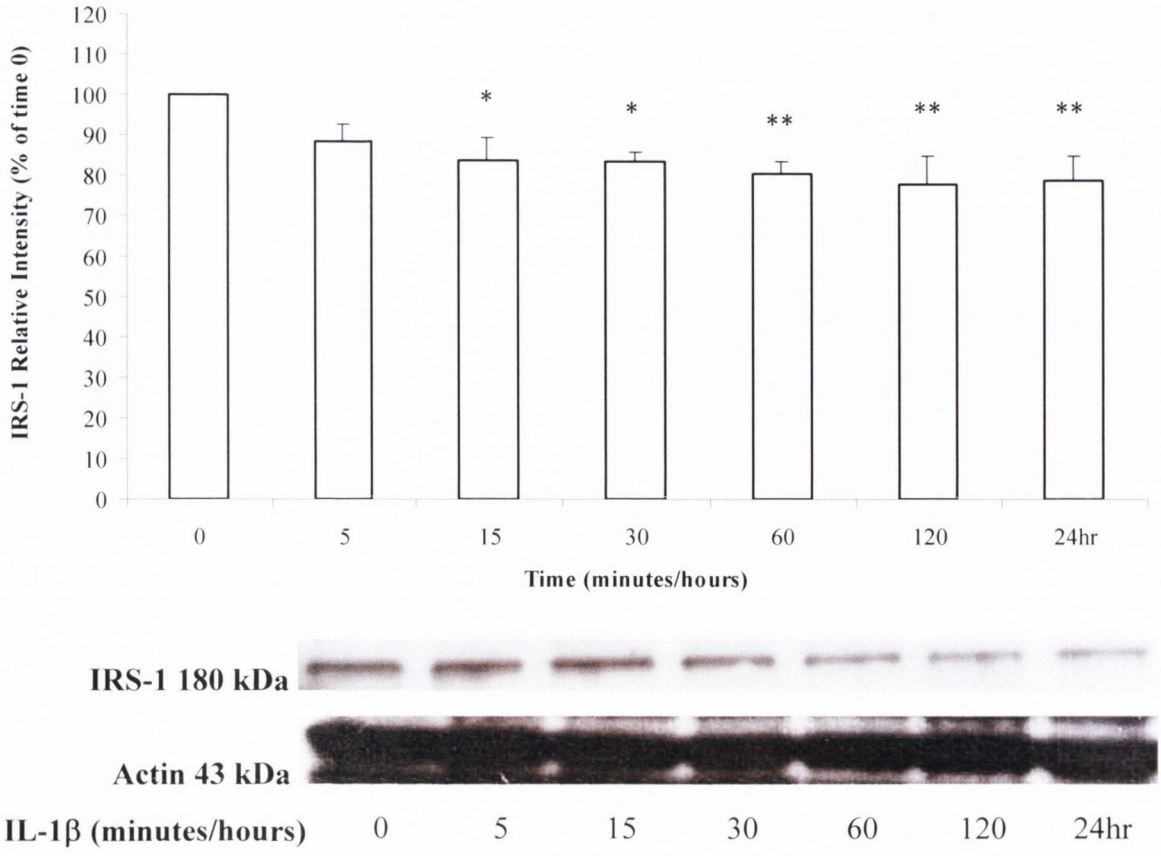

Figure 4.2 Effects of IL-1β treatment on IRS-1 protein expression in 3T3-L1 adipocyte whole cell extracts. 3T3-L1 adipocytes were treated with 10 ng/ml IL-1β for up to 24 hours. Whole cell lysates were prepared for SDS-PAGE and immunoblotting. The relative protein levels were quantified by densitometry and data expressed relative to the amount of IRS-1 at time 0 (100%). Data is presented as mean ± SEM, n = 3. A representative blot is shown below the graph. * $P \leq 0.05$, ** $P \leq 0.01$ relative to time 0. One-way ANOVA was performed within each group followed by post hoc LSD analysis. Correct loading of protein was confirmed by blotting for actin.

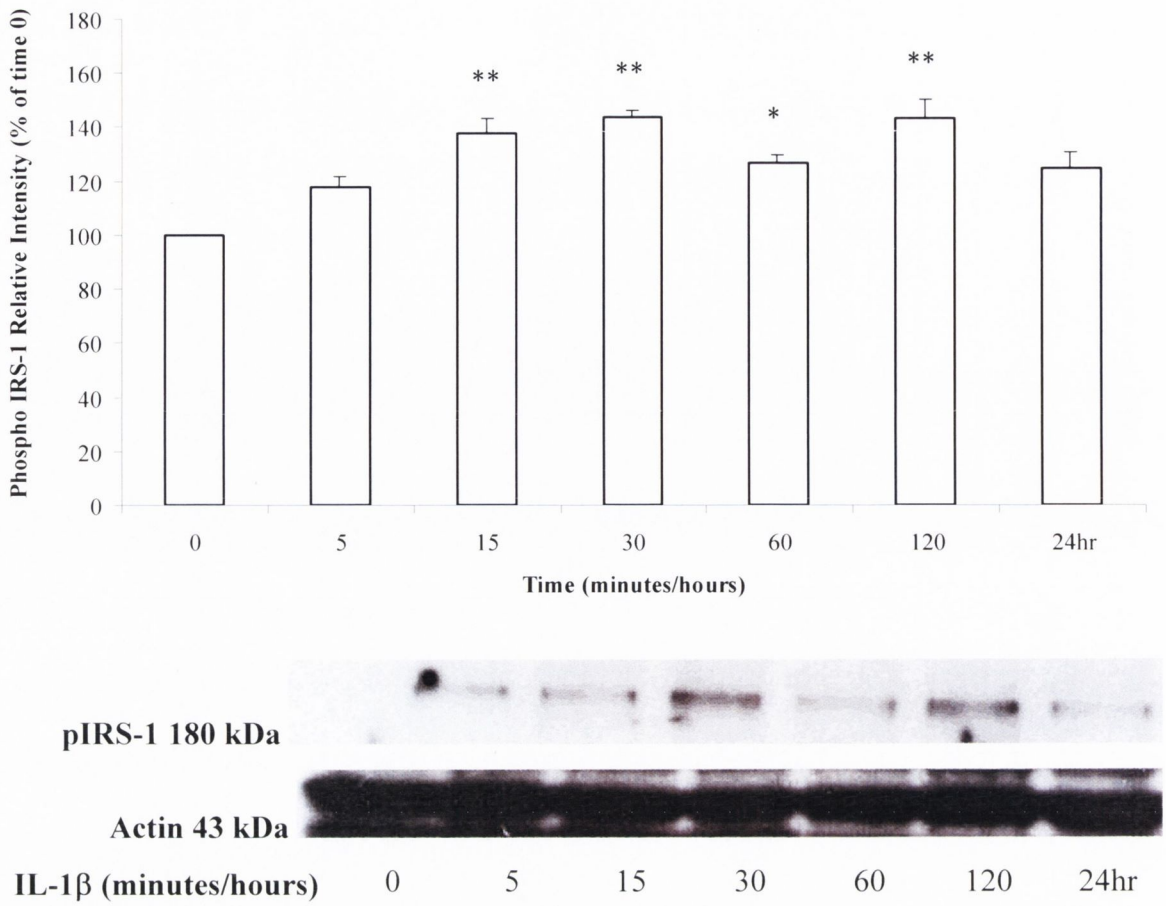

Figure 4.3 Effects of IL-1β treatment on phosphorylated IRS-1 (ser636/639) protein expression in 3T3-L1 adipocyte whole cell extracts. 3T3-L1 adipocytes were treated with 10 ng/ml IL-1β for up to 24 hours. Whole cell lysates were prepared for SDS-PAGE and immunoblotting. The relative protein levels were quantified by densitometry and data expressed relative to the amount of phosphorylated IRS-1 at time 0 (100%). Data is presented as mean ± SEM, n = 3. A representative blot is shown below the graph. * $P \leq 0.05$, ** $P \leq 0.01$ relative to time 0. One-way ANOVA was performed within each group followed by post hoc LSD analysis. Correct loading of protein was confirmed by blotting for actin.

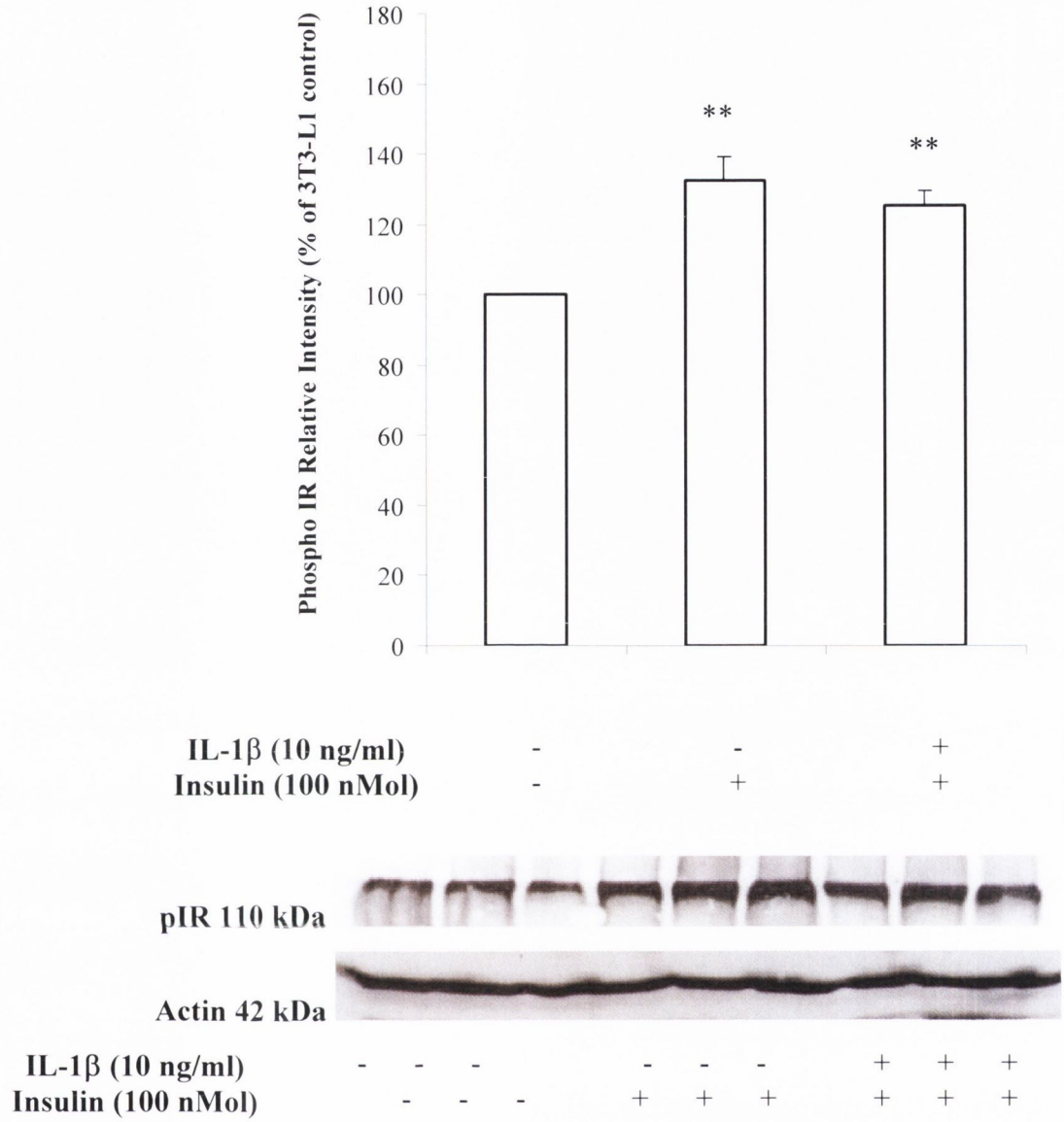

Figure 4.4 Effects of IL-1β treatment on phosphorylated insulin receptor (IR, Tyr1158, Tyr1162, Tyr1163) protein expression in 3T3-L1 adipocyte whole cell extracts. 3T3-L1 adipocytes were treated with 10 ng/ml IL-1β for 48 hours and insulin for 30 minutes. Whole cell lysates were prepared for SDS-PAGE and immunoblotting. The relative protein levels were quantified by densitometry and data expressed relative to the 3T3-L1 untreated control (100%). Data is presented as mean ± SEM, n = 3. A representative blot is shown below the graph. ** $P \leq 0.01$ relative to untreated 3T3-L1. One-way ANOVA was performed within each group followed by post hoc LSD analysis. Correct loading of protein was confirmed by blotting for actin.

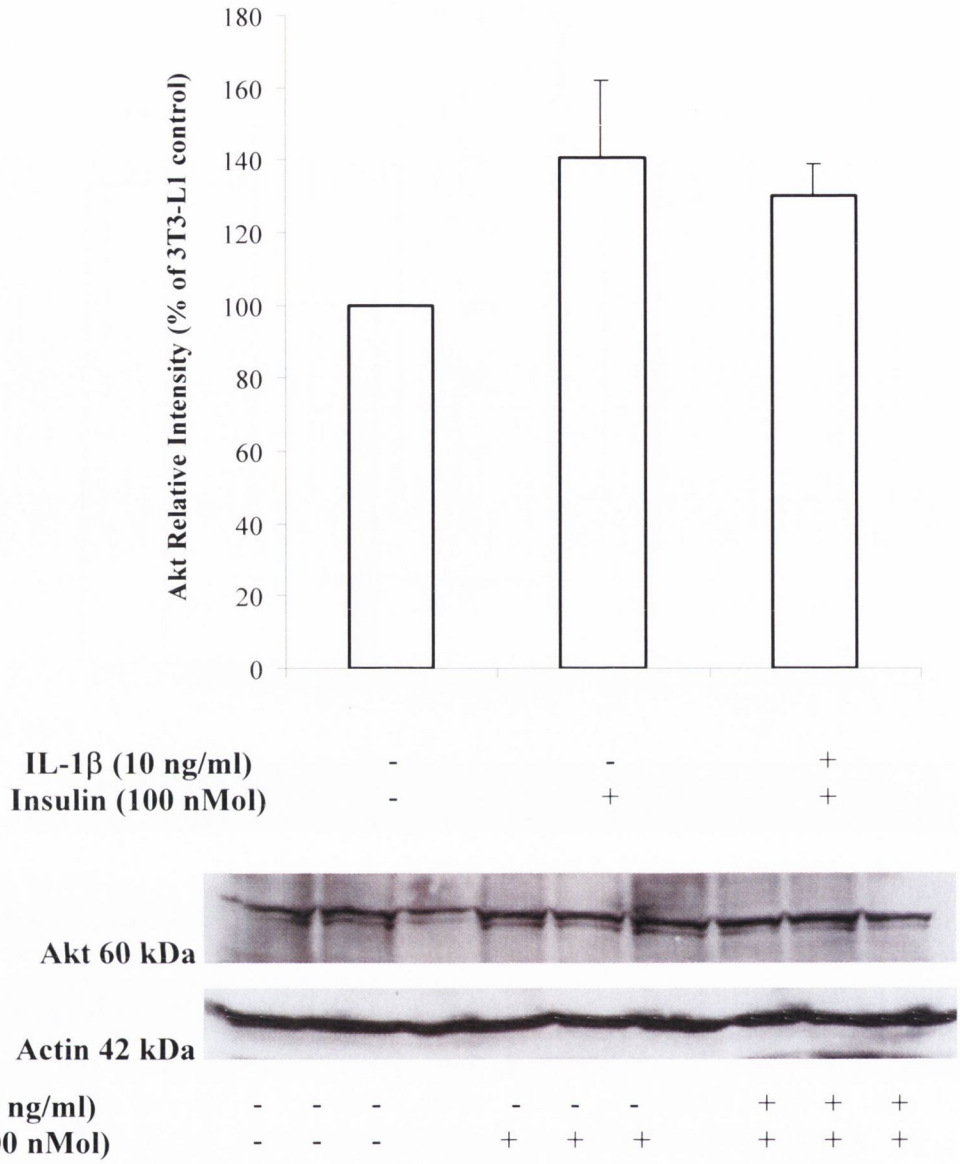

Figure 4.5 Effects of IL-1β treatment on PKB/Akt protein expression in 3T3-L1 adipocyte whole cell extracts. 3T3-L1 adipocytes were treated with 10 ng/ml IL-1β for 48 hours and insulin for 30 minutes. Whole cell lysates were prepared for SDS-PAGE and immunoblotting. The relative protein levels were quantified by densitometry and data expressed relative to untreated 3T3-L1 control (100%). Data is presented as mean ± SEM, n = 3. A representative blot is shown below the graph. Correct loading of protein was confirmed by blotting for actin.

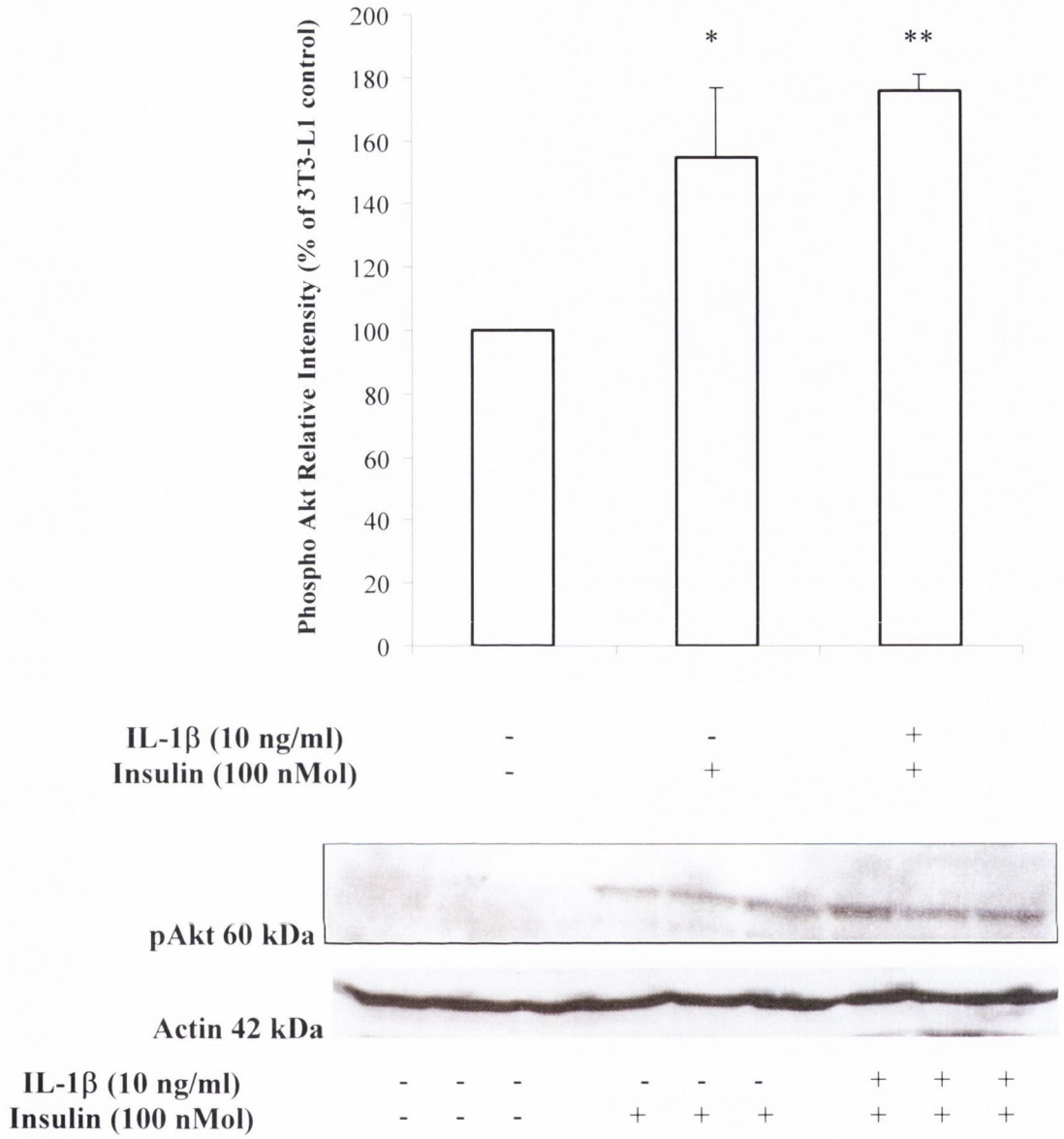

Figure 4.6 Effects of IL-1β treatment on phosphorylated PKB/Akt (Thr308) protein expression in 3T3-L1 adipocytes whole cell extracts. 3T3-L1 adipocytes were treated with 10 ng/ml IL-1β for 48 hours and insulin for 30 minutes. Whole cell lysates were prepared for SDS-PAGE and immunoblotting. The relative protein levels were quantified by densitometry and data expressed relative to the 3T3-L1 untreated control (100%). Data is presented as mean ± SEM, n = 3. A representative blot is shown below the graph. * $P \leq 0.05$, ** $P \leq 0.01$ relative to untreated 3T3-L1. One-way ANOVA was performed within each group followed by post hoc LSD analysis. Correct loading of protein was confirmed by blotting for actin.

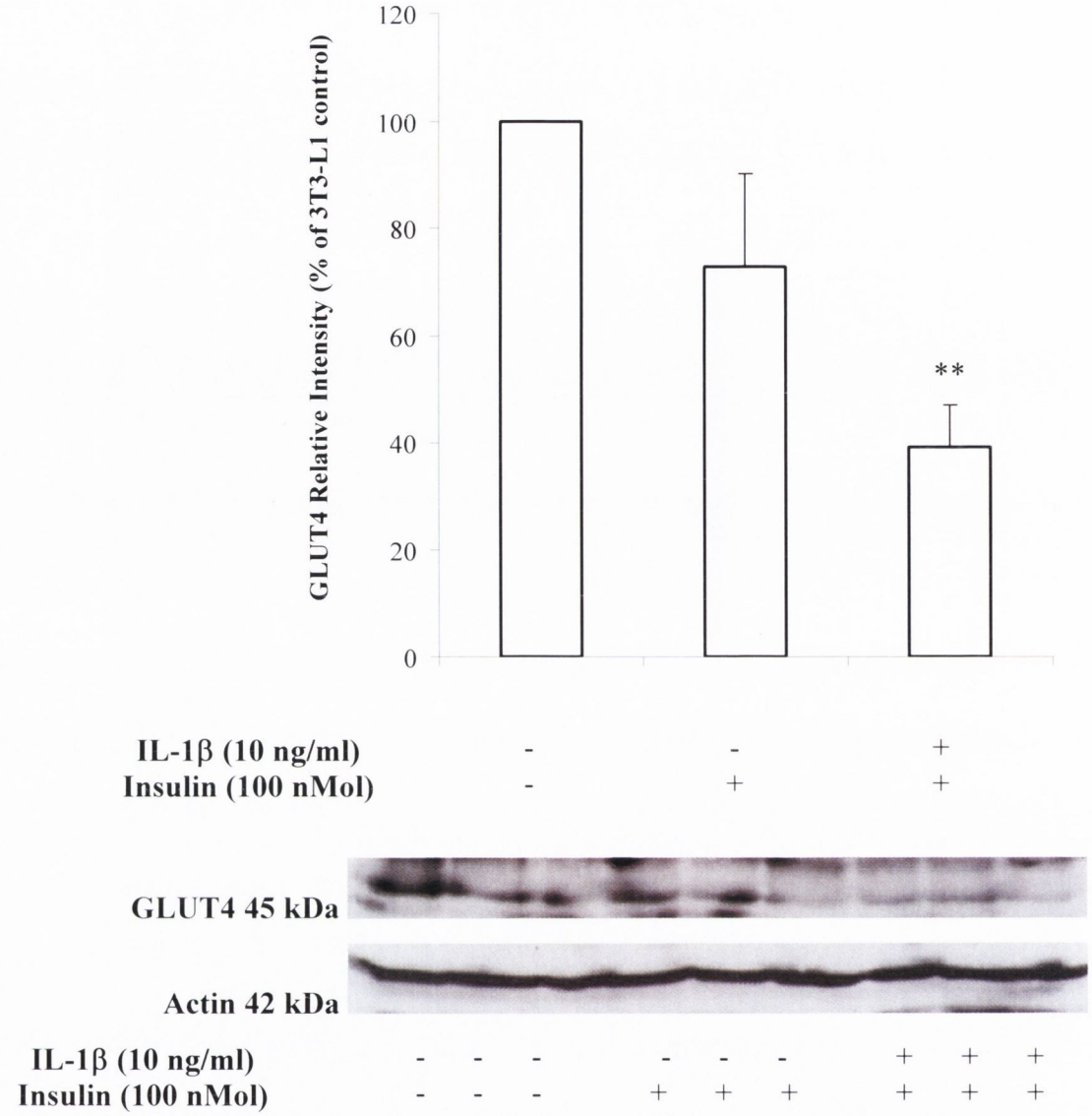

Figure 4.7 Effects of IL-1β treatment on GLUT4 protein expression in 3T3-L1 adipocytes whole cell extracts. 3T3-L1 adipocytes were treated with 10 ng/ml IL-1β for 48 hours and insulin for 30 minutes. Whole cell lysates were prepared for SDS-PAGE and immunoblotting. The relative protein levels were quantified by densitometry and data expressed relative to the 3T3-L1 untreated control (100%). Data is presented as mean ± SEM, n = 3. A representative blot is shown below the graph. ** $P \leq 0.01$ relative untreated 3T3-L1. One-way ANOVA was performed within each group followed by post hoc LSD analysis. Correct loading of protein was confirmed by blotting for actin.

4.3.2 Effects of IL-1β treatment on ^{3}H glucose uptake in 3T3-L1 adipocytes

Glucose uptake assays were performed on the fully differentiated 3T3-L1 adipocytes, which had been either left untreated or treated with 10 ng/ml IL-1β for 48 hours. Figure 4.8 illustrates that insulin induced a significant increase in glucose uptake in untreated 3T3-L1 adipocytes (5.5 fold increase, $P \leq 0.001$); glucose uptake was also elevated in IL-1β treated 3T3-L1 adipocytes (4.5 fold increase, $P \leq 0.001$) both relative to untreated adipocytes. However, glucose uptake was significantly reduced 18% in 3T3-L1 adipocytes treated with IL-1β compared to 3T3-L1 adipocytes stimulated with insulin ($P \leq 0.006$).

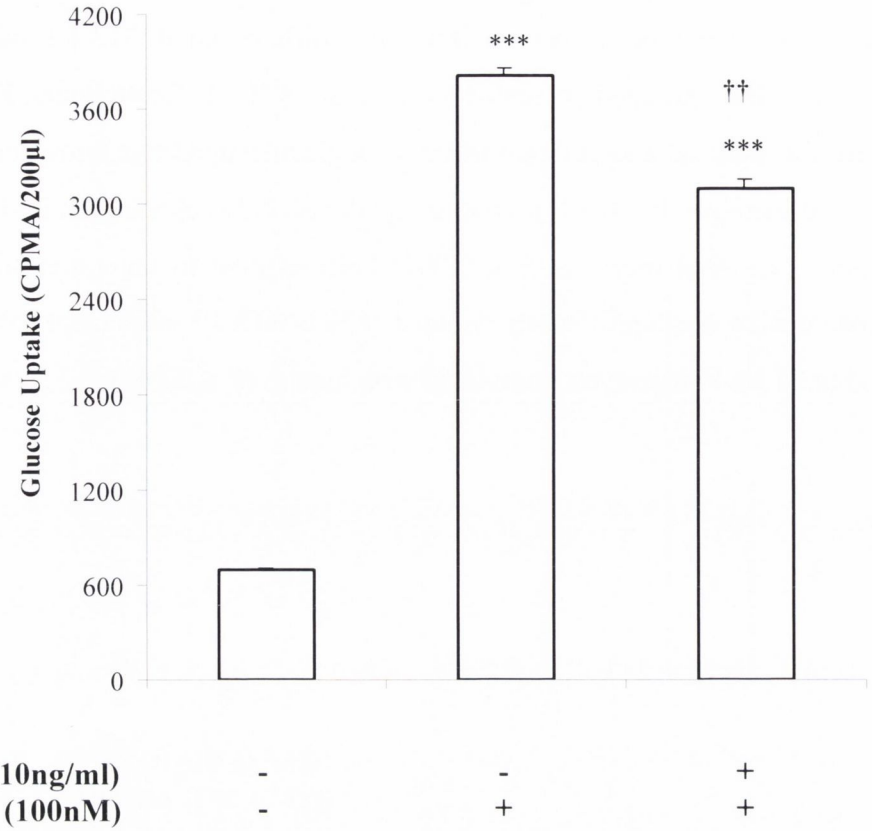

Figure 4.8 Effects of IL-1β on glucose uptake in 3T3-L1 adipocytes. Glucose uptake assays were performed on the fully differentiated 3T3-L1 adipocytes, which had been either left untreated or treated with 10 ng/ml IL-1β for 48 hours. Cells were incubated with 100 nMol of insulin for 30 minutes followed by 5 µCi/ml of ^{3}H glucose in 1 mMol glucose for 15 minutes. Cells were lysed and assayed for ^{3}H uptake as counts per minute, data is presented as mean ± SEM, n = 4 - 8. *** $P \leq 0.001$ relative to untreated 3T3-L1; †† $P \leq 0.01$ relative to 3T3-L1 adipocytes treated with insulin. One-way ANOVA was performed within each group followed by post hoc LSD analysis.

4.3.3 Effects of IL-1β treatment on lipid accumulation in 3T3-L1 adipocytes

Oil red O staining was used to assess cellular lipid content in IL-1β treated 3T3-L1 adipocytes (Figure 4.9). IL-1β treatment induced a small but significant ($P \leq 0.034$) decrease in oil red O lipid staining (9% decrease) compared to untreated 3T3-L1 adipocytes.

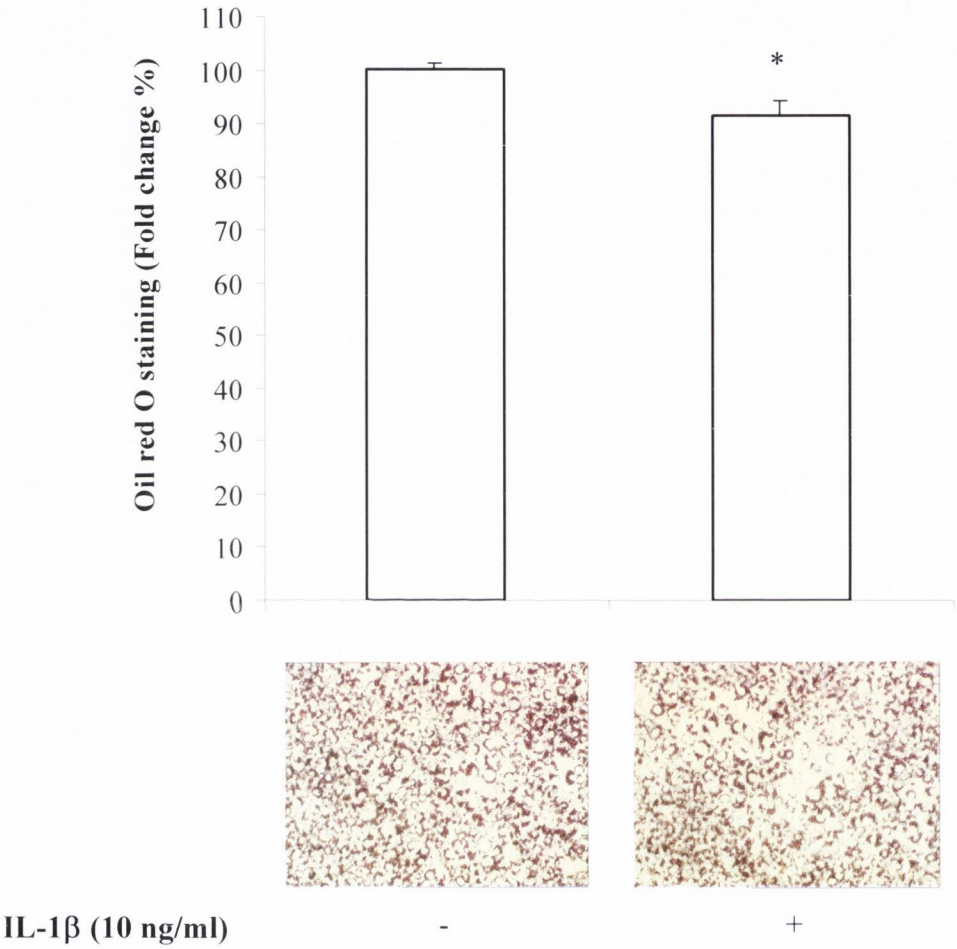

Figure 4.9 Effects of IL-1β treatment on lipid accumulation in 3T3-L1 adipocytes. Oil red O staining was used to stain accumulated lipids within adipocytes treated and untreated with IL-1β (10 ng/ml) for 48 hours. After IL-1β treatment adipocytes were fixed in 10% neutral buffered formalin and stained with oil red O. Oil red O staining was assessed within microscope images as percentage fold change. Data is presented as mean ± SEM, n = 5. * $P \leq 0.05$ relative to untreated 3T3-L1. An independent Student's t-test was performed on the IL-1β treated adipocytes vs. controls.

4.3.4 Effects of IL-1β treatment on MAPK protein expression in 3T3-L1 adipocytes

p38 MAPK, phosphorylated p38 MAPK (Thr180/Tyr182), ERK1, phosphorylated ERK1/2 (Thr202/Tyr204), JNK and phosphorylated JNK (T183/Y185) protein expression was measured in 3T3-L1 adipocytes treated with 10ng/ml IL-1β for up to 24 hours as presented in Figures 4.10 to 4.15. Whole cell p38 protein expression was not significantly changed in fully differentiated 3T3-L1 adipocytes treated with IL-1β (Figure 4.10). Interestingly, IL-1β treatment in mature 3T3-L1 adipocytes significantly increased phosphorylation of p38 (Thr180/Tyr182) at 5 minutes (72% increase, $P \leq 0.001$), 15 minutes (2.2 fold increase, $P \leq 0.001$) and 30 minutes (63% increased, $P \leq 0.002$) after which levels normalised (Figure 4.11).

There was no significant change in whole cell ERK1 protein expression in 3T3-L1 adipocytes treated with IL-1β over a 24 hour period (Figure 4.12). However, phosphorylated ERK1/2 (Thr202/Tyr204) protein expression was increased in 3T3-L1 adipocytes at 15 minutes (20% increase) and 30 minutes (17% increase) IL-1β treatment relative to adipocytes at time 0 ($P \leq 0.030$ and $P \leq 0.052$; Figure 4.13). Later in the time course phosphorylated ERK1/2 was significantly reduced in 3T3-L1 adipocytes at 60 (22% decrease) and 120 minutes (27% decrease) IL-1β treatment relative to time 0 ($P \leq 0.020$ and $P \leq 0.005$). There was no significant change in whole cell JNK or phosphorylated JNK (T183/Y185) protein expression in 3T3-L1 adipocytes treated with IL-1β over a 24 hours period (Figures 4.14 and 4.15).

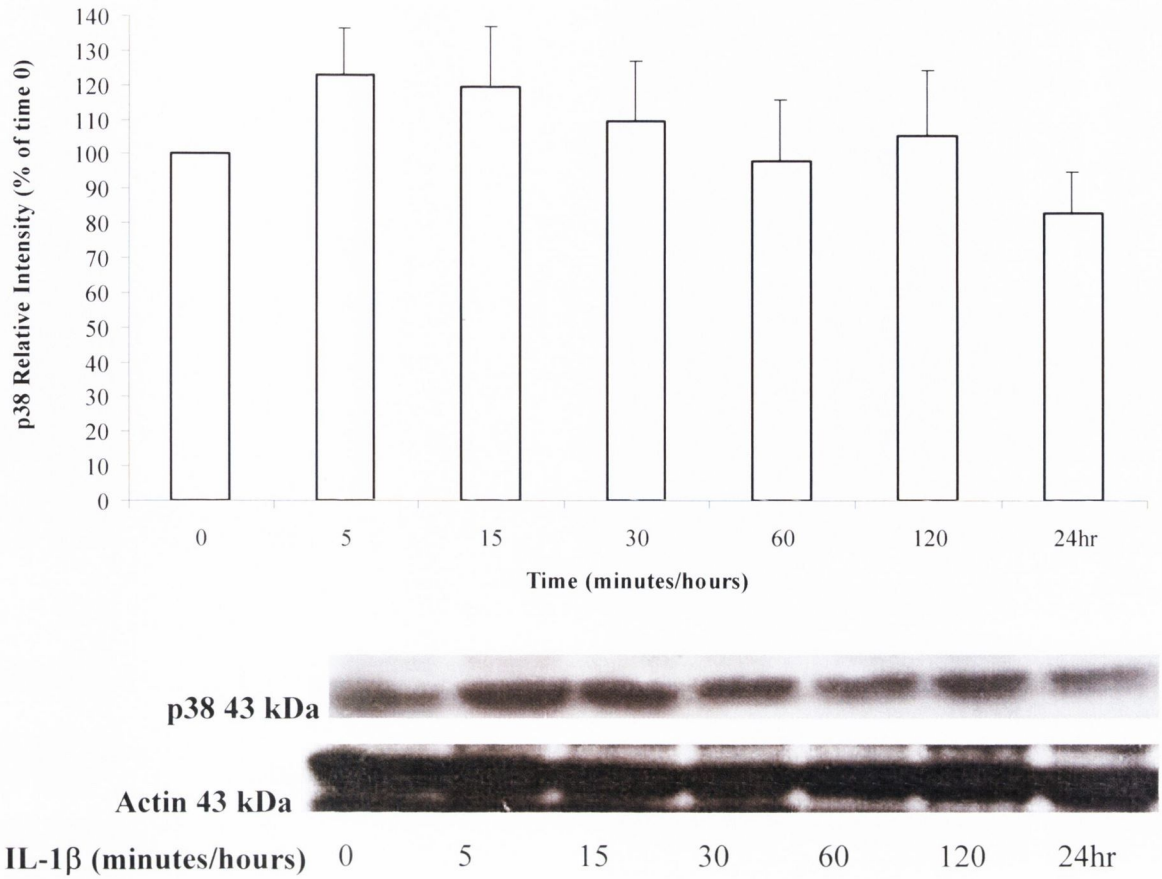

Figure 4.10 Effects of IL-1β treatment on p38 protein expression in 3T3-L1 adipocyte whole cell extracts. 3T3-L1 adipocytes were treated with 10 ng/ml IL-1β for up to 24 hours. Whole cell lysates were prepared for SDS-PAGE and immunoblotting. The relative protein levels were quantified by densitometry and data expressed relative to the amount of p38 at time 0 (100%). Data is presented as mean ± SEM, n = 3. A representative blot is shown below the graph. Correct loading of protein was confirmed by blotting for actin.

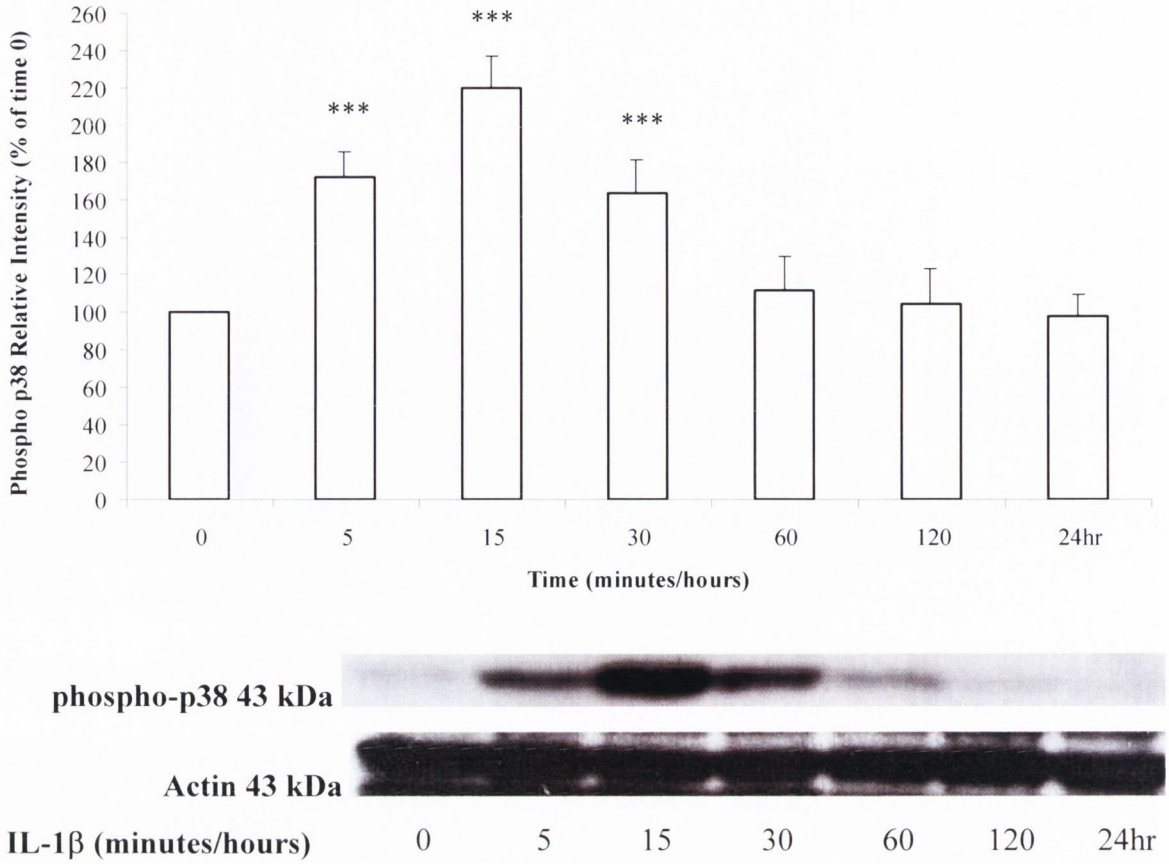

Figure 4.11 Effects of IL-1β treatment on phosphorylated p38 (Thr180/Tyr182) protein expression in 3T3-L1 adipocyte whole cell extracts. 3T3-L1 adipocytes were treated with 10 ng/ml IL-1β for up to 24 hours. Whole cell lysates were prepared for SDS-PAGE and immunoblotting. The relative protein levels were quantified by densitometry and data expressed relative to the amount of phosphorylated p38 at time 0 (100%). Data is presented as mean ± SEM, n = 3. A representative blot is shown below the graph. *** $P \leq 0.001$ relative to time 0. One-way ANOVA was performed within each group followed by post hoc LSD analysis. Correct loading of protein was confirmed by blotting for actin.

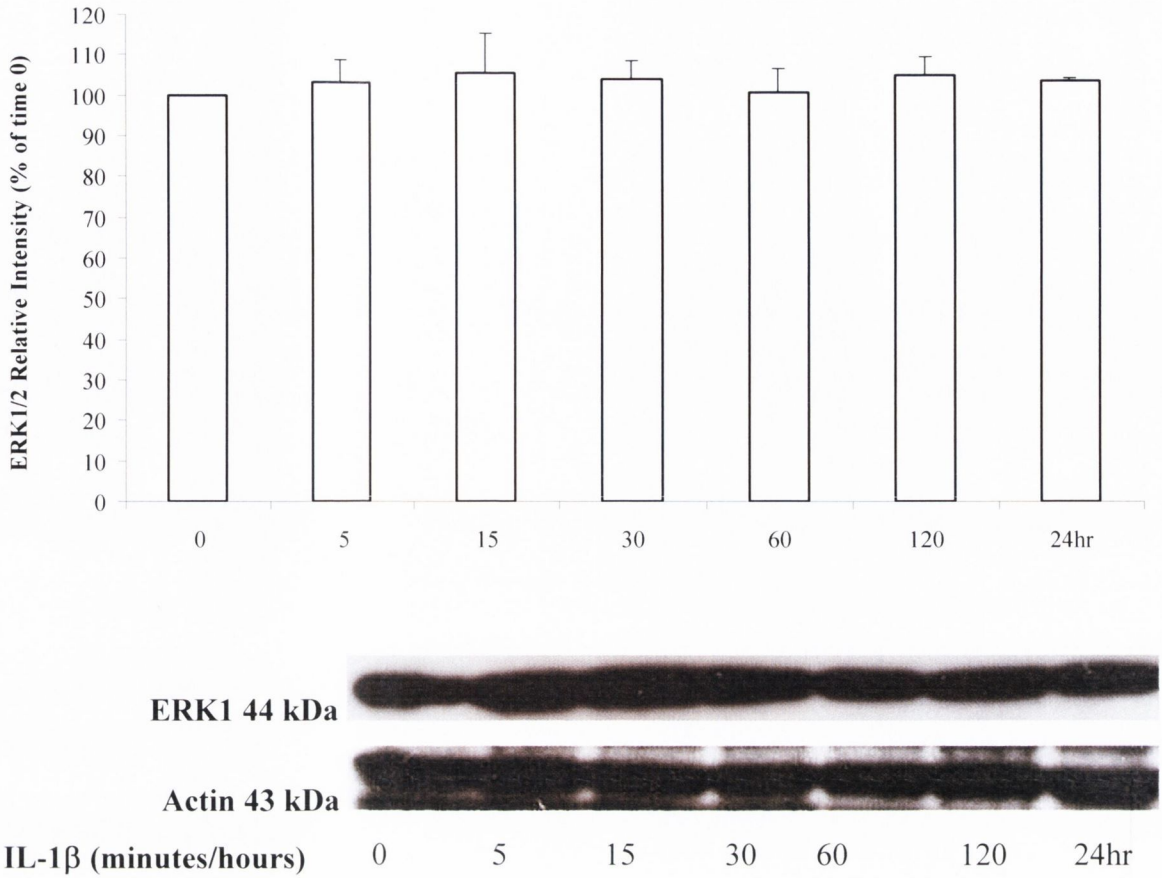

Figure 4.12 Effects of IL-1β treatment on ERK1 protein expression in 3T3-L1 adipocyte whole cell extracts. 3T3-L1 adipocytes were treated with 10 ng/ml IL-1β for up to 24 hours. Whole cell lysates were prepared for SDS-PAGE and immunoblotting. The relative protein levels were quantified by densitometry and data expressed relative to the amount of ERK1 at time 0 (100%). Data is presented as mean ± SEM, n = 3. A representative blot is shown below the graph. Correct loading of protein was confirmed by blotting for actin.

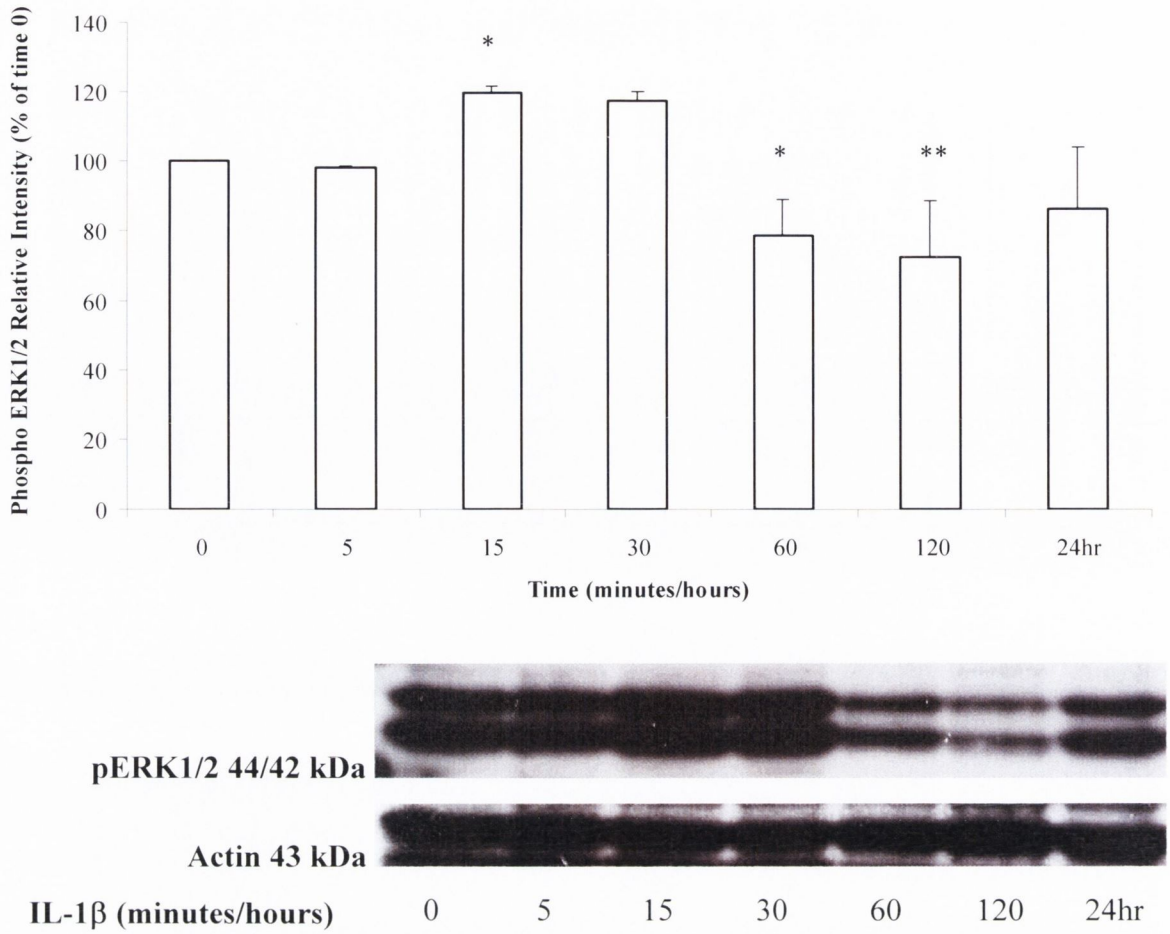

Figure 4.13 Effects of IL-1β treatment on phosphorylated ERK1/2 (Thr202/Tyr204) protein expression in 3T3-L1 adipocyte whole cell extracts. 3T3-L1 adipocytes were treated with 10 ng/ml IL-1β for up to 24 hours. Whole cell lysates were prepared for SDS-PAGE and immunoblotting. The relative protein levels were quantified by densitometry and data expressed relative to the amount of phosphorylated ERK1/2 at time 0 (100%). Data is presented as mean ± SEM, n = 3. A representative blot is shown below the graph. * $P \leq 0.05$, ** $P \leq 0.01$ relative to time 0. One-way ANOVA was performed within each group followed by post hoc LSD analysis. Correct loading of protein was confirmed by blotting for actin.

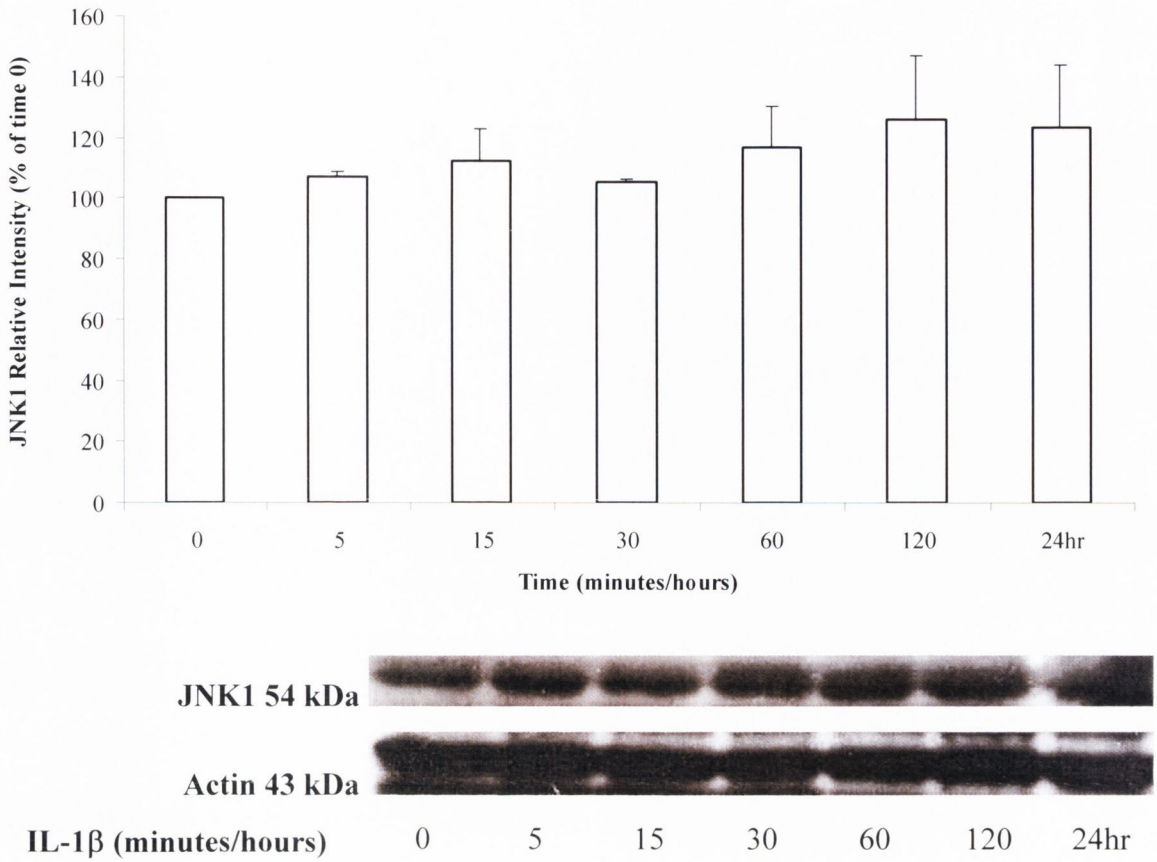

Figure 4.14 Effects of IL-1β treatment on JNK1 protein expression in 3T3-L1 adipocyte whole cell extracts. 3T3-L1 adipocytes were treated with 10 ng/ml IL-1β for up to 24 hours. Whole cell lysates were prepared for SDS-PAGE and immunoblotting. The relative protein levels were quantified by densitometry and data expressed relative to the amount of JNK at time 0 (100%). Data is presented as mean ± SEM, n = 3. A representative blot is shown below the graph. Correct loading of protein was confirmed by blotting for actin.

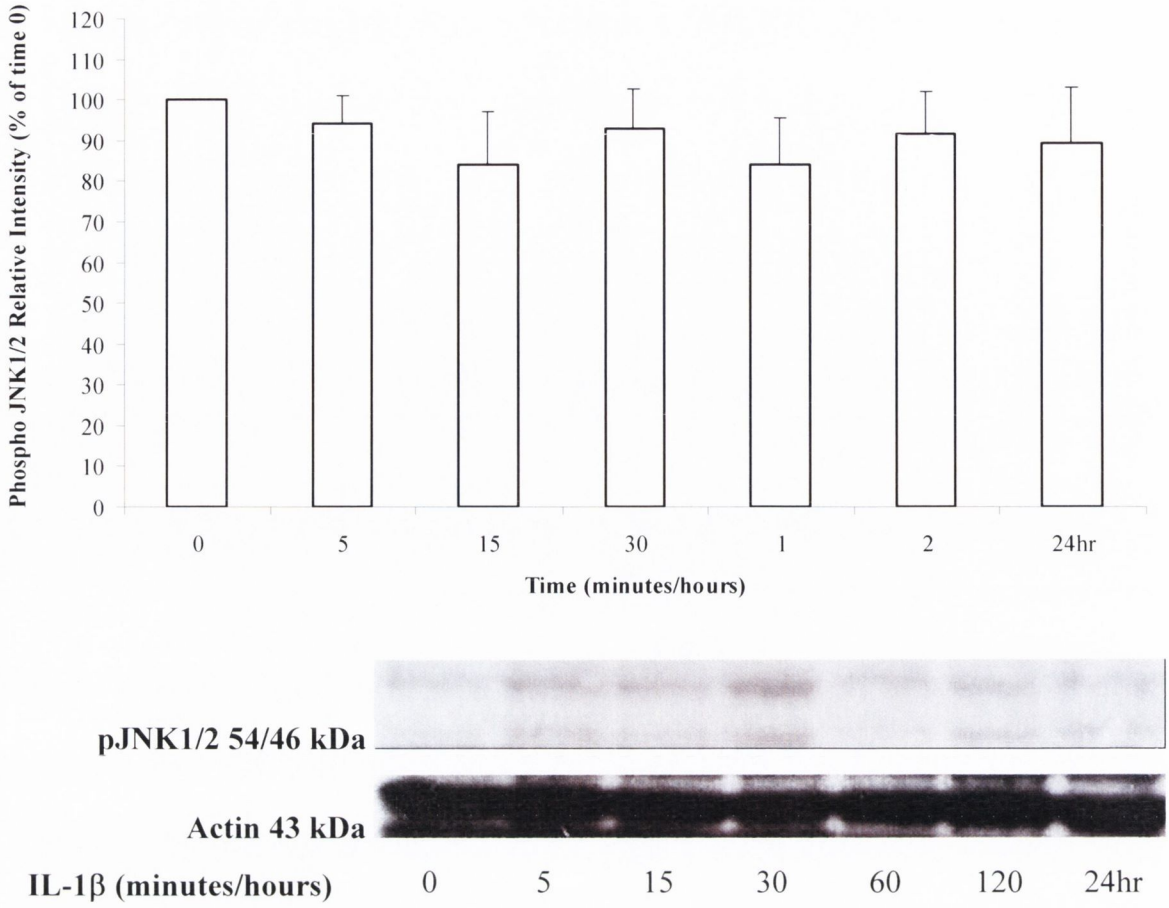

Figure 4.15 Effects of IL-1β treatment on phosphorylated JNK1/2 (Thr183/Tyr185) protein expression in 3T3-L1 adipocyte whole cell extracts. 3T3-L1 adipocytes were treated with 10 ng/ml IL-1β for up to 24 hours. Whole cell lysates were prepared for SDS-PAGE and immunoblotting. The relative protein levels were quantified by densitometry and data expressed relative to the amount of phosphorylated JNK at time 0 (100%). Data is presented as mean ± SEM, n = 3. A representative blot is shown below the graph. Correct loading of protein was confirmed by blotting for actin.

4.3.5 Effects of IL-1β treatment on IκB-α protein expression in 3T3-L1 adipocytes

IκB-α and phosphorylated IκB-α (Ser32) protein expression was measured in 3T3-L1 adipocytes treated with 10 ng/ml IL-1β for up to 24 hours as presented in Figure 4.16 and 4.17. Whole cell IκB-α protein expression was not significantly altered in fully differentiated 3T3-L1 adipocytes treated with IL-1β. However, there was an increase in IκB-α expression at 15 minutes (29% increase, $P \leq 0.063$) and 30 minutes (28% increase, $P \leq 0.074$) which correlated with a significant increase (23% increase) in phosphorylated IκB-α (ser32) at 5 minutes IL-1β treatment within 3T3-L1 adipocytes relative to time 0 ($P \leq 0.039$). Later in the time course phosphorylated IκB-α levels dropped and normalised to pre-IL-1β treatment levels.

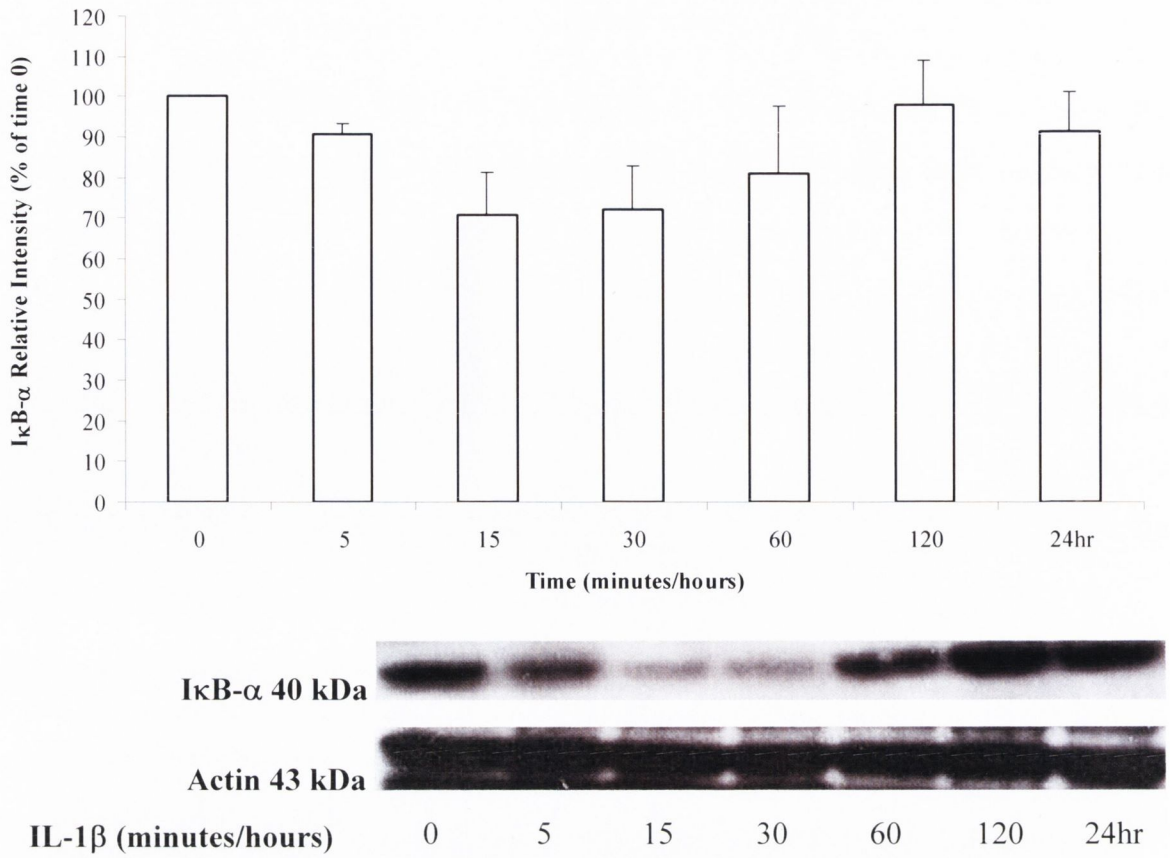

Figure 4.16 Effects of IL-1β treatment on phosphorylated IκB-α protein expression in 3T3-L1 adipocyte whole cell extracts. 3T3-L1 adipocytes were treated with 10 ng/ml IL-1β for up to 24 hours. Whole cell lysates were prepared for SDS-PAGE and immunoblotting. The relative protein levels were quantified by densitometry and data expressed relative to the amount of phosphorylated IκB-α at time 0 (100%). Data is presented as mean ± SEM, n = 3. A representative blot is shown below the graph. Correct loading of protein was confirmed by blotting for actin.

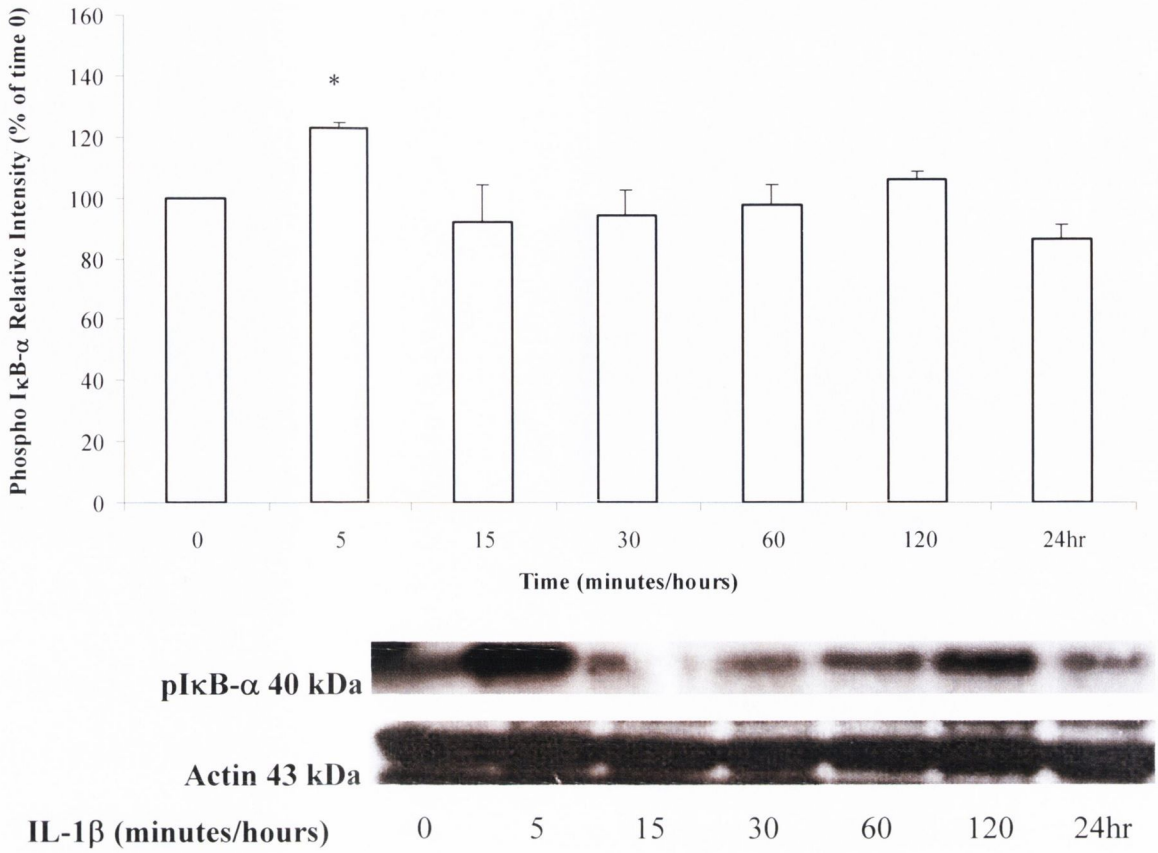

Figure 4.17 Effects of IL-1β treatment on phosphorylated IκB-α (Ser32) protein expression in 3T3-L1 adipocyte whole cell extracts. 3T3-L1 adipocytes were treated with 10 ng/ml IL-1β for up to 24 hours. Whole cell lysates were prepared for SDS-PAGE and immunoblotting. The relative protein levels were quantified by densitometry and data expressed relative to the amount of phosphorylated IκB-α at time 0 (100%). Data is presented as mean ± SEM, n = 3. A representative blot is shown below the graph. * $P \leq 0.05$ relative to time 0. One-way ANOVA was performed within each group followed by post hoc LSD analysis. Correct loading of protein was confirmed by blotting for actin.

4.3.6 Effects of IL-1β treatment on adipokine secretion in 3T3-L1 adipocytes

Adipokine protein secretion was determined by ELISA (ng/ml) in 3T3-L1 adipocytes treated with 10 ng/ml IL-1β for 24 and 48 hours. IL-6 secretion was significantly increased in 3T3-L1 adipocytes treated with IL-1β for 24 and 48 hours (30 fold increase $P \leq 0.001$ and 48 fold increase, $P \leq 0.001$ respectively (Table 4.1 and Figure 4.18). However, Adiponectin, resistin, Leptin and TNF-α secretion were not significantly changed in 3T3-L1 adipocytes treated with IL-1β for 24 hours (Table 4.1) and additionally 48 hours in the case of TNF-α secretion.

Table 4.1 Effects of IL-1β treatment on adipokine secretion from 3T3-L1 adipocytes. 3T3-L1 adipocytes were treated with 10 ng/ml IL-1β for 24 hours, supernatants were harvested and adipokine secretion determined by ELISA (pg/ml). Data is presented as mean ± SEM, n = 6, P values are shown. An independent students T test was performed on the IL-1β treated adipocytes vs. controls.

	Control		IL-1β Treatment (10 ng/ml)		
Adipokine	Mean (pg/ml)	SEM	Mean (pg/ml)	SEM	P value
IL-6	12.52	1.67	375.84	33.93	0.00
Adiponectin	1914645.10	224217.32	1740678.35	157280.52	0.54
Resistin	11961.51	406.63	12310.05	363.84	0.47
Leptin	102.47	1.50	106.11	4.58	0.54
TNF-α	8.46	3.83	6.35	2.19	0.67

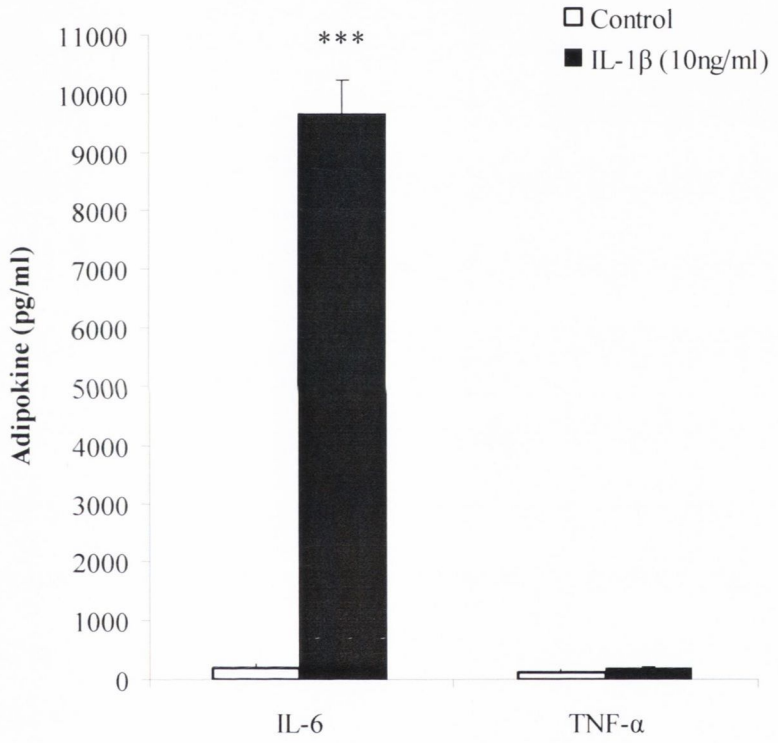

Figure 4.18 Effects of IL-1β treatment on IL-6 and TNF-α secretion from 3T3-L1 adipocytes. 3T3-L1 adipocytes were treated with 10 ng/ml IL-1β for 48 hours, supernatants were harvested and adipokine secretion determined by ELISA (pg/ml). Data is presented as mean ± SEM, n = 3. An independent Student's t test was performed on the IL-1β treated adipocytes vs. controls.

4.4 Discussion

This time course study established the inhibitory effect of IL-1β on insulin mediated glucose uptake. This time course experiment aimed to establish a working model of IL-1β activation in 3T3-L1 adipocytes while providing evidence for the mechanisms occurring within IL-1RI$^{-/-}$ mice. At the protein expression level IL-1β treatment did not significantly reduce insulin induced tyrosine phosphorylation and therefore activation of the insulin receptor. Total IRS-1 protein expression was significantly reduced by IL-1β treatment. Similarly, Jager *at el.* (2007) also determined that IL-1β decreases IRS-1 expression and found that activation of IRS-1 through tyrosine phosphorylation of IRS-1 was also reduced (Jager *et al.*, 2007). However, our study determined that phosphorylated IRS-1 (Ser636/639) was significantly up-regulated in response to Il-1β treatment. The phosphorylation of serine 636/639 is mediated by the mTOR pathway resulting in an inhibition of insulin signaling (Ozes *et al.*, 2001). Interestingly, it appears Il-1β may function to inhibit insulin signaling partially through reduction in IRS-1 protein expression or through IRS-1 serine phosphorylation via the mTOR pathway.

mTOR is an atypical serine/threonine protein kinase, belonging to the phosphatidylinositol kinase-related kinase (PIKK) family (Fingar and Blenis, 2004; Wullschleger *et al.*, 2006). mTOR regulates a variety of cellular functions including translational control, autophagy, mitochondrial metabolism and cell-cycle progression (Corradetti and Guan, 2006; Cunningham *et al.*, 2007; Wullschleger *et al.*, 2006; Yokogami *et al.*, 2000). The physiological importance of mTOR is undoubtedly demonstrated by the fact that the knockout of mTOR in mice is primordially embryonic lethal (Gangloff *et al.*, 2004; Martin and Sutherland, 2001; Murakami *et al.*, 2004). mTOR has been shown to activate S6K1. Interestingly, in cells with an elevated S6K1 activity, the expression of IRS-1 is reduced (Haruta *et al.*, 2000). Additional studies revealed that active S6K1 phosphorylates IRS-1 on multiple inhibitory sites and promotes its degradation (Greene *et al.*, 2003; Harrington *et al.*, 2004; Shah *et al.*, 2004). Taken together, the newly identified consequence of mTOR-S6K1 activation is to attenuate Akt signalling (Um *et al.*, 2004). This auto-regulatory pathway is defined as S6K1-dependent negative feedback inhibition (Manning, 2004). Furthermore, it has been demonstrated that insulin can stimulate activation of the mTOR pathway, which in turn negatively regulates insulin signals through Ser/Thr phosphorylation, subcellular redistribution and proteasomal degradation of IRS-1 in 3T3-L1 adipocytes (Haruta *et al.*, 2000; Takano *et al.*, 2001). Importantly, Ozes and colleagues (2001) demonstrated that TNF-α impairs insulin

signaling through serine phosphoylation of IRS-1 at multiple sites by activation of a PI3-kinase, Akt and mTOR pathways in NIH-3T3 fibroblasts (Ozes *et al.*, 2001). Addiotionally, Rapamycin, an inhibitor or mTOR, could partially improve insulin-stimulated glucose uptake through maintaining IRS-1 protein levels (Carlson and Rondinone, 2005). Therefore, the effects of IL-1β on the mTOR pathway within 3T3-L1 adipocytes require further analysis.

Despite the decrease in IRS-1 protein expression and the increase in serine phosphorylation of IRS-1 induced by the IL-1β treatment, insulin induced tyrosine phosphorylation of Akt after Il-1β treatment was not significantly reduced compared to insulin stimulated 3T3-L1 adipocytes. This suggests that the decrease in IRS-1 activity had no observable inhibitor affect on Akt activity. A longer IL-1β treatment may be necessary to induce a more significant reduction in IRS-1 and Akt expression or activity. However, it maybe possible that IRS-2 develops into the main docking protein in the IRS-1 reduced IL-1β treated adipocytes as suggested by Rondinone and colleagues (1997). Rondinone *et al.* examined the expression and function of IRS-1 and IRS-2 in adipocytes from healthy and diabetic individuals. Cells from subjects with T2DM had an impaired insulin effect and a marked reduction in the expression of IRS-1 protein, whereas IRS-2 was unchanged (Rondinone *et al.*, 1997). In healthy adipocytes, IRS-1 was the main docking protein for the binding and activation of insulin-stimulated PI3-kinase. In adipocytes from T2DM subjects where IRS-1 expression was reduced, IRS-2 became the main functional docking protein however, it required a higher insulin concentration for a similar binding and activation of PI3-kinase (Rondinone *et al.*, 1997). IRS-2 could therefore compensate for any down regulation in expression or activity in IRS-1 to activate Akt. Whole cell GLUT4 protein expression was significantly reduced in insulin stimulated 3T3-L1 adipocytes treated with IL-1β relative to control adipocytes. This IL-1β induced reduction in whole cell GLUT4 expression may be responsible for the decrease in glucose uptake observed in the IL-1β treated adipocytes. It would be important to examine membrane bound GLUT4 verses cytoplasmic GLUT4 in order to determine the activity of GLUT4.

Interestingly, IL-1β treatment induced a small but significant decrease in oil red O lipid staining in mature 3T3-L1 adipocytes, suggesting that these cells had reduced lipid accumulation and had undergone lipolysis. In accord, Feingold *et al.* (1992) determined TNF-α, IL-1 and IFN-α, IFN-β and IFN-γ induce lipolysis in cultured 3T3-F442A adipocytes (Feingold *et al.*, 1992). Adipose tissue lipolysis is the catabolic process in which intracellular TAG undergoes hydrolysis through the action of three major lipases:

adipose triglyceride lipase (ATGL), hormone-sensitive lipase (HSL) and monoacylglycerol lipase (MGL). Fully differentiated adipocytes exhibit increased lipid content and insulin responsiveness. Therefore, this reduction in lipid accumulation may suggest Il-1β causes a reduction in 3T3-L1 adipocyte differentiation. Furthermore, insulin resistance in adipose tissue is characterised by decreased suppression of lipolysis in adipose tissue by insulin, leading to elevated NEFA. The quantity of NEFA from adipocytes that are released into circulation corresponds to the size of the adipocytes and the overall fat mass of the adipose tissue. The consequence of increased NEFA lipolysis and reduced NEFA fractional esterification in the metabolic syndrome and T2DM is diversion of NEFA towards non adipose tissue such as liver, muscle, heart and pancreatic β cells.

Elevated activities of the ERK1/2, JNK1/2 and p38 are found in adipocytes of obese and insulin-resistant rodent and humans (Gual *et al.*, 2005) and IL-1β treatment induced many significant changes in whole cell MAPK expression and phosphorylation within fully differentiated adipocytes. p38 and JNK are more responsive to various stress stimuli from UV to cytokines and have been involved in apoptosis and the response to cellular stresses (Aouadi *et al.*, 2006).

Levels of activated p38 are elevated in the skeletal muscle, adipose tissue and kidneys of diabetic patients (Adhikary *et al.*, 2004; Carlson *et al.*, 2003; Koistinen *et al.*, 2003), suggesting that some p38 responses may be important for the pathogenesis of diabetes and its complications. A recent study by Aouadi *et al.* (2006) found a strong decrease of p38 activity in subcutaneous fat depots compared with the same tissue in lean mice within dietary and genetic (*ob/ob*) models of obesity. Furthermore, p38 activity was significantly higher in pre-adipocytes than in adipocytes, suggesting that p38 activity decreases during adipocyte differentiation (Aouadi *et al.*, 2006). In agreement with an inhibitory role of p38 in this process, Aouadi *et al.* determined that *in vitro* inhibition of p38 with the specific inhibitor PD169316 increased the expression of mature differentiated adipocyte markers. Inhibition of p38 enhanced transcriptional activity of PPAR-γ and C/EBPβ, suggesting that p38 plays a negative role in adipogenesis via inhibition of PPAR-γ and C/EBPβ transcriptional activities (Aouadi *et al.*, 2006). In this study Il-1β was observed to increase activation of p38 in the adipocytes, which correlated with an increase in lipolysis and a reduction in insulin sensitivity, further suggesting that p38 plays a negative role in adipogenesis.

Carlson *et al.* (2005) observed treatment with the specific p38 inhibitor (A304001) during the development of insulin resistance in 3T3-L1 adipocytes increased basal glucose

uptake, increased GLUT1 expression, increased glucose uptake in response to insulin stimulation and increased GLUT4 expression (Carlson and Rondinone, 2005). However, p38 inhibition did not prevent the loss of IRS-1 protein levels or insulin signalling to Akt in insulin-resistant cells (Carlson and Rondinone, 2005). This data indicates that p38 inhibition can enhance glucose uptake through regulating the expression of GLUT1 and GLUT4, although it did not prevent the development of insulin resistance. The increased activation of p38 observed in the IL-1β treated 3T3-L1 adipocytes may therefore have also induced the reduction in GLUT4 observed.

JNK activity is abnormally elevated in obesity (Hirosumi *et al.*, 2002). *In vitro* JNK-1 induced by cytokines such as TNF-α stimulates serine phosphorylation and inhibits insulin-stimulated tyrosine phosphorylation of IRS-1 (Aguirre *et al.*, 2000). Furthermore, an absence of JNK1 results in decreased adiposity, significantly improved insulin sensitivity and enhanced insulin receptor signalling capacity in obese $JNK^{-/-}$ (Hirosumi *et al.*, 2002). However, within this *in vitro* study there was only a subtle increase in whole cell JNK over the 24 hour IL-1β treatment period, while activated JNK was moderately reduced and increased in a cyclical pattern by IL-1β treatment. This suggests an IL-1β treatment of 24 hours has only subtle effects on JNK expression and activity.

The ERK pathway plays a pivotal role in many essential cellular functions, such as proliferation and differentiation (Bost *et al.*, 2005). Bost *et al.* (2005) used $ERK1^{-/-}$ mice to investigate the role of this isoform in adipose tissue development (Bost *et al.*, 2005). Mice lacking ERK1 have decreased adiposity and fewer adipocytes than WT animals. Furthermore, $ERK1^{-/-}$ mice challenged with HFD were resistant to obesity, were protected from insulin resistance and had a higher post-prandial metabolic rate. Mouse embryo fibroblasts and cultures of adult pre-adipocytes isolated from $ERK1^{-/-}$ adult animals exhibit impaired adipogenesis (Bost *et al.*, 2005). This data suggests ERK1 activity may induce an insulin resistance phenotype. Furthermore, Jager *et al.* (2007) established that pharmacological inhibition of the ERK pathway totally prevented a decrease in IRS-1 mRNA and partially prevented the inhibition of IRS-1 protein expression induced by IL-1β treatment in adipocytes (Jager *et al.*, 2007). In this current study, IL-1β treatment induced a significant increase in phosphorylated ERK1/2 (Thr202/Tyr204) protein expression in 3T3-L1 adipocytes. This suggests IL-1β treatment exerts significant control over ERK1/2 activity. The activity seems to occur in a cyclical pattern, perhaps resulting from negative feedback within the pathway. The initial increase in ERK activity within the adipocytes

may have induced the observed reduction in whole cell IRS-1 and the increase in serine phosphorylated IRS-1.

The NF-κB signaling pathway plays a key role in inflammation, immune response, cell growth control and protection against apoptosis. In most cell types, NF-κB proteins are sequestered in the cytoplasmic compartment, associated with members of the inhibitor of κB (IκB) family (IκB-α, IκB-β and IκB-ε). In response to multiple stimuli such as inflammatory cytokines, bacterial lipopolysaccharide (LPS), viral infection or stress, IkBs are phosphorylated on two critical serine residues. This modification triggers their ubiquitination and destruction via the proteasome degradation machinery. As a consequence, free NF-κB enters the nucleus and activates transcription of a variety of genes participating in immune and inflammatory responses, cell adhesion, growth control and regulation of apoptosis (Hayden and Ghosh, 2004; Karin and Ben-Neriah, 2000). At 5 minutes IL-1β treatment there was a significant and transient increase in phosphorylation of IκB-α within 3T3-L1 adipocytes, furthermore, at 120 minutes IL-1β treatment there is a second smaller phosphorylation of IκB-α. This suggests NF-κB is activated at 5 minutes and then later more moderately at 120 minutes. Whole cell IκB-α protein expression was moderately decrease in adipocytes treated with IL-1β at 15 minutes and 24 hours suggesting that IκB-α is ubiquitinated and degraded in the proteasome allowing NF-κB to become activated.

IL-6 secretion was significantly increased in 3T3-L1 adipocytes treated with IL-1β. IL-1β has been shown to up-regulate IL-6 in many cell types, however not in 3T3-L1 adipocytes. Chen *et al.* (2005) report that orbital fibroblasts, when treated with IL-1β, express high levels of IL-6. This increase in IL-6 was associated with up-regulation of IL-6 mRNA levels. In accordance with this Chen *et al.* determined that IL-1β activates both p38 and ERK1/2 components of the MAPK pathways in the fibroblast (Chen *et al.*, 2005), correlating with the observations from this current study in adipocytes. Importantly, in a study by Luo *et al.* (2003), a mouse skeletal muscle cell line was treated with IL-1β in the absence or presence of the p38 inhibitor (SB-208350) or the ERK1/2 inhibitor (PD-98059). Firstly, treatment of with IL-1β resulted in a dose- and time-dependent increase of IL-6 production accompanied by a 25-fold increase in IL-6 mRNA levels. Secondly, they established that IL-1β stimulated NF-κB DNA binding activity and gene activation in muscle cells as observed within the 3T3-L1 adipocytes. Importantly, Luo *et al.* (2003) observed that the MAPK inhibitors SB-208350 and PD-98059 inhibited the increase in IL-6 production induced by IL-1β, suggesting IL-1β regulates muscle IL-6 production at least

in part by activating the MAPK pathway and NF-κB (Luo *et al.*, 2003). It would be interesting to conduct experiments using MAPK and NF-κB inhibitors to determine the effects of IL-1β within 3T3-L1 adipocytes as it seems likely the mechanisms would be comparable. Surprisingly, adiponectin, resistin, leptin and TNF-α secretion were not significantly changed in fully differentiated 3T3-L1 adipocytes treated with IL-1β and there currently seems to be no study within the literature to refute this. However, a longer IL-1β treatment may be necessary to induce changes in adipokine expression.

In conclusion, this time course study demonstrated that IL-1β treatment reduced insulin sensitivity in 3T3-L1 adipocytes. Whole cell IRS-1 and GLUT4 protein expression was significantly reduced by IL-1β treatment in adipocytes. This study determined that serine phosphorylated IRS-1 (Ser636/639) was significantly up regulated in response to IL-1β. IL-1β may therefore function to inhibit insulin signaling partially through IRS-1 serine phosphorylation via the mTOR pathway. IL-1β treatment induced many significant changes in whole cell MAPK expression and phosphorylation within the adipocytes. Firstly, IL-1β treatment significantly increased activation of p38 in the adipocytes. Interestingly, recent studies suggest that p38 plays a negative role in adipogenesis via inhibition of PPAR-γ and C/EBPβ transcriptional activities (Aouadi *et al.*, 2006). The observed increase in p38 activity associated with the IL-1β treatment may therefore be correlated with the increased lipolysis and reduction in insulin sensitivity within the 3T3-L1 adipocytes. Studies also indicate that p38 inhibition can enhance glucose uptake through regulating the expression of GLUT1 and GLUT4 expression. Therefore, the increased p38 activity may have induced the reduction in GLUT4 observed. Secondly, IL-1β treatment induced a significant increase in ERK1/2 activity, which may have induced the reduction in whole cell IRS-1 and increase in serine phosphorylated IRS-1 observed. Lastly, IL-1β also induced a significant increase in IL-6 secretion within the adipocytes. This induction of IL-6 may be initiated by MAPK and/or NF-κB pathway activation induced by IL-1β treatment.

One limitation within this work was that a positive control such as TNF-α was not introduced as a comparison to the IL-1β treatment, to put the effects of IL-1β into context with other cytokines known to inhibit insulin sensitivity. Furthermore, a higher dose of IL-1β treatment may have been necessary to induce a more significant reduction in insulin sensitivity in 3T3-L1 adipocytes. Although, 10ng/ml of cytokines such as IL-1β and TNF-α are predominantly used within 3T3-L1 cell culture studies (He *et al.*, 2006; Li *et al.*,

2003) it would be important to conduct a dose response prior to future analysis of this model. A longer treatment of fully mature 3T3-L1 adipocytes with IL-1β may be necessary to observe an increase in insulin resistance. An experiment assessing the effects of IL-1β treament on pre-adipocyte differentiation to mature adipocytes would be valuable. IL-1β may inhibit adipocyte differentiation, reducing insulin sensitivity. Transcription factor expression and activation involved in adipocyte differentiation and insulin sensitivity such as PPAR-γ and C/EBP could be determined within total cellular and nuclear extracts of the adipocytes treated with IL-1β. Furthermore, mRNA expression of transcription factors such as PPAR-γ, adipokines such as adiponectin and lipogenic enzymes such as fatty acid synthetase (FAS) in IL-1β treated adipocytes maybe informative as to the differentiation state and insulin sensitivity of the adipocyte. It would also be of interest to understand more about how IL-1β can induce insulin resistance, perhaps with the use of specific MAPK and NF-κB inhibitors however, these inhibitors are often unspecific. Additionally, small interfering RNA (siRNA) could be used to silence specific genes within the IL-1β treated adipocytes. siRNA are a class of double-stranded RNA molecules, 20-25 nucleotides in length. siRNA are involved in the RNA interference (RNAi) pathway, where they interfere with the expression of a specific gene. siRNA gene silencing experiments in 3T3-L1 cells are often limited to pre-adipocytes because they are relatively easy to transfect using commercially available reagents. Transfection of siRNA into differentiated 3T3-L1 adipocytes can be accomplished by electroporation. However, electroporation is expensive, incompatible with high throughput assay formats and toxic to cells (Jiang *et al.*, 2003). Importantly, new kits are available in which a nano particle containing the siRNA is used. The nano particle is capable of diffusing through the cell membrane with no apparent effect on cell viability. Therefore, siRNA could be used to silence key signalling proteins such as p38 and ERK within the fully differentiated adipocytes treated with IL-1β. Additionally, mouse embryonic fibroblasts (MEFs) derived from knockout mice with deletions of specific signalling proteins of interest could be differentiated to mature adipocytes. siRNA treated adipocytes or MEFs derived adipocytes with targeted protein deletions could be used to establish novel cross talk mechanisms occurring between inflammatory and insulin signalling pathways. Importantly, the data within this chapter does indicate that IL-1β can reduce insulin sensitivity and induce inflammation within 3T3-L1 adipocytes, correlating with observations in IL-1RI$^{-/-}$ mice, which exhibited increased insulin sensitivity and reduced inflammation.

Chapter 5

The Effects of EPA and DHA Treatment on Inflammatory and Insulin Signalling *In Vitro* within 3T3-L1 Adipocytes and J774.2 Macrophages

5.1 Introduction

Inflammation is a fundamental part of the normal host response to infection and injury. However, excessive or inappropriate inflammation contributes to a range of acute and chronic human diseases such as obesity induced type 2 diabetes mellitus (T2DM). High intakes of long chain (LC) *n-3* polyunsaturated fatty acids (PUFA) such as eicosapentaenoic acid (EPA) and docosahexaenoic acid (DHA), as found in oily fish, decrease the production of inflammatory eicosanoids, cytokines and reactive oxygen species while reducing expression of adhesion molecules (Calder, 2006). LC *n-3* PUFA may therefore offer a useful anti-inflammatory strategy to decrease obesity induced insulin resistance.

Epidemiologic studies have reported a low prevalence of chronic inflammatory disease and conditions of impaired glucose tolerance, such as cardiovascular disease (CVD) and T2DM in populations consuming large amounts of LC *n-3* PUFA such as the Greenland Inuit and Alaskan natives (Adler *et al.*, 1994; Kromann and Green, 1980; Schraer *et al.*, 1999). However, human trials examining the effects of LC *n-3* PUFA supplementation in T2DM subjects have shown conflicting results (Glauber *et al.*, 1988; Malasanos and Stacpoole, 1991). This could be due to differences in the dose of LC *n-3* PUFA, the background diets, or differences in the intake of other fatty acids. Animal studies have provided more convincing evidence of the positive effects of LC *n-3* PUFA on insulin resistance however, this evidence is not conclusive and LC *n-3* PUFA seem to have variable effects within different tissues. Storlien *et al.* (1991) observed that diets high in saturated, monounsaturated (*n-9*), or polyunsaturated (*n-6*) fatty acids led to severe insulin resistance as assessed with euglycemic clamp as compared to chow fed controls. Interestingly, substituting 11% of fatty acids in the PUFA diet with LC *n-3* PUFA from fish oils was shown to normalize insulin action (Storlien *et al.*, 1991). However, Taouis *et al.* (2002) observed that a HFD containing LC *n-3* or LC *n-6* PUFA given to Wistar rats induced hyperglycemia and hyperinsulinemia, signs of insulin resistance. Although a high fat diet (HFD) enriched with LC *n-3* PUFA maintained glucose transporter (GLUT)-4 content, insulin receptor and insulin receptor substrate (IRS)-1 tyrosine phosphorylation and phosphatidylinositol-3 kinase (PI3K) activity in muscle (Glauber *et al.*, 1988)

suggesting LC *n-3* PUFA do have beneficial effects within obesity induced insulin resistance.

LC *n-3* PUFA have been shown to act through a variety of mechanisms including (1) inhibiting the inflammatory pathway of arachidonic acid (AA) and the production of eicosanoids, (2) decreasing production of pro-inflammatory cytokines and (3) reducing immune cell function (Calder and Miles, 2000; Simopoulos, 2002). Eicosanoids are key mediators and regulators of inflammation (Tilley *et al.*, 2001) and are generated from 20 carbon PUFA. Eicosanoids include prostaglandins (PGs), thromboxanes (TXs) and leukotrienes (LTs) and are generated predominantly from AA, as it is commonly the major available substrate. Increased consumption of EPA and DHA results in their incorporation into inflammatory cell phospholipids (Gibney and Hunter, 1993; Healy *et al.*, 2000), which occurs at the expense of AA. The decreased amounts of AA mean a decreased amount of substrate available for synthesis of AA derived eicosanoids (Calder, 2009). Furthermore, EPA also able act as a substrate for both cyclooxygenase (COX) and 5-lipoxygenase (LOX), giving rise to less inflammatory eicosanoids than those formed from AA (Calder, 2009). EPA is therefore able to antagonise AA metabolism and to act as a substrate for generation of less potent eicosanoids however, increasing evidence suggests this is a more complex situation. One example is PGE_2, a prostaglandin produced by AA, which is a potent inhibitor of tumour necrosis factor (TNF)-α and interleukin (IL)-1 expression from monocytes and macrophages (Miles *et al.*, 2002) and can promote the formation of anti-inflammatory lipoxins (Vachier *et al.*, 2002). However, PGE_2 is also known to induce fever, pain, vasodilation and vascular permeability (Tilley *et al.*, 2001).

Interestingly, recent studies have identified E-series resolvins, formed from EPA by a series of reactions involving COX and 5-LOX. In addition, D-series resolvins and protectin are produced by a similar series of reactions involving DHA (Serhan *et al.*, 2008). These mediators appear to enable inflamed tissue to return to a state of homeostasis and have been shown to exert potent anti-inflammatory actions in many inflammatory cell types including neutrophils, macrophages, dendritic cells and T cells (Serhan *et al.*, 2008). In a recent study the effects of resolvins and protectins within *ob/ob* mice were assessed (Gonzalez-Periz *et al.*, 2009). Dietary intake of LC *n-3* PUFA was shown to have insulin-sensitising actions in adipose tissue and liver while improving insulin tolerance in obese mice. Genes involved in insulin sensitivity such as peroxisome proliferator-activated receptor (PPAR)-γ, GLUT2, GLUT4, IRS-1 and IRS-2 were up regulated by LC *n-3* PUFA. Furthermore, LC *n-3* PUFA increased adiponectin levels and induced adenosine monophosphate-activated protein kinase (AMPK) phosphorylation. A lipidomic analysis

with liquid chromatography and mass spectrometry revealed that LC *n-3* PUFA inhibited the formation of LC *n-6* PUFA-derived eicosanoids, while triggering the formation of LC *n-3* PUFA derived resolvins and protectins, namely resolvin E1 and protectin D1 (Gonzalez-Periz *et al.*, 2009) suggesting they play a key role in preventing obesity induced insulin resistance. However, the role of resolvins and protectins remains speculative and further work is required to fully establish their function.

LC *n-3* PUFA also modify the activity of transcription factors, including NF-κB and PPAR-γ. In a recent study from Mullen *et al.* (2009) LC *n-3* PUFA were shown to decrease LPS induced pro-inflammatory cytokine production from THP-1 macrophages. Expression of the NF-κBp65 was significantly reduced in the nucleus and retained in the cytoplasm of EPA and DHA treated macrophages during LPS activation. Furthermore, nuclear IκB-α was significantly reduced, cytoplasmic NF-κBp50 significantly increased and cytoplasmic cleaving enzyme IκB inhibitor complex significantly reduced in LC *n-3* PUFA treated cells (Mullen *et al.*, 2009). This study demonstrates that EPA and DHA mediate their anti-inflammatory actions via the NF-κB signaling system. Furthermore, in macrophages obtained from a cystic fibrosis mouse model, LPS induced TNF-α and IL-6 secretion not only corresponded with increased NFκBp65 activity but was associated with low basal PPARγ expression (Andersson *et al.*, 2008).

PPAR-γ is of particular interest in relation to insulin resistance as it is a ligand dependent nuclear receptor that has a critical role in adipogenesis and glucose metabolism (Kubota *et al.*, 1999; Rosen *et al.*, 1999). This receptor is the molecular target of the thiazolidinedione (TZD) class of anti-diabetic drugs, which include rosiglitazone and pioglitazone (Lehmann *et al.*, 1995). PPAR-γ ligands include fatty acid derivatives, e.g. 15-deoxy-$\Delta^{12,14}$ prostaglandin J_2 (15d-PGJ_2) (Forman *et al.*, 1995). Furthermore, PPAR-γ is prominently expressed in activated monocytes and tissue macrophages *in vivo*, including foam cells of atherosclerotic lesions (Ricote *et al.*, 1998a) and adipose tissue macrophages (ATM) (Bassaganya-Riera *et al.*, 2009). Treatment of monocytes and macrophages with high concentrations of PPAR-γ agonists reduced secretion of inflammatory cytokines and inhibited macrophage activation (Spiegelman, 1998). Additionally, in a recent study it was confirmed that there are two phenotypically and functionally distinct subsets of ATM ($F4/80^{high}$ and $F4/80^{low}$) (Bassaganya-Riera *et al.*, 2009). $F4/80^{low}$ macrophages predominate in adipose tissue of lean mice whereas obesity causes accumulation of both $F4/80^{low}$ and $F4/80^{high}$ ATM. Moreover, accumulation of $F4/80^{high}$ ATM in adipose tissue is associated with impaired glucose tolerance. The $F4/80^{high}$ subset exhibits an enhanced

ability to express PPAR-γ, lipid scavenger receptor CD36, toll like receptor (TLR)-4 and pro-inflammatory cytokines, whereas the F4/80^{low} subset expresses IL-4 and produces lower concentrations of pro-inflammatory cytokines. Moreover, they observed that the deletion of PPAR-γ in immune cells results in enhanced expression of M1 and suppressed expression of M2 markers in WAT (Bassaganya-Riera *et al.*, 2009). This data suggests that PPAR-γ evidently plays a role in macrophage differentiation and function within obesity.

LC *n-3* PUFA and their metabolites may act in obese individuals to reduce the pro-inflammatory state of ATM, therefore improving insulin sensitivity within adipocytes of the adipose tissue. However, it is also important to consider the direct effects of LC *n-3* PUFA on other cell types, such as adipocytes, within the context of T2DM. Total body fat and abdominal and epididymal fat mass have been shown to be considerably reduced in rodents fed sources of LC *n-3* PUFA such as fish oil compared with lard or corn oil fed groups (Hainault *et al.*, 1993). Kim *et al.* (2006) observed that DHA treatment did not affect proliferation of pre-confluent pre-adipocytes; however DHA did inhibit differentiation as shown by lipid accumulation and glycerol-3-phosphate dehydrogenase (GPDH) activity of post-confluent pre-adipocytes (Kim *et al.*, 2006). It is of interest to note that post-confluent pre-adipocytes demonstrated apoptosis after 48 hour treament with 100 μMol/L DHA. In fully differentiated adipocytes, DHA increased basal lipolysis. This suggests DHA may induce anti-obesity effects by inhibiting differentiation of pre-adipocytes to mature adipocytes, inducing apoptosis in post-confluent pre-adipocytes and promoting lipolysis in mature adipocytes (Kim *et al.*, 2006). Additionally, PPAR-γ may play an important role in this anti-obesity phenotype. Interestingly, conjugated linoleic acid (CLA) isomers are also ligands for PPAR and have been shown to affect adipose development and gene expression *in vitro* (Su *et al.*, 1999). CLA has been shown to inhibit proliferation in non-confluent 3T3-L1 cells and also inhibit the induction of differentiation in 3T3-L1 cells *in vitro* (Brodie *et al.*, 1999). Furthermore, in rats fed CLA, the anti-obesity effects were accounted for by decreased lipid accumulation within the adipocytes, and therefore a decrease in cell size (Azain *et al.*, 2000).

In relation to insulin sensitivity, a recent study by Haag *et al.* (2009) examined early fatty acid action in fresh isolated adipocytes from Sprague-Dawley rats (Haag *et al.*, 2009). Adipocytes were exposed to the saturated fatty acid (SFA) stearic acid (SA), monosaturated fatty acid (MUFA) oleic acid (OA, *n-9*), LC *n-6* PUFA AA and LC *n-3* PUFA EPA and DHA for 30 minutes followed by glucose uptake analysis. Unexpectedly, SA increased insulin induced glucose uptake while the unsaturated fatty acids OA, AA, EPA and DHA depressed insulin dependent glucose uptake. Interestingly, all the fats tested

except SA and AA acids increased basal glucose uptake. This suggests unsaturated fatty acids may induce a reduction in insulin sensitivity while saturated fats improve insulin sensitivity. Due to the short term treatment it seems unlikely gene modifications were made via transcription factors within this time, therefore it appears likely the effects were induced by lipid metabolites. Longer term FA action on adipocyte glucose uptake should be examined to reach a meaningful conclusion on the efficacy of polyunsaturated fatty acids in modulation of adipocyte sensitivity to insulin (Haag *et al.*, 2009).

This study firstly examined the effects of chronic EPA and DHA treatment on mature differentiated 3T3-L1 adipocytes defining gene expression, protein expression and adipokine secretion. The effects of EPA and DHA treatment during differentiation were also examined using glucose uptake analysis. Secondly, the effects of chronic EPA and DHA treatment were determined within the LPS stimulated J774.2 macrophages, examining both MAPK and NF-κB activation in addition to cytokine secretion. Finally, the initial findings of an adipocyte and macrophage co-culture will be examined. As discussed previously, during an obese state the adipose tissue becomes inflamed with increased infiltration of immune cells such as the macrophage, which contribute to the production of pro-inflammatory cytokines. Pro-inflammatory cytokines produced in the adipose tissue are proposed to alter the endocrine function of the tissue and could impede insulin signalling and action in adipocytes leading to the development and/or aggravation of insulin resistance (Marette, 2003). Therefore, LPS stimulated and unstimulated J774.2 macrophages were treated with EPA and DHA prior to co-culture with the 3T3-L1 adipocytes. The co-culture was designed to observe the impact that EPA and DHA treated macrophages have on the adipocytes at both a gene and protein expression level relative to non-treated macrophages and to define a working model of obesity. A comprehensive series of experiments will be conducted in chapter 6 to examine the co-culture model in further detail.

5.2 Material and methods

5.2.1 Experimental design

Firstly, the effects of EPA and DHA on mature 3T3-L1 adipocytes were determined. 3T3-L1 fibroblasts were differentiated to mature adipocytes as described in section 2.2.11. Briefly, 3T3-L1 fibroblasts were grown to confluencey in 6 well plates and differentiation was initiated by culturing cells in the presence of insulin, dexamethasone and isobutyl-1-methylxanthine (IBMX) for six days as described in section 2.2.4. Differentiation media was removed and replaced with DMEM containing 10% FBS and penicillin/streptomycin for 24 hours. The fully differentiated adipocytes were treated with 50 μMol/L EPA, DHA or DMSO vehicle control in DMEM for 5 days (chronic treatment). Additionally, 3T3-L1 fibroblasts were differentiated in the presence of 50 μMol/L EPA, DHA or DMSO vehicle control for six days prior to a glucose uptake analysis. Secondly, the effects of EPA and DHA on LPS stimulated or unstimulated J774.2 macrophages. J774.2 macrophages were grown in DMEM media, J774.2 macrophages were then treated with 50 μMol/L EPA, DHA or DMSO vehicle control for 5 days (chronic treatment) prior to LPS (100 ng/ml) treatment for 15 minutes as discussed in section as described in section 2.2.10.

Finally, a contact and transwell co-culture of LPS stimulated or unstimulated J774.2 macrophages and mature 3T3-L1 adipocytes were examined as described in Figure 5.1. J774.2 macrophages were treated LPS (100 ng/ml) for 48 hours with 50 μMol/L EPA, DHA or vehicle control in DMEM media during the final 24 hour LPS treatment (acute treatment). 3T3-L1 fibroblasts were grown to confluencey in 6 well plates and differentiated for six days. Differentiation media was removed and replaced with DMEM media for 24 hours. The fully differentiated adipocytes were treated with the J774.2 macrophages for a further 24 hours in either a contact or transwell system as described in section 2.2.10. In the contact co-culture 3T3-L1 adipocytes and J774.2 macrophages were placed directly together in 6 well plates. In the transwell system 3T3-L1 adipocytes were grown in 6 well plates and J774.2 macrophages were placed in permeable inserts within the well. Inserts allowed soluble molecules to circulate between the cells however, direct cell contact was prevented.

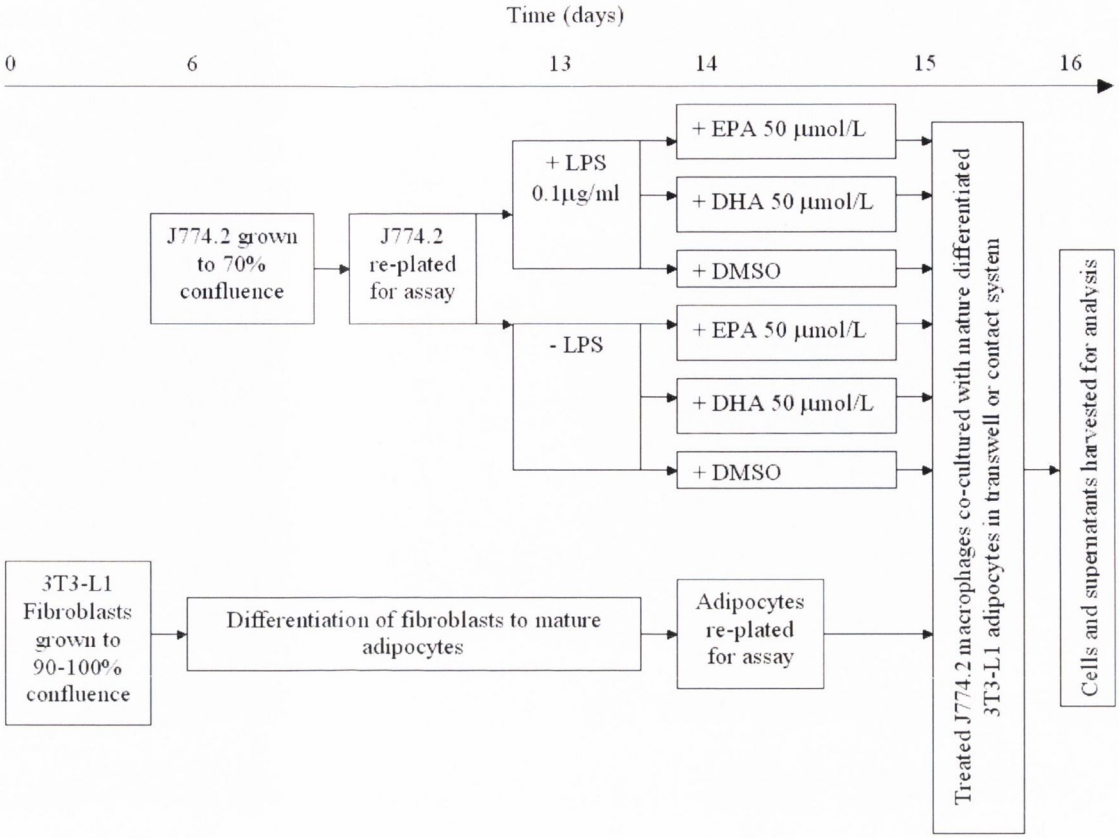

Figure 5.1 Outline of the acute EPA and DHA treatment within the co-culture experiment. J774.2 macrophages were treated LPS (100 ng/ml) for 48 hours with 50 µMol/L EPA, DHA or vehicle control in DMEM media during the final 24 hour LPS treatment. The fully differentiated adipocytes were then treated with the J774.2 macrophages for a further 24 hours in either a contact or transwell system.

5.2.2 mRNA analysis (TaqMan® RT-PCR)

Total RNA was extracted from 3T3-L1 adipocytes either by Tri reagent or using an RNeasy Mini kit from Qiagen as described in section 2.7.1. After extraction RNA was quantified and quality assessed using a Nano-Drop as described in section 2.7.2. RNA was deoxyribonuclease (DNase) treated and cDNA was synthesised using with a high capacity reverse transcription kit from Applied Biosystems or using SuperScript® VILO™ (Invitrogen Corporation) as described in section 2.7.4 and 2.7.5. Gene expression was quantified by real-time reverse transcription polymerase chain reaction (RT-PCR) on an ABI 7700 or an ABI 7900HT sequence detection system from Applied Biosystems (Warrington, UK). IRS-1, GLUT4, sterol regulatory element–binding protein (SREBP)-1c, resistin, TNF-α, IL-6, IL-1 receptor antagonist (IL-1Ra), 18S and glyceraldehydes-3-phosphates dehydrogenase (GAPDH) were investigated using pre-developed primer probe kits purchased from Applied Biosystems. The comparative Ct method, also known as the ΔΔCt method was used to calculate gene expression levels. This involves comparing the Ct

values of the samples of interest with a control; in this case DMSO vehicle control treated 3T3-L1 adipocytes. The Ct values of both the calibrator and the samples of interest are normalized to an appropriate internal control, in this case 18S. Alternatively, standard curves were constructed and the fractional cycle number of each unknown sample was used to calculate the amount of target gene relative to the standard. Both methods of analysis are described in section 2.7.6.

5.2.3 Protein analysis and Western blotting

Cells were washed in PBS and total cell lysates were extracted with RIPA buffer combined with a protease inhibitor cocktail as described in section 2.8.1. Protein concentrations were assessed using the Bradford assay. 10 μg of protein was separated by electrophoresis through SDS-PAGE gels and the proteins were then transferred to a nitrocellulose membrane as described in section 2.8.3, 2.8.4 and 2.8.5 respectively. Membranes were probed using antibodies specific to the targets GLUT4 (Millipore, MA, USA), IRS-1, inhibitor of κB (IκB)-α, phosphorylated IκB-α (Ser32), phosphorylated c-Jun N-terminal kinase (JNK)1/2 p54/46 (Thr183/Tyr185), p38 mitogen-activated protein kinase (MAPK), phosphorylated p38 (Thr180/Tyr182), phosphorylated p44/42 MAPK (extracellular signal-regulated kinases [ERK1/2], Thr202/Tyr204, Cell Signalling Technology®, MA USA), PPAR-γ (Abcam, Cambridge, UK), nuclear factor (NF)-κBp65, JNK1 p54 and p44 MAPK (ERK1; Santa Cruz Biotechnology Inc., CA, USA). Immunoreactive bands were visualized using an enhanced chemiluminescence reaction, the luminescence was then detected by photographic film and analysed using densitometry as described in section 2.8.6, 2.8.7 and 2.8.8. The position of the band was confirmed by the inclusion of suitable molecular weight markers. Correct loading of protein was confirmed by blotting for actin.

5.2.4 ELISA analysis

Supernatants were collected from the cells and ELISA analysis was carried out using commercially available kits from R and D Systems (Abington, UK) for leptin, resistin, adiponectin, TNF-α, IL-6 and IL-1β as described in section 2.9.1. Briefly, the primary or capture antibody specific to the antigen was coated to the walls of a 96 well microtiter plate. Standards were provided with the kits and were reconstituted to working concentrations by serial 1:2 dilutions in reagent diluent. Supernatant and standards were added directly to the 96 well microtiter coated with capture antibody and antigens became immobilized by the capture antibody. The secondary or detection antibody was added to the wells and binds to the immobilized antigen. The detection antibody is conjugated with

HRP. Substrate TMB was added to each well. The immobilised HRP of the detection antibody acts on the TMB causing a blue colour to develop proportionally to the amount of antigen present. H_2SO_4 stops the oxidation of TMB and changes the blue colour to yellow. Absorbance of the wells was read in the microplate reader at 450 nm with a wavelength correction of 570 nm. A standard curve was constructed for each assay and sample concentrations were calculated through the equation of the standard curve.

5.2.5 Glucose uptake assay

Glucose uptake assays were performed on the fully differentiated 3T3-L1 adipocytes, which had been treated with EPA, DHA or DMSO vehicle control during differentiation as described in section 2.6. Briefly, cells were first incubated in PBS with 0.2% BSA prior to addition of 100 nMol of Insulin in PBS for 30 minutes. After which 5 μCi/ml of ^3H glucose in 1 mMol glucose was added to the cells and incubated for 15 minutes. Cells were then washed twice and then lysed in RIPA buffer containing a protease inhibitor cocktail. Samples were assayed for ^3H uptake as counts per minute. Images of the adipocytes prior to the assay were taken.

5.2.6 Data preparation and statistical analysis

Data was reported as Mean ± SEM. Statistical analysis was performed with SPSS (SPSS Inc.). The distribution of data for each variable was assessed and variables transformed to normalise the distribution of data if necessary. Multiple comparisons were performed by one-way ANOVA. Significant inter-group differences were subsequently tested by post hoc Least Significant Difference (LSD) statistical analysis. A statistical probability of $P \leq 0.05$ was considered statistically significant.

5.3 Results

5.3.1 Effects of EPA and DHA on adipokine secretion from 3T3-L1 adipocytes

Adiponectin, leptin, IL-6, TNF-α and IL-1β protein secretion was measured from 3T3-L1 adipocytes chronically treated with EPA, DHA or vehicle control as presented in Figures 5.2 and 5.3. Leptin secretion was significantly up-regulated in 3T3-L1 adipocytes treated with EPA (2.1 fold increase) compared to DMSO treated control adipocytes ($P \leq 0.001$; Figure 5.2a). EPA treatment increased adiponectin secretion from 3T3-L1 adipocytes (88% increase) compared to DMSO treated control adipocytes ($P \leq 0.044$; Figure 5.2b). DHA treatment also increased adiponectin secretion from 3T3-L1 adipocytes (68% increase) compared to control adipocytes however, not significantly. IL-6 (Figure 5.3a), TNF-α (Figure 5.3b) and IL-1β (data not shown) secretion from 3T3-L1 adipocytes was not significantly modulated by EPA or DHA treatment relative to DMSO treated adipocytes.

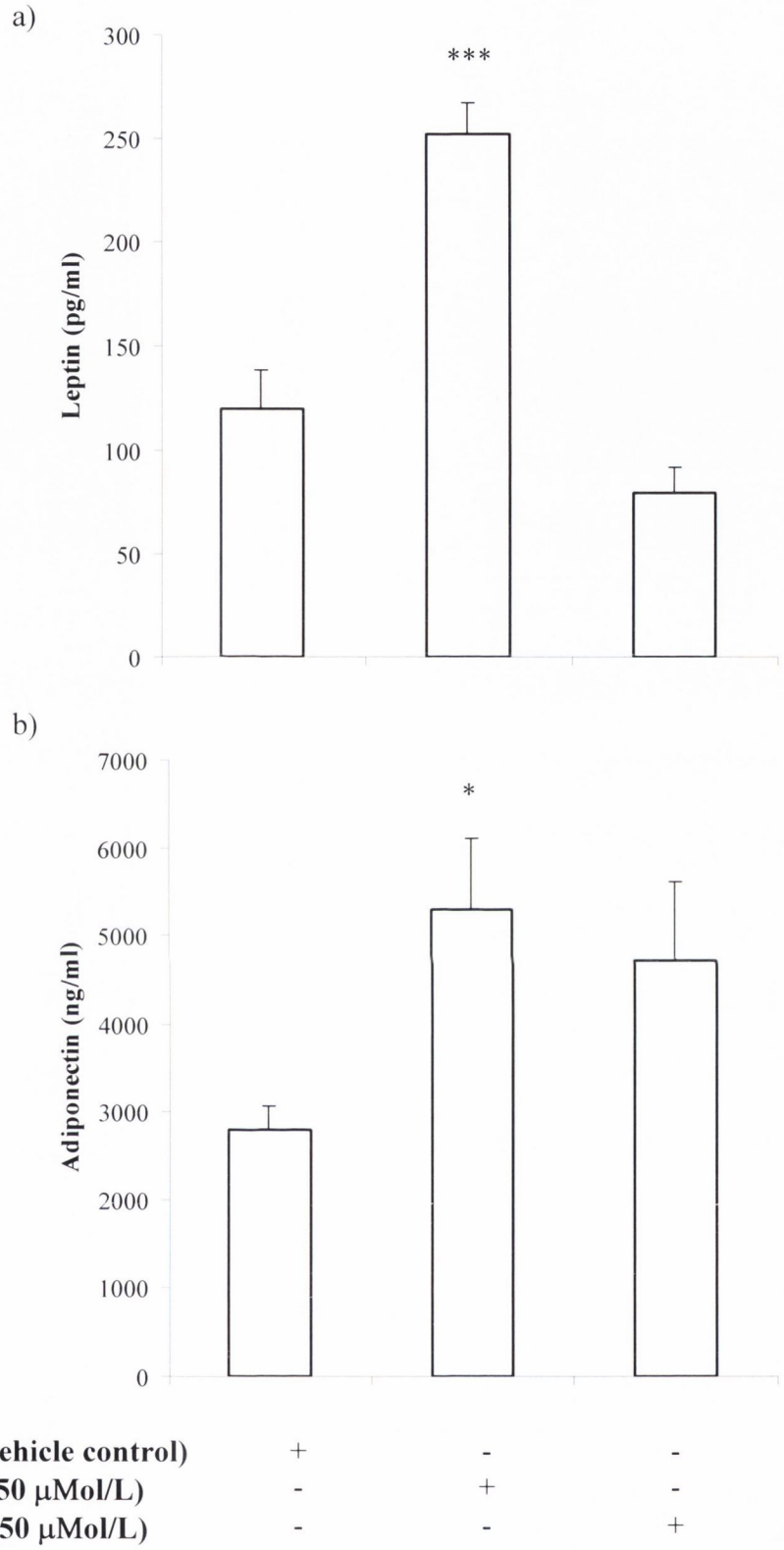

Figure 5.2 Effects of EPA and DHA on adiponectin and leptin secretion from 3T3-L1 adipocytes. 3T3-L1 adipocytes were treated with 50 μMol/L EPA, DHA or DMSO vehicle control for 5 days, supernatants were harvested and leptin (a) and adiponectin (b) secretion determined by ELISA (pg/ml or ng/ml). Data is presented as mean ± SEM, n = 3. * $P \leq 0.05$, *** $P \leq 0.001$ relative to DMSO control. For leptin a one-way ANOVA was performed within each group followed by post hoc LSD analysis. For adiponectin an independent Student's t-test was performed on the LC *n-3* PUFA treated adipocytes vs. controls.

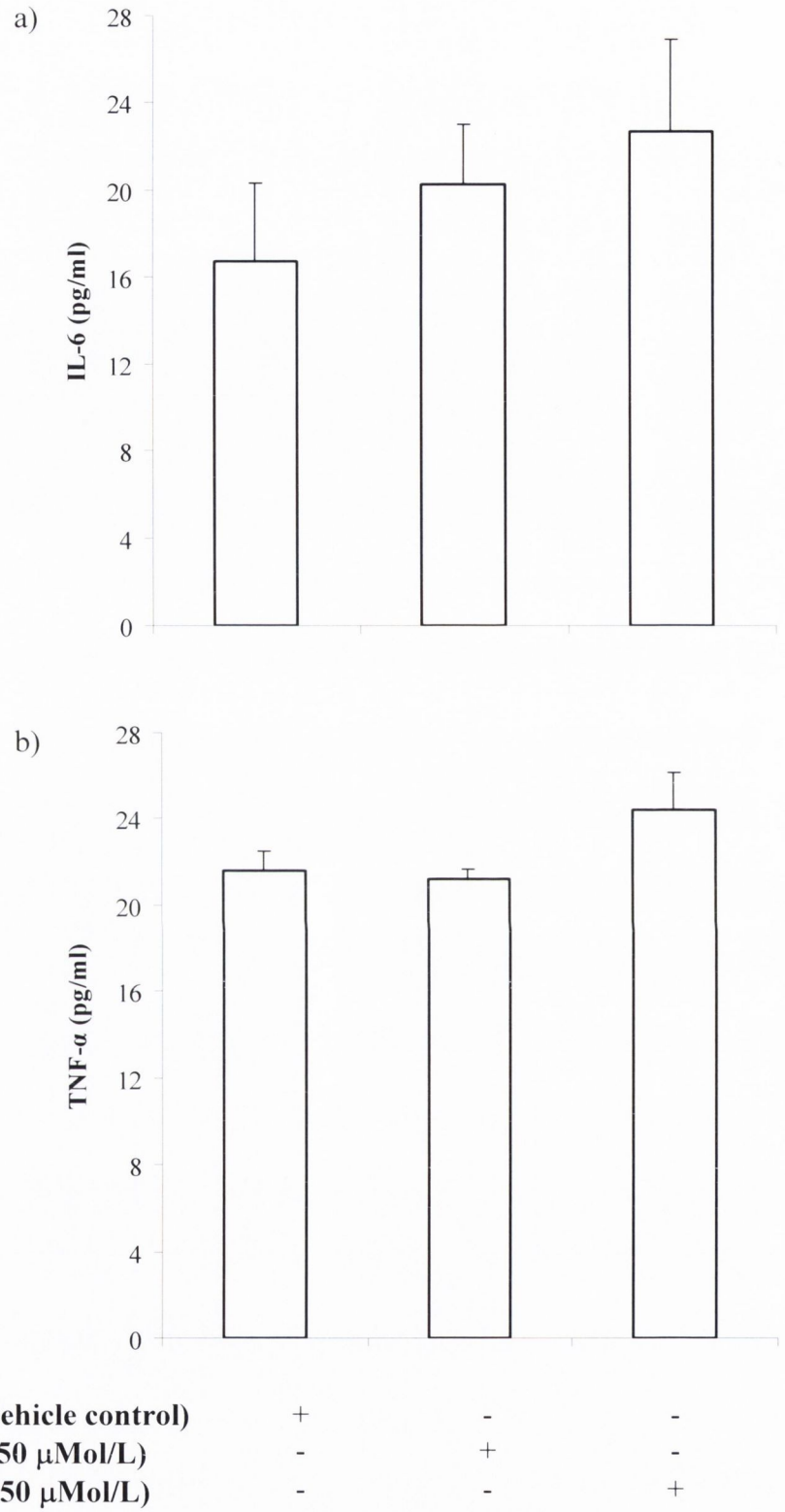

Figure 5.3 Effects of EPA and DHA on IL-6 and TNF-α secretion from 3T3-L1 adipocytes. 3T3-L1 adipocytes were treated with 50 μMol/L EPA, DHA or DMSO vehicle control for 5 days, supernatants were harvested and IL-6 (a) and TNF-α (b) secretion determined by ELISA (pg/ml). Data is presented as mean ± SEM, n = 3.

5.3.2 Effects of EPA and DHA on insulin sensitive and inflammatory target gene expression in 3T3-L1 adipocytes

GLUT4, IRS-1, resistin, SREBP-1c, TNF-α and IL-1Ra mRNA expression levels were measured within 3T3-L1 adipocytes chronically treated with EPA, DHA and DMSO vehicle control as presented in Figures 5.4, 5.5 and 5.6. GLUT4 mRNA expression was significantly reduced 52% in DHA treated 3T3-L1 adipocytes relative to DMSO treated control adipocytes ($P \leq 0.017$; Figure 5.4a). EPA and DHA treatment had no significant effect on IRS-1 gene expression within adipocytes compared to DMSO treated controls (Figure 5.4b). Resistin (Figure 5.5a) and Adiponectin (data not shown) gene expression was only moderately modulated by EPA and DHA treatment within the 3T3-L1 adipocytes however, there were similar trends between gene expression and the secretion of these adipokines from the adipocytes.

SREBP-1c (Figure 5.5b) and PPAR-γ (data not shown) gene expression was not significantly modulated by EPA and DHA. TNF-α mRNA expression was increased 76% in 3T3-L1 adipocytes treated with DHA relative to DMSO treated control adipocytes, however this was not significant (Figure 5.6a). Interestingly, while IL-1RI (data not shown) mRNA expression was not modulated by EPA and DHA treatment and IL-1β expression was undetectable IL-1Ra expression was significantly reduced 48% in 3T3-L1 adipocytes treated with both EPA and DHA relative to DMSO control adipocytes ($P \leq 0.003$; Figure 5.6b).

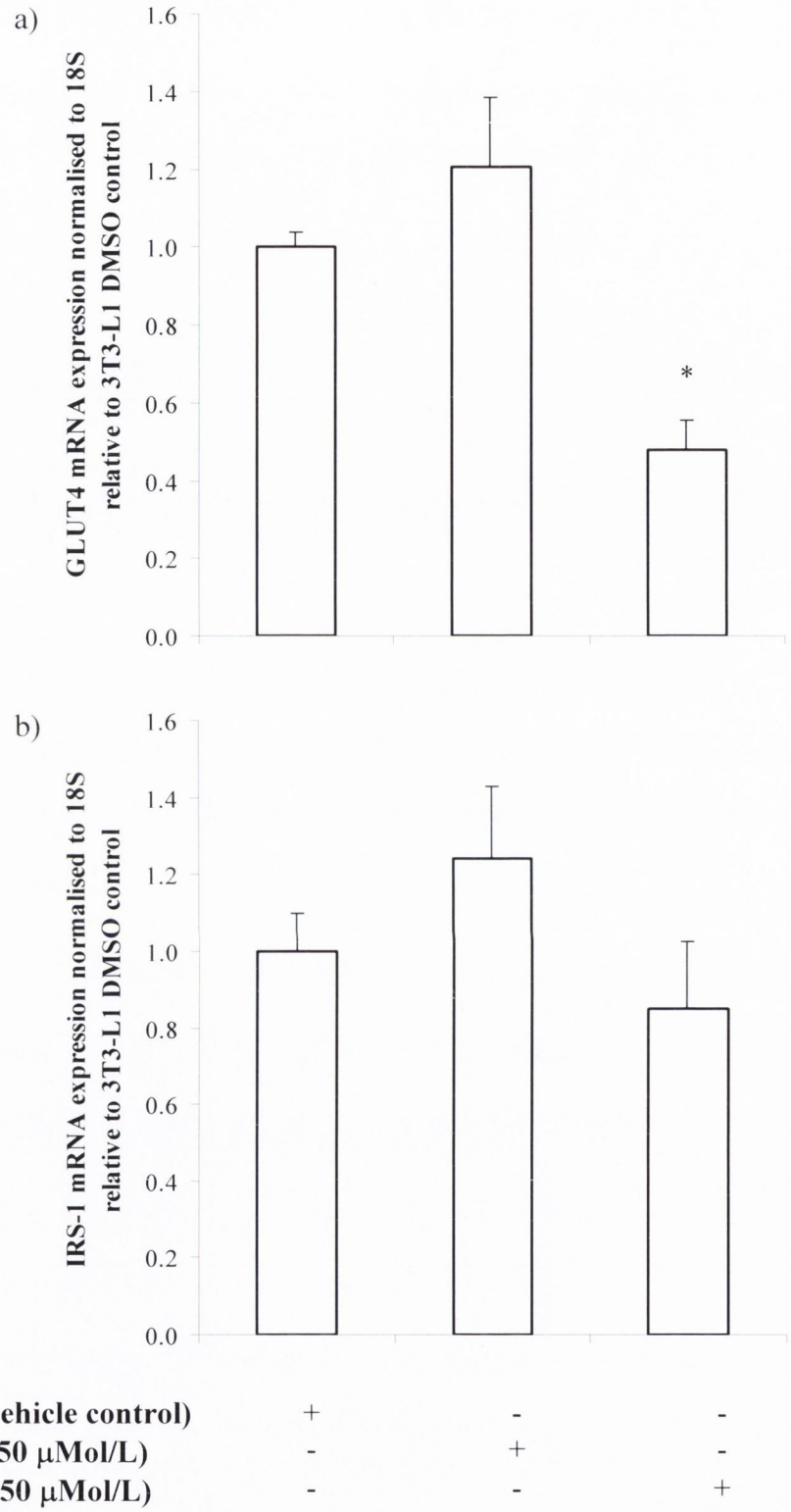

Figure 5.4 Effects of EPA and DHA on GLUT4 and IRS-1 gene expression in 3T3-L1 adipocytes. 3T3-L1 adipocytes were treated with 50mmol/L EPA, DHA or DMSO vehicle control for 5 days, GLUT4 (a) and IRS-1 (b) mRNA levels were measured using Taqman RT-PCR. mRNA levels were normalized to 18S and the results are expressed as fold induction relative to DMSO control. Data is presented as mean ± SEM, n = 3. * $P \leq 0.05$ relative to DMSO control. One-way ANOVA was performed within each group followed by post hoc LSD analysis.

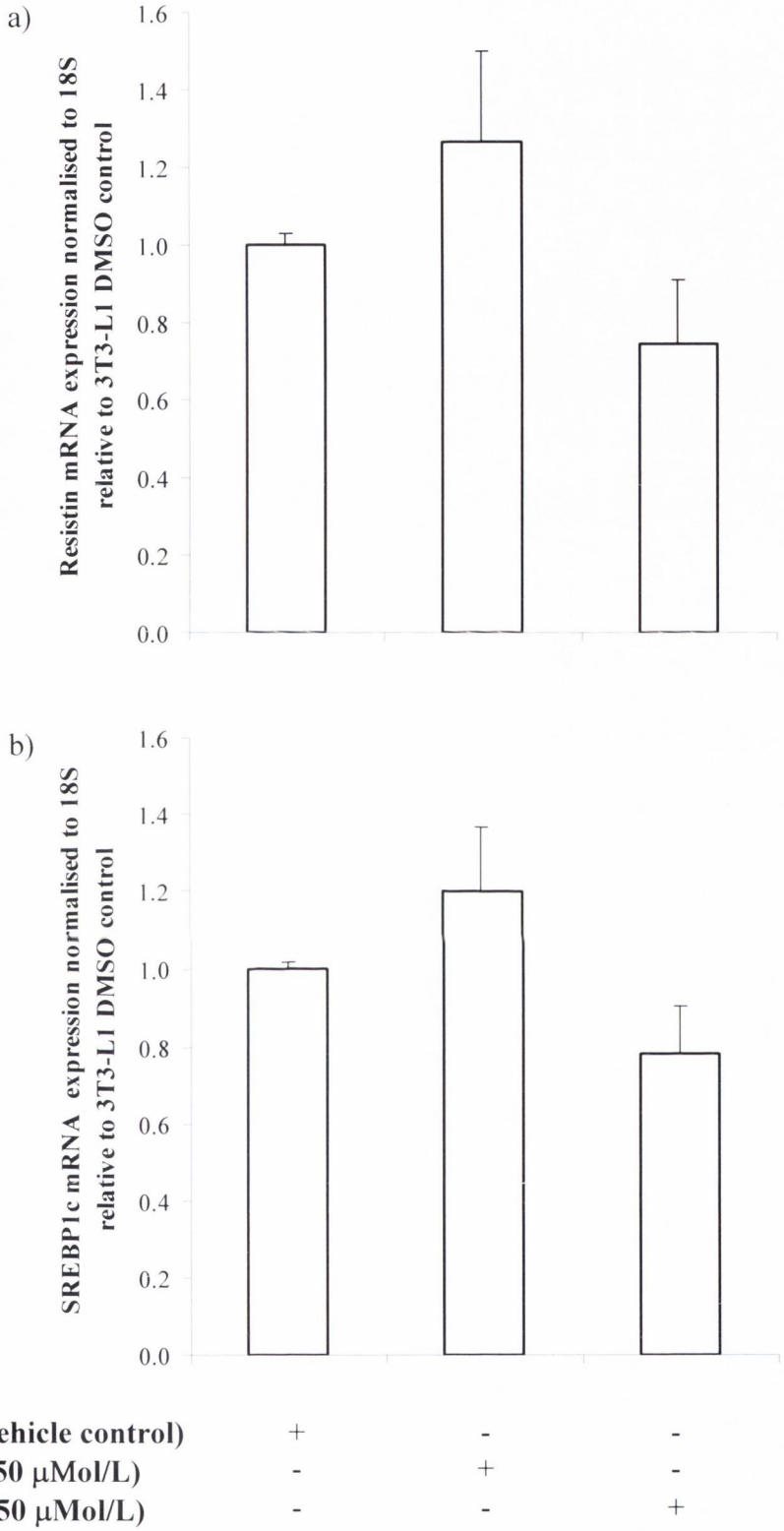

Figure 5.5 Effects of EPA and DHA on resistin and SREBP-1c gene expression in 3T3-L1 adipocytes. 3T3-L1 adipocytes were treated with 50 μMol/L EPA, DHA or DMSO vehicle control for 5 days, resistin (a) and SREBP-1c (b) mRNA levels were measured using Taqman RT-PCR. mRNA levels were normalized to 18S and the results are expressed as fold induction relative to DMSO control. Data is presented as mean ± SEM, n = 3.

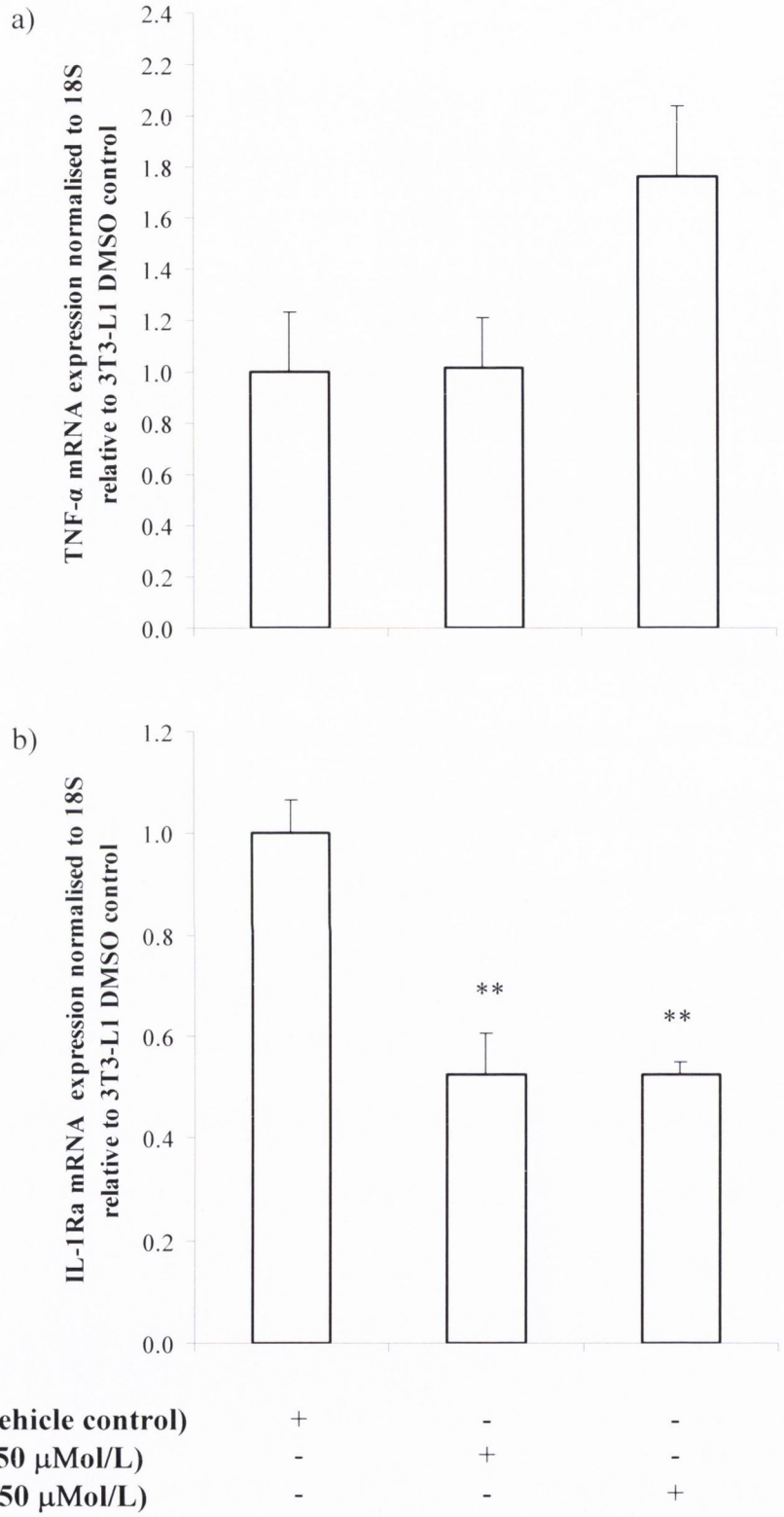

Figure 5.6 Effects of EPA and DHA on TNF-α and IL-1Ra gene expression in 3T3-L1 adipocytes. 3T3-L1 adipocytes were treated with 50 μMol/L EPA, DHA or DMSO vehicle control for 5 days, TNF-α (a) and IL-1Ra (b) mRNA levels were measured using Taqman RT-PCR. mRNA levels were normalized to 18S and the results are expressed as fold induction relative to DMSO control. Data is presented as mean ± SEM, n = 3. ** $P \leq 0.01$ relative to DMSO control. One-way ANOVA was performed within each group followed by post hoc LSD analysis.

5.3.3 Effects of EPA and DHA on insulin sensitive and inflammatory target protein expression in 3T3-L1 adipocytes

Total GLUT4, IRS-1, NF-κB, IκB-α, ERK1 and JNK1 protein expression were measured in 3T3-L1 adipocytes chronically treated with EPA, DHA or DMSO vehicle control as presented in Figures 5.7, 5.8 and 5.9. Whole cell GLUT4 protein expression was significantly reduced 43% in 3T3-L1 adipocytes treated with DHA relative to DMSO vehicle treated adipocytes ($p \leq 0.011$; Figure 5.7a). There was no significant modulation of whole cell IRS-1 (Figure 5.7b) and PPAR-γ (data not shown) by the EPA and DHA treatment in the adipocytes.

Whole cell NF-κB (Figure 5.8a) was not significantly altered by EPA and DHA treatment within the adipocytes relative to the control group. However, total IκB-α protein expression was significantly down-regulated by DHA treatment (55% decrease) relative to control adipocytes ($P \leq 0.005$; Figure 5.8b). Total ERK1 protein expression was significantly reduced 49% by DHA treatment in 3T3-L1 adipocytes compared to DMSO treated controls ($P \leq 0.015$; Figure 5.9a). Total JNK1 protein expression was unaffected by the EPA and DHA treatment compared to DMSO treated adipocytes (Figure 5.9b).

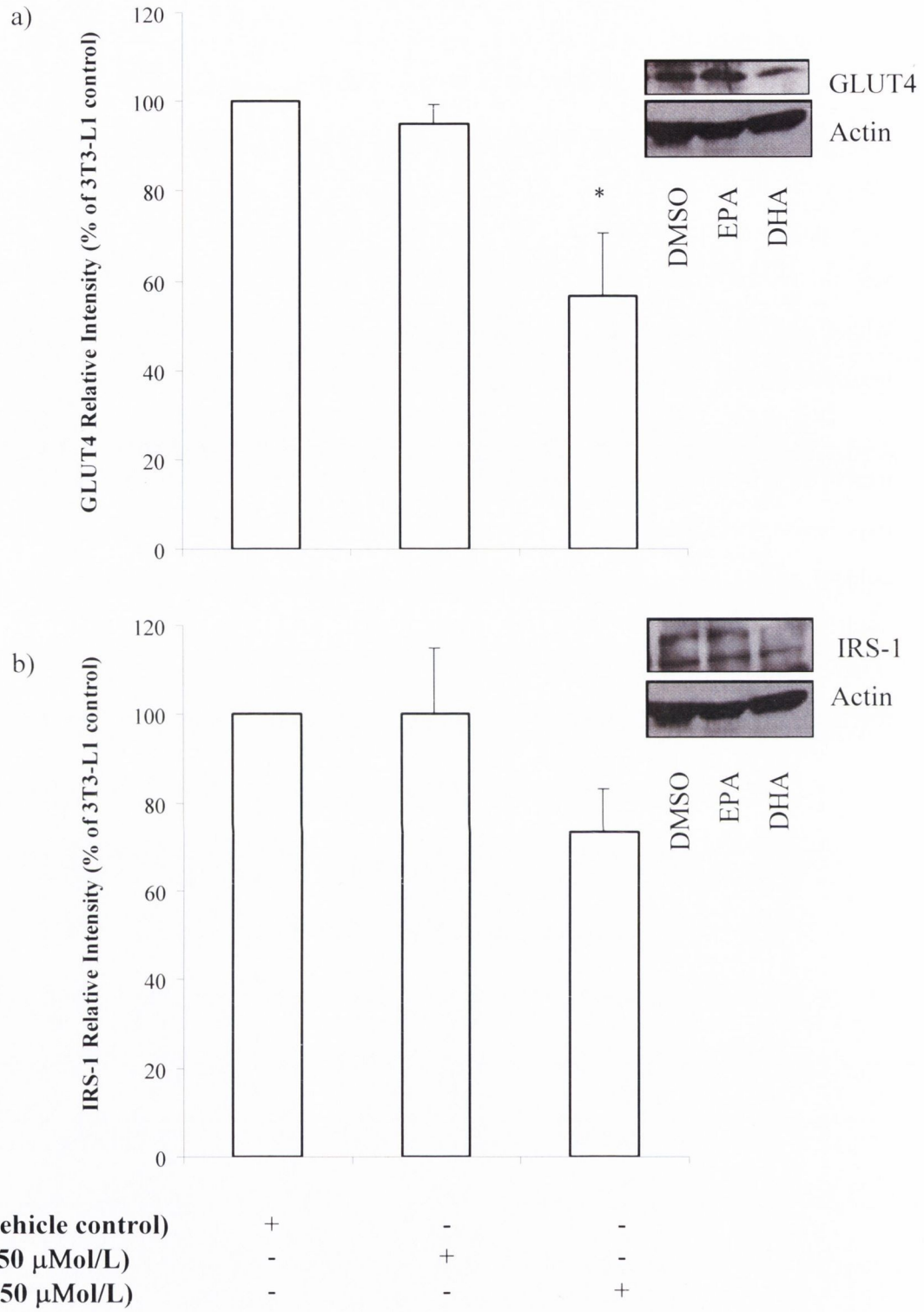

Figure 5.7 Effects of EPA and DHA on GLUT4 and IRS-1 target protein expression in 3T3-L1 adipocyte whole cell extracts. 3T3-L1 adipocytes were treated with 50 μMol/L EPA, DHA or DMSO vehicle control for 5 days. Whole cell lysates were prepared for SDS-PAGE and immunoblotting. The relative protein levels were quantified by densitometry and data expressed relative to the amount of GLUT4 (a) and IRS-1 (b) within 3T3-L1 adipocytes treated with DMSO vehicle control (100%), data is presented as mean ± SEM, n = 3. A representative blot is shown to the right of the graph. * $P \leq 0.05$ relative to DMSO control. One-way ANOVA was performed within each group followed by post hoc LSD analysis. Correct loading of protein was confirmed by blotting for actin.

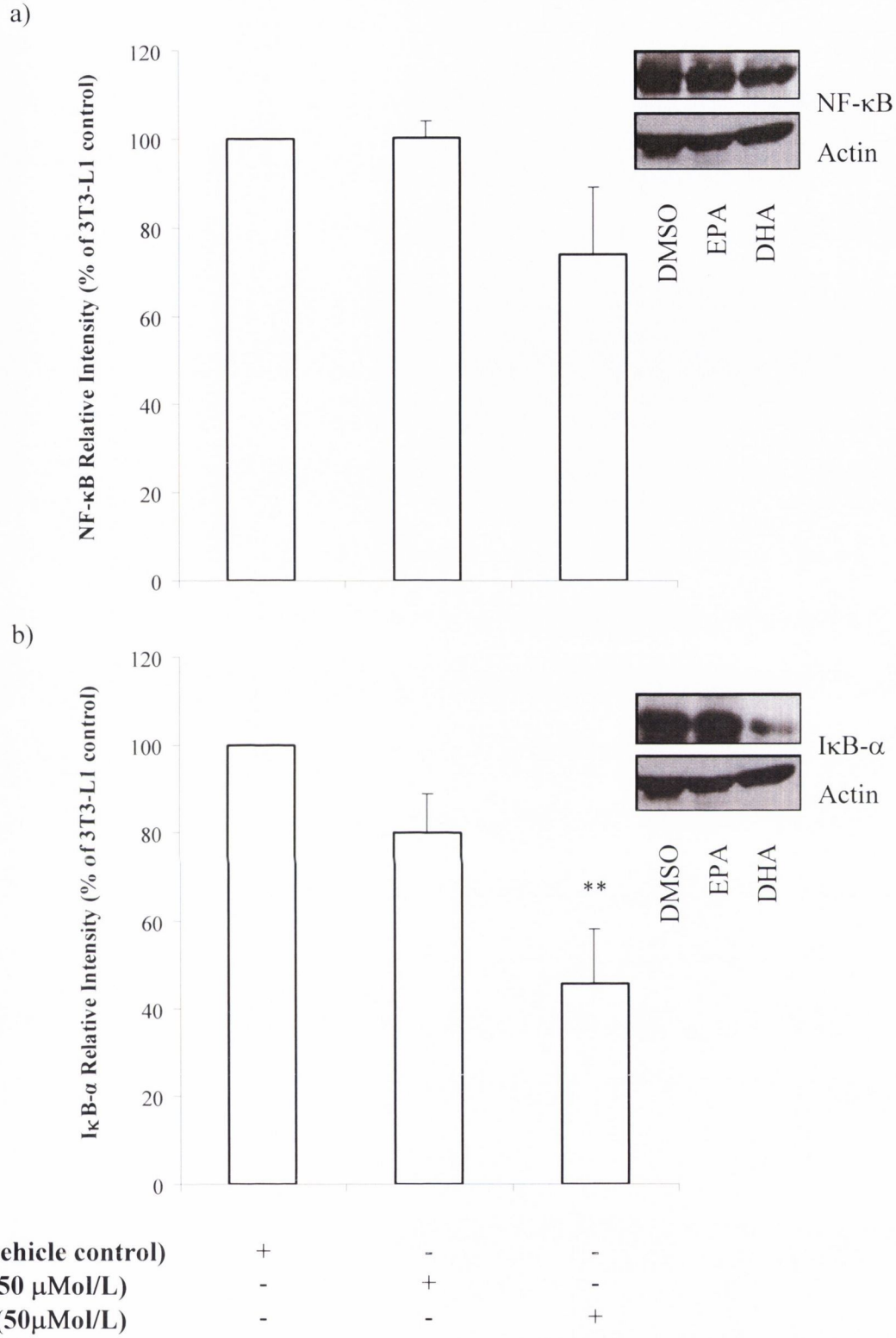

Figure 5.8 Effects of EPA and DHA on NF-κB and IKB-α protein expression in 3T3-L1 adipocyte whole cell extracts. 3T3-L1 adipocytes were treated with 50 μMol/L EPA, DHA or DMSO vehicle control for 5 days. Whole cell lysates were prepared for SDS-PAGE and immunoblotting. The relative protein levels were quantified by densitometry and data expressed relative to the amount of NF-κB (a) and IκB-α (b) within 3T3-L1 adipocytes treated with DMSO vehicle control (100%), data is presented as mean ± SEM, n = 3. A representative blot is shown to the right of the graph. ** $P \leq 0.01$ relative to DMSO control. One-way ANOVA was performed within each group followed by post hoc LSD analysis. Correct loading of protein was confirmed by blotting for actin.

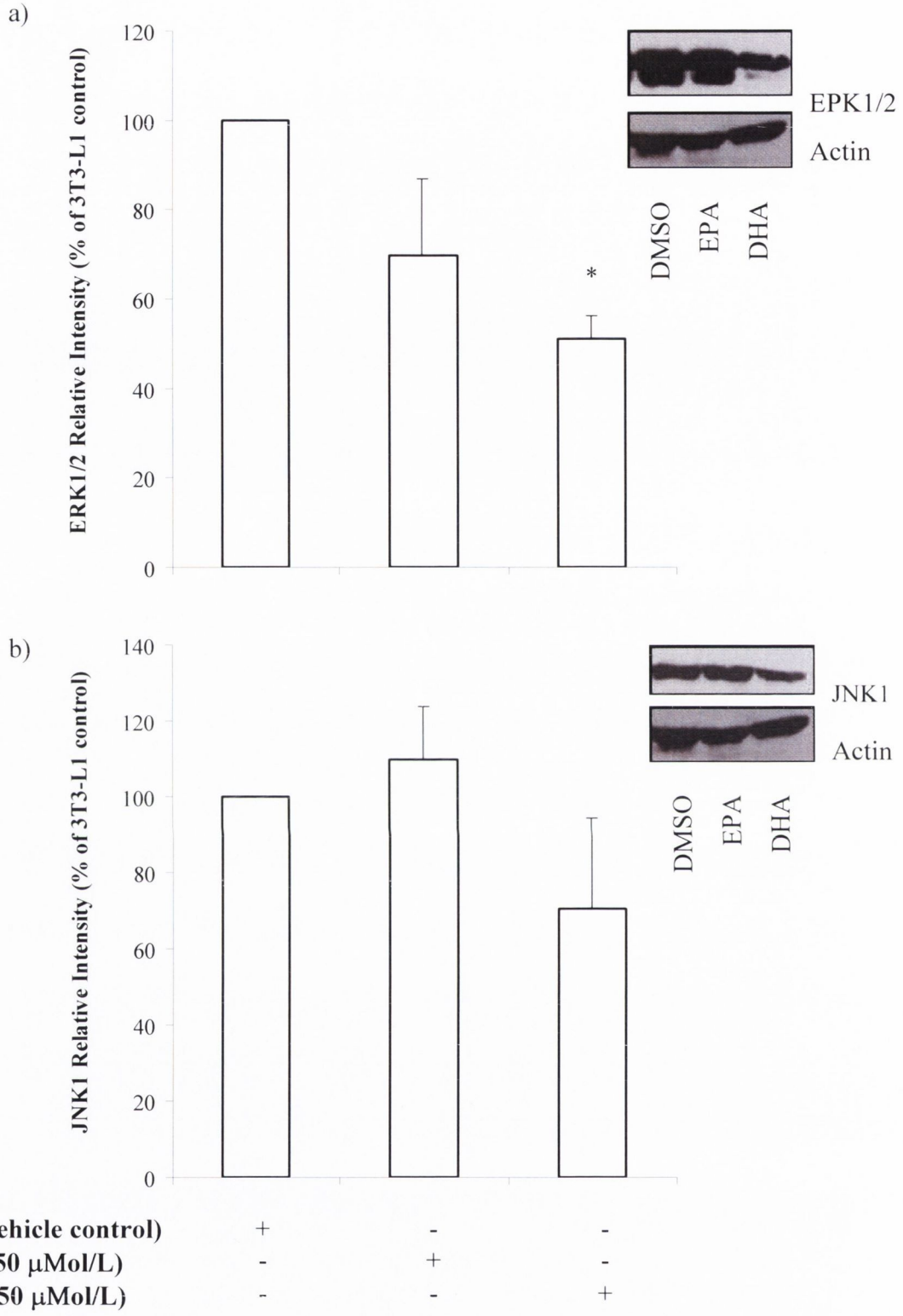

Figure 5.9 Effects of EPA and DHA on ERK1/2 and JNK1 protein expression in 3T3-L1 adipocyte whole cell extracts. 3T3-L1 adipocytes were treated with 50 μMol/L EPA, DHA or DMSO vehicle control for 5 days. Whole cell lysates were prepared for SDS-PAGE and immunoblotting. The relative protein levels were quantified by densitometry and data expressed relative to the amount of ERK1/2 (a) and JNK1 (b) within 3T3-L1 adipocytes treated with DMSO vehicle control (100%), data is presented as mean ± SEM, n = 3. A representative blot is shown to the right of the graph. * $P \leq 0.05$ relative to DMSO control. One-way ANOVA was performed within each group followed by post hoc LSD analysis. Correct loading of protein was confirmed by blotting for actin.

5.3.4 Effects of EPA and DHA on glucose uptake in 3T3-L1 adipocytes

3T3-L1 fibroblasts were differentiated in the presence of EPA, DHA or DMSO vehicle control prior to a glucose uptake assay as presented in Figure 5.10, 5.11 and 5.12. Total glucose uptake was significantly reduced (28% decrease) in 3T3-L1 adipocytes treated with DHA during differentiation compared to the DMSO treated controls ($P \leq 0.019$; Figure 5.10). EPA treatment had no effect on total glucose uptake within the adipocytes relative to controls. Both EPA and DHA treatment during differentiation induced a significant reduction (31% and 35% decrease) in basal/non-insulin dependent glucose uptake compared to the control group ($P \leq 0.046$ and $P \leq 0.030$; Figure 5.11). Additionally, EPA treatment during differentiation increased insulin dependent glucose uptake 53% compared to DMSO treated controls, although not significantly ($P \leq 0.109$) while DHA treatment moderately reduced insulin dependent glucose uptake, however not significantly (Figure 5.12).

Microscope images were taken prior to the glucose uptake analysis to examine the cellular morphology (Figure 5.13). The images show that the DMSO and EPA treatment have no observable effect on lipid accumulation and adipocytes differentiation. However, DHA treatment appeared to reduce lipid droplet accumulation with reduced differentiation as suggested by the elongated and fibroblast-like shape of the adipocytes.

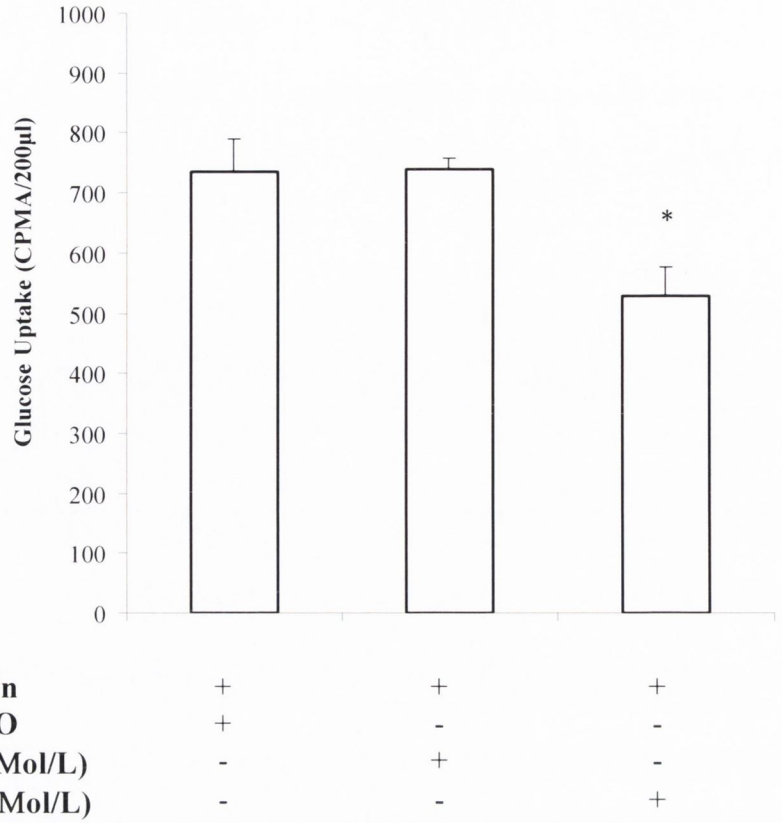

Figure 5.10 Effects of EPA and DHA on total glucose uptake in 3T3-L1 adipocytes. 3T3-L1 adipocytes were treated with 50 µMol/L EPA, DHA or DMSO vehicle control for 5 days after which insulin induced glucose uptake was determined. Cells were incubated in PBS with 0.2% BSA prior to addition of 100 nMol insulin in PBS for 15 minutes. 5 µCi/ml of ^{3}H glucose in 1 mMol glucose was added to the cells for 10 minutes. Cells were washed, lysed and assayed for ^{3}H uptake as counts per minute (CPMA), data is presented as mean ± SEM, n = 6. * $P \leq 0.05$ relative to DMSO treated adipocytes. One-way ANOVA was performed within each group followed by post hoc LSD analysis.

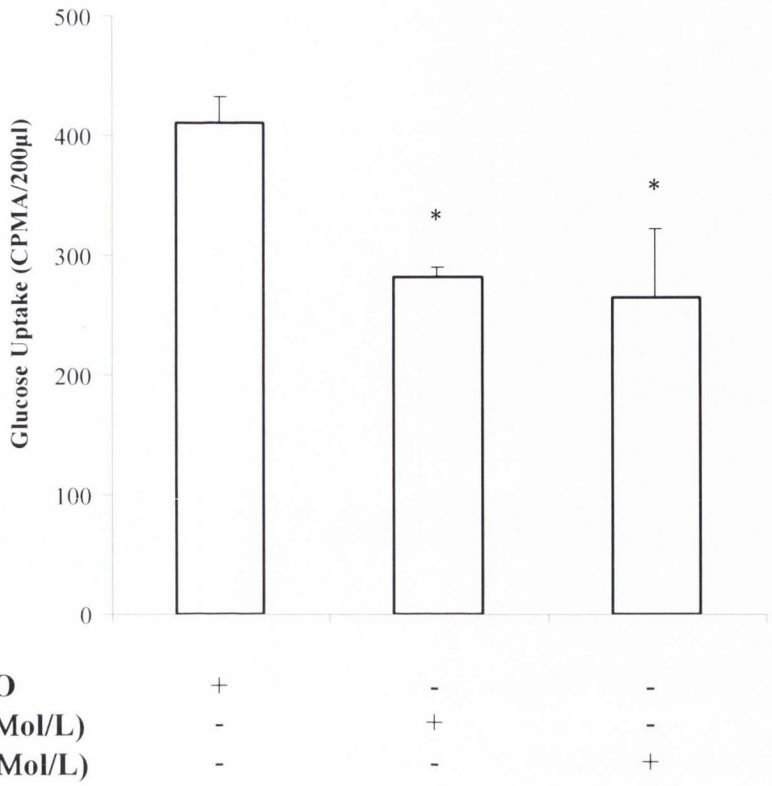

Figure 5.11 Effects of EPA and DHA on basal glucose uptake in 3T3-L1 adipocytes. 3T3-L1 adipocytes were treated with 50 µMol/L EPA, DHA or DMSO vehicle control for 5 days after which basal glucose uptake was determined. Cells were incubated in PBS with 0.2% BSA prior to addition of 5 µCi/ml of ^{3}H glucose in 1 mMol glucose for 10 minutes. Cells were washed, lysed and assayed for ^{3}H uptake as counts per minute (CPMA), data is presented as mean ± SEM, n = 6. * $P \leq 0.05$ relative to DMSO treated adipocytes. One-way ANOVA was performed within each group followed by post hoc LSD analysis.

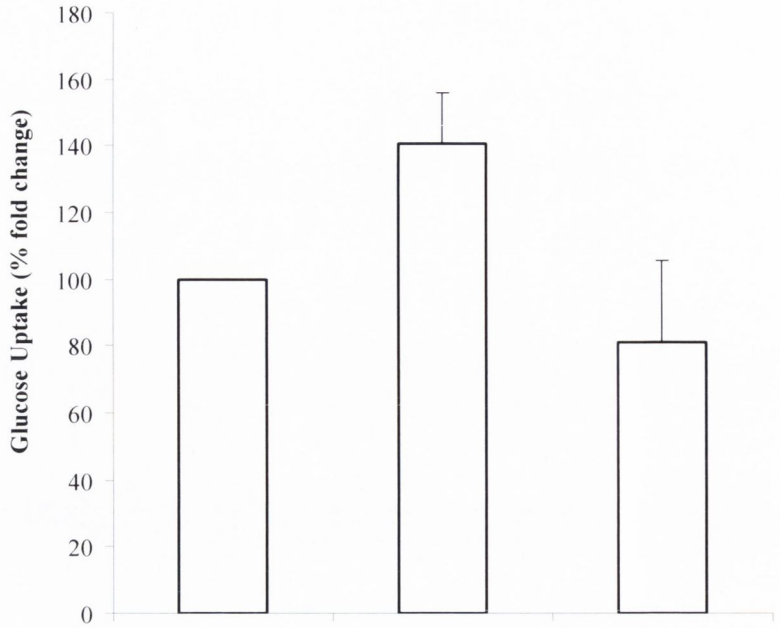

Figure 5.12 Effects of EPA and DHA on insulin induced glucose uptake in 3T3-L1 adipocytes. 3T3-L1 adipocytes were treated with 50 μMol/L EPA, DHA or DMSO vehicle control for 5 days after which insulin induced glucose uptake was determined. Cells were incubated in PBS with 0.2% BSA prior to addition of 100 nMol insulin in PBS for 15 minutes. 5 μCi/ml of ^{3}H glucose in 1 mMol glucose was added to the cells for 10 minutes. Cells were washed, lysed and assayed for ^{3}H uptake as counts per minute (CPMA). Insulin induced glucose uptake was established by subtracting total glucose uptake from basal glucose uptake, data is presented as mean ± SEM, n = 6. Data is expressed relative to the amount of insulin induced glucose uptake within DMSO treated 3T3-L1 adipocytes (100%).

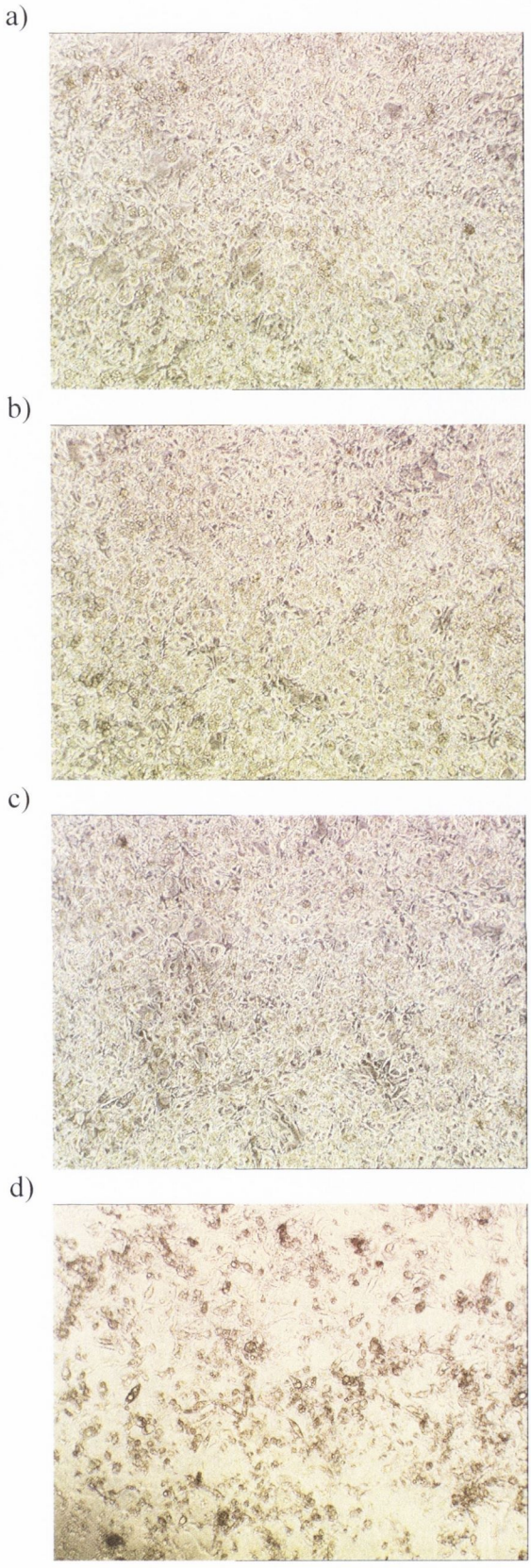

Figure 5.13 Effects of EPA and DHA on 3T3-L1 adipocyte morphology. 3T3-L1 fibroblasts were treated with 50 μMol/L EPA, DHA or DMSO vehicle control for 6 days during differentiation. Images of untreated (a), DMSO treated (b), EPA treated (c) and DHA treated (d) 3T3-L1 adipocytes are shown (100x magnification).

5.3.5 Effects of EPA and DHA treatment on cytokine secretion from LPS stimulated J774.2 macrophages

IL-6, TNF-α, IL-1β and IL-10 secretion was measured at 24 and 48 hours from LPS stimulated and unstimulated J774.2 macrophages chronically pre-treated with EPA, DHA or DMSO as presented in Figures 5.14 to 5.17. After 24 hours IL-6 secretion was significantly increased 72 fold in LPS stimulated J774.2 macrophages compared to unstimulated macrophages ($P \leq 0.001$; Figure 5.14a). IL-6 secretion was also significantly increased 67 and 68 fold in LPS stimulated J774.2 macrophages treated with EPA and DHA relative to unstimulated DMSO treated macrophages ($P \leq 0.001$ and $P \leq 0.001$). However, IL-6 secretion was significantly reduced (7% decrease) in LPS stimulated macrophages treated with EPA relative to LPS stimulated DMSO treated macrophages ($P \leq 0.032$). After a 48 hour incubation there was a significant decline in IL-6 secretion overall (Figure 5.14b). However, IL-6 secretion was still significantly increased (2.7 fold increase) in LPS stimulated DMSO treated macrophages relative to unstimulated macrophages ($P \leq 0.001$). Furthermore, after 48 hours IL-6 secretion was significantly reduced in LPS stimulated macrophages pre-treated with EPA and DHA (34% and 82% decrease) compared to LPS stimulated macrophages treated with DMSO ($P \leq 0.001$ and $P \leq 0.001$).

After a 24 hour incubation TNF-α secretion was significantly increased 9, 11 and 10 fold in LPS stimulated J774.2 macrophages treated with DMSO, EPA and DHA respectively compared to unstimulated macrophages ($P \leq 0.001$, $P \leq 0.001$ and $P \leq 0.001$; Figure 5.15a). After 48 hours TNF-α secretion had reduced to normal levels with no significant difference between LPS stimulated macrophages treated with DMSO, EPA and DHA relative to unstimulated macrophages (Figure 5.15b). Interestingly, TNF-α secretion was significantly reduced (10% decrease) in LPS stimulated macrophages pre-treated with EPA compared to untreated LPS stimulated macrophages ($P \leq 0.028$).

After a 24 hour incubation IL-1β was significantly increased 132, 119 and 98 fold in LPS stimulated J774.2 macrophages treated with DMSO, EPA and DHA respectively compared to unstimulated macrophages treated with DMSO ($P \leq 0.001$, $P \leq 0.001$ and $P \leq 0.001$; Figure 5.16a). However, IL-1β secretion was significantly reduced (10% and 26% decrease) in LPS stimulated J774.2 macrophages treated with EPA and DHA respectively relative to LPS stimulated macrophages treated with DMSO ($P \leq 0.023$ and $P \leq 0.001$). Similarly, after a 48 hour incubation IL-1β secretion had reduced significantly compared to 24 hour secretion however, IL-1β secretion was significantly higher within the LPS

stimulated macrophages treated with DMSO, EPA and DHA relative to unstimulated macrophages, which contained no detectable IL-1β ($P \leq 0.001$, $P \leq 0.001$ and $P \leq 0.001$; Figure 5.16b). Interestingly, after 48 hours IL-1β secretion was significantly reduced in LPS stimulated macrophages treated with EPA and DHA (28% and 60% decrease) compared to LPS stimulated macrophages ($P \leq 0.001$ and $P \leq 0.001$).

At 48 hours, secretion of the anti-inflammatory cytokine IL-10 was undetectable in unstimulated macrophages while LPS stimulated macrophages secreted approximately 7 pg/ml of IL-10 (Figure 5.17). Interestingly, IL-10 secretion was significantly increased in LPS stimulated macrophages treated with DHA (2.4 fold increase) compared to LPS stimulated macrophages treated with DMSO ($P \leq 0.001$).

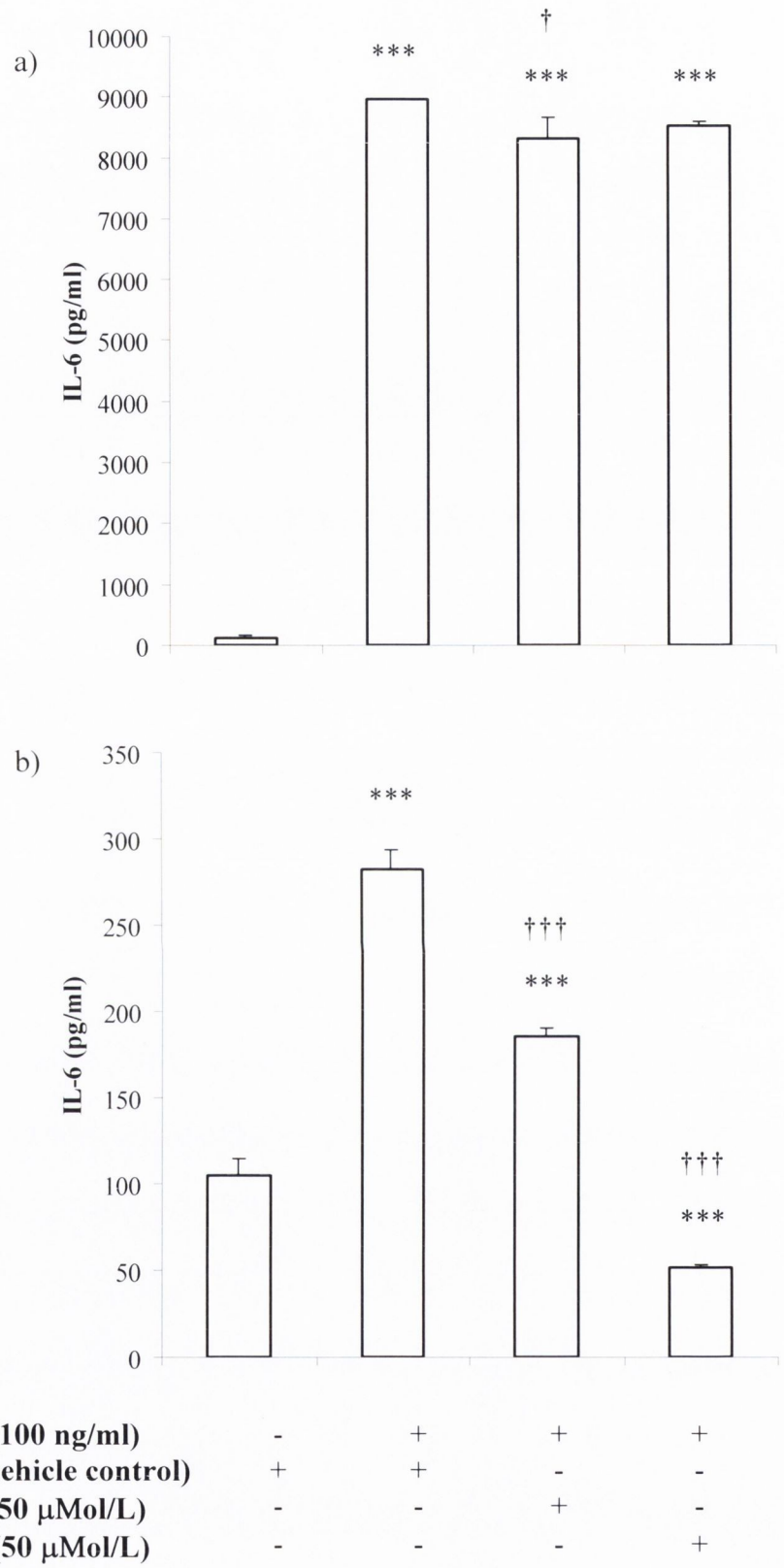

Figure 5.14 Effects of EPA and DHA on IL-6 secretion from J774.2 macrophages. J774.2 macrophages were treated with 50 μMol/L EPA, DHA or DMSO vehicle control for 5 days prior to LPS stimulation (100 ng/ml) for 15 minutes subsequently at 24 (a) and 48 (b) hours, supernatants were harvested and IL-6 secretion determined by ELISA (pg/ml). Data is presented as mean ± SEM, n = 4. *** $P \leq 0.001$ relative to DMSO control. † ≤ P 0.05, ††† ≤ P 0.001 relative to LPS stimulated DMSO control. One-way ANOVA was performed within each group followed by post hoc LSD analysis.

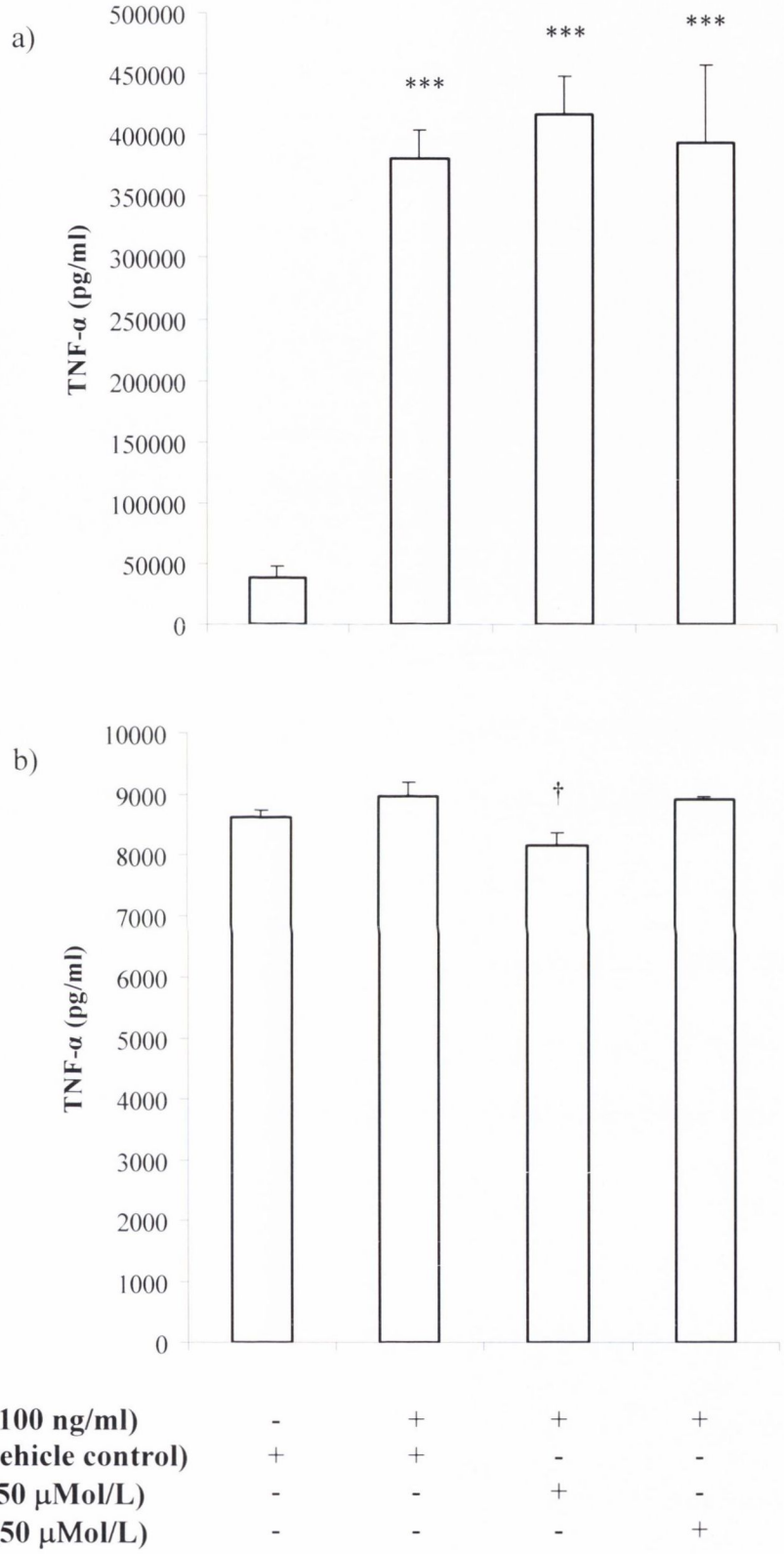

Figure 5.15 Effects of EPA and DHA on TNF-α secretion from J774.2 macrophages. J774.2 macrophages were treated with 50 μMol/L EPA, DHA or DMSO vehicle control for 5 days prior to LPS stimulation (100 ng/ml) for 15 minutes subsequently at 24 (a) and 48 (b) hours, supernatants were harvested and TNF-α secretion determined by ELISA (ng/ml). Data is presented as mean ± SEM, n = 4. *** $P \leq 0.001$ relative to DMSO control. † ≤ P 0.05 relative to LPS stimulated DMSO control. One-way ANOVA was performed within each group followed by post hoc LSD analysis.

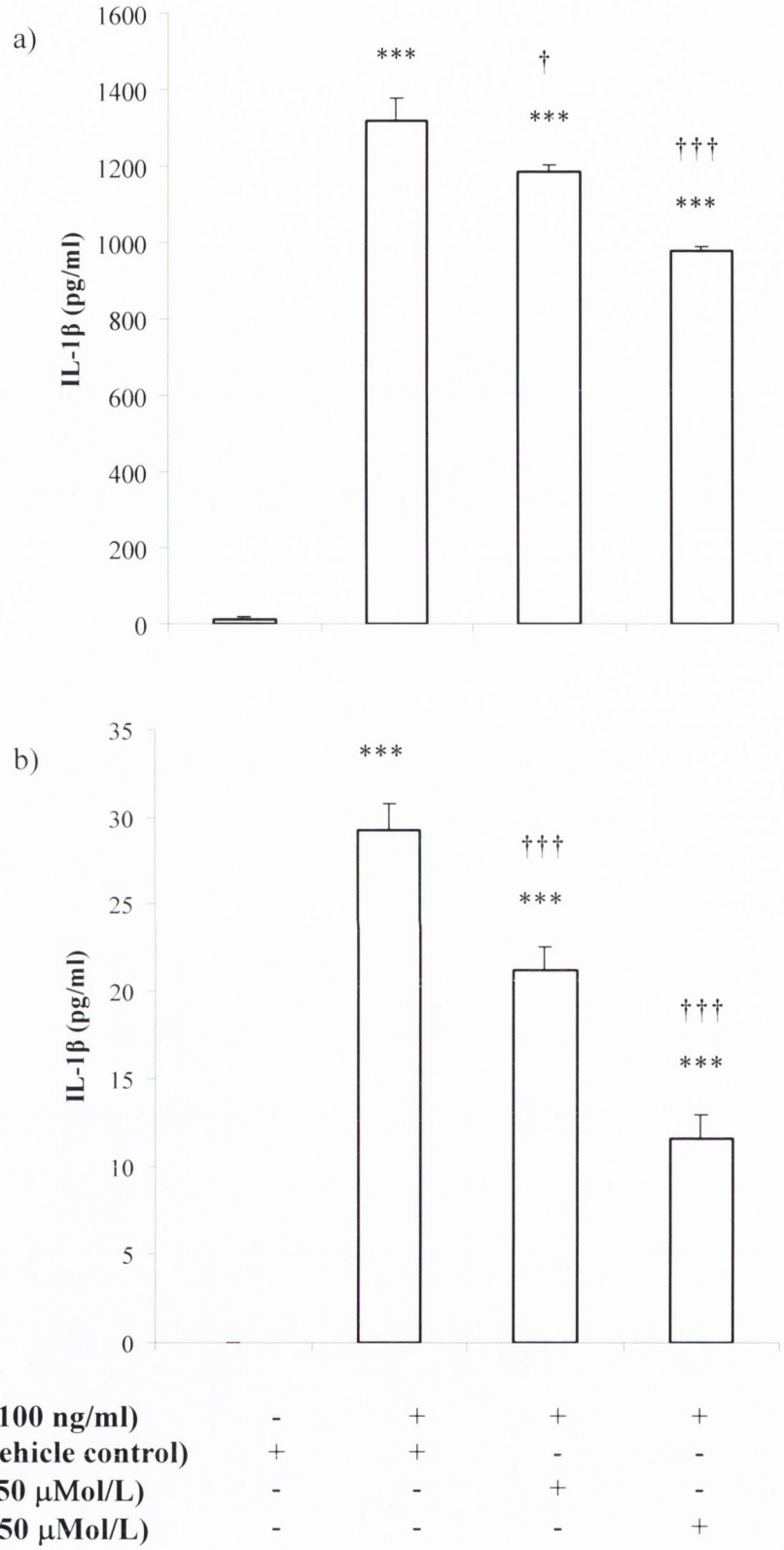

Figure 5.16 Effects of EPA and DHA on IL-1β secretion from J774.2 macrophages. J774.2 macrophages were treated with 50 μMol/L EPA, DHA or DMSO vehicle control for 5 days prior to LPS stimulation (100ng/ml) for 15 minutes subsequently at 24 (a) and 48 (b) hours, supernatants were harvested and IL-1β secretion determined by ELISA (ng/ml). Data is presented as mean ± SEM, n = 4. *** $P \leq 0.001$ relative to DMSO control. † ≤ P 0.05, ††† ≤ P 0.001 relative to LPS stimulated DMSO control. One-way ANOVA was performed within each group followed by post hoc LSD analysis.

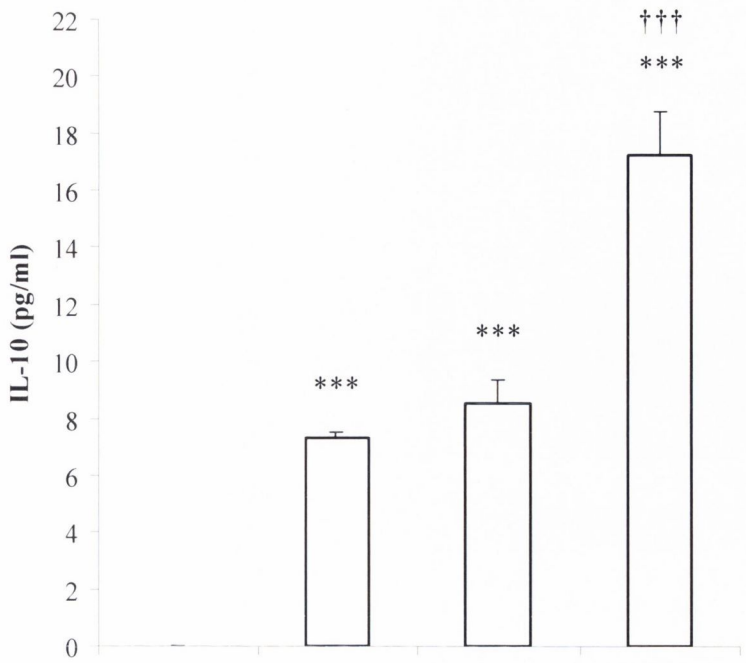

LPS (100 ng/ml)	-	+	+	+
DMSO (vehicle control)	+	+	-	-
EPA (50 μMol/L)	-	-	+	-
DHA (50 μMol/L)	-	-	-	+

Figure 5.17 Effects of EPA and DHA on IL-10 secretion from J774.2 macrophages. J774.2 macrophages were treated with 50 μMol/L EPA, DHA or DMSO vehicle control for 5 days prior to LPS stimulation (100 ng/ml) for 15 minutes subsequently at 48 hours; supernatants were harvested and IL-10 secretion determined by ELISA (ng/ml). Data is presented as mean ± SEM, n = 3. *** $P \leq 0.001$ relative to DMSO control. ††† $\leq P$ 0.001 relative to LPS stimulated DMSO control. One-way ANOVA was performed within each group followed by post hoc LSD analysis.

5.3.6 Effects of EPA and DHA treatment on inflammatory target protein expression in LPS stimulated J774.2 macrophages

p38 MAPK, phosphorylated p38 MAPK (Thr180/Tyr182), JNK1 and phosphorylated JNK1/2 (Thr183/Tyr185) and phosphorylated IκB-α (Ser32) protein expression was measured in LPS stimulated and unstimulated J774.2 macrophages chronically pre-treated with EPA, DHA and vehicle control.

Whole cell p38 protein expression was significantly increased in LPS stimulated macrophages (15% increase) relative to unstimulated macrophages ($P \leq 0.033$; Figure 5.18). Total p38 was reduced 23% and 36% in EPA pre-treated LPS stimulated macrophages compared to unstimulated and LPS stimulated control DMSO treated macrophages ($P \leq 0.005$ and $P \leq 0.001$). DHA pre-treatment significantly reduced p38 expression (17% decrease) within LPS stimulated macrophages relative to LPS stimulated DMSO treated macrophages ($P \leq 0.020$). Interestingly, phosphorylated p38 was significantly increased (2.4 fold increase) in LPS stimulated macrophages relative to unstimulated macrophages ($P \leq 0.001$; Figure 5.19). While phosphorylation of p38 expression was significantly reduced in LPS stimulated macrophages pre-treated with EPA and DHA relative to LPS stimulated macrophages treated with DMSO ($P \leq 0.001$ and $P \leq 0.005$).

Total JNK protein expression was significantly reduced in LPS stimulated macrophages pre-treated with EPA and DHA (47% and 52% decrease) relative to unstimulated macrophages and LPS stimulated macrophages ($P \leq 0.001$ and $P \leq 0.001$; $P \leq 0.006$ and $P \leq 0.003$ respectively; Figure 5.20). Phosphorylated JNK was significantly increased (21% increase) in LPS stimulated DMSO treated macrophages relative to unstimulated macrophages ($P \leq 0.003$; Figure 5.21). Interestingly, phosphorylation of JNK was not induced within LPS stimulated macrophages pre-treated with EPA and DHA relative to LPS stimulated macrophages treated with DMSO ($P \leq 0.001$ and $P \leq 0.001$). Phosphorylation of IκB-α was induced significantly (38% increase) in LPS stimulated macrophages compared to unstimulated macrophages ($P \leq 0.001$; Figure 5.22). Interestingly, there was no observable induction of IκB-α phosphorylation in LPS stimulated macrophages treated with EPA and DHA compared to LPS stimulated macrophages treated with DMSO ($P \leq 0.001$ and $P \leq 0.001$).

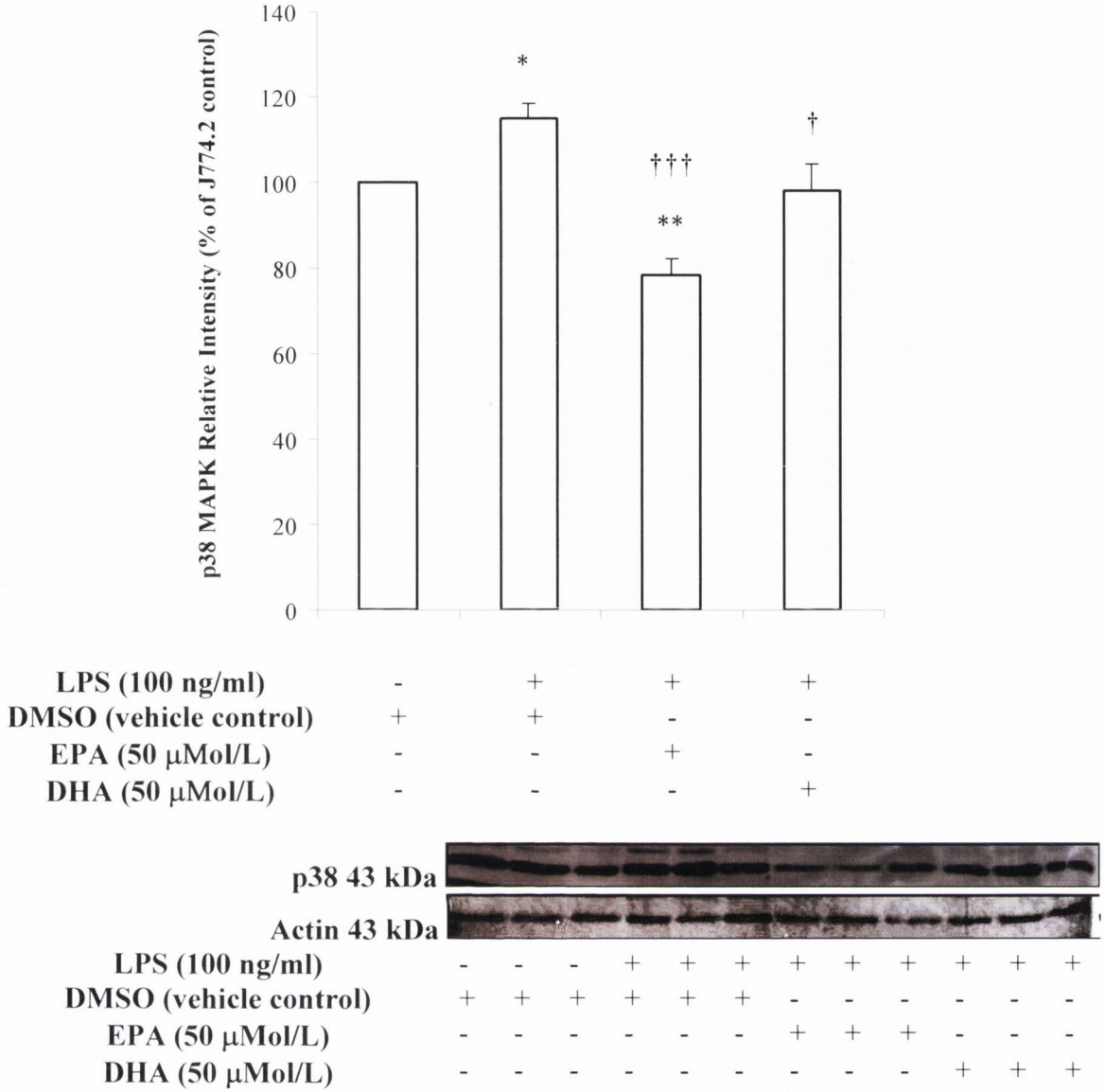

Figure 5.18 Effects of EPA and DHA on p38 MAPK protein expression within LPS stimulated J774.2 whole cell extracts. J774.2 macrophages were treated with 50 μMol/L EPA, DHA or DMSO vehicle control for 5 days prior to LPS stimulation (100 ng/ml) for 15 minutes. Whole cell lysates were prepared for SDS-PAGE and immunoblotting. The relative protein levels were quantified by densitometry and data expressed relative to the amount of p38 MAPK within J774.2 macrophages treated with DMSO vehicle control (100%), data is presented as mean ± SEM, n = 3. A representative blot is shown below the graph. * $P \leq 0.05$, ** $P \leq 0.01$ relative to DMSO control. † ≤ P 0.05, ††† ≤ P 0.001 relative to LPS stimulated DMSO control. One-way ANOVA was performed within each group followed by post hoc LSD analysis. Correct loading of protein was confirmed by blotting for actin.

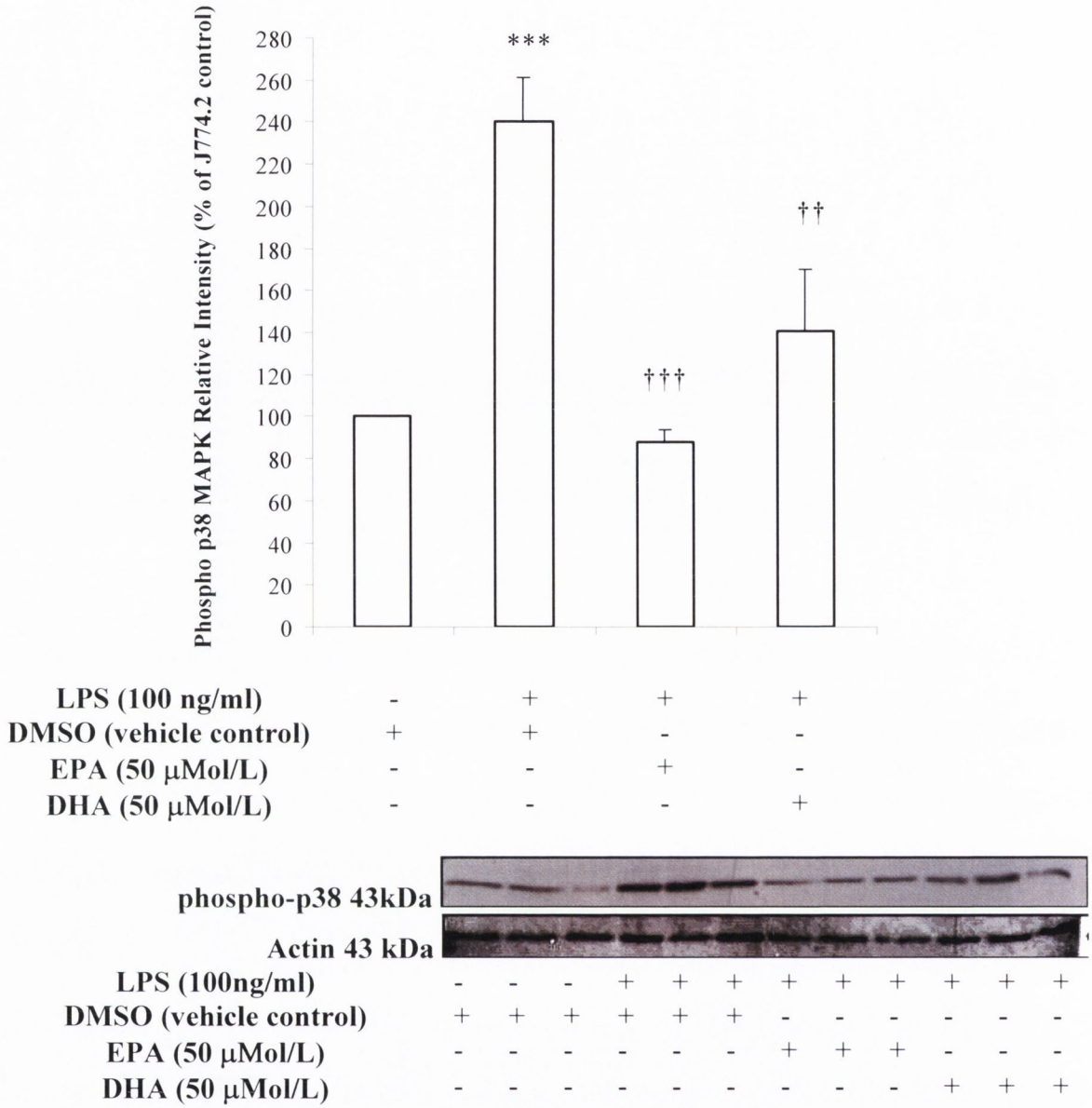

Figure 5.19 Effects of EPA and DHA on phosphorylated p38 MAPK (Thr180/Tyr182) protein expression within LPS stimulated J774.2 whole cell extracts. J774.2 macrophages were treated with 50 μMol/L EPA, DHA or DMSO vehicle control for 5 days prior to LPS stimulation (100 ng/ml) for 15 minutes. Whole cell lysates were prepared for SDS-PAGE and immunoblotting. The relative protein levels were quantified by densitometry and data expressed relative to the amount of phosphorylated p38 MAPK within J774.2 macrophages treated with DMSO vehicle control (100%), data is presented as mean ± SEM, n = 3. A representative blot is shown below the graph. *** $P \leq 0.001$ relative to DMSO control. †† $\leq$ P 0.01, ††† $P \leq 0.001$ relative to LPS stimulated DMSO control. One-way ANOVA was performed within each group followed by post hoc LSD analysis. Correct loading of protein was confirmed by blotting for actin.

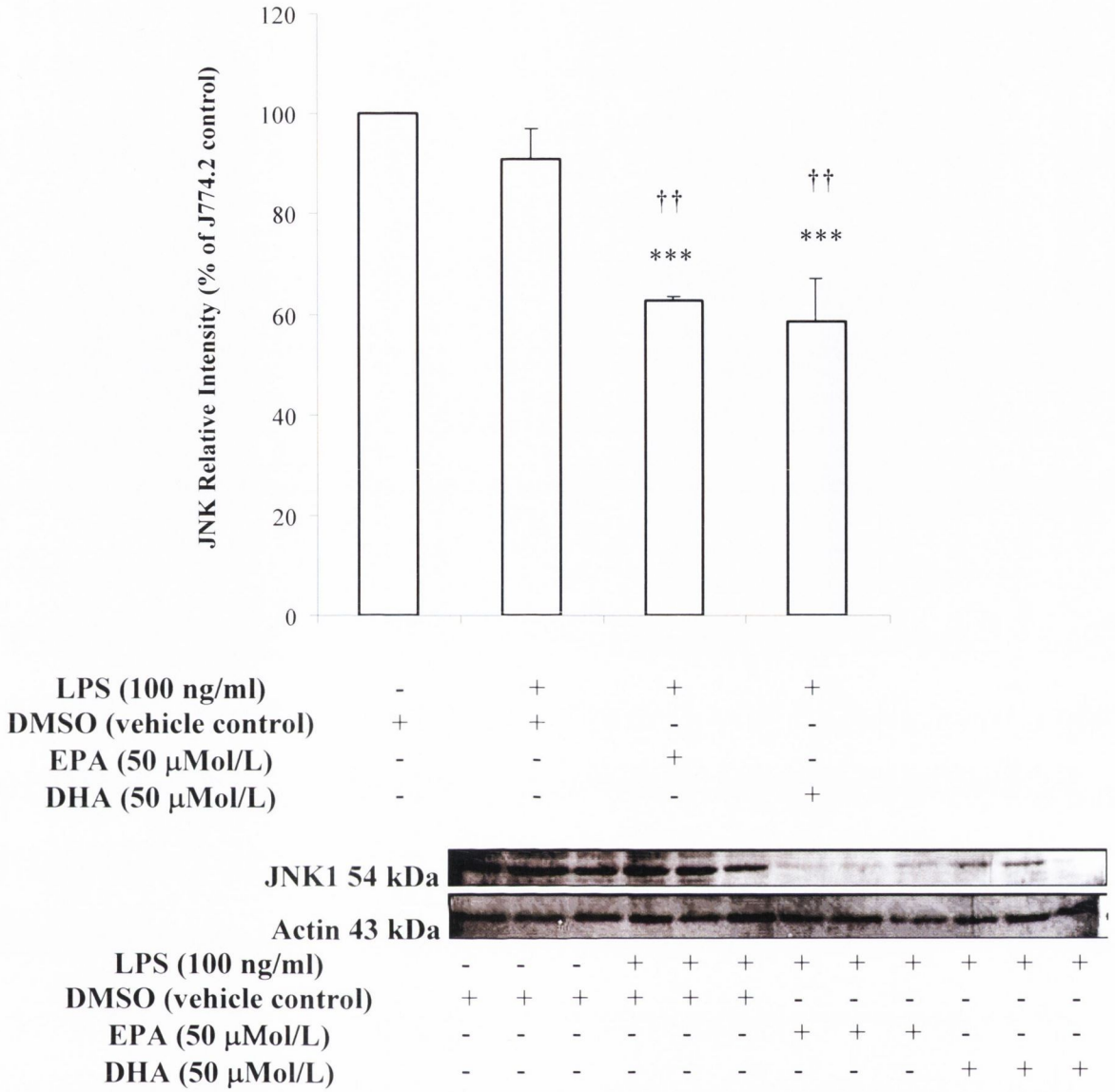

Figure 5.20 Effects of EPA and DHA on JNK1 protein expression within LPS stimulated J774.2 whole cell extracts. J774.2 macrophages were treated with 50 μMol/L EPA, DHA or DMSO vehicle control for 5 days prior to LPS stimulation (100 ng/ml) for 15 minutes. Whole cell lysates were prepared for SDS-PAGE and immunoblotting. The relative protein levels were quantified by densitometry and data expressed relative to the amount of JNK1 within J774.2 macrophages treated with DMSO vehicle control (100%), data is presented as mean ± SEM, n = 3. A representative blot is shown below the graph. *** $P \leq 0.001$ relative to DMSO control. †† $\leq P$ 0.01 relative to LPS stimulated DMSO control. One-way ANOVA was performed within each group followed by post hoc LSD analysis. Correct loading of protein was confirmed by blotting for actin.

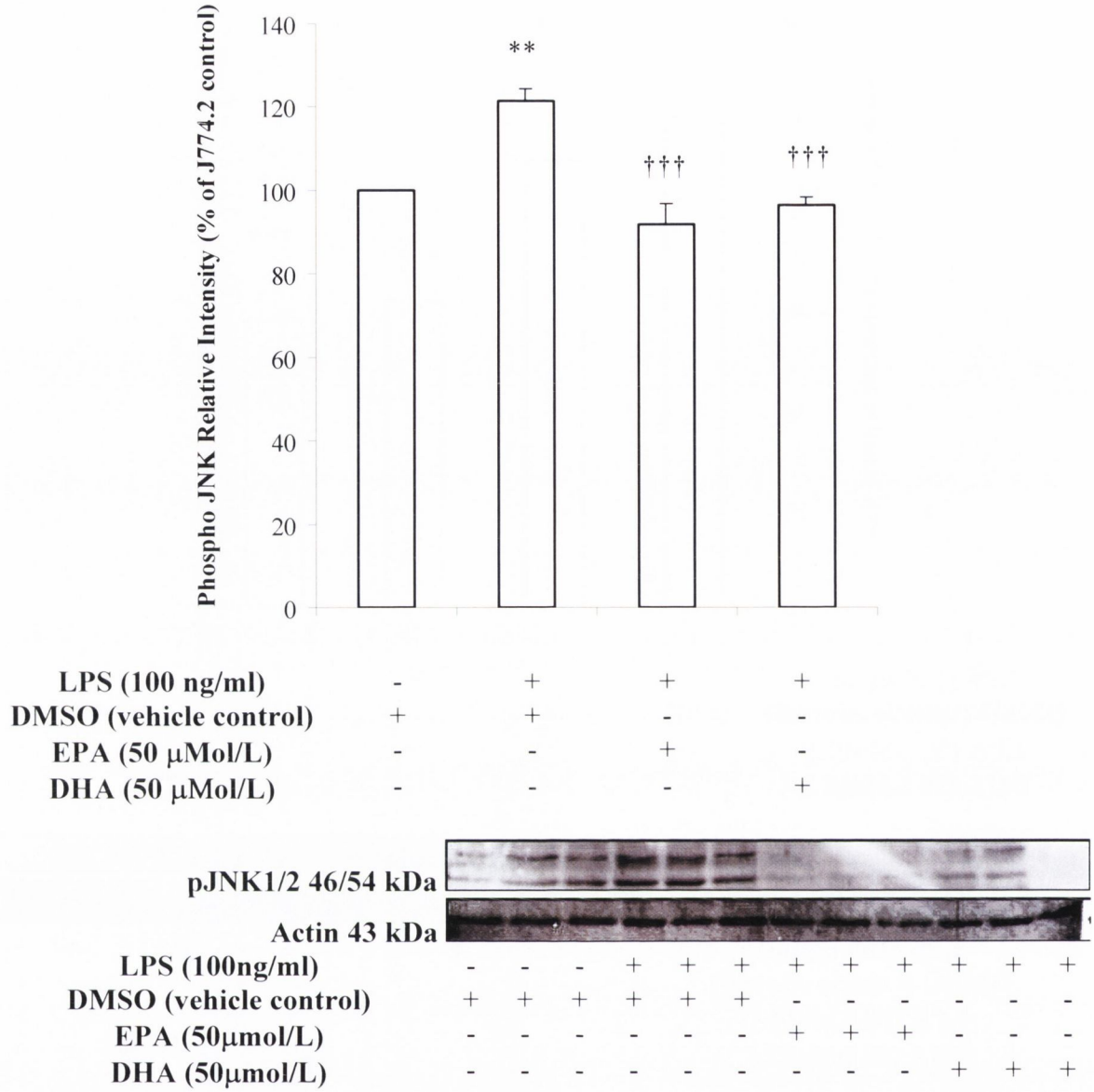

Figure 5.21 Effects of EPA and DHA on phosphorylated JNK1/2 (T183/Y185) protein expression within LPS stimulated J774.2 whole cell extracts. J774.2 macrophages were treated with 50 μMol/L EPA, DHA or DMSO vehicle control for 5 days prior to LPS stimulation (100 ng/ml) for 15 minutes. Whole cell lysates were prepared for SDS-PAGE and immunoblotting. The relative protein levels were quantified by densitometry and data expressed relative to the amount of JNK1/2 within J774.2 macrophages treated with DMSO vehicle control (100%), data is presented as mean ± SEM, n = 3. A representative blot is shown below the graph. ** $P \leq 0.01$ relative to DMSO control. ††† $\leq P$ 0.001 relative to LPS stimulated DMSO control. One-way ANOVA was performed within each group followed by post hoc LSD analysis. Correct loading of protein was confirmed by blotting for actin.

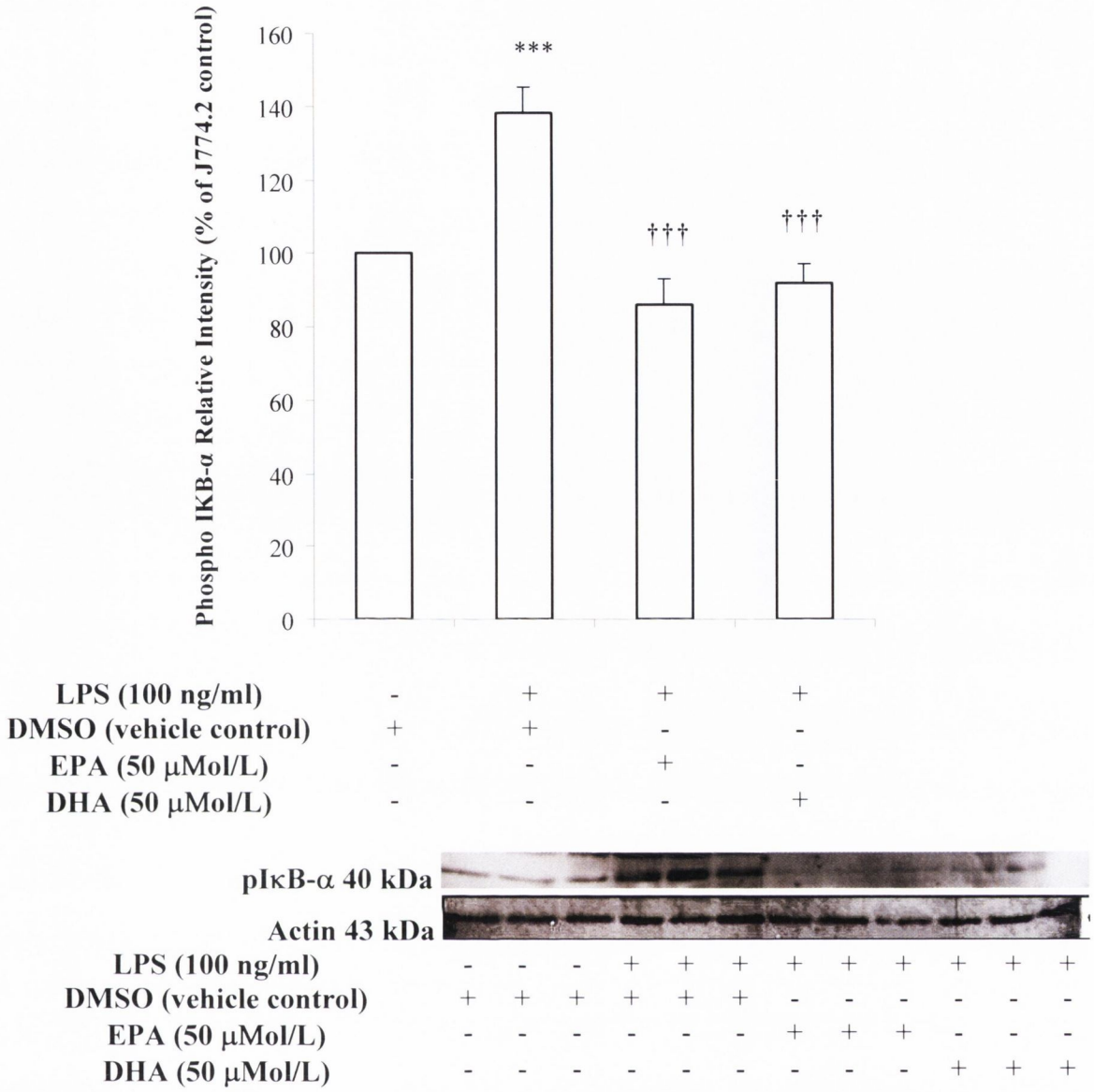

Figure 5.22 Effects of EPA and DHA on phosphorylated IKB-α (Ser32) protein expression within LPS stimulated J774.2 whole cell extracts. J774.2 macrophages were treated with 50 μMol/L EPA, DHA or DMSO vehicle control for 5 days prior to LPS stimulation (100 ng/ml) for 15 minutes. Whole cell lysates were prepared for SDS-PAGE and immunoblotting. The relative protein levels were quantified by densitometry and data expressed relative to the amount of phosphorylated IKB-α within J774.2 macrophages treated with DMSO vehicle control (100%), data is presented as mean ± SEM, n = 3. A representative blot is shown below the graph. *** $P \leq 0.001$ relative to DMSO control. ††† $\leq$ P 0.001 relative to LPS stimulated DMSO control. One-way ANOVA was performed within each group followed by post hoc LSD analysis. Correct loading of protein was confirmed by blotting for actin.

5.3.7 The effects of acute EPA and DHA treatment on cytokine and adipokine secretion within a co-culture of J774.2 macrophages and 3T3-L1 adipocytes

The effects of EPA and DHA treatment were firstly examined in 3T3-L1 adipocytes and J774.2 macrophages. This was followed by a novel co-culture of LPS stimulated and unstimulated J774.2 macrophages acutely pre-treated with EPA, DHA or DMSO vehicle control and 3T3-L1 adipocytes. The co-culture was designed to firstly observe how macrophages might act on adipocytes in an obese state. Secondly the model examined the impact that EPA and DHA treated macrophages have on the adipocytes relative to the non-LC *n-3* PUFA treated macrophages. Furthermore, the contact system and transwell system allow determination of whether macrophages are affecting adipocytes via physical contact or through soluble molecules respectively.

Within the co-culture contact system adiponectin secretion was reduced on average 66% by the presence of both unstimulated and LPS stimulated macrophages compared to adipocytes alone ($P \leq 0.001$ consistently; Figure 5.23a). EPA and DHA treatment induced no significant up-regulation in adiponectin secretion from the contact co-culture system. However, DHA treatment of the LPS stimulated macrophages within the co-culture did induce a moderate increase (40% increase) in adiponectin relative to DMSO control LPS stimulated macrophages co-cultured with the adipocytes, although not significantly. Similarly, within the transwell system the presence of both unstimulated and LPS stimulated macrophages induced a significant decrease (on average 81% decrease) in adiponectin secretion from the co-culture ($P \leq 0.001$; Figure 5.23b). Unexpectedly, within the transwell system EPA and DHA treatment of the unstimulated macrophages significantly reduced adiponectin secretion (91% and 72% decrease) within the co-culture relative to the co-culture of adipocytes and unstimulated macrophages ($P \leq 0.002$, $P \leq 0.028$).

TNF-α secretion was increased 1.6 fold and 3.1 fold within the contact co-culture of adipocytes and unstimulated or LPS stimulated macrophages compared to adipocytes alone ($P \leq 0.073$ and $P \leq 0.001$; Figure 5.24a). TNF-α secretion was increased 88% within the contact co-culture of LPS stimulated macrophages and adipocytes relative to the co-culture of adipocytes and unstimulated macrophages ($P \leq 0.001$). EPA and DHA treatment of both the unstimulated and LPS stimulated macrophages within the contact co-culture had no significant effect on TNF-α secretion. Within the transwell co-culture TNF-α secretion was increased 1.5 and 2.1 fold when adipocytes were co-cultured with unstimulated or LPS stimulated macrophages compared to adipocytes alone ($P \leq 0.010$ and $P \leq 0.001$; Figure 5.24b). TNF-α secretion was increased 34% within the co-culture of

adipocytes and LPS stimulated macrophages relative to the co-culture of adipocytes with unstimulated macrophages ($P \leq 0.022$). Importantly, EPA and DHA treatment of the unstimulated and LPS stimulated macrophages significantly reduced TNF-α secretion from the transwell co-culture (69%, 48%, 77% and 53% decrease respectively) relative to corresponding DMSO treated control groups ($P \leq 0.001$, $P \leq 0.001$, $P \leq 0.001$ and $P \leq 0.001$ correspondingly).

IL-6 secretion was increased 4.5 fold and 10.7 fold within the contact co-culture of adipocytes and unstimulated or LPS stimulated macrophages compared to adipocytes alone ($P \leq 0.001$ and $P \leq 0.001$; Figure 5.25a). EPA and DHA treatment of the unstimulated and LPS stimulated macrophages significantly reduced IL-6 secretion from the contact co-culture (31%, 10%, 51% and 14% decrease respectively) relative to corresponding DMSO treated control groups ($P \leq 0.005$, $P \leq 0.001$, $P \leq 0.027$ and $P \leq 0.003$ correspondingly). Similarly, IL-1β secretion was increased 3.7 fold and 4.5 fold within the contact co-culture of adipocytes and unstimulated or LPS stimulated macrophages compared to adipocytes alone ($P \leq 0.001$ and $P \leq 0.001$; Figure 5.25b). Furthermore, EPA and DHA treatment of the unstimulated and LPS stimulated macrophages significantly reduced IL-1β secretion from the contact co-culture (67%, 83%, 73% and 29% decrease respectively) relative to corresponding DMSO treated control groups ($P \leq 0.001$, $P \leq 0.001$, $P \leq 0.001$ and $P \leq 0.027$ respectively).

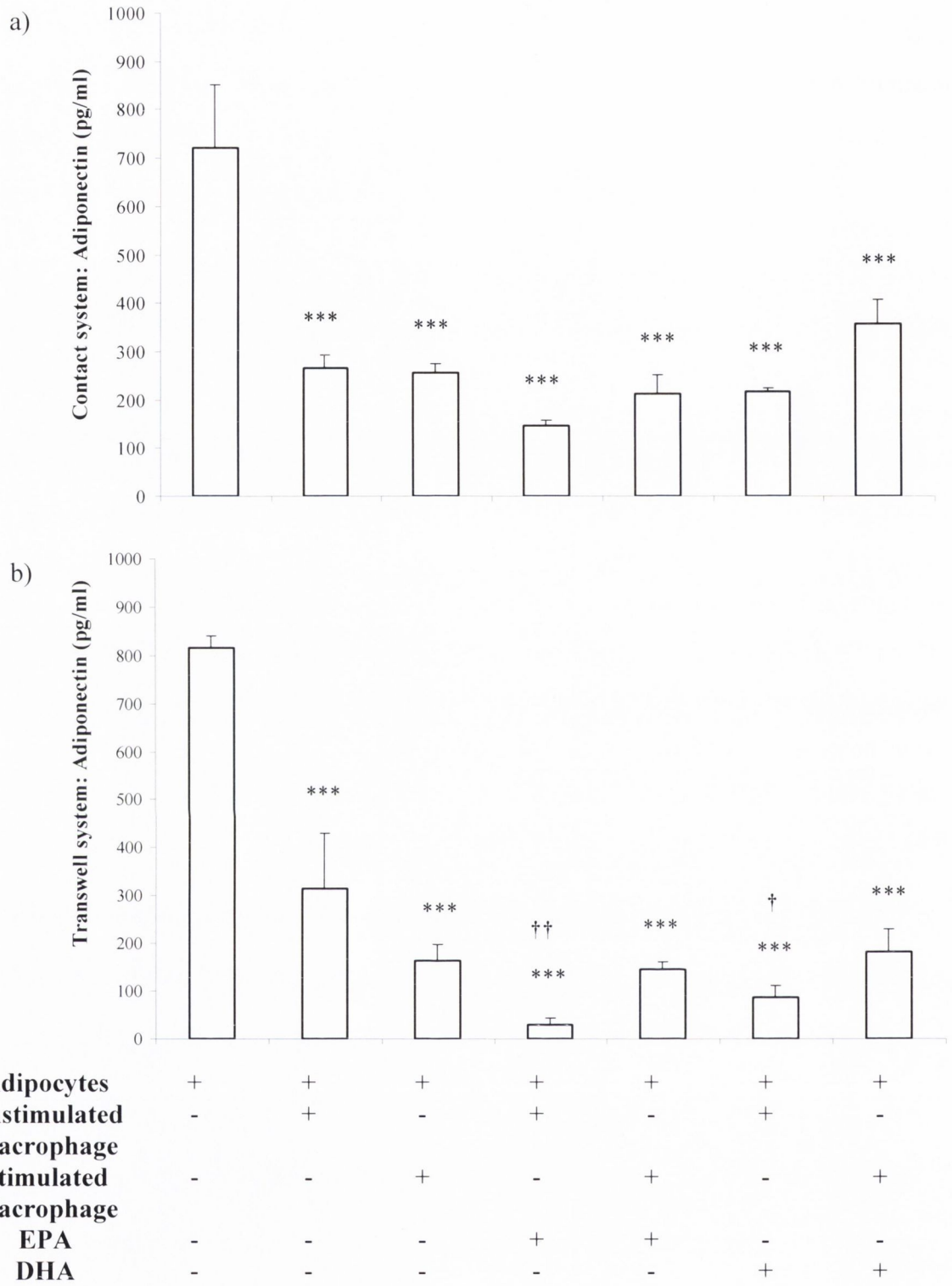

Figure 5.23 Effects of acute EPA and DHA treatment on adiponectin secretion within a co-culture of J774.2 macrophages and 3T3-L1 adipocytes. J774.2 macrophages ± LPS (100 ng/ml) for 48 hours were treated with 50 μMol/L EPA, DHA or vehicle control in DMEM for 24 hours. Fully differentiated 3T3-L1 adipocytes were co-cultured with the J774.2 macrophages for a further 24 hours, supernatants were harvested and adiponectin secretion determined by ELISA (pg/ml) in either a contact (a) or transwell (b) system. Data is presented as mean ± SEM, n = 3. *** $P \leq 0.001$ relative to adipocytes; † $P \leq 0.05$, †† $P \leq 0.01$ relative to adipocytes co-cultured with unstimulated macrophages. One-way ANOVA was performed within each group followed by post hoc LSD analysis.

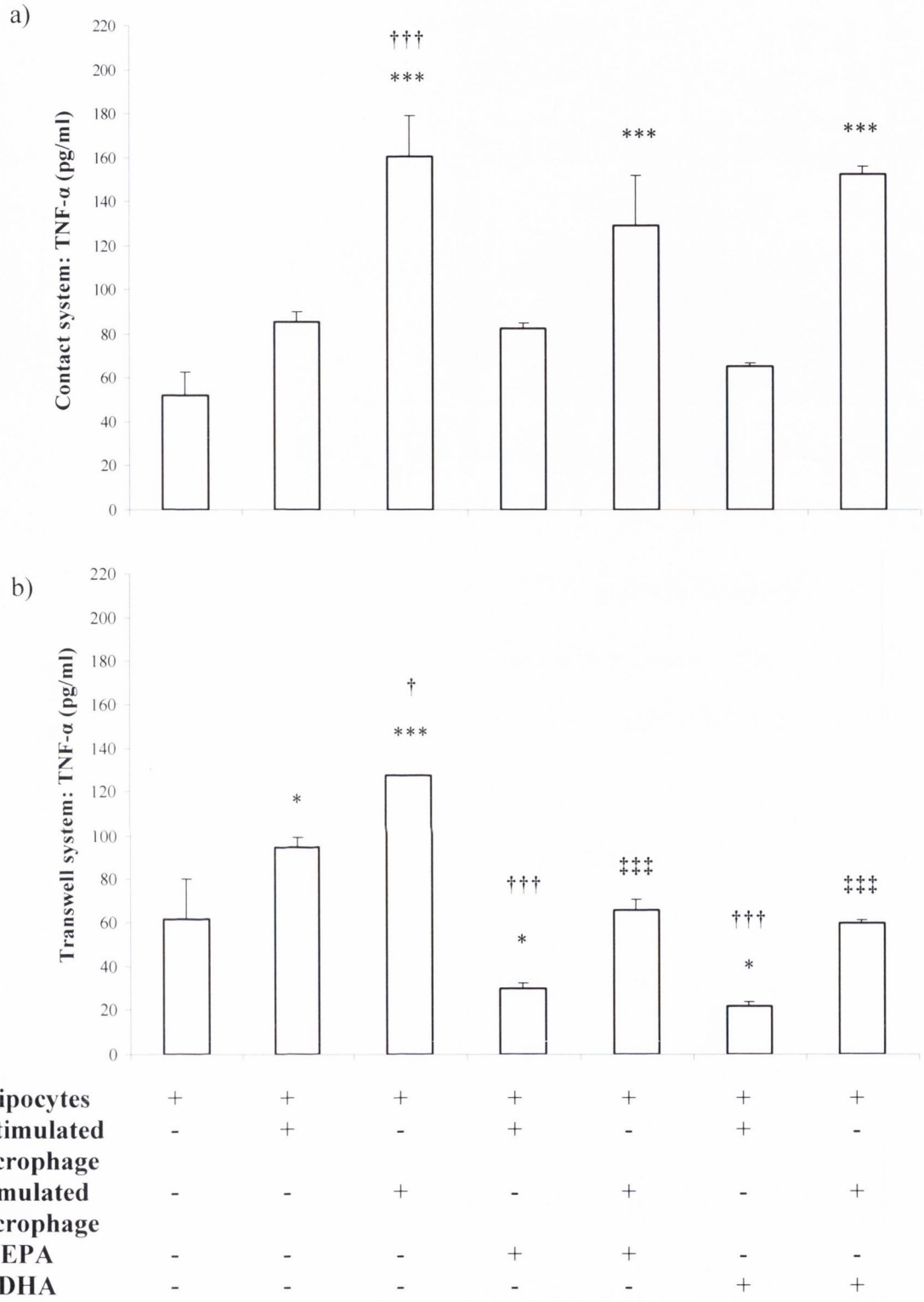

Figure 5.24 Effects of acute EPA and DHA treatment on TNF-α secretion within a co-culture of J774.2 macrophages and 3T3-L1 adipocytes. J774.2 macrophages ± LPS (100 ng/ml) for 48 hours were treated with 50 μMol/L EPA, DHA or vehicle control in DMEM for 24 hours. Fully differentiated 3T3-L1 adipocytes were co-cultured with the J774.2 macrophages for a further 24 hours, supernatants were harvested and TNF-α secretion determined by ELISA (pg/ml) in either a contact (a) or transwell (b) system. Data is presented as mean ± SEM, n = 3. * $P \leq 0.05$, *** $P \leq 0.001$ relative to adipocytes; † $P \leq 0.05$, ††† $P \leq 0.001$ relative to adipocytes co-cultured with unstimulated macrophages; ‡‡‡ $P \leq 0.001$ relative to adipocytes co-cultured with LPS stimulated macrophages. One-way ANOVA was performed within each group followed by post hoc LSD analysis.

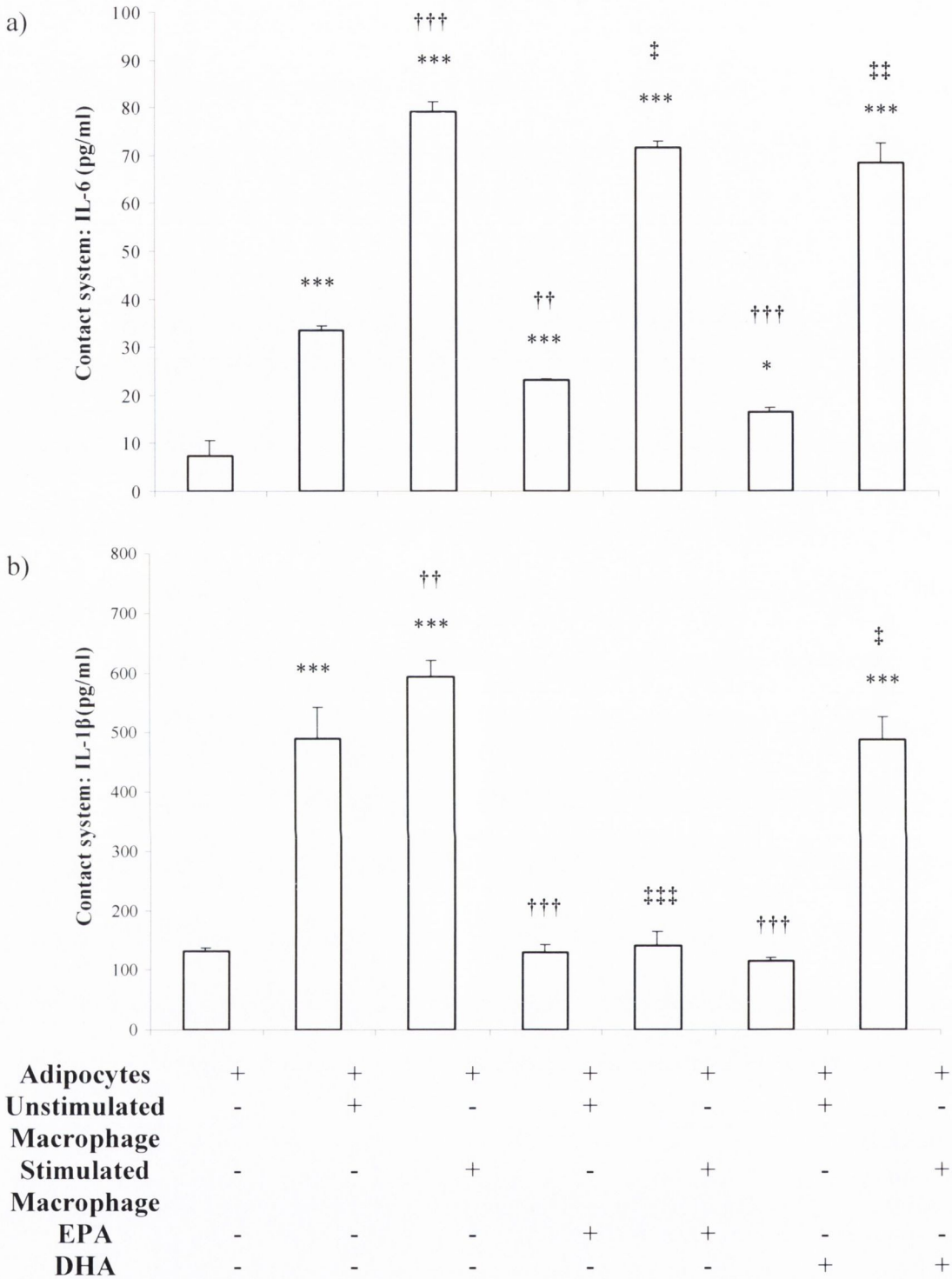

Figure 5.25 Effects of acute EPA and DHA treatment on IL-6 and IL-1β secretion within a co-culture of J774.2 macrophages and 3T3-L1 adipocytes. J774.2 macrophages ± LPS (100 ng/ml) for 48 hours were treated with 50 μMol/L EPA, DHA or vehicle control in DMEM for 24 hours. Fully differentiated 3T3-L1 adipocytes were co-cultured with the J774.2 macrophages for a further 24 hours, supernatants were harvested, IL-6 (a) and IL-1β (b) secretion was determined by ELISA (pg/ml) in a contact system. Data is presented as mean ± SEM, n = 3. * $P \leq 0.05$, *** $P \leq 0.001$ relative to adipocytes; †† $P \leq 0.01$, ††† $P \leq 0.001$ relative to adipocytes co-cultured with unstimulated macrophages; ‡ $P \leq 0.05$, ‡‡ $P \leq 0.01$, ‡‡‡ $P \leq 0.001$, relative to adipocytes co-cultured with LPS stimulated macrophages. One-way ANOVA was performed within each group followed by post hoc LSD analysis.

5.3.8 The effects of acute EPA and DHA treatment on inflammatory and insulin sensitive target gene expression within a co-culture of J774.2 macrophages and 3T3-L1 adipocytes

Within the co-culture contact and transwell system GLUT4 mRNA expression was reduced approximately 80% when adipocytes were incubated with unstimulated and LPS stimulated macrophages compared to adipocytes alone ($P \leq 0.001$ consistently; Figure 2.26a and b respectively). GLUT4 gene expression was significantly increased within the contact co-culture of adipocytes and DHA treated unstimulated macrophages relative to the co-culture of adipocytes and unstimulated macrophages ($P \leq 0.036$). Importantly, GLUT4 mRNA expression was increased 2.1 fold and 1.9 fold in adipocytes co-cultured with LPS stimulated macrophages pre-treated with EPA and DHA relative to corresponding controls ($P \leq 0.059$ and $P \leq 0.091$ respectively).

Similarly, within the contact and transwell system IRS-1 mRNA expression was significantly reduced (~80% decrease) by unstimulated and LPS stimulated macrophages compared to the adipocytes ($P \leq 0.001$ consistently; Figure 5.27a and b). Within the transwell system IRS-1 gene expression levels were increased 32% in adipocytes co-cultured with LPS stimulated macrophages treated with EPA compared to LPS stimulated DMSO treated macrophages co-cultured with adipocytes ($P \leq 0.066$).

Within the co-culture contact and transwell system TNF-α mRNA expression was not significantly regulated by the presence of unstimulated or LPS stimulated J774.2 macrophages (Figure 5.28a and b). However, there is a clear trend, with increased TNF-α mRNA expression observed when adipocytes are co-cultured with the macrophages, with these levels reduced when the macrophages are treated with EPA and DHA. It is of note that the levels of TNF-α mRNA expressed are approximately 10 fold lower within the transwell system in which adipocytes alone were analysed compared to the contact system in which both macrophages and adipocytes were analysed, an effect not observed for IL-6 mRNA expression. IL-6 mRNA expression within the contact and transwell system showed a similar trend to the TNF-α expression. However, within the contact system IL-6 mRNA expression was significantly increased 83% relative to adipocytes alone ($P \leq 0.038$; Figure 5.29a and b). Furthermore, IL-6 gene expression was significantly reduced 59% and 48% when adipocytes and LPS stimulated macrophages treated with EPA and DHA were co-cultured in a contact system ($P \leq 0.002$ and $P \leq 0.005$).

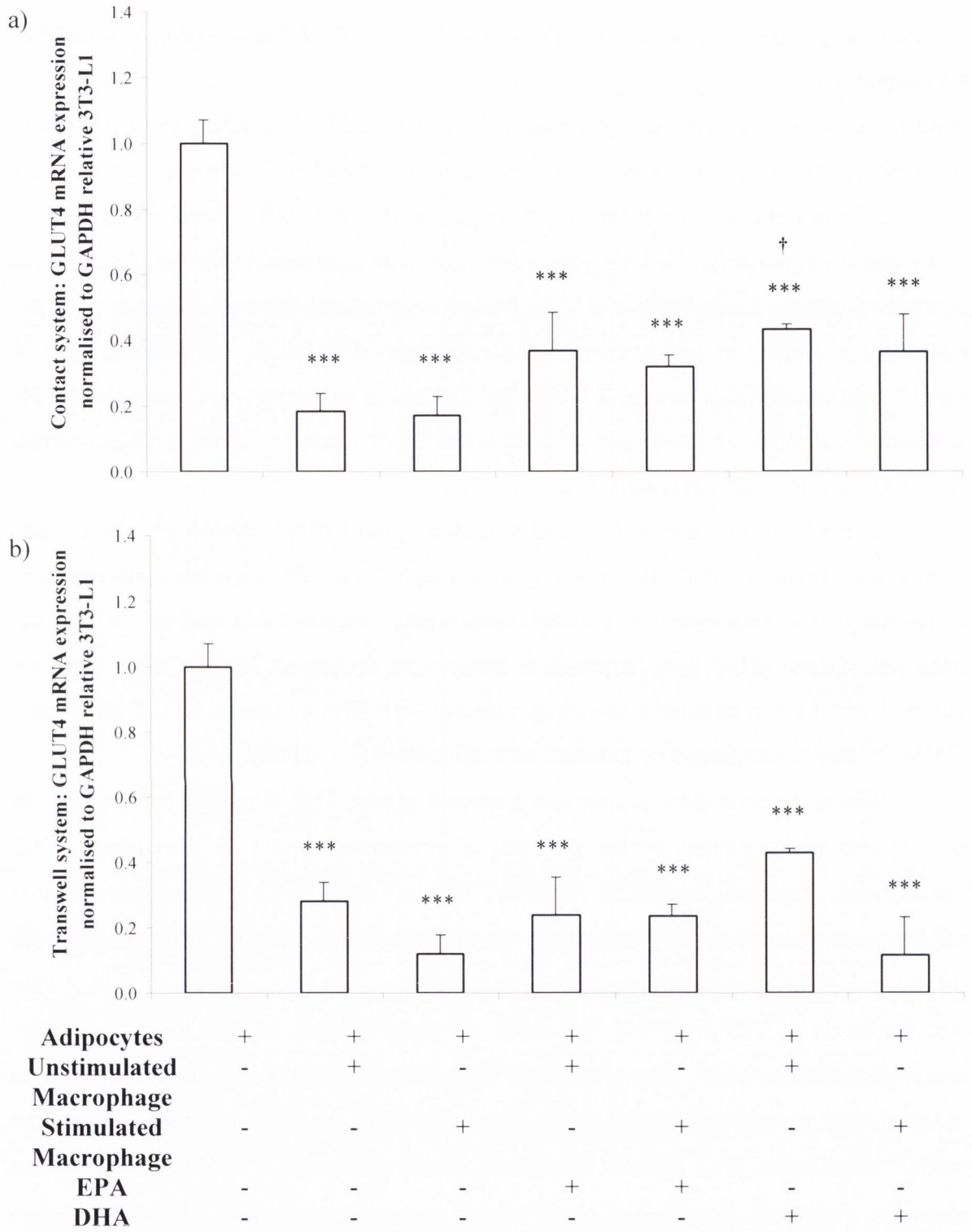

Figure 5.26 Effects of acute EPA and DHA treatment on GLUT4 gene expression within a co-culture of J774.2 macrophages and 3T3-L1 adipocytes. J774.2 macrophages ± LPS (100 ng/ml) for 48 hours were treated with 50 μMol/L EPA, DHA or vehicle control in DMEM for 24 hours. Fully differentiated 3T3-L1 adipocytes were co-cultured with the J774.2 macrophages for a further 24 hours, GLUT4 mRNA was determined by Taqman RT-PCR in either a contact (a) or transwell (b) system. mRNA levels were normalized to GAPDH and the results are expressed as fold induction relative to adipocytes. Data is presented as mean ± SEM, n = 2 - 3. *** $P \leq 0.001$ relative to adipocytes; † $P \leq 0.05$ relative to adipocytes co-cultured with unstimulated macrophages. One-way ANOVA was performed within each group followed by post hoc LSD analysis.

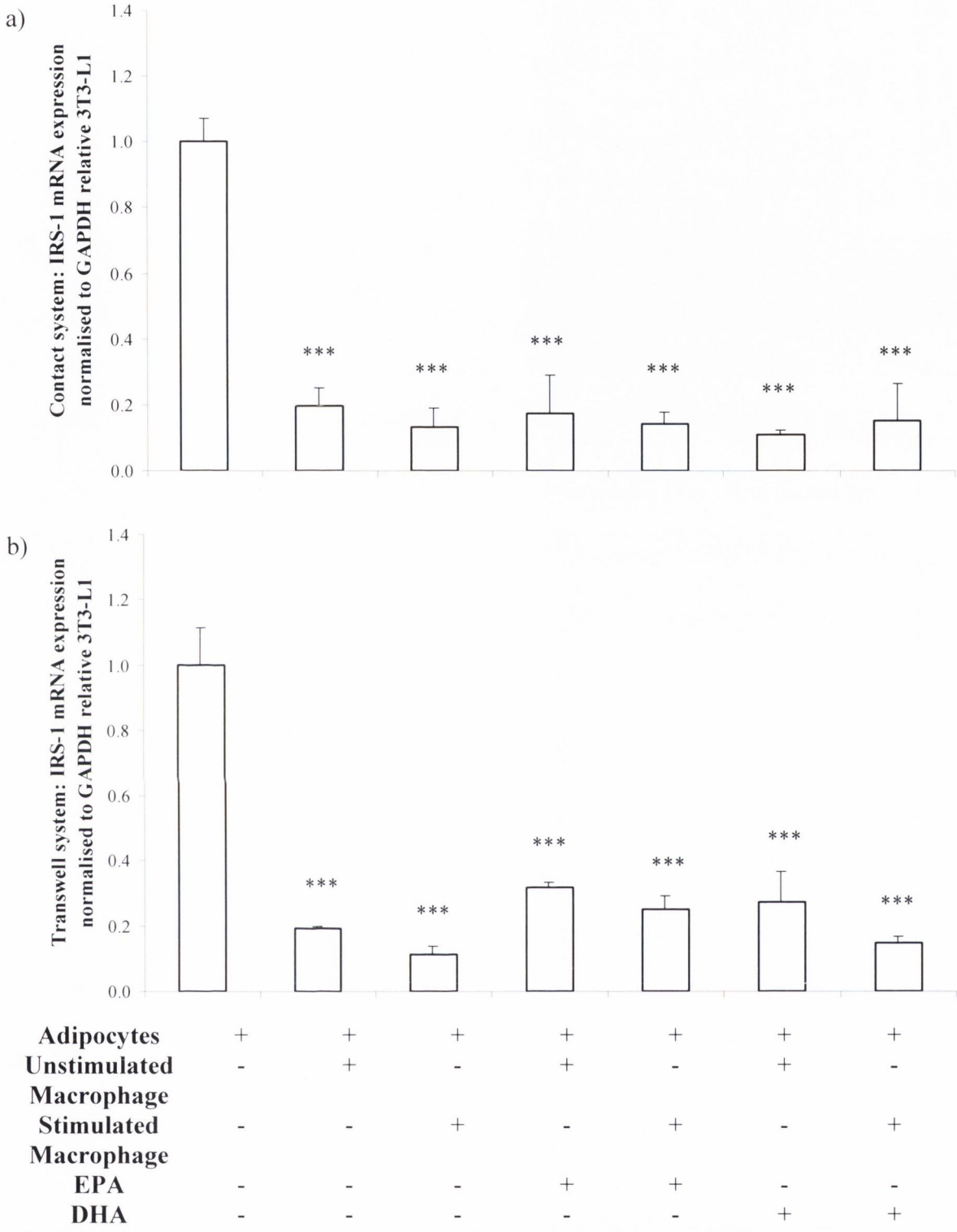

Figure 5.27 Effects of acute EPA and DHA treatment on IRS-1 gene expression within a co-culture of J774.2 macrophages and 3T3-L1 adipocytes. J774.2 macrophages ± LPS (100 ng/ml) for 48 hours were treated with 50 μMol/L EPA, DHA or vehicle control in DMEM for 24 hours. Fully differentiated 3T3-L1 adipocytes were co-cultured with the J774.2 macrophages for a further 24 hours, IRS-1 mRNA was determined by Taqman RT-PCR in either a contact (a) or transwell (b) system. mRNA levels were normalized to GAPDH and the results are expressed as fold induction relative to adipocytes. Data is presented as mean ± SEM, n = 2 - 3. *** $P \leq 0.001$ relative to adipocytes. One-way ANOVA was performed within each group followed by post hoc LSD analysis.

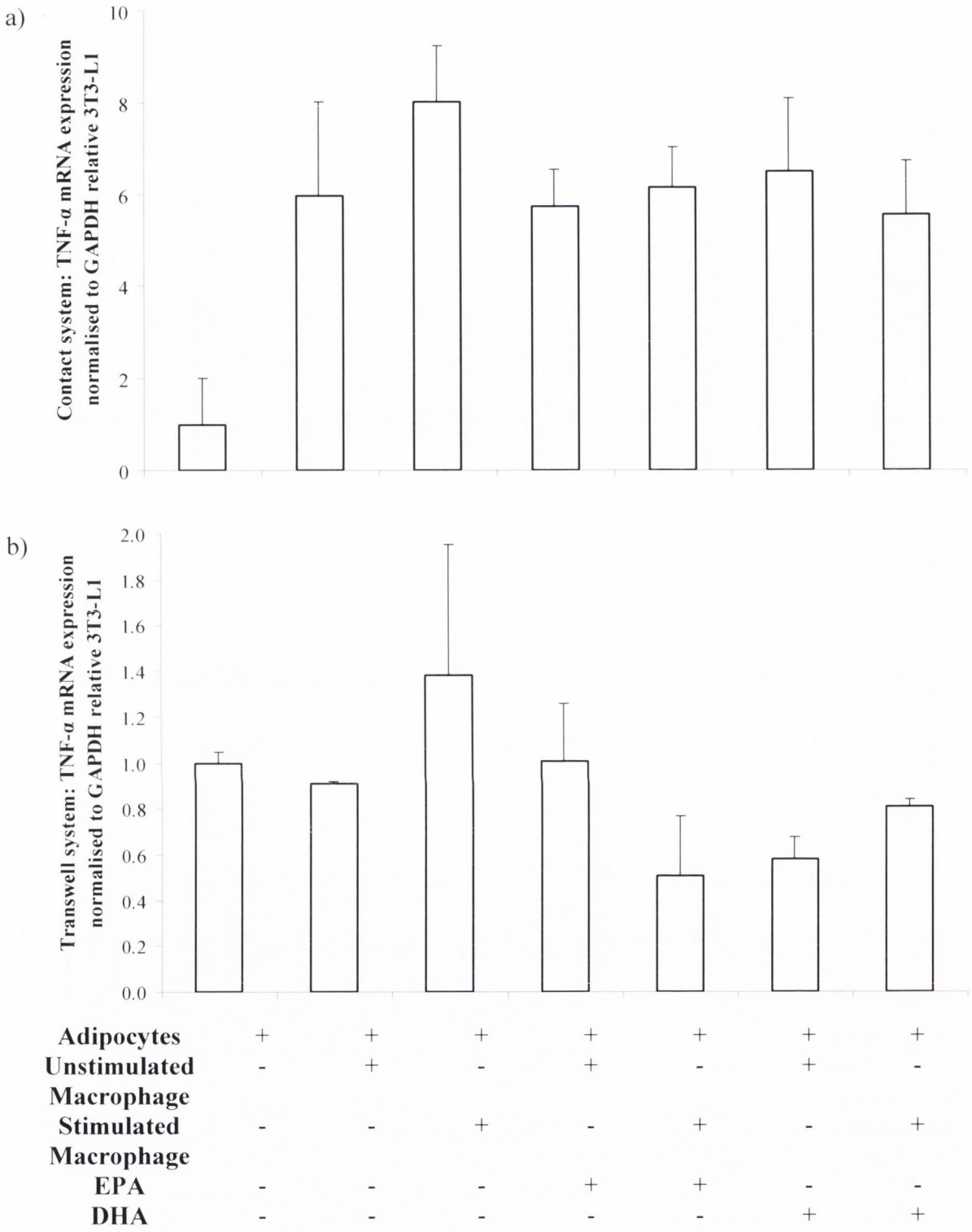

Figure 5.28 Effects of acute EPA and DHA treatment on TNF-α gene expression within a co-culture of J774.2 macrophages and 3T3-L1 adipocytes. J774.2 macrophages ± LPS (100 g/ml) for 48 hours were treated with 50 μMol/L EPA, DHA or vehicle control in DMEM for 24 hours. Fully differentiated 3T3-L1 adipocytes were co-cultured with the J774.2 macrophages for a further 24 hours, TNF-α mRNA was determined by Taqman RT-PCR in either a contact (a) or transwell (b) system. mRNA levels were normalized to GAPDH and the results are expressed as fold induction relative to adipocytes. Data is presented as mean ± SEM, n = 2 - 3.

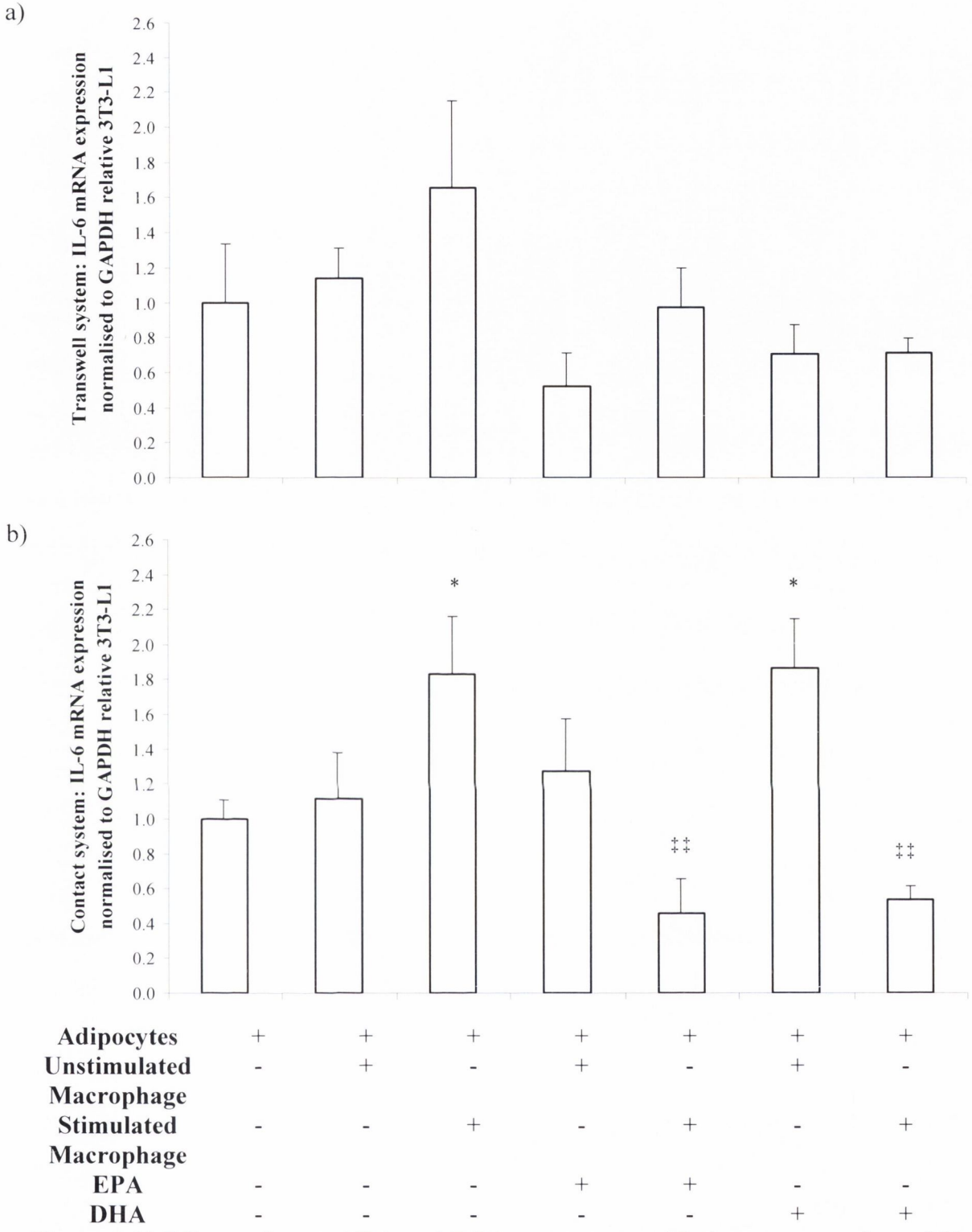

Figure 5.29 Effects of acute EPA and DHA treatment on IL-6 gene expression within a co-culture of J774.2 macrophages and 3T3-L1 adipocytes. J774.2 macrophages ± LPS (100ng/ml) for 48 hours were treated with 50μmol/L EPA, DHA or vehicle control in DMEM for 24 hours. Fully differentiated 3T3-L1 adipocytes were co-cultured with the J774.2 macrophages for a further 24 hours, IL-6 mRNA was determined by Taqman RT-PCR in either a contact (a) or transwell (b) system. mRNA levels were normalized to GAPDH and the results are expressed as fold induction relative to adipocytes. Data is presented as mean ± SEM, n = 2 - 3. * $P \leq 0.05$ relative to adipocytes; ‡‡ $P \leq 0.01$ relative to adipocytes co-cultured with LPS stimulated macrophages. One-way ANOVA was performed within each group followed by post hoc LSD analysis.

5.4 Discussion

This chapter aimed to firstly define the effects of LC *n-3* PUFA EPA and DHA on 3T3-L1 adipocytes and LPS stimulated J774.2 macrophages *in vitro*. This was followed by a novel co-culture of both J774.2 macrophages and 3T3-L1 adipocytes. In this model LPS stimulated and unstimulated J774.2 macrophages acutely pre-treated with EPA, DHA or DMSO vehicle control were co-culture with 3T3-L1 adipocytes. This model using two cell types in a co-culture mimics the condition observed in obesity induced insulin resistance. It allows the simplification of an extremely complex human state and gives a starting point to understanding some of the mechanisms occurring. Chapter 6 will examine this co-culture model in more detail. Fundamentally, EPA and DHA treatment *in vitro* appear to play a key anti-inflammatory role within LPS stimulated J774.2 macrophages. The effects of EPA and DHA treatment on 3T3-L1 adipocytes were more variable. Importantly, initial co-culture data indicates that macrophages significantly increase inflammatory target expression and reduce insulin sensitive target expression within the adipocytes of the co-culture and that these effects are attenuated by EPA and DHA pre-treatment of the macrophages prior to co-culture. The rationale for choosing the concnentrations of EPA and DHA were based on previous work conducted in our group and on current literature (Martins de Lima *et al.*, 2006). The doses used in this study are non-toxic and perhaps represent a long-term, high dose supplementation of fish oils. However, it would be important to evaluate if the EPA and DHA concentrations used in this study are achievable in human and mice fed diets high in fish oil. The lipid profiles of peripheral blood mononuclear cells (PBMC), adipose tissue macrophages (ATM) and adipocytes of humans and mice fed high levels of fish oils for long periods could be established using gas chromatography (GC).

Adipokine and cytokine expression was determined within 3T3-L1 adipocytes treated with EPA and DHA. Interestingly, EPA treatment increased secretion of leptin from 3T3-L1 adipocytes while DHA treatment moderately reduced leptin secretion. Leptin is secreted from adipose tissue, and is thought to act as a 'lipostat', signalling the body fat levels to the hypothalamus, resulting in adjustments to food intake and energy expenditure to maintain body weight homeostasis (Walder *et al.*, 1997). Administration of leptin by injection or as a constant subcutaneous infusion results in a dose-dependent decrease in body weight (Halaas *et al.*, 1997; Halaas *et al.*, 1995). In both *ob/ob* and wild-type mice, leptin was observed to induced weight loss, which was restricted to the adipose tissue (Halaas *et al.*, 1997; Halaas *et al.*, 1995). However, leptin concentrations are greatly elevated in obese subjects (Friedman and Halaas, 1998). A state of leptin resistance

develops rapidly in obese individuals, leptin becomes ineffective and leptin therapy even at high concentrations is largely ineffective in reducing the body weight of clinically obese patients (Heymsfield *et al.*, 1999). Additionally, Walder *et al.* (1997) observed that leptin reduced insulin binding to its receptor in a dose-dependent manner within adipocytes isolated from Sprague-Dawley rats (Walder *et al.*, 1997). Walder *et al.* determined that 50nMol of leptin was necessary to induce a significant decrease in insulin binding while 1nMol of leptin did not significantly reduce insulin binding. In our study leptin levels were approximately 0.008 nMol (~120 pg/ml) in EPA treated adipocytes, which is unlikely to induce a reduction in insulin binding. EPA may help to modulate body weight homeostasis through its induction of leptin in individuals gaining weight by reducing food intake, increasing energy expenditure and perhaps reducing insulin sensitivity within the adipocytes, preventing further growth of adipocytes and re-directing fatty substrates to other tissues. EPA and DHA treatment increased adiponectin secretion from 3T3-L1 adipocytes. Hu *et al.* (1996) determined that adiponectin is expressed exclusively in adipose tissue and that mRNA expression of adiponectin was reduced in an obese diabetic model, *db/db* mice (Hu *et al.*, 1996). Plasma levels of adiponectin have also been reported to be significantly reduced in obese and diabetic mice/humans (Arita *et al.*, 1999; Hu *et al.*, 1996; Yamauchi *et al.*, 2001). A recent study by Banga *et al.* (2009) observed that overnight treatment of rat adipocytes with pioglitazone, a PPAR-γ ligand, DHA or EPA triggered a two fold increase in the synthesis and secretion of high-molecular weight (HMW) adiponectin, and this increase was blocked by the addition of PPAR-γ inhibitor GW-9662 (Banga *et al.*, 2009). This indicates that EPA, DHA and their metabolites are not only PPAR-γ ligand, but that PPAR-γ activation is linked to adiponectin expression and perhaps the increased leptin expression observed in 3T3-L1 adipocytes. Furthermore, adiponectin and leptin expression was found to be up-regulated in heterozygous PPAR-γ knockout mice (Kubota *et al.*, 1999). Adiponectin has many functions within a range of organs and cell types. It induces fatty acid transport within skeletal muscle, reducing TAG content and improving insulin induced glucose uptake (Yamauchi *et al.*, 2001). Additionally, adiponectin has been shown to strongly inhibit expression of adhesion molecules and TNF-α induced NF-κB activation through inhibition of IκB-α phosphorylation (Ouchi *et al.*, 2000). Adiponectin has also been shown to regulate ERK and AMPK within muscle and endothelial cells (Arita *et al.*, 2002; Kobayashi *et al.*, 2004). EPA and DHA treatment did not significantly affect cytokine secretion from the adipocytes, which may suggest an inflammatory stimulus is required to firstly induce

inflammation before the anti-inflammatory action of LC *n-3* PUFA in adipocytes can be observed.

Gene and protein expression was also determined within the EPA and DHA treated adipocytes. Gene expression levels of the adipokines such as resistin and adiponectin within EPA and DHA treated adipocytes showed a similar trend to the secretion profiles suggesting direct gene regulation of these proteins. TNF-α gene expression was very low (ct ~36) within the 3T3-L1 adipocytes, correlating with their unstimulated state however levels of TNF-α mRNA were approximately double in adipocytes treated with DHA relative to DMSO treated adipocytes which may correlate with the subtle induction of TNF-α secretion observed in the DHA treated adipocytes. Interestingly, EPA and DHA treatment significantly reduced IL-Ra mRNA expression. IL-1Ra inhibits IL-1 agonist binding to the IL-1 receptor therefore inhibiting IL-1 signaling. Therefore, the reduction in IL-1Ra may indicate an increase in IL-1 activity due to a decrease in the receptor antagonist however, IL-1β mRNA (undetectable), IL-1RI mRNA and IL-1β secretion were not significantly up-regulated in adipocytes treated with EPA and DHA suggesting IL-1 activity is not regulated by EPA and DHA. Interestingly, DHA treatment also reduced whole cell IκB-α protein expression within adipocytes perhaps indicating an increase in NF-κB activity due to a lack of IκB-α to sequester the NF-κB within the cytoplasm. However, there was a subtle reduction in whole cell NF-κB protein expression, which could indicate a general reduction in the NF-κB pathway signaling. More work is needed to examine both cytoplasmic and nuclear levels of NF-κB to define NF-κB activity. It was also observed that ERK1 protein expression was reduced in DHA treated adipocytes. Interestingly, in a study conducted by Engelman *et al.* (2001) it was demonstrated that within 3T3-L1 adipocytes specific inhibitors of the ERK pathway restore insulin signalling to normal levels despite the presence of TNF-α. Additional experiments also observed that ERK activity is required for TNF-α-induced IRS-1 serine phosphorylation, thereby suggesting a mechanism by which these inhibitors restore insulin signaling (Engelman *et al.*, 2000). DHA may act to reduce ERK perhaps reducing its activity therefore improving insulin sensitivity, moreover this protection may be more apparent within inflamed adipocytes.

Insulin signalling target gene and protein levels were also determined within the 3T3-L1 adipocytes. Interestingly, at both the mRNA and protein expression level GLUT4 was significantly reduced in 3T3-L1 adipocytes treated with DHA. This may indicate that DHA can reduce insulin sensitivity in adipocytes. Furthermore, the effects of EPA and

DHA on differentiation and insulin sensitivity were assessed within 3T3-L1 adipocytes using a glucose uptake assay. Total glucose uptake was significantly reduced in DHA treated adipocytes while EPA had no effect relative to the DMSO treated controls. Interestingly, basal or non-insulin induced glucose uptake was significantly reduced to a similar degree by both EPA and DHA treatment of the adipocytes. Experiments performed within our group examining both non-insulin induced and insulin induced glucose uptake suggest that inflammatory stimulus such as LPS, TNF-α and IL-1β can increase non-insulin induced glucose uptake through GLUT1 signalling. Therefore, EPA and DHA may have subtly reduced inflammation and reduced basal non-insulin induced glucose uptake as a result. Importantly, there was a moderate increase in insulin induced glucose uptake within EPA treated adipocytes suggesting EPA enhances differentiation and insulin sensitivity of the adipocytes, this may also correlate with the increased secretion of leptin. Conversely, DHA moderately reduced insulin induced glucose uptake, although not significantly suggesting DHA inhibits differentiation. The reduction in glucose uptake observed within the DHA treated adipocytes may correlate with the reduction in GLUT4 mRNA and protein expression induced by DHA treatment in mature adipocytes. Furthermore, the microscope images suggest that while DMSO and EPA have no observable effect on lipid accumulation and adipocyte differentiation, DHA treatment appeared to reduce lipid droplet accumulation. DHA treatment during differentiation appeared to reduce differentiation as suggested by the elongated and fibroblast-like shape of the adipocytes. This de-differentiation may account for the subtle reduction in glucose uptake and the reduction in GLUT4. DHA may therefore induce anti-obesity effects and prevent further growth of adipocytes by inhibiting differentiation of pre-adipocytes to mature adipocytes, inducing lipolysis and reducing glucose uptake through the down regulation of GLUT4. DHA may also reduce the harmful effects of pro-inflammatory cytokines such as TNF-α on adipocyte insulin sensitivity through reduction of ERK1 signalling. However, further experiments are required to examine if EPA and DHA treatment can attenuate the pro-inflammatory state and improve insulin sensitivity associated with adipocytes treated with a pro-inflammatory stimulus such as IL-1β (as observed in chapter 4).

The effects of LC *n-3* PUFA on cytokine secretion and protein expression were defined within LPS stimulated J774.2 macrophages. LPS is a potent activator of monocytes and macrophages and activates TLR4 signalling in macrophages by binding to CD14 (a co-receptor of TLR4) in the presence of LPS-binding protein (Kielian and Blecha, 1995). Within minutes of LPS stimulation, numerous proteins become tyrosine phosphorylated

and activated, in particular ERK1/2, p38 and JNK (Hambleton *et al.*, 1996; Han *et al.*, 1994; Han *et al.*, 1993; Weinstein *et al.*, 1992). The ligation of TLRs also activates NF-κB signaling pathways (Medzhitov, 2001). Furthermore, LPS triggers the abundant secretion of many cytokines from macrophages including IL-1α/β (Dinarello, 1996), IL-6 (Akira *et al.*, 1993) and TNF-α (Tracey and Cerami, 1994). Our group has examined the effect of EPA and DHA within THP-1 macrophages, a human cell line. LC *n-3* PUFA were shown to decrease pro-inflammatory cytokine production while NF-κB activity was significantly reduced in EPA and DHA treated macrophages activated with LPS. In general EPA and DHA were shown to reduce the expression of pro-inflammatory cytokines from the LPS stimulated J774.2 macrophages. Interestingly, EPA treatment was found to down regulate IL-6 cytokine secretion from LPS stimulated J774.2 macrophages after 24 hours, which may be due to eicosanoid production and transcriptional regulation. However, both EPA and DHA significantly reduced IL-6 secretion after 48 hours, with DHA inducing a greater reduction perhaps representing the importance of resolvin D1 and protectin D1, which both regulate macrophage function and cytokine/chemokine regulation. Interestingly, Duffield and colleagues (2006) identified that resolvin D1 and protectin D1 can block TLR-mediated activation of macrophages (Duffield *et al.*, 2006). Additionally, Schwab *et al.* (2007) observed that protectin D1 like resolvin E1 can regulate the release of chemokines and cytokines during phagocytosis, reducing IFN-γ and IL-6 (Schwab *et al.*, 2007). Basal levels of TNF-α secreted by the J774.2 macrophages were higher than IL-6 (~125 pg/ml) and IL-1β (~10 pg/ml) at approximately 40 ng/ml secreted within a 24 hour time period. TNF-α secretion increased 10 fold in LPS stimulated macrophages after 24 hours. EPA and DHA treatment of the LPS stimulated macrophages did not induce a decrease in TNF-α secretion at 24 hours. However, after 48 hours the LPS stimulated macrophages treated with EPA showed a significant decline in TNF-α secretion, although levels of TNF-α in LPS stimulated macrophages were normal compared to the unstimulated macrophages. A time course experiment between 24 and 48 hours may be necessary to determine how TNF-α levels reduce in EPA and DHA pre-treated LPS stimulated macrophages. Interestingly, IL-1β levels were significantly reduced by EPA and DHA pre-treatment of the LPS stimulated macrophages after 24 and 48 hours relative to untreated LPS stimulated macrophages. DHA had a more potent effect on reducing IL-1β secretion within the LPS stimulated macrophages. Furthermore, IL-10 secretion was induced within LPS stimulated control macrophages (~8 pg/ml) after 48 hours and although low, these levels were more than doubled in DHA pre-treated LPS stimulated macrophages (~18 pg/ml). It would be

interesting to examine the production of IL-10 and perhaps other anti-inflammatory cytokines such as IL-4 over 48 hours.

At 15 minutes LPS secreted protein expression was analyzed within the macrophages. Total p38 MAPK and threonine/tyrosine phosphorylated p38, the active form of p38, were significantly up-regulated in LPS stimulated J774.2 macrophages relative to untreated controls. EPA and DHA pre-treatment of the LPS stimulated macrophages significantly reduced these levels with EPA more effective at reducing these levels. A recent study addressed the role of p38 within macrophages with the use of a p38α knockout macrophage (Kang *et al.*, 2008). Interestingly, p38α deficiency within macrophages causes a significant inhibition in the production of LPS-induced TNF-α but it had little or no effect on IL-6 production. They observed that p38α deficiency did not affect LPS-induced activation of the other major signalling pathways such as NF-κB, JNK and ERK with in macrophages. It had little inhibitory effect on LPS-induced AP-1 activity, but it significantly inhibited LPS-induced C/EBP-β and CREB activation, indicating that the role of p38α in cytokine production in macrophages is partially regulated by C/EBP-β and CREB activation (Kang *et al.*, 2008). It is therefore possible that the reduction in whole cell p38 and phosphorylated p38 induced predominately by EPA may be responsible for the reduction in TNF-α secretion observed in the LPS stimulated macrophages within this study.

Whole cell JNK1 was not up-regulated in LPS stimulated macrophages relative to the unstimulated control macrophages. However, whole cell JNK levels were significantly reduced in LPS stimulated macrophages pre-treated with EPA and DHA relative to LPS stimulated control macrophages. Interestingly, activated threonine/tyrosine phosphorylated JNK expression was significantly induced in LPS stimulated macrophages compared to the unstimulated DMSO treated macrophages. Pre-treatment of EPA and DHA significantly reduced phosphorylated JNK expression within the LPS stimulated macrophages. JNK activation leads to the phosphorylation of transcription factors, most importantly the c-Jun component of AP-1 (Tournier *et al.*, 2000; Ventura *et al.*, 2003) leading to expression of a variety of cytokines such as TNF-α and IL-6 (Tsutsumi *et al.*, 2002). Therefore, the reduction in LPS induced cytokine secretion may be in part due to the reduction in JNK activity induced by EPA and DHA pre-treatment of the macrophages. Interestingly, through the use of a JNK inhibitor Nieminen *et al.* (2006) determined that the JNK pathway is involved in the up-regulation of COX-2 expression in J774 macrophages

(Nieminen *et al.*, 2006). It seems likely EPA and DHA may down regulate JNK activity therefore modulating prostaglandin production by inhibiting the COX-2 pathway.

Serine phosphorylation and activation of IκB-α was induced by LPS stimulation. NF-κB proteins are sequestered in the cytoplasmic compartment by IκBs such as IκB-α, once IκB-α is serine phosphorylated it is degraded allowing free NF-κB to enter the nucleus and activate transcription. Pre-treatment of EPA and DHA significantly reduces the phosphorylation of IκB-α within the LPS stimulated macrophages suggesting NF-κB transcriptional activation is reduced. Further analysis is required to obtain more information on the transcriptional activity of NF-κB within the J774.2 macrophages by establishing NF-κBp65 expression within the cytoplasm and nucleus. Furthermore, it would be interesting to examine expression of TLR4 in addition to expression of downstream molecules of the TLR4 such as MyD88 and TRAF6 (which are upstream of JNK, p38 and NF-κB) in EPA and DHA pre-treated macrophages. Additionally, it would be important to observe what effect EPA and DHA have on unstimulated macrophages and cytokine stimulated macrophages to determine which effects of EPA and DHA are LPS/TLR4 specific.

After the initial adipocyte and macrophage experiments examining the effects of EPA and DHA, a co-culture of adipocytes and macrophages was developed. The co-culture acts as a model for obesity induced insulin resistance in which ATM accumulation and therefore increased pro-inflammatory cytokine production is associated with a reduction in insulin sensitivity through down-regulation and modulation of the insulin signalling molecules within adipocytes. Firstly, cytokine and adipokine secretion was determined within the co-culture. Interestingly, treatment of adipocytes with unstimulated and stimulated macrophages resulted in a significant decrease in adipocyte adiponectin secretion in the contact and transwell co-culture systems compared to adipocytes alone suggesting these adipocytes may be less insulin sensitive. Furthermore, there was very little difference between the contact and transwell systems suggesting the macrophages affect the adipocytes via soluble molecules. Unexpectedly, the data suggests that acute EPA and DHA treatment of the macrophages in an unstimulated state has a negative effect on adipocyte adiponectin secretion in the co-culture. However, DHA pre-treatment of the LPS stimulated macrophages had a positive effect on adipocyte adiponectin secretion within the contact co-culture system, suggesting DHA pre-treatment of the macrophages reduce inflammatory and attenuates the insulin resistant sate within the adipocytes. Treatment of adipocytes with unstimulated and LPS stimulated macrophages resulted in a

significant increase in TNF-α, IL-6 and IL-1β secretion from the co-culture systems compared to adipocytes alone. Treatment of adipocytes with unstimulated and LPS stimulated macrophages treated with EPA and DHA showed a significant decrease in these cytokines suggesting EPA and DHA reduce inflammation within the co-culture model.

Within the acute co-culture system gene expression analysis determined that adipocytes treated with LPS stimulated and unstimulated macrophages results in a significant decline in insulin sensitive markers GLUT4 and IRS-1. The macrophages clearly induce a strong effect on the adipocytes of the co-culture in significantly reducing gene expression of insulin sensitive markers. Interestingly, both the LPS stimulated and unstimulated macrophages induce a very similar effect on insulin sensitive markers within the adipocytes suggesting that the inflammatory state of the macrophage is not necessarily important for inhibiting insulin sensitive gene expression within the adipocyte. Insulin resistance in obesity and T2DM is manifested by decreased insulin-stimulated glucose transport and metabolism (Reaven, 1995), therefore these results suggest that macrophages may play a strong role in obesity induced insulin resistance and T2DM by inhibiting gene expression of the insulin sensitive markers. DHA treatment of the unstimulated macrophages enhanced GLUT4 expression within the adipocytes of the co-culture system, similar trends were observed for IRS-1 suggesting EPA and DHA may attenuate the insulin resistant effects induced by the macrophages.

Adipocytes co-cultured with LPS stimulated macrophages resulted in an increase in TNF-α and IL-6 mRNA expression compared to adipocytes alone. Interestingly, unlike the gene expression of the insulin sensitive markers, LPS stimulation of the macrophages is important to inducing an increase in gene expression of inflammatory markers within the adipocytes of the co-culture. However, within the contact system RNA was extracted from a combination of adipocytes and macrophages, therefore the significant up-regulation in inflammatory mRNA may be due to the macrophages and not the adipocytes within this system. However, trends are similar within the transwell system suggesting the adipocytes are also pro-inflammatory with increased expression of cytokine mRNA. Adipocytes co-cultured with LPS stimulated macrophages pre-treated with EPA and DHA showed a decline in TNF-α and IL-6 mRNA in both the contact and transwell systems which may suggest that LC *n-3* PUFA may have a therapeutic effect on reducing inflammation in obesity. EPA and DHA had intriguing but moderate affects on insulin sensitive and pro-inflammatory target expression within this co-culture system. However, a chronic EPA and DHA treatment (5 day treatment) may show more significant effects within this co-culture system and will be examined extensively in chapter 6.

In conclusion, within 3T3-L1 adipocytes chronic EPA and DHA treatment had variable effects. EPA treatment increased leptin secretion levels and improved insulin induced glucose uptake suggesting EPA may have insulin sensitising effects. Conversely, DHA reduced GLUT4 significantly and reduced insulin induced glucose uptake moderately. This may suggest DHA has negative effects on insulin sensitivity with adipocytes. DHA also appeared to induce lipolysis and reduce differentiation, which may also account for the subtle reduction in insulin induced glucose uptake. Therefore, DHA may induce anti-obesity effects and prevent further growth of adipocytes by inhibiting differentiation of pre-adipocytes, inducing lipolysis and reducing glucose uptake through the down regulation of GLUT4. DHA may also reduce the harmful effects of pro-inflammatory cytokines such as TNF-α on adipocyte insulin sensitivity through reduction of ERK signalling. However, further experiments are required to examine if EPA and DHA treatment can attenuate the pro-inflammatory state and reduced insulin sensitivity associated within inflamed adipocytes. In general, the effects of EPA and DHA on J774.2 macrophages were more consistent, with EPA and DHA reducing inflammatory cytokine production while down-regulating and reducing phosphorylation of p38, JNK1/2 and IκB-α. A co-culture of adipocytes and macrophages was then developed as a model of obesity induced insulin resistance. The co-culture data suggests that obesity is associated with the generation of macrophage-derived soluble factors that promote a pro-inflammatory environment leading to insulin-resistant adipocyte function. Furthermore, this work has shown that pre-culturing macrophages with EPA and DHA can attenuate the inflammatory effect as well as increasing insulin sensitive markers. However, an experiment using a longer pre-treatment of the macrophages with LC *n-3* PUFA within the co-culture system will be used to define the effects more extensively. A broader spectrum of genes and proteins will be examined within this chronic treatment co-culture model to identify the effects of LPS stimulated macrophages pre-treated with EPA and DHA on adipocytes within the co-culture.

Chapter 6

The Effects of LPS Stimulated Macrophages Pre-treated with EPA and DHA on Inflammatory and Insulin Signalling within 3T3-L1 Adipocytes of a Co-culture System

6.1 Introduction

A major advancement in our understanding of obesity came in 2003 when Weisberg and colleagues noted that obesity alters adipose tissue metabolic and endocrine function leading to an increased release of free fatty acid (FFA), hormones and pro-inflammatory molecules that contribute to obesity associated complications (Weisberg *et al.*, 2003). To further characterize the changes that occur in adipose tissue with increasing adiposity, Weisberg *et al.* (2003) performed microarray analyses comparing adipose tissue RNA profiles of various mouse models of obesity and identified a subset of genes consistently expressed in obese mice. Further analyses determined that this gene set, not typically expressed in adipocytes, was macrophage-derived (Weisberg *et al.*, 2003). Xu *et al.* (2003) reported similar findings and also observed that thiazolidinedione (TZD) treatment could repress the expression of macrophage-specific genes, providing an additional mechanism by which TZD treatment improves insulin sensitivity (Xu *et al.*, 2003). Weisberg *et al.* (2003) used immunohistochemical analysis of various adipose tissue depots to demonstrate that the percentage of cells expressing the macrophage marker F4/80 (F4/80+) was significant and positively correlated with both adipocyte size and body mass. They established that the F4/80+ cells are colony stimulating factor (CSF)-1 dependent, bone marrow-derived adipose tissue macrophages (ATM) (Weisberg *et al.*, 2003).

The importance of macrophage accumulation in obesity induced insulin resistance was revealed in mice deficient in CC chemokine receptor (CCR)-2, the receptor for monocyte chemotactic protein (MCP)-1. CCR2 regulates monocyte and macrophage recruitment and Weisberg *et al.* (2006) examined $CCR2^{-/-}$ mice. These mice showed reduced food intake with attenuated development of obesity in mice fed a high fat diet (HFD) (Weisberg *et al.*, 2006). Importantly, in obese mice matched for adiposity, CCR2 deficiency reduced macrophage content while reducing the inflammatory profile within the adipose tissue, adiponectin expression was increased, hepatic steatosis ameliorated and systemic glucose homeostasis and insulin sensitivity was improved (Weisberg *et al.*, 2006). This data indicates that CCR2 and the associated reduction in ATM influences the development of obesity induced insulin resistance. Similarly, $IL\text{-}1RI^{-/-}$ mice, which are though to have reduced macrophage activity, were observed to be more insulin sensitive

during a HFD as discussed in chapter 3. Furthermore, mice with a macrophage-specific deletion of peroxisome proliferator-activated receptor (PPAR)-γ were shown to have impaired M2 activation. These mice were predisposed to diet-induced obesity, insulin resistance, and glucose intolerance suggesting that macrophage polarization towards M2 might be a useful strategy for treating type 2 diabetes mellitus (T2DM) (Odegaard *et al.*, 2007b).

Importantly, ATM have been shown to produce many of the pro-inflammatory molecules released by adipose tissue including tumour necrosis factor (TNF)-α and a significant portion of nitric oxide synthase (NOS) -2 and interleukin (IL)-6 gene expression (Weisberg *et al.*, 2003). As discussed in chapter 4 these pro-inflammatory molecules are capable of inducing insulin resistance within adipocytes through cross talk with insulin signalling pathways. However, it is also important to note that other immune cells such as cytotoxic T cells are also thought to contribute to the local and generalised inflammatory state observed in obesity. Consequently, whether the influx of macrophages or other immune cells proves upstream, these processes must be downstream of an initiating event, such as hypoxia or adipocyte cell death. Briefly, Weisberg *et al.* (2007) determined that obesity in male C57BL/6J mice is associated with increased expression of hypoxia-inducible factor (HIF) isoforms in adipose tissue (Rausch *et al.*, 2008) suggesting hypoxia is elevated in obesity. Immunohistochemistry revealed hypoxic areas co-localize predominantly with F4/80+ macrophages indicating macrophages may infiltrate into adipose tissue to stimulate angiogenesis and reduce hypoxia (Pang *et al.*, 2008). Additionally, Cinti *et al.* (2005) demonstrated that more than 90% of all macrophages in white adipose tissue (WAT) are localized to dead adipocytes, suggesting that scavenging of adipocyte debris is an important function of the ATM in obese individuals (Cinti *et al.*, 2005).

Most notably Suganami and Lumeng have explored the effects of macrophages on adipocytes within co-culture models. Suganami *et al.* (2005) co-cultured differentiated 3T3-L1 adipocytes and RAW 264 macrophages and observed a marked up-regulation of pro-inflammatory cytokines, such as TNF-α, and the down-regulation of adiponectin (Suganami *et al.*, 2005). Importantly, production of TNF-α from the macrophages was markedly increased by palmitate, a major FFA released from 3T3-L1, suggesting FFA may be important adipocyte-derived mediators of macrophage inflammation (Suganami *et al.*, 2005). Later in 2007 Suganami *et al.* determined that the co-culture resulted in the activation of NF-κB in both macrophages and adipocytes (Suganami *et al.*, 2007b).

Interestingly, pharmacological inhibition of NF-κB markedly suppressed the co-culture induced production of pro-inflammatory cytokines and adipocyte lipolysis (Suganami *et al.*, 2007b). Furthermore, peritoneal macrophages obtained from toll like receptor (TLR)-4 mutant mice exhibited significant attenuation of TNF-α production in response to saturated fatty acids (SFA). Notably, co-culture of hypertrophied adipocytes and TLR4-mutant macrophages resulted in inhibition of pro-inflammatory cytokine production and adipocyte lipolysis (Suganami *et al.*, 2007b). Additionally, they determined that the inflammatory changes induced by the co-culture of adipocytes and macrophages are significantly abolished by inhibiting mitogen-activated protein kinase (MAPK) activity suggesting that MAPK pathways are involved in the induction of inflammatory changes associated with adipocytes and macrophages (Suganami *et al.*, 2005). Fundamentally, these findings suggest that SFA released from hypertrophied adipocytes via the macrophage-induced adipocyte lipolysis serves as a naturally occurring ligand for TLR4, thereby inducing the inflammatory changes in both adipocytes and macrophages through NF-κB and MAPK activation.

Additionally, in 2007 Lumeng and colleagues examined whether macrophages can modify insulin responsiveness and glucose metabolism in adipocytes of a co-culture system. They observed that macrophage-secreted factors reduced insulin-stimulated glucose uptake in adipocytes via down-regulation of glucose transporter (GLUT)-4 and insulin receptor substrate (IRS)-1. Consistent with this, insulin-stimulated GLUT4 plasma membrane translocation was attenuated by macrophage-secreted factors. GLUT1 transporters were up-regulated, correlating with increased basal glucose uptake. Treatment of macrophage-conditioned medium with TNF-α-blocking antibodies partially reversed this inhibitory effect, which was also seen during direct and indirect co-culture. Essentially, they demonstrate that macrophage derived factors can limit the ability of adipocytes to take up glucose upon insulin stimulation (Lumeng *et al.*, 2007b). Interestingly, adipocytes conditioned medium (CM) containing various adipokines such as IL-6, MCP-1 and resistin can induce insulin resistance with a significant decrease in insulin-stimulated phosphorylation of protein kinase B (PKB/Akt) and glycogen synthase kinase (GSK)-3 within a human liver cell line HepG2 (Zhou *et al.*, 2007). This suggests that adipocyte derived factors may play an important systemic role in whole body insulin resistance and inflammation, which may be exacerbated by the presence of ATM.

New studies suggest that therapeutic strategies for obesity induced insulin resistance may be to reduce the pro-inflammation environment induced by the ATM. A recent study examined the effects of salicylate on the cross-talk between the macrophages

and adipocytes (An *et al.*, 2009). Exposure to RAW 264 macrophage media (CM) resulted in an increase in gene expression and/or protein secretion of TNF-α, IL-6 and resistin with a decrease in the gene expression of PPAR-γ and adiponectin in 3T3-L1 adipocytes (An *et al.*, 2009). Salicylate effectively reversed these changes inhibiting phosphorylation of NF-κB in adipocytes incubated with the CM suggesting salicylate blocks inflammatory process in the pathogenesis of inflammation-related insulin resistance (An *et al.*, 2009). Furthermore, in a co-culture of 3T3-L1 adipocytes and RAW 264 macrophages, PPAR-α ligands (Wy14643) were observed to reduce MCP-1 and TNF-α mRNA expression and secretion *in vitro* relative to the vehicle control treated group (Toyoda *et al.*, 2008).

Long chain (LC) *n-3* polyunsaturated fatty acids (PUFA) may also be able to attenuate the pro-inflammatory phenotype of the macrophages, therefore improving insulin sensitivity within adipocytes of the co-culture system. LC *n-3* PUFA such as eicosapentaenoic acid (EPA) and docosahexaenoic acid (DHA) have been shown to decrease the production of inflammatory eicosanoids, cytokines, and reactive oxygen species while reducing expression of adhesion molecules (Calder, 2006) from many different cells including the macrophage as discussed in chapter 5. However, relatively little is known about the ability of LC *n-3* PUFA to attenuate inflammation and therefore improve insulin signaling within a co-culture of macrophages and adipocytes. However, Itoh *et al.* (2007) examined the effect of EPA on adiponectin production in an *in vitro* co-culture of 3T3-L1 adipocytes and RAW 264 macrophages (Itoh *et al.*, 2007). Adiponectin mRNA expression and secretion to the media were significantly reduced in adipocytes co-cultured with macrophages (Itoh *et al.*, 2007). Treatment with EPA reversed significantly the co-culture induced decrease in adiponectin secretion in a dose-dependent manner whereas adiponectin mRNA expression was unchanged (Itoh *et al.*, 2007). Furthermore, EPA did not significantly affect adiponectin secretion and mRNA expression in 3T3-L1 adipocytes alone. Additionally, it was determined that treatment with EPA at doses of 100 and 200 μMol/L suppresses significantly the co-culture induced increase in TNF-α mRNA expression, which occurs predominantly in the RAW 264 macrophages of the co-culture system (Itoh *et al.*, 2007).

Within this chapter the interaction between LPS stimulated macrophages and adipocytes *in vitro* were examined within the context of a transwell co-culture system and with the incubation of macrophage conditioned media (CM) with adipocytes. These models allow the simplification of an extremely complex human disease state and give a foundation to understanding some of the mechanisms taking place between adipocytes and macrophages within obesity induced insulin resistance. Importantly, the co-culture system

was used to determine if LC *n-3* PUFA can attenuate the pro-inflammatory phenotype of the LPS stimulated macrophages, reducing macrophage induced inflammation on the adipocytes therefore increasing expression of insulin sensitive targets such as GLUT4, IRS-1 and adiponectin and finally improving insulin sensitivity within adipocytes of the co-culture system.

6.2 Material and methods

6.2.1 Experimental design

A transwell co-culture of LPS stimulated J774.2 macrophages pre-treated with EPA, DHA or DMSO vehicle control and mature 3T3-L1 adipocytes were examined as described in section 2.2.11. Briefly, J774.2 macrophages were pre-treated with 50 μMol/L EPA, DHA or an equivalent volume of DMSO vehicle control in DMEM with 10% FCS for 5 days termed the chronic treatment. Macrophages were stimulated with 100 ng/ml LPS during the final 48 hours of the LC *n-3* PUFA chronic treatment. Within the transwell co-cultured system 3T3-L1 adipocytes were grown to confluencey and differentiated for six days in 6-well plates as described in section 2.2.4. Treated macrophages were transferred to permeable inserts above the differentiated adipocytes for 24 hours.

The conditioned media from LPS stimulated J774.2 macrophages (CM) pre-treated with EPA, DHA or DMSO vehicle control was collected and incubated with mature 3T3-L1 adipocytes for 48 hours as discussed in section 2.2.11. Briefly, Macrophages were pre-treated with 50 μMol/L EPA, DHA or vehicle control in DMEM with 1% FCS for 3 days. Macrophages were then stimulated with 100 ng/ml LPS for 30 minutes, washed twice and DMEM with 1% serum and 50 μMol/L EPA, DHA or vehicle control replaced for a further 48 hours. 3T3-L1 adipocytes were grown to confluencey and differentiated for six days in 12 well plates as described in section 2.2.4. Macrophage CM was collected and incubated with mature differentiated 3T3-L1 adipocytes in 12 well plates for 24 hours. Additionally, macrophages were pre-treated with 50 μMol/L EPA, DHA or vehicle control in DMEM with 1% FCS for 4 days. Macrophages were then stimulated with 100 ng/ml LPS for 30 minutes, washed twice and DMEM with 1% serum and 50 μMol/L EPA, DHA or vehicle control replaced for a further 24 hours. 3T3-L1 adipocytes were grown to confluencey and differentiated for six days in 12 well plates as described in section 2.2.4. Macrophage CM was collected and incubated with mature differentiated 3T3-L1 adipocytes in 12 well plates for 48 hours. Figure 6.1 illustrates an outline of cell culture experiment conditions.

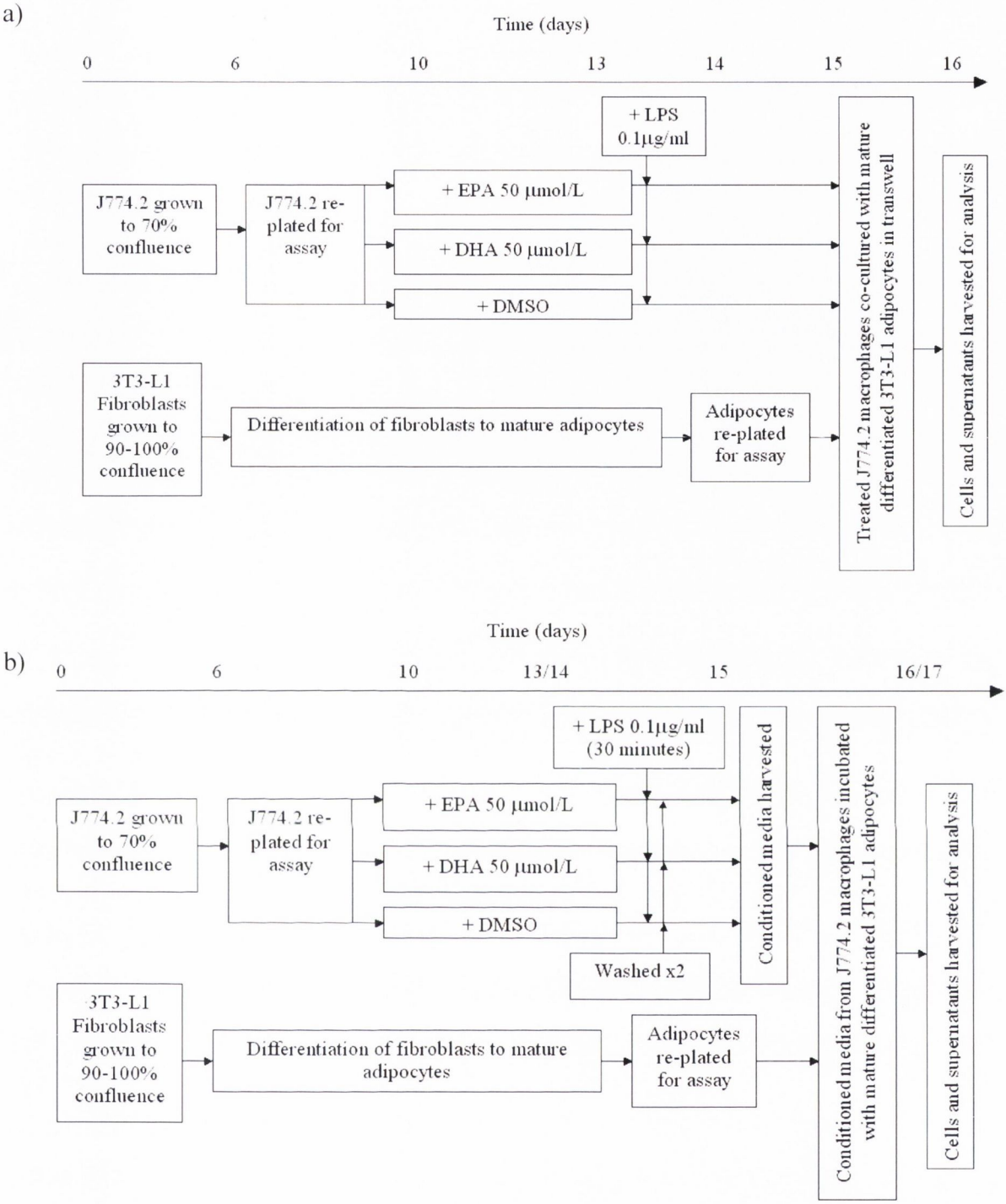

Figure 6.1 In the chronic system (a), macrophages were pre-treated with EPA/DHA for 5 days and stimulated with LPS (100 ng/ml) for 48 hours prior to co-culture in a transwell system for 24 hours. In the conditioned media (CM) experiments (b), macrophages were pre-treated with EPA/DHA for a total of 5 days. The macrophages were stimulated with LPS for 30 minutes, washed and incubated for 24/48 hours in media containing EPA/DHA. CM was collected and incubated with the adipocytes for 24/48 hours.

6.2.2 Macrophage and adipocyte fatty acid composition analysis

To ensure that exogenous fatty acids were incorporated into J774.2 macrophages, the fatty acid composition of the EPA and DHA treated macrophages was assessed. The fatty acid composition of the 3T3-L1 adipocytes within the co-culture was also assessed by gas chromatography (GC) as described in section 2.4. Briefly, Lipid was isolated from cells in accordance to the Bligh and Dyer method (Bligh and Dyer, 1959; Byrdwell *et al.*, 2002). Total lipids were transmethylated and fatty acids were then separated and detected by a Shimadzu GC 2010 (Mason Technologies) equipped with a flame ionisation detector, a fused silica capillary column (Omegawax, 30 m x 0.25 mm inner diameter, 0.2 μm film; Supelco Inc.) and GC solutions software (Mason Technologies). Fatty acids were identified according to their retention times in comparison to two FAME standards (Supelco Inc.). The fatty acid composition was represented as a relative percentage of the total quantified fatty acids.

6.2.3 mRNA analysis (TaqMan® RT-PCR)

Total RNA was extracted from 3T3-L1 adipocytes using an RNeasy Mini kit from Qiagen as described in section 2.7.1. After extraction RNA was quantified and quality assessed using a Nano-Drop as described in section 2.7.2. RNA was deoxyribonuclease (DNase) treated and cDNA was synthesised using SuperScript® VILO™ (Invitrogen Corporation) as described in section 2.7.4 and 2.75 respectively. Gene expression was quantified by real-time RT-PCR on an ABI PRISM 7900HT sequence detection system from Applied Biosystems as described in section 2.7.6. IRS-1, GLUT4, PPARγ, sterol regulatory element–binding protein (SREBP)-1c, fatty acid binding protein (FABP)-4, TLR4, resistin, adiponectin, TNF-α, IL-6, IL-1 receptor I (IL-1RI), IL-1RII, IL-1β, IL-1 receptor antagonist (IL-1Ra), and 18S were investigated using pre-developed primer probe kits purchased from Applied Biosystems. The comparative Ct method also known as the ΔΔ Ct method was used to calculate gene expression levels. This involves comparing the Ct values of the samples of interest with a control in this case 3T3-L1 adipocytes. The Ct values of both the calibrator and the samples of interest were normalized to an appropriate endogenous housekeeping gene in this case 18S.

6.2.4 Protein analysis and Western blotting

Cells were washed in PBS and total cell lysates were extracted with RIPA buffer with protease inhibitor cocktail (Sigma-Aldrich) as described in section 2.8.1. Protein concentrations were assessed using the Bradford assay. 10μg of protein was separated by

electrophoresis through sodium dodecyl sulphate polyacrylamide (SDS-PAGE) gels and the proteins were then transferred to a nitrocellulose membrane as described in section 2.8.3 and 2.8.4. Details of the Western blotting and antigen detection techniques are described in section 2.8.5 and 2.8.6. Briefly, membranes were blocked using 5% BSA in TBS with 0.1% tween 20 and then incubated overnight at 4°C with antibodies specific to GLUT4 (Millipore), IRS-1, inhibitor of κB (IκB)-α, phosphorylated-IκB-α (Ser32), phosphorylated-c-Jun N-terminal kinase (JNK)1/2 p54/46 (Thr183/Tyr185), p38 mitogen-activated protein kinase (MAPK), phosphorylated-p38 (Thr180/Tyr182), phosphorylated-p44/42 MAPK (extracellular signal-regulated kinases [ERK1/2], Thr202/Tyr204; Cell Signalling Technology®), PPAR-γ (Abcam), nuclear factor (NF)-κBp65, JNK1 p83, p44 MAPK (ERK1; Santa Cruz Biotechnology Inc.). Correct loading of protein was confirmed by blotting for actin (Sigma-Aldrich). Membranes were washed in TBS with 0.1% tween (Sigma-Aldrich) and then incubated with peroxidase conjugate anti-rabbit antibody (Santa Cruz Biotechnology Inc.) for 2 hours at room temperature. After further washing, immunoreactive bands were visualized using an enhanced chemiluminescence reaction (Supersignal® West Pico Cemiluminescent Substrate, Pierce Biotechnology). Membranes were exposed to film for 1 to 10 minutes and processed using a XoGraph automatic X-ray processor (Healthcare Ltd.). The position of the band was confirmed by the inclusion of suitable molecular weight markers (Bio-Rad Laboratories). Protein bands were quantified by densitometry using the TINA software version 2.09c (Raytest, Straubenhardt, Germany) and protein levels were expressed as percentage change relative to adipocytes alone.

6.2.5 ELISA analysis

Supernatants were collected from the cells and ELISA analysis was carried out using commercially available kits from R and D Systems for leptin, resistin, adiponectin, TNF-α, IL-6 and IL-1β as described in section 2.9.1. Briefly, the primary or capture antibody specific to the antigen was coated to the walls of a 96 well microtiter plate. Standards were provided with the kits and were reconstituted to working concentrations by serial 1:2 dilutions in reagent diluent. Supernatant and standards were added directly to the 96-well microtiter coated with capture antibody and antigens became immobilized by the capture antibody. The secondary or detection antibody was added to the wells and bound to the immobilized antigen. The detection antibody was conjugated with horseradish peroxidase (HRP) and substrate tetramethylbenzidine (TMB) was added to each well. The immobilised HRP of the detection antibody acts on the TMB causing a blue colour to develop proportionally to the amount of antigen present. H_2SO_4 stops the oxidation of

TMB and changes the blue colour to yellow. Absorbance of the wells was read in the microplate reader at 450 nm with a wavelength correction of 570 nm. A standard curve was constructed for each assay and sample concentrations were calculated through the equation of the standard curve.

6.2.6 Oil red O staining

A fresh working solution of oil red O was prepared as described in section 2.5. Adipocytes were washed in PBS and fixed in 10% neutral buffered formalin (Sigma-Aldrich). Cells were washed again and the working solution of oil red O was added. Cells were washed and observed under microscope (Nikon Corporation); images were taken using Matrox Intellicam (Matrox Electronic Systems Ltd.). Oil red O staining was extracted from the adipocytes with 100% isopropanol. Isopropanol was used as a blank and optical density was measured at 500 nm. Values were expressed as percentage change relative to adipocytes.

6.2.7 Glucose uptake assay

Glucose uptake was analyzed in 3T3-L1 adipocytes as described in section 2.6. Cells were incubated in serum free media with 0.2% BSA for 4 hours. Cells were then incubated in PBS with 0.2% BSA for 30 minutes prior to addition of 100 nMol of Insulin (Sigma-Aldrich) in PBS for 15 minutes, after which 5 μCi/ml of Deoxy-D-glucose, 2-[^{3}H(N)] (Perkin-Elmer) in 1 mMol glucose (Sigma-Aldrich) was added to the cells and incubated for 10 minutes. Cells were then washed twice and then lysed in RIPA buffer containing protease inhibitor cocktail (Sigma-Aldrich). The samples were added to scintillation fluid (National Diagnostics Inc.) and assayed for ^{3}H uptake as counts per minute (Tri-Carb 2900TR low activity liquid scintillation analyzer, Perkin-Elmer).

6.2.8 Confocal GLUT4 translocation analysis

Mature differentiated 3T3-L1 adipocytes were cultured on a 13 mm cover glass within the lower compartment of a transwell co-cultured system. J774.2 macrophages were pre-treated with 50 μMol/L EPA, DHA or DMSO vehicle control for 5 days and stimulated with 100 ng/ml LPS during the final 48 hours of the LC *n-3* PUFA chronic treatment. The mature adipocytes were then co-cultured with the macrophages in a transwell system for 24 hours. The transwell insert containing macrophages was removed and 10 nMol of insulin was added to each well and incubated for 40 minutes. The adipocytes were washed and fixed with 4% paraformalderhyde (Sigma-Aldrich). Cells were incubated with 5%

BSA to minimise non-specific background staining. The cell surface IgG was labelled with 0.5 mg/ml EZ-link Sulfo-NHS-LC-biotin followed by Texas red avidin D (Peirce Biotechnology). The cells were permeabilised using triton x-100 (0.1%, Sigma-Aldrich) and then incubated with BSA (5%). Cells were incubated with GLUT4 (Millipore) followed by a corresponding FITC conjugated secondary antibody (Abcam). The cover glass was mounted onto slides using a Dako mounting medium (Dako). Images were taken and co-localisation was analysed using a LSM510 META confocal microscope (Carl Zeiss MicroImaging Inc.) as described in chapter 2.10.

Briefly, using confocal microscopy specimens were recorded as a digital image composed of a multi-dimensional array containing many volume elements termed voxels that represent three-dimensional pixels. An argon-ion laser and helium-neon laser are switched on and a multi-track configuration selected, allowing detection of two or more fluorophores. The adipocytes of interest with good staining are selected. Gain and offset is used to adjust light intensities to match the dynamic range of the detector. A stack of images (z stack) focused at regularly placed intervals through the depth of the object of interest was taken allowing one to subsequently create renderings to visualize the entire sample in one or three dimensional. The co-localization of the two fluorescent probes within the adipocytes FITC (fluoresces at ~488 nm with absorption at ~495 nm), which has green emission, and Texas red (fluoresces at ~615 nm with absorption at ~589 nm), which has red emission, was represented in the image by pixels containing both red and green colour contributions. Graphical display for co-localization analysis of the pseudocolored specimen image was represented by a scatterplot, which correlates the relationship or association between two sets of data. Pearson's correlation coefficient was used to describe the degree of overlap between the two patterns i.e. the co-localisation. The value of this coefficient ranges from -1 to 1, with a value of -1 representing a total lack of overlap between pixels from the images and a value of 1 indicating perfect image registration. However, the potentially negative values are difficult to interpret. Values between –1 and 0 indicate some form of inverse relationship between the channels as may occur when one channel is very dim and the other bright (Pawley, 2006). Other coefficients provide further information regarding the nature of the co-localisation as well as being less sensitive to channel imbalances, however represent other problems and issues to the analysis (Pawley, 2006).

6.2.9 Data preparation and statistical analysis

Data was reported as Mean ± SEM. Statistical analysis was performed with SPSS (SPSS Inc.). The distribution of data for each variable was assessed and variables transformed to normalise the distribution of data if necessary. Multiple comparisons were performed by one-way ANOVA. Individual inter-group differences were subsequently tested by post hoc LSD statistical analysis. A statistical probability of $P \leq 0.05$ was considered statistically significant.

6.3 Results

6.3.1 Effects of EPA and DHA treatment on J774.2 macrophage fatty acid composition

Fatty acid composition was analysed within J774.2 macrophages pre-treated with EPA, DHA and DMSO vehicle control as presented in Table 6.1 and Figures 6.2a, 6.2b and 6.3. Essentially, EPA concentrations were increased 8 fold in macrophages treated with EPA while DHA concentrations were increased 11 fold in DHA treated macrophages.

However, chronic EPA and DHA treatment significantly reduced myristate (C14:0) levels approximately 4% and 3% respectively within the J774.2 macrophages relative to DMSO treated controls ($P \leq 0.017$ and $P \leq 0.030$). EPA and DHA treatment of the macrophages reduced palmitoleic acid (C16:1 *n-7*) concentrations 17% and 20% relative to DMSO treated macrophages ($P \leq 0.068$ and $P \leq 0.045$). Oleic acid (OA, C18:1) levels were significantly reduced 5% and 6% within macrophages treated with EPA and DHA relative to DMSO treated controls ($P \leq 0.009$ and $P \leq 0.002$). Linoleic acid (LA, C18:2 *n-6*) concentrations were significantly reduced 4% and 5% in EPA and DHA treated macrophages compared to DMSO treated controls ($P \leq 0.009$ and $P \leq 0.004$). Chronic DHA treatment of the macrophages significantly reduced α-Linolenic acid (ALA, C18:3 *n-3*) and gondoic acid (C20:1 *n-9*) concentrations 0.09% and 0.05% compared to DMSO treated macrophages ($P \leq 0.046$ and $P \leq 0.051$). Eicosatrienoic acid levels were significantly reduced ~0.07% in both EPA and DHA treated macrophages relative to DMSO treated control macrophages ($P \leq 0.010$ and $P \leq 0.007$). Interestingly, both EPA and DHA treatment significantly increased EPA levels approximately 6% and 3% respectively within the J774.2 macrophages relative to DMSO treated controls ($P \leq 0.001$ and $P \leq 0.001$). Furthermore, docosapentaenoic acid (DPA, C22:5 *n-3*) levels were increase 16% in EPA treated macrophages relative to DMSO treated macrophages ($P \leq 0.001$). Importantly, both EPA and DHA treatment significantly increased DHA levels 2% and 27% respectively within the J774.2 macrophages relative to DMSO treated controls ($P \leq 0.001$ and $P \leq 0.001$).

Total SFA concentrations were not significantly altered in macrophages treated with LC *n-3* PUFA however, total MUFA levels were significantly reduced 22% and 26% in macrophages treated with EPA and DHA respectively relative to DMSO treated macrophages ($P \leq 0.009$ and $P \leq 0.004$; Figure 6.3). Total PUFA concentrations were increased approximately 23% and 24% within macrophages treated with EPA and DHA respectively ($P \leq 0.001$ and $P \leq 0.001$). Interestingly, total *n-6* PUFA levels were significantly reduced 7% in DHA treated macrophages ($P \leq 0.011$) while total *n-3* PUFA

levels were significantly increased within EPA (26% increase) and DHA (30% increase) treated macrophages relative to DMSO treated control macrophages ($P \leq 0.001$ and $P \leq 0.001$).

Table 6.1 The effects of EPA and DHA treatment on fatty acid composition within J774.2 macrophages. J774.2 macrophages were treated with 50 μMol/L EPA, DHA or DMSO vehicle control for 5 days prior to fatty acid analysis by gas liquid chromatography. The fatty acid composition is represented as a relative percentage of the total quantified fatty acids. Data is presented as mean ± SEM, n = 5. *** $P \leq 0.001$, ** $P \leq 0.01$, * $P \leq 0.05$ relative to DMSO treated macrophages. One-way ANOVA was performed within each group followed by post hoc LSD analysis.

			Macrophage Treatment					
			DMSO		EPA		DHA	
			Mean	SEM	Mean	SEM	Mean	SEM
Myristate	**SFA**	**C14:0**	7.72	1.43	4.24*	0.43	4.62*	0.39
Palmitic acid	**SFA**	**C16:0**	29.57	5.94	32.56	1.10	34.02	0.33
Palmitoleic acid	**MUFA**	**C16:1 (*n-7*)**	26.41	10.73	8.80	0.16	6.80*	0.06
Stearic acid	**SFA**	**C18:0**	6.62	0.73	6.60	0.47	7.19	0.11
Oleic acid	**MUFA**	**C18:1**	9.97	1.88	5.17**	0.07	3.89**	0.11
Linoleic acid	**PUFA**	**C18:2 (*n-6*)**	7.70	1.60	3.59**	0.25	2.99**	0.04
γ-Linolenic acid	**PUFA**	**C18:3 (*n-6*)**	2.11	0.52	2.22	0.16	1.88	0.12
α-Linolenic acid	**PUFA**	**C18:3 (*n-3*)**	0.12	0.05	0.10	0.04	0.01*	0.00
Stearidonic acid	**PUFA**	**C18:4 (*n-3*)**	0.10	0.03	1.75	1.72	0.03	0.00
Gondoic acid	**PUFA**	**C20:1 (*n-9*)**	0.07	0.02	0.05	0.02	0.02*	0.00
Eicosatrienoic acid	**PUFA**	**C20:3 (*n-6*)**	0.78	0.26	0.12**	0.02	0.08**	0.01
Arachidonic acid	**PUFA**	**C20:4 (*n-6*)**	3.24	1.09	3.51	0.10	2.13	0.48
Eicosatetraenoic acid	**PUFA**	**C20:4 (*n-3*)**	0.14	0.07	0.14	0.01	0.14	0.01
Eicosapentaenoic acid	**PUFA**	**C20:5 (*n-3*)**	0.85	0.18	7.05***	0.29	3.66***	0.04
Docosatetraenoic acid	**PUFA**	**C22:4 (*n-6*)**	0.23	0.13	1.68	1.06	0.06	0.01
Docosapentaenoic acid	**PUFA**	**C22:5 (*n-3*)**	1.89	0.37	18.01***	1.00	3.04	0.09
Docosahexaenoic acid	**PUFA**	**C22:6 (*n-3*)**	2.74	0.41	4.43***	0.09	29.45***	0.23

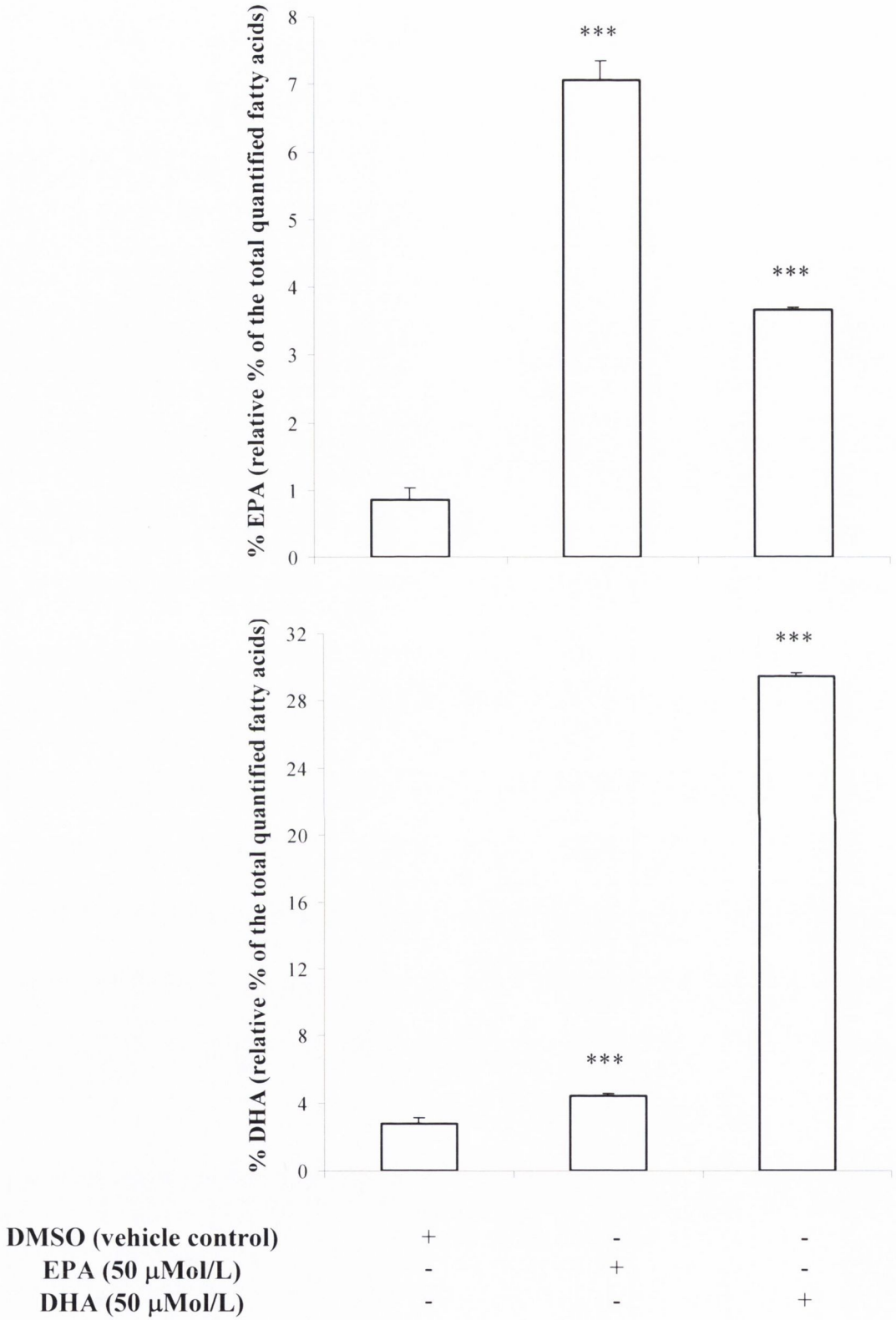

Figure 6.2 The effects of EPA and DHA treatment on EPA and DHA composition within J774.2 macrophages. J774.2 macrophages were treated with 50 μMol/L EPA, DHA or DMSO vehicle control for 5 days prior to fatty acid analysis by gas liquid chromatography. The fatty acid composition is represented as a relative percentage of the total quantified fatty acids. Data is presented as mean ± SEM, n = 5. *** $P \leq 0.001$, relative to DMSO treated macrophages. One-way ANOVA was performed within each group followed by post hoc LSD analysis.

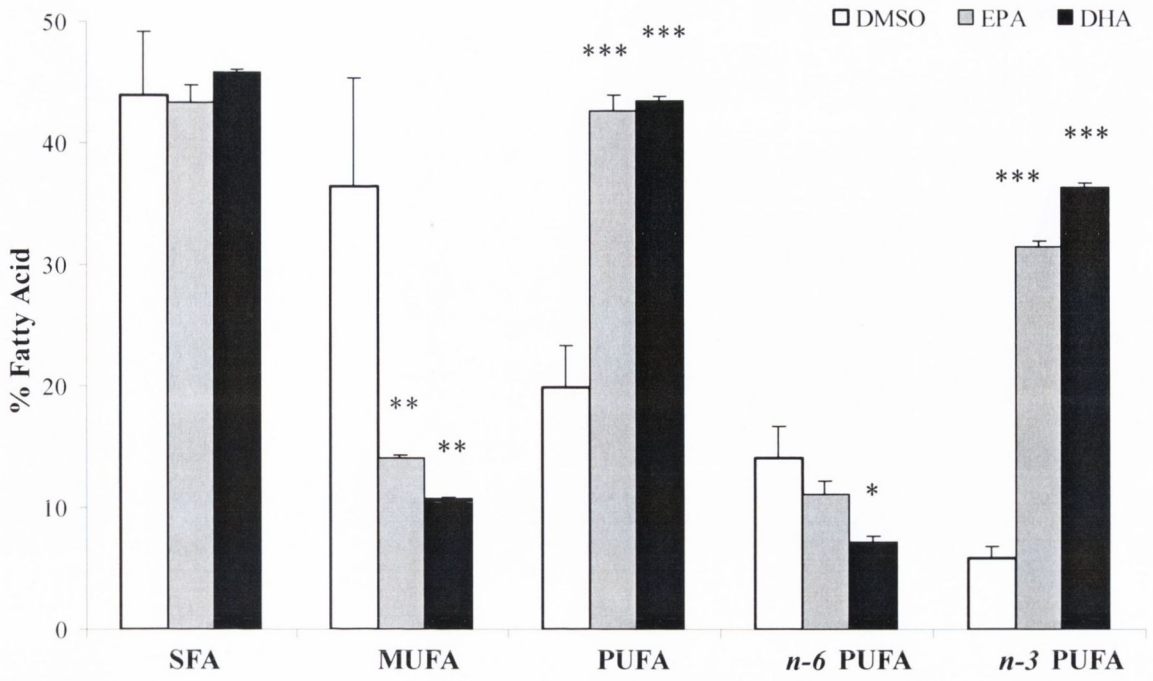

Figure 6.3 The effects of EPA and DHA treatment on total SFA, MUFA and PUFA composition within J774.2 macrophages. J774.2 macrophages were treated with 50 μMol/L EPA, DHA or DMSO vehicle control for 5 days prior to fatty acid analysis by gas liquid chromatography. The fatty acid composition is represented as a relative percentage of the total quantified fatty acids. Data is presented as mean ± SEM, n = 5. *** $P \leq 0.001$, ** $P \leq 0.01$, * $P \leq 0.05$ relative to DMSO treated macrophages. One-way ANOVA was performed within each group followed by post hoc LSD analysis.

6.3.2 Effects of J774.2 macrophages pre-treated with EPA and DHA on 3T3-L1 adipocyte fatty acid composition within a transwell co-culture system

Fatty acid composition was analysed within 3T3-L1 adipocytes co-cultured with J774.2 macrophages pre-treated with EPA, DHA and DMSO vehicle control as presented in Table 6.2 and Figure 6.4. Palmitic acid (PA, C16:0) levels were significantly increased approximately 4% in 3T3-L1 adipocytes co-cultured with J774.2 macrophages pre-treated with DMSO, EPA and DHA relative to adipocytes alone ($P \leq 0.022$, $P \leq 0.008$ and $P \leq 0.027$). Palmitoleic acid concentrations were reduced 5%, 7% and 6% in adipocytes co-cultured with macrophages pre-treated with DMSO, EPA and DHA respectively relative to adipocytes alone ($P \leq 0.054$, $P \leq 0.015$ and $P \leq 0.028$). Stearic acid (C18:0) concentrations were significantly reduced 0.4% and 0.7% in adipocytes co-cultured with macrophages pre-treated with EPA and DHA respectively relative to adipocytes alone ($P \leq 0.036$ and $P \leq 0.002$). Furthermore, stearic acid concentrations were significantly reduced in adipocytes co-cultured with macrophages pre-treated with DHA relative to adipocytes co-cultured with DMSO pre-treated macrophages ($P \leq 0.032$).

Total SFA concentrations were significantly increased 4%, 4% and 3% in adipocytes co-cultured with macrophages pre-treated with DMSO, EPA and DHA respectively relative to adipocytes alone ($P \leq 0.022$, $P \leq 0.008$ and $P \leq 0.027$; Figure 6.4). Total MUFA levels were significantly reduced 4%, 5% and 4% in adipocytes co-cultured with macrophages pre-treated with DMSO, EPA and DHA respectively relative to adipocytes ($P \leq 0.003$, $P \leq 0.001$ and $P \leq 0.002$). Total PUFA and *n-6* PUFA concentrations were not significantly modified in adipocytes co-cultured with macrophages. However, *n-3* PUFA levels were significantly reduced in adipocytes co-cultured with macrophages pre-treated with DMSO and EPA relative to adipocytes alone ($P \leq 0.005$ and $P \leq 0.052$).

Table 6.2 The effects of J774.2 macrophages pre-treated with EPA and DHA on 3T3-L1 adipocytes fatty acid composition within a transwell co-culture system. Fully differentiated 3T3-L1 adipocytes were co-cultured in a transwell system with J774.2 macrophages chronically pre-treated with 50 μMol/L EPA, DHA or DMSO for 24 hours. Fatty acid composition was assessed within the 3T3-L1 adipocytes of the co-culture using gas liquid chromatography. The fatty acid composition is represented as a relative percentage of the total quantified fatty acids. Data is presented as mean ± SEM, n = 4. *** $P \leq 0.001$, ** $P \leq 0.01$, * $P \leq 0.05$ relative to DMSO treated macrophages; † $P \leq 0.05$ relative to adipocytes co-cultured with DMSO treated macrophages. One-way ANOVA was performed within each group followed by post hoc LSD analysis.

			Adipocytes		Adipocytes co-cultured with DMSO treated macrophages		Adipocytes co-cultured with EPA treated macrophages		Adipocytes co-cultured with DHA treated macrophages	
			Mean	SEM	Mean	SEM	Mean	SEM	Mean	SEM
Myristate	**C14:0**	**SFA**	8.77	2.08	8.54	0.08	7.72	0.26	7.92	0.06
Palmitic acid	**C16:0**	**SFA**	26.65	2.12	30.36*	0.39	31.12**	0.83	30.22*	0.06
Palmitoleic acid	**C16:1 (*n-7*)**	**MUFA**	47.89	3.59	42.85*	0.33	41.24**	1.24	42.01*	0.57
Stearic acid	**C18:0**	**SFA**	4.01	0.06	4.26	0.06	4.40*	0.18	4.66**,†	0.18
Oleic acid	**C18:1**	**MUFA**	6.72	2.13	7.70	0.13	8.41	0.37	8.21	0.21
Linoleic acid	**C18:2 (*n-6*)**	**PUFA**	1.94	0.67	2.27	0.08	2.65	0.10	2.61	0.10
γ-Linolenic acid	**C18:3 (*n-6*)**	**PUFA**	0.46	0.18	0.58	0.08	0.66	0.06	0.62	0.05
α-Linolenic acid	**C18:3 (*n-3*)**	**PUFA**	0.01	0.00	0.00	0.00	0.02	0.03	0.02	0.03
Stearidonic acid	**C18:4 (*n-3*)**	**PUFA**	0.00	0.00	0.00	0.00	0.00	0.00	0.00	0.00
Gondoic acid	**C20:1 (*n-9*)**	**PUFA**	0.03	0.03	0.01	0.00	0.00	0.00	0.00	0.00
Eicosatrienoic acid	**C20:3 (*n-6*)**	**PUFA**	0.37	0.20	0.23	0.01	0.25	0.02	0.25	0.02
Arachidonic acid	**C20:4 (*n-6*)**	**PUFA**	1.41	0.54	1.53	0.03	1.75	0.08	1.67	0.03
Eicosatetraenoic acid	**C20:4 (*n-3*)**	**PUFA**	0.07	0.08	0.00	0.00	0.01	0.01	0.00	0.00
Eicosapentaenoic acid	**C20:5 (*n-3*)**	**PUFA**	0.41	0.16	0.44	0.01	0.48	0.01	0.47	0.02
Docosatetraenoic acid	**C22:4 (*n-6*)**	**PUFA**	0.06	0.07	0.00	0.00	0.00	0.00	0.00	0.00
Docosapentaenoic	**C22:5 (*n-3*)**	**PUFA**	0.44	0.04	0.33	0.04	0.37	0.04	0.38	0.02
Docosahexaenoic acid	**C22:6 (*n-3*)**	**PUFA**	1.08	0.11	0.91	0.03	0.92	0.04	0.95	0.09

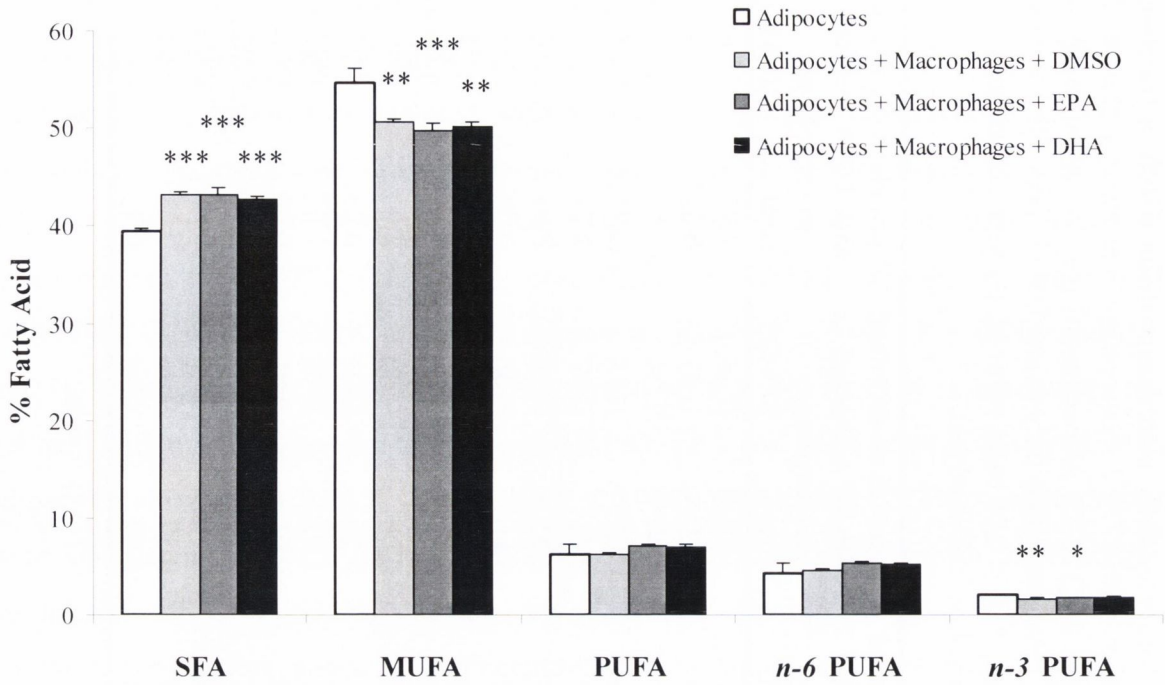

Figure 6.4 The effects of J774.2 macrophages pre-treated with EPA and DHA on total SFA, MUFA and PUFA composition within 3T3-L1 adipocytes of a transwell co-culture system. Fully differentiated 3T3-L1 adipocytes were co-cultured in a transwell system with J774.2 macrophages chronically pre-treated with 50 μMol/L EPA, DHA or DMSO for 24 hours. Fatty acid composition was assessed within the 3T3-L1 adipocytes of the co-culture using gas liquid chromatography. The fatty acid composition is represented as a relative percentage of the total quantified fatty acids. Data is presented as mean ± SEM, n = 4. *** $P \leq 0.001$, ** $P \leq 0.01$, * $P \leq 0.05$ relative to DMSO treated macrophages. One-way ANOVA was performed within each group followed by post hoc LSD analysis.

6.3.3 Effects of chronic EPA and DHA treatment on cytokine and adipokine secretion within a co-culture of J774.2 macrophages and 3T3-L1 adipocytes

TNF-α, IL-6, adiponectin and leptin protein secretion was measured within a transwell co-culture of 3T3-L1 adipocytes and LPS stimulated J774.2 macrophages pre-treated with EPA, DHA and DMSO vehicle control for 5 days as presented in Figures 6.5a, 6.5b, 6.6a and 6.6b. TNF-α secretion was significantly increased 4.5 fold, 4.7 fold and 3.8 fold in adipocytes co-cultured with LPS stimulated macrophages pre-treated with DMSO, EPA and DHA respectively relative to adipocytes alone ($P \leq 0.001$ consistently; Figure 6.5a). Interestingly, pre-incubation of the LPS stimulated macrophages with DHA prior to co-culture reduced TNF-α secretion (15% decrease) relative to adipocytes co-cultured with DMSO treated LPS stimulated macrophages ($P \leq 0.006$). IL-6 secretion was significantly increased 7.4 fold, 3.5 fold and 2.6 fold in adipocytes co-cultured with LPS stimulated macrophages pre-treated with DMSO, EPA and DHA respectively relative to adipocytes alone ($P \leq 0.001$, $P \leq 0.001$ and $P \leq 0.007$; Figure 6.5b). However, IL-6 secretion was significantly reduced in LPS stimulated macrophages pre-treated with EPA (52% decrease) and DHA (64% decrease) prior to co-culture with the adipocytes relative to adipocytes co-cultured with LPS stimulated vehicle control treated macrophages. IL-1β secretion (data not shown) was increased in the co-culture of adipocytes and LPS stimulated macrophages relative to adipocytes. However, IL-1β secretion was not significantly attenuated by pre-incubation of the LPS stimulated macrophages with EPA and DHA prior to co-culture.

Interestingly, leptin secretion was significantly reduced 26% in adipocytes co-cultured with LPS stimulated macrophages pre-treated with DMSO relative to adipocytes alone ($P \leq 0.009$; Figure 6.6a). EPA pre-treatment of the macrophages prior to co-culture with the adipocytes had no effect on leptin secretion. However, leptin secretion was moderately increased 17% in adipocytes co-cultured with LPS stimulated macrophages pre-treated with DHA, although not significantly ($P \leq 0.135$). Adiponectin (Figure 6.6b) and resistin (data not shown) secretion were not significantly altered within the co-culture system.

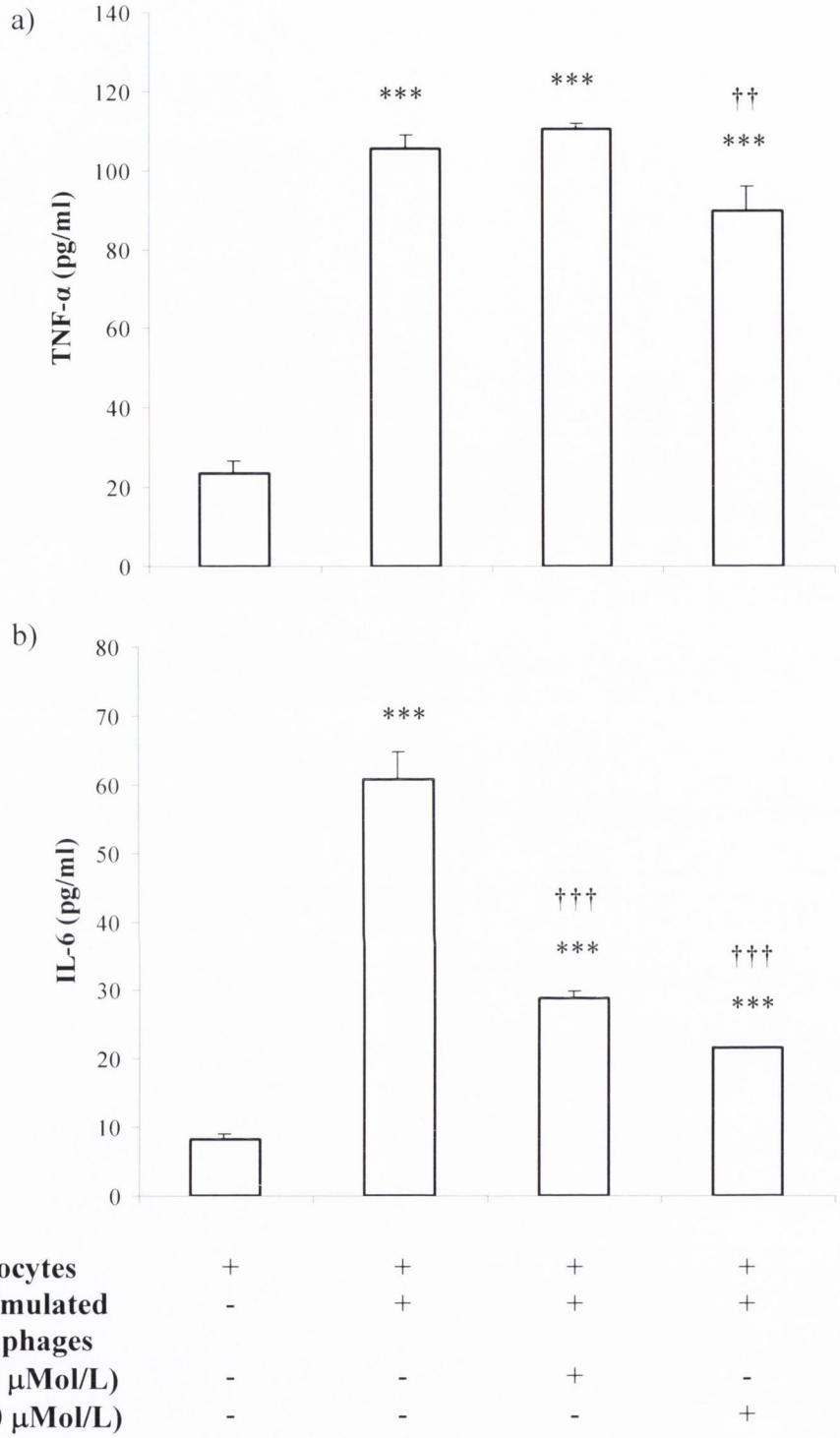

Figure 6.5 Effects of EPA and DHA treatment on cytokine secretion within a co-culture of J774.2 macrophages and 3T3-L1 adipocytes. J774.2 macrophages were treated with 50 μMol/L EPA, DHA or DMSO vehicle control for 5 days with LPS stimulation (100 ng/ml) for 48 hours. Fully differentiated 3T3-L1 adipocytes were co-cultured with the macrophages for a further 24 hours in a transwell system. Supernatants were harvested and TNF-α (a) and IL-6 (b) secretion determined by ELISA (pg/ml). Data presented as mean ± SEM, n = 3. *** $P \leq 0.001$ relative to adipocytes; †† $P \leq 0.01$, ††† $P \leq 0.001$ relative to adipocytes co-cultured with DMSO treated macrophages. One-way ANOVA was performed within each group followed by post hoc LSD analysis.

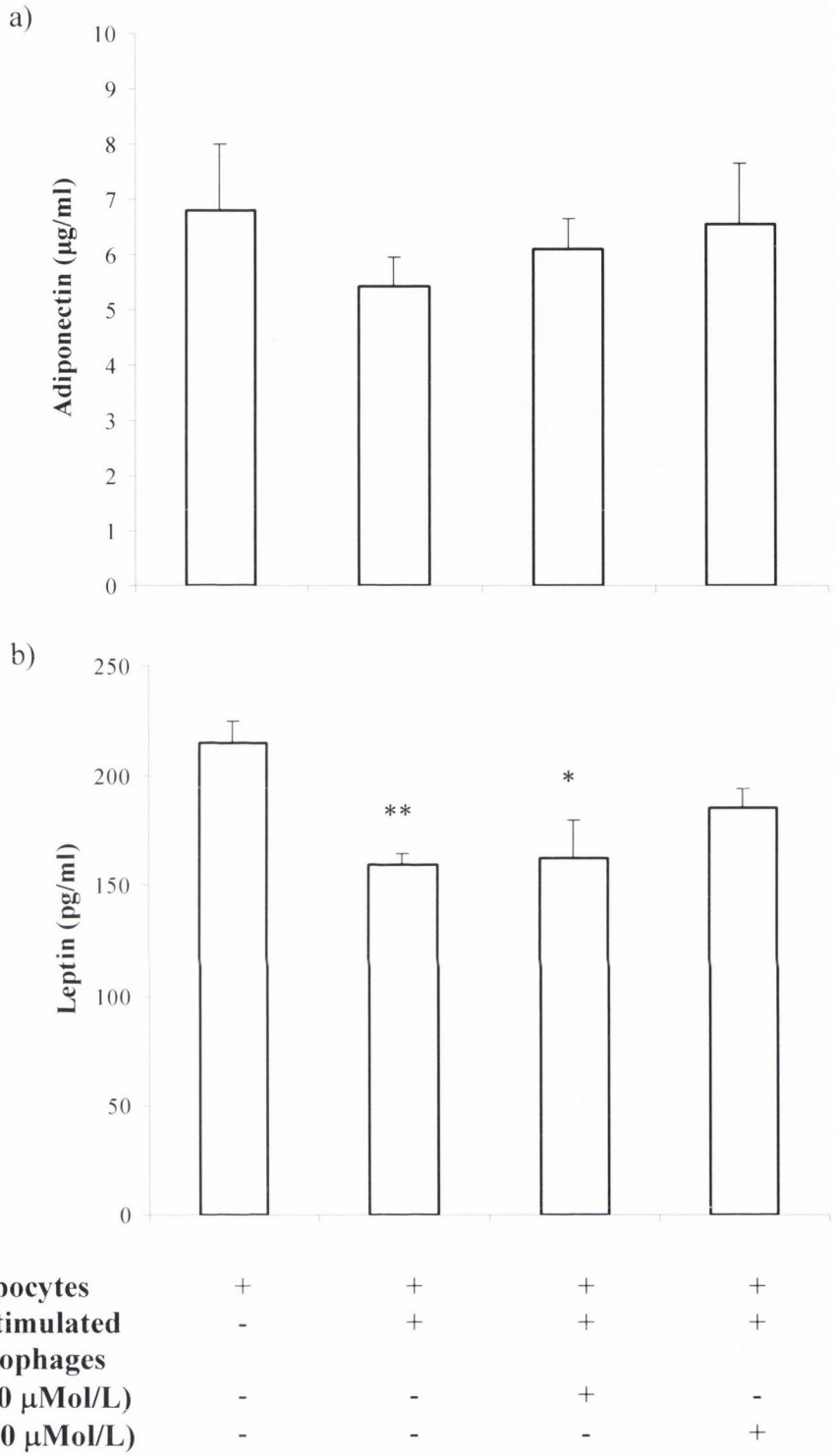

Figure 6.6 Effects of LPS stimulated macrophages pre-treated with EPA and DHA on adipokine secretion from 3T3-L1 adipocytes of a co-culture system. J774.2 macrophages were treated with 50 µMol/L EPA, DHA or DMSO vehicle control for 5 days with LPS stimulation (100 ng/ml) for 48 hours. Fully differentiated 3T3-L1 adipocytes were co-cultured with the macrophages for a further 24 hours in a transwell system. Supernatants were harvested and adiponectin (a) and leptin (b) secretion determined by ELISA (pg/ml). Data is presented as mean ± SEM, n = 3. * $P \leq 0.05$, ** $P \leq 0.01$ relative to adipocytes. One-way ANOVA was performed within each group followed by post hoc LSD analysis.

6.3.4 Effects of LPS stimulated J774.2 macrophages pre-treated with EPA or DHA on inflammatory and insulin sensitive target gene expression within 3T3-L1 adipocytes of a transwell co-culture

IRS-1, GLUT4, IL-6 and IL-1Ra mRNA expression was examined within 3T3-L1 adipocytes co-culture in a transwell system with LPS stimulated J774.2 macrophages pre-treated with EPA, DHA and DMSO vehicle control as presented in figure 6.7a, 6.7b, 6.8a and 6.8b. The presence of LPS stimulated macrophages significantly reduced IRS-1 mRNA 54% within the co-cultured adipocytes ($P \leq 0.001$; Figure 6.7a). EPA pre-treatment of the LPS stimulated macrophages prior to co-culture only moderately increased levels of IRS-1 mRNA (12% increase) within the adipocytes relative to adipocytes co-cultured with LPS stimulated macrophages. However, DHA pre-treatment of the LPS stimulated macrophages prior to co-culture significantly increased IRS-1 mRNA expression 36% within the adipocytes relative to adipocytes co-cultured with LPS stimulated macrophages pre-treated with DMSO vehicle control ($P \leq 0.011$). There was a similar trend in GLUT4 gene expression, with LPS stimulated macrophages reducing GLUT4 expression within the adipocytes of the co-culture while pre-treatment of the macrophages with EPA and DHA increased GLUT4 mRNA expression within the adipocytes, although not significantly (Figure 6.7b).

IL-6 mRNA was significantly increased 80% and 78% in adipocytes co-cultured with LPS stimulated macrophages pre-treated with DMSO and EPA respectively relative to adipocytes alone ($P \leq 0.001$ consistently; Figure 6.8a). However, IL-6 gene expression was significantly reduced to normal levels in adipocytes co-cultured with LPS stimulated macrophages pre-treated with DHA relative to adipocytes co-cultured with LPS stimulated vehicle control treated macrophages ($P \leq 0.001$). IL-1Ra mRNA expression was significantly reduced 68%, 58% and 52% in adipocytes co-cultured with LPS stimulated macrophages pre-incubated with DMSO, EPA or DHA respectively ($P \leq 0.001$ consistently; Figure 6.8b). Although not significant there was an increase in IL-1Ra levels within adipocytes co-cultured with LPS stimulated macrophages pre-treated with EPA (30% increase) and DHA (51% increase) relative to adipocytes co-cultured with untreated LPS stimulated macrophages ($P \leq 0.266$ and $P \leq 0.079$).

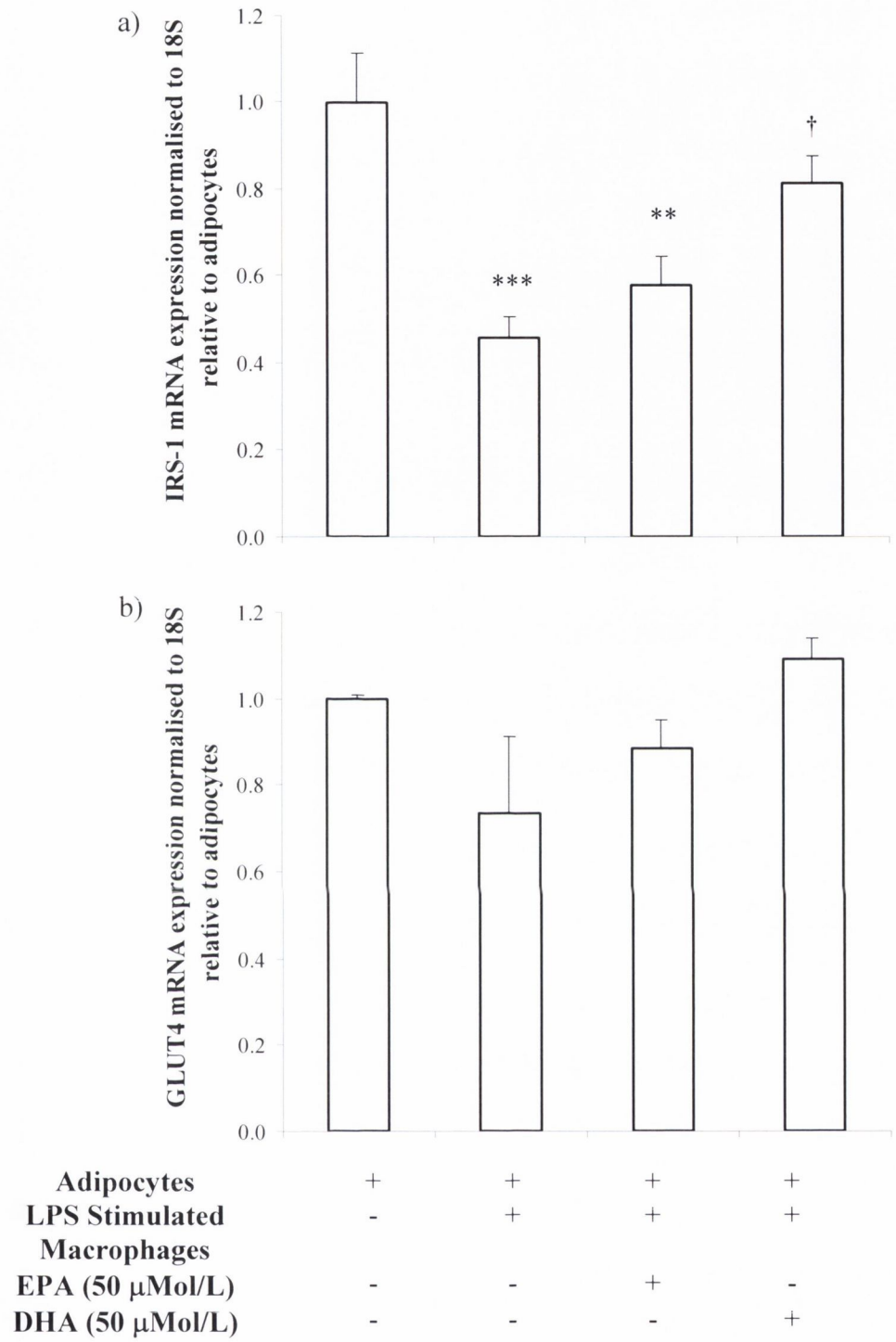

Figure 6.7 Effects of LPS stimulated macrophages pre-treated with EPA and DHA on insulin sensitive target gene expression within 3T3-L1 adipocytes of a co-culture system. J774.2 macrophages were treated with 50 μMol/L EPA, DHA or DMSO vehicle control for 5 days with LPS stimulation (100 ng/ml) for 48 hours. Fully differentiated 3T3-L1 adipocytes were treated with the macrophages for a further 24 hours, IRS-1 (a) and GLUT4 (b) mRNA levels were measured using Taqman RT-PCR. mRNA levels were normalized to 18S and the results are expressed as fold induction relative to DMSO control. Data is presented as mean ± SEM, n = 3. *** $P \leq 0.001$, ** $P \leq 0.01$ relative to adipocytes; † $P \leq 0.05$ relative to adipocytes co-cultured with DMSO treated LPS stimulated macrophages. One-way ANOVA was performed within each group followed by post hoc LSD analysis.

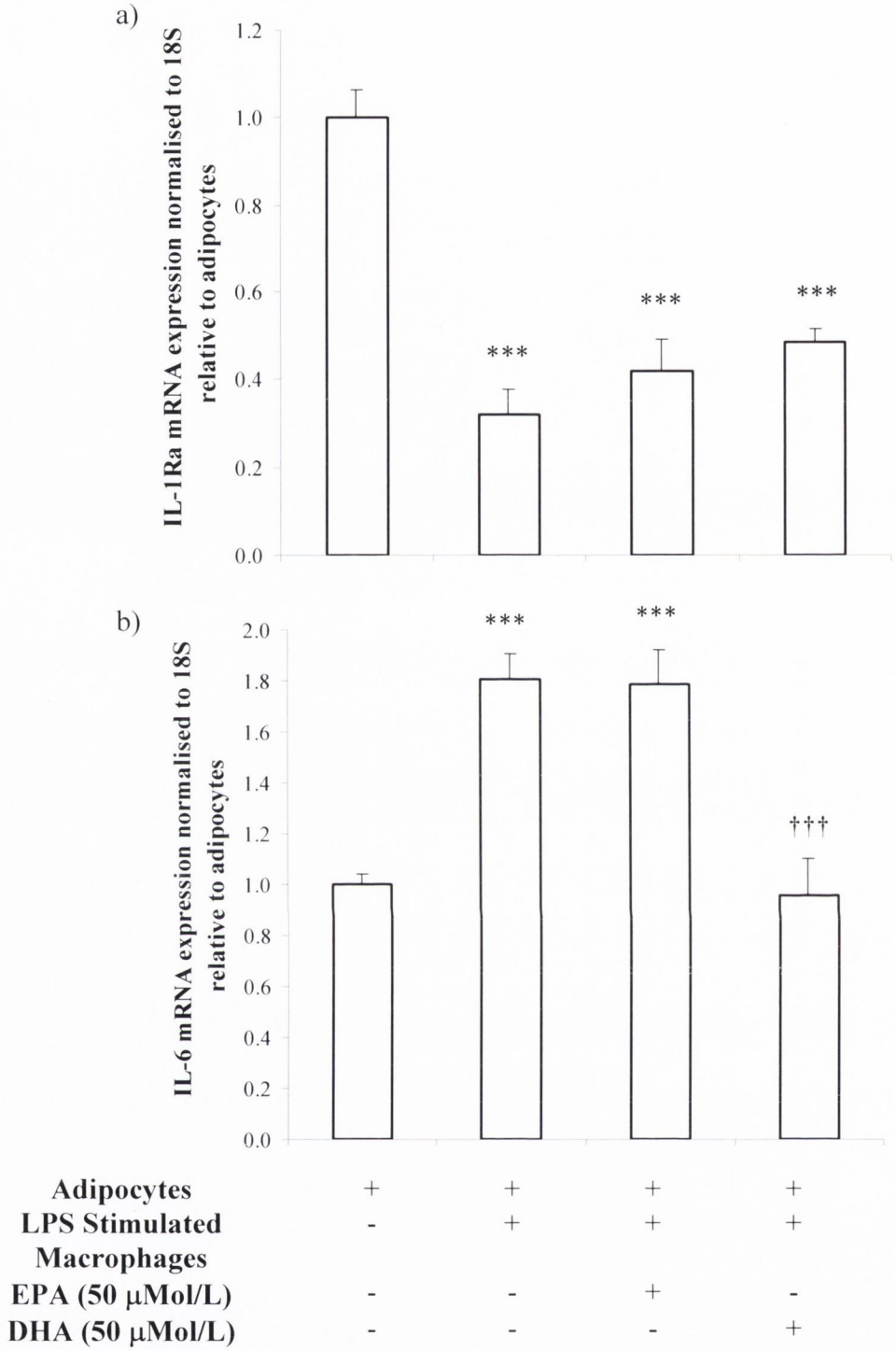

Figure 6.8 Effects of LPS stimulated macrophages pre-treated with EPA and DHA on inflammatory target gene expression within 3T3-L1 adipocytes of a co-culture system. J774.2 macrophages were treated with 50 μMol/L EPA, DHA or DMSO vehicle control for 5 days with LPS stimulation (100 ng/ml) for 48 hours. Fully differentiated 3T3-L1 adipocytes were treated with the macrophages for a further 24 hours, IL-6 (a) and IL-1Ra (b) mRNA levels were measured using Taqman RT-PCR. mRNA levels were normalized to 18S and the results are expressed as fold induction relative to DMSO control. Data is presented as mean ± SEM, n = 3. *** $P \leq 0.001$, ** $P \leq 0.01$ relative to adipocytes; ††† $P \leq 0.001$ relative to adipocytes co-cultured with DMSO treated LPS stimulated macrophages. One-way ANOVA was performed within each group followed by post hoc LSD analysis.

6.3.5 Effects of LPS stimulated macrophages pre-treated with EPA and DHA on GLUT4 and IRS-1 protein expression in 3T3-L1 adipocytes

GLUT4 protein expression was measured in 3T3-L1 adipocytes treated with the CM LPS stimulated J774.2 macrophages pre-treated with EPA, DHA and DMSO vehicle control for 30 minutes as presented in Figure 6.9. Whole cell GLUT4 protein expression was significantly reduced 72% in adipocytes incubated for 30 minutes with the CM of LPS stimulated macrophages pre-treated with DMSO vehicle control relative to adipocytes ($P \leq 0.001$). Similarly, GLUT4 expression was also reduced in adipocytes incubated for 30 minutes with CM from LPS stimulated macrophages pre-treated with EPA (83% decrease) and DHA (80% decrease) relative to adipocytes alone ($P \leq 0.001$ and $P \leq 0.001$). Unexpectedly, whole cell GLUT4 was significantly reduced 43% in adipocytes incubated for 30 minutes with the CM of LPS stimulated macrophages pre-treated with EPA relative to adipocytes incubated with CM of LPS stimulated macrophages pre-treated with DMSO vehicle control ($P \leq 0.037$).

Furthermore, GLUT4 and IRS-1 expression was measured in adipocytes co-cultured with LPS stimulated macrophages pre-treated with EPA and DHA in a transwell system for 24 hours as shown in Figures 6.10 and 6.11. Whole cell IRS-1 protein expression was significantly reduced 36% in adipocytes co-cultured for 24 hours with LPS stimulated macrophages pre-treated with DMSO vehicle control and EPA relative to adipocytes alone ($P \leq 0.001$ and $P \leq 0.001$). However, whole cell IRS-1 was significantly increased 42% in adipocytes co-cultured with LPS stimulated macrophages pre-treated with DHA relative to adipocytes co-cultured with LPS stimulated macrophages pre-treated with DMSO vehicle control ($P \leq 0.004$). Whole cell GLUT4 displayed a similar however, not significant, trend to IRS-1 within adipocytes of the transwell system.

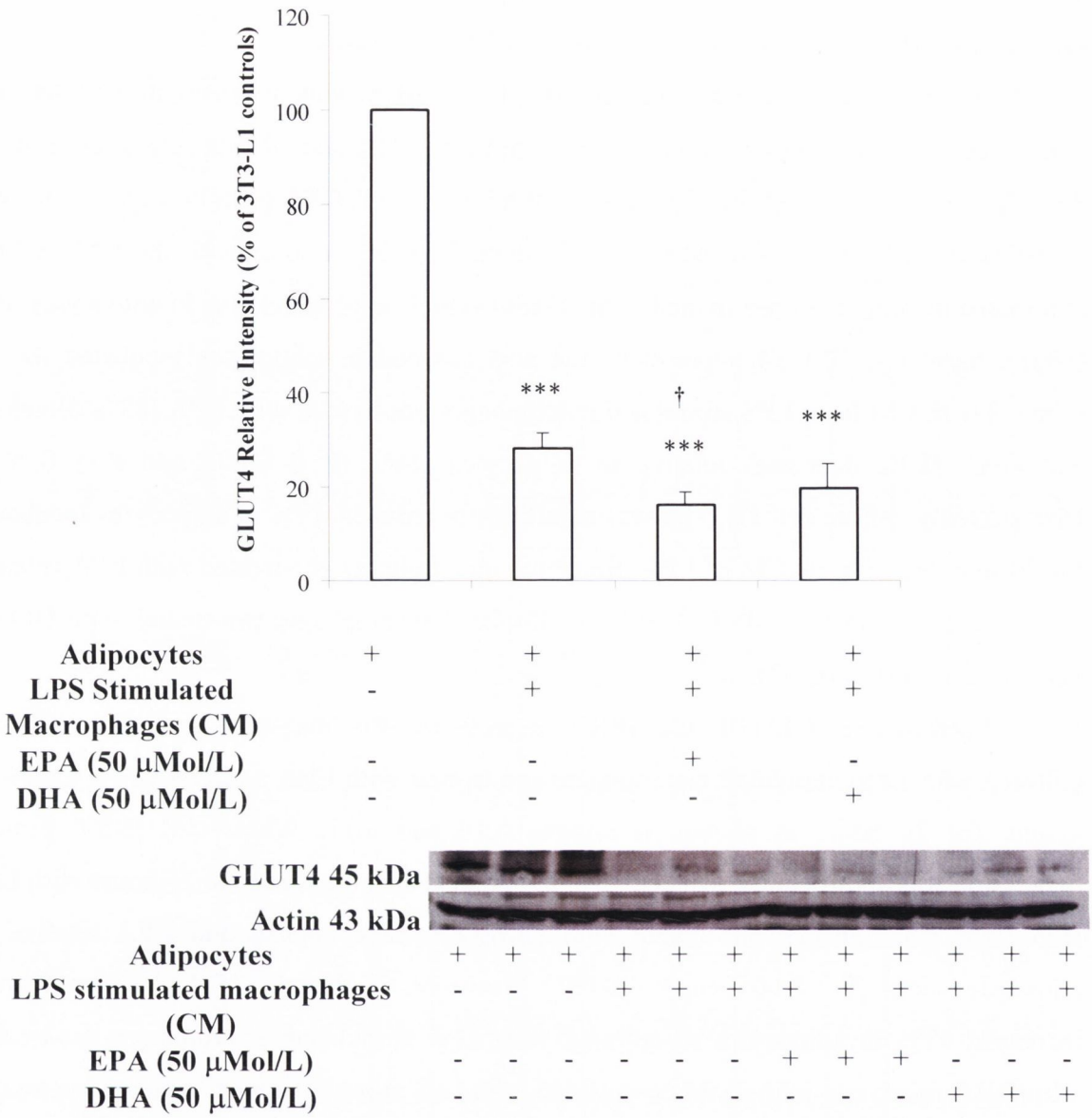

Figure 6.9 Effects of conditioned media from LPS stimulated macrophages (CM) pre-treated with EPA and DHA on GLUT4 protein expression within 3T3-L1 adipocytes. J774.2 macrophages were treated with 50 μMol/L EPA, DHA or DMSO vehicle control for 5 days prior to LPS stimulation (100 ng/ml) for 24 hours. The conditioned media (CM) was harvested and incubated with fully differentiated 3T3-L1 adipocytes for 30 minutes. Whole cell lysates were prepared for SDS-PAGE and immunoblotting. The relative protein levels were quantified by densitometry and data expressed relative to the amount of GLUT4 within adipocytes alone (100%), data is presented as mean ± SEM, n = 3. *** $P \leq 0.001$ relative to adipocytes. † $P \leq 0.05$ relative to adipocytes co-cultured with CM of DMSO treated LPS stimulated macrophages. One-way ANOVA was performed within each group followed by post hoc LSD analysis.

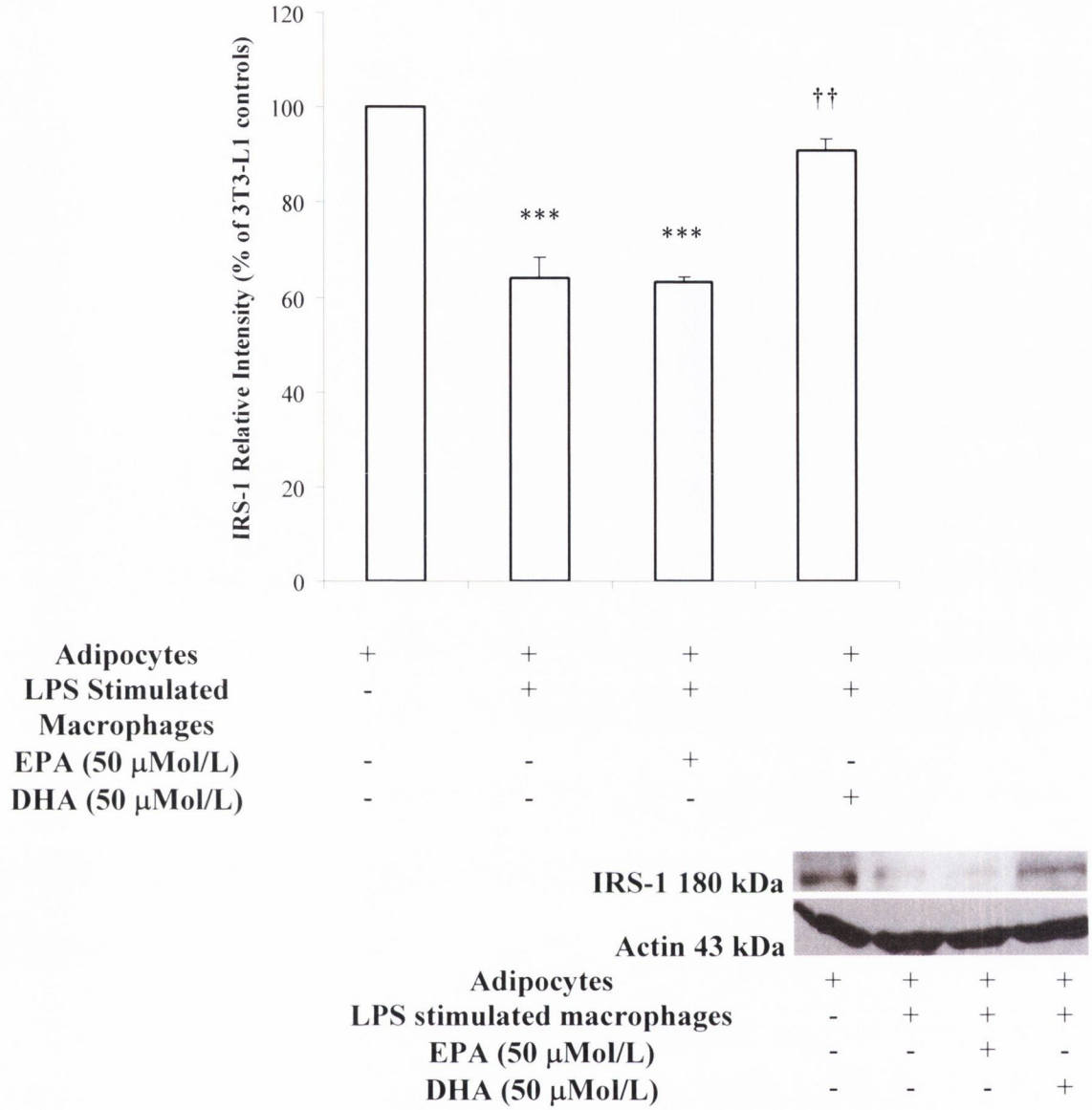

Figure 6.10 Effects of conditioned media from LPS stimulated macrophages (CM) pre-treated with EPA and DHA on IRS-1 protein expression within 3T3-L1 adipocytes. J774.2 macrophages were treated with 50 μMol/L EPA, DHA or DMSO vehicle control for 5 days with LPS stimulation (100 ng/ml) for 48 hours. Fully differentiated 3T3-L1 adipocytes were co-cultured with the macrophages for a further 24 hours in a transwell system. Whole cell lysates were prepared for SDS-PAGE and immunoblotting. A representative blot is shown below the graph. The relative protein levels were quantified by densitometry and data expressed relative to the amount of IRS-1 within adipocytes alone (100%), data is presented as mean ± SEM, n = 2. *** $P \leq 0.001$, relative to adipocytes; †† $P \leq 0.01$ relative to adipocytes co-cultured with CM of DMSO treated LPS stimulated macrophages. One-way ANOVA was performed within each group followed by post hoc LSD analysis. Correct loading of protein was confirmed by blotting for actin.

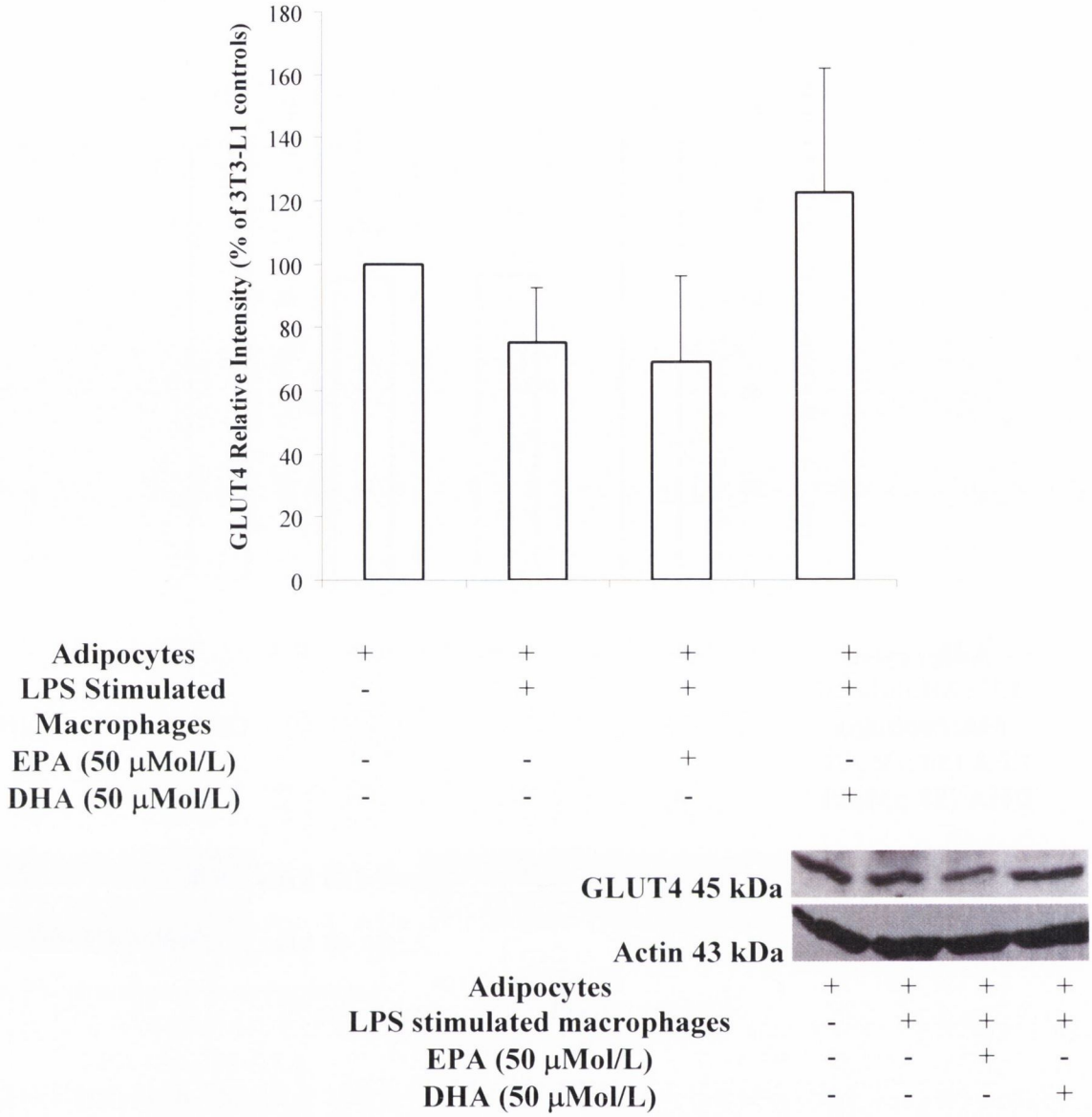

Figure 6.11 Effects of conditioned media from LPS stimulated macrophages (CM) pre-treated with EPA and DHA on GLUT4 protein expression within 3T3-L1 adipocytes. J774.2 macrophages were treated with 50 μMol/L EPA, DHA or DMSO vehicle control for 5 days with LPS stimulation (100 ng/ml) for 48 hours. Fully differentiated 3T3-L1 adipocytes were co-cultured with the macrophages for a further 24 hours in a transwell system. Whole cell lysates were prepared for SDS-PAGE and immunoblotting. A representative blot is shown below the graph. The relative protein levels were quantified by densitometry and data expressed relative to the amount of GLUT4 within adipocytes alone (100%), data is presented as mean ± SEM, n = 3. Correct loading of protein was confirmed by blotting for actin.

6.3.6 Effects of LPS stimulated macrophages pre-treated with EPA and DHA on insulin induced GLUT4 translocation to the membrane within 3T3-L1 adipocytes of a co-culture system

Insulin induced GLUT4 translocation to the membrane was determined within 3T3-L1 adipocytes co-cultured with LPS stimulated J774.2 macrophages pre-treated with EPA, DHA and DMSO vehicle control using confocal microscopy as presented in Figures 6.12 and 6.13. Co-localization was expressed as Pearson's correlation coefficient (R), which is one of the standard techniques applied in pattern recognition for matching one image to another in order to describe the degree of overlap between the two patterns. The value of this coefficient ranges from -1 to 1, with a value of -1 representing a total lack of overlap between pixels from the images and a value of 1 indicating perfect image registration.

Within this study adipocytes, which were unstimulated with insulin show very low levels of co-localization (R = 0.068). Importantly, within adipocytes stimulated with insulin there was a significant increase in co-localization of GLUT4 to the membrane with a coefficient value of R = 0.191 relative to adipocytes unstimulated with insulin ($P \leq 0.001$). Interestingly, within adipocytes co-cultured with LPS stimulated macrophages pre-treated with DMSO there was a significant reduction in insulin induced GLUT4 translocation to the membrane (R = 0.046) relative to insulin-stimulated adipocytes ($P \leq 0.001$). Furthermore, within adipocytes co-cultured with LPS stimulated macrophages pre-treated with EPA and DHA there was also a significant reduction in insulin induced GLUT4 translocation to the membrane (R = 0.004 and R = 0.105 respectively) relative to adipocytes alone stimulated with insulin ($P \leq 0.001$ and $P \leq 0.001$). Interestingly, EPA pre-treatment of the LPS stimulated macrophages prior to co-culture reduced adipocytes GLUT4 translocation to the membrane significantly relative to adipocytes unstimulated with insulin ($P \leq 0.022$), although not relative to adipocytes co-cultured with LPS stimulated macrophages pre-treated with DMSO and stimulated with insulin ($P \leq 0.341$). Whereas DHA pre-treatment of the LPS stimulated macrophages prior to co-culture significantly increased adipocytes GLUT4 translocation to the membrane (R = 0.105) relative to adipocytes co-cultured with LPS stimulated macrophages pre-treated with vehicle control ($P \leq 0.017$).

The images show GLUT4 labeled with FITC (green; first column) and the membrane labeled with Texas red (red; second column). Co-localization of GLUT4 and the membrane is shown as a mixture of the two fluorophores and is visualized as yellow. Adipocytes alone (a) show a more red or orange membrane outline this indicates that GLUT4 has not translocated to the membrane and the fluorophores remain separate. The

adipocytes stimulated with insulin (b) show a yellow outline, which indicates an overlap of the fluorophores and translocation of GLUT4 to the membrane. Adipocytes stimulated with insulin and co-cultured with LPS stimulated macrophages (c) show a more red or orange membrane outline; this indicates that GLUT4 has not translocated to the membrane and the fluorophores remain separate. Pre-treated of the macrophages with EPA prior to co-culture (d) does not attenuate the effect and a red outline is still observed. However, in adipocytes co-cultured with LPS stimulated macrophages pre-treated with DHA (e) there is an observable increase in yellow around the adipocytes indicating GLUT4 translocation to the membrane and overlap of fluorophores.

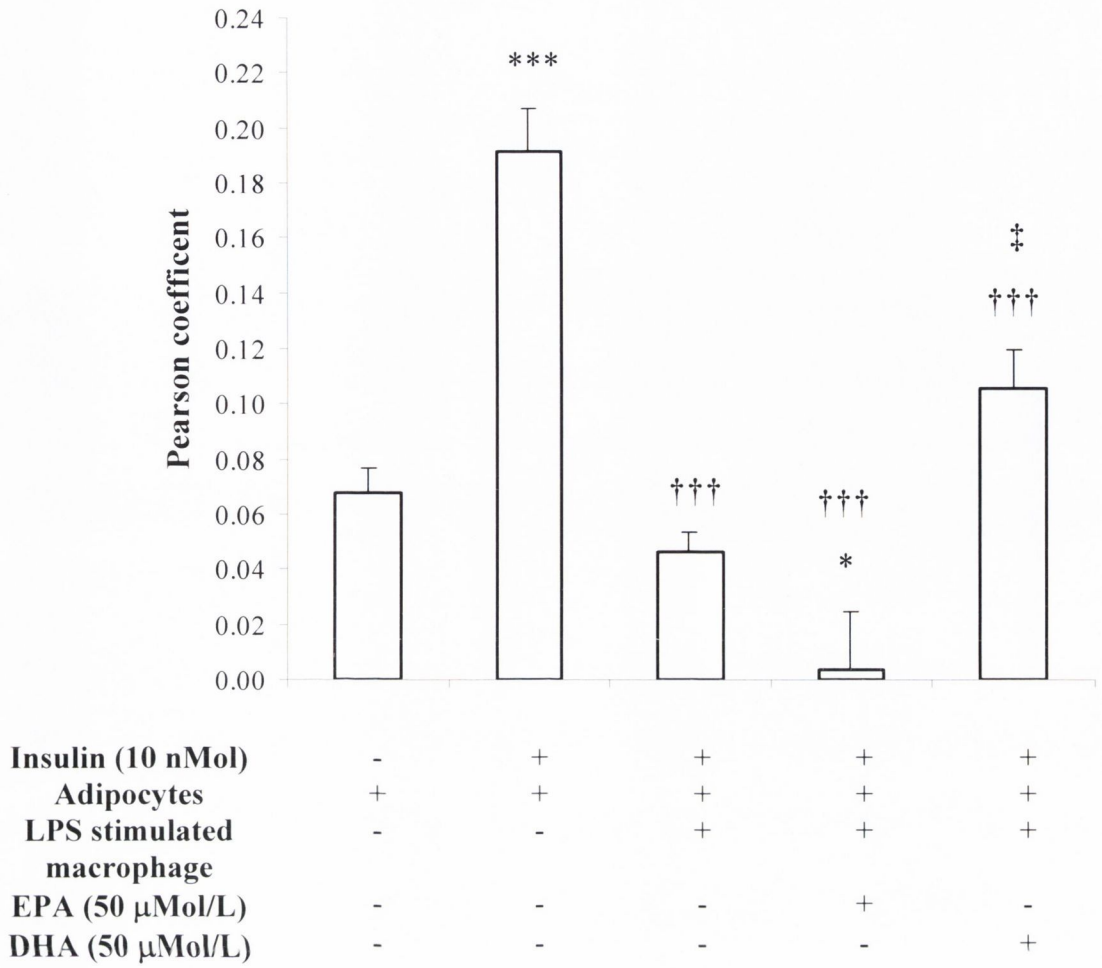

Figure 6.12 Effects of LPS stimulated macrophages pre-treated with EPA and DHA on insulin induced GLUT4 translocation to the membrane within 3T3-L1 adipocytes of a co-culture system. J774.2 macrophages were treated with 50 μMol/L EPA, DHA or DMSO vehicle control for 5 days prior to LPS stimulation (100 ng/ml) for 48 hours. Fully differentiated 3T3-L1 adipocytes were co-cultured with the macrophages for a further 24 hours in a transwell system. Adipocytes were incubated for 40 minutes with 10 nMol of insulin. The adipocyte membrane was then labelled with Texas red (red) and GLUT4 was labelled with FITC (green). Images were taken and co-localisation analysed using a LSM510 META Zeiss confocal microscope. Colocalization was measured in voxels within each confocal stack and expressed as Pearson's correlation coefficient. Data is presented as mean ± SEM, n = 168 – 251 confocal stacks within 8 – 16 cells. * $P \leq 0.05$ relative to adipocytes. ††† $P \leq 0.001$ relative to adipocytes + insulin. ‡ $P \leq 0.05$ relative to adipocytes co-cultured with LPS stimulated macrophages pre-treated with DMSO + insulin. One-way ANOVA was performed within each group followed by post hoc Bonferroni analysis. Representative Images are shown in Figure 6.30.

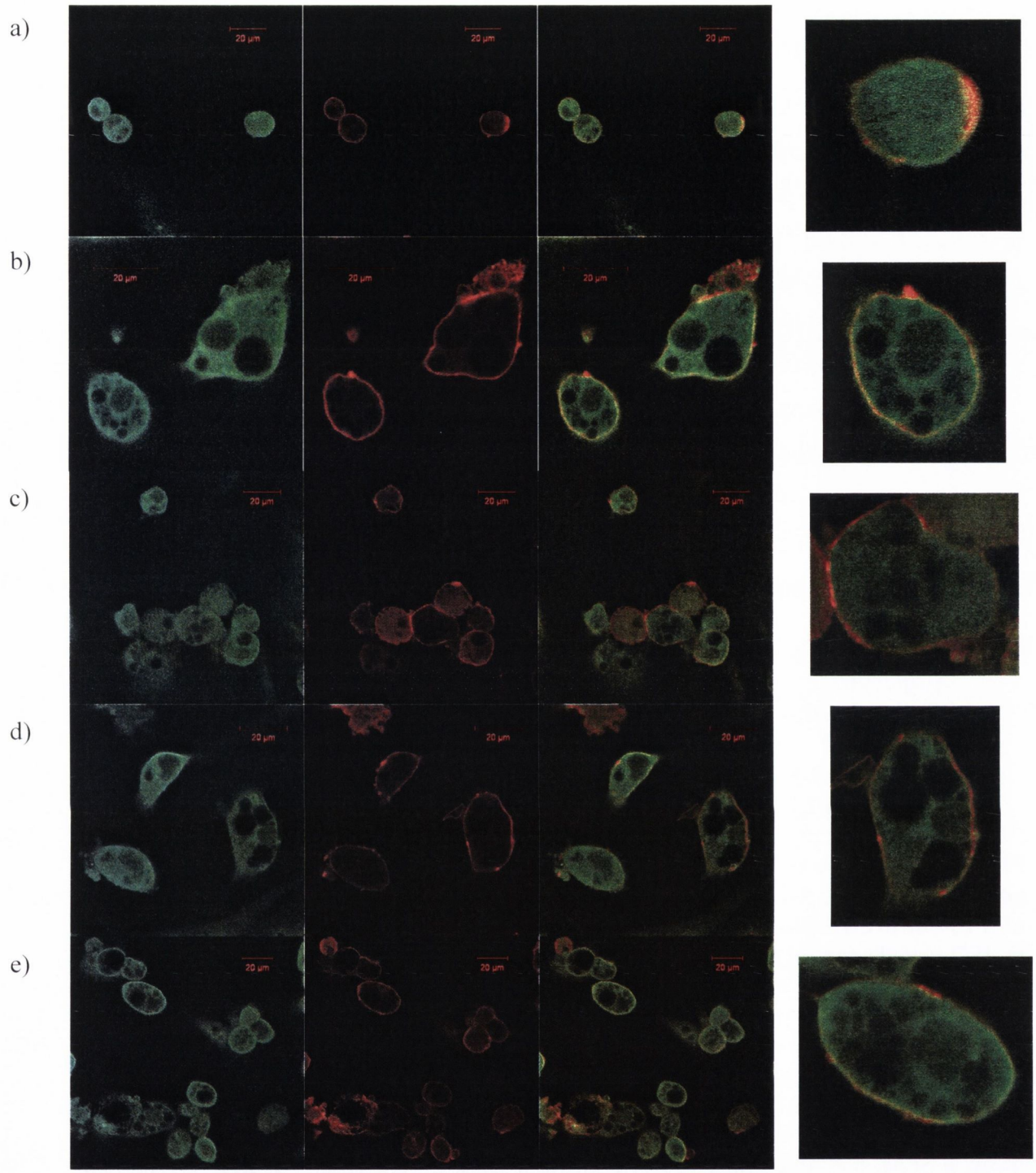

Figure 6.13 Effects of LPS stimulated macrophages pre-treated with EPA and DHA on insulin induced GLUT4 translocation to the membrane within 3T3-L1 adipocytes of a co-culture system. J774.2 macrophages were treated with 50 µMol/L EPA, DHA or DMSO vehicle control for 5 days with LPS stimulation (100 ng/ml) for 48 hours. Fully differentiated 3T3-L1 adipocytes were co-cultured with the macrophages for a further 24 hours in a transwell system. Adipocytes were incubated for 40 minutes with 10nMol of insulin. The adipocyte membrane was labelled with Texas red (red) and GLUT4 was labelled with FITC (green). Translocation of GLUT4 to the membrane is shown as yellow. Images were taken using confocal microscope and images show adipocytes (a), adipocytes + insulin (b), adipocytes co-cultured with LPS stimulated macrophages pre-treated with DMSO + insulin (c), adipocytes co-cultured with LPS stimulated macrophages pre-treated with EPA + insulin (d), adipocytes co-cultured with LPS stimulated macrophages pre-treated with DHA + insulin (e; 630x magnification)

6.3.7 Effects of conditioned media from LPS stimulated macrophages (CM) pre-treated with EPA and DHA on ^{3}H glucose uptake within 3T3-L1 adipocytes

Glucose uptake was examined within 3T3-L1 adipocytes incubated with CM from LPS stimulated J774.2 macrophages pre-treated with EPA, DHA and DMSO vehicle control as presented in Figures 6.14 to 6.17.

Firstly, conditioned media (CM) was harvested from macrophages pre-treated with EPA, DHA or vehicle control and stimulated with LPS for 48 hours. CM was incubated with mature differentiated 3T3-L1 adipocytes for 24 hours. This system is similar to the design of the transwell co-culture experiments. Basal glucose uptake was significantly up-regulated in adipocytes incubated with CM from LPS stimulated macrophages pre-treated with DMSO vehicle control (21% increase) or EPA (34% increase) relative to adipocytes alone ($P \leq 0.028$ and $P \leq 0.005$; Figure 6.14). Conversely, DHA pre-treated LPS stimulated macrophage CM had no significant effect on basal glucose uptake in adipocytes. Insulin induced glucose uptake was significantly reduced 37% in adipocytes incubated with the CM of LPS stimulated macrophages pre-treated with vehicle control or DHA relative to adipocytes alone ($P \leq 0.007$ and $P \leq 0.019$; Figure 1.5). Interestingly, insulin induced glucose uptake was significantly increased in adipocytes incubated with CM from LPS stimulated macrophages pre-treated with EPA relative to adipocytes incubated with CM of LPS stimulated macrophages pre-treated with DMSO vehicle control ($P \leq 0.005$).

Secondly, CM was harvested from macrophages pre-treated with EPA, DHA or vehicle control and stimulated with LPS for 24 hours. CM was incubated with mature differentiated 3T3-L1 adipocytes for 48 hours. This gives the EPA and DHA pre-treated macrophages less time to recover and attenuate the LPS induced inflammation while longer CM incubation with the adipocytes models a more chronic inflammatory environment for the adipocytes. Basal glucose uptake was significantly reduced in adipocytes treated for 48 hours with the CM of LPS stimulated macrophages pre-treated with DMSO (27% decrease) or EPA (32% decrease) relative to adipocytes alone ($P \leq 0.001$ and $P \leq 0.002$; Figure 1.6). However, basal glucose uptake was unaffected in adipocytes incubated with the CM of LPS stimulated macrophages pre-treated with DHA relative to adipocytes alone and was increased relative to adipocytes incubated with the CM of LPS stimulated macrophages treated with vehicle control ($P \leq 0.002$). Insulin induced glucose uptake was significantly reduced in adipocytes incubated for 48 hours with CM of LPS stimulated macrophages treated with vehicle control (81% decrease) or EPA (70% decrease) relative to adipocytes alone ($P \leq 0.001$ and $P \leq 0.001$; Figure 1.7). Importantly, insulin induced glucose uptake was significantly increased in adipocytes

incubated for 48 hours with the CM from DHA pre-treated LPS stimulated macrophages relative to adipocytes incubated with the CM of LPS stimulated macrophages pre-treated with vehicle control ($P \leq 0.001$).

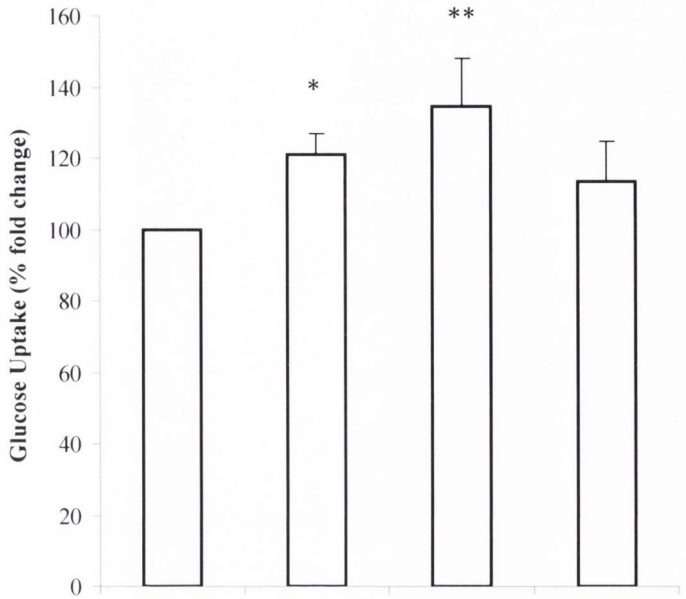

Insulin (100 nMol)	-	-	-	-
Adipocytes	+	+	+	+
LPS stimulated macrophage (CM)	-	+	+	+
EPA (50 μMol/L)	-	-	+	-
DHA (50 μMol/L)	-	-	-	+

Figure 6.14 Short-term (24 hour) effects of conditioned media from LPS stimulated macrophages (CM) pre-treated with EPA and DHA on basal glucose uptake in 3T3-L1 adipocytes. J774.2 macrophages were treated with 50 μMol/L EPA, DHA or DMSO vehicle control for 5 days with LPS stimulation (100 ng/ml) for 48 hours. The conditioned media was harvested and incubated with fully differentiated 3T3-L1 adipocytes for 24 hours. Cells were incubated in PBS with 0.2% BSA prior to addition of 5 μCi/ml of ^{3}H glucose in 1 mMol glucose for 10 minutes. Cells were washed, lysed and assayed for ^{3}H uptake as counts per minute (CPMA). Data is expressed relative to basal glucose uptake within 3T3-L1 adipocytes (100%) and presented as mean ± SEM, n = 3 - 6. * $P \leq 0.05$, ** $P \leq 0.01$ relative to adipocytes. One-way ANOVA was performed within each group followed by post hoc LSD analysis

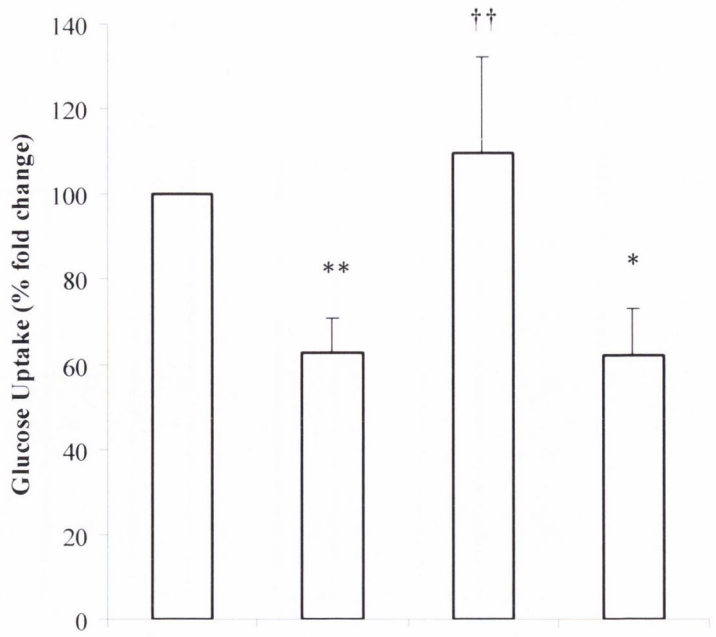

Insulin (100 nMol)	+	+	+	+
Adipocytes	+	+	+	+
LPS stimulated macrophage (CM)	-	+	+	+
EPA (50 μMol/L)	-	-	+	-
DHA (50μMol/L)	-	-	-	+

Figure 6.15 Short-term (24 hour) effects of conditioned media from LPS stimulated macrophages (CM) pre-treated with EPA and DHA on insulin induced glucose uptake in 3T3-L1 adipocytes. J774.2 macrophages were treated with 50 μMol/L EPA, DHA or DMSO vehicle control for 5 days with LPS stimulation (100 ng/ml) for 48 hours. The conditioned media (CM) was harvested and incubated with fully differentiated 3T3-L1 adipocytes for 24 hours. Cells were incubated in PBS with 0.2% BSA prior to addition of 100nM insulin in PBS for 15 minutes. 5 μCi/ml of ^{3}H glucose in 1 mMol glucose was added to the cells for 10 minutes. Cells were washed, lysed and assayed for ^{3}H uptake as counts per minute (CPMA). Insulin induced glucose uptake was established by subtracting total glucose uptake from basal glucose uptake. Data is expressed relative to insulin induced glucose uptake within 3T3-L1 adipocytes (100%) and presented as mean ± SEM, n = 3 - 6. * $P \leq 0.05$, ** $P \leq 0.01$ relative to adipocytes; †† $P \leq 0.01$ relative to adipocytes co-cultured with CM of LPS stimulated macrophages pre-treated with DMSO. One-way ANOVA was performed within each group followed by post hoc LSD analysis.

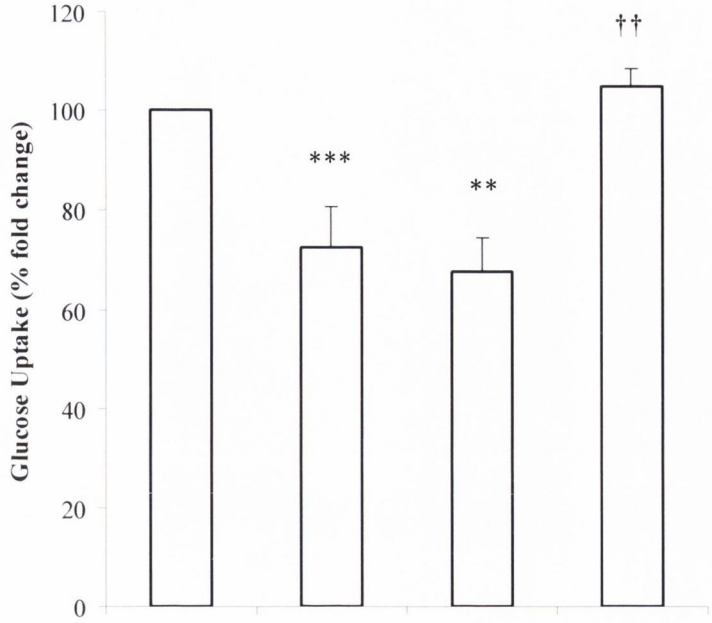

Insulin (100 nMol)	-	-	-	-
Adipocytes	+	+	+	+
LPS stimulated macrophage (CM)	-	+	+	+
EPA (50 μMol/L)	-	-	+	-
DHA (50 μMol/L)	-	-	-	+

Figure 6.16 Long-term (48 hour) effects of conditioned media from LPS stimulated macrophages (CM) pre-treated with EPA and DHA on basal glucose uptake in 3T3-L1 adipocytes. J774.2 macrophages were treated with 50 μMol/L EPA, DHA or DMSO vehicle control for 5 days with LPS stimulation (100 ng/ml) for 24 hours. The conditioned media (CM) was harvested and incubated with fully differentiated 3T3-L1 adipocytes for 48 hours. Cells were incubated in PBS with 0.2% BSA prior to addition of 5 μCi/ml of ^{3}H glucose in 1 mMol glucose for 10 minutes. Cells were washed, lysed and assayed for ^{3}H uptake as counts per minute (CPMA). Data is expressed relative to basal glucose uptake within 3T3-L1 adipocytes (100%) and presented as mean ± SEM, n = 4 - 8. ** $P \leq 0.01$, *** $P \leq 0.001$ relative to adipocytes; †† $P \leq 0.01$ relative to adipocytes co-cultured with CM of LPS stimulated macrophages pre-treated with DMSO. One-way ANOVA was performed within each group followed by post hoc LSD analysis

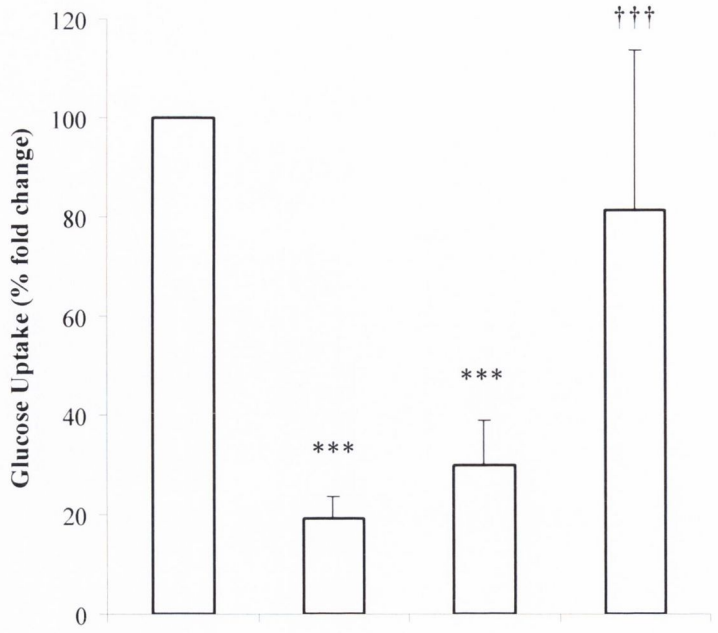

Insulin (100 nMol)	+	+	+	+
Adipocytes	+	+	+	+
LPS stimulated macrophage (CM)	-	+	+	+
EPA (50 μMol/L)	-	-	+	-
DHA (50 μMol/L)	-	-	-	+

Figure 6.17 Long-term (48 hour) effects of conditioned media from LPS stimulated macrophages (CM) pre-treated with EPA and DHA on insulin induced glucose uptake in 3T3-L1 adipocytes. J774.2 macrophages were treated with 50 μMol/L EPA, DHA or DMSO vehicle control for 5 days prior to LPS stimulation (100 ng/ml) for 24 hours. The conditioned media (CM) was harvested and incubated with fully differentiated 3T3-L1 adipocytes for 48 hours. Cells were incubated in PBS with 0.2% BSA prior to addition of 100nM insulin in PBS for 15 minutes. 5 μCi/ml of ^{3}H glucose in 1 mMol glucose was added to the cells for 10 minutes. Cells were washed, lysed and assayed for ^{3}H uptake as counts per minute (CPMA). Insulin induced glucose uptake was established by subtracting total glucose uptake from basal glucose uptake. Data is expressed relative to insulin induced glucose uptake within 3T3-L1 adipocytes (100%) and presented as mean ± SEM, n = 4 - 8. *** $P \leq 0.001$ relative to adipocytes; ††† $P \leq 0.01$ relative to adipocytes co-cultured with CM of LPS stimulated macrophages pre-treated with DMSO. One-way ANOVA was performed within each group followed by post hoc LSD analysis

6.3.8 Effects of conditioned media from LPS stimulated macrophages (CM) pre-treated with EPA and DHA on 3T3-L1 adipocyte lipid accumulation and cell morphology

Lipid accumulation and cell morphology was examined within 3T3-L1 adipocytes incubated with CM from LPS stimulated J774.2 macrophages pre-treated with EPA, DHA and DMSO vehicle control as presented in figure 6.18, 6.19 and 6.20. Lipid accumulation was assessed using oil red O staining. For this analysis CM was harvested from macrophages pre-treated with EPA, DHA or vehicle control and stimulated with LPS for 24 hours. CM was then incubated with mature differentiated 3T3-L1 adipocytes for 48 hours. Lipid accumulation was significantly reduced 20% in adipocytes incubated with CM for 48 hours ($P \leq 0.001$ consistently; Figure 6.18). EPA and DHA pre-treatment of the LPS stimulated macrophages did not attenuate the reduction in lipid accumulation induced by CM. A similar trend is observed in the oil red O images as shown in Figure 6.19. Adipocytes treated with CM for 48 hours appear to have reduced lipid droplet accumulation with reduced differentiation as suggested by the elongated and fibroblast-like shape of the adipocytes. The images within Figure 6.20 suggest that lipid accumulation and differentiation of the adipocytes reduces over time during incubation with the CM. Interestingly, adipocytes treated with the CM of LPS stimulated macrophages pre-treated with EPA for 24 hours retained their mature adipocyte round structure however, after 48 hours these adipocytes develop a more fibroblast-like shape. Additionally, adipocytes incubated with the CM of LPS stimulated macrophages pre-treated with DHA for 48 hours appear to recover and develop a rounder more mature morphology.

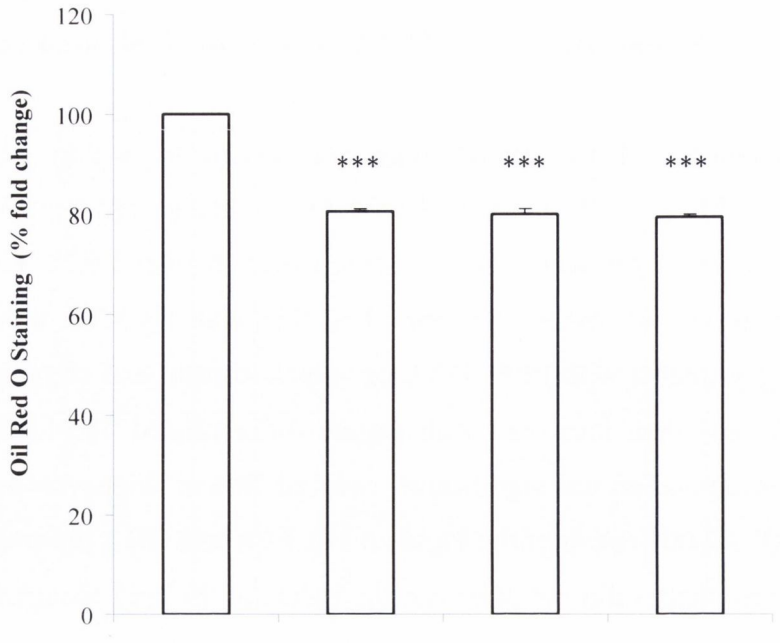

Adipocytes	+	+	+	+
LPS stimulated macrophage (CM)	-	+	+	+
EPA (50 μMol/L)	-	-	+	-
DHA (50 μMol/L)	-	-	-	+

Figure 6.18 Effects of conditioned media from LPS stimulated macrophages (CM) pre-treated with EPA and DHA on lipid accumulation within 3T3-L1 adipocytes. J774.2 macrophages were treated with 50 μMol/L EPA, DHA or DMSO vehicle control for 5 days prior to LPS stimulation (100 ng/ml) for 24 hours. The conditioned media (CM) was harvested and incubated with fully differentiated 3T3-L1 adipocytes for 48 hours. After CM treatment adipocytes were fixed in 10% neutral buffered formalin and stained with oil red O. 100% isopropanol was used to extract oil red O from the adipocytes and optical density measured at 500nm. Data is presented as percentage fold change relative to 3T3-L1 adipocytes (100%); mean ± SEM, n = 2. *** $P \leq 0.001$ relative to adipocytes. One-way ANOVA was performed within each group followed by post hoc LSD analysis.

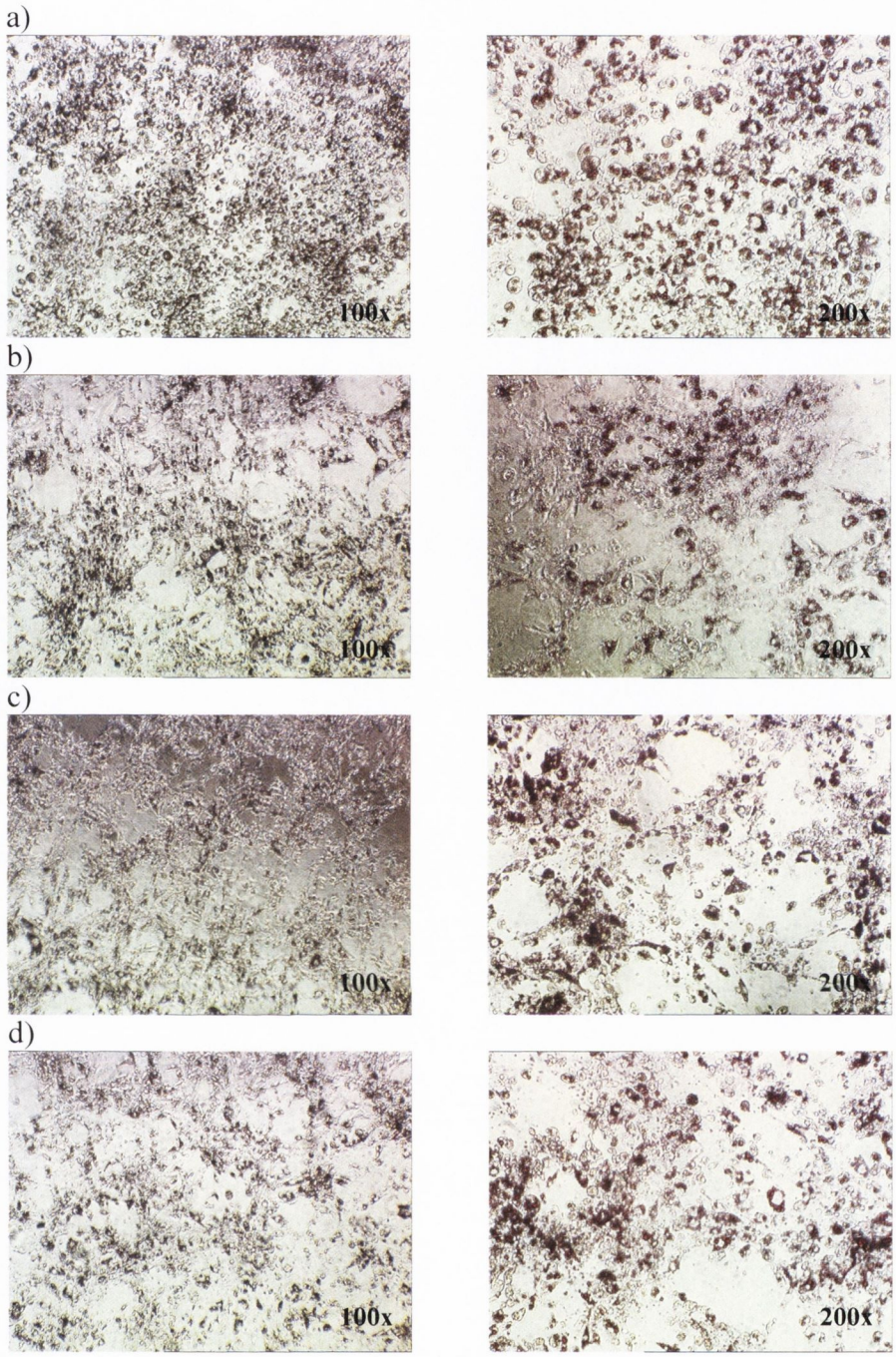

Figure 6.19 Effects of conditioned media from LPS stimulated macrophages (CM) pre-treated with EPA and DHA on lipid accumulation within 3T3-L1 adipocytes at 48 hours post incubation. J774.2 macrophages were treated with 50 μMol/L EPA, DHA or DMSO vehicle control for 5 days prior to LPS stimulation (100 ng/ml) for 24 hours. The conditioned media (CM) was harvested and incubated with fully differentiated 3T3-L1 adipocytes for 48 hours. Oil red O staining was used to stain accumulated lipids within the adipocytes. Images show adipocytes alone (a), adipocytes incubated with CM of LPS stimulated macrophages pre-treated with DMSO (b), adipocytes incubated with CM of LPS stimulated macrophages pre-treated with EPA (c), adipocytes incubated with CM of LPS stimulated macrophages pre-treated with DHA (d; 100x and 200x magnification)

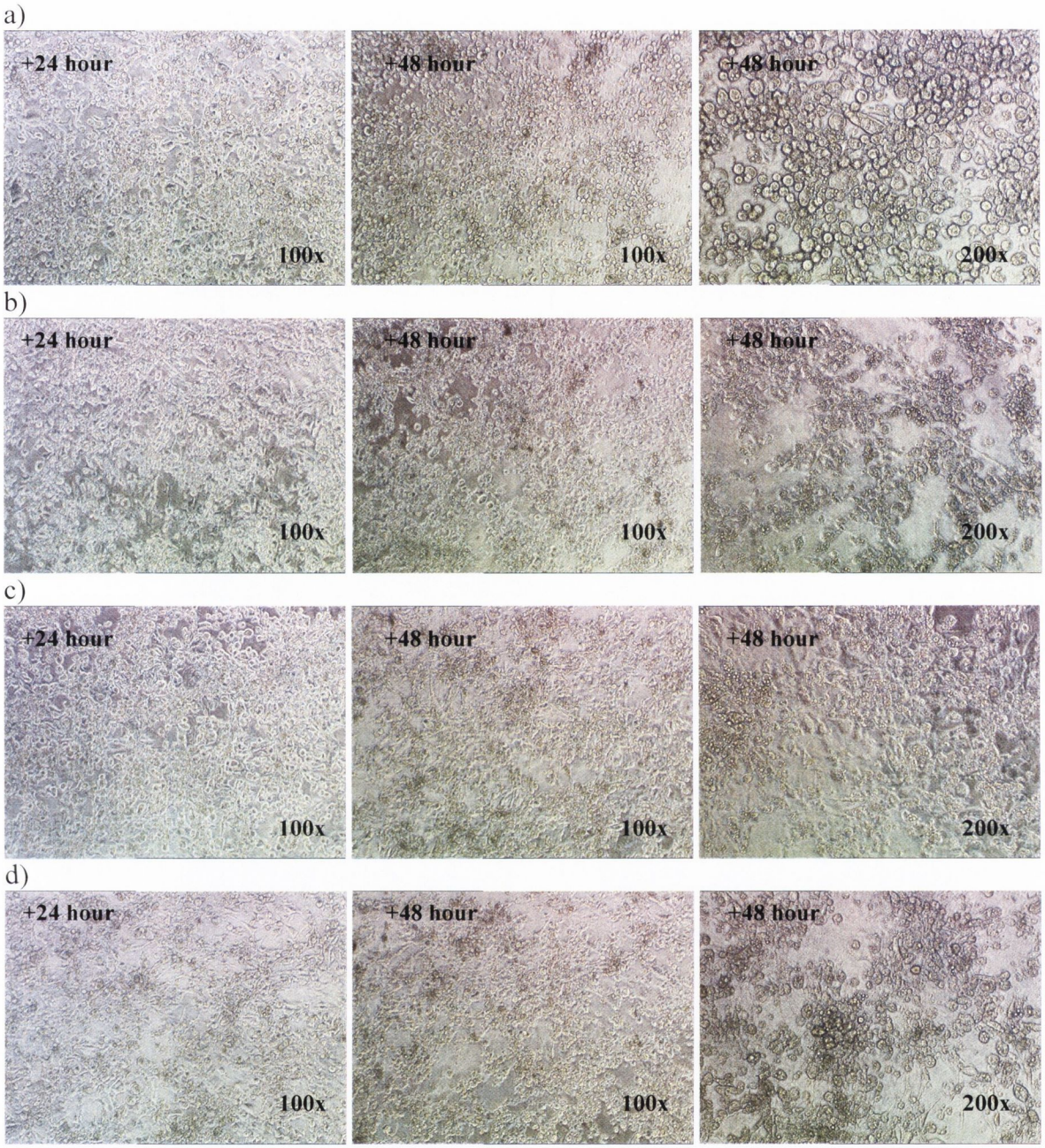

Figure 6.20 Effects of conditioned media from LPS stimulated macrophages (CM) pre-treated with EPA and DHA on 3T3-L1 adipocytes morphology at 24 and 48 hours post incubation. J774.2 macrophages were treated with 50mMol/L EPA, DHA or DMSO vehicle control for 5 days prior to LPS stimulation (100ng/ml) for 24 hours. The conditioned media (CM) was harvested and incubated with fully differentiated 3T3-L1 adipocytes for 24 (right) and 48 hours (centre and left). Images show adipocytes alone (a), adipocytes incubated with CM of LPS stimulated macrophages pre-treated with DMSO (b), adipocytes incubated with CM of LPS stimulated macrophages pre-treated with EPA (c), adipocytes incubated with CM of LPS stimulated macrophages pre-treated with DHA (d; 100x and 200x magnification)

6.3.9 Effects of conditioned media from LPS stimulated macrophages (CM) pre-treated with EPA and DHA on MAPK protein expression in 3T3-L1 adipocytes

ERK1, phosphorylated ERK1/2 (Thr202/Tyr204), p38, phosphorylated p38 (Thr180/Tyr182) JNK1 and phosphorylated JNK (T183/Y185) protein expression was measured in 3T3-L1 adipocytes treated with the CM of LPS stimulated J774.2 macrophages pre-treated with EPA, DHA and DMSO vehicle control for 30 minutes as presented in Figures 6.21, 6.22, 6.23, 6.24, 6.25 and 6.26 respectively.

Total ERK1 was subtlety increased in adipocytes incubated with the CM of LPS stimulated macrophages pre-treated with DMSO (8% increase) and EPA (9% increase) relative to adipocytes, although not significantly ($P \leq 0.110$ and $P \leq 0.063$; Figure 2.21). EPA pre-treatment of the macrophages prior to incubation with the adipocytes did not modulate ERK1 protein expression relative to adipocytes alone. Although ERK1 was reduced significantly in adipocytes incubated with LPS stimulated macrophages pre-treated with DHA (10% decrease) relative to adipocytes incubated with CM of LPS stimulated macrophages pre-treated with DMSO ($P \leq 0.031$). ERK1/2 phosphorylation was significantly increased 2.3 fold in adipocytes incubated with CM of LPS stimulated macrophages pre-treated with vehicle control relative to adipocytes alone ($P \leq 0.001$; Figure 2.22). ERK1/2 phosphorylation was also significantly increased 2.0 and 1.9 fold in adipocytes incubated with CM of LPS stimulated macrophages pre-treated with EPA and DHA relative to adipocytes ($P \leq 0.001$ and $P \leq 0.001$). Interestingly, ERK1/2 phosphorylation was significantly reduced in adipocytes incubated with CM of LPS stimulated macrophages pre-treated with EPA (13% decrease) and DHA (19% decrease) relative to adipocytes incubated with CM of LPS stimulated macrophages pre-treated with DMSO ($P \leq 0.001$ and $P \leq 0.001$).

Total p38 MAPK was not significantly regulated in adipocytes treated with the CM of LPS stimulated macrophages (Figure 2.23). However, there was a trend towards an increase in p38 in adipocytes incubated with the CM of LPS stimulated macrophages pre-treated with DMSO relative to adipocytes. While total p38 was reduced in adipocytes incubated with CM of LPS stimulated macrophages pre-treated with EPA and DHA. p38 MAPK phosphorylation was increased 3.0 fold in adipocytes incubated with the CM of LPS stimulated macrophages pre-treated with DMSO relative to adipocytes ($P \leq 0.001$; Figure 2.24). p38 phosphorylation was also significantly increased in adipocytes incubated with CM of LPS stimulated macrophages pre-treated with EPA (2.5 fold increase) and DHA (2.3 fold increase) relative to adipocytes ($P \leq 0.001$ and $P \leq 0.001$). Interestingly, p38 phosphorylation was significantly reduced in adipocytes incubated with CM of LPS

stimulated macrophages pre-treated with EPA (17% reduced) and DHA (22% reduced) relative to adipocytes incubated with CM of LPS stimulated macrophages pre-treated with DMSO ($P \leq 0.001$ and $P \leq 0.001$).

Total JNK1 protein expression was not significantly regulated in adipocytes incubated with CM of LPS stimulated macrophages pre-treated with DMSO vehicle control. However, total JNK1 expression was reduced in adipocytes incubated with LPS stimulated macrophages pre-treated with EPA (5% decrease) or DHA (14% decrease) relative to adipocytes ($P \leq 0.056$ and $P \leq 0.001$). Additionally, total JNK1 expression was reduced in adipocytes incubated with LPS stimulated macrophages pre-treated with DHA (12% decrease) relative to adipocytes incubated with LPS stimulated macrophages pre-treated with vehicle control ($P \leq 0.001$). JNK1/2 phosphorylation was not significantly modulated in adipocytes incubated with CM of LPS stimulated macrophages pre-treated with DMSO relative to adipocytes. Interestingly, JNK1/2 phosphorylation was significantly reduced in adipocytes incubated with CM of LPS stimulated macrophages pre-treated with EPA (22% and 18% decrease) and DHA (50% and 53% decrease) relative to both adipocytes ($P \leq 0.008$ and $P \leq 0.001$) and adipocytes incubated with CM of LPS stimulated macrophages pre-treated with DMSO ($P \leq 0.025$ and $P \leq 0.001$).

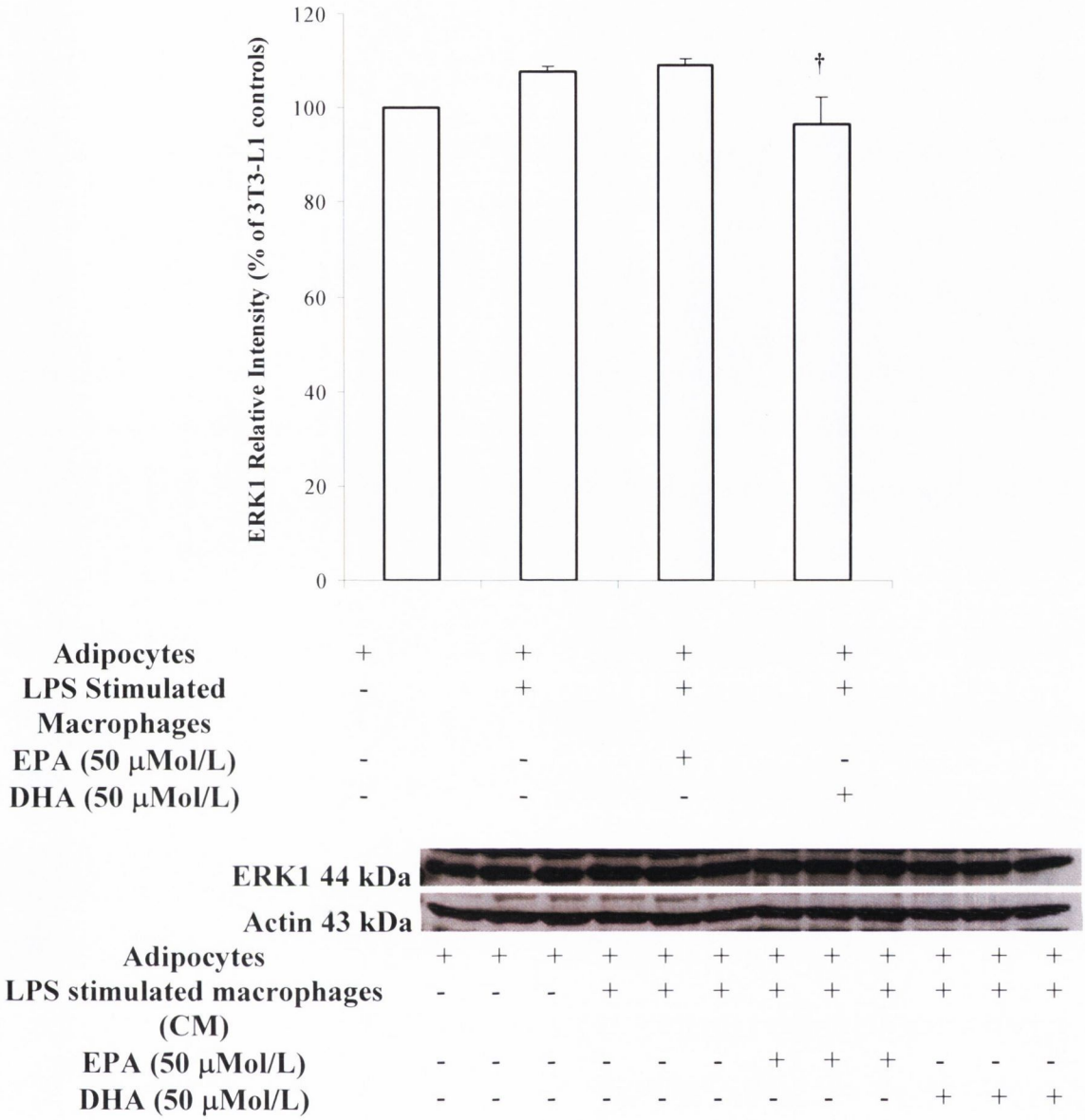

Figure 6.21 Effects of conditioned media from LPS stimulated macrophages (CM) pre-treated with EPA and DHA on ERK1 protein expression within 3T3-L1 adipocytes. J774.2 macrophages were treated with 50 μMol/L EPA, DHA or DMSO vehicle control for 5 days prior to LPS stimulation (100 ng/ml) for 24 hours. The conditioned media (CM) was harvested and incubated with fully differentiated 3T3-L1 adipocytes for 30 minutes. Whole cell lysates were prepared for SDS-PAGE and immunoblotting. The relative protein levels were quantified by densitometry and data expressed relative to the amount of ERK1 within adipocytes alone (100%), data is presented as mean ± SEM, n = 3. † $P \leq 0.05$ relative to adipocytes co-cultured with CM of LPS stimulated macrophages pre-treated with DMSO. One-way ANOVA was performed within each group followed by post hoc LSD analysis.

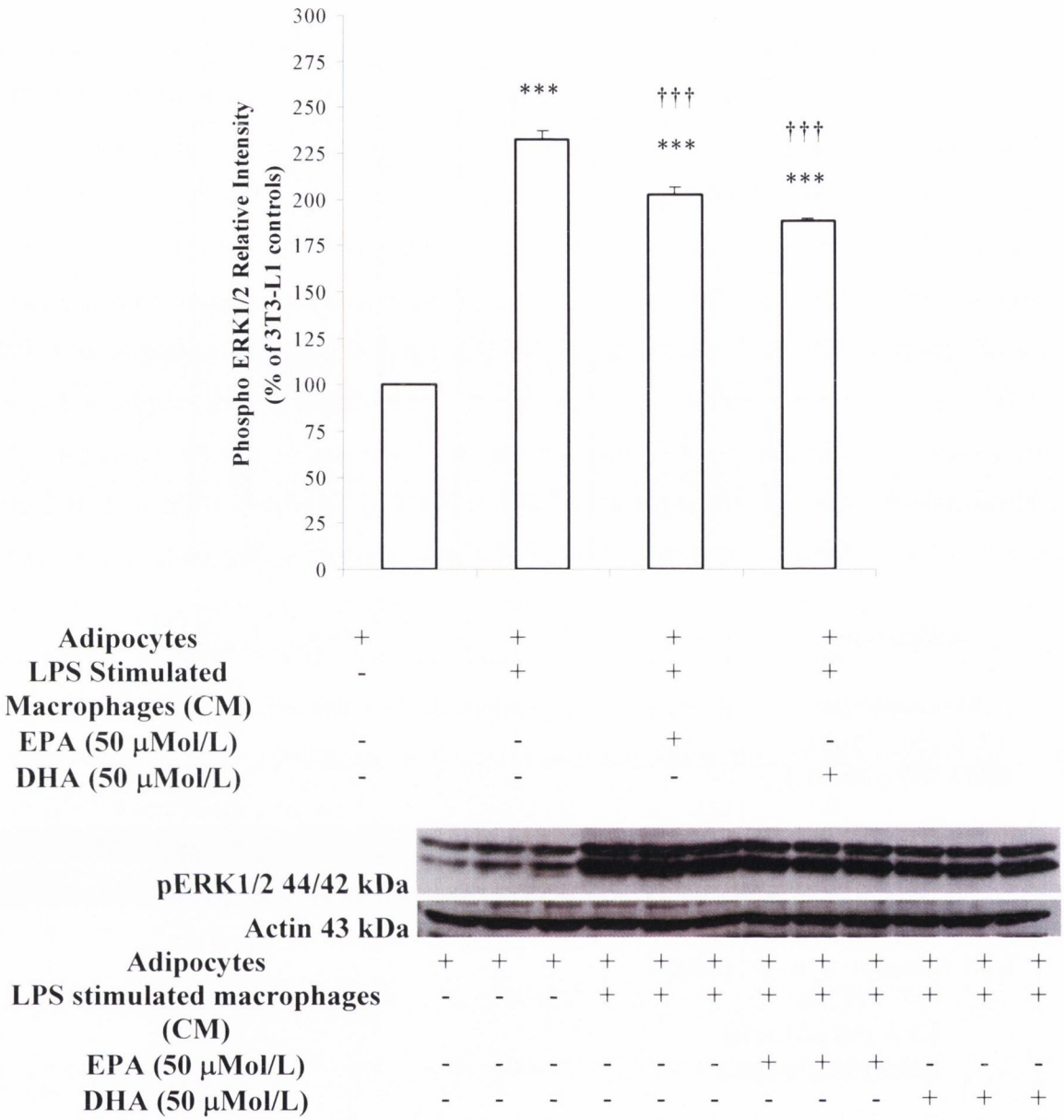

Figure 6.22 Effects of conditioned media from LPS stimulated macrophages (CM) pre-treated with EPA and DHA on phosphorylated ERK1/2 (Thr202/Tyr204) protein expression within 3T3-L1 adipocytes. J774.2 macrophages were treated with 50 μMol/L EPA, DHA or DMSO vehicle control for 5 days prior to LPS stimulation (100 ng/ml) for 24 hours. The conditioned media (CM) was harvested and incubated with fully differentiated 3T3-L1 adipocytes for 30 minutes. Whole cell lysates were prepared for SDS-PAGE and immunoblotting. The relative protein levels were quantified by densitometry and data expressed relative to the amount of phosphorylated ERK1/2 within adipocytes alone (100%), data is presented as mean ± SEM, n = 3. *** $P \leq 0.001$ relative to adipocytes. ††† $P \leq 0.001$ relative to adipocytes co-cultured with CM of DMSO treated LPS stimulated macrophages. One-way ANOVA was performed within each group followed by post hoc LSD analysis.

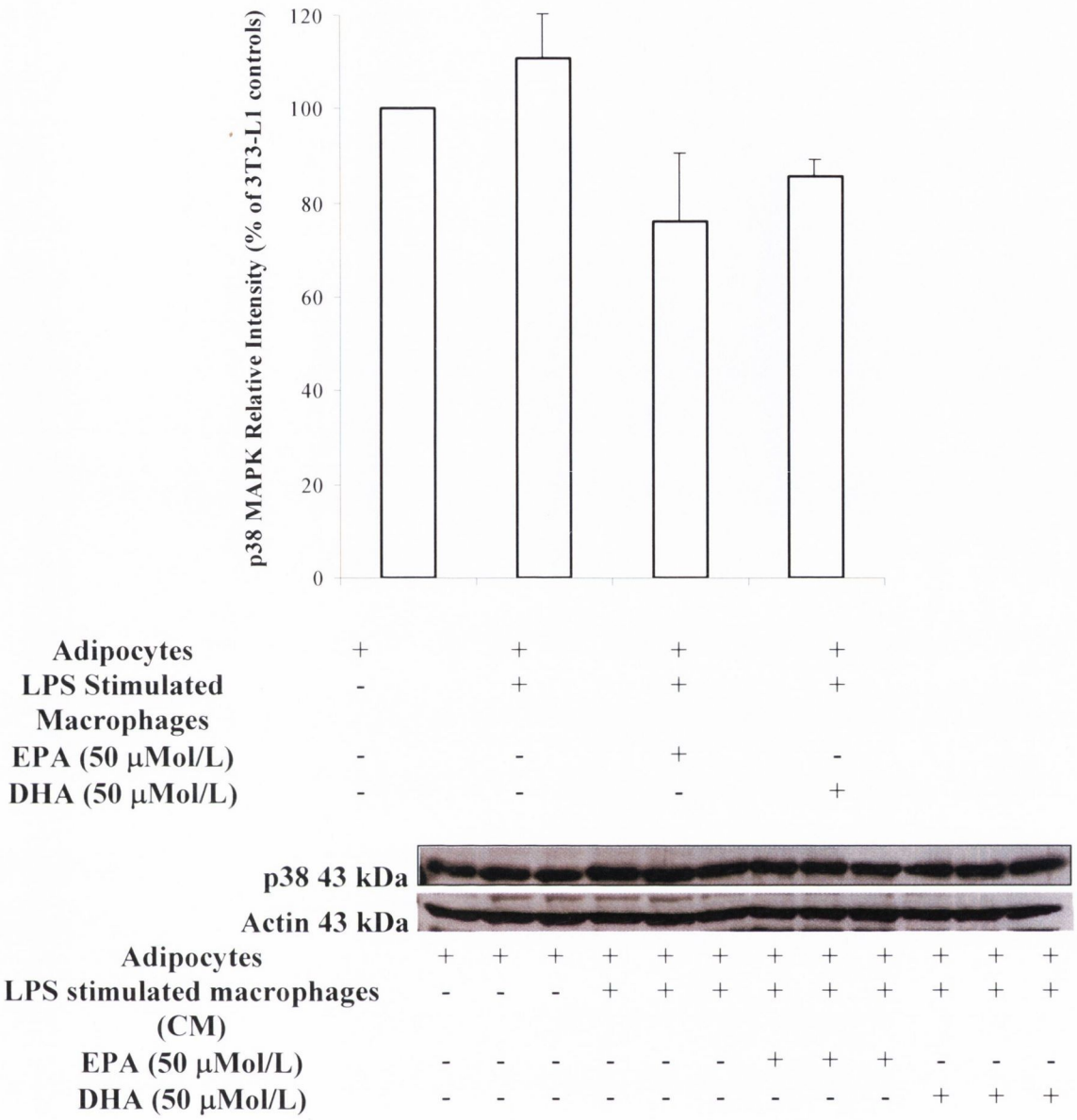

Figure 6.23 Effects of conditioned media from LPS stimulated macrophages (CM) pre-treated with EPA and DHA on p38 protein expression within 3T3-L1 adipocytes. J774.2 macrophages were treated with 50 μMol/L EPA, DHA or DMSO vehicle control for 5 days prior to LPS stimulation (100 ng/ml) for 24 hours. The conditioned media (CM) was harvested and incubated with fully differentiated 3T3-L1 adipocytes for 30 minutes. Whole cell lysates were prepared for SDS-PAGE and immunoblotting. The relative protein levels were quantified by densitometry and data expressed relative to the amount of p38 within adipocytes alone (100%), data is presented as mean ± SEM, n = 3.

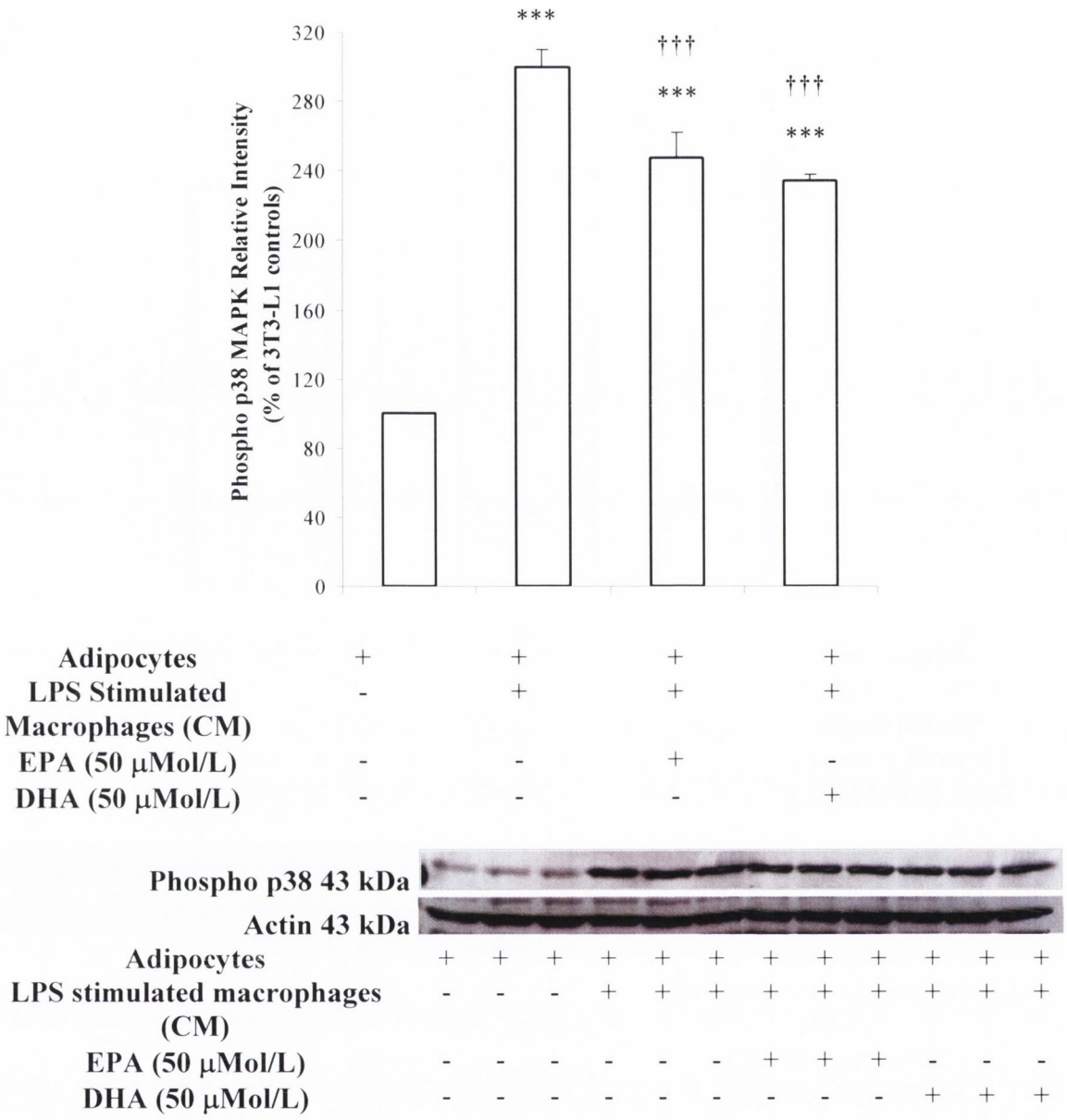

Figure 6.24 Effects of conditioned media from LPS stimulated macrophages (CM) pre-treated with EPA and DHA on phosphorylated p38 (Thr180/Tyr182) protein expression within 3T3-L1 adipocytes. J774.2 macrophages were treated with 50 μMol/L EPA, DHA or DMSO vehicle control for 5 days prior to LPS stimulation (100 ng/ml) for 24 hours. The conditioned media (CM) was harvested and incubated with fully differentiated 3T3-L1 adipocytes for 30 minutes. Whole cell lysates were prepared for SDS-PAGE and immunoblotting. The relative protein levels were quantified by densitometry and data expressed relative to the amount of phosphorylated p38 within adipocytes alone (100%), data is presented as mean ± SEM, n = 3. *** $P \leq 0.001$ relative to adipocytes. ††† relative to adipocytes co-cultured with CM of DMSO treated LPS stimulated macrophages. One-way ANOVA was performed within each group followed by post hoc LSD analysis.

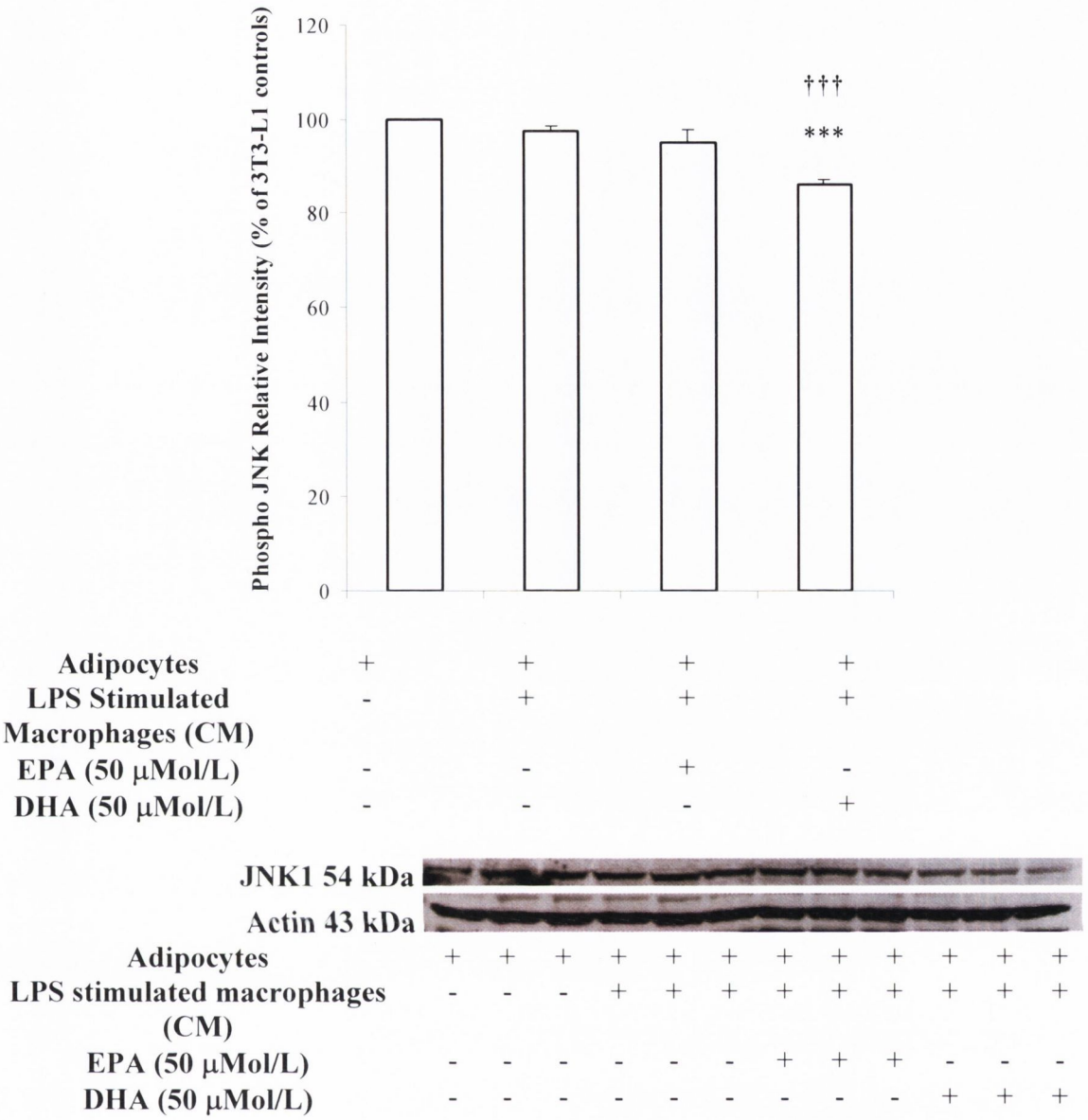

Figure 6.25 Effects of conditioned media from LPS stimulated macrophages (CM) pre-treated with EPA and DHA on JNK1 protein expression within 3T3-L1 adipocytes. J774.2 macrophages were treated with 50 μMol/L EPA, DHA or DMSO vehicle control for 5 days prior to LPS stimulation (100 ng/ml) for 24 hours. The conditioned media (CM) was harvested and incubated with fully differentiated 3T3-L1 adipocytes for 30 minutes. Whole cell lysates were prepared for SDS-PAGE and immunoblotting. The relative protein levels were quantified by densitometry and data expressed relative to the amount of JNK1 within adipocytes alone (100%), data is presented as mean ± SEM, n = 3. *** $P \leq 0.001$ relative to adipocytes. ††† $P \leq 0.001$ relative to adipocytes co-cultured with CM of DMSO treated LPS stimulated macrophages. One-way ANOVA was performed within each group followed by post hoc LSD analysis.

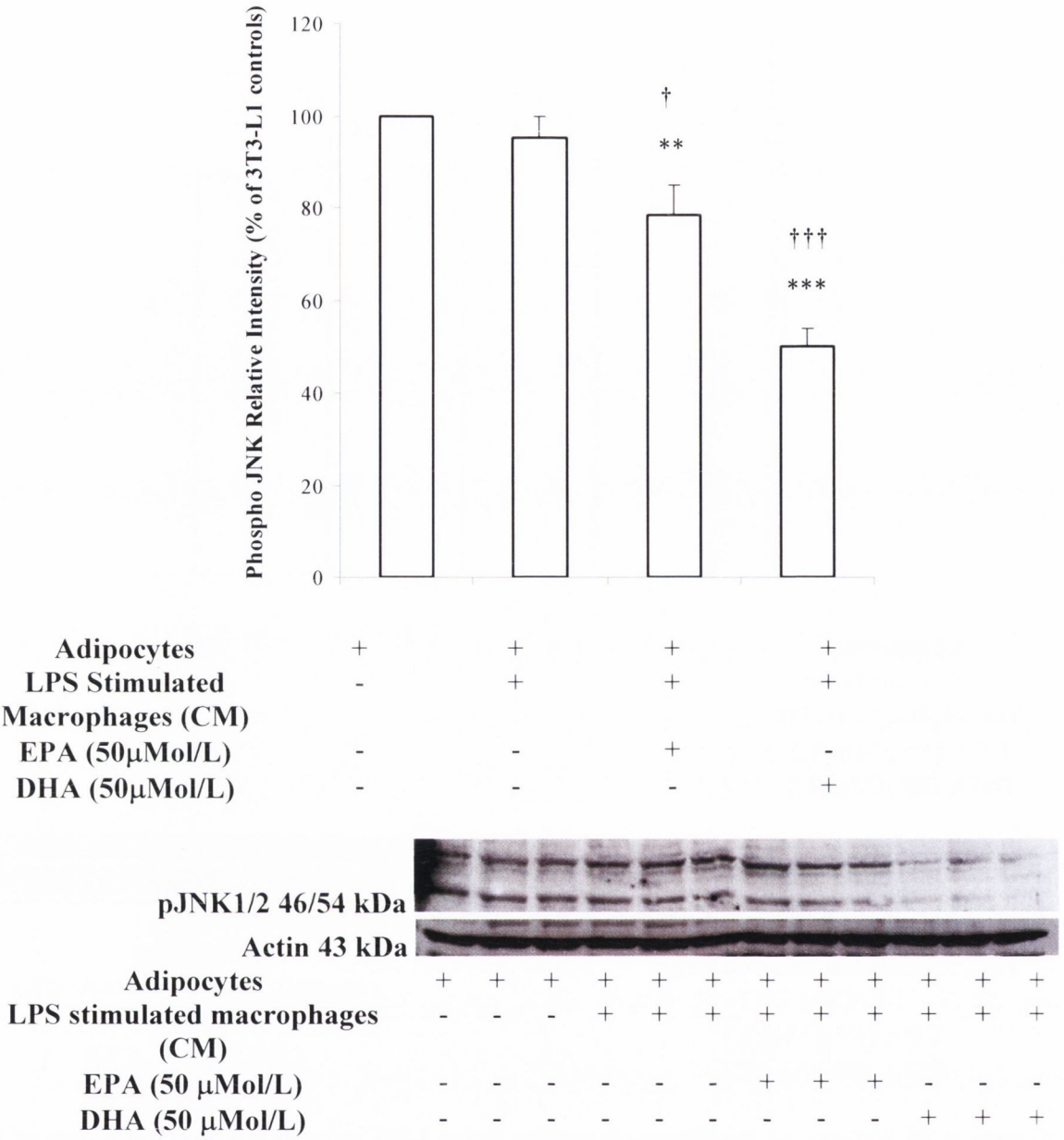

Figure 6.26 Effects of conditioned media from LPS stimulated macrophages (CM) pre-treated with EPA and DHA on phosphorylated JNK1/2 (T183/Y185) protein expression within 3T3-L1 adipocytes. J774.2 macrophages were treated with 50 μMol/L EPA, DHA or DMSO vehicle control for 5 days prior to LPS stimulation (100 ng/ml) for 24 hours. The conditioned media (CM) was harvested and incubated with fully differentiated 3T3-L1 adipocytes for 30 minutes. Whole cell lysates were prepared for SDS-PAGE and immunoblotting. The relative protein levels were quantified by densitometry and data expressed relative to the amount of phosphorylated JNK1/2 within adipocytes alone (100%), data is presented as mean ± SEM, n = 3. *** $P \leq 0.001$, ** $P \leq 0.01$ relative to adipocytes; † $P \leq 0.05$, ††† relative to adipocytes co-cultured with CM of DMSO treated LPS stimulated macrophages. One-way ANOVA was performed within each group followed by post hoc LSD analysis.

6.3.10 Effects of conditioned media from LPS stimulated macrophages (CM) pre-treated with EPA and DHA on IκB-α protein expression in 3T3-L1 adipocytes

IκB-α and phosphorylated IκB-α (Ser32) protein expression was measured in 3T3-L1 adipocytes treated with the CM of LPS stimulated J774.2 macrophages pre-treated with EPA, DHA and DMSO vehicle control for 30 minutes as presented in Figures 6.27 and 6.28. Total IκB-α was significantly reduced in adipocytes incubated with the CM of LPS stimulated macrophages pre-treated with DMSO (38% reduced) relative to adipocytes alone ($P \leq 0.001$; Figure 6.27). Similarly, Total IκB-α protein expression was also significantly reduced in adipocytes incubated with the CM of LPS stimulated macrophages pre-treated with EPA (47% reduced) and DHA (32% reduced) relative to adipocytes ($P \leq 0.001$ and $P \leq 0.001$). There was no significant increased in IκB-α expression within adipocytes incubated with LPS stimulated macrophages pre-treated with EPA and DHA relative to adipocytes incubated with LPS stimulated pre-treated with vehicle control ($P \leq 0.234$ and $P \leq 0.381$).

IκB-α phosphorylation was increased 8.1 fold in adipocytes incubated with the CM of LPS stimulated macrophages pre-treated with DMSO relative to adipocytes ($P \leq 0.001$; Figure 6.28). IκB-α phosphorylation was also increased in adipocytes incubated with CM of LPS stimulated macrophages pre-treated with EPA (10.4 fold increase) and DHA (6.3 fold increase) relative to adipocytes alone ($P \leq 0.001$ and $P \leq 0.001$). IκB-α phosphorylation was increased 28% in adipocytes incubated with CM of LPS stimulated macrophages pre-treated with EPA relative to adipocytes incubated with the CM of LPS stimulated macrophages pre-treated with DMSO, although not significantly ($P \leq 0.066$). Conversely, IκB-α phosphorylation was reduced 23% in adipocytes incubated with CM of LPS stimulated macrophages pre-treated with DHA relative to adipocytes incubated with the CM of LPS stimulated macrophages pre-treated with DMSO, although not significantly ($P \leq 0.128$).

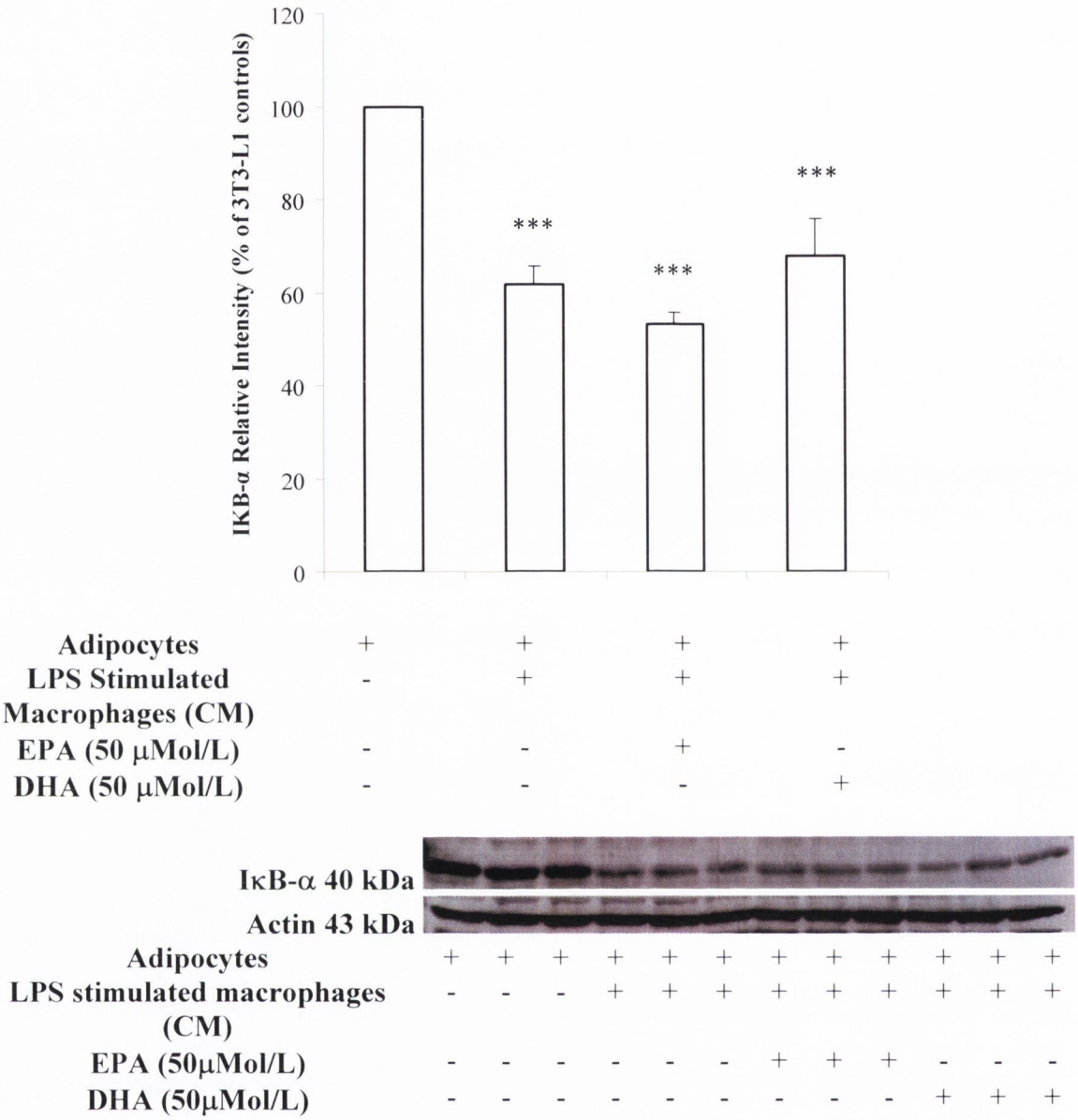

Figure 6.27 Effects of conditioned media from LPS stimulated macrophages (CM) pre-treated with EPA and DHA on IκB-α protein expression within 3T3-L1 adipocytes. J774.2 macrophages were treated with 50 μMol/L EPA, DHA or DMSO vehicle control for 5 days prior to LPS stimulation (100 ng/ml) for 24 hours. The conditioned media (CM) was harvested and incubated with fully differentiated 3T3-L1 adipocytes for 30 minutes. Whole cell lysates were prepared for SDS-PAGE and immunoblotting. The relative protein levels were quantified by densitometry and data expressed relative to the amount of IκB-α within adipocytes alone (100%), data is presented as mean ± SEM, n = 3. *** $P \leq 0.001$ relative to adipocytes. One-way ANOVA was performed within each group followed by post hoc LSD analysis.

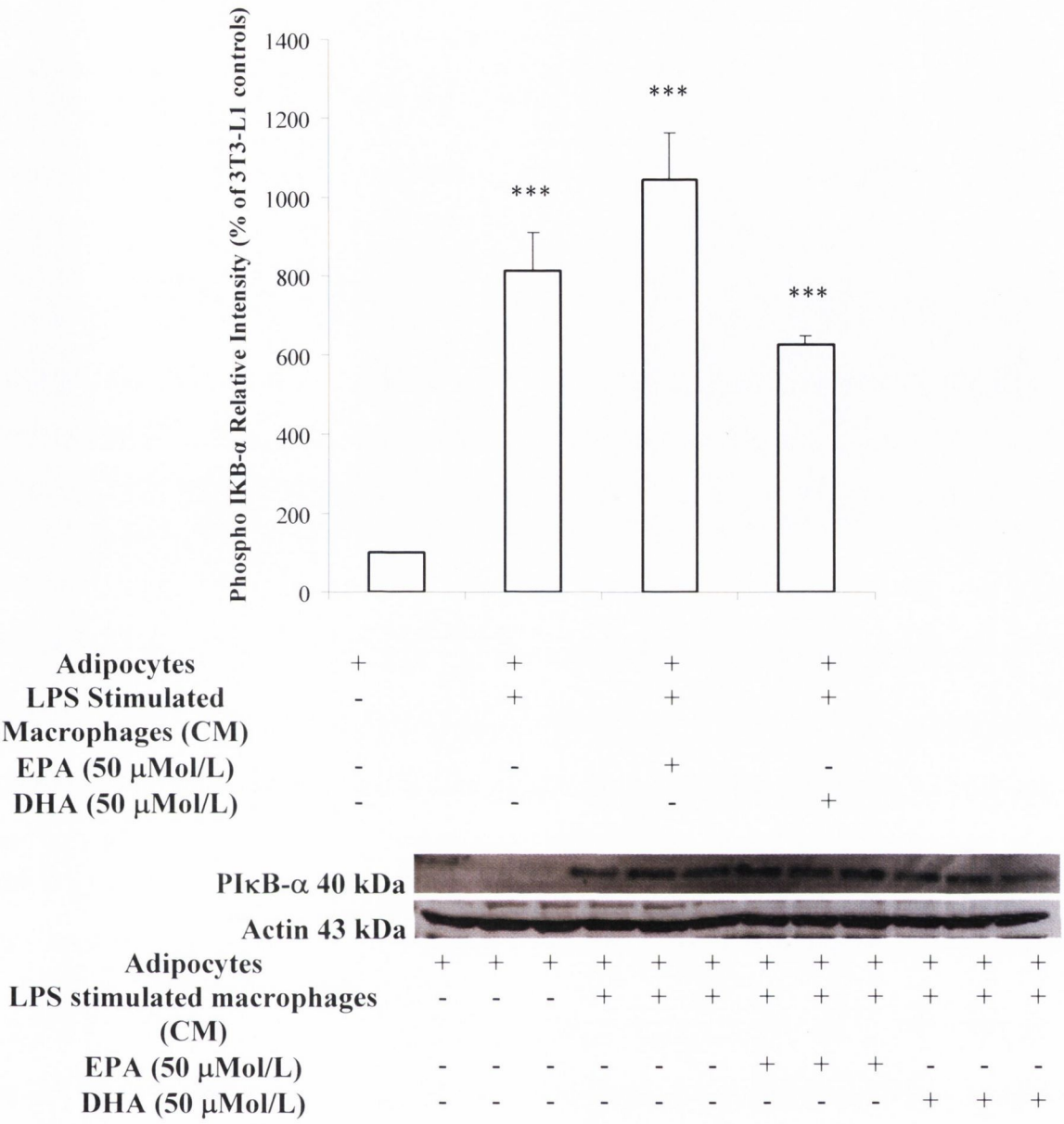

Figure 6.28 Effects of conditioned media from LPS stimulated macrophages (CM) pre-treated with EPA and DHA on phosphorylated IκB-α (Ser32) protein expression within 3T3-L1 adipocytes. J774.2 macrophages were treated with 50 μMol/L EPA, DHA or DMSO vehicle control for 5 days prior to LPS stimulation (100 ng/ml) for 24 hours. The conditioned media (CM) was harvested and incubated with fully differentiated 3T3-L1 adipocytes for 30 minutes. Whole cell lysates were prepared for SDS-PAGE and immunoblotting. The relative protein levels were quantified by densitometry and data expressed relative to the amount of phosphorylated IKB-α within adipocytes alone (100%), data is presented as mean ± SEM, n = 3. *** $P \leq 0.001$ relative to adipocytes. One-way ANOVA was performed within each group followed by post hoc LSD analysis.

6.4 Discussion

In this study, presence of macrophage-derived soluble factors were found to promote a pro-inflammatory environment within adipocytes in which inflammatory pathways such as NF-κB and MAPK became up regulated. This inflammation leads to a down regulation of insulin sensitive markers such as GLUT4 and IRS-1 causing insulin-resistant adipocyte function. Pre-treatment of the macrophages with EPA and DHA prior to co-culture partially attenuated the inflammation and insulin resistance within the adipocytes.

Initially fatty acid composition was assessed to ensure that exogenous fatty acids were incorporated into macrophages treated with EPA and DHA. EPA treatment increased EPA and DHA levels. Additionally, DPA levels were increase within EPA treated macrophages. DHA treatment significantly increased EPA and DHA. Essentially, EPA concentrations were increased 8 fold in macrophages treated with EPA while DHA concentrations were increased 11 fold in DHA treated macrophages suggesting direct incorporation of the fatty acids into the macrophages. The lower levels of EPA relative to DHA within the LC *n-3* PUFA treated macrophages may indicate that EPA is being utilized in the metabolism of eicosanoids. However, total *n-3* PUFA levels were significantly increased within EPA and DHA treated macrophages relative to control macrophages. However, this data also suggests there was conversion between EPA to DHA occurring within the J774.2 macrophages.

Interestingly, this significantly correlates with a study conducted by Leslie *et al.* (Leslie *et al.*, 1985). Within this study fatty acid composition of macrophage phospholipids were assessed from mice fed a standard diet supplied with either fish oil (17% EPA, 12% DHA, 0% AA and 2% linoleic acid) or corn oil (0% EPA, 0% DHA, 0% AA, and 65% linoleic acid) (Leslie *et al.*, 1985). Mice fed a chow diet showed similar phospholipid profiles to mice fed a corn oil diet. However, after 1 week on the fish oil diet, the macrophage phospholipids contained EPA (4%) and DHA (10%) as well as significant quantities of DPA (10%) as observed in the J774.2 macrophages treated with EPA. Only mice receiving fish oil in their diet had significant quantities of DPA in their phospholipid pool. Trace amount were detected in the phospholipid pool of chow-fed mice and none was detected in the corn oil-fed mice. Since DPA was present only in small quantities in the fish oil diet, it must have be derived from the LC *n-3* PUFA, perhaps by chain elongation of EPA (Leslie *et al.*, 1985). The DHA present in the macrophages of fish oil-fed mice must also be either incorporated directly from the fish oil diet or by further desaturation of DPA (Leslie *et al.*, 1985). Therefore, it also seems likely that EPA is converted to either

DPA though chain elongation or to DHA through desaturation of DPA within the J774.2 macrophages.

Furthermore, there also appears to be conversion of DHA to EPA within the J774.2 macrophages. In isolated rat liver cell retroconversion of DHA to EPA was observed via β-oxidation (Gronn *et al.*, 1991). Retroconversion of DHA to EPA has also been observed in the tumors of rats fed diets rich in DHA (Nasrollahzadeh *et al.*, 2008). Additionally, Vidgren *et al.* (1997) examined the effects of LC *n-3* PUFA supplementation in the form of fresh fish, fish oil and DHA oil on the fatty acid composition of plasma lipid fractions in addition to platelets and erythrocyte membranes of young healthy males (Vidgren *et al.*, 1997). As expected LC *n-3* PUFA supplementation increased the amounts of LC *n-3* PUFA and reduced LC *n-6* PUFA significantly in plasma, platelets and erythrocytes. Importantly, they observed that the proportion of EPA in plasma, platelets and erythrocyte membranes was increased by DHA supplementation (Vidgren *et al.*, 1997). These results suggest retroconversion of DHA to EPA is possible within mammals.

Within this study the increase in *n-3* PUFA coincided with a displacement of *n-6* PUFA such as linoleic acid and eicosatrienoic acid levels within the J774.2 macrophages pre-treated with EPA and DHA. This was also observed in the studies by Leslie *et al.* (Leslie *et al.*, 1985) and Vidgren *et al.* (Vidgren *et al.*, 1997). Increased consumption of these LC *n-3* PUFA results in their incorporation into inflammatory cell phospholipids which occurs in a dose-response fashion and is partly at the expense of AA and other *n-6* PUFA (Calder, 2009). Chronic DHA treatment of the macrophages reduced *n-3* (α-Linolenic acid) and *n-9* (gondoic acid) PUFA concentrations suggesting DHA may interfere with linoleic and gondoic acid metabolism specifically. Chronic EPA and DHA treatment also significantly reduced myristate concentrations within the macrophages, however total SFA concentrations were not significantly altered in macrophages treated with LC *n-3* PUFA. MUFA such as palmitoleic acid and oleic acid were significantly displaced or reduced in EPA and DHA pre-treated macrophages leading to a significant total reduction in MUFA concentrations. Therefore, increased incorporation and production of EPA, DHA and DPA within J774.2 macrophages treated with LC *n-3* PUFA may have inhibited production of other fatty acids such as the SFA and MUFA through competitive inhibition of the enzymes.

Fatty acid composition was also analysed within 3T3-L1 adipocytes co-cultured with J774.2 macrophages pre-treated with EPA and DHA. In contrast to the LC *n-3* PUFA treated macrophages total SFA concentrations (palmitic acid and stearic acid) were significantly increased in adipocytes co-cultured with macrophages. Although the DMEM

media contained no fatty acids it is possible that the FBS used within the media acts as a source of fatty acids. It is therefore possible that presence of macrophages increased uptake of SFA within adipocytes from the media. However, FBS has been shown to contain high levels of linoleic acid (Stoll and Spector, 1984), which was not significantly increased within the adipocytes and was significantly reduced within the macrophages treated with LC *n-3* PUFA suggesting uptake of fatty acids from the FBS is not significant within this model. Therefore, it seems likely that fatty acid synthesis is up-regulated within adipocytes co-cultured with macrophages perhaps because of increased enzymatic activities of FAS to produce palmitic acid. Beyond the 16-C length of the palmitic acid fatty acid synthesis is mainly catalyzed by fatty acid elongases associated with the ER. ER enzymes lengthen fatty acids as well as dietary polyunsaturated fatty acids. It therefore seems likely the enzymatic activities of elongases are also increased to produce stearic acid. Protein expression of enzymes such as FAS could be assessed within adipocytes of the transwell co-culture model to address this hypothesis. Oil red O was examined with adipocytes incubated with the CM of LPS stimulated macrophages; lipid accumulation was significantly reduced and this effect was not attenuated by pre-treatment of the macrophages with LC *n-3* PUFA. This suggests the adipocytes are undergoing lipoysis of TAG through activation of lipases with release of FFA. The increased percentage of SFA could therefore be due to a loss of other lipids within the adipocytes.

Importantly, SFA are though to have inflammatory and insulin-antagonizing effects, which contribute to the development of metabolic syndrome. Mechanisms responsible for these unhealthy effects of SFA include: 1) accumulation of diacylglycerol and ceramide; 2) activation of NF-κB and MAPK with subsequent induction of inflammatory genes in white adipose tissue and immune cells; 3) decreased PPAR activation and adiponectin production, which decreases the oxidation of glucose and FA; and 4) recruitment of immune cells such as macrophages, neutrophils, and bone marrow-derived dendritic cells to WAT and muscle (Kennedy *et al.*, 2009). Therefore the increase in SFA observed within adipocytes co-cultured with macrophages may cause inflammation and a reduction in insulin sensitivity within adipocytes. Additionally, Suganami *et al.* (2007) proposed that SFA released from hypertrophied adipocytes via the macrophage-induced adipocyte lipolysis, serve as a naturally occurring ligand for TLR4, thereby inducing the inflammatory changes in both adipocytes and macrophages through NF-κB and MAPK activation (Suganami et al., 2007b).

Total MUFA levels (palmitoleic acid) were significantly reduced in adipocytes co-cultured with macrophages. Interestingly, MUFA profiles of obese subjects showed a

significantly higher content of palmitoleic acid and oleic acid than in non-obese controls. Plasma palmitoleic acid content has a significant relation with abdominal adiposity in obese children (Okada *et al.*, 2005). Perhaps as obesity develops and macrophages infiltrate the adipose tissue this courses adipocytes to secrete MUFA raising plasma levels. Interestingly, *n-3* PUFA levels were significantly reduced in adipocytes co-cultured with macrophages. Although, *n-3* PUFA levels were not decreased in adipocytes co-cultured with macrophages pre-treated with DHA suggesting that DHA may have a protective effect on *n-3* PUFA synthesis within this system. Furthermore, the increased lipoysis induced by the presence of macrophages within adipocytes may have lead to a reduction in total MUFA or *n-3* PUFA. Alternatively, it is possible that increased production of SFA within the adipocytes co-cultured with macrophages may have inhibited production of other fatty acids such as the MUFA and *n-3* PUFA through competitive inhibition of the enzymes.

Inflammation was then assessed within the co-culture and CM experiments. Cytokine secretion and gene expression was determined within the supernatants and the adipocytes of the transwell co-culture respectively. TNF-α and IL-6 secretion were significantly increased within the co-culture of adipocytes and LPS stimulated macrophages. Interestingly, pre-treatment of the LPS stimulated macrophages with DHA significantly reduced TNF-α secretion within the co-culture while pre-treatment with EPA and DHA reduced IL-6 secretion within the co-culture. This suggests EPA and DHA pre-treatment of the macrophages prior to co-culture can attenuate the inflammatory phenotype induced by the macrophages within this model. Data from chapter 5 demonstrated that EPA and DHA can reduce cytokine secretion from J774.2 macrophages therefore supporting this concept. This data demonstrate that two closely related LC *n-3* PUFA differentially impact pro-inflammatory responses of J774.2 macrophages leading to differential effects in the 3T3-L1 adipocytes.

Importantly, IL-6 gene expression was significantly increased within the adipocytes co-cultured with LPS stimulated macrophages and reduced to normal levels in adipocytes co-cultured with LPS stimulated macrophages pre-treated with DHA. This suggests DHA pre-treatment of the macrophages attenuates the inflammatory effects induced by the macrophages within the adipocytes. However, this does not concur with the IL-6 secretion profiles in which LPS stimulated macrophages pre-treatment with both EPA and DHA attenuated IL-6 secretion from the 3T3-L1 adipocytes. This may indicate that DHA acts to modulate IL-6 gene expression through activation of transcription factors such as PPAR-γ while EPA may act post-transcriptionally through the regulation of proteins that control either translational initiation or mRNA stability. IL-1Ra mRNA expression was

significantly reduced in adipocytes co-cultured with LPS stimulated macrophages and increased in adipocytes co-cultured with LPS stimulated macrophages pre-treated with DHA. IL-1Ra inhibits IL-1 agonist binding to the IL-1 receptor therefore inhibiting IL-1 signalling. Therefore, the reduction in IL-1Ra may indicate an increase in IL-1 activity due to a decrease in the receptor antagonist. DHA pre-treatment of the macrophages prior to co-culture increased IL-1Ra levels perhaps reducing IL-1 signalling indicating that DHA has protective effects within this model of obesity. This data suggests that presence of LPS stimulated macrophages induces a pro-inflammatory environment within adipocytes, which is then attenuated by pre-treatment of the macrophages with LC *n-3* PUFA. This is further confirmed by evaluation of MAPK and NF-κB activity within 3T3-L1 adipocytes treated with the CM of LPS stimulated J774.2 macrophages pre-treated with EPA and DHA.

Total ERK1/2 and p38 expression was not increased within adipocytes incubated with the CM of LPS stimulated macrophages. However, ERK1/2 activation as determined by Threonine/Tyrosine phosphorylation at specific sites was significantly increased in adipocytes incubated with CM of LPS stimulated macrophages. Interestingly, pre-treated of the macrophages with EPA and DHA significantly reduced ERK1/2 phosphorylation and activation within the adipocytes. Similarly, Threonine/Tyrosine p38 phosphorylation was increased in adipocytes incubated with the CM of LPS stimulated macrophages. p38 MAPK phosphorylation was significantly reduced in adipocytes incubated with CM of LPS stimulated macrophages pre-treated with EPA and DHA. This data clearly demonstrates that pre-treatment of the macrophages with EPA and DHA prior to co-culture attenuates the activation of MAPK within adipocytes. ERK1/2 and p38 are activated by extracellular stimuli such as growth factors and cytokines (Foltz *et al.*, 1997; Lewis *et al.*, 1998; Raingeaud *et al.*, 1995). It is therefore probable that adipocytes ERK1/2 and p38 become activated by pro-inflammatory molecules secreted by the macrophages such as TNF-α and IL-6. The decreased activation of the MAPK molecules within adipocytes incubated with the CM of LPS stimulated macrophages pre-treated with LC *n-3* PUFA may be due to the reduction in cytokines associated with the EPA and DHA pre-treatment. Interestingly SFA, specifically palmitic acid which was significantly up-regulated within adipocytes co-cultured with the macrophages has been shown to activate MAPK signaling within 3T3-L1 adipocytes (Ajuwon and Spurlock, 2005). Therefore, increased SFA content of the adipocytes could lead to increased MAPK activation. However, there is no significant reduction in SFA content in adipocytes co-cultured with macrophages pre-

treated with LC *n-3* PUFA, therefore this does not explain the reduction in MAPK activity associated with the LC *n-3* PUFA pre-treatment.

Elevated activities of the MAPKs, ERK1/2, JNK1/2, and p38 are found in adipocytes of obese and insulin-resistant rodent and humans (Gual *et al.*, 2005) . Jager *et al.* (2007) established that pharmacological inhibition of the ERK pathway totally prevented a decrease in IRS-1 mRNA and partially prevented the inhibition of IRS-1 protein expression induced by IL-1β treatment in 3T3-L1 adipocytes (Jager *et al.*, 2007). This suggests ERK1/2 activity may play a critical role in IRS-1 reduction in obesity. In this study CM of LPS stimulated macrophages induced a significant increase in phosphorylated ERK1/2 protein expression in 3T3-L1 adipocytes, which may have induced the reduction in whole cell IRS-1 observed. Additionally, Carlson *et al.* (2003) observed that elevated MAPK activity with adipocytes from T2DM was associated with decreased IRS-1 and GLUT4 (Carlson *et al.*, 2003). Inhibition of the p38 pathway prevented the insulin-stimulated decrease in GLUT4 protein levels suggesting up-regulation of the p38 pathway might contribute to the loss of GLUT4 expression observed in adipose tissue from obese T2DM patients (Carlson *et al.*, 2003). Aouadi *et al.* (2006) determined that *in vitro* inhibition of p38 increased the expression of mature differentiated adipocyte markers. Furthermore, inhibition of p38 enhanced transcriptional activity of PPAR-γ and C/EBPβ suggest that p38 plays a negative role in adipogenesis via inhibition of PPAR-γ and C/EBPβ transcriptional activities (Aouadi *et al.*, 2006). Interestingly, in this study CM from LPS stimulated macrophages was observed to increase activation of p38 in the 3T3-L1 adipocytes, which correlated with an increase in lipolysis and a reduction in insulin sensitivity. Furthermore, EPA and DHA pre-treatment of the macrophages reduced p38 MAPK levels while insulin sensitivity was moderately improved.

Conversely, JNK activation was not increased within adipocytes incubated with the CM of LPS stimulated macrophages. This seems counterintuitive as JNK is activated, as are ERK1/2 and p38 by pro-inflammatory cytokines (Manning and Davis, 2003). It is possible that JNK phosphorylation may have occurred prior to the 30 minutes CM incubation or may have occurred subsequently; a time course may be necessary to capture JNK activation. However, total JNK and activated JNK were reduced in adipocytes incubated with the CM of LPS stimulated macrophages pre-treated with DHA relative to adipocytes alone. JNK is associated with IRS-1 and phosphorylates serine^{307} (Aguirre *et al.*, 2000; Aguirre *et al.*, 2002) leading to inhibition of the insulin signalling cascade. Therefore, the reduction in JNK activity observed in adipocytes incubated with the CM of LPS stimulated macrophages pre-treated with DHA may improve insulin sensitivity.

Total IκB-α was significantly reduced in adipocytes incubated with the CM of LPS stimulated macrophages, which correlates with a significant increase in IκB-α serine phosphorylation. These effects were not attenuated by pre-treatment of the macrophages with EPA and DHA. As discussed in chapter 4, in response to multiple stimuli such as inflammatory cytokines or stress, IkBs are phosphorylated on two critical serine residues. This modification triggers their ubiquitination and destruction via the proteasome degradation machinery. As a consequence, free NF-κB enters the nucleus and activates transcription of a variety of genes participating in immune and inflammatory responses, cell adhesion, growth control and regulation of apoptosis (Hayden and Ghosh, 2004; Karin and Ben-Neriah, 2000). Therefore, this data indicates that NF-κB activity and therefore inflammation is increased within adipocytes incubated with the CM, which is not attenuated by pre-incubation of the macrophages with EPA and DHA. It is probable that IKB-α became phosphorylated by cytokines secreted from the macrophages of the co-culture. However, SFA have also been shown to activate TLR signaling in murine adipocytes (Song *et al.*, 2006; Suganami *et al.*, 2007a; Suganami *et al.*, 2007b) leading to NF-κB and JNK activation with cytokine production. Consistent with these data, TLR4 knockout mice were protected against the adverse effects of feeding a HFD rich in Palmitic acid (Davis *et al.*, 2008). The increased production of SFA within the adipocytes co-cultured with the macrophages may have induced in part the NF-κB activation observed. Furthermore, SFA content was not reduced in adipocytes co-cultured with macrophages pre-treated with LC *n-3* PUFA consistent with the lack of attenuation of IKB-α phosphorylation.

After establishing the pro-inflammatory state of the adipocytes co-cultured in incubated with the CM of LPS stimulated macrophages pre-treated with LC *n-3* PUFA insulin sensitivity was assessed. Adipokine secretion was determined within the supernatants of co-culture adipocytes and macrophages. Interestingly, leptin secretion was significantly reduced in adipocytes co-cultured with LPS stimulated macrophages. This effect was not attenuated by pre-treatment of the macrophages with either EPA or DHA. Leptin is secreted from adipocytes and has been implicated in the regulation of food intake, energy expenditure and whole-body energy balance in rodents and humans. The *ob/ob* knockout mouse, which produces no leptin, has severe obesity. In both *ob/ob* and wild-type mice, leptin administration was observed to induced weight loss, which was restricted to the adipose tissue (Halaas *et al.*, 1997; Halaas *et al.*, 1995). The mice show decreased food intake with an elevated metabolic rate. Therefore, within the context of obesity a reduction

in leptin secretion from adipocytes due to macrophage infiltration in the adipose tissue, as our in vitro study suggests, could lead to increased food intake and a reduction in the energy metabolism.

In the fed, steady-state leptin expression and secretion reflect body fat mass in rodents and humans (Considine *et al.*, 1996; Frederich *et al.*, 1995; Maffei *et al.*, 1995) and are highly correlated with adipocyte size in lean and obese mice (Houseknecht *et al.*, 1996). However, more subtle changes in energy balance have profound effects on leptin expression. A 10% reduction in body weight in obese human subjects results in a 53% reduction in serum leptin (Considine *et al.*, 1996) and a 10% increase in body weight causes a 300% increase in serum leptin (Kolaczynski *et al.*, 1996b). *In vitro* Asada *et al.* (2001) studied the effects of human growth hormone (hGH) on leptin production and lipolysis stimulation in 3T3-L1-hGHR adipocytes, which efficiently express human growth hormone receptor. Importantly, they clarified that hGH decreases leptin secretion after hGH-induced lipolysis stimulation. This could indicate that an increase in lipolysis or drop in lipid accumulation could lead to a reduction in leptin secretion. Oil red O staining of 3T3-L1 adipocytes incubated with the media from LPS stimulated macrophages demonstrated that lipid content was significantly reduced suggesting an up-regulation in lipolysis. Consistent with the leptin data, lipid accumulation as shown by oil red O staining was not increased when macrophages are pre-treated with LC *n-3* PUFA.

Insulin signalling target gene and protein levels were also determined within the 3T3-L1 adipocytes of the co-culture and CM models. The presence of LPS stimulated macrophages for 24 hours significantly reduced IRS-1 mRNA within the co-cultured adipocytes. DHA pre-treatment of the LPS stimulated macrophages prior to co-culture significantly increase IRS-1 mRNA expression within the adipocytes. There was a similar trend in GLUT4 gene expression, although not significantly. At the protein expression level similar trends were observed. Whole cell IRS-1 was significantly reduced in adipocytes co-cultured for 24 hours with LPS stimulated macrophages. However, whole cell IRS-1 was significantly increased in adipocytes co-cultured with LPS stimulated macrophages pre-treated with DHA. Whole cell GLUT4 protein expression correlated with the GLUT4 mRNA gene expression data. Interestingly, GLUT4 protein expression was significantly reduced in adipocytes incubated for 30 minutes with the CM of LPS stimulated macrophages. Indicating the swiftness at which the CM media acts on the adipocytes. It is possible that DHA and EPA may not prevent the reduction in insulin signalling proteins initially but may enable the adipocytes to recover and become more insulin sensitive perhaps though the production of resolvins and protectin.

Overall these findings concur with a study conducted by Lumeng *et al* (2007) in which macrophage-secreted factors were shown to reduce insulin-stimulated glucose uptake in adipocytes via down-regulation of GLUT4 and IRS-1. As discussed in chapter 4 many cytokines such as TNF-α, IL-6 and IL-1β can decrease the expression of insulin signaling protein as well as increasing the serine phosphorylation of IRS-1, thus impairing downstream insulin signaling (Rui *et al.*, 2001). Studies indicate that cytokines may induce insulin resistance through activation of MAPK. Interestingly, ERK1/2 activation may be linked to the reduction in IRS-1 while p38 activation maybe linked to GLUT4 reduction (Aouadi *et al.*, 2006; Jager *et al.*, 2007). However, further analysis is required of the insulin signaling pathway within this model. It would be valuable to determine whether the macrophages can induce serine phosphorylation of IRS-1 therefore inhibiting insulin signaling in addition to looking at insulin receptor and AKT phosphorylation. Furthermore, it would be interesting to examine expression of SOCS proteins which are activated by cytokines and attenuate insulin signalling by sterically hindering coupling of insulin receptor with IRS-1 (Ueki *et al.*, 2004b) or by binding directly to IRS-1 facilitating its ubiquitation and subsequent degradation by the proteasome (Shi *et al.*, 2006a). Additionally, this study could be taken further by determining whether specific inhibitor of MAPK can attenuate the reduction in insulin signaling molecules induced by the LPS stimulated macrophages within adipocytes of the co-culture model.

Insulin sensitivity was assessed within the adipocytes of the co-culture and CM experiments using confocal microscopy and glucose uptake assays. Insulin induced GLUT4 translocation to the membrane was determined within the co-culture using confocal microscopy. As expected, adipocytes unstimulated with insulin showed very low levels of co-localization or transocation of GLUT4 to the membrane. Within adipocytes stimulated with insulin there was a significant increase in co-localization of GLUT4 to the membrane suggesting the adipocytes were insulin sensitive. However, within adipocytes co-cultured with LPS stimulated macrophages there was a significant reduction in insulin induced GLUT4 translocation to the membrane with levels similar to the non-insulin stimulated adipocytes. This suggests that macrophages induce insulin resistance within the adipocytes. DHA pre-treatment of the LPS stimulated macrophages prior to co-culture significantly increased adipocyte GLUT4 translocation to the membrane suggesting an increase in insulin sensitivity although levels of translocation remained lower than normal. Pre-treatment of the LPS stimulated macrophages with EPA reduced translocation of GLUT4 to the membrane to levels below those observed for adipocytes unstimulated with insulin, furthermore many of the values were negative. Co-localization was expressed as

Pearson's correlation coefficient, which is one of the standard techniques applied in pattern recognition for matching one image to another in order to describe the degree of overlap between the two patterns. The value of this coefficient ranges from -1 to 1, with a value of -1 representing a total lack of overlap between pixels from the images and a value of 1 indicating perfect image registration. However, negative values are ambiguous and difficult to interpret. Values between –1 and 0 indicate some form of inverse relationship between the channels as may occur when one channel is very dim and the other bright (Pawley, 2006). This suggests the adipocytes co-cultured with LPS stimulated macrophages pre-treated with EPA require re-analysis. Other coefficients provide subsequent information regarding the nature of the co-localisation as well as being less sensitive to channel imbalances (Pawley, 2006). However, these coefficients were not sensitive enough for this analysis. This confocal technique required a large amount of optimisation, the effects induced by the insulin and macrophages are subtle compared to the effects normally measured using the confocal microscope, therefore the data obtained is particularly difficult to interpret.

Glucose uptake was then examined within 3T3-L1 adipocytes incubated for 24 hours with CM (short term treatment) from macrophages pre-treated with LC *n-3* PUFA and stimulated with LPS for 48 hours. Interestingly, basal glucose uptake was significantly up-regulated in adipocytes incubated with CM from LPS stimulated macrophages for 24 hours. Cytokines such as IL-6 and TNF-α have been shown to up-regulate glucose uptake by increasing insulin dependent GLUT-1 activity (Phillips *et al.*, 2005; Stephens *et al.*, 1992; Stouthard *et al.*, 1996; Wieman *et al.*, 2007). However, DHA pre-treated LPS stimulated macrophage CM had no significant effect on basal glucose, which may reflect attenuation in pro-inflammatory cytokine production from the DHA pre-treated macrophages. Insulin induced glucose uptake was significantly reduced in adipocytes incubated with the CM of LPS stimulated macrophages for 24 hours which coincided with the development of a more fibroblast-like shape and a reduction in differentiation. Interestingly, insulin induced glucose uptake was significantly increased in adipocytes incubated for 24 hours with CM from LPS stimulated macrophages pre-treated with EPA. This suggests pre-treatment of the macrophages with EPA prior to incubation of the CM with adipocytes for 24 hours increases insulin sensitivity while DHA had no attenuating effect. Interestingly, adipocytes treated with the CM of LPS stimulated macrophages pre-treated with EPA for 24 hours retained their mature adipocyte round structure.

In continuation of the glucose uptake assay CM was then harvested from macrophages pre-treated with LC *n-3* PUFA and stimulated with LPS for 24 hours. CM

was incubated with mature differentiated 3T3-L1 adipocytes for 48 hours (long term treatment). This gives the EPA and DHA pre-treated macrophages less time to recover and attenuate the LPS induced inflammation while longer CM incubation with the adipocytes models a more chronic inflammatory environment for the adipocytes. Basal glucose uptake was significantly reduced in adipocytes treated for 48 hours with the CM of LPS stimulated macrophages. This suggests that GLUT1 activity induced in the adipocytes initially by the macrophage soluble factors is lost after 48 hours incubation. However, basal glucose uptake was unaffected in adipocytes incubated with the CM of LPS stimulated macrophages pre-treated with DHA for 48 hours as observed at 24 hours, indicating DHA does not induce GLUT1 activity. Insulin induced glucose uptake was significantly reduced in adipocytes incubated for 48 hours with CM of LPS stimulated macrophages, which coincides with a reduction in lipid accumulation and differentiation observed. Importantly, insulin induced glucose uptake was significantly increased in adipocytes incubated for 48 hours with the CM from DHA pre-treated LPS stimulated macrophages and suggests insulin sensitivity is improved in these adipocytes. These adipocytes developed a rounder more mature morphology coinciding with the increase in insulin induced glucose uptake. This improved insulin sensitivity is further demonstrated by the increased GLUT4 translocation to the membrane in adipocytes co-cultured with LPS stimulated macrophages pre-treated with DHA as observed in the confocal microscope images. Furthermore, treatment of adipocytes with LPS stimulated macrophages chronically pre-treated with DHA showed a significant up-regulation in adipocyte IRS-1 and GLUT4 gene and protein expression in the transwell system compared to adipocytes treated with LPS stimulated macrophages, indicating that these adipocytes may be more insulin sensitive.

In conclusion, the presence of macrophages was found to increase SFA accumulation within co-cultured adipocytes perhaps due to increased activity of FAS and elongases. The macrophage-derived soluble factors such as TNF-α and IL-6 were established to promote a pro-inflammatory environment within adipocytes in which inflammatory pathways NF-κB, ERK1/2 and p38 became up regulated. Interestingly, SFA, specifically palmitic acid has been shown to activate NF-κB and MAPK signaling within 3T3-L1 adipocytes (Ajuwon and Spurlock, 2005). Macrophage-secreted factors were shown to reduced insulin-stimulated glucose uptake in adipocytes via down-regulation of GLUT4 and IRS-1. Interestingly, studies indicate that cytokines may induce insulin resistance through activation of MAPK. Specifically, ERK1/2 activation may be linked to the reduction in IRS-1 while p38 activation may be linked to GLUT4 reduction (Aouadi *et*

al., 2006; Jager *et al.*, 2007). Leptin secretion was significantly reduced in adipocytes co-cultured with LPS stimulated macrophages. This effect was not attenuated by pre-treatment of the macrophages with either EPA or DHA. The reduction in leptin may be associated with the increased lipolysis and de-differentiation observed within adipocytes incubated with the media from LPS stimulated macrophages.

EPA and DHA pre-treatment of the macrophages prior to co-culture attenuate the inflammatory phenotype induced by the macrophages within this model. Insulin induced glucose uptake was significantly reduced in adipocytes incubated with the CM of LPS stimulated macrophages for 24 or 48 hours. Interestingly, insulin induced glucose uptake was significantly increased in adipocytes incubated with CM from LPS stimulated macrophages pre-treated with EPA for 24 hours but not 48 hours. Insulin induced glucose uptake was significantly increased in adipocytes incubated for 48 hours, but not 24 hours, with the CM from DHA pre-treated LPS stimulated macrophages. This improved insulin sensitivity is corroborated by the up-regulation in adipocyte IRS-1 and GLUT4 gene and protein expression in addition to the increased GLUT4 translocation to the membrane within adipocytes co-cultured with LPS stimulated macrophages pre-treated with DHA. DHA pre-treatment seems to have a greater attenuating effect on inflammation and insulin sensitivity within adipocytes of the co-culture. However, this greater attenuating effect of DHA may reflect the greater incorporation of DHA relative to EPA in the LC *n-3* PUFA treated macrophages. EPA concentrations were increased 8 fold in macrophages treated with EPA while DHA concentrations were increased 11 fold in DHA treated macrophages. The differential effects of EPA and DHA within this study may also be due to the type and quantity of metabolites produced. It is expected that LC *n-3* PUFA cause changes in membrane lipid composition and fluidity. These changes therefore modulate metabolite and secondary lipid messenger production, resulting in alterations in cell signalling mechanisms. It would be important to examine expression of ecosanoids, resolvins, protectins and isoeicosanoids in a full lipidomic analysis, to gain insight into the metabolism of EPA and DHA. Furthermore, electrospray tandem mass spectrometry (ESI-MS/MS) could be used to detect low abundant metabolites such as secondary lipid messengers e.g. ceramide. Modifications in the membrane lipid composition may also regulate transporters, receptors and enzymes, leading to changes in intracellular signal transduction. It would be valuable to examine TLR4 and CD14 expression as these proteins mediate LPS signaling. A time-course experiment may determine at which point the macrophages induce insulin resistance within the adipocytes and establish the time point at which the EPA and DHA pre-treatment attenuate these effects. Furthermore,

cytokine neutralizing antibodies, MAPK inhibitors or NF-κB inhibitors, in addition to siRNA gene silencing (as discussed in chapter 4) in either the macrophages or adipocytes could be introduced into the co-culture system to establish the role of these pathways within insulin resistance.

Chapter 7

General Discussion

During an obese state, white adipose tissue (WAT) becomes inflamed, with increased infiltration of immune cells such as macrophages, which contribute to the production of pro-inflammatory cytokines (Weisberg *et al.*, 2003; Xu *et al.*, 2003). These adipose derived pro-inflammatory cytokines are proposed to alter the endocrine function of the adipose tissue and impinge insulin signalling (Lumeng *et al.*, 2007b; Marette, 2003). Importantly, obesity is now considered a major contributor to the global burden of chronic disease and disability (WHO, 2004). Therefore a greater understanding of obesity induced insulin resistance is necessary to determine the mechanisms occurring in obese subjects, with the aim of developing better treatments for T2DM by identifying potential molecular targets for drug treatment and assessing the therapeutic potential of functional foods such as eicosapentaenoic acid (EPA) and docosahexaenoic acid (DHA). This thesis aimed to investigate the molecular mechanisms that mediate the interaction between macrophages and adipocytes using both *in vivo* and *in vitro* models. The therapeutic potential of LC *n-3* PUFA treatment was then assessed *in vitro*.

Firstly, this thesis aimed to establish an *in vivo* time-course experiment to study the molecular mechanisms involved in the development of obesity-induced insulin resistance in immune compromised IL-1 type 1 receptor knock out mice (IL-1RI$^{-/-}$). In light of current literature, we hypothesized that IL-1RI$^{-/-}$ mice will not only have a general reduction in inflammation, but also a specific reduction in adipose tissue macrophages (ATM) due to a lack in IL-1 signalling. Furthermore, we speculated that this reduction in ATM would lead to increased insulin sensitivity within the WAT. Previous work from our group indicated that IL-1RI$^{-/-}$ mice are partially protected against obesity induced insulin resistance (De Roos *et al.*, 2009). However, other studies examining the effects of IL-1 signalling in obesity-induced insulin resistance have produced mixed results (Garcia *et al.*, 2006; Larsen *et al.*, 2007; Matsuki *et al.*, 2003; Somm *et al.*, 2005).

In this thesis it was established that both IL-1RI$^{-/-}$ and wild type (WT) groups showed deterioration in their glucose uptake response during the glucose tolerance test (GTT) throughout the 16 week high fat diet (HFD). However, in the WT control group there was a more significant deterioration in the glucose response. At week 6 of the HFD it was established that the IL-1RI$^{-/-}$ group showed enhanced glucose uptake response relative to the WT group, suggesting IL-1RI$^{-/-}$ mice are more insulin sensitive. However, IL-1RI$^{-/-}$ mice also showed significantly lower body weight at week 6 compared to WT. This may

indicate that the increased insulin sensitivity within IL-1RI$^{-/-}$ mice at week 6 is weight dependent. However, at week 16, IL-1RI$^{-/-}$ mice exhibited increased insulin sensitivity with no significant difference between body weights. This may signify that at week 16 of the HFD, the IL-1RI$^{-/-}$ group had reduced inflammation with reduced ATM infiltration, leading to improved insulin signalling relative to the WT group. Adipose tissue specimines could be examined using immunohistochemistry or flow cytometry to directly demonstrate that ATM and other immune cells, such as T cells, were altered throughout the 16 week HFD intervention. Importantly, this hypothesis was supported by a reduction in pro-inflammatory cytokine and chemokine concentrations in the plasma, specifically IL-1β and CCL5, in addition to reduced TNF-α and MCP-1 gene expression levels in the epididymal adipose tissue (EAT) of IL-1RI$^{-/-}$ mice relative to WT. Additionally, IL-1RI$^{-/-}$ mice exhibited lower fasting plasma insulin and triacylglycerol (TAG) concentrations relative to the WT mice. This indicates that the HFD induced a state of hyperinsulinemia and dyslipidemia in WT mice. IL-1RI$^{-/-}$ mice appear to be partially protected from these effects, suggesting that they may be more insulin sensitive. Furthermore, IL-1R1$^{-/-}$ mice exhibited significantly higher EAT levels of insulin sensitive target genes such as glucose transporter (GLUT)-4 and insulin receptor substrate (IRS)-1 at week 0, also signifying that these mice are more insulin sensitive. Notably, IL-1RI$^{-/-}$ mice fed a HFD showed lower body weight and WAT mass with higher food intake, suggesting IL-1RI$^{-/-}$ mice have increased metabolic activity and lean body mass. Additionally, IL-1R1$^{-/-}$ mice exhibited smaller adipocyte size within their EAT, a common feature of highly insulin sensitive lean adipose tissue. Further work is ongoing to elucidate this model in more depth. In future studies a metabolic cage or pair-feeding could be introduced to elucidate if WT and IL-1RI$^{-/-}$ mice have different metabolic rates or appetite/food intake levels. Analysis of body composition in IL-1RI$^{-/-}$ and WT controls could be examined using dual-energy X-ray absorptiometry (DEXA) or magnetic resonance imaging (MRI).

The insulin resistant state could be further examined by correctly determining plasma insulin measurements during the GTT or with the use of insulin tolerance tests (ITT) and hyperinsulinemic euglycemic clamps. Furthermore, it would be important to successfully determine plasma cytokine levels such as IL-6 and MCP-1 in the mice to elucidate the inflammatory phenotype further. Western blot analysis of WAT proteins would provide insight into the insulin signalling mechanisms, as activity of the insulin targets is not necessarily regulated only through transcriptional expression, but also through post-translational modification. Several studies have indicated that abdominal WAT, particularly visceral adipose tissue (VAT), is a strong independent predictor of the

MetS. Therefore, it would be important to examine gene and protein expression levels in the VAT tissue and adipocytes. Other organs such as the liver and muscle may play a crucial role in the phenotypes observed and will need to be analysed to build a more comprehensive understanding of the IL-1R1$^{-/-}$ model.

In future studies, conditional gene targeting applying the Cre/loxP-mediated recombination system could be used to evaluate how deletion of the IL-1RI gene in a specific cell-type such as macrophages can affect the onset of obesity induced insulin resistance. Another system for examining IL-1 signalling in an obesity induced insulin resistance mouse model is to lethally irradiate, from a cesium gamma source, WT recipient mice and inject them with bone marrow cells from corresponding IL-1RI$^{-/-}$ mice. Correspondingly, irradiated IL-1RI$^{-/-}$ mice could be injected with the bone marrow of WT mice. These studies could add insight into the IL-1RI$^{-/-}$ model and perhaps establish if lack of IL-1 signalling in bone marror derived immune cells could protect against diet induced insulin resistnace.

Following this *in vivo* study, a series of cell culture experiments were used to examine and verify the findings of the IL-1R1$^{-/-}$ study. Therefore the direct effects of IL-1β treatment over time on adipocytes *in vitro* were explored. This time-course study demonstrated that IL-1β treatment reduced insulin sensitivity in 3T3-L1 adipocytes. Whole cell IRS-1 and GLUT4 protein expression was significantly reduced by IL-1β treatment in adipocytes, while serine phosphorylated IRS-1 (Serine 636/639) was significantly up-regulated in response to IL-1β, indicating that IL-1β may inhibit insulin signalling partially through IRS-1 serine phosphorylation via the mammalian target of the rapamycin (mTOR) pathway. IL-1β treatment significantly increased activation of p38 and extracellular signal-regulated kinases (ERK) in the 3T3-L1 adipocytes. Interestingly, studies indicate that p38 activity may regulate GLUT1 and GLUT4 expression, while ERK regulates IRS-1 expression. It would therefore be of interest to use a specific mitogen-activated protein kinase (MAPK) inhibitor to understand more about how IL-1β can induce insulin resistance via MAPK regulated mechanisms. In future studies, siRNA could be used to silence key signalling proteins such as p38 and ERK in fully mature adipocytes treated with IL-1β. Additionally, mouse embryonic fibroblasts (MEFs) derived from knockout mice with deletions of specific signalling proteins of interest could be differentiated to mature adipocytes. siRNA treated adipocytes or MEFs derived adipocytes with targeted protein deletions could therefore be used to establish novel cross talk mechanisms occurring between inflammatory and insulin signalling pathways.

IL-1β treatment was found to induce lipolysis and reduce the differentiation state of 3T3-L1 adipocytes. Interestingly, IL-1β induced a significant and specific up-regulation in IL-6 secretion within the adipocytes. This induction of IL-6 may have been initiated by MAPK and/or NF-κB pathway activation induced by the IL-1β treatment. Studies indicate that IL-6 regulates the expression and activation of insulin signalling targets such as IRS-1. Therefore, the induction of IL-6 by IL-1β may have initiated the reduction in insulin sensitivity within the 3T3-L1 adipocytes. IL-6 neutralizing antibody could be introduced during the IL-1β treatment to ensure the effects observed on inflammatory and insulin signaling are due to IL-1β and not IL-6 signaling. Further studies could also define the effects of IL-1 receptor antagonist (IL-1Ra) on 3T3-L1 both independently and in combination with IL-1 agonists. In conclusion, the data from this time-course experiment indicate that IL-1β can reduce insulin sensitivity and induce inflammation within 3T3-L1 adipocytes, correlating with observations in IL-1RI$^{-/-}$ mice, which exhibited increased insulin sensitivity and reduced inflammation.

High intakes of long chain (LC) *n-3* polyunsaturated fatty acids (PUFA) such as EPA and DHA, as found in oily fish, decrease the production of inflammatory eicosanoids, cytokines, reactive oxygen species (ROS) and adhesion molecules while increasing expression of anti-inflammatory eicosanoids, isoeicosanoids, resolvins and protectin (Calder, 2009; Miles *et al.*, 2002; Mullen *et al.*, 2009). Importantly, LC *n-3* PUFA also cause changes in membrane lipid composition and fluidity leading to alterations in cell signalling mechanisms via modulation of metabolites and secondary lipid messenger production. Modifications in the membrane lipid composition may also regulate transporters, receptors and enzymes, leading to changes in intracellular signal transduction. Through these mechanisms, LC *n-3* PUFA may offer a useful anti-inflammatory strategy to decrease obesity induced insulin resistance. Consequently, this thesis aimed to define the effects of EPA and DHA on 3T3-L1 adipocytes and LPS stimulated J774.2 macrophages *in vitro*. Furthermore, this was followed by a novel co-culture of both J774.2 macrophages and 3T3-L1 adipocytes.

Within 3T3-L1 adipocytes, chronic EPA and DHA treatment had variable effects. EPA treatment increased leptin and adiponectin secretion levels and improved insulin induced glucose uptake, suggesting EPA may have insulin sensitising effects. Conversely, DHA reduced GLUT4, inducing lipolysis and reducing the differentiation state of the 3T3-L1 adipocytes. This may suggest DHA has negative effects on adipocyte insulin sensitivity. However, DHA may induce anti-obesity effects and prevent further growth of

adipocytes by inhibiting differentiation of pre-adipocytes, inducing lipolysis and reducing glucose uptake through the down-regulation of GLUT4. DHA may also reduce the harmful effects of pro-inflammatory cytokines such as TNF-α on adipocyte insulin sensitivity through reduction of ERK signalling. EPA and DHA treatment did not significantly affect cytokine secretion from the adipocytes, which may suggest an inflammatory stimulus is required to firstly induce inflammation before the anti-inflammatory action of LC *n-3* PUFA in adipocytes can be observed. Therefore, further experiments are required to examine if EPA and DHA treatment can attenuate the pro-inflammatory state and reduce insulin sensitivity associated within inflamed adipocytes.

In general, the effects of EPA and DHA on J774.2 macrophages were more consistent, with EPA and DHA reducing inflammatory cytokine production while down-regulating and reducing phosphorylation of p38, JNK1/2 and IκB-α. These results correspond with previous work from our group which established that LC *n-3* PUFA reduces LPS induced pro-inflammatory cytokine production and NF-κB activity in THP-1 macrophages. Once the effects of EPA and DHA had been established within macrophages and adipocytes, a co-culture of both cell types was developed. This model mimics the condition observed in obesity-induced insulin resistance in which macrophages infiltrate into the WAT. It allows the simplification of an extremely complex human state and gives a starting point to understanding some of the mechanisms involved. Initially, this model examined LPS stimulated and unstimulated J774.2 macrophages acutely treated with EPA, DHA or DMSO vehicle control (24 hour treatment) in co-culture with 3T3-L1 adipocytes. Overall, the data from this co-culture, in which macrophages were acutely treated with LC *n-3* PUFA, suggests that obesity is associated with the generation of macrophage-derived soluble factors such as TNF-α, IL-6 and IL-1β that promote a pro-inflammatory environment. This leads to a reduction in adipocyte insulin signalling molecules such as GLUT4 and IRS-1, indicating that the adipocytes have become less insulin sensitive. Of particular note, this work has shown that pre-culturing macrophages with EPA and DHA can partially attenuate the inflammatory effect while moderately increasing insulin sensitive markers.

Finally, this thesis aimed to determine if chronic (5 day) LC *n-3* PUFA pre-treatment of the LPS stimulated J774.2 macrophages can attenuate the pro-inflammatory phenotype further and improve insulin action within the 3T3-L1 adipocytes of the co-culture system. This chronic pre-treatment perhaps mimics a long-term high intake of LC *n-3* PUFA in human and animal models. A transwell system was selected for on-going analysis of the co-culture. The transwell system enables protein and gene expression to be

examined within isolated adipocytes of the co-culture, while the contact system is a combination of adipocytes and macrophages, making analysis of the separate cell types more difficult. The co-culture experiments were combined with a set of condition media (CM) experiments in which adipocytes were incubated with the CM of LPS stimulated macrophages chronically pre-treated with LC *n-3* PUFA.

As observed within the acute co-culture model, the presence of macrophages induced production of pro-inflammatory cytokines. Interestingly, EPA pre-treatment of LPS stimulated macrophages was observed to attenuate IL-6 secretion within the co-culture while IL-6 mRNA expression was not modulated. However, DHA pre-treatment of LPS stimulated macrophages attenuated IL-6 expression at both a gene and protein level. These differences indicate that DHA acts to modulate IL-6 gene expression through activation of transcription factors such as PPAR-γ, while EPA may act post-transcriptionally through the regulation of proteins that control either translational initiation or mRNA stability. Macrophage-derived soluble factors such as TNF-α and IL-6 were considered to promote a pro-inflammatory environment within adipocytes in which inflammatory pathways NF-κB, ERK1/2 and p38 became up-regulated. Interestingly, the presence of macrophages was found to increase saturated fatty acid (SFA) accumulation within co-cultured adipocytes. Importantly, SFA, specifically palmitic acid (PA), has been shown to activate NF-κB and MAPK signalling within 3T3-L1 adipocytes via toll like receptor (TLR)-4 (Suganami *et al.*, 2007a; Suganami *et al.*, 2007b). TLR4 inhibitors could be introduced into the co-culture system to establish the role of these pathways. Importantly, macrophage-secreted factors were shown to reduce insulin-stimulated glucose uptake in adipocytes, which correlated with down-regulation of GLUT4 and IRS-1.

Chronic pre-treatment of LPS stimulated macrophages with EPA and DHA significantly reduced ERK1/2 and p38 activation in adipocytes of the co-culture, while GLUT4 and IRS-1 expression was increased within adipocytes co-cultured with LPS stimulated macrophages pre-treated with LC *n-3* PUFA, specifically DHA. It would be of interest to use a specific MAPK inhibitor to examine how macrophages can induce insulin resistance via MAPK regulated mechanisms.

In the conditioned media (CM) experiments, the presence of macrophage-derived soluble factors significantly up-regulated basal GLUT1 glucose uptake in adipocytes incubated with CM from LPS stimulated macrophages for 24 hours, however this increased GLUT1 activity was lost after 48 hours incubation. Interestingly, DHA pre-treated LPS stimulated macrophage CM had no significant effect on basal glucose after 24 or 48 hours, which may reflect attenuation in pro-inflammatory cytokine production from

the DHA pre-treated macrophages. Insulin-induced glucose uptake was significantly reduced in adipocytes incubated with the CM of LPS stimulated macrophages at 24 and 48 hours. Importantly, EPA pre-treatment had protective effects on insulin induced glucose uptake at 24 hours while DHA pre-treatment attenuated the effects at 48 hours. These data demonstrate that two closely related LC *n-3* PUFA differentially impact pro-inflammatory responses of J774.2 macrophages and adipocytes in co-culture, therefore differentially impacting insulin signalling and sensitivity in adipocytes. The proposed cell signalling mechanisms, which mediate the cross talk between adipocytes and macrophages in the co-culture experiments, are outlined in Figure 7.1

In future studies, specific inhibitors of the COX and LOX pathways could be used in the co-culture system to examine the effects of eicosanoid production. Fatty acid metabolites such as eicosanoids, isoeicosanoids, resolvins, protectins and secondary lipid messengers could be assessed using lipidomics. Furthermore, it would be interesting to examine the activity of transcription factors such as C/EBP, PPAR-γ and SREBP-1c in the adipocytes of the co-culture. Specific cytokine inhibitors or neutralizing agents could be used individually or in combination to establish which cytokines are most active in inducing insulin resistance within the adipocytes of the co-culture model. In future studies, siRNA could be used to silence key signalling proteins such as p38 and ERK in adipocytes or macrophages of the co-culture.

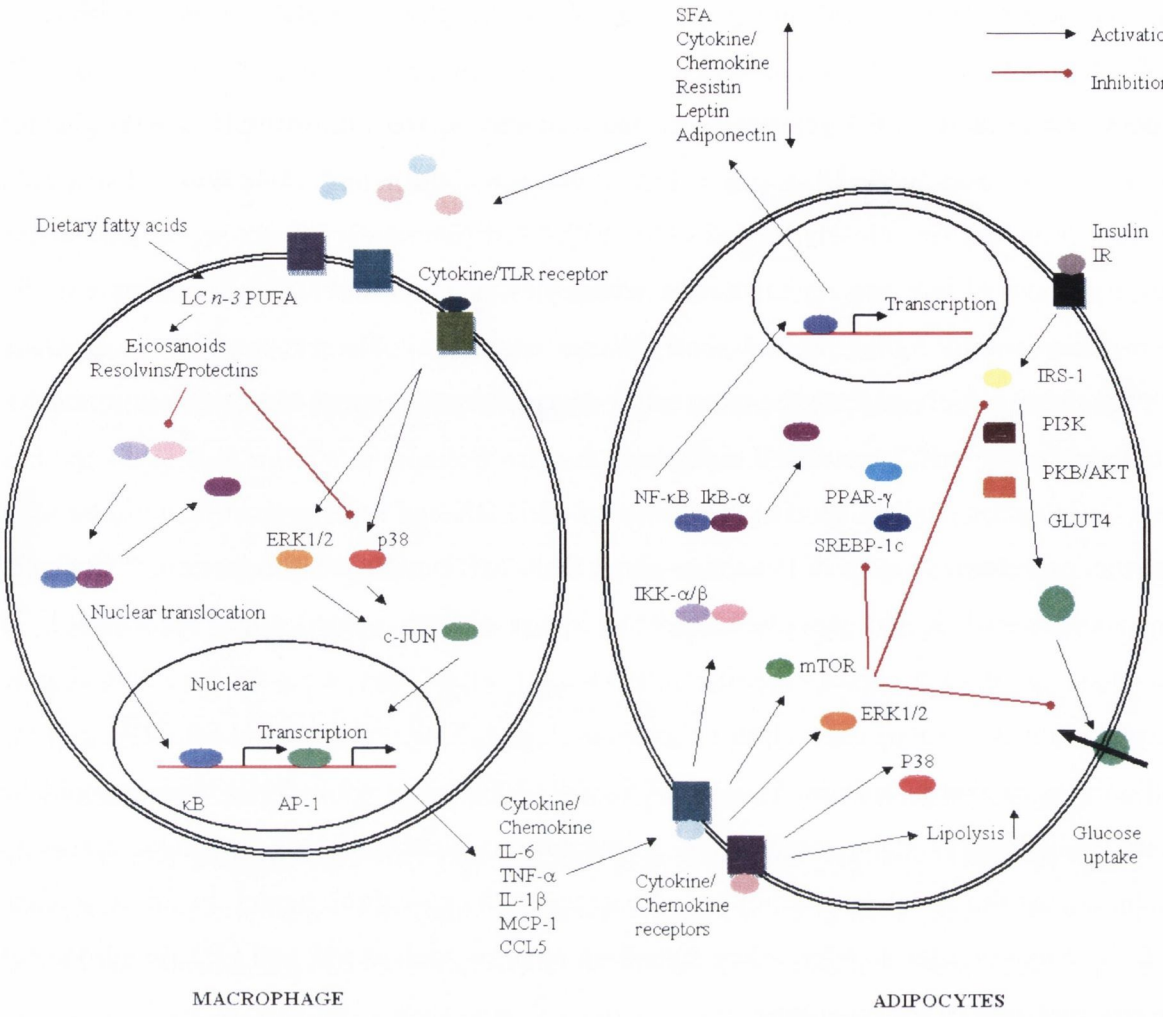

Figure 7.1 Proposed cell signalling mechanisms between adipocytes and macrophages in a co-culture system.

The results from this thesis stress the importance of inflammation and adipose tissue macrophages (ATM) in the progression of obesity-induced insulin resistance. Essentially, IL-1R1$^{-/-}$ mice remain more insulin sensitive after a 16 week HFD, most likely due to a reduced pro-inflammatory state and less ATM accumulation. However, more work is necessary to identify the underlying mechanisms within this model. The results of this thesis also demonstrated that macrophages produce pro-inflammatory cytokines such as TNF-α, IL-6 and IL-1β. These secreted factors enhance the activation of MAPK and NF-κB signalling within adipocytes. Up-regulation in pro-inflammatory pathway signalling appears to cross talk with the insulin signalling pathway, resulting in down-regulation of insulin sensitive targets such as GLUT4 and IRS-1, while initiating serine phosphorylation of IRS-1, blocking tyrosine phosphorylation and reducing insulin induced GLUT4 translocation to the membrane. LC *n-3* PUFA have been shown to attenuate many of the deleterious effects within adipocytes and macrophages such as reducing the pro-

inflammatory state, up-regulating insulin signalling molecules and improving insulin sensitivity, indicating that they may have therapeutic potential within the context of the obese insulin resistant state. However, further work is required to continue investigating the molecular mechanisms that mediate the interaction between macrophages and adipocytes, and to examine whether LC *n-3* PUFA treatment can attenuate the pro-inflammatory phenotype and improve insulin action within obesity.

References

Accili, D., Nakae, J., Kim, J. J., Park, B. C., and Rother, K. I. (1999): Targeted gene mutations define the roles of insulin and IGF-I receptors in mouse embryonic development. *J Pediatr Endocrinol Metab* **12**, 475-85.

Adachi, O., Kawai, T., Takeda, K., Matsumoto, M., Tsutsui, H., Sakagami, M., Nakanishi, K., and Akira, S. (1998): Targeted disruption of the MyD88 gene results in loss of IL-1- and IL-18-mediated function. *Immunity* **9**, 143-50.

Adhikary, L., Chow, F., Nikolic-Paterson, D. J., Stambe, C., Dowling, J., Atkins, R. C., and Tesch, G. H. (2004): Abnormal p38 mitogen-activated protein kinase signalling in human and experimental diabetic nephropathy. *Diabetologia* **47**, 1210-22.

Adler, A. I., Boyko, E. J., Schraer, C. D., and Murphy, N. J. (1994): Lower prevalence of impaired glucose tolerance and diabetes associated with daily seal oil or salmon consumption among Alaska Natives. *Diabetes Care* **17**, 1498-501.

Aggarwal, B. B., and Natarajan, K. (1996): Tumor necrosis factors: developments during the last decade. *Eur Cytokine Netw* **7**, 93-124.

Aguilera, A. A., Diaz, G. H., Barcelata, M. L., Guerrero, O. A., and Ros, R. M. (2004): Effects of fish oil on hypertension, plasma lipids, and tumor necrosis factor-alpha in rats with sucrose-induced metabolic syndrome. *J Nutr Biochem* **15**, 350-7.

Aguirre, V., Uchida, T., Yenush, L., Davis, R., and White, M. F. (2000): The c-Jun NH(2)-terminal kinase promotes insulin resistance during association with insulin receptor substrate-1 and phosphorylation of Ser(307). *J Biol Chem* **275**, 9047-54.

Aguirre, V., Werner, E. D., Giraud, J., Lee, Y. H., Shoelson, S. E., and White, M. F. (2002): Phosphorylation of Ser307 in insulin receptor substrate-1 blocks interactions with the insulin receptor and inhibits insulin action. *J Biol Chem* **277**, 1531-7.

Ahima, R. S., Saper, C. B., Flier, J. S., and Elmquist, J. K. (2000): Leptin regulation of neuroendocrine systems. *Front Neuroendocrinol* **21**, 263-307.

Ahmadian, M., Duncan, R. E., Jaworski, K., Sarkadi-Nagy, E., and Sul, H. S. (2007): Triacylglycerol metabolism in adipose tissue. *Future Lipidol* **2**, 229-237.

Ajuwon, K. M., and Spurlock, M. E. (2005): Palmitate activates the NF-kappaB transcription factor and induces IL-6 and TNFalpha expression in 3T3-L1 adipocytes. *J Nutr* **135**, 1841-6.

Akira, S., Taga, T., and Kishimoto, T. (1993): Interleukin-6 in biology and medicine. *Adv Immunol* **54**, 1-78.

Alessi, D. R., and Downes, C. P. (1998): The role of PI 3-kinase in insulin action. *Biochim Biophys Acta* **1436**, 151-64.

Alonzi, T., Mancone, C., Amicone, L., and Tripodi, M. (2008): Elucidation of lipoprotein particles structure by proteomic analysis. *Expert Rev Proteomics* **5**, 91-104.

An, Y., Liu, K., Zhou, Y., and Liu, B. (2009): Salicylate Inhibits Macrophage-Secreted Factors Induced Adipocyte Inflammation and Changes of Adipokines in 3T3-L1 Adipocytes. *Inflammation.*

Anderson, P. D., Mehta, N. N., Wolfe, M. L., Hinkle, C. C., Pruscino, L., Comiskey, L. L., Tabita-Martinez, J., Sellers, K. F., Rickels, M. R., Ahima, R. S., and Reilly, M. P. (2007): Innate immunity modulates adipokines in humans. *J Clin Endocrinol Metab* **92**, 2272-9.

Andersson, C., Zaman, M. M., Jones, A. B., and Freedman, S. D. (2008): Alterations in immune response and PPAR/LXR regulation in cystic fibrosis macrophages. *J Cyst Fibros* **7**, 68-78.

Antuna-Puente, B., Faraj, M., Karelis, A. D., Garrel, D., Prud'homme, D., Rabasa-Lhoret, R., and Bastard, J. P. (2008): HOMA or QUICKI: is it useful to test the reproducibility of formulas? *Diabetes Metab* **34**, 294-6.

Aouadi, M., Laurent, K., Prot, M., Le Marchand-Brustel, Y., Binetruy, B., and Bost, F. (2006): Inhibition of p38MAPK increases adipogenesis from embryonic to adult stages. *Diabetes* **55**, 281-9.

Appay, V., and Rowland-Jones, S. L. (2001): RANTES: a versatile and controversial chemokine. *Trends Immunol* **22**, 83-7.

Arab, L. (2003): Biomarkers of fat and fatty acid intake. *J Nutr* **133 Suppl 3**, 925S-932S.

Araki, E., Lipes, M. A., Patti, M. E., Bruning, J. C., Haag, B., 3rd, Johnson, R. S., and Kahn, C. R. (1994): Alternative pathway of insulin signalling in mice with targeted disruption of the IRS-1 gene. *Nature* **372**, 186-90.

Arena, F. P., Dugowson, C., and Saudek, C. D. (1978): Salicylate-induced hypoglycemia and ketoacidosis in a nondiabetic adult. *Arch Intern Med* **138**, 1153-4.

Arita, Y., Kihara, S., Ouchi, N., Maeda, K., Kuriyama, H., Okamoto, Y., Kumada, M., Hotta, K., Nishida, M., Takahashi, M., Nakamura, T., Shimomura, I., Muraguchi, M., Ohmoto, Y., Funahashi, T., and Matsuzawa, Y. (2002): Adipocyte-derived plasma protein adiponectin acts as a platelet-derived growth factor-BB-binding protein and regulates growth factor-induced common postreceptor signal in vascular smooth muscle cell. *Circulation* **105**, 2893-8.

Arita, Y., Kihara, S., Ouchi, N., Takahashi, M., Maeda, K., Miyagawa, J., Hotta, K., Shimomura, I., Nakamura, T., Miyaoka, K., Kuriyama, H., Nishida, M., Yamashita, S., Okubo, K., Matsubara, K., Muraguchi, M., Ohmoto, Y., Funahashi, T., and Matsuzawa, Y. (1999): Paradoxical decrease of an adipose-specific protein, adiponectin, in obesity. *Biochem Biophys Res Commun* **257**, 79-83.

Arkan, M. C., Hevener, A. L., Greten, F. R., Maeda, S., Li, Z. W., Long, J. M., Wynshaw-Boris, A., Poli, G., Olefsky, J., and Karin, M. (2005): IKK-beta links inflammation to obesity-induced insulin resistance. *Nat Med* **11**, 191-8.

Arora, P. D., Ma, J., Min, W., Cruz, T., and McCulloch, C. A. (1995): Interleukin-1-induced calcium flux in human fibroblasts is mediated through focal adhesions. *J Biol Chem* **270**, 6042-9.

Asensio, C., Cettour-Rose, P., Theander-Carrillo, C., Rohner-Jeanrenaud, F., and Muzzin, P. (2004): Changes in glycemia by leptin administration or high- fat feeding in rodent models of obesity/type 2 diabetes suggest a link between resistin expression and control of glucose homeostasis. *Endocrinology* **145**, 2206-13.

Auron, P. E. (1998): The interleukin 1 receptor: ligand interactions and signal transduction. *Cytokine Growth Factor Rev* **9**, 221-37.

Azain, M. J., Hausman, D. B., Sisk, M. B., Flatt, W. P., and Jewell, D. E. (2000): Dietary conjugated linoleic acid reduces rat adipose tissue cell size rather than cell number. *J Nutr* **130**, 1548-54.

Azzout-Marniche, D., Becard, D., Guichard, C., Foretz, M., Ferre, P., and Foufelle, F. (2000): Insulin effects on sterol regulatory-element-binding protein-1c (SREBP-1c) transcriptional activity in rat hepatocytes. *Biochem J* **350 Pt 2**, 389-93.

Bagga, D., Wang, L., Farias-Eisner, R., Glaspy, J. A., and Reddy, S. T. (2003): Differential effects of prostaglandin derived from omega-6 and omega-3 polyunsaturated fatty acids on COX-2 expression and IL-6 secretion. *Proc Natl Acad Sci U S A* **100**, 1751-6.

Ballou, L. R., Laulederkind, S. J., Rosloniec, E. F., and Raghow, R. (1996): Ceramide signalling and the immune response. *Biochim Biophys Acta* **1301**, 273-87.

Banerjee, R. R., Rangwala, S. M., Shapiro, J. S., Rich, A. S., Rhoades, B., Qi, Y., Wang, J., Rajala, M. W., Pocai, A., Scherer, P. E., Steppan, C. M., Ahima, R. S., Obici, S., Rossetti, L., and Lazar, M. A. (2004): Regulation of fasted blood glucose by resistin. *Science* **303**, 1195-8.

Banga, A., Unal, R., Tripathi, P., Pokrovskaya, I., Owens, R. J., Kern, P. A., and Ranganathan, G. (2009): Adiponectin translation is increased by the PPARgamma

agonists pioglitazone and omega-3 fatty acids. *Am J Physiol Endocrinol Metab* **296**, E480-9.

Baqui, M., Botero, D., Gereben, B., Curcio, C., Harney, J. W., Salvatore, D., Sorimachi, K., Larsen, P. R., and Bianco, A. C. (2003): Human type 3 iodothyronine selenodeiodinase is located in the plasma membrane and undergoes rapid internalization to endosomes. *J Biol Chem* **278**, 1206-11.

Baron, S. H. (1982): Salicylates as hypoglycemic agents. *Diabetes Care* **5**, 64-71.

Bartz, R., Zehmer, J. K., Zhu, M., Chen, Y., Serrero, G., Zhao, Y., and Liu, P. (2007): Dynamic activity of lipid droplets: protein phosphorylation and GTP-mediated protein translocation. *J Proteome Res* **6**, 3256-65.

Bassaganya-Riera, J., Misyak, S., Guri, A. J., and Hontecillas, R. (2009): PPAR gamma is highly expressed in F4/80(hi) adipose tissue macrophages and dampens adipose-tissue inflammation. *Cell Immunol* **258**, 138-46.

Bays, H. E., Gonzalez-Campoy, J. M., Bray, G. A., Kitabchi, A. E., Bergman, D. A., Schorr, A. B., Rodbard, H. W., and Henry, R. R. (2008): Pathogenic potential of adipose tissue and metabolic consequences of adipocyte hypertrophy and increased visceral adiposity. *Expert Rev Cardiovasc Ther* **6**, 343-68.

Beeson, M., Sajan, M. P., Dizon, M., Grebenev, D., Gomez-Daspet, J., Miura, A., Kanoh, Y., Powe, J., Bandyopadhyay, G., Standaert, M. L., and Farese, R. V. (2003): Activation of protein kinase C-zeta by insulin and phosphatidylinositol-3,4,5-(PO4)3 is defective in muscle in type 2 diabetes and impaired glucose tolerance: amelioration by rosiglitazone and exercise. *Diabetes* **52**, 1926-34.

Beinke, S., and Ley, S. C. (2004): Functions of NF-kappaB1 and NF-kappaB2 in immune cell biology. *Biochem J* **382**, 393-409.

Belluzzi, A., Brignola, C., Campieri, M., Pera, A., Boschi, S., and Miglioli, M. (1996): Effect of an enteric-coated fish-oil preparation on relapses in Crohn's disease. *N Engl J Med* **334**, 1557-60.

Benatti, P., Peluso, G., Nicolai, R., and Calvani, M. (2004): Polyunsaturated fatty acids: biochemical, nutritional and epigenetic properties. *J Am Coll Nutr* **23**, 281-302.

Bendtzen, K., Mandrup-Poulsen, T., Nerup, J., Nielsen, J. H., Dinarello, C. A., and Svenson, M. (1986): Cytotoxicity of human pI 7 interleukin-1 for pancreatic islets of Langerhans. *Science* **232**, 1545-7.

Berchtold, P., Bjorntorp, P., Gustafson, A., Lindholm, B., Tibblin, G., and Wilhelmsen, L. (1972): Glucose tolerance, plasma insulin and lipids in relation to adipose tissue cellularity in men after myocardial infarction. *Acta Med Scand* **191**, 35-41.

Berg, A. H., Combs, T. P., Du, X., Brownlee, M., and Scherer, P. E. (2001): The adipocyte-secreted protein Acrp30 enhances hepatic insulin action. *Nat Med* **7**, 947-53.

Berg, J., Tymoczko JL, Stryer L. (2002): *Biochemistry*. W.H. Freeman and Co.

Berger, J., and Moller, D. E. (2002): The mechanisms of action of PPARs. *Annu Rev Med* **53**, 409-35.

Bergman, R. N., Ider, Y. Z., Bowden, C. R., and Cobelli, C. (1979): Quantitative estimation of insulin sensitivity. *Am J Physiol* **236**, E667-77.

Bergman, R. N., Phillips, L. S., and Cobelli, C. (1981): Physiologic evaluation of factors controlling glucose tolerance in man: measurement of insulin sensitivity and beta-cell glucose sensitivity from the response to intravenous glucose. *J Clin Invest* **68**, 1456-67.

Bertolani, C., Sancho-Bru, P., Failli, P., Bataller, R., Aleffi, S., DeFranco, R., Mazzinghi, B., Romagnani, P., Milani, S., Gines, P., Colmenero, J., Parola, M., Gelmini, S., Tarquini, R., Laffi, G., Pinzani, M., and Marra, F. (2006): Resistin as an intrahepatic cytokine: overexpression during chronic injury and induction of proinflammatory actions in hepatic stellate cells. *Am J Pathol* **169**, 2042-53.

Birnbaum, M. J., Haspel, H. C., and Rosen, O. M. (1986): Cloning and characterization of a cDNA encoding the rat brain glucose-transporter protein. *Proc Natl Acad Sci U S A* **83**, 5784-8.

Bjorntorp, P. (1971): Sjostrom L,+SJOSTROM L: Number and size of adipose tissue fat cells in relation to metabolism in human obesity. *Metabolism* **20**, 703-13.

Bjorntorp, P., Jonsson, A., and Berchtold, P. (1972): Adipose tissue cellularity in maturity onset diabetes mellitus. *Acta Med Scand* **191**, 129-32.

Bligh, E. G., and Dyer, W. J. (1959): A rapid method of total lipid extraction and purification. *Can J Biochem Physiol* **37**, 911-7.

Bo, S., Gambino, R., Pagani, A., Guidi, S., Gentile, L., Cassader, M., and Pagano, G. F. (2005): Relationships between human serum resistin, inflammatory markers and insulin resistance. *Int J Obes (Lond)* **29**, 1315-20.

Bobrowski, W. F., McDuffie, J. E., Sobocinski, G., Chupka, J., Olle, E., Bowman, A., and Albassam, M. (2005): Comparative methods for multiplex analysis of cytokine protein expression in plasma of lipopolysaccharide-treated mice. *Cytokine* **32**, 194-8.

Bodmer, M. W., Angal, S., Yarranton, G. T., Harris, T. J., Lyons, A., King, D. J., Pieroni, G., Riviere, C., Verger, R., and Lowe, P. A. (1987): Molecular cloning of a human gastric lipase and expression of the enzyme in yeast. *Biochim Biophys Acta* **909**, 237-44.

Boizard, M., Le Liepvre, X., Lemarchand, P., Foufelle, F., Ferre, P., and Dugail, I. (1998): Obesity-related overexpression of fatty-acid synthase gene in adipose tissue involves sterol regulatory element-binding protein transcription factors. *J Biol Chem* **273**, 29164-71.

Bokarewa, M., Nagaev, I., Dahlberg, L., Smith, U., and Tarkowski, A. (2005): Resistin, an adipokine with potent proinflammatory properties. *J Immunol* **174**, 5789-95.

Bost, F., Aouadi, M., Caron, L., Even, P., Belmonte, N., Prot, M., Dani, C., Hofman, P., Pages, G., Pouyssegur, J., Le Marchand-Brustel, Y., and Binetruy, B. (2005): The extracellular signal-regulated kinase isoform ERK1 is specifically required for in vitro and in vivo adipogenesis. *Diabetes* **54**, 402-11.

Bourlier, V., Zakaroff-Girard, A., Miranville, A., De Barros, S., Maumus, M., Sengenes, C., Galitzky, J., Lafontan, M., Karpe, F., Frayn, K. N., and Bouloumie, A. (2008): Remodeling phenotype of human subcutaneous adipose tissue macrophages. *Circulation* **117**, 806-15.

Bouzakri, K., Roques, M., Gual, P., Espinosa, S., Guebre-Egziabher, F., Riou, J. P., Laville, M., Le Marchand-Brustel, Y., Tanti, J. F., and Vidal, H. (2003): Reduced activation of phosphatidylinositol-3 kinase and increased serine 636 phosphorylation of insulin receptor substrate-1 in primary culture of skeletal muscle cells from patients with type 2 diabetes. *Diabetes* **52**, 1319-25.

Bradford, M. M. (1976): A rapid and sensitive method for the quantitation of microgram quantities of protein utilizing the principle of protein-dye binding. *Anal Biochem* **72**, 248-54.

Braissant, O., Foufelle, F., Scotto, C., Dauca, M., and Wahli, W. (1996): Differential expression of peroxisome proliferator-activated receptors (PPARs): tissue distribution of PPAR-alpha, -beta, and -gamma in the adult rat. *Endocrinology* **137**, 354-66.

Brissova, M., Fowler, M. J., Nicholson, W. E., Chu, A., Hirshberg, B., Harlan, D. M., and Powers, A. C. (2005): Assessment of human pancreatic islet architecture and composition by laser scanning confocal microscopy. *J Histochem Cytochem* **53**, 1087-97.

Brodie, A. E., Manning, V. A., Ferguson, K. R., Jewell, D. E., and Hu, C. Y. (1999): Conjugated linoleic acid inhibits differentiation of pre- and post- confluent 3T3-L1

preadipocytes but inhibits cell proliferation only in preconfluent cells. *J Nutr* **129**, 602-6.

Broughton, K. S., Johnson, C. S., Pace, B. K., Liebman, M., and Kleppinger, K. M. (1997): Reduced asthma symptoms with n-3 fatty acid ingestion are related to 5-series leukotriene production. *Am J Clin Nutr* **65**, 1011-7.

Brown, M. S., and Goldstein, J. L. (1997): The SREBP pathway: regulation of cholesterol metabolism by proteolysis of a membrane-bound transcription factor. *Cell* **89**, 331-40.

Brozinick, J. T., Jr., McCoid, S. C., Reynolds, T. H., Nardone, N. A., Hargrove, D. M., Stevenson, R. W., Cushman, S. W., and Gibbs, E. M. (2001): GLUT4 overexpression in db/db mice dose-dependently ameliorates diabetes but is not a lifelong cure. *Diabetes* **50**, 593-600.

Bruun, J. M., Lihn, A. S., Pedersen, S. B., and Richelsen, B. (2005): Monocyte chemoattractant protein-1 release is higher in visceral than subcutaneous human adipose tissue (AT): implication of macrophages resident in the AT. *J Clin Endocrinol Metab* **90**, 2282-9.

Byrdwell, W. C., Sato, H., Schwarz, A. K., Borchman, D., Yappert, M. C., and Tang, D. (2002): 31P NMR quantification and monophasic solvent purification of human and bovine lens phospholipids. *Lipids* **37**, 1087-92.

Cabrera, O., Berman, D. M., Kenyon, N. S., Ricordi, C., Berggren, P. O., and Caicedo, A. (2006): The unique cytoarchitecture of human pancreatic islets has implications for islet cell function. *Proc Natl Acad Sci U S A* **103**, 2334-9.

Cai, D., Yuan, M., Frantz, D. F., Melendez, P. A., Hansen, L., Lee, J., and Shoelson, S. E. (2005): Local and systemic insulin resistance resulting from hepatic activation of IKK-beta and NF-kappaB. *Nat Med* **11**, 183-90.

Calabro, P., Samudio, I., Willerson, J. T., and Yeh, E. T. (2004): Resistin promotes smooth muscle cell proliferation through activation of extracellular signal-regulated kinase 1/2 and phosphatidylinositol 3-kinase pathways. *Circulation* **110**, 3335-40.

Calder, P. C. (2006): n-3 polyunsaturated fatty acids, inflammation, and inflammatory diseases. *Am J Clin Nutr* **83**, 1505S-1519S.

Calder, P. C. (2009): Polyunsaturated fatty acids and inflammatory processes: New twists in an old tale. *Biochimie* **91**, 791-5.

Calder, P. C., and Miles, E. A. (2000): Fatty acids and atopic disease. *Pediatr Allergy Immunol* **11 Suppl 13**, 29-36.

Canaan, S., Roussel, A., Verger, R., and Cambillau, C. (1999): Gastric lipase: crystal structure and activity. *Biochim Biophys Acta* **1441**, 197-204.

Cancello, R., Henegar, C., Viguerie, N., Taleb, S., Poitou, C., Rouault, C., Coupaye, M., Pelloux, V., Hugol, D., Bouillot, J. L., Bouloumie, A., Barbatelli, G., Cinti, S., Svensson, P. A., Barsh, G. S., Zucker, J. D., Basdevant, A., Langin, D., and Clement, K. (2005): Reduction of macrophage infiltration and chemoattractant gene expression changes in white adipose tissue of morbidly obese subjects after surgery-induced weight loss. *Diabetes* **54**, 2277-86.

Cancello, R., Tordjman, J., Poitou, C., Guilhem, G., Bouillot, J. L., Hugol, D., Coussieu, C., Basdevant, A., Bar Hen, A., Bedossa, P., Guerre-Millo, M., and Clement, K. (2006): Increased infiltration of macrophages in omental adipose tissue is associated with marked hepatic lesions in morbid human obesity. *Diabetes* **55**, 1554-61.

Carlson, C. J., Koterski, S., Sciotti, R. J., Poccard, G. B., and Rondinone, C. M. (2003): Enhanced basal activation of mitogen-activated protein kinases in adipocytes from type 2 diabetes: potential role of p38 in the downregulation of GLUT4 expression. *Diabetes* **52**, 634-41.

Carlson, C. J., and Rondinone, C. M. (2005): Pharmacological inhibition of p38 MAP kinase results in improved glucose uptake in insulin-resistant 3T3-L1 adipocytes. *Metabolism* **54**, 895-901.

Cerasi, E., and Luft, R. (1967): "What is inherited--what is added" hypothesis for the pathogenesis of diabetes mellitus. *Diabetes* **16**, 615-27.

Chahinian, H., Snabe, T., Attias, C., Fojan, P., Petersen, S. B., and Carriere, F. (2006): How gastric lipase, an interfacial enzyme with a Ser-His-Asp catalytic triad, acts optimally at acidic pH. *Biochemistry* **45**, 993-1001.

Chan, J. M., Rimm, E. B., Colditz, G. A., Stampfer, M. J., and Willett, W. C. (1994): Obesity, fat distribution, and weight gain as risk factors for clinical diabetes in men. *Diabetes Care* **17**, 961-9.

Chawla, A., Schwarz, E. J., Dimaculangan, D. D., and Lazar, M. A. (1994): Peroxisome proliferator-activated receptor (PPAR) gamma: adipose-predominant expression and induction early in adipocyte differentiation. *Endocrinology* **135**, 798-800.

Chen, B., Tsui, S., and Smith, T. J. (2005): IL-1 beta induces IL-6 expression in human orbital fibroblasts: identification of an anatomic-site specific phenotypic attribute relevant to thyroid-associated ophthalmopathy. *J Immunol* **175**, 1310-9.

Chen, F., Castranova, V., Shi, X., and Demers, L. M. (1999): New insights into the role of nuclear factor-kappaB, a ubiquitous transcription factor in the initiation of diseases. *Clin Chem* **45**, 7-17.

Chinetti, G., Fruchart, J. C., and Staels, B. (2000): Peroxisome proliferator-activated receptors (PPARs): nuclear receptors at the crossroads between lipid metabolism and inflammation. *Inflamm Res* **49**, 497-505.

Chomczynski, P., and Sacchi, N. (1987): Single-step method of RNA isolation by acid guanidinium thiocyanate-phenol-chloroform extraction. *Anal Biochem* **162**, 156-9.

Christiansen, T., Richelsen, B., and Bruun, J. M. (2005): Monocyte chemoattractant protein-1 is produced in isolated adipocytes, associated with adiposity and reduced after weight loss in morbid obese subjects. *Int J Obes (Lond)* **29**, 146-50.

Christman, J. W., Lancaster, L. H., and Blackwell, T. S. (1998): Nuclear factor kappa B: a pivotal role in the systemic inflammatory response syndrome and new target for therapy. *Intensive Care Med* **24**, 1131-8.

Cinti, S. (2005): The adipose organ. *Prostaglandins Leukot Essent Fatty Acids* **73**, 9-15.

Cinti, S., Mitchell, G., Barbatelli, G., Murano, I., Ceresi, E., Faloia, E., Wang, S., Fortier, M., Greenberg, A. S., and Obin, M. S. (2005): Adipocyte death defines macrophage localization and function in adipose tissue of obese mice and humans. *J Lipid Res* **46**, 2347-55.

Clifford, G. M., Londos, C., Kraemer, F. B., Vernon, R. G., and Yeaman, S. J. (2000): Translocation of hormone-sensitive lipase and perilipin upon lipolytic stimulation of rat adipocytes. *J Biol Chem* **275**, 5011-5.

Coenen, K. R., Gruen, M. L., Lee-Young, R. S., Puglisi, M. J., Wasserman, D. H., and Hasty, A. H. (2009): Impact of macrophage toll-like receptor 4 deficiency on macrophage infiltration into adipose tissue and the artery wall in mice. *Diabetologia* **52**, 318-28.

Colditz, G. A., Willett, W. C., Rotnitzky, A., and Manson, J. E. (1995): Weight gain as a risk factor for clinical diabetes mellitus in women. *Ann Intern Med* **122**, 481-6.

Coleman, R. A., and Lee, D. P. (2004): Enzymes of triacylglycerol synthesis and their regulation. *Prog Lipid Res* **43**, 134-76.

Coleman, R. A., Lewin, T. M., and Muoio, D. M. (2000): Physiological and nutritional regulation of enzymes of triacylglycerol synthesis. *Annu Rev Nutr* **20**, 77-103.

Collins, T. J. (2007): ImageJ for microscopy. *Biotechniques* **43**, 25-30.

Colotta, F., Dower, S. K., Sims, J. E., and Mantovani, A. (1994): The type II 'decoy' receptor: a novel regulatory pathway for interleukin 1. *Immunol Today* **15**, 562-6.

Combs, T. P., Berg, A. H., Rajala, M. W., Klebanov, S., Iyengar, P., Jimenez-Chillaron, J. C., Patti, M. E., Klein, S. L., Weinstein, R. S., and Scherer, P. E. (2003): Sexual differentiation, pregnancy, calorie restriction, and aging affect the adipocyte-specific secretory protein adiponectin. *Diabetes* **52**, 268-76.

Combs, T. P., Wagner, J. A., Berger, J., Doebber, T., Wang, W. J., Zhang, B. B., Tanen, M., Berg, A. H., O'Rahilly, S., Savage, D. B., Chatterjee, K., Weiss, S., Larson, P. J., Gottesdiener, K. M., Gertz, B. J., Charron, M. J., Scherer, P. E., and Moller, D. E. (2002): Induction of adipocyte complement-related protein of 30 kilodaltons by PPARgamma agonists: a potential mechanism of insulin sensitization. *Endocrinology* **143**, 998-1007.

Compton, S. J., and Jones, C. G. (1985): Mechanism of dye response and interference in the Bradford protein assay. *Anal Biochem* **151**, 369-74.

Considine, R. V., Sinha, M. K., Heiman, M. L., Kriauciunas, A., Stephens, T. W., Nyce, M. R., Ohannesian, J. P., Marco, C. C., McKee, L. J., Bauer, T. L., and et al. (1996): Serum immunoreactive-leptin concentrations in normal-weight and obese humans. *N Engl J Med* **334**, 292-5.

Cornelius, P., MacDougald, O. A., and Lane, M. D. (1994): Regulation of adipocyte development. *Annu Rev Nutr* **14**, 99-129.

Corradetti, M. N., and Guan, K. L. (2006): Upstream of the mammalian target of rapamycin: do all roads pass through mTOR? *Oncogene* **25**, 6347-60.

Cowherd, R. M., Lyle, R. E., and McGehee, R. E., Jr. (1999): Molecular regulation of adipocyte differentiation. *Semin Cell Dev Biol* **10**, 3-10.

Cross, D. A., Alessi, D. R., Cohen, P., Andjelkovich, M., and Hemmings, B. A. (1995): Inhibition of glycogen synthase kinase-3 by insulin mediated by protein kinase B. *Nature* **378**, 785-9.

Cunningham, J. T., Rodgers, J. T., Arlow, D. H., Vazquez, F., Mootha, V. K., and Puigserver, P. (2007): mTOR controls mitochondrial oxidative function through a YY1-PGC-1alpha transcriptional complex. *Nature* **450**, 736-40.

Cusin, I., Sainsbury, A., Doyle, P., Rohner-Jeanrenaud, F., and Jeanrenaud, B. (1995): The ob gene and insulin. A relationship leading to clues to the understanding of obesity. *Diabetes* **44**, 1467-70.

Dalla Man, C., Campioni, M., Polonsky, K. S., Basu, R., Rizza, R. A., Toffolo, G., and Cobelli, C. (2005): Two-hour seven-sample oral glucose tolerance test and meal protocol: minimal model assessment of beta-cell responsivity and insulin sensitivity in nondiabetic individuals. *Diabetes* **54**, 3265-73.

Davies, M. J. (2005): Post-prandial hyperglycaemia and prevention of cardiovascular disease. *Diabet Med* **22 Suppl 1**, 6-9.

Davis, J. E., Gabler, N. K., Walker-Daniels, J., and Spurlock, M. E. (2008): Tlr-4 deficiency selectively protects against obesity induced by diets high in saturated fat. *Obesity (Silver Spring)* **16**, 1248-55.

De Meyts, P., Urso, B., Christoffersen, C. T., and Shymko, R. M. (1995): Mechanism of insulin and IGF-I receptor activation and signal transduction specificity. Receptor dimer cross-linking, bell-shaped curves, and sustained versus transient signaling. *Ann N Y Acad Sci* **766**, 388-401.

De Roos, B., Rungapamestry, V., Ross, K., Rucklidge, G., Reid, M., Duncan, G., Horgan, G., Toomey, S., Browne, J., Loscher, C. E., Mills, K. H., and Roche, H. M. (2009): Attenuation of inflammation and cellular stress-related pathways maintains insulin sensitivity in obese type I interleukin-1 receptor knockout mice on a high-fat diet. *Proteomics* **9**, 3244-56.

DeFronzo, R. A., and Ferrannini, E. (1991): Insulin resistance. A multifaceted syndrome responsible for NIDDM, obesity, hypertension, dyslipidemia, and atherosclerotic cardiovascular disease. *Diabetes Care* **14**, 173-94.

DeFronzo, R. A., Tobin, J. D., and Andres, R. (1979): Glucose clamp technique: a method for quantifying insulin secretion and resistance. *Am J Physiol* **237**, E214-23.

Degawa-Yamauchi, M., Bovenkerk, J. E., Juliar, B. E., Watson, W., Kerr, K., Jones, R., Zhu, Q., and Considine, R. V. (2003): Serum resistin (FIZZ3) protein is increased in obese humans. *J Clin Endocrinol Metab* **88**, 5452-5.

Delerive, P., Fruchart, J. C., and Staels, B. (2001): Peroxisome proliferator-activated receptors in inflammation control. *J Endocrinol* **169**, 453-9.

Despres, J. P., Moorjani, S., Lupien, P. J., Tremblay, A., Nadeau, A., and Bouchard, C. (1990): Regional distribution of body fat, plasma lipoproteins, and cardiovascular disease. *Arteriosclerosis* **10**, 497-511.

Despres, J. P., Nadeau, A., Tremblay, A., Ferland, M., Moorjani, S., Lupien, P. J., Theriault, G., Pinault, S., and Bouchard, C. (1989): Role of deep abdominal fat in the association between regional adipose tissue distribution and glucose tolerance in obese women. *Diabetes* **38**, 304-9.

Desvergne, B., and Wahli, W. (1999): Peroxisome proliferator-activated receptors: nuclear control of metabolism. *Endocr Rev* **20**, 649-88.

Devary, Y., Rosette, C., DiDonato, J. A., and Karin, M. (1993): NF-kappa B activation by ultraviolet light not dependent on a nuclear signal. *Science* **261**, 1442-5.

Dinarello, C. A. (1996): Biologic basis for interleukin-1 in disease. *Blood* **87**, 2095-147.

Dinarello, C. A. (2009): Immunological and inflammatory functions of the interleukin-1 family. *Annu Rev Immunol* **27**, 519-50.

Duffield, J. S., Hong, S., Vaidya, V. S., Lu, Y., Fredman, G., Serhan, C. N., and Bonventre, J. V. (2006): Resolvin D series and protectin D1 mitigate acute kidney injury. *J Immunol* **177**, 5902-11.

Eaton, S. B., and Konner, M. (1985): Paleolithic nutrition. A consideration of its nature and current implications. *N Engl J Med* **312**, 283-9.

Elgazar-Carmon, V., Rudich, A., Hadad, N., and Levy, R. (2008): Neutrophils transiently infiltrate intra-abdominal fat early in the course of high-fat feeding. *J Lipid Res* **49**, 1894-903.

Elmhurst, J. L., Betti, P. A., and Rangachari, P. K. (1997): Intestinal effects of isoprostanes: evidence for the involvement of prostanoid EP and TP receptors. *J Pharmacol Exp Ther* **282**, 1198-205.

Emanuelli, B., Peraldi, P., Filloux, C., Sawka-Verhelle, D., Hilton, D., and Van Obberghen, E. (2000): SOCS-3 is an insulin-induced negative regulator of insulin signaling. *J Biol Chem* **275**, 15985-91.

Engelman, J. A., Berg, A. H., Lewis, R. Y., Lisanti, M. P., and Scherer, P. E. (2000): Tumor necrosis factor alpha-mediated insulin resistance, but not dedifferentiation, is abrogated by MEK1/2 inhibitors in 3T3-L1 adipocytes. *Mol Endocrinol* **14**, 1557-69.

Ericsson, A., Liu, C., Hart, R. P., and Sawchenko, P. E. (1995): Type 1 interleukin-1 receptor in the rat brain: distribution, regulation, and relationship to sites of IL-1-induced cellular activation. *J Comp Neurol* **361**, 681-98.

Faggioni, R., Fantuzzi, G., Fuller, J., Dinarello, C. A., Feingold, K. R., and Grunfeld, C. (1998): IL-1 beta mediates leptin induction during inflammation. *Am J Physiol* **274**, R204-8.

Fain, J. N. (1975): Isolation of free brown and white fat cells. *Methods Enzymol* **35**, 555-61.

Fajas, L., Schoonjans, K., Gelman, L., Kim, J. B., Najib, J., Martin, G., Fruchart, J. C., Briggs, M., Spiegelman, B. M., and Auwerx, J. (1999): Regulation of peroxisome proliferator-activated receptor gamma expression by adipocyte differentiation and determination factor 1/sterol regulatory element binding protein 1: implications for adipocyte differentiation and metabolism. *Mol Cell Biol* **19**, 5495-503.

Fantin, V. R., Wang, Q., Lienhard, G. E., and Keller, S. R. (2000): Mice lacking insulin receptor substrate 4 exhibit mild defects in growth, reproduction, and glucose homeostasis. *Am J Physiol Endocrinol Metab* **278**, E127-33.

Feige, J. N., Gelman, L., Michalik, L., Desvergne, B., and Wahli, W. (2006): From molecular action to physiological outputs: peroxisome proliferator-activated receptors are nuclear receptors at the crossroads of key cellular functions. *Prog Lipid Res* **45**, 120-59.

Feingold, K. R., Doerrler, W., Dinarello, C. A., Fiers, W., and Grunfeld, C. (1992): Stimulation of lipolysis in cultured fat cells by tumor necrosis factor, interleukin-1, and the interferons is blocked by inhibition of prostaglandin synthesis. *Endocrinology* **130**, 10-6.

Feinstein, D. L., Spagnolo, A., Akar, C., Weinberg, G., Murphy, P., Gavrilyuk, V., and Dello Russo, C. (2005): Receptor-independent actions of PPAR thiazolidinedione agonists: is mitochondrial function the key? *Biochem Pharmacol* **70**, 177-88.

Feinstein, R., Kanety, H., Papa, M. Z., Lunenfeld, B., and Karasik, A. (1993): Tumor necrosis factor-alpha suppresses insulin-induced tyrosine phosphorylation of insulin receptor and its substrates. *J Biol Chem* **268**, 26055-8.

Fernandis, A. Z., and Wenk, M. R. (2007): Membrane lipids as signaling molecules. *Curr Opin Lipidol* **18**, 121-8.

Feuerer, M., Herrero, L., Cipolletta, D., Naaz, A., Wong, J., Nayer, A., Lee, J., Goldfine, A. B., Benoist, C., Shoelson, S., and Mathis, D. (2009): Lean, but not obese, fat is enriched for a unique population of regulatory T cells that affect metabolic parameters. *Nat Med* **15**, 930-9.

Fingar, D. C., and Blenis, J. (2004): Target of rapamycin (TOR): an integrator of nutrient and growth factor signals and coordinator of cell growth and cell cycle progression. *Oncogene* **23**, 3151-71.

Flier, J. S. (1997): Leptin expression and action: new experimental paradigms. *Proc Natl Acad Sci U S A* **94**, 4242-5.

Flier, J. S., and Hollenberg, A. N. (1999): ADD-1 provides major new insight into the mechanism of insulin action. *Proc Natl Acad Sci U S A* **96**, 14191-2.

Foltz, I. N., Lee, J. C., Young, P. R., and Schrader, J. W. (1997): Hemopoietic growth factors with the exception of interleukin-4 activate the p38 mitogen-activated protein kinase pathway. *J Biol Chem* **272**, 3296-301.

Fong, Y., Moldawer, L. L., Marano, M., Wei, H., Barber, A., Manogue, K., Tracey, K. J., Kuo, G., Fischman, D. A., Cerami, A., and et al. (1989): Cachectin/TNF or IL-1 alpha induces cachexia with redistribution of body proteins. *Am J Physiol* **256**, R659-65.

Foretz, M., Guichard, C., Ferre, P., and Foufelle, F. (1999a): Sterol regulatory element binding protein-1c is a major mediator of insulin action on the hepatic expression of glucokinase and lipogenesis-related genes. *Proc Natl Acad Sci U S A* **96**, 12737-42.

Foretz, M., Pacot, C., Dugail, I., Lemarchand, P., Guichard, C., Le Liepvre, X., Berthelier-Lubrano, C., Spiegelman, B., Kim, J. B., Ferre, P., and Foufelle, F. (1999b): ADD1/SREBP-1c is required in the activation of hepatic lipogenic gene expression by glucose. *Mol Cell Biol* **19**, 3760-8.

Forman, B. M., Tontonoz, P., Chen, J., Brun, R. P., Spiegelman, B. M., and Evans, R. M. (1995): 15-Deoxy-delta 12, 14-prostaglandin J2 is a ligand for the adipocyte determination factor PPAR gamma. *Cell* **83**, 803-12.

Frayn, K. N., and Coppack, S. W. (1992): Insulin resistance, adipose tissue and coronary heart disease. *Clin Sci (Lond)* **82**, 1-8.

Frederich, R. C., Hamann, A., Anderson, S., Lollmann, B., Lowell, B. B., and Flier, J. S. (1995): Leptin levels reflect body lipid content in mice: evidence for diet-induced resistance to leptin action. *Nat Med* **1**, 1311-4.

Fredrikson, G., Stralfors, P., Nilsson, N. O., and Belfrage, P. (1981): Hormone-sensitive lipase of rat adipose tissue. Purification and some properties. *J Biol Chem* **256**, 6311-20.

Fried, S. K., Appel, B., and Zechner, R. (1993): Interleukin 1 alpha decreases the synthesis and activity of lipoprotein lipase in human adipose tissue. *Horm Metab Res* **25**, 129-30.

Fried, S. K., Bunkin, D. A., and Greenberg, A. S. (1998): Omental and subcutaneous adipose tissues of obese subjects release interleukin-6: depot difference and regulation by glucocorticoid. *J Clin Endocrinol Metab* **83**, 847-50.

Friedman, J. M., and Halaas, J. L. (1998): Leptin and the regulation of body weight in mammals. *Nature* **395**, 763-70.

Fritsche, L., Weigert, C., Haring, H. U., and Lehmann, R. (2008): How insulin receptor substrate proteins regulate the metabolic capacity of the liver--implications for health and disease. *Curr Med Chem* **15**, 1316-29.

Fujioka, S., Matsuzawa, Y., Tokunaga, K., and Tarui, S. (1987): Contribution of intra-abdominal fat accumulation to the impairment of glucose and lipid metabolism in human obesity. *Metabolism* **36**, 54-9.

Fukumoto, H., Seino, S., Imura, H., Seino, Y., Eddy, R. L., Fukushima, Y., Byers, M. G., Shows, T. B., and Bell, G. I. (1988): Sequence, tissue distribution, and chromosomal localization of mRNA encoding a human glucose transporter-like protein. *Proc Natl Acad Sci U S A* **85**, 5434-8.

Furtado, L. M., Somwar, R., Sweeney, G., Niu, W., and Klip, A. (2002): Activation of the glucose transporter GLUT4 by insulin. *Biochem Cell Biol* **80**, 569-78.

Gangloff, Y. G., Mueller, M., Dann, S. G., Svoboda, P., Sticker, M., Spetz, J. F., Um, S. H., Brown, E. J., Cereghini, S., Thomas, G., and Kozma, S. C. (2004): Disruption of the mouse mTOR gene leads to early postimplantation lethality and prohibits embryonic stem cell development. *Mol Cell Biol* **24**, 9508-16.

Ganon, W. (2005): *Review of medical physiology*. The McGraw-Hill Companies.

Gao, C. L., Zhao, D. Y., Qiu, J., Zhang, C. M., Ji, C. B., Chen, X. H., Liu, F., and Guo, X. R. (2009): Resistin induces rat insulinoma cell RINm5F apoptosis. *Mol Biol Rep* **36**, 1703-8.

Garcia, M. C., Wernstedt, I., Berndtsson, A., Enge, M., Bell, M., Hultgren, O., Horn, M., Ahren, B., Enerback, S., Ohlsson, C., Wallenius, V., and Jansson, J. O. (2006): Mature-onset obesity in interleukin-1 receptor I knockout mice. *Diabetes* **55**, 1205-13.

Gearing, K. L., Gottlicher, M., Teboul, M., Widmark, E., and Gustafsson, J. A. (1993): Interaction of the peroxisome-proliferator-activated receptor and retinoid X receptor. *Proc Natl Acad Sci U S A* **90**, 1440-4.

Geusens, P., Wouters, C., Nijs, J., Jiang, Y., and Dequeker, J. (1994): Long-term effect of omega-3 fatty acid supplementation in active rheumatoid arthritis. A 12-month, double-blind, controlled study. *Arthritis Rheum* **37**, 824-9.

Gibney, M. J., and Hunter, B. (1993): The effects of short- and long-term supplementation with fish oil on the incorporation of n-3 polyunsaturated fatty acids into cells of the immune system in healthy volunteers. *Eur J Clin Nutr* **47**, 255-9.

Ginsberg, B. H., Brown, T. J., Simon, I., and Spector, A. A. (1981): Effect of the membrane lipid environment on the properties of insulin receptors. *Diabetes* **30**, 773-80.

Ginsberg, B. H., Jabour, J., and Spector, A. A. (1982): Effect of alterations in membrane lipid unsaturation on the properties of the insulin receptor of Ehrlich ascites cells. *Biochim Biophys Acta* **690**, 157-64.

Glaccum, M. B., Stocking, K. L., Charrier, K., Smith, J. L., Willis, C. R., Maliszewski, C., Livingston, D. J., Peschon, J. J., and Morrissey, P. J. (1997): Phenotypic and functional characterization of mice that lack the type I receptor for IL-1. *J Immunol* **159**, 3364-71.

Glauber, H., Wallace, P., Griver, K., and Brechtel, G. (1988): Adverse metabolic effect of omega-3 fatty acids in non-insulin-dependent diabetes mellitus. *Ann Intern Med* **108**, 663-8.

Gonzalez-Periz, A., Horrillo, R., Ferre, N., Gronert, K., Dong, B., Moran-Salvador, E., Titos, E., Martinez-Clemente, M., Lopez-Parra, M., Arroyo, V., and Claria, J. (2009): Obesity-induced insulin resistance and hepatic steatosis are alleviated by omega-3 fatty acids: a role for resolvins and protectins. *Faseb J* **23**, 1946-57.

Goodpaster, B. H., and Kelley, D. E. (1998): Role of muscle in triglyceride metabolism. *Curr Opin Lipidol* **9**, 231-6.

Goodpaster, B. H., Krishnaswami, S., Resnick, H., Kelley, D. E., Haggerty, C., Harris, T. B., Schwartz, A. V., Kritchevsky, S., and Newman, A. B. (2003): Association between regional adipose tissue distribution and both type 2 diabetes and impaired glucose tolerance in elderly men and women. *Diabetes Care* **26**, 372-9.

Goodpaster, B. H., Thaete, F. L., Simoneau, J. A., and Kelley, D. E. (1997): Subcutaneous abdominal fat and thigh muscle composition predict insulin sensitivity independently of visceral fat. *Diabetes* **46**, 1579-85.

Gordon, S., and Taylor, P. R. (2005): Monocyte and macrophage heterogeneity. *Nat Rev Immunol* **5**, 953-64.

Green, H., and Kehinde, O. (1975): An established preadipose cell line and its differentiation in culture. II. Factors affecting the adipose conversion. *Cell* **5**, 19-27.

Green, H., and Kehinde, O. (1979): Formation of normally differentiated subcutaneous fat pads by an established preadipose cell line. *J Cell Physiol* **101**, 169-71.

Greene, M. W., Sakaue, H., Wang, L., Alessi, D. R., and Roth, R. A. (2003): Modulation of insulin-stimulated degradation of human insulin receptor substrate-1 by Serine 312 phosphorylation. *J Biol Chem* **278**, 8199-211.

Greenfeder, S. A., Nunes, P., Kwee, L., Labow, M., Chizzonite, R. A., and Ju, G. (1995): Molecular cloning and characterization of a second subunit of the interleukin 1 receptor complex. *J Biol Chem* **270**, 13757-65.

Gregoire, F., De Broux, N., Hauser, N., Heremans, H., Van Damme, J., and Remacle, C. (1992): Interferon-gamma and interleukin-1 beta inhibit adipoconversion in cultured rodent preadipocytes. *J Cell Physiol* **151**, 300-9.

Gronn, M., Christensen, E., Hagve, T. A., and Christophersen, B. O. (1991): Peroxisomal retroconversion of docosahexaenoic acid (22:6(n-3)) to eicosapentaenoic acid (20:5(n-3)) studied in isolated rat liver cells. *Biochim Biophys Acta* **1081**, 85-91.

Gual, P., Gremeaux, T., Gonzalez, T., Le Marchand-Brustel, Y., and Tanti, J. F. (2003): MAP kinases and mTOR mediate insulin-induced phosphorylation of insulin receptor substrate-1 on serine residues 307, 612 and 632. *Diabetologia* **46**, 1532-42.

Gual, P., Le Marchand-Brustel, Y., and Tanti, J. F. (2005): Positive and negative regulation of insulin signaling through IRS-1 phosphorylation. *Biochimie* **87**, 99-109.

Guo, D., and Donner, D. B. (1996): Tumor necrosis factor promotes phosphorylation and binding of insulin receptor substrate 1 to phosphatidylinositol 3-kinase in 3T3-L1 adipocytes. *J Biol Chem* **271**, 615-8.

Haag, M., Malipa, A. C., van Papendorp, D. H., Stivaktas, P. I., Alummoottil, S., and Koorts, A. M. (2009): Short-term fatty acid effects on adipocyte glucose uptake: mechanistic insights. *Prostaglandins Leukot Essent Fatty Acids* **80**, 247-53.

Hainault, I., Carolotti, M., Hajduch, E., Guichard, C., and Lavau, M. (1993): Fish oil in a high lard diet prevents obesity, hyperlipemia, and adipocyte insulin resistance in rats. *Ann N Y Acad Sci* **683**, 98-101.

Halaas, J. L., Boozer, C., Blair-West, J., Fidahusein, N., Denton, D. A., and Friedman, J. M. (1997): Physiological response to long-term peripheral and central leptin infusion in lean and obese mice. *Proc Natl Acad Sci U S A* **94**, 8878-83.

Halaas, J. L., Gajiwala, K. S., Maffei, M., Cohen, S. L., Chait, B. T., Rabinowitz, D., Lallone, R. L., Burley, S. K., and Friedman, J. M. (1995): Weight-reducing effects of the plasma protein encoded by the obese gene. *Science* **269**, 543-6.

Hambleton, J., Weinstein, S. L., Lem, L., and DeFranco, A. L. (1996): Activation of c-Jun N-terminal kinase in bacterial lipopolysaccharide-stimulated macrophages. *Proc Natl Acad Sci U S A* **93**, 2774-8.

Han, J., Lee, J. D., Bibbs, L., and Ulevitch, R. J. (1994): A MAP kinase targeted by endotoxin and hyperosmolarity in mammalian cells. *Science* **265**, 808-11.

Han, J., Lee, J. D., Tobias, P. S., and Ulevitch, R. J. (1993): Endotoxin induces rapid protein tyrosine phosphorylation in 70Z/3 cells expressing CD14. *J Biol Chem* **268**, 25009-14.

Hannun, Y. A., and Obeid, L. M. (1995): Ceramide: an intracellular signal for apoptosis. *Trends Biochem Sci* **20**, 73-7.

Hardie, D. G. (2003): Minireview: the AMP-activated protein kinase cascade: the key sensor of cellular energy status. *Endocrinology* **144**, 5179-83.

Harrington, L. S., Findlay, G. M., Gray, A., Tolkacheva, T., Wigfield, S., Rebholz, H., Barnett, J., Leslie, N. R., Cheng, S., Shepherd, P. R., Gout, I., Downes, C. P., and Lamb, R. F. (2004): The TSC1-2 tumor suppressor controls insulin-PI3K signaling via regulation of IRS proteins. *J Cell Biol* **166**, 213-23.

Haruta, T., Uno, T., Kawahara, J., Takano, A., Egawa, K., Sharma, P. M., Olefsky, J. M., and Kobayashi, M. (2000): A rapamycin-sensitive pathway down-regulates insulin signaling via phosphorylation and proteasomal degradation of insulin receptor substrate-1. *Mol Endocrinol* **14**, 783-94.

Haugen, F., Jorgensen, A., Drevon, C. A., and Trayhurn, P. (2001): Inhibition by insulin of resistin gene expression in 3T3-L1 adipocytes. *FEBS Lett* **507**, 105-8.

Hauner, H., Petruschke, T., Russ, M., Rohrig, K., and Eckel, J. (1995): Effects of tumour necrosis factor alpha (TNF alpha) on glucose transport and lipid metabolism of newly-differentiated human fat cells in cell culture. *Diabetologia* **38**, 764-71.

Havel, P. J. (2002): Control of energy homeostasis and insulin action by adipocyte hormones: leptin, acylation stimulating protein, and adiponectin. *Curr Opin Lipidol* **13**, 51-9.

Hayden, M. S., and Ghosh, S. (2004): Signaling to NF-kappaB. *Genes Dev* **18**, 2195-224.

He, J., Usui, I., Ishizuka, K., Kanatani, Y., Hiratani, K., Iwata, M., Bukhari, A., Haruta, T., Sasaoka, T., and Kobayashi, M. (2006): Interleukin-1alpha inhibits insulin signaling with phosphorylating insulin receptor substrate-1 on serine residues in 3T3-L1 adipocytes. *Mol Endocrinol* **20**, 114-24.

Healy, D. A., Wallace, F. A., Miles, E. A., Calder, P. C., and Newsholm, P. (2000): Effect of low-to-moderate amounts of dietary fish oil on neutrophil lipid composition and function. *Lipids* **35**, 763-8.

Heilbronn, L. K., Rood, J., Janderova, L., Albu, J. B., Kelley, D. E., Ravussin, E., and Smith, S. R. (2004): Relationship between serum resistin concentrations and insulin resistance in nonobese, obese, and obese diabetic subjects. *J Clin Endocrinol Metab* **89**, 1844-8.

Henke, B. R., Blanchard, S. G., Brackeen, M. F., Brown, K. K., Cobb, J. E., Collins, J. L., Harrington, W. W., Jr., Hashim, M. A., Hull-Ryde, E. A., Kaldor, I., Kliewer, S. A., Lake, D. H., Leesnitzer, L. M., Lehmann, J. M., Lenhard, J. M., Orband-Miller, L. A., Miller, J. F., Mook, R. A., Jr., Noble, S. A., Oliver, W., Jr., Parks, D. J., Plunket, K. D., Szewczyk, J. R., and Willson, T. M. (1998): N-(2-Benzoylphenyl)-L-tyrosine PPARgamma agonists. 1. Discovery of a novel series of potent antihyperglycemic and antihyperlipidemic agents. *J Med Chem* **41**, 5020-36.

Herder, C., Haastert, B., Muller-Scholze, S., Koenig, W., Thorand, B., Holle, R., Wichmann, H. E., Scherbaum, W. A., Martin, S., and Kolb, H. (2005): Association of systemic chemokine concentrations with impaired glucose tolerance and type 2 diabetes: results from the Cooperative Health Research in the Region of Augsburg Survey S4 (KORA S4). *Diabetes* **54 Suppl 2**, S11-7.

Herman, M. A., and Kahn, B. B. (2006): Glucose transport and sensing in the maintenance of glucose homeostasis and metabolic harmony. *J Clin Invest* **116**, 1767-75.

Heymsfield, S. B., Greenberg, A. S., Fujioka, K., Dixon, R. M., Kushner, R., Hunt, T., Lubina, J. A., Patane, J., Self, B., Hunt, P., and McCamish, M. (1999): Recombinant leptin for weight loss in obese and lean adults: a randomized, controlled, dose-escalation trial. *Jama* **282**, 1568-75.

Hirosumi, J., Tuncman, G., Chang, L., Gorgun, C. Z., Uysal, K. T., Maeda, K., Karin, M., and Hotamisligil, G. S. (2002): A central role for JNK in obesity and insulin resistance. *Nature* **420**, 333-6.

Holgado-Madruga, M., Emlet, D. R., Moscatello, D. K., Godwin, A. K., and Wong, A. J. (1996): A Grb2-associated docking protein in EGF- and insulin-receptor signalling. *Nature* **379**, 560-4.

Holm, C. (2003): Molecular mechanisms regulating hormone-sensitive lipase and lipolysis. *Biochem Soc Trans* **31**, 1120-4.

Horton, J. D., and Shimomura, I. (1999): Sterol regulatory element-binding proteins: activators of cholesterol and fatty acid biosynthesis. *Curr Opin Lipidol* **10**, 143-50.

Hosogai, N., Fukuhara, A., Oshima, K., Miyata, Y., Tanaka, S., Segawa, K., Furukawa, S., Tochino, Y., Komuro, R., Matsuda, M., and Shimomura, I. (2007): Adipose tissue hypoxia in obesity and its impact on adipocytokine dysregulation. *Diabetes* **56**, 901-11.

Hotamisligil, G. S., Arner, P., Atkinson, R. L., and Spiegelman, B. M. (1997): Differential regulation of the p80 tumor necrosis factor receptor in human obesity and insulin resistance. *Diabetes* **46**, 451-5.

Hotamisligil, G. S., Arner, P., Caro, J. F., Atkinson, R. L., and Spiegelman, B. M. (1995): Increased adipose tissue expression of tumor necrosis factor-alpha in human obesity and insulin resistance. *J Clin Invest* **95**, 2409-15.

Hotamisligil, G. S., Budavari, A., Murray, D., and Spiegelman, B. M. (1994a): Reduced tyrosine kinase activity of the insulin receptor in obesity-diabetes. Central role of tumor necrosis factor-alpha. *J Clin Invest* **94**, 1543-9.

Hotamisligil, G. S., Murray, D. L., Choy, L. N., and Spiegelman, B. M. (1994b): Tumor necrosis factor alpha inhibits signaling from the insulin receptor. *Proc Natl Acad Sci U S A* **91**, 4854-8.

Hotamisligil, G. S., Peraldi, P., Budavari, A., Ellis, R., White, M. F., and Spiegelman, B. M. (1996): IRS-1-mediated inhibition of insulin receptor tyrosine kinase activity in TNF-alpha- and obesity-induced insulin resistance. *Science* **271**, 665-8.

Hotamisligil, G. S., Shargill, N. S., and Spiegelman, B. M. (1993): Adipose expression of tumor necrosis factor-alpha: direct role in obesity-linked insulin resistance. *Science* **259**, 87-91.

Hotta, K., Funahashi, T., Bodkin, N. L., Ortmeyer, H. K., Arita, Y., Hansen, B. C., and Matsuzawa, Y. (2001): Circulating concentrations of the adipocyte protein

adiponectin are decreased in parallel with reduced insulin sensitivity during the progression to type 2 diabetes in rhesus monkeys. *Diabetes* **50**, 1126-33.

Houseknecht, K. L., Baile, C. A., Matteri, R. L., and Spurlock, M. E. (1998): The biology of leptin: a review. *J Anim Sci* **76**, 1405-20.

Houseknecht, K. L., Mantzoros, C. S., Kuliawat, R., Hadro, E., Flier, J. S., and Kahn, B. B. (1996): Evidence for leptin binding to proteins in serum of rodents and humans: modulation with obesity. *Diabetes* **45**, 1638-43.

Hu, E., Liang, P., and Spiegelman, B. M. (1996): AdipoQ is a novel adipose-specific gene dysregulated in obesity. *J Biol Chem* **271**, 10697-703.

Hu, F. B., Cho, E., Rexrode, K. M., Albert, C. M., and Manson, J. E. (2003): Fish and long-chain omega-3 fatty acid intake and risk of coronary heart disease and total mortality in diabetic women. *Circulation* **107**, 1852-7.

Huang, J., Gao, X., Li, S., and Cao, Z. (1997): Recruitment of IRAK to the interleukin 1 receptor complex requires interleukin 1 receptor accessory protein. *Proc Natl Acad Sci U S A* **94**, 12829-32.

Hubbard, S. R. (1997): Crystal structure of the activated insulin receptor tyrosine kinase in complex with peptide substrate and ATP analog. *Embo J* **16**, 5572-81.

Hubbard, S. R., Wei, L., Ellis, L., and Hendrickson, W. A. (1994): Crystal structure of the tyrosine kinase domain of the human insulin receptor. *Nature* **372**, 746-54.

Huggins, K. W., Boileau, A. C., and Hui, D. Y. (2002): Protection against diet-induced obesity and obesity- related insulin resistance in Group 1B PLA2-deficient mice. *Am J Physiol Endocrinol Metab* **283**, E994-E1001.

Hulbert, A. J., Turner, N., Storlien, L. H., and Else, P. L. (2005): Dietary fats and membrane function: implications for metabolism and disease. *Biol Rev Camb Philos Soc* **80**, 155-69.

IDF (2009): International Diabetes Federation. Diabetes atlas: Diabetic complecations www.eatlas.idf.org.

Ikezu, T., Okamoto, T., Yonezawa, K., Tompkins, R. G., and Martyn, J. A. (1997): Analysis of thermal injury-induced insulin resistance in rodents. Implication of postreceptor mechanisms. *J Biol Chem* **272**, 25289-95.

Ilyin, S. E., and Plata-Salaman, C. R. (1996): In vivo regulation of the IL-1 beta system (ligand, receptors I and II, receptor accessory protein, and receptor antagonist) and TNF-alpha mRNAs in specific brain regions. *Biochem Biophys Res Commun* **227**, 861-7.

Imbeault, P., Lemieux, S., Prud'homme, D., Tremblay, A., Nadeau, A., Despres, J. P., and Mauriege, P. (1999): Relationship of visceral adipose tissue to metabolic risk factors for coronary heart disease: is there a contribution of subcutaneous fat cell hypertrophy? *Metabolism* **48**, 355-62.

Israel, A., Le Bail, O., Hatat, D., Piette, J., Kieran, M., Logeat, F., Wallach, D., Fellous, M., and Kourilsky, P. (1989): TNF stimulates expression of mouse MHC class I genes by inducing an NF kappa B-like enhancer binding activity which displaces constitutive factors. *Embo J* **8**, 3793-800.

Itoh, M., Suganami, T., Satoh, N., Tanimoto-Koyama, K., Yuan, X., Tanaka, M., Kawano, H., Yano, T., Aoe, S., Takeya, M., Shimatsu, A., Kuzuya, H., Kamei, Y., and Ogawa, Y. (2007): Increased adiponectin secretion by highly purified eicosapentaenoic acid in rodent models of obesity and human obese subjects. *Arterioscler Thromb Vasc Biol* **27**, 1918-25.

Itoh, M., Yoshida, Y., Nishida, K., Narimatsu, M., Hibi, M., and Hirano, T. (2000): Role of Gab1 in heart, placenta, and skin development and growth factor- and cytokine-induced extracellular signal-regulated kinase mitogen-activated protein kinase activation. *Mol Cell Biol* **20**, 3695-704.

Iwaki, M., Matsuda, M., Maeda, N., Funahashi, T., Matsuzawa, Y., Makishima, M., and Shimomura, I. (2003): Induction of adiponectin, a fat-derived antidiabetic and antiatherogenic factor, by nuclear receptors. *Diabetes* **52**, 1655-63.

Jackson, S. M., Parhami, F., Xi, X. P., Berliner, J. A., Hsueh, W. A., Law, R. E., and Demer, L. L. (1999): Peroxisome proliferator-activated receptor activators target human endothelial cells to inhibit leukocyte-endothelial cell interaction. *Arterioscler Thromb Vasc Biol* **19**, 2094-104.

Jacobs, N. J., and Vandemark, P. J. (1960): Comparison of the mechanism of glycerol oxidation in aerobically and anaerobically grown Streptococcus faecalis. *J Bacteriol* **79**, 532-8.

Jager, J., Gremeaux, T., Cormont, M., Le Marchand-Brustel, Y., and Tanti, J. F. (2007): Interleukin-1beta-induced insulin resistance in adipocytes through down-regulation of insulin receptor substrate-1 expression. *Endocrinology* **148**, 241-51.

Jain, S., Pulikuri, S., Zhu, Y., Qi, C., Kanwar, Y. S., Yeldandi, A. V., Rao, M. S., and Reddy, J. K. (1998): Differential expression of the peroxisome proliferator-activated receptor gamma (PPARgamma) and its coactivators steroid receptor coactivator-1 and PPAR-binding protein PBP in the brown fat, urinary bladder, colon, and breast of the mouse. *Am J Pathol* **153**, 349-54.

Janke, J., Engeli, S., Gorzelniak, K., Luft, F. C., and Sharma, A. M. (2002): Resistin gene expression in human adipocytes is not related to insulin resistance. *Obes Res* **10**, 1-5.

Jequier, E., and Tappy, L. (1999): Regulation of body weight in humans. *Physiol Rev* **79**, 451-80.

Jiang, C., Ting, A. T., and Seed, B. (1998): PPAR-gamma agonists inhibit production of monocyte inflammatory cytokines. *Nature* **391**, 82-6.

Jiang, Z. Y., Zhou, Q. L., Coleman, K. A., Chouinard, M., Boese, Q., and Czech, M. P. (2003): Insulin signaling through Akt/protein kinase B analyzed by small interfering RNA-mediated gene silencing. *Proc Natl Acad Sci U S A* **100**, 7569-74.

Jones, J. R., Barrick, C., Kim, K. A., Lindner, J., Blondeau, B., Fujimoto, Y., Shiota, M., Kesterson, R. A., Kahn, B. B., and Magnuson, M. A. (2005): Deletion of PPARgamma in adipose tissues of mice protects against high fat diet-induced obesity and insulin resistance. *Proc Natl Acad Sci U S A* **102**, 6207-12.

Jones, S. A., Horiuchi, S., Topley, N., Yamamoto, N., and Fuller, G. M. (2001): The soluble interleukin 6 receptor: mechanisms of production and implications in disease. *Faseb J* **15**, 43-58.

Jue, D. M., Sherry, B., Luedke, C., Manogue, K. R., and Cerami, A. (1990): Processing of newly synthesized cachectin/tumor necrosis factor in endotoxin-stimulated macrophages. *Biochemistry* **29**, 8371-7.

Juge-Aubry, C. E., Henrichot, E., and Meier, C. A. (2005): Adipose tissue: a regulator of inflammation. *Best Pract Res Clin Endocrinol Metab* **19**, 547-66.

Juge-Aubry, C. E., Somm, E., Chicheportiche, R., Burger, D., Pernin, A., Cuenod-Pittet, B., Quinodoz, P., Giusti, V., Dayer, J. M., and Meier, C. A. (2004): Regulatory effects of interleukin (IL)-1, interferon-beta, and IL-4 on the production of IL-1 receptor antagonist by human adipose tissue. *J Clin Endocrinol Metab* **89**, 2652-8.

Jump, D. B. (2002): Dietary polyunsaturated fatty acids and regulation of gene transcription. *Curr Opin Lipidol* **13**, 155-64.

Jump, D. B., and Clarke, S. D. (1999): Regulation of gene expression by dietary fat. *Annu Rev Nutr* **19**, 63-90.

Kahn, B. B., and Rossetti, L. (1998): Type 2 diabetes--who is conducting the orchestra? *Nat Genet* **20**, 223-5.

Kamimura, D., Ishihara, K., and Hirano, T. (2003): IL-6 signal transduction and its physiological roles: the signal orchestration model. *Rev Physiol Biochem Pharmacol* **149**, 1-38.

Kaneto, H., Fujii, J., Seo, H. G., Suzuki, K., Matsuoka, T., Nakamura, M., Tatsumi, H., Yamasaki, Y., Kamada, T., and Taniguchi, N. (1995): Apoptotic cell death triggered by nitric oxide in pancreatic beta-cells. *Diabetes* **44**, 733-8.

Kang, Y. J., Chen, J., Otsuka, M., Mols, J., Ren, S., Wang, Y., and Han, J. (2008): Macrophage deletion of p38alpha partially impairs lipopolysaccharide-induced cellular activation. *J Immunol* **180**, 5075-82.

Kappes, A., and Loffler, G. (2000): Influences of ionomycin, dibutyryl-cycloAMP and tumour necrosis factor-alpha on intracellular amount and secretion of apM1 in differentiating primary human preadipocytes. *Horm Metab Res* **32**, 548-54.

Karin, M., and Ben-Neriah, Y. (2000): Phosphorylation meets ubiquitination: the control of NF-[kappa]B activity. *Annu Rev Immunol* **18**, 621-63.

Karin, M., Yamamoto, Y., and Wang, Q. M. (2004): The IKK NF-kappa B system: a treasure trove for drug development. *Nat Rev Drug Discov* **3**, 17-26.

Kaser, S., Kaser, A., Sandhofer, A., Ebenbichler, C. F., Tilg, H., and Patsch, J. R. (2003): Resistin messenger-RNA expression is increased by proinflammatory cytokines in vitro. *Biochem Biophys Res Commun* **309**, 286-90.

Katsuki, A., Sumida, Y., Murashima, S., Murata, K., Takarada, Y., Ito, K., Fujii, M., Tsuchihashi, K., Goto, H., Nakatani, K., and Yano, Y. (1998): Serum levels of tumor necrosis factor-alpha are increased in obese patients with noninsulin-dependent diabetes mellitus. *J Clin Endocrinol Metab* **83**, 859-62.

Katz, A., Nambi, S. S., Mather, K., Baron, A. D., Follmann, D. A., Sullivan, G., and Quon, M. J. (2000): Quantitative insulin sensitivity check index: a simple, accurate method for assessing insulin sensitivity in humans. *J Clin Endocrinol Metab* **85**, 2402-10.

Kayano, T., Fukumoto, H., Eddy, R. L., Fan, Y. S., Byers, M. G., Shows, T. B., and Bell, G. I. (1988): Evidence for a family of human glucose transporter-like proteins. Sequence and gene localization of a protein expressed in fetal skeletal muscle and other tissues. *J Biol Chem* **263**, 15245-8.

Kelley, D. E., Thaete, F. L., Troost, F., Huwe, T., and Goodpaster, B. H. (2000): Subdivisions of subcutaneous abdominal adipose tissue and insulin resistance. *Am J Physiol Endocrinol Metab* **278**, E941-8.

Kennedy, A., Martinez, K., Chuang, C. C., LaPoint, K., and McIntosh, M. (2009): Saturated fatty acid-mediated inflammation and insulin resistance in adipose tissue: mechanisms of action and implications. *J Nutr* **139**, 1-4.

Kennedy, E. P. (1961): Biosynthesis of complex lipids. *Fed Proc* **20**, 934-40.

Kershaw, E. E., Hamm, J. K., Verhagen, L. A., Peroni, O., Katic, M., and Flier, J. S. (2006): Adipose triglyceride lipase: function, regulation by insulin, and comparison with adiponutrin. *Diabetes* **55**, 148-57.

Kesavulu, M. M., Kameswararao, B., Apparao, C., Kumar, E. G., and Harinarayan, C. V. (2002): Effect of omega-3 fatty acids on lipid peroxidation and antioxidant enzyme status in type 2 diabetic patients. *Diabetes Metab* **28**, 20-6.

Khan, A. H., and Pessin, J. E. (2002): Insulin regulation of glucose uptake: a complex interplay of intracellular signalling pathways. *Diabetologia* **45**, 1475-83.

Kieffer, T. J., and Habener, J. F. (2000): The adipoinsular axis: effects of leptin on pancreatic beta-cells. *Am J Physiol Endocrinol Metab* **278**, E1-E14.

Kielian, T. L., and Blecha, F. (1995): CD14 and other recognition molecules for lipopolysaccharide: a review. *Immunopharmacology* **29**, 187-205.

Kim, H. K., Della-Fera, M., Lin, J., and Baile, C. A. (2006): Docosahexaenoic acid inhibits adipocyte differentiation and induces apoptosis in 3T3-L1 preadipocytes. *J Nutr* **136**, 2965-9.

Kim, J. B., Sarraf, P., Wright, M., Yao, K. M., Mueller, E., Solanes, G., Lowell, B. B., and Spiegelman, B. M. (1998a): Nutritional and insulin regulation of fatty acid synthetase and leptin gene expression through ADD1/SREBP1. *J Clin Invest* **101**, 1-9.

Kim, J. B., and Spiegelman, B. M. (1996): ADD1/SREBP1 promotes adipocyte differentiation and gene expression linked to fatty acid metabolism. *Genes Dev* **10**, 1096-107.

Kim, J. B., Wright, H. M., Wright, M., and Spiegelman, B. M. (1998b): ADD1/SREBP1 activates PPARgamma through the production of endogenous ligand. *Proc Natl Acad Sci U S A* **95**, 4333-7.

Kim, J. K., Kim, Y. J., Fillmore, J. J., Chen, Y., Moore, I., Lee, J., Yuan, M., Li, Z. W., Karin, M., Perret, P., Shoelson, S. E., and Shulman, G. I. (2001a): Prevention of fat-induced insulin resistance by salicylate. *J Clin Invest* **108**, 437-46.

Kim, K. H., Lee, K., Moon, Y. S., and Sul, H. S. (2001b): A cysteine-rich adipose tissue-specific secretory factor inhibits adipocyte differentiation. *J Biol Chem* **276**, 11252-6.

Kinsella, J. E., Lokesh, B., Broughton, S., and Whelan, J. (1990): Dietary polyunsaturated fatty acids and eicosanoids: potential effects on the modulation of inflammatory and immune cells: an overview. *Nutrition* **6**, 24-44; discussion 59-62.

Kissebah, A. H., Vydelingum, N., Murray, R., Evans, D. J., Hartz, A. J., Kalkhoff, R. K., and Adams, P. W. (1982): Relation of body fat distribution to metabolic complications of obesity. *J Clin Endocrinol Metab* **54**, 254-60.

Kleeberg, J. (1971): [The discovery of gastric lipase by Franz Volhard (1901)]. *Z Gastroenterol* **9**, 646-7.

Kliewer, S. A., Forman, B. M., Blumberg, B., Ong, E. S., Borgmeyer, U., Mangelsdorf, D. J., Umesono, K., and Evans, R. M. (1994): Differential expression and activation of a family of murine peroxisome proliferator-activated receptors. *Proc Natl Acad Sci U S A* **91**, 7355-9.

Klip, A., Tsakiridis, T., Marette, A., and Ortiz, P. A. (1994): Regulation of expression of glucose transporters by glucose: a review of studies in vivo and in cell cultures. *Faseb J* **8**, 43-53.

Kobayashi, H., Ouchi, N., Kihara, S., Walsh, K., Kumada, M., Abe, Y., Funahashi, T., and Matsuzawa, Y. (2004): Selective suppression of endothelial cell apoptosis by the high molecular weight form of adiponectin. *Circ Res* **94**, e27-31.

Koditschek, L. K., and Umbreit, W. W. (1969): Alpha-glycerophosphate oxidase in Streptococcus faecium F 24. *J Bacteriol* **98**, 1063-8.

Koerner, A., Kratzsch, J., and Kiess, W. (2005): Adipocytokines: leptin--the classical, resistin--the controversical, adiponectin--the promising, and more to come. *Best Pract Res Clin Endocrinol Metab* **19**, 525-46.

Koistinen, H. A., Chibalin, A. V., and Zierath, J. R. (2003): Aberrant p38 mitogen-activated protein kinase signalling in skeletal muscle from Type 2 diabetic patients. *Diabetologia* **46**, 1324-8.

Kolaczynski, J. W., Considine, R. V., Ohannesian, J., Marco, C., Opentanova, I., Nyce, M. R., Myint, M., and Caro, J. F. (1996a): Responses of leptin to short-term fasting and refeeding in humans: a link with ketogenesis but not ketones themselves. *Diabetes* **45**, 1511-5.

Kolaczynski, J. W., Ohannesian, J. P., Considine, R. V., Marco, C. C., and Caro, J. F. (1996b): Response of leptin to short-term and prolonged overfeeding in humans. *J Clin Endocrinol Metab* **81**, 4162-5.

Kolehmainen, M., Vidal, H., Alhava, E., and Uusitupa, M. I. (2001): Sterol regulatory element binding protein 1c (SREBP-1c) expression in human obesity. *Obes Res* **9**, 706-12.

Kopelman, P. G. (2000): Obesity as a medical problem. *Nature* **404**, 635-43.

Kopp, E., and Ghosh, S. (1994): Inhibition of NF-kappa B by sodium salicylate and aspirin. *Science* **265**, 956-9.

Kops, G. J., and Burgering, B. M. (1999): Forkhead transcription factors: new insights into protein kinase B (c-akt) signaling. *J Mol Med* **77**, 656-65.

Koyama, K., Chen, G., Lee, Y., and Unger, R. H. (1997): Tissue triglycerides, insulin resistance, and insulin production: implications for hyperinsulinemia of obesity. *Am J Physiol* **273**, E708-13.

Krief, S., Bazin, R., Dupuy, F., and Lavau, M. (1988): Increased in vivo glucose utilization in 30-day-old obese Zucker rat: role of white adipose tissue. *Am J Physiol* **254**, E342-8.

Kromann, N., and Green, A. (1980): Epidemiological studies in the Upernavik district, Greenland. Incidence of some chronic diseases 1950-1974. *Acta Med Scand* **208**, 401-6.

Kubota, N., Terauchi, Y., Miki, H., Tamemoto, H., Yamauchi, T., Komeda, K., Satoh, S., Nakano, R., Ishii, C., Sugiyama, T., Eto, K., Tsubamoto, Y., Okuno, A., Murakami, K., Sekihara, H., Hasegawa, G., Naito, M., Toyoshima, Y., Tanaka, S., Shiota, K., Kitamura, T., Fujita, T., Ezaki, O., Aizawa, S., Kadowaki, T., and et al. (1999): PPAR gamma mediates high-fat diet-induced adipocyte hypertrophy and insulin resistance. *Mol Cell* **4**, 597-609.

Kunapuli, P., Lawson, J. A., Rokach, J. A., Meinkoth, J. L., and FitzGerald, G. A. (1998): Prostaglandin F2alpha (PGF2alpha) and the isoprostane, 8, 12-iso-isoprostane F2alpha-III, induce cardiomyocyte hypertrophy. Differential activation of downstream signaling pathways. *J Biol Chem* **273**, 22442-52.

Kushiyama, A., Shojima, N., Ogihara, T., Inukai, K., Sakoda, H., Fujishiro, M., Fukushima, Y., Anai, M., Ono, H., Horike, N., Viana, A. Y., Uchijima, Y., Nishiyama, K., Shimosawa, T., Fujita, T., Katagiri, H., Oka, Y., Kurihara, H., and Asano, T. (2005): Resistin-like molecule beta activates MAPKs, suppresses insulin signaling in hepatocytes, and induces diabetes, hyperlipidemia, and fatty liver in transgenic mice on a high fat diet. *J Biol Chem* **280**, 42016-25.

Lagathu, C., Yvan-Charvet, L., Bastard, J. P., Maachi, M., Quignard-Boulange, A., Capeau, J., and Caron, M. (2006): Long-term treatment with interleukin-1beta induces insulin resistance in murine and human adipocytes. *Diabetologia* **49**, 2162-73.

Lang, C. H., Dobrescu, C., and Bagby, G. J. (1992): Tumor necrosis factor impairs insulin action on peripheral glucose disposal and hepatic glucose output. *Endocrinology* **130**, 43-52.

Larsen, C. M., Faulenbach, M., Vaag, A., Volund, A., Ehses, J. A., Seifert, B., Mandrup-Poulsen, T., and Donath, M. Y. (2007): Interleukin-1-receptor antagonist in type 2 diabetes mellitus. *N Engl J Med* **356**, 1517-26.

Latasa, M. J., Moon, Y. S., Kim, K. H., and Sul, H. S. (2000): Nutritional regulation of the fatty acid synthase promoter in vivo: sterol regulatory element binding protein functions through an upstream region containing a sterol regulatory element. *Proc Natl Acad Sci U S A* **97**, 10619-24.

Lavan, B. E., Fantin, V. R., Chang, E. T., Lane, W. S., Keller, S. R., and Lienhard, G. E. (1997a): A novel 160-kDa phosphotyrosine protein in insulin-treated embryonic kidney cells is a new member of the insulin receptor substrate family. *J Biol Chem* **272**, 21403-7.

Lavan, B. E., Lane, W. S., and Lienhard, G. E. (1997b): The 60-kDa phosphotyrosine protein in insulin-treated adipocytes is a new member of the insulin receptor substrate family. *J Biol Chem* **272**, 11439-43.

Laws, A., and Reaven, G. M. (1992): Evidence for an independent relationship between insulin resistance and fasting plasma HDL-cholesterol, triglyceride and insulin concentrations. *J Intern Med* **231**, 25-30.

Lawson, J. A., Rokach, J., and FitzGerald, G. A. (1999): Isoprostanes: formation, analysis and use as indices of lipid peroxidation in vivo. *J Biol Chem* **274**, 24441-4.

Le Good, J. A., Ziegler, W. H., Parekh, D. B., Alessi, D. R., Cohen, P., and Parker, P. J. (1998): Protein kinase C isotypes controlled by phosphoinositide 3-kinase through the protein kinase PDK1. *Science* **281**, 2042-5.

Le Marchand, Y., Freychet, P., and Jeanrenaud, B. (1978): Longitudinal study on the establishment of insulin resistance in hypothalamic obese mice. *Endocrinology* **102**, 74-85.

Lee, J. Y., Plakidas, A., Lee, W. H., Heikkinen, A., Chanmugam, P., Bray, G., and Hwang, D. H. (2003): Differential modulation of Toll-like receptors by fatty acids: preferential inhibition by n-3 polyunsaturated fatty acids. *J Lipid Res* **44**, 479-86.

Lee, J. Y., Sohn, K. H., Rhee, S. H., and Hwang, D. (2001): Saturated fatty acids, but not unsaturated fatty acids, induce the expression of cyclooxygenase-2 mediated through Toll-like receptor 4. *J Biol Chem* **276**, 16683-9.

Lee, Y., Yu, X., Gonzales, F., Mangelsdorf, D. J., Wang, M. Y., Richardson, C., Witters, L. A., and Unger, R. H. (2002): PPAR alpha is necessary for the lipopenic action of hyperleptinemia on white adipose and liver tissue. *Proc Natl Acad Sci U S A* **99**, 11848-53.

Lehmann, J. M., Lenhard, J. M., Oliver, B. B., Ringold, G. M., and Kliewer, S. A. (1997): Peroxisome proliferator-activated receptors alpha and gamma are activated by indomethacin and other non-steroidal anti-inflammatory drugs. *J Biol Chem* **272**, 3406-10.

Lehmann, J. M., Moore, L. B., Smith-Oliver, T. A., Wilkison, W. O., Willson, T. M., and Kliewer, S. A. (1995): An antidiabetic thiazolidinedione is a high affinity ligand for peroxisome proliferator-activated receptor gamma (PPAR gamma). *J Biol Chem* **270**, 12953-6.

Lehrke, M., Reilly, M. P., Millington, S. C., Iqbal, N., Rader, D. J., and Lazar, M. A. (2004): An inflammatory cascade leading to hyperresistinemia in humans. *PLoS Med* **1**, e45.

Leonard, A. E., Bobik, E. G., Dorado, J., Kroeger, P. E., Chuang, L. T., Thurmond, J. M., Parker-Barnes, J. M., Das, T., Huang, Y. S., and Mukerji, P. (2000): Cloning of a human cDNA encoding a novel enzyme involved in the elongation of long-chain polyunsaturated fatty acids. *Biochem J* **350 Pt 3**, 765-70.

Leslie, C. A., Gonnerman, W. A., Ullman, M. D., Hayes, K. C., Franzblau, C., and Cathcart, E. S. (1985): Dietary fish oil modulates macrophage fatty acids and decreases arthritis susceptibility in mice. *J Exp Med* **162**, 1336-49.

Levin, N., Nelson, C., Gurney, A., Vandlen, R., and de Sauvage, F. (1996): Decreased food intake does not completely account for adiposity reduction after ob protein infusion. *Proc Natl Acad Sci U S A* **93**, 1726-30.

Lewis, G. F. (1997): Fatty acid regulation of very low density lipoprotein production. *Curr Opin Lipidol* **8**, 146-53.

Lewis, R. A., Austen, K. F., and Soberman, R. J. (1990): Leukotrienes and other products of the 5-lipoxygenase pathway. Biochemistry and relation to pathobiology in human diseases. *N Engl J Med* **323**, 645-55.

Lewis, T. S., Shapiro, P. S., and Ahn, N. G. (1998): Signal transduction through MAP kinase cascades. *Adv Cancer Res* **74**, 49-139.

Li, X., Commane, M., Jiang, Z., and Stark, G. R. (2001): IL-1-induced NFkappa B and c-Jun N-terminal kinase (JNK) activation diverge at IL-1 receptor-associated kinase (IRAK). *Proc Natl Acad Sci U S A* **98**, 4461-5.

Li, Y., Totsune, K., Takeda, K., Furuyama, K., Shibahara, S., and Takahashi, K. (2003): Differential expression of adrenomedullin and resistin in 3T3-L1 adipocytes treated with tumor necrosis factor-alpha. *Eur J Endocrinol* **149**, 231-8.

Lindsay, R. S., Funahashi, T., Hanson, R. L., Matsuzawa, Y., Tanaka, S., Tataranni, P. A., Knowler, W. C., and Krakoff, J. (2002): Adiponectin and development of type 2 diabetes in the Pima Indian population. *Lancet* **360**, 57-8.

Lindsay, R. S., Funahashi, T., Krakoff, J., Matsuzawa, Y., Tanaka, S., Kobes, S., Bennett, P. H., Tataranni, P. A., Knowler, W. C., and Hanson, R. L. (2003): Genome-wide linkage analysis of serum adiponectin in the Pima Indian population. *Diabetes* **52**, 2419-25.

Listenberger, L. L., Han, X., Lewis, S. E., Cases, S., Farese, R. V., Jr., Ory, D. S., and Schaffer, J. E. (2003): Triglyceride accumulation protects against fatty acid-induced lipotoxicity. *Proc Natl Acad Sci U S A* **100**, 3077-82.

Liu, L. S., Spelleken, M., Rohrig, K., Hauner, H., and Eckel, J. (1998): Tumor necrosis factor-alpha acutely inhibits insulin signaling in human adipocytes: implication of the p80 tumor necrosis factor receptor. *Diabetes* **47**, 515-22.

Liu, S. C., Wang, Q., Lienhard, G. E., and Keller, S. R. (1999): Insulin receptor substrate 3 is not essential for growth or glucose homeostasis. *J Biol Chem* **274**, 18093-9.

Loewen, C. J., Gaspar, M. L., Jesch, S. A., Delon, C., Ktistakis, N. T., Henry, S. A., and Levine, T. P. (2004): Phospholipid metabolism regulated by a transcription factor sensing phosphatidic acid. *Science* **304**, 1644-7.

Londos, C., Brasaemle, D. L., Gruia-Gray, J., Servetnick, D. A., Schultz, C. J., Levin, D. M., and Kimmel, A. R. (1995): Perilipin: unique proteins associated with intracellular neutral lipid droplets in adipocytes and steroidogenic cells. *Biochem Soc Trans* **23**, 611-5.

Londos, C., Brasaemle, D. L., Schultz, C. J., Segrest, J. P., and Kimmel, A. R. (1999): Perilipins, ADRP, and other proteins that associate with intracellular neutral lipid droplets in animal cells. *Semin Cell Dev Biol* **10**, 51-8.

Long, S. D., and Pekala, P. H. (1996): Lipid mediators of insulin resistance: ceramide signalling down-regulates GLUT4 gene transcription in 3T3-L1 adipocytes. *Biochem J* **319 (Pt 1)**, 179-84.

Luheshi, G. N., Gardner, J. D., Rushforth, D. A., Loudon, A. S., and Rothwell, N. J. (1999): Leptin actions on food intake and body temperature are mediated by IL-1. *Proc Natl Acad Sci U S A* **96**, 7047-52.

Lumeng, C. N., Bodzin, J. L., and Saltiel, A. R. (2007a): Obesity induces a phenotypic switch in adipose tissue macrophage polarization. *J Clin Invest* **117**, 175-84.

Lumeng, C. N., Deyoung, S. M., and Saltiel, A. R. (2007b): Macrophages block insulin action in adipocytes by altering expression of signaling and glucose transport proteins. *Am J Physiol Endocrinol Metab* **292**, E166-74.

Luo, G., Hershko, D. D., Robb, B. W., Wray, C. J., and Hasselgren, P. O. (2003): IL-1beta stimulates IL-6 production in cultured skeletal muscle cells through activation of MAP kinase signaling pathway and NF-kappa B. *Am J Physiol Regul Integr Comp Physiol* **284**, R1249-54.

Luo, L., Cruz, T., and McCulloch, C. (1997): Interleukin 1-induced calcium signalling in chondrocytes requires focal adhesions. *Biochem J* **324 (Pt 2)**, 653-8.

Lynch, L., O'Shea, D., Winter, D. C., Geoghegan, J., Doherty, D. G., and O'Farrelly, C. (2009): Invariant NKT cells and CD1d(+) cells amass in human omentum and are depleted in patients with cancer and obesity. *Eur J Immunol* **39**, 1893-901.

Lyon, C. J., Law, R. E., and Hsueh, W. A. (2003): Minireview: adiposity, inflammation, and atherogenesis. *Endocrinology* **144**, 2195-200.

Ma, W., Lim, W., Gee, K., Aucoin, S., Nandan, D., Kozlowski, M., Diaz-Mitoma, F., and Kumar, A. (2001): The p38 mitogen-activated kinase pathway regulates the human interleukin-10 promoter via the activation of Sp1 transcription factor in lipopolysaccharide-stimulated human macrophages. *J Biol Chem* **276**, 13664-74.

Maeda, N., Takahashi, M., Funahashi, T., Kihara, S., Nishizawa, H., Kishida, K., Nagaretani, H., Matsuda, M., Komuro, R., Ouchi, N., Kuriyama, H., Hotta, K., Nakamura, T., Shimomura, I., and Matsuzawa, Y. (2001): PPARgamma ligands increase expression and plasma concentrations of adiponectin, an adipose-derived protein. *Diabetes* **50**, 2094-9.

Maffei, M., Halaas, J., Ravussin, E., Pratley, R. E., Lee, G. H., Zhang, Y., Fei, H., Kim, S., Lallone, R., Ranganathan, S., and et al. (1995): Leptin levels in human and rodent: measurement of plasma leptin and ob RNA in obese and weight-reduced subjects. *Nat Med* **1**, 1155-61.

Maffeis, C., Silvagni, D., Bonadonna, R., Grezzani, A., Banzato, C., and Tato, L. (2007): Fat cell size, insulin sensitivity, and inflammation in obese children. *J Pediatr* **151**, 647-52.

Malasanos, T. H., and Stacpoole, P. W. (1991): Biological effects of omega-3 fatty acids in diabetes mellitus. *Diabetes Care* **14**, 1160-79.

Malmstrom, R., Taskinen, M. R., Karonen, S. L., and Yki-Jarvinen, H. (1996): Insulin increases plasma leptin concentrations in normal subjects and patients with NIDDM. *Diabetologia* **39**, 993-6.

Mandrup, S., and Lane, M. D. (1997): Regulating adipogenesis. *J Biol Chem* **272**, 5367-70.

Manning, A. M., and Davis, R. J. (2003): Targeting JNK for therapeutic benefit: from junk to gold? *Nat Rev Drug Discov* **2**, 554-65.

Manning, B. D. (2004): Balancing Akt with S6K: implications for both metabolic diseases and tumorigenesis. *J Cell Biol* **167**, 399-403.

Mantovani, A., Sica, A., Sozzani, S., Allavena, P., Vecchi, A., and Locati, M. (2004): The chemokine system in diverse forms of macrophage activation and polarization. *Trends Immunol* **25**, 677-86.

Mantzoros, C. S. (1999): The role of leptin in human obesity and disease: a review of current evidence. *Ann Intern Med* **130**, 671-80.

Marangou, A. G., Weber, K. M., Boston, R. C., Aitken, P. M., Heggie, J. C., Kirsner, R. L., Best, J. D., and Alford, F. P. (1986): Metabolic consequences of prolonged hyperinsulinemia in humans. Evidence for induction of insulin insensitivity. *Diabetes* **35**, 1383-9.

Marette, A. (2003): Molecular mechanisms of inflammation in obesity-linked insulin resistance. *Int J Obes Relat Metab Disord* **27 Suppl 3**, S46-8.

Marignani, P. A., and Sebaldt, R. J. (1995): Formation of second messenger diradylglycerol in murine peritoneal macrophages is altered after in vivo (n-3) polyunsaturated fatty acid supplementation. *J Nutr* **125**, 3030-40.

Martin, M. U., and Wesche, H. (2002): Summary and comparison of the signaling mechanisms of the Toll/interleukin-1 receptor family. *Biochim Biophys Acta* **1592**, 265-80.

Martin, P. M., and Sutherland, A. E. (2001): Exogenous amino acids regulate trophectoderm differentiation in the mouse blastocyst through an mTOR-dependent pathway. *Dev Biol* **240**, 182-93.

Martinez-Botas, J., Anderson, J. B., Tessier, D., Lapillonne, A., Chang, B. H., Quast, M. J., Gorenstein, D., Chen, K. H., and Chan, L. (2000): Absence of perilipin results in leanness and reverses obesity in Lepr(db/db) mice. *Nat Genet* **26**, 474-9.

Martins de Lima, T., Cury-Boaventura, M. F., Giannocco, G., Nunes, M. T., and Curi, R. (2006): Comparative toxicity of fatty acids on a macrophage cell line (J774). *Clin Sci (Lond)* **111**, 307-17.

Marx, N., Bourcier, T., Sukhova, G. K., Libby, P., and Plutzky, J. (1999): PPARgamma activation in human endothelial cells increases plasminogen activator inhibitor type-1 expression: PPARgamma as a potential mediator in vascular disease. *Arterioscler Thromb Vasc Biol* **19**, 546-51.

Mason, M. M., He, Y., Chen, H., Quon, M. J., and Reitman, M. (1998): Regulation of leptin promoter function by Sp1, C/EBP, and a novel factor. *Endocrinology* **139**, 1013-22.

Matsubara, C., Nishikawa, Y., Yoshida, Y., and Takamura, K. (1983): A spectrophotometric method for the determination of free fatty acid in serum using acyl-coenzyme A synthetase and acyl-coenzyme A oxidase. *Anal Biochem* **130**, 128-33.

Matsui, H., Okumura, K., Kawakami, K., Hibino, M., Toki, Y., and Ito, T. (1997): Improved insulin sensitivity by bezafibrate in rats: relationship to fatty acid composition of skeletal-muscle triglycerides. *Diabetes* **46**, 348-53.

Matsuki, T., Horai, R., Sudo, K., and Iwakura, Y. (2003): IL-1 plays an important role in lipid metabolism by regulating insulin levels under physiological conditions. *J Exp Med* **198**, 877-88.

Matthews, D. R., Hosker, J. P., Rudenski, A. S., Naylor, B. A., Treacher, D. F., and Turner, R. C. (1985): Homeostasis model assessment: insulin resistance and beta-cell function from fasting plasma glucose and insulin concentrations in man. *Diabetologia* **28**, 412-9.

Mayser, P., Mrowietz, U., Arenberger, P., Bartak, P., Buchvald, J., Christophers, E., Jablonska, S., Salmhofer, W., Schill, W. B., Kramer, H. J., Schlotzer, E., Mayer, K., Seeger, W., and Grimminger, F. (1998): Omega-3 fatty acid-based lipid infusion in patients with chronic plaque psoriasis: results of a double-blind, randomized, placebo-controlled, multicenter trial. *J Am Acad Dermatol* **38**, 539-47.

McCall, J. L., Tuckey, J. A., and Parry, B. R. (1992): Serum tumour necrosis factor alpha and insulin resistance in gastrointestinal cancer. *Br J Surg* **79**, 1361-3.

McCall, R. E., and Tankersley, C. M. (2008): *Phlebotomy essentials*. Lippincott Williams and Wilkins, a Wolters Kluwer business.

McTernan, C. L., McTernan, P. G., Harte, A. L., Levick, P. L., Barnett, A. H., and Kumar, S. (2002a): Resistin, central obesity, and type 2 diabetes. *Lancet* **359**, 46-7.

McTernan, P. G., McTernan, C. L., Chetty, R., Jenner, K., Fisher, F. M., Lauer, M. N., Crocker, J., Barnett, A. H., and Kumar, S. (2002b): Increased resistin gene and protein expression in human abdominal adipose tissue. *J Clin Endocrinol Metab* **87**, 2407.

Medzhitov, R. (2001): Toll-like receptors and innate immunity. *Nat Rev Immunol* **1**, 135-45.

Medzhitov, R., Preston-Hurlburt, P., and Janeway, C. A., Jr. (1997): A human homologue of the Drosophila Toll protein signals activation of adaptive immunity. *Nature* **388**, 394-7.

Meier, C. A., Bobbioni, E., Gabay, C., Assimacopoulos-Jeannet, F., Golay, A., and Dayer, J. M. (2002): IL-1 receptor antagonist serum levels are increased in human obesity: a possible link to the resistance to leptin? *J Clin Endocrinol Metab* **87**, 1184-8.

Memon, R. A., Fuller, J., Moser, A. H., Smith, P. J., Grunfeld, C., and Feingold, K. R. (1999): Regulation of putative fatty acid transporters and Acyl-CoA synthetase in liver and adipose tissue in ob/ob mice. *Diabetes* **48**, 121-7.

Meyer, K. A., Kushi, L. H., Jacobs, D. R., Jr., and Folsom, A. R. (2001): Dietary fat and incidence of type 2 diabetes in older Iowa women. *Diabetes Care* **24**, 1528-35.

Meyer zu Heringdorf, D., and Jakobs, K. H. (2007): Lysophospholipid receptors: signalling, pharmacology and regulation by lysophospholipid metabolism. *Biochim Biophys Acta* **1768**, 923-40.

Miles, E. A., Allen, E., and Calder, P. C. (2002): In vitro effects of eicosanoids derived from different 20-carbon Fatty acids on production of monocyte-derived cytokines in human whole blood cultures. *Cytokine* **20**, 215-23.

Mohamed-Ali, V., Goodrick, S., Rawesh, A., Katz, D. R., Miles, J. M., Yudkin, J. S., Klein, S., and Coppack, S. W. (1997): Subcutaneous adipose tissue releases interleukin-6, but not tumor necrosis factor-alpha, in vivo. *J Clin Endocrinol Metab* **82**, 4196-200.

Moldawer, L. L., Andersson, C., Gelin, J., and Lundholm, K. G. (1988): Regulation of food intake and hepatic protein synthesis by recombinant-derived cytokines. *Am J Physiol* **254**, G450-6.

Montague, C. T., Farooqi, I. S., Whitehead, J. P., Soos, M. A., Rau, H., Wareham, N. J., Sewter, C. P., Digby, J. E., Mohammed, S. N., Hurst, J. A., Cheetham, C. H., Earley, A. R., Barnett, A. H., Prins, J. B., and O'Rahilly, S. (1997): Congenital leptin deficiency is associated with severe early-onset obesity in humans. *Nature* **387**, 903-8.

Monteiro, R., de Castro, P. M., Calhau, C., and Azevedo, I. (2006): Adipocyte size and liability to cell death. *Obes Surg* **16**, 804-6.

Moon, B., Kwan, J. J., Duddy, N., Sweeney, G., and Begum, N. (2003): Resistin inhibits glucose uptake in L6 cells independently of changes in insulin signaling and GLUT4 translocation. *Am J Physiol Endocrinol Metab* **285**, E106-15.

Moran, O., and Phillip, M. (2003): Leptin: obesity, diabetes and other peripheral effects--a review. *Pediatr Diabetes* **4**, 101-9.

Morin, C. L., Gayles, E. C., Podolin, D. A., Wei, Y., Xu, M., and Pagliassotti, M. J. (1998): Adipose tissue-derived tumor necrosis factor activity correlates with fat cell size but not insulin action in aging rats. *Endocrinology* **139**, 4998-5005.

Morrow, J. D., Awad, J. A., Boss, H. J., Blair, I. A., and Roberts, L. J., 2nd (1992): Non-cyclooxygenase-derived prostanoids (F2-isoprostanes) are formed in situ on phospholipids. *Proc Natl Acad Sci U S A* **89**, 10721-5.

Morrow, J. D., Hill, K. E., Burk, R. F., Nammour, T. M., Badr, K. F., and Roberts, L. J., 2nd (1990): A series of prostaglandin F2-like compounds are produced in vivo in humans by a non-cyclooxygenase, free radical-catalyzed mechanism. *Proc Natl Acad Sci U S A* **87**, 9383-7.

Morrow, J. D., and Roberts, L. J., 2nd (1996): The isoprostanes. Current knowledge and directions for future research. *Biochem Pharmacol* **51**, 1-9.

Mu, H., Ohashi, R., Yan, S., Chai, H., Yang, H., Lin, P., Yao, Q., and Chen, C. (2006): Adipokine resistin promotes in vitro angiogenesis of human endothelial cells. *Cardiovasc Res* **70**, 146-57.

Mulder, C., Schouten, J. A., and Popp-Snijders, C. (1983): Determination of free fatty acids: a comparative study of the enzymatic versus the gas chromatographic and the colorimetric method. *J Clin Chem Clin Biochem* **21**, 823-7.

Mullen, A., Loscher, C. E., and Roche, H. M. (2009): Anti-inflammatory effects of EPA and DHA are dependent upon time and dose-response elements associated with LPS stimulation in THP-1-derived macrophages. *J Nutr Biochem.*

Muniyappa, R., Lee, S., Chen, H., and Quon, M. J. (2008): Current approaches for assessing insulin sensitivity and resistance in vivo: advantages, limitations, and appropriate usage. *Am J Physiol Endocrinol Metab* **294**, E15-26.

Muoio, D. M., Dohm, G. L., Fiedorek, F. T., Jr., Tapscott, E. B., and Coleman, R. A. (1997): Leptin directly alters lipid partitioning in skeletal muscle. *Diabetes* **46**, 1360-3.

Murakami, M., Ichisaka, T., Maeda, M., Oshiro, N., Hara, K., Edenhofer, F., Kiyama, H., Yonezawa, K., and Yamanaka, S. (2004): mTOR is essential for growth and proliferation in early mouse embryos and embryonic stem cells. *Mol Cell Biol* **24**, 6710-8.

Murphy, D. J., and Vance, J. (1999): Mechanisms of lipid-body formation. *Trends Biochem Sci* **24**, 109-15.

Muse, E. D., Obici, S., Bhanot, S., Monia, B. P., McKay, R. A., Rajala, M. W., Scherer, P. E., and Rossetti, L. (2004): Role of resistin in diet-induced hepatic insulin resistance. *J Clin Invest* **114**, 232-9.

Mussig, K., Fiedler, H., Staiger, H., Weigert, C., Lehmann, R., Schleicher, E. D., and Haring, H. U. (2005): Insulin-induced stimulation of JNK and the PI 3-kinase/mTOR pathway leads to phosphorylation of serine 318 of IRS-1 in C2C12 myotubes. *Biochem Biophys Res Commun* **335**, 819-25.

Muzio, M., Ni, J., Feng, P., and Dixit, V. M. (1997): IRAK (Pelle) family member IRAK-2 and MyD88 as proximal mediators of IL-1 signaling. *Science* **278**, 1612-5.

Nadal, A., Alonso-Magdalena, P., Soriano, S., Quesada, I., and Ropero, A. B. (2009): The pancreatic beta-cell as a target of estrogens and xenoestrogens: Implications for blood glucose homeostasis and diabetes. *Mol Cell Endocrinol* **304**, 63-8.

Nadler, S. T., Stoehr, J. P., Schueler, K. L., Tanimoto, G., Yandell, B. S., and Attie, A. D. (2000): The expression of adipogenic genes is decreased in obesity and diabetes mellitus. *Proc Natl Acad Sci U S A* **97**, 11371-6.

Nagaev, I., Bokarewa, M., Tarkowski, A., and Smith, U. (2006): Human resistin is a systemic immune-derived proinflammatory cytokine targeting both leukocytes and adipocytes. *PLoS One* **1**, e31.

Nagamatsu, S., Kornhauser, J. M., Burant, C. F., Seino, S., Mayo, K. E., and Bell, G. I. (1992): Glucose transporter expression in brain. cDNA sequence of mouse GLUT3, the brain facilitative glucose transporter isoform, and identification of sites of expression by in situ hybridization. *J Biol Chem* **267**, 467-72.

Nasrollahzadeh, J., Siassi, F., Doosti, M., Eshraghian, M. R., Shokri, F., Modarressi, M. H., Mohammadi-Asl, J., Abdi, K., Nikmanesh, A., and Karimian, S. M. (2008): The influence of feeding linoleic, gamma-linolenic and docosahexaenoic acid rich oils on rat brain tumor fatty acids composition and fatty acid binding protein 7 mRNA expression. *Lipids Health Dis* **7**, 45.

Newgard, C. B., and McGarry, J. D. (1995): Metabolic coupling factors in pancreatic beta-cell signal transduction. *Annu Rev Biochem* **64**, 689-719.

Nguyen, M. T., Satoh, H., Favelyukis, S., Babendure, J. L., Imamura, T., Sbodio, J. I., Zalevsky, J., Dahiyat, B. I., Chi, N. W., and Olefsky, J. M. (2005): JNK and tumor necrosis factor-alpha mediate free fatty acid-induced insulin resistance in 3T3-L1 adipocytes. *J Biol Chem* **280**, 35361-71.

Nieminen, R., Lahti, A., Jalonen, U., Kankaanranta, H., and Moilanen, E. (2006): JNK inhibitor SP600125 reduces COX-2 expression by attenuating mRNA in activated murine J774 macrophages. *Int Immunopharmacol* **6**, 987-96.

Ninomiya-Tsuji, J., Kishimoto, K., Hiyama, A., Inoue, J., Cao, Z., and Matsumoto, K. (1999): The kinase TAK1 can activate the NIK-I kappaB as well as the MAP kinase cascade in the IL-1 signalling pathway. *Nature* **398**, 252-6.

Nolte, R. T., Wisely, G. B., Westin, S., Cobb, J. E., Lambert, M. H., Kurokawa, R., Rosenfeld, M. G., Willson, T. M., Glass, C. K., and Milburn, M. V. (1998): Ligand binding and co-activator assembly of the peroxisome proliferator-activated receptor-gamma. *Nature* **395**, 137-43.

Novikoff, A. B., Novikoff, P. M., Rosen, O. M., and Rubin, C. S. (1980): Organelle relationships in cultured 3T3-L1 preadipocytes. *J Cell Biol* **87**, 180-96.

O'Brien, R. M., Streeper, R. S., Ayala, J. E., Stadelmaier, B. T., and Hornbuckle, L. A. (2001): Insulin-regulated gene expression. *Biochem Soc Trans* **29**, 552-8.

Oatey, P. B., Van Weering, D. H., Dobson, S. P., Gould, G. W., and Tavare, J. M. (1997): GLUT4 vesicle dynamics in living 3T3 L1 adipocytes visualized with green-fluorescent protein. *Biochem J* **327 (Pt 3)**, 637-42.

Odegaard, J. I., Ricardo-Gonzalez, R. R., Goforth, M. H., Morel, C. R., Subramanian, V., Mukundan, L., Eagle, A. R., Vats, D., Brombacher, F., Ferrante, A. W., and Chawla, A. (2007a): Macrophage-specific PPARgamma controls alternative activation and improves insulin resistance. *Nature* **447**, 1116-20.

Odegaard, J. I., Ricardo-Gonzalez, R. R., Goforth, M. H., Morel, C. R., Subramanian, V., Mukundan, L., Red Eagle, A., Vats, D., Brombacher, F., Ferrante, A. W., and Chawla, A. (2007b): Macrophage-specific PPARgamma controls alternative activation and improves insulin resistance. *Nature* **447**, 1116-20.

Ohsumi, J., Sakakibara, S., Yamaguchi, J., Miyadai, K., Yoshioka, S., Fujiwara, T., Horikoshi, H., and Serizawa, N. (1994): Troglitazone prevents the inhibitory effects of inflammatory cytokines on insulin-induced adipocyte differentiation in 3T3-L1 cells. *Endocrinology* **135**, 2279-82.

Okada, T., Furuhashi, N., Kuromori, Y., Miyashita, M., Iwata, F., and Harada, K. (2005): Plasma palmitoleic acid content and obesity in children. *Am J Clin Nutr* **82**, 747-50.

Osborne, T. F. (2000): Sterol regulatory element-binding proteins (SREBPs): key regulators of nutritional homeostasis and insulin action. *J Biol Chem* **275**, 32379-82.

Ouchi, N., Kihara, S., Arita, Y., Maeda, K., Kuriyama, H., Okamoto, Y., Hotta, K., Nishida, M., Takahashi, M., Nakamura, T., Yamashita, S., Funahashi, T., and Matsuzawa, Y. (1999): Novel modulator for endothelial adhesion molecules: adipocyte-derived plasma protein adiponectin. *Circulation* **100**, 2473-6.

Ouchi, N., Kihara, S., Arita, Y., Okamoto, Y., Maeda, K., Kuriyama, H., Hotta, K., Nishida, M., Takahashi, M., Muraguchi, M., Ohmoto, Y., Nakamura, T., Yamashita, S., Funahashi, T., and Matsuzawa, Y. (2000): Adiponectin, an adipocyte-derived plasma protein, inhibits endothelial NF-kappaB signaling through a cAMP-dependent pathway. *Circulation* **102**, 1296-301.

Ouchi, N., Ohishi, M., Kihara, S., Funahashi, T., Nakamura, T., Nagaretani, H., Kumada, M., Ohashi, K., Okamoto, Y., Nishizawa, H., Kishida, K., Maeda, N., Nagasawa, A., Kobayashi, H., Hiraoka, H., Komai, N., Kaibe, M., Rakugi, H., Ogihara, T., and Matsuzawa, Y. (2003): Association of hypoadiponectinemia with impaired vasoreactivity. *Hypertension* **42**, 231-4.

Ouchi, N., and Walsh, K. (2007): Adiponectin as an anti-inflammatory factor. *Clin Chim Acta* **380**, 24-30.

Ozes, O. N., Akca, H., Mayo, L. D., Gustin, J. A., Maehama, T., Dixon, J. E., and Donner, D. B. (2001): A phosphatidylinositol 3-kinase/Akt/mTOR pathway mediates and PTEN antagonizes tumor necrosis factor inhibition of insulin signaling through insulin receptor substrate-1. *Proc Natl Acad Sci U S A* **98**, 4640-5.

Pang, C., Gao, Z., Yin, J., Zhang, J., Jia, W., and Ye, J. (2008): Macrophage infiltration into adipose tissue may promote angiogenesis for adipose tissue remodeling in obesity. *Am J Physiol Endocrinol Metab* **295**, E313-22.

Pardridge, W. M., Boado, R. J., and Farrell, C. R. (1990): Brain-type glucose transporter (GLUT-1) is selectively localized to the blood-brain barrier. Studies with quantitative western blotting and in situ hybridization. *J Biol Chem* **265**, 18035-40.

Patel, L., Buckels, A. C., Kinghorn, I. J., Murdock, P. R., Holbrook, J. D., Plumpton, C., Macphee, C. H., and Smith, S. A. (2003): Resistin is expressed in human macrophages and directly regulated by PPAR gamma activators. *Biochem Biophys Res Commun* **300**, 472-6.

Pawley, J. B. (2006): *Handbook of biological confocal microscopy*. Springer.

Pelleymounter, M. A., Cullen, M. J., Baker, M. B., Hecht, R., Winters, D., Boone, T., and Collins, F. (1995): Effects of the obese gene product on body weight regulation in ob/ob mice. *Science* **269**, 540-3.

Penicaud, L., Ferre, P., Terretaz, J., Kinebanyan, M. F., Leturque, A., Dore, E., Girard, J., Jeanrenaud, B., and Picon, L. (1987): Development of obesity in Zucker rats. Early insulin resistance in muscles but normal sensitivity in white adipose tissue. *Diabetes* **36**, 626-31.

Permutt, M. A., and Rotwein, P. (1983): Analysis of the insulin gene in noninsulin-dependent diabetes. *Am J Med* **75**, 1-7.

Perreault, M., and Marette, A. (2001): Targeted disruption of inducible nitric oxide synthase protects against obesity-linked insulin resistance in muscle. *Nat Med* **7**, 1138-43.

Peschon, J. J., Torrance, D. S., Stocking, K. L., Glaccum, M. B., Otten, C., Willis, C. R., Charrier, K., Morrissey, P. J., Ware, C. B., and Mohler, K. M. (1998): TNF receptor-deficient mice reveal divergent roles for p55 and p75 in several models of inflammation. *J Immunol* **160**, 943-52.

Pfeiffer, A., Janott, J., Mohlig, M., Ristow, M., Rochlitz, H., Busch, K., Schatz, H., and Schifferdecker, E. (1997): Circulating tumor necrosis factor alpha is elevated in male but not in female patients with type II diabetes mellitus. *Horm Metab Res* **29**, 111-4.

Phillips, H. J., and Terryberry, J. E. (1957): Counting actively metabolizing tissue cultured cells. *Exp Cell Res* **13**, 341-7.

Phillips, T., Ferraz, I., Bell, S., Clegg, P. D., Carter, S. D., and Mobasheri, A. (2005): Differential regulation of the GLUT1 and GLUT3 glucose transporters by growth factors and pro-inflammatory cytokines in equine articular chondrocytes. *Vet J* **169**, 216-22.

Pickup, J. C. (2004): Inflammation and activated innate immunity in the pathogenesis of type 2 diabetes. *Diabetes Care* **27**, 813-23.

Plata-Salaman, C. R. (1988): Food intake suppression by growth factors and platelet peptides by direct action in the central nervous system. *Neurosci Lett* **94**, 161-6.

Plata-Salaman, C. R. (1989): Immunomodulators and feeding regulation: a humoral link between the immune and nervous systems. *Brain Behav Immun* **3**, 193-213.

Plata-Salaman, C. R. (1992): Interferons and central regulation of feeding. *Am J Physiol* **263**, R1222-7.

Plata-Salaman, C. R. (1994): Meal patterns in response to the intracerebroventricular administration of interleukin-1 beta in rats. *Physiol Behav* **55**, 727-33.

Plata-Salaman, C. R. (1996): Anorexia induced by activators of the signal transducer gp 130. *Neuroreport* **7**, 841-4.

Plata-Salaman, C. R., and Borkoski, J. P. (1993): Interleukin-8 modulates feeding by direct action in the central nervous system. *Am J Physiol* **265**, R877-82.

Plata-Salaman, C. R., and Borkoski, J. P. (1994): Chemokines/intercrines and central regulation of feeding. *Am J Physiol* **266**, R1711-5.

Plata-Salaman, C. R., and Ffrench-Mullen, J. M. (1992): Intracerebroventricular administration of a specific IL-1 receptor antagonist blocks food and water intake suppression induced by interleukin-1 beta. *Physiol Behav* **51**, 1277-9.

Plata-Salaman, C. R., Oomura, Y., and Kai, Y. (1988): Tumor necrosis factor and interleukin-1 beta: suppression of food intake by direct action in the central nervous system. *Brain Res* **448**, 106-14.

Plata-Salaman, C. R., Sonti, G., Borkoski, J. P., Wilson, C. D., and French-Mullen, J. M. b. (1996): Anorexia induced by chronic central administration of cytokines at estimated pathophysiological concentrations. *Physiol Behav* **60**, 867-75.

Poitout, V., Hagman, D., Stein, R., Artner, I., Robertson, R. P., and Harmon, J. S. (2006): Regulation of the insulin gene by glucose and fatty acids. *J Nutr* **136**, 873-6.

Poynter, M. E., and Daynes, R. A. (1998): Peroxisome proliferator-activated receptor alpha activation modulates cellular redox status, represses nuclear factor-kappaB signaling, and reduces inflammatory cytokine production in aging. *J Biol Chem* **273**, 32833-41.

Prado, C. L., Pugh-Bernard, A. E., Elghazi, L., Sosa-Pineda, B., and Sussel, L. (2004): Ghrelin cells replace insulin-producing beta cells in two mouse models of pancreas development. *Proc Natl Acad Sci U S A* **101**, 2924-9.

Pratico, D., Barry, O. P., Lawson, J. A., Adiyaman, M., Hwang, S. W., Khanapure, S. P., Iuliano, L., Rokach, J., and FitzGerald, G. A. (1998): IPF2alpha-I: an index of lipid peroxidation in humans. *Proc Natl Acad Sci U S A* **95**, 3449-54.

Pratico, D., Smyth, E. M., Violi, F., and FitzGerald, G. A. (1996): Local amplification of platelet function by 8-Epi prostaglandin F2alpha is not mediated by thromboxane receptor isoforms. *J Biol Chem* **271**, 14916-24.

Pravenec, M., Kazdova, L., Landa, V., Zidek, V., Mlejnek, P., Jansa, P., Wang, J., Qi, N., and Kurtz, T. W. (2003): Transgenic and recombinant resistin impair skeletal muscle glucose metabolism in the spontaneously hypertensive rat. *J Biol Chem* **278**, 45209-15.

Price, S. R., Mizel, S. B., and Pekala, P. H. (1986): Regulation of lipoprotein lipase synthesis and 3T3-L1 adipocyte metabolism by recombinant interleukin 1. *Biochim Biophys Acta* **889**, 374-81.

Pullen, N., Dennis, P. B., Andjelkovic, M., Dufner, A., Kozma, S. C., Hemmings, B. A., and Thomas, G. (1998): Phosphorylation and activation of p70s6k by PDK1. *Science* **279**, 707-10.

Quan, N., Sundar, S. K., and Weiss, J. M. (1994): Induction of interleukin-1 in various brain regions after peripheral and central injections of lipopolysaccharide. *J Neuroimmunol* **49**, 125-34.

Raingeaud, J., Gupta, S., Rogers, J. S., Dickens, M., Han, J., Ulevitch, R. J., and Davis, R. J. (1995): Pro-inflammatory cytokines and environmental stress cause p38 mitogen-activated protein kinase activation by dual phosphorylation on tyrosine and threonine. *J Biol Chem* **270**, 7420-6.

Rajala, M. W., Obici, S., Scherer, P. E., and Rossetti, L. (2003): Adipose-derived resistin and gut-derived resistin-like molecule-beta selectively impair insulin action on glucose production. *J Clin Invest* **111**, 225-30.

Ralph, P., and Nakoinz, I. (1975): Phagocytosis and cytolysis by a macrophage tumour and its cloned cell line. *Nature* **257**, 393-4.

Rausch, M. E., Weisberg, S., Vardhana, P., and Tortoriello, D. V. (2008): Obesity in C57BL/6J mice is characterized by adipose tissue hypoxia and cytotoxic T-cell infiltration. *Int J Obes (Lond)* **32**, 451-63.

Reaven, G. M. (1995): Pathophysiology of insulin resistance in human disease. *Physiol Rev* **75**, 473-86.

Reid, J., Macdougall, A. I., and Andrews, M. M. (1957): Aspirin and diabetes mellitus. *Br Med J* **2**, 1071-4.

Reisner, A. H., Nemes, P., and Bucholtz, C. (1975): The use of Coomassie Brilliant Blue G250 perchloric acid solution for staining in electrophoresis and isoelectric focusing on polyacrylamide gels. *Anal Biochem* **64**, 509-16.

Ricote, M., Huang, J., Fajas, L., Li, A., Welch, J., Najib, J., Witztum, J. L., Auwerx, J., Palinski, W., and Glass, C. K. (1998a): Expression of the peroxisome proliferator-activated receptor gamma (PPARgamma) in human atherosclerosis and regulation in macrophages by colony stimulating factors and oxidized low density lipoprotein. *Proc Natl Acad Sci U S A* **95**, 7614-9.

Ricote, M., Li, A. C., Willson, T. M., Kelly, C. J., and Glass, C. K. (1998b): The peroxisome proliferator-activated receptor-gamma is a negative regulator of macrophage activation. *Nature* **391**, 79-82.

Rock, F. L., Hardiman, G., Timans, J. C., Kastelein, R. A., and Bazan, J. F. (1998): A family of human receptors structurally related to Drosophila Toll. *Proc Natl Acad Sci U S A* **95**, 588-93.

Rodbell, M. (1964): Metabolism of Isolated Fat Cells. I. Effects of Hormones on Glucose Metabolism and Lipolysis. *J Biol Chem* **239**, 375-80.

Rondinone, C. M., Wang, L. M., Lonnroth, P., Wesslau, C., Pierce, J. H., and Smith, U. (1997): Insulin receptor substrate (IRS) 1 is reduced and IRS-2 is the main docking protein for phosphatidylinositol 3-kinase in adipocytes from subjects with non-insulin-dependent diabetes mellitus. *Proc Natl Acad Sci U S A* **94**, 4171-5.

Rosen, E. D., Sarraf, P., Troy, A. E., Bradwin, G., Moore, K., Milstone, D. S., Spiegelman, B. M., and Mortensen, R. M. (1999): PPAR gamma is required for the differentiation of adipose tissue in vivo and in vitro. *Mol Cell* **4**, 611-7.

Rosen, E. D., and Spiegelman, B. M. (2006): Adipocytes as regulators of energy balance and glucose homeostasis. *Nature* **444**, 847-53.

Rotter, V., Nagaev, I., and Smith, U. (2003): Interleukin-6 (IL-6) induces insulin resistance in 3T3-L1 adipocytes and is, like IL-8 and tumor necrosis factor-alpha, overexpressed in human fat cells from insulin-resistant subjects. *J Biol Chem* **278**, 45777-84.

Rui, L., Aguirre, V., Kim, J. K., Shulman, G. I., Lee, A., Corbould, A., Dunaif, A., and White, M. F. (2001): Insulin/IGF-1 and TNF-alpha stimulate phosphorylation of IRS-1 at inhibitory Ser307 via distinct pathways. *J Clin Invest* **107**, 181-9.

Rui, L., Yuan, M., Frantz, D., Shoelson, S., and White, M. F. (2002): SOCS-1 and SOCS-3 block insulin signaling by ubiquitin-mediated degradation of IRS1 and IRS2. *J Biol Chem* **277**, 42394-8.

Russell, T. R., and Ho, R. (1976): Conversion of 3T3 fibroblasts into adipose cells: triggering of differentiation by prostaglandin F2alpha and 1-methyl-3-isobutyl xanthine. *Proc Natl Acad Sci U S A* **73**, 4516-20.

Sacre, S. M., Andreakos, E., Taylor, P., Feldmann, M., and Foxwell, B. M. (2005): Molecular therapeutic targets in rheumatoid arthritis. *Expert Rev Mol Med* **7**, 1-20.

Saghizadeh, M., Ong, J. M., Garvey, W. T., Henry, R. R., and Kern, P. A. (1996): The expression of TNF alpha by human muscle. Relationship to insulin resistance. *J Clin Invest* **97**, 1111-6.

Sakai, J., Duncan, E. A., Rawson, R. B., Hua, X., Brown, M. S., and Goldstein, J. L. (1996): Sterol-regulated release of SREBP-2 from cell membranes requires two sequential cleavages, one within a transmembrane segment. *Cell* **85**, 1037-46.

Saladin, R., De Vos, P., Guerre-Millo, M., Leturque, A., Girard, J., Staels, B., and Auwerx, J. (1995): Transient increase in obese gene expression after food intake or insulin administration. *Nature* **377**, 527-9.

Salmenniemi, U., Ruotsalainen, E., Pihlajamaki, J., Vauhkonen, I., Kainulainen, S., Punnonen, K., Vanninen, E., and Laakso, M. (2004): Multiple abnormalities in glucose and energy metabolism and coordinated changes in levels of adiponectin, cytokines, and adhesion molecules in subjects with metabolic syndrome. *Circulation* **110**, 3842-8.

Saltiel, A. R., and Olefsky, J. M. (1996): Thiazolidinediones in the treatment of insulin resistance and type II diabetes. *Diabetes* **45**, 1661-9.

Samad, F., Yamamoto, K., and Loskutoff, D. J. (1996): Distribution and regulation of plasminogen activator inhibitor-1 in murine adipose tissue in vivo. Induction by tumor necrosis factor-alpha and lipopolysaccharide. *J Clin Invest* **97**, 37-46.

Samad, F., Yamamoto, K., Pandey, M., and Loskutoff, D. J. (1997): Elevated expression of transforming growth factor-beta in adipose tissue from obese mice. *Mol Med* **3**, 37-48.

Sarraf, P., Frederich, R. C., Turner, E. M., Ma, G., Jaskowiak, N. T., Rivet, D. J., 3rd, Flier, J. S., Lowell, B. B., Fraker, D. L., and Alexander, H. R. (1997): Multiple cytokines and acute inflammation raise mouse leptin levels: potential role in inflammatory anorexia. *J Exp Med* **185**, 171-5.

Sartipy, P., and Loskutoff, D. J. (2003): Monocyte chemoattractant protein 1 in obesity and insulin resistance. *Proc Natl Acad Sci U S A* **100**, 7265-70.

Sauter, N. S., Schulthess, F. T., Galasso, R., Castellani, L. W., and Maedler, K. (2008): The antiinflammatory cytokine interleukin-1 receptor antagonist protects from high-fat diet-induced hyperglycemia. *Endocrinology* **149**, 2208-18.

Savage, D. B., Sewter, C. P., Klenk, E. S., Segal, D. G., Vidal-Puig, A., Considine, R. V., and O'Rahilly, S. (2001): Resistin / Fizz3 expression in relation to obesity and peroxisome proliferator-activated receptor-gamma action in humans. *Diabetes* **50**, 2199-202.

Savill, J., Dransfield, I., Gregory, C., and Haslett, C. (2002): A blast from the past: clearance of apoptotic cells regulates immune responses. *Nat Rev Immunol* **2**, 965-75.

Scherer, P. E., Williams, S., Fogliano, M., Baldini, G., and Lodish, H. F. (1995): A novel serum protein similar to C1q, produced exclusively in adipocytes. *J Biol Chem* **270**, 26746-9.

Schittmayer, M., and Birner-Gruenberger, R. (2009): Functional proteomics in lipid research: lipases, lipid droplets and lipoproteins. *J Proteomics* **72**, 1006-18.

Schley, P. D., Brindley, D. N., and Field, C. J. (2007): (n-3) PUFA alter raft lipid composition and decrease epidermal growth factor receptor levels in lipid rafts of human breast cancer cells. *J Nutr* **137**, 548-53.

Schmitz, G., and Ecker, J. (2008): The opposing effects of n-3 and n-6 fatty acids. *Prog Lipid Res* **47**, 147-55.

Schneider, A., Martin-Villalba, A., Weih, F., Vogel, J., Wirth, T., and Schwaninger, M. (1999): NF-kappaB is activated and promotes cell death in focal cerebral ischemia. *Nat Med* **5**, 554-9.

Schober, A., Manka, D., von Hundelshausen, P., Huo, Y., Hanrath, P., Sarembock, I. J., Ley, K., and Weber, C. (2002): Deposition of platelet RANTES triggering monocyte recruitment requires P-selectin and is involved in neointima formation after arterial injury. *Circulation* **106**, 1523-9.

Schopfer, F. J., Lin, Y., Baker, P. R., Cui, T., Garcia-Barrio, M., Zhang, J., Chen, K., Chen, Y. E., and Freeman, B. A. (2005): Nitrolinoleic acid: an endogenous peroxisome proliferator-activated receptor gamma ligand. *Proc Natl Acad Sci U S A* **102**, 2340-5.

Schraer, C. D., Risica, P. M., Ebbesson, S. O., Go, O. T., Howard, B. V., and Mayer, A. M. (1999): Low fasting insulin levels in Eskimos compared to American Indians: are Eskimos less insulin resistant? *Int J Circumpolar Health* **58**, 272-80.

Schreuder, H., Tardif, C., Trump-Kallmeyer, S., Soffientini, A., Sarubbi, E., Akeson, A., Bowlin, T., Yanofsky, S., and Barrett, R. W. (1997): A new cytokine-receptor binding mode revealed by the crystal structure of the IL-1 receptor with an antagonist. *Nature* **386**, 194-200.

Schwab, J. M., Chiang, N., Arita, M., and Serhan, C. N. (2007): Resolvin E1 and protectin D1 activate inflammation-resolution programmes. *Nature* **447**, 869-74.

Semeriva, M., and Desnuelle, P. (1976): Pancreatic lipase and colipase: an example of heterogeneous biocatalysis. *Horiz Biochem Biophys* **2**, 32-59.

Serhan, C. N., Chiang, N., and Van Dyke, T. E. (2008): Resolving inflammation: dual anti-inflammatory and pro-resolution lipid mediators. *Nat Rev Immunol* **8**, 349-61.

Serhan, C. N., Haeggstrom, J. Z., and Leslie, C. C. (1996): Lipid mediator networks in cell signaling: update and impact of cytokines. *Faseb J* **10**, 1147-58.

Seufert, J. (2004): Leptin effects on pancreatic beta-cell gene expression and function. *Diabetes* **53 Suppl 1**, S152-8.

Shah, O. J., Wang, Z., and Hunter, T. (2004): Inappropriate activation of the TSC/Rheb/mTOR/S6K cassette induces IRS1/2 depletion, insulin resistance, and cell survival deficiencies. *Curr Biol* **14**, 1650-6.

Shi, H., Cave, B., Inouye, K., Bjorbaek, C., and Flier, J. S. (2006a): Overexpression of suppressor of cytokine signaling 3 in adipose tissue causes local but not systemic insulin resistance. *Diabetes* **55**, 699-707.

Shi, H., Kokoeva, M. V., Inouye, K., Tzameli, I., Yin, H., and Flier, J. S. (2006b): TLR4 links innate immunity and fatty acid-induced insulin resistance. *J Clin Invest* **116**, 3015-25.

Shimizu, S., Tani, Y., Yamada, H., Tabata, M., and Murachi, T. (1980): Enzymatic determination of serum-free fatty acids: a colorimetric method. *Anal Biochem* **107**, 193-8.

Shimomura, I., Bashmakov, Y., Ikemoto, S., Horton, J. D., Brown, M. S., and Goldstein, J. L. (1999): Insulin selectively increases SREBP-1c mRNA in the livers of rats with streptozotocin-induced diabetes. *Proc Natl Acad Sci U S A* **96**, 13656-61.

Shimomura, I., Shimano, H., Horton, J. D., Goldstein, J. L., and Brown, M. S. (1997): Differential expression of exons 1a and 1c in mRNAs for sterol regulatory element binding protein-1 in human and mouse organs and cultured cells. *J Clin Invest* **99**, 838-45.

Siegrist-Kaiser, C. A., Pauli, V., Juge-Aubry, C. E., Boss, O., Pernin, A., Chin, W. W., Cusin, I., Rohner-Jeanrenaud, F., Burger, A. G., Zapf, J., and Meier, C. A. (1997): Direct effects of leptin on brown and white adipose tissue. *J Clin Invest* **100**, 2858-64.

Siiteri, P. K. (1987): Adipose tissue as a source of hormones. *Am J Clin Nutr* **45**, 277-82.

Sijben, J. W., and Calder, P. C. (2007): Differential immunomodulation with long-chain n-3 PUFA in health and chronic disease. *Proc Nutr Soc* **66**, 237-59.

Silswal, N., Singh, A. K., Aruna, B., Mukhopadhyay, S., Ghosh, S., and Ehtesham, N. Z. (2005): Human resistin stimulates the pro-inflammatory cytokines TNF-alpha and IL-12 in macrophages by NF-kappaB-dependent pathway. *Biochem Biophys Res Commun* **334**, 1092-101.

Simopoulos, A. P. (2002): Omega-3 fatty acids in inflammation and autoimmune diseases. *J Am Coll Nutr* **21**, 495-505.

Simopoulos, A. P., Norman, H. A., and Gillaspy, J. E. (1995): Purslane in human nutrition and its potential for world agriculture. *World Rev Nutr Diet* **77**, 47-74.

Slieker, L. J., Sloop, K. W., Surface, P. L., Kriauciunas, A., LaQuier, F., Manetta, J., Bue-Valleskey, J., and Stephens, T. W. (1996): Regulation of expression of ob mRNA and protein by glucocorticoids and cAMP. *J Biol Chem* **271**, 5301-4.

Smirnova, E., Goldberg, E. B., Makarova, K. S., Lin, L., Brown, W. J., and Jackson, C. L. (2006): ATGL has a key role in lipid droplet/adiposome degradation in mammalian cells. *EMBO Rep* **7**, 106-13.

Somm, E., Henrichot, E., Pernin, A., Juge-Aubry, C. E., Muzzin, P., Dayer, J. M., Nicklin, M. J., and Meier, C. A. (2005): Decreased fat mass in interleukin-1 receptor antagonist-deficient mice: impact on adipogenesis, food intake, and energy expenditure. *Diabetes* **54**, 3503-9.

Somwar, R., Koterski, S., Sweeney, G., Sciotti, R., Djuric, S., Berg, C., Trevillyan, J., Scherer, P. E., Rondinone, C. M., and Klip, A. (2002): A dominant-negative p38

MAPK mutant and novel selective inhibitors of p38 MAPK reduce insulin-stimulated glucose uptake in 3T3-L1 adipocytes without affecting GLUT4 translocation. *J Biol Chem* **277**, 50386-95.

Somwar, R., Perreault, M., Kapur, S., Taha, C., Sweeney, G., Ramlal, T., Kim, D. Y., Keen, J., Cote, C. H., Klip, A., and Marette, A. (2000): Activation of p38 mitogen-activated protein kinase alpha and beta by insulin and contraction in rat skeletal muscle: potential role in the stimulation of glucose transport. *Diabetes* **49**, 1794-800.

Song, M. J., Kim, K. H., Yoon, J. M., and Kim, J. B. (2006): Activation of Toll-like receptor 4 is associated with insulin resistance in adipocytes. *Biochem Biophys Res Commun* **346**, 739-45.

Sonti, G., Ilyin, S. E., and Plata-Salaman, C. R. (1996): Anorexia induced by cytokine interactions at pathophysiological concentrations. *Am J Physiol* **270**, R1394-402.

Soukas, A., Cohen, P., Socci, N. D., and Friedman, J. M. (2000): Leptin-specific patterns of gene expression in white adipose tissue. *Genes Dev* **14**, 963-80.

Souza, S. C., de Vargas, L. M., Yamamoto, M. T., Lien, P., Franciosa, M. D., Moss, L. G., and Greenberg, A. S. (1998): Overexpression of perilipin A and B blocks the ability of tumor necrosis factor alpha to increase lipolysis in 3T3-L1 adipocytes. *J Biol Chem* **273**, 24665-9.

Spector, A. A., and Yorek, M. A. (1985): Membrane lipid composition and cellular function. *J Lipid Res* **26**, 1015-35.

Spiegelman, B. M. (1998): PPARgamma in monocytes: less pain, any gain? *Cell* **93**, 153-5.

Spranger, J., Kroke, A., Mohlig, M., Hoffmann, K., Bergmann, M. M., Ristow, M., Boeing, H., and Pfeiffer, A. F. (2003): Inflammatory cytokines and the risk to develop type 2 diabetes: results of the prospective population-based European Prospective Investigation into Cancer and Nutrition (EPIC)-Potsdam Study. *Diabetes* **52**, 812-7.

Stauffacher, W., and Renold, A. E. (1969): Effect of insulin in vivo on diaphragm and adipose tissue of obese mice. *Am J Physiol* **216**, 98-105.

Steensberg, A., Fischer, C. P., Keller, C., Moller, K., and Pedersen, B. K. (2003): IL-6 enhances plasma IL-1ra, IL-10, and cortisol in humans. *Am J Physiol Endocrinol Metab* **285**, E433-7.

Steinberger, J., and Daniels, S. R. (2003): Obesity, insulin resistance, diabetes, and cardiovascular risk in children: an American Heart Association scientific statement from the Atherosclerosis, Hypertension, and Obesity in the Young Committee (Council on Cardiovascular Disease in the Young) and the Diabetes Committee (Council on Nutrition, Physical Activity, and Metabolism). *Circulation* **107**, 1448-53.

Stenbit, A. E., Tsao, T. S., Li, J., Burcelin, R., Geenen, D. L., Factor, S. M., Houseknecht, K., Katz, E. B., and Charron, M. J. (1997): GLUT4 heterozygous knockout mice develop muscle insulin resistance and diabetes. *Nat Med* **3**, 1096-101.

Stephens, J. M., Carter, B. Z., Pekala, P. H., and Malter, J. S. (1992): Tumor necrosis factor alpha-induced glucose transporter (GLUT-1) mRNA stabilization in 3T3-L1 preadipocytes. Regulation by the adenosine-uridine binding factor. *J Biol Chem* **267**, 8336-41.

Stephens, J. M., and Pekala, P. H. (1991): Transcriptional repression of the GLUT4 and C/EBP genes in 3T3-L1 adipocytes by tumor necrosis factor-alpha. *J Biol Chem* **266**, 21839-45.

Stephens, L., Anderson, K., Stokoe, D., Erdjument-Bromage, H., Painter, G. F., Holmes, A. B., Gaffney, P. R., Reese, C. B., McCormick, F., Tempst, P., Coadwell, J., and

Hawkins, P. T. (1998): Protein kinase B kinases that mediate phosphatidylinositol 3,4,5-trisphosphate-dependent activation of protein kinase B. *Science* **279**, 710-4.

Steppan, C. M., Bailey, S. T., Bhat, S., Brown, E. J., Banerjee, R. R., Wright, C. M., Patel, H. R., Ahima, R. S., and Lazar, M. A. (2001): The hormone resistin links obesity to diabetes. *Nature* **409**, 307-12.

Steppan, C. M., Wang, J., Whiteman, E. L., Birnbaum, M. J., and Lazar, M. A. (2005): Activation of SOCS-3 by resistin. *Mol Cell Biol* **25**, 1569-75.

Stoll, L. L., and Spector, A. A. (1984): Changes in serum influence the fatty acid composition of established cell lines. *In Vitro* **20**, 732-8.

Storlien, L. H., Jenkins, A. B., Chisholm, D. J., Pascoe, W. S., Khouri, S., and Kraegen, E. W. (1991): Influence of dietary fat composition on development of insulin resistance in rats. Relationship to muscle triglyceride and omega-3 fatty acids in muscle phospholipid. *Diabetes* **40**, 280-9.

Stouthard, J. M., Oude Elferink, R. P., and Sauerwein, H. P. (1996): Interleukin-6 enhances glucose transport in 3T3-L1 adipocytes. *Biochem Biophys Res Commun* **220**, 241-5.

Straczkowski, M., Kowalska, I., Nikolajuk, A., Krukowska, A., and Gorska, M. (2005): Plasma interleukin-10 concentration is positively related to insulin sensitivity in young healthy individuals. *Diabetes Care* **28**, 2036-7.

Stryer, L. (2000): *Biochemistry*. W.H. Freeman and Company. New York.

Su, C. G., Wen, X., Bailey, S. T., Jiang, W., Rangwala, S. M., Keilbaugh, S. A., Flanigan, A., Murthy, S., Lazar, M. A., and Wu, G. D. (1999): A novel therapy for colitis utilizing PPAR-gamma ligands to inhibit the epithelial inflammatory response. *J Clin Invest* **104**, 383-9.

Suganami, T., Mieda, T., Itoh, M., Shimoda, Y., Kamei, Y., and Ogawa, Y. (2007a): Attenuation of obesity-induced adipose tissue inflammation in C3H/HeJ mice carrying a Toll-like receptor 4 mutation. *Biochem Biophys Res Commun* **354**, 45-9.

Suganami, T., Nishida, J., and Ogawa, Y. (2005): A paracrine loop between adipocytes and macrophages aggravates inflammatory changes: role of free fatty acids and tumor necrosis factor alpha. *Arterioscler Thromb Vasc Biol* **25**, 2062-8.

Suganami, T., Tanimoto-Koyama, K., Nishida, J., Itoh, M., Yuan, X., Mizuarai, S., Kotani, H., Yamaoka, S., Miyake, K., Aoe, S., Kamei, Y., and Ogawa, Y. (2007b): Role of the Toll-like receptor 4/NF-kappaB pathway in saturated fatty acid-induced inflammatory changes in the interaction between adipocytes and macrophages. *Arterioscler Thromb Vasc Biol* **27**, 84-91.

Sun, X. J., Rothenberg, P., Kahn, C. R., Backer, J. M., Araki, E., Wilden, P. A., Cahill, D. A., Goldstein, B. J., and White, M. F. (1991): Structure of the insulin receptor substrate IRS-1 defines a unique signal transduction protein. *Nature* **352**, 73-7.

Sun, X. J., Wang, L. M., Zhang, Y., Yenush, L., Myers, M. G., Jr., Glasheen, E., Lane, W. S., Pierce, J. H., and White, M. F. (1995): Role of IRS-2 in insulin and cytokine signalling. *Nature* **377**, 173-7.

Surmi, B. K., and Hasty, A. H. (2008): Macrophage infiltration into adipose tissue: initiation, propagation and remodeling. *Future Lipidol* **3**, 545-556.

Suzawa, M., Takada, I., Yanagisawa, J., Ohtake, F., Ogawa, S., Yamauchi, T., Kadowaki, T., Takeuchi, Y., Shibuya, H., Gotoh, Y., Matsumoto, K., and Kato, S. (2003): Cytokines suppress adipogenesis and PPAR-gamma function through the TAK1/TAB1/NIK cascade. *Nat Cell Biol* **5**, 224-30.

Takahashi, K., Nammour, T. M., Fukunaga, M., Ebert, J., Morrow, J. D., Roberts, L. J., 2nd, Hoover, R. L., and Badr, K. F. (1992): Glomerular actions of a free radical-generated novel prostaglandin, 8-epi-prostaglandin F2 alpha, in the rat. Evidence for interaction with thromboxane A2 receptors. *J Clin Invest* **90**, 136-41.

Takano, A., Usui, I., Haruta, T., Kawahara, J., Uno, T., Iwata, M., and Kobayashi, M. (2001): Mammalian target of rapamycin pathway regulates insulin signaling via

subcellular redistribution of insulin receptor substrate 1 and integrates nutritional signals and metabolic signals of insulin. *Mol Cell Biol* **21**, 5050-62.

Takano, H., Nagai, T., Asakawa, M., Toyozaki, T., Oka, T., Komuro, I., Saito, T., and Masuda, Y. (2000): Peroxisome proliferator-activated receptor activators inhibit lipopolysaccharide-induced tumor necrosis factor-alpha expression in neonatal rat cardiac myocytes. *Circ Res* **87**, 596-602.

Tamemoto, H., Kadowaki, T., Tobe, K., Yagi, T., Sakura, H., Hayakawa, T., Terauchi, Y., Ueki, K., Kaburagi, Y., Satoh, S., and et al. (1994): Insulin resistance and growth retardation in mice lacking insulin receptor substrate-1. *Nature* **372**, 182-6.

Tanti, J. F., Gremeaux, T., van Obberghen, E., and Le Marchand-Brustel, Y. (1994): Serine/threonine phosphorylation of insulin receptor substrate 1 modulates insulin receptor signaling. *J Biol Chem* **269**, 6051-7.

Taouis, M., Dagou, C., Ster, C., Durand, G., Pinault, M., and Delarue, J. (2002): N-3 polyunsaturated fatty acids prevent the defect of insulin receptor signaling in muscle. *Am J Physiol Endocrinol Metab* **282**, E664-71.

Taylor, S. I. (1999): Deconstructing type 2 diabetes. *Cell* **97**, 9-12.

Terao, S., Yilmaz, G., Stokes, K. Y., Ishikawa, M., Kawase, T., and Granger, D. N. (2008): Inflammatory and injury responses to ischemic stroke in obese mice. *Stroke* **39**, 943-50.

Thorens, B., Sarkar, H. K., Kaback, H. R., and Lodish, H. F. (1988): Cloning and functional expression in bacteria of a novel glucose transporter present in liver, intestine, kidney, and beta-pancreatic islet cells. *Cell* **55**, 281-90.

Tietz, N. W. (1990): *Clinical Guide to Laboratory Tests*. Saunders Company. Philadelphia, USA.

Tilg, H., and Moschen, A. R. (2006): Adipocytokines: mediators linking adipose tissue, inflammation and immunity. *Nat Rev Immunol* **6**, 772-83.

Tilg, H., Trehu, E., Atkins, M. B., Dinarello, C. A., and Mier, J. W. (1994): Interleukin-6 (IL-6) as an anti-inflammatory cytokine: induction of circulating IL-1 receptor antagonist and soluble tumor necrosis factor receptor p55. *Blood* **83**, 113-8.

Tilley, S. L., Coffman, T. M., and Koller, B. H. (2001): Mixed messages: modulation of inflammation and immune responses by prostaglandins and thromboxanes. *J Clin Invest* **108**, 15-23.

Todoric, J., Loffler, M., Huber, J., Bilban, M., Reimers, M., Kadl, A., Zeyda, M., Waldhausl, W., and Stulnig, T. M. (2006): Adipose tissue inflammation induced by high-fat diet in obese diabetic mice is prevented by n-3 polyunsaturated fatty acids. *Diabetologia* **49**, 2109-19.

Tolon, R. M., Castillo, A. I., and Aranda, A. (1998): Activation of the prolactin gene by peroxisome proliferator-activated receptor-alpha appears to be DNA binding-independent. *J Biol Chem* **273**, 26652-61.

Tomas, E., Tsao, T. S., Saha, A. K., Murrey, H. E., Zhang Cc, C., Itani, S. I., Lodish, H. F., and Ruderman, N. B. (2002): Enhanced muscle fat oxidation and glucose transport by ACRP30 globular domain: acetyl-CoA carboxylase inhibition and AMP-activated protein kinase activation. *Proc Natl Acad Sci U S A* **99**, 16309-13.

Tontonoz, P., and Spiegelman, B. M. (2008): Fat and beyond: the diverse biology of PPARgamma. *Annu Rev Biochem* **77**, 289-312.

Tournier, C., Hess, P., Yang, D. D., Xu, J., Turner, T. K., Nimnual, A., Bar-Sagi, D., Jones, S. N., Flavell, R. A., and Davis, R. J. (2000): Requirement of JNK for stress-induced activation of the cytochrome c-mediated death pathway. *Science* **288**, 870-4.

Towbin, H., Staehelin, T., and Gordon, J. (1979): Electrophoretic transfer of proteins from polyacrylamide gels to nitrocellulose sheets: procedure and some applications. *Proc Natl Acad Sci U S A* **76**, 4350-4.

Toyoda, T., Kamei, Y., Kato, H., Sugita, S., Takeya, M., Suganami, T., and Ogawa, Y. (2008): Effect of peroxisome proliferator-activated receptor-alpha ligands in the interaction between adipocytes and macrophages in obese adipose tissue. *Obesity (Silver Spring)* **16**, 1199-207.

Tracey, K. J., and Cerami, A. (1994): Tumor necrosis factor: a pleiotropic cytokine and therapeutic target. *Annu Rev Med* **45**, 491-503.

Trayhurn, P., and Wood, I. S. (2004): Adipokines: inflammation and the pleiotropic role of white adipose tissue. *Br J Nutr* **92**, 347-55.

Trinder, P. (1969): Determination of blood glucose using an oxidase-peroxidase system with a non-carcinogenic chromogen. *J Clin Pathol* **22**, 158-61.

Tsutsumi, T., Suzuki, T., Moriya, K., Yotsuyanagi, H., Shintani, Y., Fujie, H., Matsuura, Y., Kimura, S., Koike, K., and Miyamura, T. (2002): Alteration of intrahepatic cytokine expression and AP-1 activation in transgenic mice expressing hepatitis C virus core protein. *Virology* **304**, 415-24.

Tzameli, I., Fang, H., Ollero, M., Shi, H., Hamm, J. K., Kievit, P., Hollenberg, A. N., and Flier, J. S. (2004): Regulated production of a peroxisome proliferator-activated receptor-gamma ligand during an early phase of adipocyte differentiation in 3T3-L1 adipocytes. *J Biol Chem* **279**, 36093-102.

Ueki, K., Kondo, T., and Kahn, C. R. (2004a): Suppressor of cytokine signaling 1 (SOCS-1) and SOCS-3 cause insulin resistance through inhibition of tyrosine phosphorylation of insulin receptor substrate proteins by discrete mechanisms. *Mol Cell Biol* **24**, 5434-46.

Ueki, K., Kondo, T., Tseng, Y. H., and Kahn, C. R. (2004b): Central role of suppressors of cytokine signaling proteins in hepatic steatosis, insulin resistance, and the metabolic syndrome in the mouse. *Proc Natl Acad Sci U S A* **101**, 10422-7.

Um, S. H., Frigerio, F., Watanabe, M., Picard, F., Joaquin, M., Sticker, M., Fumagalli, S., Allegrini, P. R., Kozma, S. C., Auwerx, J., and Thomas, G. (2004): Absence of S6K1 protects against age- and diet-induced obesity while enhancing insulin sensitivity. *Nature* **431**, 200-5.

Unger, R. H., Zhou, Y. T., and Orci, L. (1999): Regulation of fatty acid homeostasis in cells: novel role of leptin. *Proc Natl Acad Sci U S A* **96**, 2327-32.

Utriainen, T., Malmstrom, R., Makimattila, S., and Yki-Jarvinen, H. (1996): Supraphysiological hyperinsulinemia increases plasma leptin concentrations after 4 h in normal subjects. *Diabetes* **45**, 1364-6.

Uysal, K. T., Wiesbrock, S. M., Marino, M. W., and Hotamisligil, G. S. (1997): Protection from obesity-induced insulin resistance in mice lacking TNF-alpha function. *Nature* **389**, 610-4.

Vachier, I., Chanez, P., Bonnans, C., Godard, P., Bousquet, J., and Chavis, C. (2002): Endogenous anti-inflammatory mediators from arachidonate in human neutrophils. *Biochem Biophys Res Commun* **290**, 219-24.

Van der Poll, T., Romijn, J. A., Endert, E., Borm, J. J., Buller, H. R., and Sauerwein, H. P. (1991): Tumor necrosis factor mimics the metabolic response to acute infection in healthy humans. *Am J Physiol* **261**, E457-65.

van Meer, G., and Lisman, Q. (2002): Sphingolipid transport: rafts and translocators. *J Biol Chem* **277**, 25855-8.

van Meer, G., Voelker, D. R., and Feigenson, G. W. (2008): Membrane lipids: where they are and how they behave. *Nat Rev Mol Cell Biol* **9**, 112-24.

Van Obberghen, E., Baron, V., Delahaye, L., Emanuelli, B., Filippa, N., Giorgetti-Peraldi, S., Lebrun, P., Mothe-Satney, I., Peraldi, P., Rocchi, S., Sawka-Verhelle, D., Tartare-Deckert, S., and Giudicelli, J. (2001): Surfing the insulin signaling web. *Eur J Clin Invest* **31**, 966-77.

Vanhaesebroeck, B., and Alessi, D. R. (2000): The PI3K-PDK1 connection: more than just a road to PKB. *Biochem J* **346 Pt 3**, 561-76.

Vazquez-Vela, M. E., Torres, N., and Tovar, A. R. (2008): White adipose tissue as endocrine organ and its role in obesity. *Arch Med Res* **39**, 715-28.

Ventura, J. J., Kennedy, N. J., Lamb, J. A., Flavell, R. A., and Davis, R. J. (2003): c-Jun NH(2)-terminal kinase is essential for the regulation of AP-1 by tumor necrosis factor. *Mol Cell Biol* **23**, 2871-82.

Vidal, H., Auboeuf, D., De Vos, P., Staels, B., Riou, J. P., Auwerx, J., and Laville, M. (1996): The expression of ob gene is not acutely regulated by insulin and fasting in human abdominal subcutaneous adipose tissue. *J Clin Invest* **98**, 251-5.

Vidgren, H. M., Agren, J. J., Schwab, U., Rissanen, T., Hanninen, O., and Uusitupa, M. I. (1997): Incorporation of n-3 fatty acids into plasma lipid fractions, and erythrocyte membranes and platelets during dietary supplementation with fish, fish oil, and docosahexaenoic acid-rich oil among healthy young men. *Lipids* **32**, 697-705.

Vigers, G. P., Anderson, L. J., Caffes, P., and Brandhuber, B. J. (1997): Crystal structure of the type-I interleukin-1 receptor complexed with interleukin-1beta. *Nature* **386**, 190-4.

Villena, J. A., Roy, S., Sarkadi-Nagy, E., Kim, K. H., and Sul, H. S. (2004): Desnutrin, an adipocyte gene encoding a novel patatin domain-containing protein, is induced by fasting and glucocorticoids: ectopic expression of desnutrin increases triglyceride hydrolysis. *J Biol Chem* **279**, 47066-75.

Visser, M., Bouter, L. M., McQuillan, G. M., Wener, M. H., and Harris, T. B. (1999): Elevated C-reactive protein levels in overweight and obese adults. *Jama* **282**, 2131-5.

Voronov, E., Shouval, D. S., Krelin, Y., Cagnano, E., Benharroch, D., Iwakura, Y., Dinarello, C. A., and Apte, R. N. (2003): IL-1 is required for tumor invasiveness and angiogenesis. *Proc Natl Acad Sci U S A* **100**, 2645-50.

Voros, G., Maquoi, E., Demeulemeester, D., Clerx, N., Collen, D., and Lijnen, H. R. (2005): Modulation of angiogenesis during adipose tissue development in murine models of obesity. *Endocrinology* **146**, 4545-54.

Walder, K., Filippis, A., Clark, S., Zimmet, P., and Collier, G. R. (1997): Leptin inhibits insulin binding in isolated rat adipocytes. *J Endocrinol* **155**, R5-7.

Wang, A. C., Dai, X., Luu, B., and Conrad, D. J. (2001): Peroxisome proliferator-activated receptor-gamma regulates airway epithelial cell activation. *Am J Respir Cell Mol Biol* **24**, 688-93.

Wang, D., Paz-Priel, I., and Friedman, A. D. (2009): NF-kappa B p50 regulates C/EBP alpha expression and inflammatory cytokine-induced neutrophil production. *J Immunol* **182**, 5757-62.

Wang, F., Li, S. S., Segersvard, R., Strommer, L., Sundqvist, K. G., Holgersson, J., and Permert, J. (2007): Hypoxia inducible factor-1 mediates effects of insulin on pancreatic cancer cells and disturbs host energy homeostasis. *Am J Pathol* **170**, 469-77.

Wang, W., and Zhang, J. (2008): Induction of renoprotective gene expression by hypoxia-inducible transcription factor-1alpha ameliorates renal damage. *Med Hypotheses* **70**, 948-50.

Watowich, S. S., Wu, H., Socolovsky, M., Klingmuller, U., Constantinescu, S. N., and Lodish, H. F. (1996): Cytokine receptor signal transduction and the control of hematopoietic cell development. *Annu Rev Cell Dev Biol* **12**, 91-128.

Weinstein, S. L., Sanghera, J. S., Lemke, K., DeFranco, A. L., and Pelech, S. L. (1992): Bacterial lipopolysaccharide induces tyrosine phosphorylation and activation of mitogen-activated protein kinases in macrophages. *J Biol Chem* **267**, 14955-62.

Weisberg, S. P., Hunter, D., Huber, R., Lemieux, J., Slaymaker, S., Vaddi, K., Charo, I., Leibel, R. L., and Ferrante, A. W., Jr. (2006): CCR2 modulates inflammatory and metabolic effects of high-fat feeding. *J Clin Invest* **116**, 115-24.

Weisberg, S. P., McCann, D., Desai, M., Rosenbaum, M., Leibel, R. L., and Ferrante, A. W., Jr. (2003): Obesity is associated with macrophage accumulation in adipose tissue. *J Clin Invest* **112**, 1796-808.

Weiss, S. B., Kennedy, E. P., and Kiyasu, J. Y. (1960): The enzymatic synthesis of triglycerides. *J Biol Chem* **235**, 40-4.

Weldon, S. M., Mullen, A. C., Loscher, C. E., Hurley, L. A., and Roche, H. M. (2007): Docosahexaenoic acid induces an anti-inflammatory profile in lipopolysaccharide-stimulated human THP-1 macrophages more effectively than eicosapentaenoic acid. *J Nutr Biochem* **18**, 250-8.

Wesche, H., Henzel, W. J., Shillinglaw, W., Li, S., and Cao, Z. (1997): MyD88: an adapter that recruits IRAK to the IL-1 receptor complex. *Immunity* **7**, 837-47.

Weyer, C., Foley, J. E., Bogardus, C., Tataranni, P. A., and Pratley, R. E. (2000): Enlarged subcutaneous abdominal adipocyte size, but not obesity itself, predicts type II diabetes independent of insulin resistance. *Diabetologia* **43**, 1498-506.

Weyer, C., Funahashi, T., Tanaka, S., Hotta, K., Matsuzawa, Y., Pratley, R. E., and Tataranni, P. A. (2001): Hypoadiponectinemia in obesity and type 2 diabetes: close association with insulin resistance and hyperinsulinemia. *J Clin Endocrinol Metab* **86**, 1930-5.

White, M. F., Maron, R., and Kahn, C. R. (1985): Insulin rapidly stimulates tyrosine phosphorylation of a Mr-185,000 protein in intact cells. *Nature* **318**, 183-6.

White, M. F., and Yenush, L. (1998): The IRS-signaling system: a network of docking proteins that mediate insulin and cytokine action. *Curr Top Microbiol Immunol* **228**, 179-208.

WHO (2004): Global strategy on diet, physical activity and health. 57th World Health Assembly, World Health Organization.

WHO (2006): *European Charter on counteracting obesity, World Health Organization: Istanbul, Turkey*

Wieman, H. L., Wofford, J. A., and Rathmell, J. C. (2007): Cytokine stimulation promotes glucose uptake via phosphatidylinositol-3 kinase/Akt regulation of Glut1 activity and trafficking. *Mol Biol Cell* **18**, 1437-46.

Willson, T. M., Brown, P. J., Sternbach, D. D., and Henke, B. R. (2000): The PPARs: from orphan receptors to drug discovery. *J Med Chem* **43**, 527-50.

Withers, D. J., Gutierrez, J. S., Towery, H., Burks, D. J., Ren, J. M., Previs, S., Zhang, Y., Bernal, D., Pons, S., Shulman, G. I., Bonner-Weir, S., and White, M. F. (1998): Disruption of IRS-2 causes type 2 diabetes in mice. *Nature* **391**, 900-4.

Wu, H., Ghosh, S., Perrard, X. D., Feng, L., Garcia, G. E., Perrard, J. L., Sweeney, J. F., Peterson, L. E., Chan, L., Smith, C. W., and Ballantyne, C. M. (2007): T-cell accumulation and regulated on activation, normal T cell expressed and secreted upregulation in adipose tissue in obesity. *Circulation* **115**, 1029-38.

Wullschleger, S., Loewith, R., and Hall, M. N. (2006): TOR signaling in growth and metabolism. *Cell* **124**, 471-84.

Wulster-Radcliffe, M. C., Ajuwon, K. M., Wang, J., Christian, J. A., and Spurlock, M. E. (2004): Adiponectin differentially regulates cytokines in porcine macrophages. *Biochem Biophys Res Commun* **316**, 924-9.

Xing, H., Northrop, J. P., Grove, J. R., Kilpatrick, K. E., Su, J. L., and Ringold, G. M. (1997): TNF alpha-mediated inhibition and reversal of adipocyte differentiation is accompanied by suppressed expression of PPARgamma without effects on Pref-1 expression. *Endocrinology* **138**, 2776-83.

Xu, H., Barnes, G. T., Yang, Q., Tan, G., Yang, D., Chou, C. J., Sole, J., Nichols, A., Ross, J. S., Tartaglia, L. A., and Chen, H. (2003): Chronic inflammation in fat plays a crucial role in the development of obesity-related insulin resistance. *J Clin Invest* **112**, 1821-30.

Xu, H. E., Lambert, M. H., Montana, V. G., Plunket, K. D., Moore, L. B., Collins, J. L., Oplinger, J. A., Kliewer, S. A., Gampe, R. T., Jr., McKee, D. D., Moore, J. T., and Willson, T. M. (2001): Structural determinants of ligand binding selectivity between the peroxisome proliferator-activated receptors. *Proc Natl Acad Sci U S A* **98**, 13919-24.

Yamaguchi, N., Argueta, J. G., Masuhiro, Y., Kagishita, M., Nonaka, K., Saito, T., Hanazawa, S., and Yamashita, Y. (2005): Adiponectin inhibits Toll-like receptor family-induced signaling. *FEBS Lett* **579**, 6821-6.

Yamauchi, T., Kamon, J., Minokoshi, Y., Ito, Y., Waki, H., Uchida, S., Yamashita, S., Noda, M., Kita, S., Ueki, K., Eto, K., Akanuma, Y., Froguel, P., Foufelle, F., Ferre, P., Carling, D., Kimura, S., Nagai, R., Kahn, B. B., and Kadowaki, T. (2002): Adiponectin stimulates glucose utilization and fatty-acid oxidation by activating AMP-activated protein kinase. *Nat Med* **8**, 1288-95.

Yamauchi, T., Kamon, J., Waki, H., Terauchi, Y., Kubota, N., Hara, K., Mori, Y., Ide, T., Murakami, K., Tsuboyama-Kasaoka, N., Ezaki, O., Akanuma, Y., Gavrilova, O., Vinson, C., Reitman, M. L., Kagechika, H., Shudo, K., Yoda, M., Nakano, Y., Tobe, K., Nagai, R., Kimura, S., Tomita, M., Froguel, P., and Kadowaki, T. (2001): The fat-derived hormone adiponectin reverses insulin resistance associated with both lipoatrophy and obesity. *Nat Med* **7**, 941-6.

Yang, W. S., Jeng, C. Y., Wu, T. J., Tanaka, S., Funahashi, T., Matsuzawa, Y., Wang, J. P., Chen, C. L., Tai, T. Y., and Chuang, L. M. (2002): Synthetic peroxisome proliferator-activated receptor-gamma agonist, rosiglitazone, increases plasma levels of adiponectin in type 2 diabetic patients. *Diabetes Care* **25**, 376-80.

Yang, Y., Xiao, M., Mao, Y., Li, H., Zhao, S., Gu, Y., Wang, R., Yu, J., Zhang, X., Irwin, D. M., Niu, G., and Tan, H. (2009): Resistin and insulin resistance in hepatocytes: resistin disturbs glycogen metabolism at the protein level. *Biomed Pharmacother* **63**, 366-74.

Ye, J., Gao, Z., Yin, J., and He, Q. (2007): Hypoxia is a potential risk factor for chronic inflammation and adiponectin reduction in adipose tissue of ob/ob and dietary obese mice. *Am J Physiol Endocrinol Metab* **293**, E1118-28.

Yin, M. J., Yamamoto, Y., and Gaynor, R. B. (1998): The anti-inflammatory agents aspirin and salicylate inhibit the activity of I(kappa)B kinase-beta. *Nature* **396**, 77-80.

Yokogami, K., Wakisaka, S., Avruch, J., and Reeves, S. A. (2000): Serine phosphorylation and maximal activation of STAT3 during CNTF signaling is mediated by the rapamycin target mTOR. *Curr Biol* **10**, 47-50.

Yokota, T., Oritani, K., Takahashi, I., Ishikawa, J., Matsuyama, A., Ouchi, N., Kihara, S., Funahashi, T., Tenner, A. J., Tomiyama, Y., and Matsuzawa, Y. (2000): Adiponectin, a new member of the family of soluble defense collagens, negatively regulates the growth of myelomonocytic progenitors and the functions of macrophages. *Blood* **96**, 1723-32.

Yokoyama, C., Wang, X., Briggs, M. R., Admon, A., Wu, J., Hua, X., Goldstein, J. L., and Brown, M. S. (1993): SREBP-1, a basic-helix-loop-helix-leucine zipper protein that controls transcription of the low density lipoprotein receptor gene. *Cell* **75**, 187-97.

Yu, J. G., Javorschi, S., Hevener, A. L., Kruszynska, Y. T., Norman, R. A., Sinha, M., and Olefsky, J. M. (2002): The effect of thiazolidinediones on plasma adiponectin levels in normal, obese, and type 2 diabetic subjects. *Diabetes* **51**, 2968-74.

Yuan, M., Konstantopoulos, N., Lee, J., Hansen, L., Li, Z. W., Karin, M., and Shoelson, S. E. (2001): Reversal of obesity- and diet-induced insulin resistance with salicylates or targeted disruption of Ikkbeta. *Science* **293**, 1673-7.

Zeyda, M., Farmer, D., Todoric, J., Aszmann, O., Speiser, M., Gyori, G., Zlabinger, G. J., and Stulnig, T. M. (2007): Human adipose tissue macrophages are of an anti-inflammatory phenotype but capable of excessive pro-inflammatory mediator production. *Int J Obes (Lond)* **31**, 1420-8.

Zhang, H., DiBaise, J. K., Zuccolo, A., Kudrna, D., Braidotti, M., Yu, Y., Parameswaran, P., Crowell, M. D., Wing, R., Rittmann, B. E., and Krajmalnik-Brown, R. (2009): Human gut microbiota in obesity and after gastric bypass. *Proc Natl Acad Sci U S A* **106**, 2365-70.

Zhang, J., Qin, Y., Zheng, X., Qiu, J., Gong, L., Mao, H., Jia, W., and Guo, J. (2002): [The relationship between human serum resistin level and body fat content, plasma glucose as well as blood pressure]. *Zhonghua Yi Xue Za Zhi* **82**, 1609-12.

Zhou, L., Sell, H., Eckardt, K., Yang, Z., and Eckel, J. (2007): Conditioned medium obtained from in vitro differentiated adipocytes and resistin induce insulin resistance in human hepatocytes. *FEBS Lett* **581**, 4303-8.

Zhou, L., Xia, T., Li, Y., Chen, X., Peng, Y., and Yang, Z. (2006): Transcriptional regulation of the resistin gene. *Domest Anim Endocrinol* **30**, 98-107.

Zick, Y. (2001): Insulin resistance: a phosphorylation-based uncoupling of insulin signaling. *Trends Cell Biol* **11**, 437-41.

Zimmermann, R., Strauss, J. G., Haemmerle, G., Schoiswohl, G., Birner-Gruenberger, R., Riederer, M., Lass, A., Neuberger, G., Eisenhaber, F., Hermetter, A., and Zechner, R. (2004): Fat mobilization in adipose tissue is promoted by adipose triglyceride lipase. *Science* **306**, 1383-6.

Zimmet, P., Hodge, A., Nicolson, M., Staten, M., de Courten, M., Moore, J., Morawiecki, A., Lubina, J., Collier, G., Alberti, G., and Dowse, G. (1996): Serum leptin concentration, obesity, and insulin resistance in Western Samoans: cross sectional study. *Bmj* **313**, 965-9.

Zweytick, D., Athenstaedt, K., and Daum, G. (2000): Intracellular lipid particles of eukaryotic cells. *Biochim Biophys Acta* **1469**, 101-20.